Current Status and Perspectives of Human Mesenchymal Stem Cell Therapy

Lead Guest Editor: Jane Ru Choi
Guest Editors: Kar Wey Yong and Hui Yin Nam

Current Status and Perspectives of Human Mesenchymal Stem Cell Therapy

Current Status and Perspectives of Human Mesenchymal Stem Cell Therapy

Lead Guest Editor: Jane Ru Choi
Guest Editors: Kar Wey Yong and Hui Yin Nam

Editorial Board

Qingzhong Xiao, UK
Takao Yasuhara, Japan
Zhaohui Ye, USA
Holm Zaehres, Germany

Elias T. Zambidis, USA
Ludovic Zimmerlin, USA
Ewa K. Zuba-Surma, Poland
Eder Zucconi, Brazil

Maurizio Zuccotti, Italy
Nicole Isolde zur Nieden, USA

Contents

Editorial

Current Status and Perspectives of Human Mesenchymal Stem Cell Therapy

Jane Ru Choi [iD],[1,2] **Kar Wey Yong** [iD],[3,4] **and Hui Yin Nam** [iD][5]

[1]*University of British Columbia, Department of Mechanical Engineering, 2054-6250 Applied Science Lane, Vancouver, BC, Canada V6T 1Z4*
[2]*University of British Columbia, Centre for Blood Research, Life Sciences Centre, 2350 Health Sciences Mall, Vancouver, BC, Canada V6T 1Z3*
[3]*University of Calgary, Pharmaceutical Production Research Facility, Department of Chemical and Petroleum Engineering, Schulich School of Engineering, 2500 University Drive NW, Calgary, AB, Canada T2N 1N4*
[4]*University of Calgary, BioMEMS and Bioinspired Microfluidic Laboratory, Department of Mechanical and Manufacturing Engineering, Schulich School of Engineering, 2500 University Drive NW, Calgary, AB, Canada T2N 1N4*
[5]*Tissue Engineering Group (TEG), National Orthopaedic Centre of Excellence in Research and Learning (NOCERAL), Department of Orthopaedic Surgery, Faculty of Medicine, University of Malaya, Lembah Pantai, 50603 Kuala Lumpur, Malaysia*

Correspondence should be addressed to Jane Ru Choi; janeruchoi@gmail.com and Kar Wey Yong; karwey.yong@ucalgary.ca

Human mesenchymal stem cells (MSCs) hold tremendous potential in cell-based therapies and regenerative medicine [1]. These cells can be readily isolated from multiple sources including bone marrow, fat, umbilical cord, and menstrual blood, enabling the ease of their procurement [2, 3]. They are relatively free from ethical concerns and have the capability of secreting bioactive factors and differentiating into specialized cells of the tissues they reside in [4, 5]. These make them a prospective medical therapy to treat diseases such as musculoskeletal, ischemic, and respiratory diseases [6–8]. While numerous preclinical and clinical studies suggested the therapeutic potential of MSCs in various clinical fields, multiple challenges are yet to be addressed to achieve successful clinical translations [9, 10]. This special issue highlights the recent advances in the clinical use of MSCs, which allows better understanding of their therapeutic impact. The development of new strategies to improve their therapeutic effects especially in the aspects of bioprocessing, safety and efficacy assessment, cell administration route, and delivery strategies has been discussed.

A total of 14 articles introduced the use of MSCs for the treatment of multiple types of diseases, including musculoskeletal, ischemic, respiratory, neurological, autoimmune, and retinal degeneration diseases. A number of comprehensive review articles highlighted the current status and perspectives of MSC therapy in diverse scientific areas including tissue engineering, dentistry, and ischemic and autoimmune diseases. For example, R. E. B. Fitzsimmons et al. reviewed the recent advances of MSC therapy in tissue engineering. The history of MSCs, their sources, and the challenges remained in cell bioprocessing, including cell isolation, cell expansion, and downstream processes for clinical applications, were comprehensively discussed. A. G. Paz et al. reviewed the use of stem cell therapy in dentistry. Various sources and unique properties of MSCs and their potential clinical applications in the field of dentistry, including regeneration of tooth, salivary glands, and mandibular condyle, were briefly discussed.

W. Chen et al. reviewed the use of MSCs for the treatment of primary Sjögren's syndrome (pSS). MSCs are known to suppress autoimmunity and improve the secretory function of the salivary gland in patients with pSS by upregulating regulatory T cells, inactivating proinflammatory T cells, and differentiating themselves into salivary epithelial cells. Furthermore, K. W. Yong et al. discussed the potential therapeutic roles of human MSCs in ischemic diseases.

Generally, MSCs repair ischemic tissues and restore the tissue function mainly via angiogenesis and immunomodulation through paracrine secretion of bioactive factors. However, there are some remaining formidable challenges, including poor engraftment and persistence in the host and limited accessibility of the functional *in vitro* ischemic disease model. The possible solutions and future perspectives were discussed for ischemic disease therapy. Moreover, B. Xie et al. performed meta-analysis on randomized controlled clinical trials of critical limb ischemia (CLI) to assess the efficacy and safety of human autologous stem cell therapy, including bone marrow-derived MSCs (BMMSCs) in CLI. It was found that stem cell therapy reduces the ulcer size and the limb amputation rate, improves angiogenesis, and restores limb function and limb perfusion without any adverse effects. The authors also revealed that cell administration route, cell dosage, and cell type are critical factors in stem cell therapy of CLI.

A number of research articles in this issue have reported the therapeutic effects of MSCs in several diseases, such as ischemic stroke, neurological disease, acute lung injury, retinal degeneration, and cartilage repair. Y. Guan et al. demonstrated the use of BMMSCs to reduce the overall number of infiltrated monocytes (Ly6C$^+$ cells) in rat ischemic stroke models induced by distal middle cerebral artery occlusion. Interestingly, there was an increase in the proportions of Ly6C$^+$ cells that express brain-derived neurotrophic factor or proinflammatory cytokines (tumor necrosis factor-α or interleukin-1β) in the ischemic areas, which could contribute to the neuroprotection and recovery of ischemic stroke. In addition, D. Y. Lee et al. reported the use of BMMSCs to suppress inflammatory activity of activated microglia for the treatment of neurological diseases. Interestingly, coculturing BMMSCs with lipopolysaccharide-stimulated primary rat microglia increases the migration of BMMSCs to the microglia and hence reduces the inflammatory response. The outcome of this study will improve understanding of the relationship between activated microglia and MSCs, which may lead to a new therapeutic strategy using MSCs for neurological diseases.

In another study, H. Ren et al. compared the therapeutic effects of umbilical cord- and menstrual blood-derived MSCs using the mouse acute lung injury models. The authors found that both sources of MSCs are able to repair the lung tissues by suppressing the inflammation via paracrine release of bioactive factors. Interestingly, umbilical cord-derived MSCs secreted higher levels of anti-inflammatory cytokines (keratinocyte growth factor and interleukin-10) as compared to those derived from menstrual blood, resulting in a better recovery of the lung tissues. A. Barzelay et al. demonstrated that adipose-derived MSCs are able to migrate to retinal pigment epithelial cells to protect them against cell death induced by oxidative stress. This finding suggests that MSCs are extremely useful in future retinal degeneration treatment. Besides that, S. Zheng et al. reported that type 3 transforming growth factor-beta receptor (TGF-βR3) plays a vital role in regulating chondrogenic differentiation of BMMSCs. Silencing the activity of TGF-βR3 using TGF-βR3 RNA interference increased TGF-β-smad2/3 signaling and hence enhanced the chondrogenic differentiation of MSCs. It was suggested that MSCs could be modified by TGF-βR3 knockdown, which serves as a potential strategy for cartilage regeneration.

Other research articles have suggested some effective methods to improve therapeutic efficacy of MSCs. For instance, S. Baig et al. used chitosan nanoparticles as a carrier for *Thymus serpyllum* extract to evaluate its protective effects on BMMSCs against oxidative stress. This herb extract was able to reduce oxidative stress-induced apoptosis of MSCs as it contains antioxidant compounds (*e.g.*, polyphenol). This finding suggests that chitosan nanoparticles can be used to control the release of *Thymus serpyllum* extract for improving the survival rate of MSC transplant and hence enhancing therapeutic efficacy of MSCs. Furthermore, X. Yang et al. investigated the effects of hydroxyapatite nanoparticles (HA NPs) on osteogenesis of BMMSCs. It was found that HA NPs enhanced osteogenic potential of MSCs in a size-dependent manner. HA NPs with sizes of 50 nm and 100 nm were particularly effective in promoting osteogenic differentiation of MSCs, which appear promising for bone regeneration. S. Sancilio et al. developed a scaffold made up of alginate and HA NPs for encapsulating dental pulp-derived MSCs to create a dental pulp construct. This scaffold supported osteogenic differentiation of MSCs and enhanced bone mineralization, suggesting its potential use in developing dental pulp tissue construct for tooth regeneration. Additionally, H. Y. Nam et al. applied uniaxial cyclic stretching on BMMSCs to induce tenogenic differentiation. It was observed that 8% tensile strain at 1 Hz specifically mediates tenogenic differentiation of MSCs for tendon regeneration.

In summary, this special issue has provided unprecedented insights into the roles of human MSC in treating numerous diseases and highlighted the remaining challenges and possible strategies to enhance their therapeutic potential. Despite significant advancements in MSC therapy, a deeper understanding of the nature, function, mechanism, mode of isolation, and route of administration as well as experimental handling of MSCs is critical to improve the therapeutic efficacy of MSCs. While there are many obstacles remain to be overcome, we envision that the therapeutic potential of MSCs will attract further research investments in this area to resolve the challenges and improve the effectiveness of medical treatment.

Jane Ru Choi
Kar Wey Yong
Hui Yin Nam

Conflicts of Interest

The authors declare no conflict of interest.

References

[1] P. Bianco, X. Cao, P. S. Frenette et al., "The meaning, the sense and the significance: translating the science of mesenchymal

stem cells into medicine," *Nature Medicine*, vol. 19, no. 1, pp. 35–42, 2013.

[2] Y. Wang, X. Chen, W. Cao, and Y. Shi, "Plasticity of mesenchymal stem cells in immunomodulation: pathological and therapeutic implications," *Nature Immunology*, vol. 15, no. 11, pp. 1009–1016, 2014.

[3] L. Chen, B. Xiang, X. Wang, and C. Xiang, "Exosomes derived from human menstrual blood-derived stem cells alleviate fulminant hepatic failure," *Stem Cell Research & Therapy*, vol. 8, no. 1, p. 9, 2017.

[4] B. Lindroos, R. Suuronen, and S. Miettinen, "The potential of adipose stem cells in regenerative medicine," *Stem Cell Reviews and Reports*, vol. 7, no. 2, pp. 269–291, 2011.

[5] J. Phelps, A. Sanati-Nezhad, M. Ungrin, N. A. Duncan, and A. Sen, "Bioprocessing of mesenchymal stem cells and their derivatives: toward cell-free therapeutics," *Stem Cells International*, vol. 2018, Article ID 9415367, 23 pages, 2018.

[6] J. R. Choi, K. W. Yong, and J. Y. Choi, "Effects of mechanical loading on human mesenchymal stem cells for cartilage tissue engineering," *Journal of Cellular Physiology*, vol. 233, no. 3, pp. 1913–1928, 2018.

[7] J. Zhu, Q. Liu, Y. Jiang, L. Wu, G. Xu, and X. Liu, "Enhanced angiogenesis promoted by human umbilical mesenchymal stem cell transplantation in stroked mouse is Notch1 signaling associated," *Neuroscience*, vol. 290, pp. 288–299, 2015.

[8] M. N. Islam, S. R. Das, M. T. Emin et al., "Mitochondrial transfer from bone-marrow–derived stromal cells to pulmonary alveoli protects against acute lung injury," *Nature Medicine*, vol. 18, no. 5, pp. 759–765, 2012.

[9] J. Galipeau and L. Sensébé, "Mesenchymal stromal cells: clinical challenges and therapeutic opportunities," *Cell Stem Cell*, vol. 22, no. 6, pp. 824–833, 2018.

[10] K. W. Yong, J. R. Choi, A. S. Dolbashid, and W. K. Z. Wan Safwani, "Biosafety and bioefficacy assessment of human mesenchymal stem cells: what do we know so far?," *Regenerative Medicine*, vol. 13, no. 2, pp. 219–232, 2018.

Research Article

Effect of Chitosan Nanoparticle-Loaded *Thymus serpyllum* on Hydrogen Peroxide-Induced Bone Marrow Stromal Cell Damage

Salma Baig,[1] **Ainnul Hamidah Syahadah Azizan,**[2,3]
Hanumantha Rao Balaji Raghavendran ⓘ**,**[1] **Elango Natarajan** ⓘ**,**[4] **Sangeetha Naveen,**[1]
Malliga Raman Murali ⓘ**,**[1] **Hui Yin Nam** ⓘ**,**[1] **and Tunku Kamarul** ⓘ[1]

[1]*Tissue Engineering Group (TEG), National Orthopaedic Centre of Excellence in Research and Learning (NOCERAL), Department of Orthopaedic Surgery, Faculty of Medicine, University of Malaya, Lembah Pantai, 50603 Kuala Lumpur, Malaysia*
[2]*Research Centre for Crystalline Materials, School of Science and Technology, Sunway University, 47500 Selangor, Malaysia*
[3]*Department of Chemistry, Faculty of Science, University of Malaya, 50603 Kuala Lumpur, Malaysia*
[4]*Faculty of Engineering, UCSI University, Kuala Lumpur, Malaysia*

Correspondence should be addressed to Elango Natarajan; cad.elango.n@gmail.com and Tunku Kamarul; tkzrea@um.edu.my

We have determined the protective effects of *Thymus serpyllum* (TS) extract and nanoparticle-loaded TS on hydrogen peroxide-induced cell death of mesenchymal stromal cells (MSCs) *in vitro*. Gas chromatography–mass spectroscopy confirmed the spectrum of active components in the extract. Out of the three different extracts, the hexane extract showed significant free radical scavenging activity. Treatment of MSCs with H_2O_2 (hydrogen peroxide) significantly increased intracellular cell death; however, pretreatment with TS extract and nanoparticle-loaded TS (200 μg/ml) suppressed H_2O_2-induced elevation of Cyt-c and MMP13 and increased the survival rates of MSCs. H_2O_2-induced (0.1 mM) changes in cytokines were attenuated in the extract and nanoparticles by pretreatment and cotreatment at two time points ($p < 0.05$). H_2O_2 increased cell apoptosis. In contrast, treatment with nanoparticle-loaded TS suppressed the percentage of apoptosis considerably ($p < 0.05$). Therefore, TS may be considered as a potential candidate for enhancing the effectiveness of MSC transplantation in cell therapy.

1. Introduction

Thymus serpyllum is traditionally used as a culinary herb. In folk medicine, it is used for the prevention or treatment of certain diseases [1]. The phenolic monoterpenes, thymol and carvacrol, are the major components of the plant. Some studies have indicated that this herb contains a polyphenol which is the main reason for its antioxidant effect when used as an aqueous tea [2]. For decades, naturally derived antioxidants have been gaining more attention in the natural medical domain. Among the antioxidants, polyphenols are widely used as a source of alternative and complimentary therapy for various diseases, including cancers. Polyphenols extracted from rice or isolated polyphenols manifest specific biological properties such as antimicrobial, antifungal, anti-inflammatory, and free radical scavenging activities in vitro and in vivo.

Previous studies have shown that the water extract of the plant *Thymus serpyllum* has potential antioxidant and antihypersensitive effects in vitro. In traditional practice, plants rich in polyphenols have been consumed in the form of water extracts, especially as herbal teas. Despite the advantage of these plant-based polyphenols, some limitations do exist, like loss of its biological property due to poor storage conditions and the unpleasant taste of phenol. These limitations were resolved by encapsulating plant extracts into nanoparticles which would reduce the decomposition of the polyphenol and improve the slow release of polyphenols in the gastrointestinal system [3].

Encapsulated formulations of *T. serpyllum* have a potential to be used as additives to new functional food products. Upon intake of such products, it is possible to achieve a synergistic action of different polyphenolic compounds. Numerous studies have proved the pharmacological properties

of polyphenols, including antioxidative, anti-inflammatory, and antimutagenic properties. Polyphenols are plant metabolites which act as powerful antioxidants, i.e., they neutralize the harmful effects of free radicals and thus provide support to the immune system. Among the more than 8000 phenolic compounds, each one is structurally very different, and the majority are presented in the form of phenolic acids, flavanols, flavonoids, and dihydrochalcones. The main feature of these compounds is the presence of one aryl ring attached with the hydroxyl group [4, 5].

Oxidative stress is one of the major factors underlying the pathogenesis of many diseases. Hence, the excessive production of free radicals could have a negative effect on the survival of transplanted stromal cells. Increased levels of reactive oxygen/nitrogen species (ROS/RNS) are associated with tissue injury and inflammation; they affect a number of cellular processes, including cell adhesion, migration, and proliferation; and they have been linked to cellular senescence in MSCs, potentially compromising their activities [6]. Though the use of stem cells as a therapeutic tool has shown great promise for treating various ailments such as cornea repair, blood vessel damage linked to heart attacks, or diseases such as critical limb ischemia, the efficacy of these treatments has not been established yet. Nevertheless, the major limitation seems to be the poor viability of the transplanted stromal cells in the injured site affecting its therapeutic efficacy [7]. Naturally occurring polyphenolic compounds (polyphenols), such as epigallocatechin-3-gallate (EGCG) and curcumin, block ROS/RNS and are potent inflammation-modulating agents [8].

A previous study has stated that chitosan/polyphenol systems could be a very promising functional food additive when used in combination with polymers with protective and mucoadhesive properties. In addition to the existing studies, incorporation of polyphenolic compounds in chitosan micro-/nanoparticles has been achieved by spray drying or ionic gelation in the presence of polyphenolic compounds [9, 10], while other encapsulation technologies have not yet been explored enough. This study was designed to investigate the protective effect of Thymus serpyllum extract and nanoparticle-loaded plant extract on H_2O_2-induced damage of MSC.

2. Materials and Methods

2.1. Reagents.
Analytical grade n-hexane and ascorbic acid were purchased from Sigma-Aldrich (Karlsruhe, Germany). All spectrophotometric data were collected using a Jasco V-530 UV-vis spectrophotometer (Jasco International Co. Ltd., Tokyo, Japan).

2.2. Preparation of Extract- and Nanoparticle-Loaded Thymus serpyllum.
Dried plant material (Thymus serpyllum) was purchased during the flowering period (June-August) from a local market and was stored under cool and dark conditions. For the purpose of extract preparation, 60 g of dried plant material (flowers and leaves of Thymus serpyllum) were ground and weighed. The plant material was soaked in 800 ml of n-hexane for 72 hr at room temperature with occasional shaking. This was repeated five times and the mixture

was subsequently filtered (Whatman Filter Paper No. 1, UK). The extract was concentrated to dryness using a rotary evaporator. The extract was stored at 4°C till further use. Chitosan beads were synthesized by applying the emulsion technique, with the addition of a crosslinking agent. For the preparation and encapsulation of Thymus serpyllum in chitosan nanoparticles, the protocol of Kata et al. [11] was followed. Briefly, chitosan microparticles (about 0.25 g) were immersed in 10 ml of thyme extract and the pH was adjusted to 3.5 with itaconic acid and left for 24 h in a mild orbital shaker. This will improve the capacity of the nanomaterials to absorb polyphenols from the aqueous extract. After that, the microparticles were filtered from the solution and dried in an oven at 37°C and subsequently in a vacuum until reaching constant weight; then, it was stored in a desiccator at room temperature.

2.3. Bone Marrow Stromal Cell Culture.
Human bone marrow mesenchymal cells were isolated from bone marrow samples from donors at the University of Malaya Medical Center. The patient samples were collected based on written informed consent, and other approved guidelines were followed. 2.5 ml of bone marrow was diluted with 2 ml of phosphate-buffered saline (PBS; pH 7.2), and Ficoll-Paque Premium was used to layer the sample (GE Healthcare Life Sciences, Sweden). The sample was subjected to gradient centrifugation at 1800 rpm for 30 min (Eppendorf 5810R). The collected monolayer was washed twice with low-glucose Dulbecco's modified Eagle's medium (DMEM) (Invitrogen--Gibco, USA) containing 1% antibiotic/antimycotic (v/v; Invitrogen-Gibco). The isolated mononuclear cells were cultured in a low-glucose DMEM containing 10% fetal bovine serum with antibiotics and GlutaMAX (Invitrogen-Gibco). Cells were transferred into tissue culture flasks (Nunc™, USA) and cultured periodically every 3 days of media change.

Human bone marrow-derived mesenchymal stromal cells were isolated in accordance with the standard laboratory protocol. For the control group, cells were untreated. Another group of cells were treated with H_2O_2 (0.05 mM and 0.1 mM for a 2 hr incubation period). Following isolation, these cells were cultured in the DMEM medium (Invitrogen, Carlsbad, CA, USA) and supplemented with 10% stem cell-specified fetal bovine serum (FBS, Invitrogen), 100 U/ml penicillin (Sigma-Aldrich, USA), and 100 mg/ml streptomycin (Sigma-Aldrich). Cells were cultivated in tissue culture flasks at 37°C in a humidified atmosphere of 5% CO_2. Upon achieving 80% confluence, cells were harvested with trypsin (Cell Applications, San Diego, CA, USA) and passaged. Cells used in this study were obtained from a control donor (28- to 40-year age group). Exclusion criteria include the following: emergency operation for infection (skin, soft tissue, or bone) and chronic osteoarthritis, history of osteosarcoma, medical history contraindicating bone marrow aspiration, history of prior or concurrent diagnosis of HIV, hepatitis-B, or hepatitis-C infection, and diagnosis of diabetes or autoimmune disease. Inclusion criteria include the following: patients under total knee replacement, ACL reconstruction, and fracture treatment and patients whose donors are able to understand and accept the aspiration procedure.

2.4. Cell Seeding. Human mesenchymal stromal cells were trypsinized and detached at passage 3 and seeded onto a 35 mm petri dish with a cell density of 30,000–40,000 cells. The medium was changed at specific time points (24, 48, and 72 hr) according to the respective treatment plan.

2.5. Gas Chromatography–Mass Spectroscopic (GC–MS) Analysis. An Agilent Technologies 7890A Network Gas Chromatographic (GC) system equipped with a TOF-MS (mass selective) detector and an Agilent Technologies 7693 series automatic liquid sampler were used for the analysis of the hexane extract. The injection volume was $1.0\,\mu l$ with split ratio of 1 : 10. An electron ionization system producing an ionization energy of 70 eV was used for GS-MS analysis of the sample. Initial temperature was set at 40°C (hold time of 5-minute interval). Furthermore, the settings of 4°C/min at 160°C and 5°C/min at 280°C with a 10-minute hold time were used. Gas (helium) was provided at a flow rate of 1.0 ml/min and at the mass scanning range (50–1000 m/z). The temperatures for the injector (250°C) and MS transfer line (300°C) were set.

2.5.1. Free Radical Scavenging Activity. The free radical scavenging potential of the hexane extract was assessed by measuring its ability to scavenge 2,2′-diphenyl-1-picrylhydrazyl stable radicals (DPPH). The samples (2 to 10 mg/ml) were mixed with 1 ml of 90 μmol/l DPPH solution and made up with 95% methanol to attain a final volume of 4 ml. Ascorbic acid was used as control. After an incubation period of 30 minutes at room temperature, the absorbance was recorded at 515 nm. Percent of radical scavenging concentration was calculated using the following formula:

$$\text{Radical scavenging}(\%) = 100 \times \left(\frac{A\,\text{blank} - A\,\text{sample}}{A\,\text{blank}} \right), \quad (1)$$

where (A blank) is the absorbance of the control (ascorbic acid)—containing all reagents except the test extract—and (A sample) is the absorbance of each tested extract. IC50 values representing the concentration of the extract that caused 50% scavenging were calculated from the plot of percentage scavenging against concentration.

2.6. Immunocytochemistry. Cells on each grid plate were fixed with 4% (w/v) paraformaldehyde (PFA, Sigma-Aldrich) in 1x phosphate-buffered saline for 20 min at room temperature. Cells were treated for 5 min and thrice washed with the PBS 0.1% (v/v) Triton X-100 (Sigma-Aldrich) in $1 \times$ PBS. To block nonspecific binding, the cells were incubated with 2% (v/v) goat serum (Sigma-Aldrich) in $1 \times$ PBS for 30 min at room temperature and washed thrice with the PBS. The cells were incubated with primary antibodies at 4°C for 3 h. The following primary antibodies (anti-FN antibody IST-9) were used for incubation (1 : 1000; Abcam, England): B-cell lymphoma 2 (BCL2), cytochrome c (Cyt-c), and matrix metalloproteinase 13 (MMP13). After the incubation, the cells were washed thrice with $1 \times$ PBS for 5 min each. Polyclonal secondary antibody (chicken) was added to Anti-Mouse IgG FITC labelled (Abcam, England), and $1 \times$ PBS was added

for double staining. These cells were incubated for 1 h at room temperature and counterstained using Hoechst dye and kept for 15 minutes. The signals were observed under a microscope (Nikon C-HGFI, Japan), and the images were taken documented NIS elemental imaging software using the NIS-Elements Documentation software.

2.7. Cytokine Assay and Flow Cytometry. ProcartaPlex™ Multiplex Immunoassays for serum, plasma, and cell culture supernatants were used to examine the cytokine levels. The cells were collected by centrifugation, and the supernatant was aspirated. The cells were resuspended in 0.5–1.0 ml $1 \times$ PBS, and formaldehyde was added to obtain a final concentration of 45%. This was fixed for 10 min at 37°C. The tubes were chilled on ice for 1 min. Cells were permeabilized by adding ice-cold methanol slowly to prechilled cells, while gently vortexing to a final concentration of 90% methanol. It was further incubated for 30 min on ice. Immunostaining was done with Section D, or cells were stored at −20°C in 90% methanol. $0.5–1 \times 10^5$ cells were aliquoted into each assay tube, and 2–3 ml incubation buffer was added to each tube and washed by centrifugation. Cells were resuspended in 100 μl of primary antibody (prepared in incubation buffer as directed) and incubated for 1 hour at room temperature. Washing by centrifugation in 2–3 ml of incubation buffer resuspended the cells in 0.5 ml $1 \times$ PBS and this was analyzed on a flow cytometer. Cells were resuspended in 0.5 ml of DNA dye (propidium iodide) and incubated for at least 30 min at room temperature. Cells were analyzed in DNA staining solution on a flow cytometer.

2.8. Statistical Analysis. All the experiments were performed in triplicate and the data are presented as mean values ± standard deviation of triplicate findings. Statistical analysis of the data was performed using the SPSS Program, and a probability value of $p \leq 0.001$ was considered to show a statistically significant difference.

3. Results

The extract was subjected to GC-MS chromatography. The list of the chemical compositions is shown in Table 1, and their respective spectra are shown in Figure 1. In vitro free radical scavenging activity was examined using a different extra hexane extract, dichloromethane extract, and methanol extract, with ascorbic acid used as a positive control as shown in Figure 2(d). The concentration of 10,000 μg/ml showed approximately 90% free radical scavenging activity, while 5000 μg/ml of hexane extract (Figure 2(a)) showed approximately 40–50% free radical scavenging activity. While dichloromethane (Figure 2(b)) and methanol (Figure 2(c)) extract at 5000 μg/ml showed around 20–25% free radical scavenging activity, increased concentrations showed around 80–90%, respectively.

Initially, bone marrow stromal cells were exposed to each of the two concentrations of hydrogen peroxide (0.05 mM and 0.1 mM, 2 h) at 37°C to test the potential of the extract and nanoparticle-loaded plant extract (Figures 3–6). Expression of BCL2, MMP13, and cytochrome c was examined. The

TABLE 1: List of chemical compounds identified in the hexane extract of *Thymus serpyllum* using GC-MS.

Compounds	Formula	Retention time (s)	Similarity	Weight	Area %
Benzene, 1-methyl-3-(1-methylethyl)-	$C_{10}H_{14}$	926.85	971	134	2.3176
Thymoquinone	$C_{10}H_{12}O_2$	1444.55	950	164	8.8140
Thymol	$C_{10}H_{14}O$	1540.2	956	150	35.2661
Carvacrol	$C_{10}H_{14}O$	1559.65	954	150	30.9641
p-*tert*-Butyl catechol	$C_{10}H_{14}O_2$	1830.75	788	166	9.8301
2(4H)-Benzofuranone, 5,6,7,7a-Tetrahydro-4,4,7a-trimethyl-	$C_{11}H_{16}O_2$	1984.85	899	180	1.4065
2-Methyloctacosane	$C_{29}H_{60}$	3840.35	931	408	1.5172
Hexacosane	$C_{26}H_{54}$	4127.25	961	366	2.3650
Heptacosane	$C_{27}H_{56}$	4310.75	960	380	7.4996
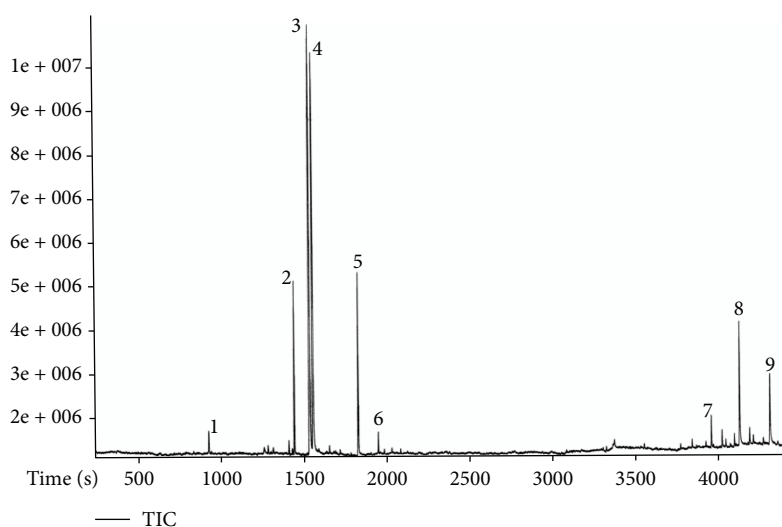
FIGURE 1: Gas chromatography–mass spectroscopy chromatogram of *Thymus serpyllum* hexane extract. Peak numbers indicate the type of active component present in the extract.

control group showed no or very less percentage of cells positive for FITC BCL2 expression. The H_2O_2 treatment induced 40–50% of cells to be positive for FITC BCL2 expression, when compared with those of the extract treatment group. The cells treated with nanoparticle-loaded plant extract showed BCL2 expression, however it was statistically not significant. We also examined the expression of the other two important factors of apoptosis, cytochrome c and MMP13. The bone marrow stromal cells treated with H_2O_2 induced 72–86% cell expression of cytochrome c, while the cotreatment with extract and nanoparticles induced 47% and 38% cell expression, respectively, which was statistically ($p < 0.05$) less significant when compared to cells treated with H_2O_2 alone. The percentage of cells that appeared to be positive for FITC cells of the MMP13 antibody was around 88–98%, while for the cotreatment groups, either extract or nanoparticles, it was around 45% and 38%, respectively. These results indicated that the extract and nanoparticles cotreated against hydrogen peroxide were effective. When the concentration of hydrogen peroxide was increased and cotreated with the extract and nanoparticles, the expression of BCL2 was almost similar with the H_2O_2-treated group. However, the Cyto-c

and MMP13 expression was considerably less when compared with the H_2O_2-only group. This is indicative that the extract and nanoparticles could be protective against apoptosis in cells. However, the nonexpressive level of BCL2 against apoptosis was not evident which needs further investigation.

Isolated human bone marrow stromal cells were pretreated with extract and nanoparticles and challenged against H_2O_2. There was no difference between the cells positive for FITC (BCL2) when treated with H_2O_2 only and pretreated with extract and nanoparticles. However, the extract pretreatment significantly reduced the expression of Cyt-c (26%–31%) and MMP13 (39%–43%), while the nanoparticle pretreatment showed the expression of Cyt-c (27%–30%) and MMP13 (32%–39%) when compared with the cells treated with H_2O_2.

Furthermore, the levels of cytokines were examined in bone marrow stromal cells treated with H_2O_2 at two time points, namely 24 h and 72 h. The cells treated with H_2O_2 induced the release of IL8 (Figure 7(a)) by approximately 2-fold when compared to the untreated control cells. Furthermore, the cells cotreated with nanoparticles inhibited the release when compared with those that were treated with
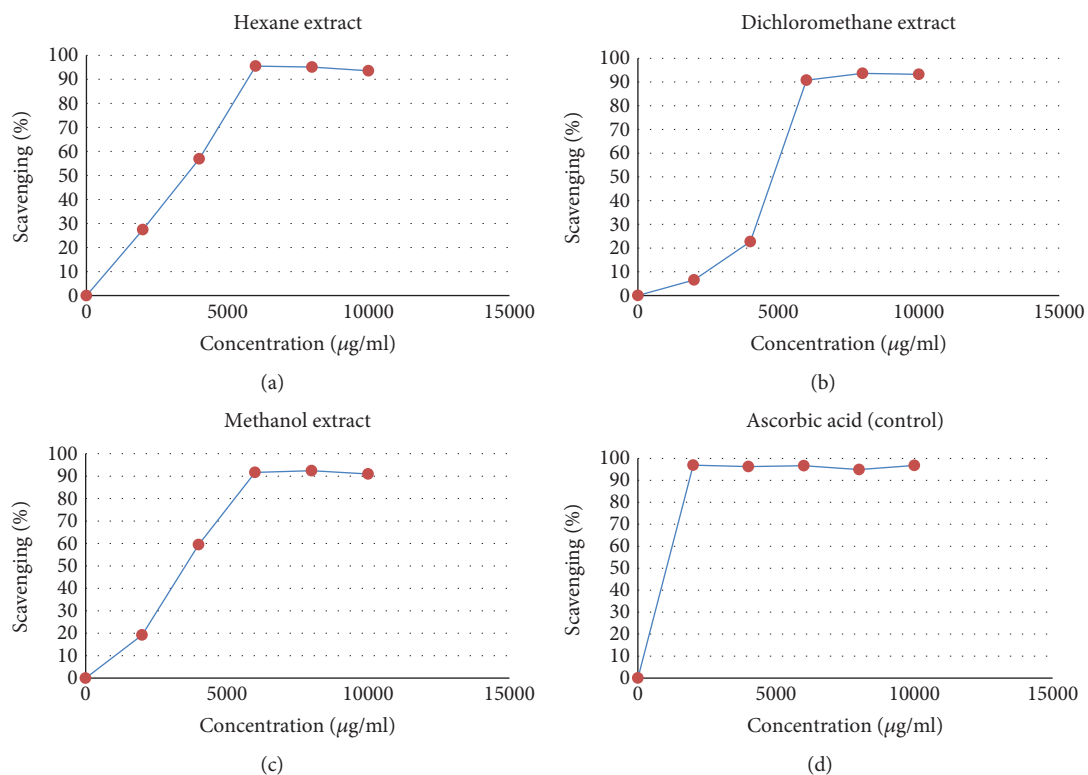
FIGURE 2: Free radical scavenging potential of (a) hexane extract, (b) dichloromethane extract, (c) methanol extract, and (d) ascorbic acid (control). The percentage of scavenging activity has been compared with ascorbic acid used as control.
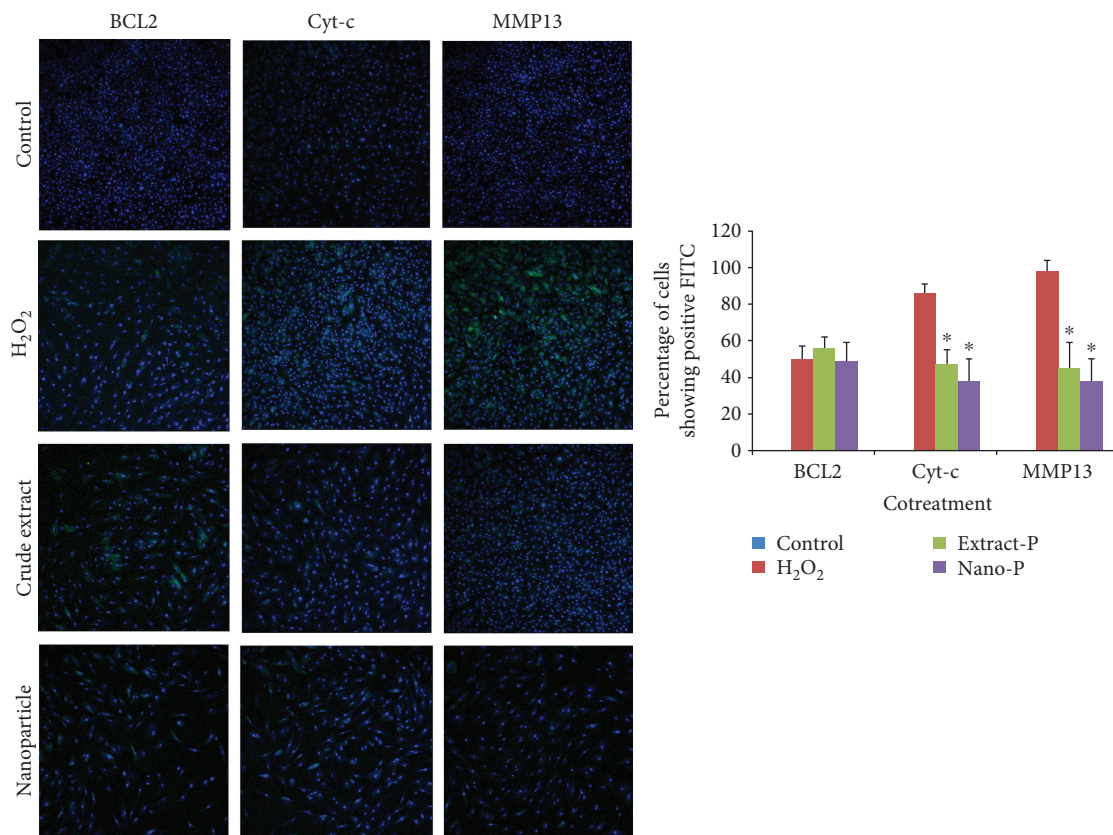
FIGURE 3: Expression of BCL2, cytochrome c (Cyt-c), and matrix metalloproteinase (MMP13) in control (untreated) and experimental groups (Extract-S and Nano-S represent cotreatment with hydrogen peroxide (H_2O_2–0.5 mM)).
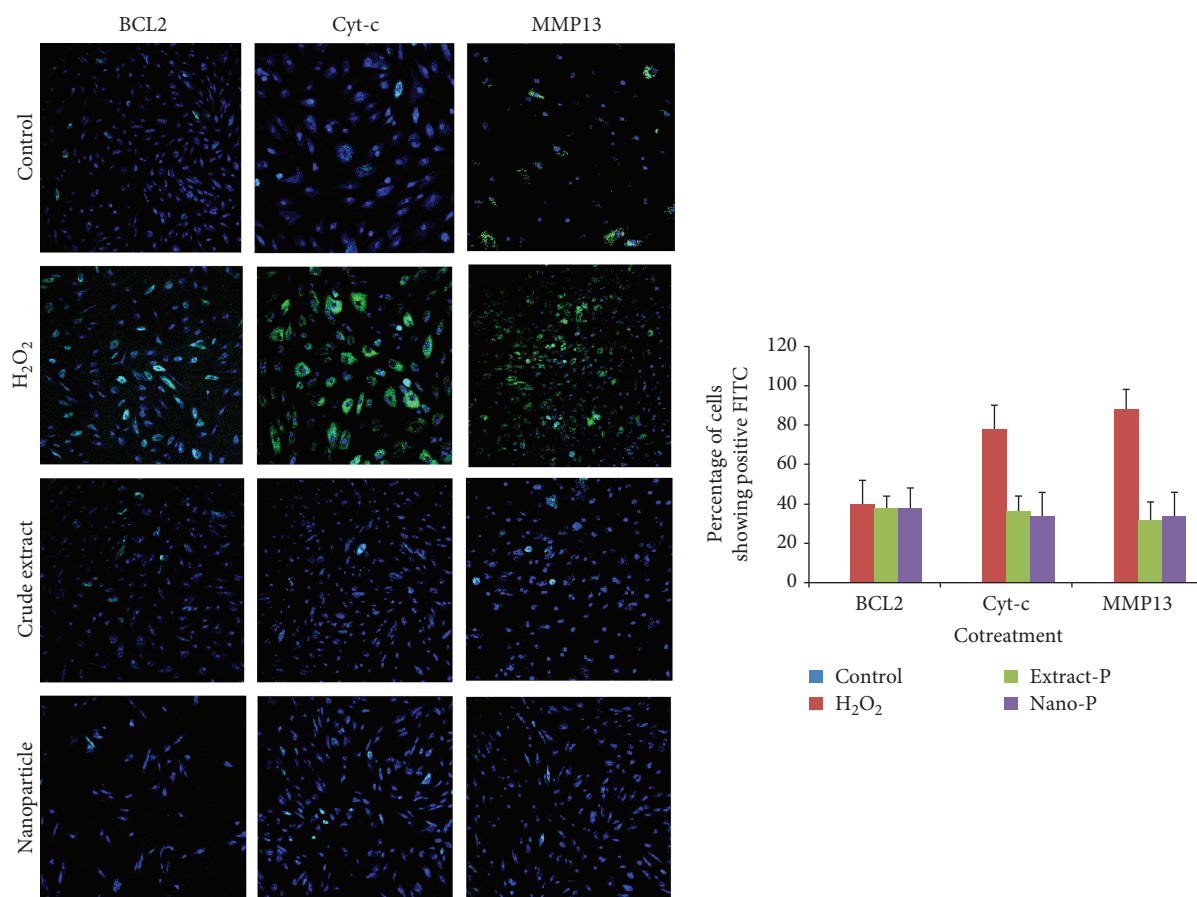
FIGURE 4: Expression of BCL2, cytochrome c (Cyt-c), and matrix metalloproteinase (MMP13) in control (untreated) and experimental groups (Extract-S and Nano-S represent cotreatment with hydrogen peroxide (H_2O_2—1 mM)).

H_2O_2 only. At 72 h, the release was considerably reduced ($p < 0.05$) in extract pretreatment and nanoparticle cotreatment. No significant changes were observed in the levels of IL2 (Figure 7(b)). ILβ1 was significantly increased by 2-fold in the cells treated with H_2O_2 at 24 h and 72 h time points compared to the control (Figure 7(c)). It was also observed that the cotreatment and pretreatment with extract and nanoparticles significantly reduced the increase in IL2 by 2-fold ($p < 0.05$). Next, the vascular endothelial growth factor was significantly decreased by 2-fold when compared with the control. The levels were considerably reduced in cotreatment and pretreatment with extract and nanoparticles at 72 h (Figure 7(d)). Cells cotreated with nanoparticles did not prevent the decrease significantly at 24 h time, while the extract cotreatment, extract pretreatment, and nanoparticle pretreatment prevented the decrease.

In addition, we examined the levels of IL6 (Figure 8(a)), which showed that the cells treated with H_2O_2 induced the release of IL6, a proinflammatory factor, by approximately 3-fold in comparison to the control. In response to this, the levels were reduced in nanoparticle cotreatment and pretreatment while the extract showed a protective role at 72 h ($p < 0.05$) when compared with the cells treated with H_2O_2 only.

The levels of TNF-α in the cells treated with H_2O_2 (Figure 8(b)) increased significantly when compared to

control cells. In contrast, the levels did not increase significantly in the cells treated with extract and nanoparticles in both cotreatment and pretreatment. The levels of MCP in the cells treated with H_2O_2 considerably decreased (Figure 8(c)) when compared with the untreated control cells. These decreases were significantly prevented when the cell extract or nanoparticles were cotreated or pretreated. The levels of IL3 in the cells treated with H_2O_2 decreased when compared with the control cells. In contrast, extract and nanoparticle-loaded plant extract were not decreased ($p < 0.05$) compared with untreated cells at the 24 h and 72 h time points (Figure 8(d)).

All the hMSCs were treated similarly with both nanoparticle and extract preparations, and the distribution of cells in different phases of the cell cycle was analyzed (Figure 9(a)–9(e)). Treatment with nanoparticle-loaded plant extract led to a marginal accumulation of cells in the G2/M phase following pretreatment time. However, after 72 h of similar treatment, the arrest of the cells in the G1 and S phases of the cell cycle was observed. In the case of cotreatment with extracted cells, both 24 h and 72 h had no effect on the G2/M phase of the cell cycle, except for a marginal increase in the S phase (in case of 72 h). Together, these results clearly show that the observed cell growth effects of both nanoparticle and extract preparations were associated with their cell cycle arrest activity. The percentage of apoptosis was also
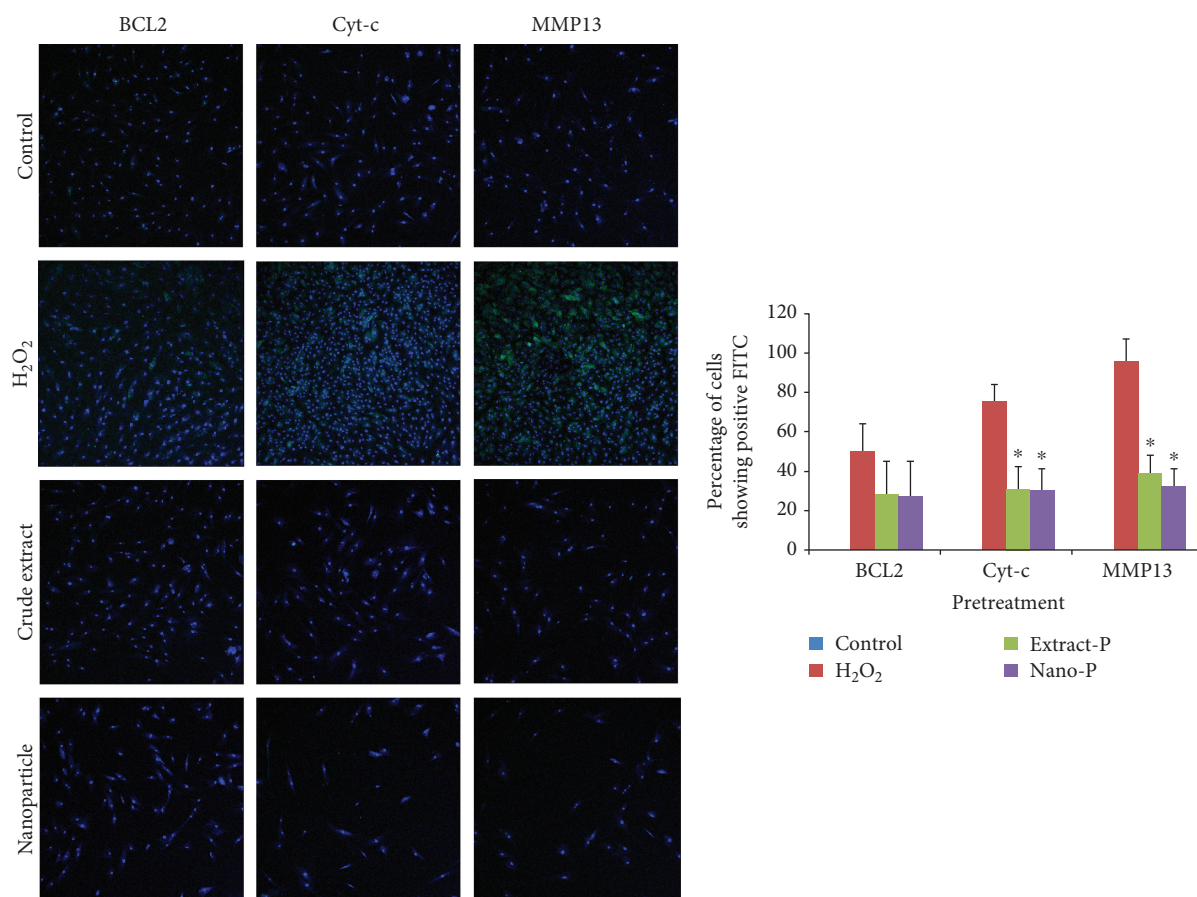
FIGURE 5: Expression of BCL2, cytochrome c (Cyt-c), and matrix metalloproteinase (MMP13) in control (untreated) and experimental groups (Extract-P and Nano-P represent pretreatment with hydrogen peroxide (H_2O_2–0.05 mM)).

calculated from FACS data, as shown in Figure 9(f). The control- (H_2O_2) treated cells showed a high percentage of cells undergoing apoptosis, while nanoparticle-loaded plant extract-treated cells and plant extract-treated cells showed a low apoptosis percentage at 72 h; however, no effect was observed at 24 h.

4. Discussion

For decades, the use of polyphenols involves an aqueous extraction process of herbs and preparation of herbal tea [7]. During this preparation, the biological effects may be affected due to the presence of oxygen moisture and storage conditions. In addition, the consumption of polyphenols is limited due to their taste. Such limitations can be improved via encapsulation methods like converting liquid to solid forms for easier consumption. A further advantage of encapsulation is having a slow release formula. These methods have potential in new functional food products [12]. Previous studies on aqueous *Thymus serpyllum* L. extract have proved that it has a pronounced antioxidant and free radical scavenging activity in vitro and an antihypertensive effect. So, for different compounds like PLGA and PLA, hydrogen has been used for the encapsulation of active molecules [13]. Although chitosan/polyphenol systems could be very

promising as a functional food additive, to our knowledge there has been only one report on the entrapment of thyme polyphenols into chitosan microbeads. In addition, in the existing studies, incorporation of polyphenolic compounds in chitosan micro/nanoparticles has been performed by spray drying or ionic gelation in the presence of polyphenolic compounds, while other encapsulation technologies have not yet been explored adequately enough. A previous study attempted to load polyphenolic compounds into chitosan microbeads that were obtained by an emulsion crosslinking technique (ready-made support) by the so-called postloading entrapment. They have examined the physiochemical properties of the bead, while the biological property or radical quenching property was not examined [14, 15].

Among different cell sources, mesenchymal stem cells show an extensive differentiation potential abundant in bone marrow tissue, adipose tissue, and several other tissues. The adipose or bone marrow stromal cells are a good source for potential applications due to their abundance, accessibility, and low immunogenicity [16]. Their survival and rate of differentiation at the injured site of transplantation is limited due to apoptosis in the stress environment. Therefore, the identification of a strategy for the protection of transplanted MSCs is key for the development of MSC-based therapy for regenerative therapy [17].
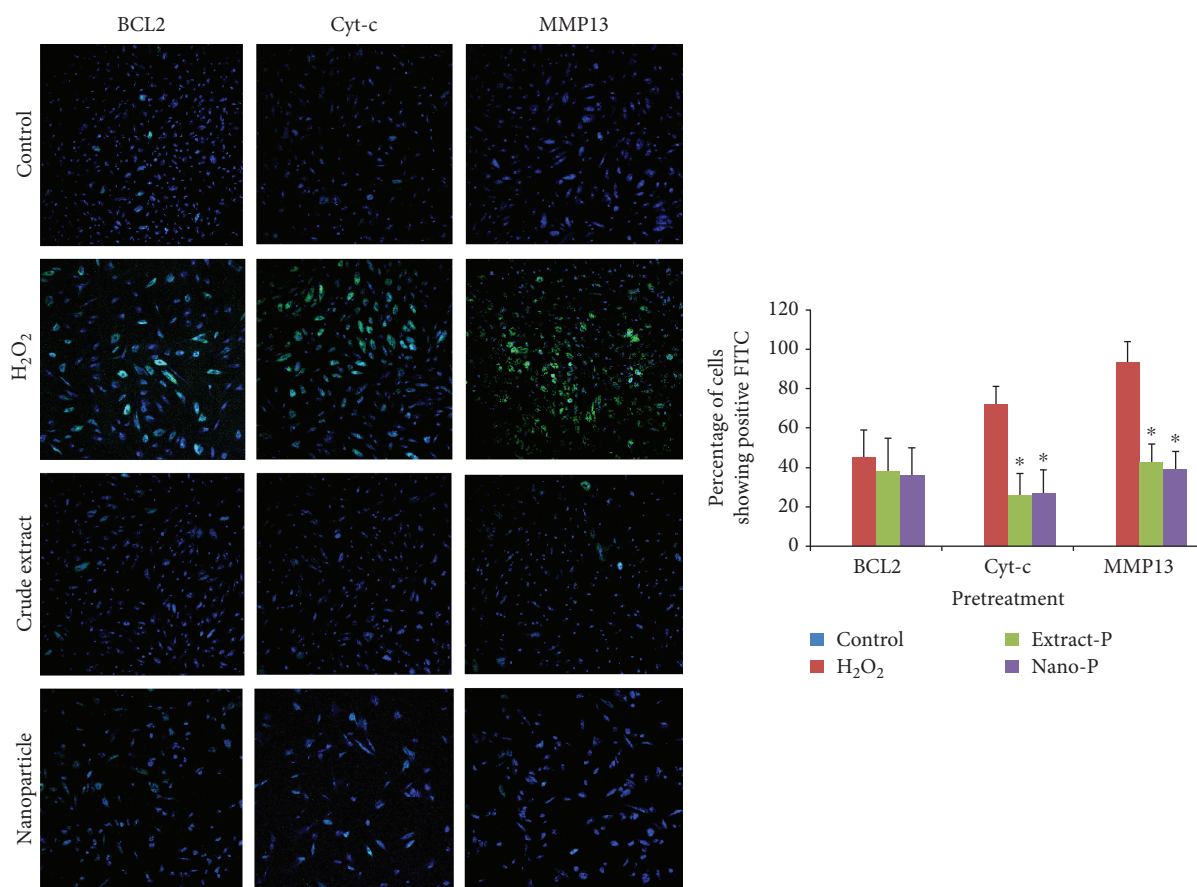
FIGURE 6: Expression of BCL2, cytochrome c (Cyt-c), and matrix metalloproteinase (MMP13) in control (untreated) and experimental groups (Extract-P and Nano-P represent pretreatment with hydrogen peroxide (H_2O_2—0.1 mM)).

In the present study, the HPLC chromatogram detected polyphenols in the *Thymus serpyllum* extract. Despite the wide spectrum of attractive biological properties, the protective effects of *Thymus serpyllum* on hydrogen peroxide-induced changes in MSCs have yet to be fully elucidated. The BCL2 family of proteins is composed of the antiapoptotic proteins and proapoptotic proteins, of which their relative proportions control the fine balance between cell survival and cell death via the intrinsic apoptotic pathway [18]. The present study indicated that fluorescence microscopy could reverse the reduction of the antiapoptotic protein BCL2 following treatment with H_2O_2, but the level of reduction was not significant. In addition, cotreatment with extract and nanoparticle-loaded extract with H_2O_2 significantly reduced the Cyto-c and MMP13 levels compared with cells treated with H_2O_2 alone, showing the protective effects of the extract or nanoparticle of *Thymus serpyllum*. Reactive oxygen species (ROS) excessively produced by the respiratory chain can also cause progressive mitochondrial damage leading to apoptosis. All of the proposed cytochrome c releasing mechanisms, however, remain hypothetical, and fail to provide a physiological basis for the underlying naturally occurring apoptosis. In support of our data, the change in the expressions of *MMP13* was remarkably directly upregulated by the oxidant, and their activities were implicated in the invasive potential induced in cells [19]. The activation of *MMP* probably occurs by the reaction of ROS with thiol groups in the protease catalytic domain. In addition to their role as key regulators of *MMP* activation, ROS have been implicated in *MMP* gene expression [20]. Since treatment reduced their elevation in the MMP, it is an indication of its protective role on oxidative stress-mediated damage to the cells.

Interleukin (IL8) is a cytokine with potent chemotactic properties for neutrophils and T lymphocytes, and thus serves to amplify the inflammatory cascade. IL8 is produced by a wide variety of cell types including mononuclear cells, endothelial cells, and epithelial cells [21], and it has been implicated as an important mediator of neutrophil infiltration. However, some studies have shown no direct relation with apoptosis in other cell lines, and the increase in stromal cells upon H_2O_2 treatment was indicative of apoptosis in relation with the increase in TNF-alpha when compared to the control group left untreated. As shown in the previous study on other cell lines, we speculate that as a potent chemoattractant IL8 secretion stimulated by the Fas ligation might be associated with inflammation, and that it might participate in the pathophysiology of apoptosis. MSCs secrete cytokines either "spontaneously" or after induction by other cytokines, the most important being IL6, TNFα, and IL1β

(a)

(b)

(c)

(d)
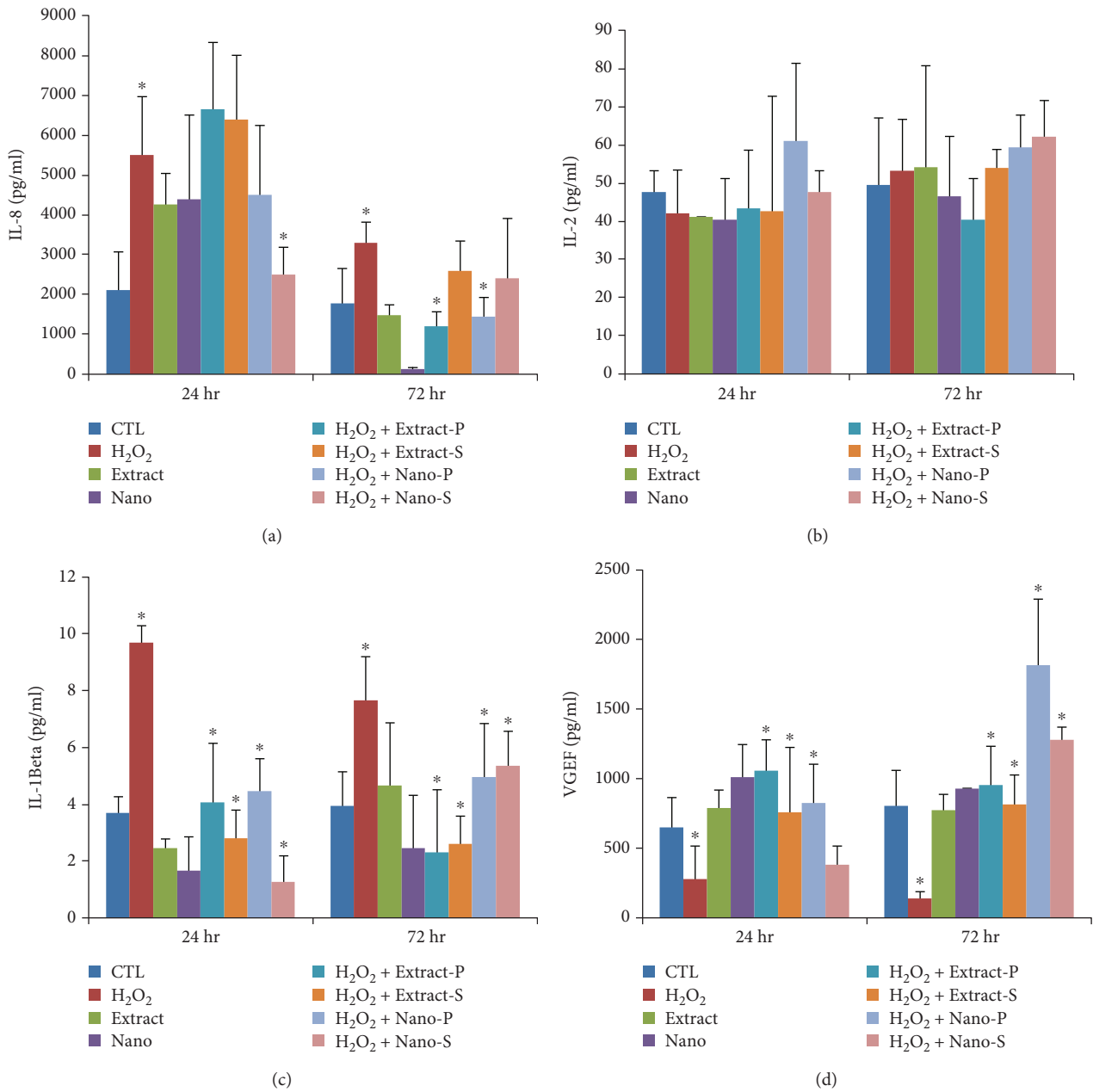
FIGURE 7: (a–d) Levels (pg/ml) of IL8, IL2, IL1beta, and VEGF in control (untreated) and experimental groups (S—cotreatment, P—pretreatment), as well nano- and extract-treated cells at two different time points, 24 hr and 72 hr.

[22, 23], and it should be underlined that MSCs are not always immunosuppressive. It is assumed that their effects are determined by the local conditions of the microenvironment, and sometimes the proinflammatory IL6, TNFα, and IL1β cytokines may induce cell death upon H_2O_2 treatment, which could have been considerably prevented upon the treatment with *Thymus serpyllum*, indicative of protective property. However, the mechanism of action is undisclosed and further studies are warranted. The induction of other proinflammatory factors by IL6 has been regarded as part of an attempt to maintain homeostasis. Similarly, the coincidence of the induction of necrotic cell death signaling with the induction of proinflammatory signaling

molecules, such as IL6, may function to alert the cells of the occurrence of necrotic cell death with consequent removal of the necrotic cells during the cell cycle. *Thymus serpyllum* treatment showed considerable protection in maintaining the homeostasis against hydrogen peroxide-induced changes in cytokine levels.

Previous studies have demonstrated that MSC secreted paracrine factors that are able to induce angiogenesis and affect cellular migration. Unique to our study, we quantified the secretion of VEGF and MCP1 by MSCs into the surrounding media, and we were able to detect the same factors in MSCs, while these factors declined after H_2O_2 treatment. A report has shown that [24] human embryonic stem cells

(a)

(b)

(c)

(d)
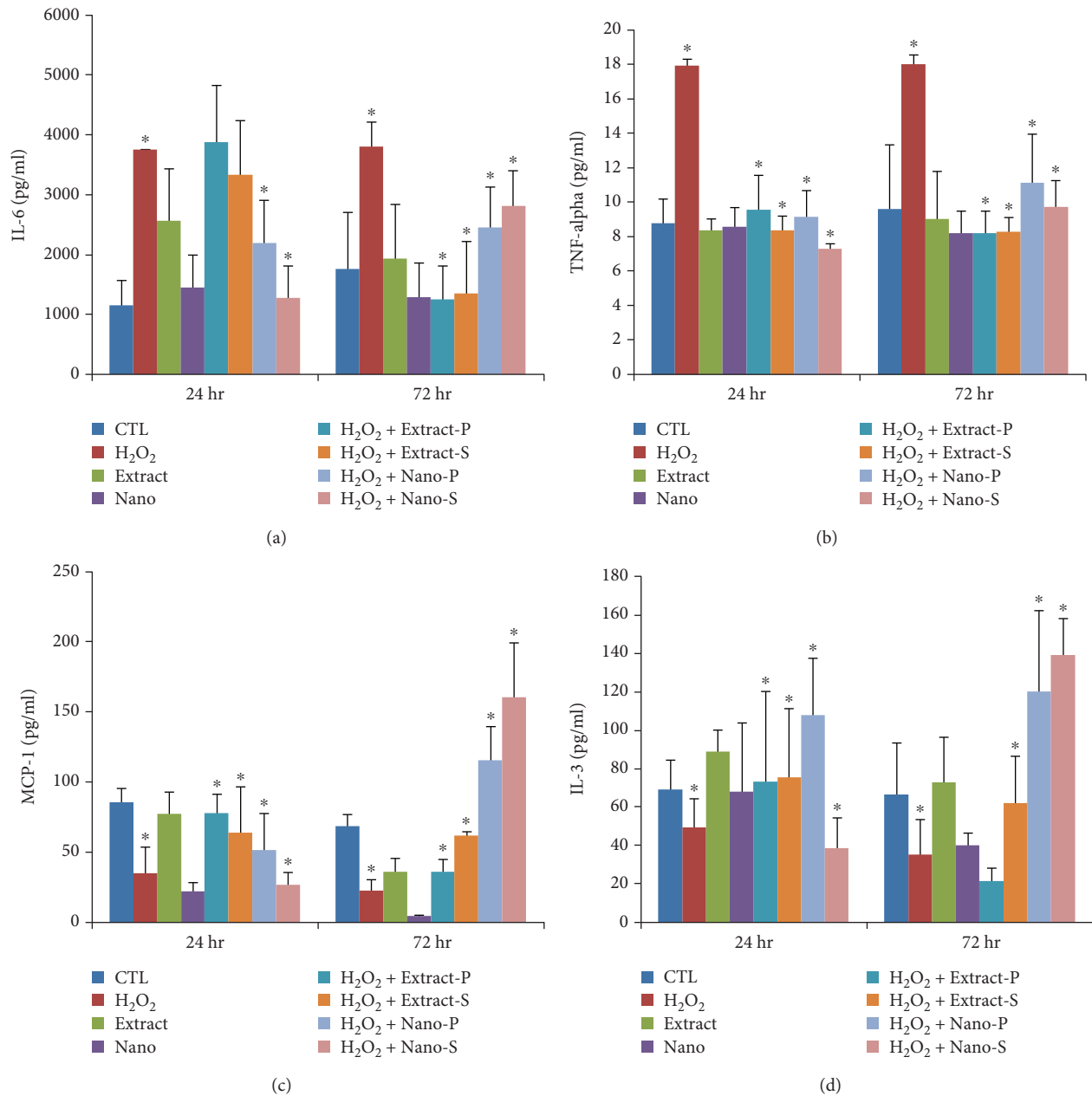
Figure 8: (a–d) Levels (pg/ml) of IL6, IL2, TNF-alpha, MCP1, and IL3 in control (untreated) and experimental groups (S—cotreatment, P—pretreatment), as well nano- and extract-treated cells at two different time points, 24 hr and 72 hr.

released paracrine factors that reduced apoptosis in H9c2 cells, and it focused on TIMP-1 (tissue inhibitor of metalloproteinase) as an important molecule in this process. Other investigators have identified a number of factors secreted by cord blood-derived [25] and embryonic stem cell-derived [26] MSCs including VEGF and MCP1, but they did not determine their specific biological effects. The treatment with extract and nanoparticles showed a positive improvement in the levels of antiapoptotic factors. Interleukin (IL3), a cytokine secreted by activated T lymphocytes, is known to regulate hematopoiesis. Previously, reports have shown that IL3 prevents bone and cartilage damage in animal models of human rheumatoid arthritis and osteoarthritis [27, 28]. IL3 also promotes the differentiation of human MSCs into

functional osteoblasts and increases their in vivo regenerative potential in immunocompromised mice. However, the role of IL3 in the migration and motility of MSCs is not yet known. In this study, we investigated the role of IL3 on human MSCs isolated from BM treated with H_2O_2 following pre- and cotreatment with extract or with nanoparticles of *Thymus serpyllum*. We found that IL3 significantly enhanced the migration and motility of MSCs, which can help the cells treated with the extract or nanoparticles.

5. Conclusion

Both *Thymus serpyllum* extract and nanoparticles showed considerable protection against hydrogen peroxide-induced
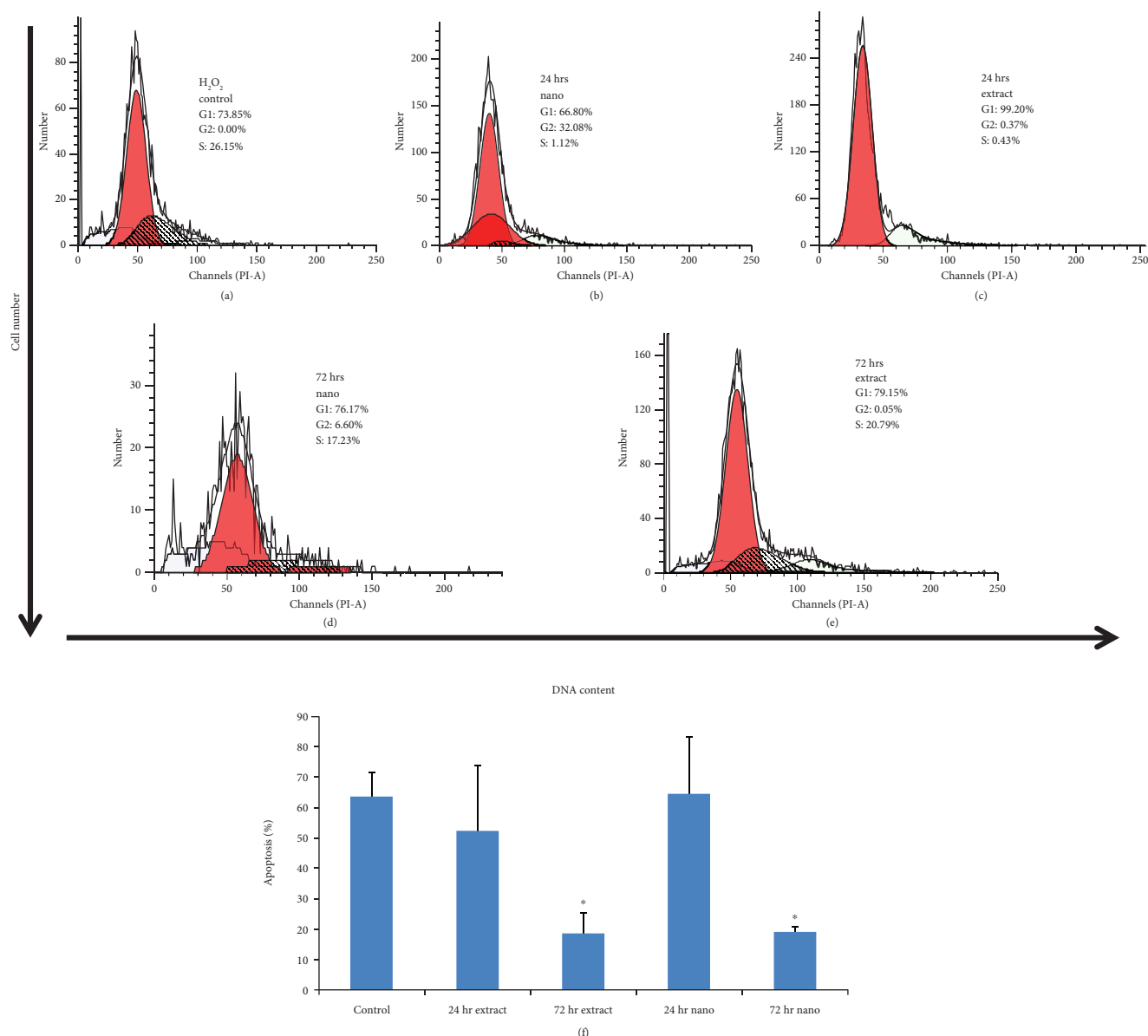
FIGURE 9: Flow cytometric analysis of H_2O_2 control and experimental groups such as extract- and nanoparticle-loaded *Thymus serpyllum* treated to cells at two different time points, 24 hr and 72 hr, as cotreatment against H_2O_2 (a–e). Relative percentage of apoptosis (f) in control and experimental groups such as extract- and nanoparticle-loaded *Thymus serpyllum* treated to cells at two different time points, 24 hr and 72 hr, as cotreatment against H_2O_2.

mesenchymal stromal cell damage in vitro. Hence, this nanoparticle-loaded *Thymus serpyllum* can be a potential candidate to use as an adjuvant treatment with stem cell treatment.

Data Availability

The data used to support the findings of this study are available from the corresponding author upon request. We assure data availability on reviewer's request.

Conflicts of Interest

Authors declare that no conflicts of interest exist.

References

[1] E. Stahl-Biskup and F. Sáez, *Thyme: The Genus Thymus*, Taylor and Francis, London, New York, USA, 2002.

[2] S. Aziz and H. Ur-Rehman, "Studies on the chemical constituents of *Thymus serpyllum*," *Turkish Journal of Chemistry*, vol. 32, pp. 605–614, 2008.

[3] S. Jaric, M. Mitrovic, and P. Pavlovic, "Review of ethnobotanical, phytochemical, and pharmacological study of *Thymus serpyllum* L.," *Evidence-based Complementary and Alternative Medicine: Ecam*, vol. 2015, Article ID 101978, 10 pages, 2015.

[4] Alamgeer, M. N. Mushtaq, S. Bashir et al., "Comparative hypoglycemic activity of different fractions of *Thymus serpyllum* L. in alloxan induced diabetic rabbits," *Pakistan Journal of Pharmaceutical Sciences*, vol. 29, no. 5, pp. 1483–1488, 2016.

[5] R. Rohban and T. R. Pieber, "Mesenchymal stem and progenitor cells in regeneration: tissue specificity and regenerative potential," *Stem Cells International*, vol. 2017, Article ID 5173732, 16 pages, 2017.

[6] M. Valko, D. Leibfritz, J. Moncol, M. T. D. Cronin, M. Mazur, and J. Telser, "Free radicals and antioxidants in normal physiological functions and human disease," *The International Journal of Biochemistry & Cell Biology*, vol. 39, no. 1, pp. 44–84, 2007.

[7] H. Yagi, J. Tan, and R. S. Tuan, "Polyphenols suppress hydrogen peroxide-induced oxidative stress in human bone-marrow derived mesenchymal stem cells," *Journal of Cellular Biochemistry*, vol. 114, no. 5, pp. 1163–1173, 2013.

[8] R. Harris, E. Lecumberri, I. Mateos-Aparicio, M. Mengíbar, and A. Heras, "Chitosan nanoparticles and microspheres for the encapsulation of natural antioxidants extracted from *Ilex paraguariensis*," *Carbohydrate Polymers*, vol. 84, no. 2, pp. 803–806, 2011.

[9] J. Liang, F. Li, Y. Fang et al., "Synthesis, characterization and cytotoxicity studies of chitosan-coated tea polyphenols nanoparticles," *Colloids and Surfaces B: Biointerfaces*, vol. 82, no. 2, pp. 297–301, 2011.

[10] P. Gardiner, "Complementary, holistic, and integrative medicine: chamomile," *Pediatrics in Review*, vol. 28, no. 4, pp. E16–E18, 2007.

[11] K. T. Trifković, N. Z. Milašinović, V. B. Djordjević et al., "Chitosan microbeads for encapsulation of thyme (*Thymus serpyllum* L.) polyphenols," *Carbohydrate Polymers*, vol. 111, pp. 901–907, 2014.

[12] P. Anand, H. B. Nair, B. Sung et al., "Design of curcumin-loaded PLGA nanoparticles formulation with enhanced cellular uptake, and increased bioactivity in vitro and superior bioavailability in vivo," *Biochemical Pharmacology*, vol. 79, no. 3, pp. 330–338, 2010.

[13] S. L. Kosaraju, L. D'ath, and A. Lawrence, "Preparation and characterisation of chitosan microspheres for antioxidant delivery," *Carbohydrate Polymers*, vol. 64, no. 2, pp. 163–167, 2006.

[14] D. Chiou and T. A. G. Langrish, "Development and characterisation of novel nutraceuticals with spray drying technology," *Journal of Food Engineering*, vol. 82, no. 1, pp. 84–91, 2007.

[15] C. R. Fellows, C. Matta, R. Zakany, I. M. Khan, and A. Mobasheri, "Adipose, bone marrow and synovial joint-derived mesenchymal stem cells for cartilage repair," *Frontiers in Genetics*, vol. 7, 2016.

[16] M. Zhang, D. Methot, V. Poppa, Y. Fujio, K. Walsh, and C. E. Murry, "Cardiomyocyte grafting for cardiac repair: graft cell death and anti-death strategies," *Journal of Molecular and Cellular Cardiology*, vol. 33, no. 5, pp. 907–921, 2001.

[17] J. A. Wells and C. L. McClendon, "Reaching for high-hanging fruit in drug discovery at protein-protein interfaces," *Nature*, vol. 450, no. 7172, pp. 1001–1009, 2007.

[18] S. H. Lee, Y. J. Lee, and H. J. Han, "Effect of arachidonic acid on hypoxia-induced IL-6 production in mouse ES cells: involvement of MAPKs, NF-κB, and HIF-1α," *Journal of Cellular Physiology*, vol. 222, no. 3, pp. n/a–585, 2010.

[19] S. Gencer, A. Cebeci, and M. B. Irmak-Yazicioglu, "Matrix metalloproteinase gene expressions might be oxidative stress targets in gastric cancer cell lines," *Chinese Journal of Cancer Research*, vol. 25, no. 3, pp. 322–333, 2013.

[20] M. E. Bernardo and W. E. Fibbe, "Mesenchymal stromal cells: sensors and switchers of inflammation," *Cell Stem Cell*, vol. 13, no. 4, pp. 392–402, 2013.

[21] F. Dazzi and M. Krampera, "Mesenchymal stem cells and autoimmune diseases," *Best Practice & Research Clinical Haematology*, vol. 24, no. 1, pp. 49–57, 2011.

[22] T. Vanden Berghe, M. Kalai, G. Denecker, A. Meeus, X. Saelens, and P. Vandenabeele, "Necrosis is associated with IL-6 production but apoptosis is not," *Cellular Signalling*, vol. 18, no. 3, pp. 328–335, 2006.

[23] D. K. Singla, R. D. Singla, and D. E. McDonald, "Factors released from embryonic stem cells inhibit apoptosis in H9c2 cells through PI3K/Akt but not ERK pathway," *American Journal of Physiology-Heart and Circulatory Physiology*, vol. 295, no. 2, pp. H907–H913, 2008.

[24] C.-H. Liu and S.-M. Hwang, "Cytokine interactions in mesenchymal stem cells from cord blood," *Cytokine*, vol. 32, no. 6, pp. 270–279, 2005.

[25] S. K. Sze, D. P. V. de Kleijn, R. C. Lai et al., "Elucidating the secretion proteome of human embryonic stem cell-derived mesenchymal stem cells," *Molecular & Cellular Proteomics*, vol. 6, no. 10, pp. 1680–1689, 2007.

[26] R. K. Srivastava, G. B. Tomar, A. P. Barhanpurkar et al., "IL-3 attenuates collagen-induced arthritis by modulating the development of Foxp3^{+} regulatory T cells," *Journal of Immunology*, vol. 186, no. 4, pp. 2262–2272, 2011.

[27] S. Kour, M. G. Garimella, D. A. Shiroor et al., "IL-3 decreases cartilage degeneration by downregulating matrix metalloproteinases and reduces joint destruction in osteoarthritic mice," *Journal of Immunology*, vol. 196, no. 12, pp. 5024–5035, 2016.

[28] A. P. Barhanpurkar, N. Gupta, R. K. Srivastava et al., "IL-3 promotes osteoblast differentiation and bone formation in human mesenchymal stem cells," *Biochemical and Biophysical Research Communications*, vol. 418, no. 4, pp. 669–675, 2012.

Research Article

Uniaxial Cyclic Tensile Stretching at 8% Strain Exclusively Promotes Tenogenic Differentiation of Human Bone Marrow-Derived Mesenchymal Stromal Cells

Hui Yin Nam [iD],[1] Belinda Pingguan-Murphy [iD],[2] Azlina Amir Abbas [iD],[1] Azhar Mahmood Merican [iD],[1] and Tunku Kamarul [iD][1]

[1]*Tissue Engineering Group, Department of Orthopaedic Surgery (NOCERAL), Faculty of Medicine, University of Malaya, 50603 Kuala Lumpur, Malaysia*
[2]*Department of Biomedical Engineering, Faculty of Engineering, University of Malaya, 50603 Kuala Lumpur, Malaysia*

Correspondence should be addressed to Hui Yin Nam; huiyin26@yahoo.com and Tunku Kamarul; tkzrea@um.edu.my

The present study was conducted to establish the amount of mechanical strain (uniaxial cyclic stretching) required to provide optimal tenogenic differentiation expression in human mesenchymal stromal cells (hMSCs) *in vitro*, in view of its potential application for tendon maintenance and regeneration. *Methods*. In the present study, hMSCs were subjected to 1 Hz uniaxial cyclic stretching for 6, 24, 48, and 72 hours; and were compared to unstretched cells. Changes in cell morphology were observed under light and atomic force microscopy. The tenogenic, osteogenic, adipogenic, and chondrogenic differentiation potential of hMSCs were evaluated using biochemical assays, extracellular matrix expressions, and selected mesenchyme gene expression markers; and were compared to primary tenocytes. *Results*. Cells subjected to loading displayed cytoskeletal coarsening, longer actin stress fiber, and higher cell stiffness as early as 6 hours. At 8% and 12% strains, an increase in collagen I, collagen III, fibronectin, and N-cadherin production was observed. Tenogenic gene expressions were highly expressed ($p < 0.05$) at 8% (highest) and 12%, both comparable to tenocytes. In contrast, the osteoblastic, chondrogenic, and adipogenic marker genes appeared to be downregulated. *Conclusion*. Our study suggests that mechanical loading at 8% strain and 1 Hz provides exclusive tenogenic differentiation; and produced comparable protein and gene expression to primary tenocytes.

1. Introduction

Bone marrow-derived mesenchymal stromal cells (MSCs) have the ability to undergo multilineage differentiation and, when introduced into damaged tendon, have been shown to result in superior repair outcomes [1, 2]. Despite demonstrating good efficacy, there have been concerns that undifferentiated cells may possibly progress towards unwanted cell lineages when transplanted into tissues, resulting in patient morbidity [3, 4]. An example to demonstrate such phenomenon would be in the formation of osteoblastic cells when human MSCs (hMSCs) are transplanted into the cartilage tissue [5]. It has been suggested that lineage-committed or predifferentiated hMSCs may be the answer to this problem [6]. Several methods can be employed to direct hMSCs

towards a particular lineage. In the past, these have included hormonal, ionic, and environmental manipulation [7]. However, one of the mechanisms that can be readily used on these cells but not often described in literature is mechanical signalling [8].

It is suggested that the ability of cells to respond to mechanical stimuli is controlled by a series of mechanosensitive receptors or structures that sense and convert mechanical signals into biochemical signalling events [9]. This process, commonly known as mechanotransduction, translates mechanical cues that are perceived from the environment into intracellular signals. This ultimately regulates the complex processes involved in cell proliferation and differentiation [10]. It has been described that during this process, the complex interaction of signals generated

from the binding of integrins to signalling molecules, the opening of stretch sensitive ion channels, and the resultant cytoskeletal deformation are simultaneously activated [11]. However, the order of sequence of these events, as well as the relationship between the activated pathways and outcome, remains to be rationalized [12, 13].

Although previous works have indicated that mechanical stimulation in general guides MSC differentiation in different ways, these studies have predominantly involved cells other than those found responsible for tendon or ligament homeostasis, such as osteoblast, neuron-like cells, and chondrogenic cells [14–16]. In addition, there appears to be very few studies investigating the effects of cyclic uniaxial tensile loading on progenitor cells, although this stimulus is physiologically relevant to the musculoskeletal system. It is worth noting that this stimulus is probably the single most important signal that regulates the proliferation and functions of both ligament and tendon cells [17, 18]. However, we also need to be mindful that because of their multipotential ability, it is possible that stimulating stem cells mechanically at an inappropriate manner can result in undesirable outcomes as previously mentioned. It is therefore paramount that the characteristics of the mechanical loading applied be established so as to eliminate these unwanted outcomes. Sadly, studies related to this area appears lacking as previous studies have been mainly focused on a narrow range of frequency and strain rates which do to mimic the scenario observed during physiological loading [19–22].

In order to establish these characteristics, the present study was conducted to examine the effects of uniaxial cyclic stretching in different durations and strain rates on hMSCs. The focus of this study is to determine the mesenchymal lineage differentiation potential of these cells using gene expression and extracellular matrix (ECM) production related to mesenchymal lineage-related specific markers. These were also compared to tenocytes in order to determine if the tenogenic expression potential of hMSCs subjected to these loading conditions was comparable to that of native tendon cells. These would then indicate that progenitor cells would have undergone tenogenic differentiation. Tenogenic differentiation is defined as cells that exhibit tenocyte-lineage marker genes at both mRNA and protein levels [23]. Amongst the genes that have been identified as described in many literatures include scleraxis, tenomodulin, tenascin-C, collagen type I, collagen type III, and decorin [19, 23–25]. Protein expressions for tenogenic differentiation on the other hand are less specific and not well described. However, from available literature, frequently quoted proteins that appear to be relevant to the tenogenic differentiation process have included collagen I and collagen III [23, 26].

We hypothesize also that the regulation of extracellular matrix remodelling as well as the expression of the differentiation of hMSCs to a particular cell lineage is dependent on the degree of tensile forces; the morphology and stiffness of the cells were also investigated. Since the focus of this study is relating to the tenogenic differentiation potential of cyclic-loaded hMSCs, the expression of tenogenic genes and proteins as mentioned above was thus investigated. It is hoped that by determining the effects of mechanical stretch on hMSCs using quantitative measurements, we may be able to have better understanding on the mechanical characteristics that govern tendon homeostasis thus enabling future potential therapies for tendons and ligaments to be advocated.

2. Materials and Methods

All experimental protocols were approved by the University Malaya Medical Centre Institutional Review Board (Reference no: 369.19) and performed in accordance with the guidelines for Medical Ethics Committee of the University Malaya Medical Centre.

2.1. Isolation and Culture of Human Bone Marrow-Derived MSCs. To isolate bone marrow-derived MSCs, the bone marrow was aspirated from the femoral canal of 10 patients/donors undergoing orthopaedic-related surgeries such as total joint arthroplasty in the University Malaya Medical Centre. Each bone marrow sample was kept on ice throughout the transportation to the laboratory and processed for cell isolation as described in our previous publication [27]. The cells were subcultured until passage 2 to be used in our experiments.

To determine whether the cells obtained were hMSCs, various tests including flow cytometry analysis for specific cell surface markers, cell morphological images, and the ability of the isolated cells to undergo trilineage differentiation were conducted. The methods used in this study are described in our previous publications [27, 28]. The isolated cells appeared to conform to the characteristics expected of MSCs (Figure 1), i.e., (1) spindle-shaped plastic adherent features; (2) positive markers for CD29, CD44, CD73, CD90, and CD105 while being devoid of CD14, CD34, CD45, and HLA-DR [28]; and (3) able to undergo trilineage differentiation, namely, chondrogenic, osteogenic, and adipogenic differentiation.

2.2. Isolation and Culture of Human Tenocytes. Human primary tenocytes were isolated from hamstring tendons of adult donors, who underwent surgery for joint arthroplasty. Tendon tissues were harvested to the required size by the operating surgeon and transferred aseptically into containers and immersed with saline solution. Once the tendons were harvested, cell isolation was immediately performed, using the methods modified from the study of Zhang and Wang [29]. Briefly, the tendons were minced into approximately 1 mm^3 in size under a sterile condition, and then phosphate buffered saline (PBS) was added (Gibco, USA). Subsequently, the mixture was added with 0.4 mg/mL type I collagenase and incubated at 37°C for 2 h to allow the enzymatic digestion process to occur. After digestion, the suspension was centrifuged at 1800 rpm for 5 min to remove the collagenase solution, then the pellet was washed 2 times with PBS by centrifugation. The pellet was then resuspended with 1 mL of DMEM high glucose (4.5 g/L glucose) supplemented with 10% fetal bovine serum (FBS), 1% penicillin-streptomycin, and 1% GlutaMAX™-I (Gibco, USA), and transferred into a T25 flask which was added with 5 mL of culture medium.

(a)

(b)

(c)

(d)
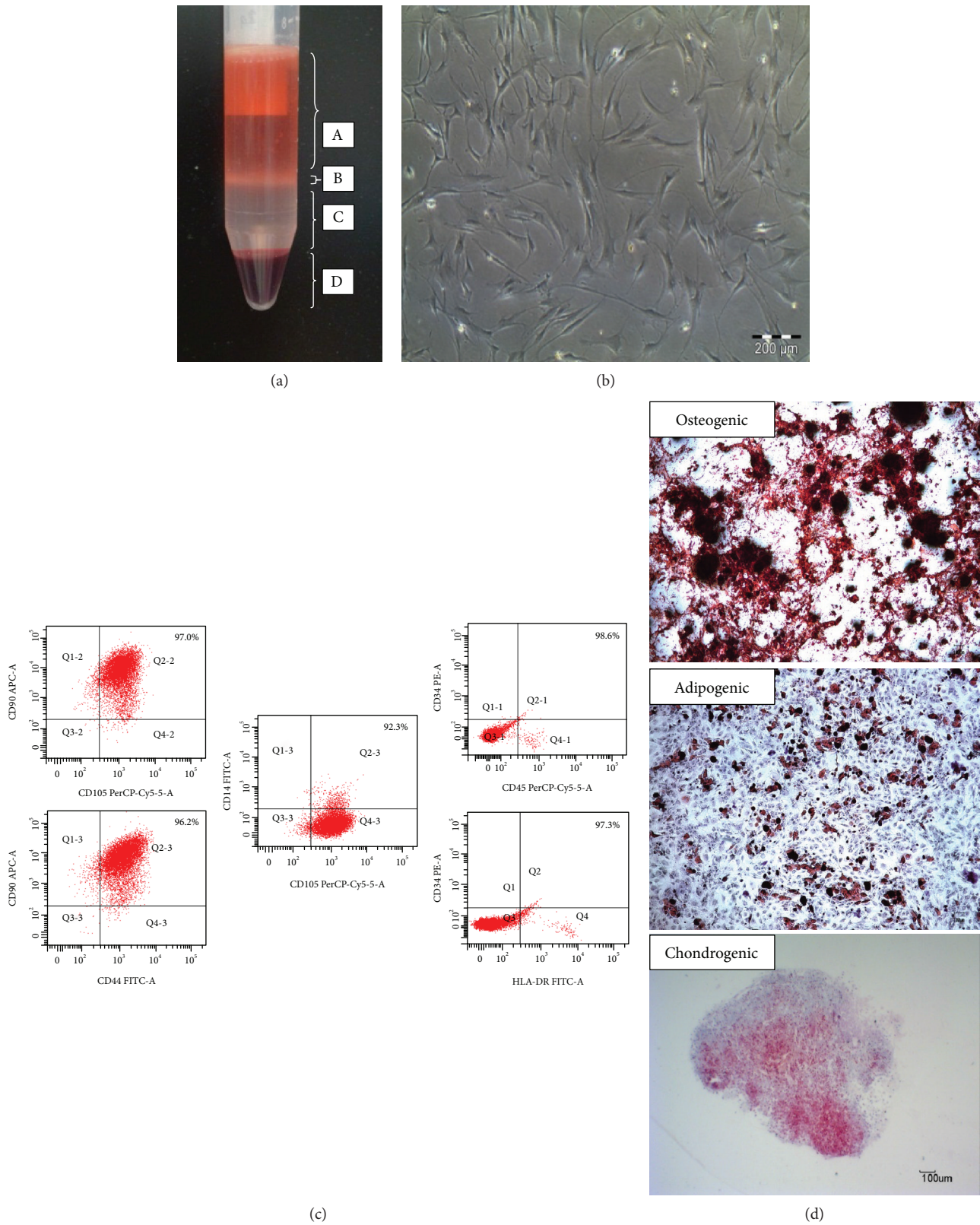
FIGURE 1: Characterization of hMSCs was confirmed. (a) Density gradient separation of human bone marrow: (A) plasma, (B) mononuclear cells, (C) ficoll paque, (D) erythrocytes, and granulocytes. (b) Morphology of replated cells showed homogeneous and fibroblastic shape. (c) Representative images of multicolour CD markers by flow cytometry. The results showed that hMSCs expressed at least 90% of double-positive expression, double-negative, or coexpressed positive and negative markers. (d) Trilineage differentiation potential of the hMSCs into osteogenic, adipogenic, and chondrogenic lineage.

Cultures were incubated at 37°C and 5% CO_2 incubator for 24 h. The digested tissues were then removed from the cell culture flask and discarded completely. The culture medium was changed every third day, until 80–85% confluency for subculture using trypsin digestion. These primary native human tenocyte cultures (passage 3) were used as positive controls in the subsequent experiments.

2.3. Application of Cyclic Uniaxial Tensile Strain. A commercial loading device (STREX, Japan) fitted with elastic silicone chambers was used to conduct experiments that determine the effect of cyclic uniaxial strain on hMSCs. hMSCs were seeded on the collagen type I (Sigma, USA)-coated silicone chamber at the density of $10^4/cm^2$ and allowed to set at 37°C in complete growth medium for 48 h. The medium was then changed to 1% FBS for 24 h and proceeded with complete growth medium before being assembled into the uniaxial strain device. Control cells were treated similarly but were not subjected to cyclic stimulation. The medium and cells were harvested after 6, 24, 48, and 72 h of cyclic loading for downstream analyses, which included (1) biochemical assay, (2) immunostaining, (3) immunophenotyping, (4) topography imaging and elasticity measurement, and (5) gene expression assay.

2.4. Cellular Morphology by Microscopy. Phase-contrast microscopic images of unstrained and strained hMSCs were obtained (Olympus, Japan) in at least four randomly selected sites from our visual field. To observe the effect of cyclic loading on cytoskeletal actin arrangements, hMSCs at all conditions were stained with fluorescent phallotoxins (Molecular Probes, Oregon, USA) for 30 min and then the nucleus stained with Hoechst (Molecular Probes, Oregon, USA) for 10 min in the dark. Fluorescence was recorded using a laser scanning confocal attachment (Leica TCS SP5 II, Germany) and measured by LAS AF image software (Leica, Germany). Images of unstrained MSCs on silicone membrane served as control.

2.5. Quantification of ECM Components. At the end of each time point of the experiment, the total amount of collagen, sulfated glycosaminoglycan (sGAG), and elastin of the resulting samples was determined using Sircol™ Collagen assay kit, Blyscan™ sGAG assay kit, and Fastin™ Elastin assay kit, respectively. The technique used in each measurement was according to the manufacturer's (Biocolor, UK) protocol. These kits used quantitative dye-binding methods to determine the total quantity of the respective ECM component in the sample which released to medium. An enzyme immunoassay kit (Chondrex Inc., USA) was used to measure the levels of type I collagen in strained hMSC lysate (1 Hz, 8%) following the manufacturer's instructions. The concentration of collagen type I was obtained by measuring the absorbance at 490 nm on the microplate reader.

2.6. Immunocytochemical and Fluorescent Immunostaining for ECM Analysis. Membranes with hMSCs subjected to the uniaxial straining or in unstrained conditions were rinsed using PBS, followed by fixation process in methanol for 20 min. After rinsing using Tris-buffered saline (Dako,

Denmark), peroxidase block was applied for 5 min to reduce nonspecific background signalling. Cells were then incubated with primary antibodies, which included rabbit anti-collagen type I, rabbit anti-collagen type II, or rat anti-collagen type III (Calbiochem-Daiichi Fine Chemical Co., Japan) diluted at 1 : 100 for 30 min. The cells were then incubated with streptavidin-peroxidase secondary antibody (Dako, Denmark) for 30 min. At last, the collagens in the cells were visualized by reaction with diaminobenzidine (Dako, Denmark).

For direct visualization of the adhesion molecules fibronectin matrix and N-cadherin, 4% paraformaldehyde was used to fixed cells and was permeabilized with −20°C acetone. Cells were then incubated with 1% bovine serum albumin to block nonspecific binding of antibodies, before being incubated with primary antibody, anti-fibronectin (Abcam, UK) diluted 1 : 300 for 1 h. The primary antibody was then detected by a secondary antibody specific to rabbit IgG (Abcam, UK) diluted 1 : 600 for 1 h. Hoechst staining was performed at the end of the staining process and examined under laser scanning confocal microscope (Leica TCS SP5 II, Germany).

2.7. Stimulated Cell Surface Antigen Analysis by a Fluorescence-Activated Cell Sorter (FACS). Antibodies against the human antigen, CD44, CD73, CD90, and CD105 (BD Biosciences, USA), were used to characterize the surface antigen expressions of stretched hMSCs. Briefly, the loaded cells were resuspended in 100 μL of PBS and incubated with fluorescein isothiocyanate- (FITC-) or phycoerythrin- (PE-) conjugated antibodies in the dark for 15 min at room temperature. The fluorescence intensity of the cells was evaluated using a flow cytometer (BD FACS Cantor II, BD Biosciences, USA). Data were analysed using CELLQUEST software (BD Sciences, USA). The presence or absence of staining in cells was determined by comparing strained cells to the matched unstrained control.

2.8. Histologic Assessment of Differentiation after Mechanical Stimulation. The presence of bone-forming nodules was used to determine the occurrence of osteoblast differentiation. This was further assessed using Alizarin Red S dye (Sigma, USA), which stains calcium phosphate deposits. The accumulation of lipid droplets was used to denote adipocyte differentiation. It was determined by incubating paraformaldehyde-fixed cells with 60% isopropanol and followed by freshly prepared Oil Red O solution (Sigma, USA). Unstrained samples were treated as controls. All samples were then captured using a light microscope (Nikon Eclipse TE2000-S, Japan).

2.9. Atomic Force Microscopy Measurement of Young's Modulus. Atomic force microscopy (AFM) images were obtained by scanning the cell surface under ambient conditions using AFM (Bruker Nano, USA) that was set at PeakForce QNM mode. The AFM measurements were obtained using ScanAsyst-air probes. However, the spring constant (nominal 0.4 N/m) and deflection sensitivity were first calibrated but not the tip radius (the nominal value has

TABLE 1: The genes of interest were determined in this study.

Related marker	Gene name	Abbreviation
	Matrix metallopeptidase 3 (stromelysin 1, progelatinase)	MMP3
	Proline rich 16	PRR16
ECM component	Collagen type I, α1	COL1
	Collagen type III, α1	COL3
	Decorin	DCN
Tendon lineage	Tenascin C	TNC
	Scleraxis homolog A	SCX
	Tenomodulin	TNMD
Bone lineage	Runt-related transcription factor 2	RUNX2
	Alkaline phosphatase, liver/bone, kidney	ALP
	Osteocalcin	OCN
Cartilage lineage	Collagen type II, α1	COL2
	Cartilage oligomeric matrix protein	COMP
	SRY- (sex-determining region Y-) box 9	SOX9
Fat lineage	Peroxisome proliferator-activated receptor, gamma	PPARG
Smooth muscle lineage	Transgelin	TAGLN
Housekeeping gene	Phosphoglycerate kinase 1	PGK1

been used, 3.5 nm). AFM images were collected from each sample and at random spot (at least five areas per sample). The quantitative mechanical data was obtained by measuring DMT modulus/Pa using Bruker software (NanoScope Analysis). To obtain Young's modulus, the retracted curve was fit using the Derjaguin-Muller-Toporov model or abbreviated as DMT modulus [30].

2.10. Multiplex Gene Expression Assay. Total RNA was extracted from unstrained and strained hMSCs using RNeasy mini kit (Qiagen, USA). The purity and concentration of the RNA were assessed by determining the absorbance ratio, measured at 260 and 280 nm wave bands. RNA integrity was assessed by visualizing 18S and 28S rRNA bands on formaldehyde-agarose gels. Only samples with high quality were selected for microsphere-based multiplex-branched DNA downstream analysis. The mRNA expression of mesenchymal lineages (Table 1) was quantified by the Quanti-Gene 2.0 Plex assay (Panomics/Affymetrix Inc., USA). Individual bead-based oligonucleotide probe sets specific for each gene examined were developed by the manufacturer (the 2.0 plex set 12082). In this assay, each lysate was measured in triplicate wells. Controls are also included for genomic DNA contamination, RNA quality, and general assay performance. The housekeeping gene was PGK1 (phosphoglycerate kinase 1) previously validated as the best housekeeping for accurate gene expression analysis in our study.

2.11. Statistical Analysis. The assays were carried out with a minimum number of technical triplicates ($n = 3$) per experimental run, using six independent samples from different donors ($N = 6$) for each group of the experiments. Data were presented as mean ± standard deviation (SD). For Young's modulus experiment, Student's t-test was carried out to compare the differences in mean values. While for the other experiments, statistical significance was analysed by one-way analysis of variance (ANOVA), using the least significant difference (LSD). A confidence level of 95% ($p < 0.05$) was chosen for determining statistical significance using the SPSS 15.0 software (SPSS Inc., USA).

3. Results

3.1. Uniaxial Mechanical Strain Induces MSC Alignment Perpendicular to the Direction of Stretching. To determine the effects of uniaxial cyclic strain on cell morphology and organization, hMSCs were exposed to uniaxial strain under predetermined experimental conditions. The degree of cells' responsiveness was affected at different strain magnitude and duration (Figure 2(a)). Cells that were exposed to the highest strain magnitude (12%) aligned themselves faster than cells at other strain rates. After 72 h, cells under cyclic strain aligned themselves perpendicular to the direction of strain and these cells look more elongated and were slender in shape, while unstrained cells remain randomly oriented.

Confocal images showed the reorganization of actin filaments perpendicular to the direction of strain whilst random organization of actin filaments for unstrained cells. It also showed that stained actin filaments were denser in the stimulated hMSCs compared to the nonstimulated groups (Figure 2(c)). hMSCs on 8% uniaxial strained at 1 Hz (Figure 2(b)) lead to spindle-shaped cells similar in shape to tenocytes in vitro. All these results indicated that the cellular cytoskeletal development was associated with strain magnitude.

3.2. Uniaxial Tensile Loading Enhances Collagen and Elastin Production but Not GAG. The total collagen and elastin production appears to be influenced by the strain magnitude. Our results showed that uniaxial stretching increased collagen production (Figure 3(a)), with the exception of the 4% strained group. Higher collagen production was measured as early as 6 h in the 12% strained group. For the 8% strained group, the collagen production was enhanced significantly only after 48 h, which is close to the collagen content in tenoctyes (ratio of human tenoctyes/unstrained hMSCs = 1.43, graph not shown). Compared to collagen, elastin was only increased after 72 h at the higher strained group (Figure 3(c)). However, no enhancement of GAG production in any of the strained groups was observed (Figure 3(b)).

Since collagen type I was reported to be abundant in tendon, ligament, and muscle cells, the 8% strained cells at 1 Hz were further tested using ELISA assay. The results showed that the collagen type I level in medium was increased in mechanically stimulated cells as compared to unstrained

(a)

(b)

(c)
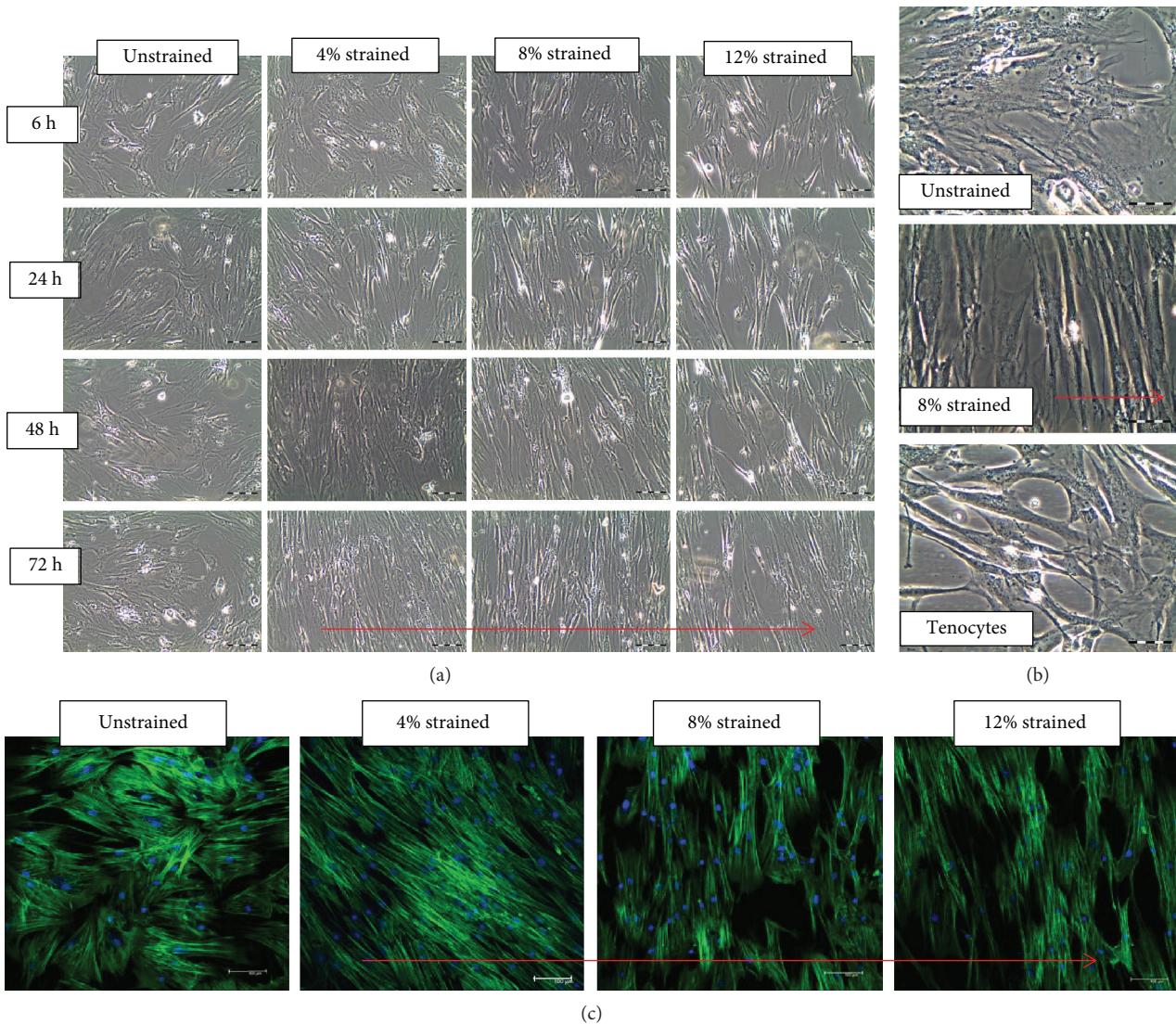
FIGURE 2: Microscopy images of unstrained and strained hMSCs. (a) Phase-contrast photomicrographs of hMSCs subjected to cyclic uniaxial stretching in different magnitude and duration of stretching. (b) Higher magnification of phase contrast of unstrained and 8% strained hMSCs at 72 h and tenocytes. (c) Confocal laser scanning micrographs showing actin stress fibers (green) and nuclei (blue) of unstrained cells and 4%, 8%, and 12% strained cells at 72 h. The substrate was stretched in the red arrow direction.

cells. The content of collagen type I increased with the duration of stretching (Figure 3(d)).

3.3. Mechanical Stimulation Promotes Collagen Type I, Collagen Type III, Fibronectin, and N-Cadherin Expressions.
Immunocytochemical assay showed that the uniaxial cyclic straining promoted the synthesis of collagen type I in MSCs. In the unstrained control group, there was only a light brown collagen staining in the cytoplasm, while a more intense staining was observed in the 72 h strained group for collagen type I (Figure 4(a)). This was in line with the result of collagen type I obtained from ELISA. Collagen I and collagen III staining showed positive protein expression on both unstrained and strained hMSCs but denser in strained cells especially in the 8% and 12% groups. In contrast, collagen II was not expressed when hMSCs were stretched. These

results appear comparable to the level of collagen expressed from primary tenocytes.

When unstrained, fibronectin was arranged in random web-like structures, which distributed mainly at the cell periphery. The peripheral fibronectin staining appears to be upregulated when cells are stretched. Fibronectin fibril formation also appears to be enhanced with the increase in strain magnitude (Figure 4(b)). Furthermore, unstimulated or unstretched cells appeared to have thin fibronectin fibrils clustered and distributed throughout the entire basal surface of the cell, while cells exposed to 72 h at 8% and 12% uniaxial stretching appeared to form thicker fibronectin fibrils and to have an observable increase in fibronectin fluorescence intensity (Figure 4(c)). To view cell-cell contacts after stretching, we found that the expression level of N-cadherin was higher on strained cells (Figure 4(b)). However, this level of expression was lower in the 12% strained group.

(a)

(b)

(c)

(d)
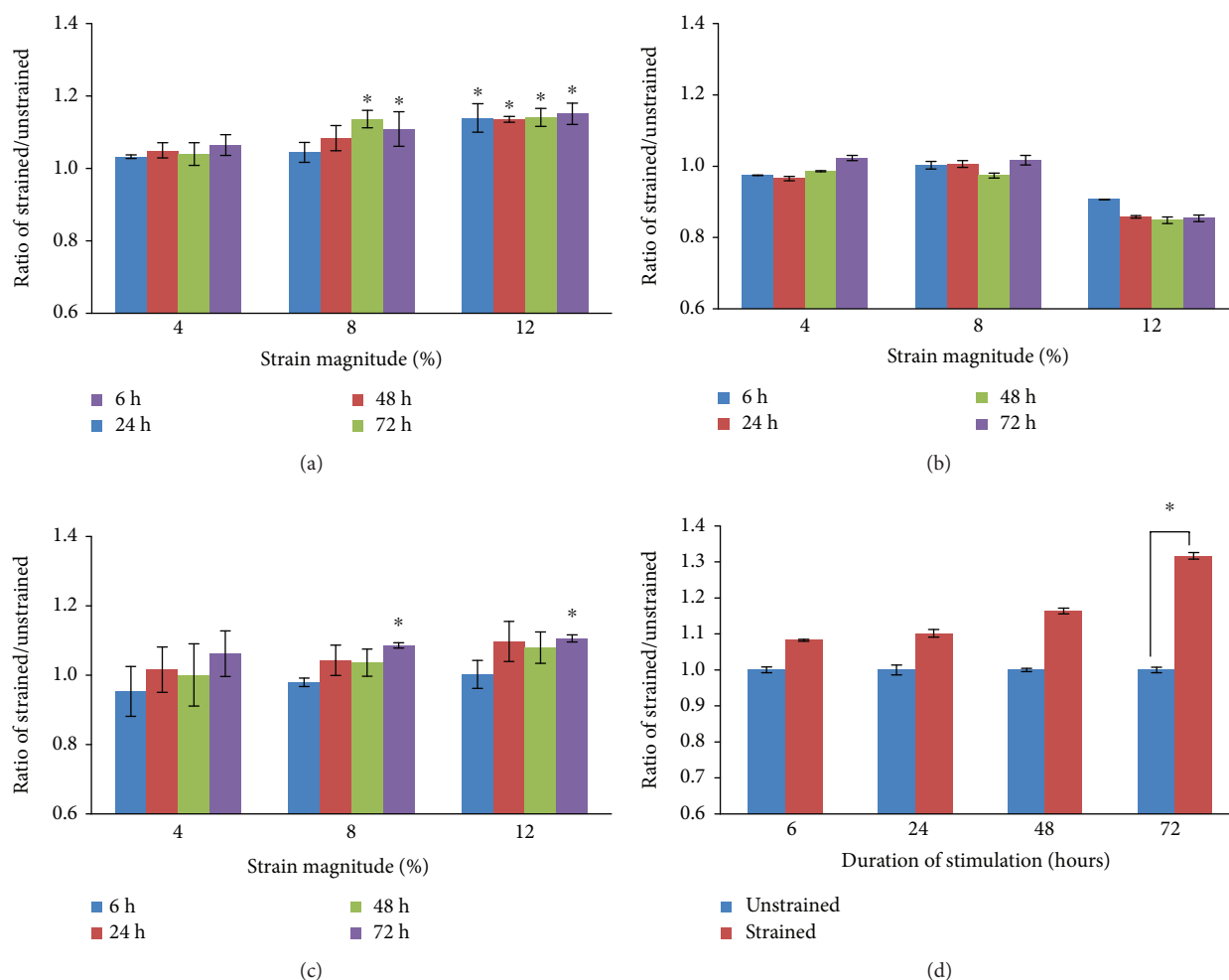
FIGURE 3: Biochemical analysis of MSCs subjected to various mechanical stimuli for different duration of stimulation. Content of (a) total collagen, (b) GAG, and (c) elastin of strained cells was measured to determine the total quantity of the respective ECM component in the sample which released to medium. (d) The level of collagen type I in the medium was measured by ELISA. The ratio of the ECM expression was counted by normalizing to the expression amount of corresponding unstrained groups (indicated as 1). Significance $p < 0.05$ was represented by * which compared to unstrained. $N = 6$, $n = 3$, error bar ± SD.

3.4. Mechanical Stretching Induces the Alteration in hMSC Surface Antigen Expression. The expression of the CD markers in hMSCs appears positive in nonstimulated cells on silicone chambers, as with hMSCs cultured on plastic culture flasks. After 72 h of cyclic loading, CD markers in 4% strained cells appear comparable to unstrained cells. However, when subjected to 8% and 12% strains, the expression of CD markers was reduced, suggesting that appropriate levels of mechanical stretch may induce the alterations in MSC surface antigen expression (Figure 5(a)). It was observed that CD44 and CD105 were significantly reduced in both 8% and 12% strained groups, while CD73 and CD90 reduced significantly at 8% and 12% strains, respectively. Figure 5(b) demonstrates examples of the expression of the multicolour CD markers in different strain magnitude.

3.5. Mechanical Stretching Did Not Express Osteogenesis and Adipogenesis Histological Staining. Mineralization of hMSCs was observed in the osteogenic medium induction hMSCs (21 days) after being stained with Alizarin Red S

(Figure 5(c)A), but this was not shown in mechanical induction hMSCs (8% strained, 72 h), with only slightly brown stained around the nucleus of the cells (Figure 5(c)B). Negative results were shown in 4% and 12% strained cells (figure not shown). The effect of tensile loading on adipogenic differentiation of hMSCs was studied using Oil Red O staining of the lipid droplets. The lipid droplet formation under adipogenic differentiation was found in adipogenic medium induction hMSCs (14 days) (Figure 5(c)C), whereas the mechanical-stimulated hMSCs showed no lipid droplet (8% strained, 72 h) (Figure 5(c)D). Similar result also appeared on the other 2 strained groups (photo not shown).

3.6. Topographical Changes Observed in Mechanically Stimulated Cells. The changes in cell topography of unstrained and strained hMSCs were analysed using an AFM. Topographical images were obtained in both height and deflection channels (Figure 6(a)). Results of AFM analysis revealed that strained cells appeared elongated, with spindle-like morphology and microfilament bundles running

(a)

(b)

(c)
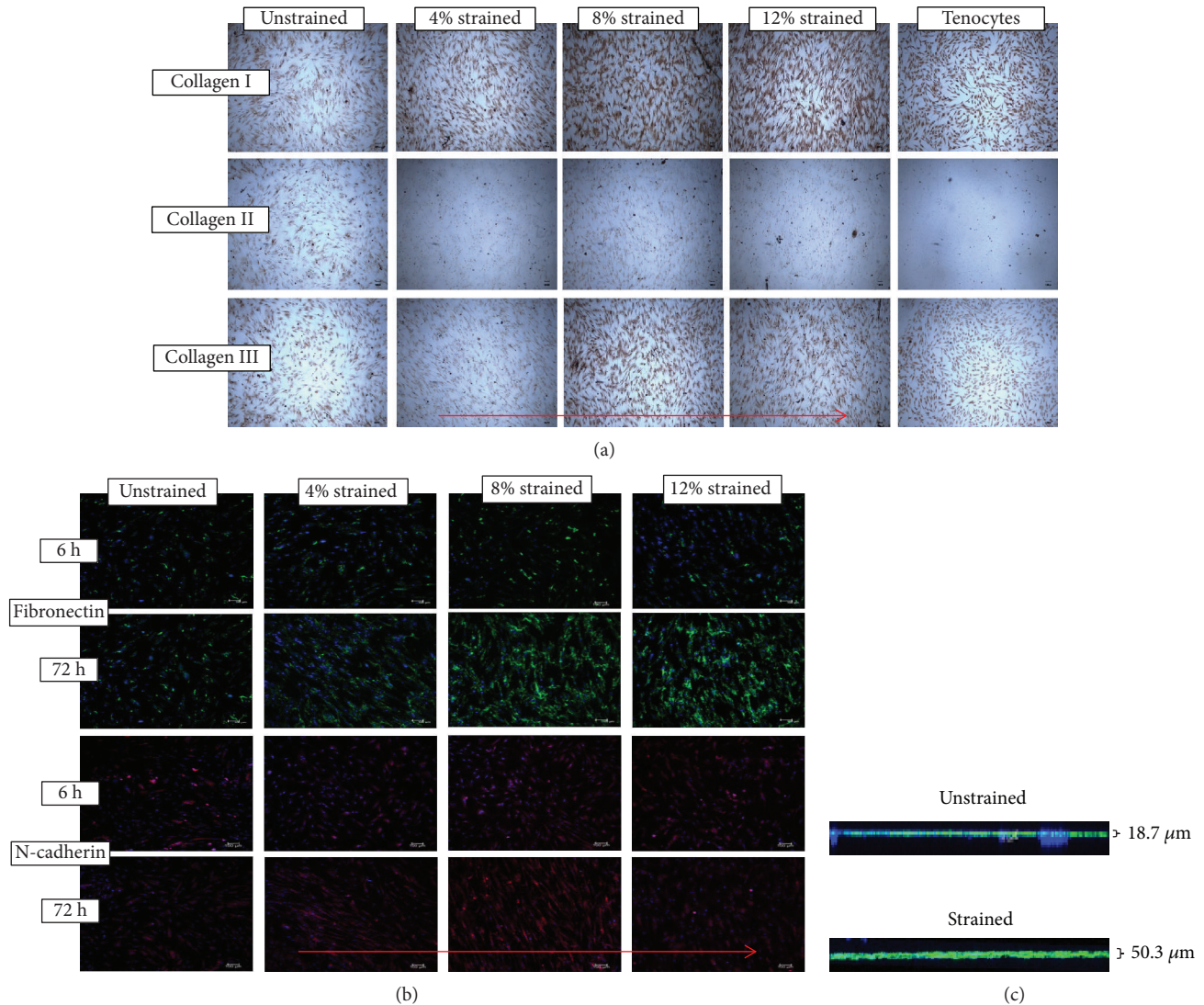
FIGURE 4: ECM expression on unstrained and strained cells. (a) Comparison of different collagen staining on various mechanical stimuli hMSCs at 72 h and tenocytes as positive control. (b) Immunofluorescence staining of fibronectin and N-cadherin on unstrained and strained hMSC for 6 h or 72 h. The expression of fibronectin and N-cadherin was enhanced by the cyclic stretch and magnitude strain dependent. The substrate was stretched in the red arrow direction. (c) Thicker fibronectin fibrils were formed by cyclic mechanical stimulation.

parallel to their long axes, while unstrained cells appeared large and flat. Height image showed larger height scale for strained cells than unstrained cells. This was apparently related to the thicker actin stress fibers of the strained cells than the unstrained hMSCs, which could be visualized in detail in the deflection channel. In unstrained cells, deflection image revealed the fine cytoskeletal structure (presumably actin) just under the cell membrane at detail. The fine cytoskeleton structure began integrating when mechanical stimulation was applied on the cells. The cytoskeleton of the stimulated cells became more pronounced. This effect was much evident with the higher magnitude strain to hMSCs, compatible with tenocytes.

The elasticity measurements (Young's modulus) were performed on the cytoskeleton regions surrounding the nuclei. Figure 6(b) shows the average Young's modulus of fixed unstrained and strained hMSCs from 3 independent

cultures with 5 different areas. The Young's moduli values of strained hMSC groups were greater than those of unstrained hMSC groups, with a significant increase observed in the 8% and 12% strained group. These results demonstrate that as the strain rate is increased, Young's modulus and therefore stiffness of the cytoskeleton of hMSCs increase. The unstrained hMSCs are supple when compared to strained hMSCs, especially in the 8% strained group.

3.7. Mechanical Stimulation Influences the Expression of MMP3 and PRR16. The mRNA expression of PRR16, an indicator of stem cell differentiation, when cells were subjected to mechanical loading is shown in Figure 7(a). At 1 Hz stretching, downregulation of the PRR16 gene was noted in both 8% and 12% strained groups. This effect was more obvious after the cells were stretched for a longer period. These results appear to occur in parallel to the reduction in

(a)

(b)

(c)
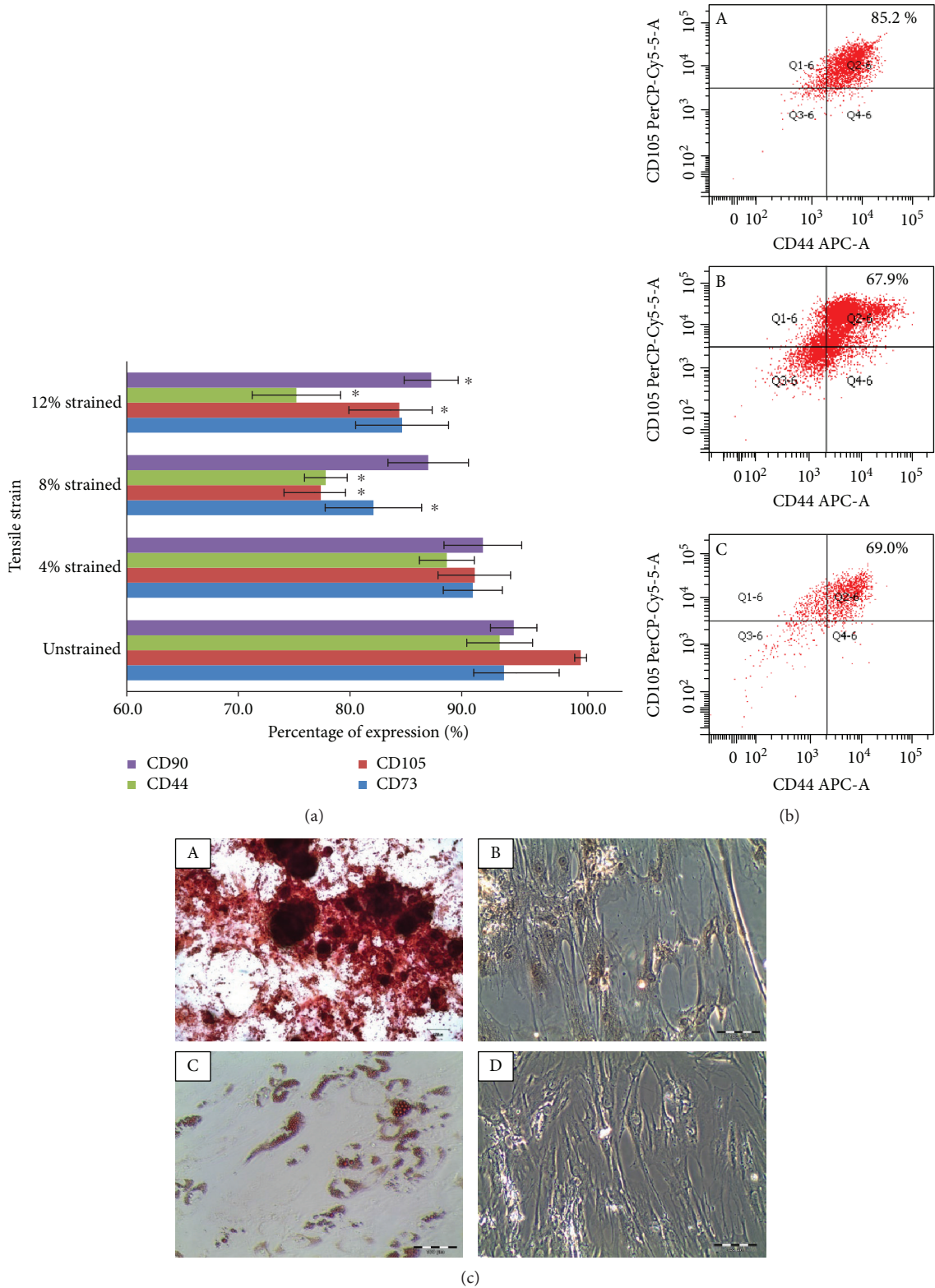
Figure 5: Mechanical stretching altered hMSC surface antigen expression but did not express osteogenesis and adipogenesis. (a) Expression levels of the CD markers of hMSCs cultured in mechanical stretching with different strains. Significance ($p < 0.05$) was represented by * which compared to unstrained. $n = 3$, error bar ± SD. (b) Percentage of multicolour expression for lymphocyte adhesion molecule CD44 and endoglin CD105. Fluorescent expression intensity and area of CD44 and CD105 in (A) 4%, (B) 8%, and (C) 12% strain magnitudes. (c) Representative images of Alizarin Red- and Oil Red O-stained hMSCs: (A) positive Alizarin Red staining on osteogenic medium cultured hMSCs, (B) negative Alizarin Red result on mechanical stimulated hMSCs, (C) positive Oil Red O staining on adipogenic medium cultured hMSCs, (D) negative Oil Red O result on strained hMSCs.

(a)   (b)
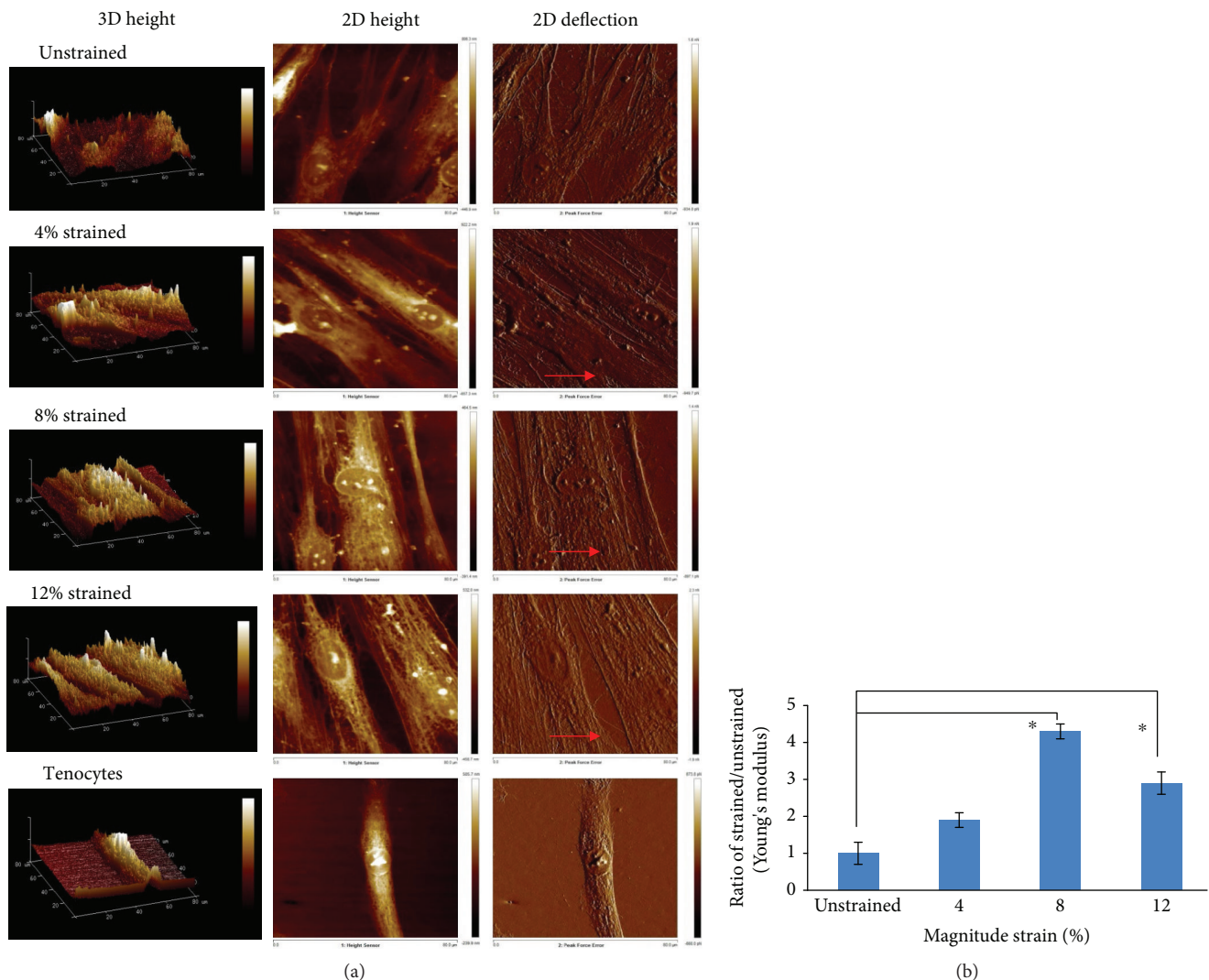
FIGURE 6: The comparison of cell surface topography between the unstrained hMSCs, strained hMSCs, and tenocytes, visualized by AFM. (a) Representative AFM height and deflection scans of unstrained hMSCs and 4%, 8%, and 12% strained hMSCs, and tenocytes. In height images, brighter colour indicates higher distance of substrate. In deflection images, the detailed structure of presumably the stress fiber could be observed with AFM in different cell groups. The direction of uniaxial strain was in the red arrow direction. (b) Young's modulus on the cytoskeleton of the cells subjected to 4%, 8%, or 12% cyclic stretching for 72 h as indicated. The ratio was counted by normalizing to the expression amount of corresponding unstrained groups (indicated as 1). Statistical significance ($p < 0.05$) was represented by * relative to the unstrained group. $n = 3$, error bar $\pm$ SD.

the expressed CD markers described previously. Although there is a downregulation of *PRR16*, the mRNA expression of *MMP3* was upregulated in 8% strain (Figure 7(a)). The exhibitory effect on *MMP3* mRNA expression was not obvious in the 12% strained group after 48 h.

3.8. High Mechanical Strain Upregulated Genes for Macromolecular Components of ECM and Induced Differentiation Markers for Tendon-Like Cell. Uniaxial strain regulated matrix remodelling, as observed from the increasing levels of *COL1* and *COL3* expression, in a liner fashion and parallel to the amount of strain (Figure 7(b)). A significant increase was induced by strains of 8% and 12%, but this upregulation was not significant for the 4% strained group. The expression of *COL3* showed a pattern

similar to that of *COL1*, but the increase was slightly higher than that of *COL1* at 8% strain (at 24 h). *DCN* expression was significantly upregulated at 8% and 12% strains (>24 h and 48 h), respectively.

The differentiation of hMSCs towards tendon-like cells was further examined by measuring the expression of several genes (Figure 7(c)). The results demonstrated that the tenogenic marker (*TNC*, *SCX*, and *TNMD*) expression was upregulated in all groups. However, this was only significantly increased in the 8% and 12% strained groups, most notable being in the 8% group after 24 h, i.e., which was closer to the gene expressions from tenocytes (*DCN* = 1.50, *COL1* = 1.59, *COL3* = 1.37, *TNC* = 2.22, *SCX* = 2.65, and *TNMD* = 1.80; fold change of human tenoctyes vs. unstrained hMSCs; graph not shown). After 2 days of stretching, the
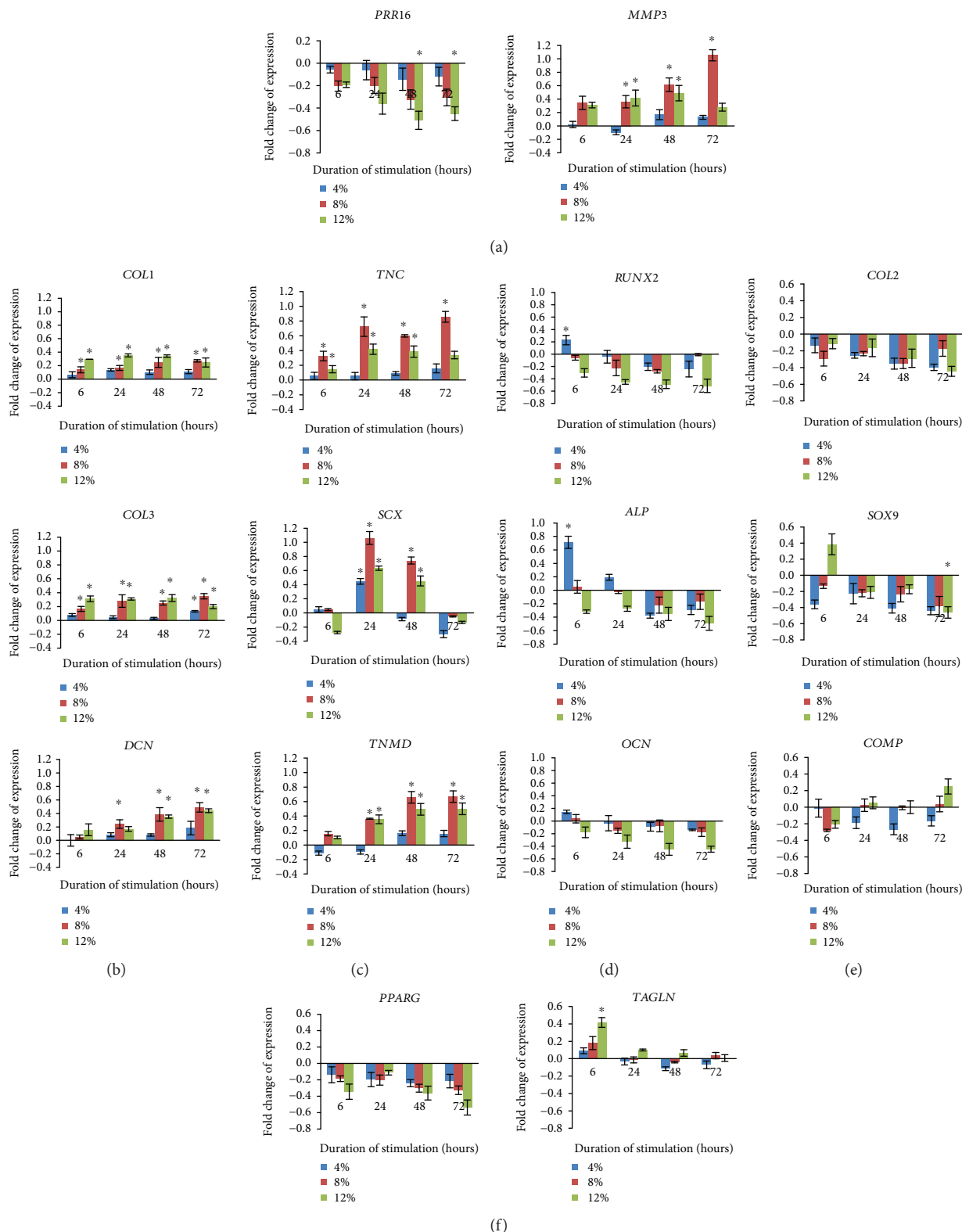
Figure 7: mRNA expression level of different genes subjected to different strain for different time point. (a) mRNA expression of *MMP3* and *PRR16*. (b) ECM component (*COL1*, *COL3*, and *DCN*). (c) Tendon cell lineage (*TNC*, *SCX*, and *TNMD*). (d) Bone cell lineage (*RUNX2*, *ALP*, and *OCN*). (e) Cartilage cell lineage (*COL2*, *SOX9*, and *COMP*). (f) Adipose cell (*PPARG*) and smooth muscle cell (*TAGLN*). The expression level of each gene was normalized with the level of housekeeping gene. The value of fold change was presented as the ratio of strained group with unstrained group. Statistical significance ($p < 0.05$) was represented by * which compared to unstrained. $N = 6$, $n = 3$, error bar $\pm$ SD.

gene expression levels of *SCX* returned to the basal level as with the unstrained group, suggesting that the observed increase in gene expression was transient.

3.9. Uniaxial Mechanical Strain Did Not Induce Chondrogenic, Adipogenic, and Osteogenic Differentiation Markers. To determine the global differentiation responses of hMSCs when subjected to uniaxial mechanical strain and to ascertain the possible expression of nontendon differentiation markers, the expressions of nontendon genes were also investigated in this study. These included gene markers for the bone, cartilage, and fat. We found that at 4% strain, osteogenic genes (*RUNX2*, *ALP*, and *OCN*) were transiently upregulated (Figure 7(d)). However, at 8% and 12% strains, these genes were downregulated suggesting that at low mechanical strain levels, osteoblastic differentiation is transiently enhanced. Consistent with our immunostaining results, uniaxial strain did not increase *COL2* (Figure 7(e)) and *PPARG* (Figure 7(f)) genes related to chondrogenesis and adipogenesis processes in these progenitor cells. Several molecules involved in chondrogenesis (i.e., *SOX9* and *COMP*) were influenced by the changes in strain magnitude and duration of cyclic stretching (Figure 7(e)). *SOX9* gene was downregulated when uniaxial strain was applied, although at 12% it was observed that a transient increase can be expected at the early stages of stretching (6 h) but is not present thereafter. In contrast, *COMP* was upregulated in the 12% strained group at 72 h. One reason to this may be due to the fact that *COMP* is not a specific gene for chondrogenesis and can be found in tendon cells as per observed in other studies [16]. Uniaxial cyclic stimulation also increased the smooth muscle contractile marker, *TAGLN*, transiently at 12% strain (Figure 7(f)).

Despite the evidences from this study suggesting that a transient increase in nontendon-related genes can occur when hMSCs are subjected to cyclic loading, the functional significance of these changes may be insignificant since only low levels and short duration of these genes were expressed throughout our experiments. We can therefore conclude that uniaxial cyclic loading generally results in tenogenic differentiation and results in the insignificant increase in other downstream musculoskeletal lineages.

4. Discussion

Our current study demonstrates that uniaxial stretching over a period of time provides exclusive tenogenic lineage differentiation ability in hMSCs. The genes and proteins expressed from these cells were within the defined characteristics of tenogenic differentiation, as mentioned earlier. We can also conclude that the action of cyclic stretching also stimulates superior cell proliferation based on our previous pilot study [28]. However, an increase in strain magnitude does not necessarily result in higher differentiation as demonstrated in this study, where 8% strain resulted in the highest tenogenic expression and not at 4% or 12% strain. Yet, based on our previous pilot study [28], hMSCs subjected to 4% strain at 1 Hz provides the best cell proliferation. The choice of strain rate, i.e., 1 Hz in this study was based on our previous study

which showed that at this rate the best cellular differentiation in hMSCs was observed [28]. It is worth noting that uniaxial cyclic loading does not result in chondrogenic, adipogenic, or osteogenic differentiation and that, at the prescribed loading regime, cells tend to form distinctive tendon-like cell phenotype. As far as the authors of this paper are aware, these observations have not been previously reported. Another novelty of this study is that specific combinations of strain amounts and rate of tensile loading provide specific hMSC tenogenic differentiation responses as mentioned earlier. It is important to note here that as far as the authors of this paper are aware, there is no consensus on the proper definition of tenogenic differentiation. In trying to ensure that the work done in our study incorporates any characteristics of tenogenic differentiation possible using gene and protein expressions, the work of several studies from different laboratories was used as reference [25, 26, 31, 32]. It is hoped that in doing this, a more global definition of what defines tenogenic differentiation can be made [23].

Our study corroborates previous findings that cell orientation is altered when subjected to cyclic loading [20, 33]. The cell appears to reorientate in a longitudinal axis perpendicular to its original orientation as well as the direction of cyclic loading. This phenomenon appears to be necessary for the reduction of excessive strain that is applied to the cellular structures. In addition, this also results in the increase in specific phenotypic expressions from these cells as previously described [34, 35]. It has been suggested that the mechanisms involved in promoting cellular realignment are dependent on various factors, which includes the rearrangement of intracellular stress fibers due to energy dissipation and the fluctuations in the ionic exchange mechanisms such as the depolarization of voltage-gated channels [36, 37]. Based on our observations, it is likely that the actin stress fibers, which are a major cytoskeletal constituent, may be responsible for the proliferation and differentiation of hMSCs [38, 39]. The AFM and confocal fluorescence microscopic analyses demonstrate these changes occurring in the actin stress fibers which, if based on previous findings, suggest that the change in Young's modulus was ascribable to the development of the cellular cytoskeleton during the differentiation process [40].

Another finding that corroborates previous studies is the fact that hMSCs subjected to tensile cyclic loading result in the apparent increase in the synthesis of collagen type I and type III, and potentially other tenogenic protein expressions [31, 32, 41]. However, whilst our study did not demonstrate any chondrogenic, osteogenic, or adipogenic expressions, these have been reported in others [42–45]. We hypothesized that these differences may be attributable to the different loading types, magnitude, rates, and even the device used to create the mechanical strained environments employed in each of these studies, since it has been shown that different types of mechanical signals will produce different outcomes, i.e., resulting in the differentiation of hMSCs towards a specific lineage [46]. For example, low-amplitude or low-frequency mechanical loading has been shown to promote osteogenic (1 Hz, 3%, 48 h) [31], myogenic (1 Hz, 4%, 24 h) [47], and neuronal (0.5 Hz, 0.5%, 8 h) [15] differentiation of hMSCs. In addition, the action of cyclic compression

appears to be a major contributing factor required for MSCs to undergo chondrogenesis [48]. Apparently, loading cells in a uniaxial and biaxial manner will result in different outcomes. In another study using similar rate and magnitudes to ours but employing biaxial loading, MSCs tend to differentiate towards osteogenic lineage [49]. Thus, it is not unexpected that uniaxial cyclic stretch is believed to be of paramount importance in the development of functional musculoskeletal tissues [50] especially for the differentiation of MSCs into tendon/ligament fibroblasts. One aspect that needs to be considered is that the differences observed between our study and that of previous reports [51–53] may have been related to the Flexcell system used in their studies. In contrast to the Strex machine used in our study, this device employs a suction mechanism at the centre of the elastomeric cell culture surface to create the stretching effect. It may be the case that the radial stretching effect of the Flexcell system could have produced compounding compressive forces to the attached cells thus resulting in the osteogenic lineage differentiation. This however remains speculative and would require further supportive findings in future studies. Thus, it can be concluded that different types of mechanical signals will produce different outcomes, i.e., resulting in the differentiation of hMSCs towards a specific lineage [54].

The clinical implication of the study is apparent and may lead to several potential applications. Although further studies are required, it is now possible to extrapolate the data obtained from our study to be applied into patients. In fact, this is not new since many studies have demonstrated that mechanical loading is beneficial to the musculoskeletal system [55]. This particularly applies to the tendon which has been shown to undergo tissue reparative process when subjected to stretching exercises [56, 57]. What is new here in this study is the fact that only a certain combination of strain and cyclic loading rates may be beneficial for multipotent cells such as hMSCs, while other combinations may not be or in fact quite the opposite, may even result in detrimental outcomes. Once the optimal combination has been established, such as that which is observed in the present study, stretching will elicit anabolic responses from the tendon cells. This in turn increases the production of type I collagen in the peritendinous tissues as demonstrated previously [58].

Tendons, being viscoelastic tissues that are stiffer than most other soft tissues, allow the transfer of large tensile forces to occur without causing tissue or cell damage [59]. Indeed, although resistant to tensile forces, tenocytes are still subjected to high mechanical stresses enclaved within a highly mechanoactive environment [60]. However, to study the mechanical processes underpinning the cellular response within an *in vivo* environment would be technically unmanageable; hence, a model such as the one employed in the present study may be more realistic, appropriate, and informative. We recognize the limitations of a system that do not truly mimic the *in vivo* environment; however, these have been considered during our analyses and have not overstated the findings of the present study. We also recognized that although the present study was well designed, several

limitations were unavoidable and thus need to be highlighted here. Firstly, it needs to be reminded that as with any *in vitro* studies, the present study does not take into account the complexities of surrounding tissues, and thus, translating the findings into clinical applications would need to be done with caution. Secondly, the present study assumes that the effect of the stretching occurs in a uniform manner, which in reality may not be the case. More so when certain areas within the substrate are subjected to a phenomenon known as differential stretching, as suggested in previous studies [61–64]. Limited by the size of the cell culture flask and the maximal rate of which cells can proliferate, the present study could only be conducted up to 72 hours. There is a downside to this, since it is possible that certain gene expressions such as osteogenic expressions may not have been detected. In previous studies, it appears that culturing MSCs up to 14 days may be needed for these changes to be observed. Hence, it may be the case that the tests from our experiment may have shown false-negative results. It needs to be reminded however that these changes may be better applied for static cultures and probably not applicable to our stretching cultures [65, 66]. Results from other studies seem to suggest that this is the case [53, 67, 68]. Notwithstanding these limitations, the findings of the present study are still valid and useful owing to the robust study design employed. It is however hoped that future studies can be conducted using more advanced techniques that are not subjected to the limitations mentioned above.

5. Conclusions

Cells subjected to 1 Hz cyclic uniaxial stretching demonstrated significant maximal tenogenic expression observed but not of other mesenchyme lineages when stretched at 8% strain. No dose-related responses were observed as the result of increased strain magnitude, and it is more likely to be the case that a specific combination of rate and strain magnitude will elicit specific cell responses as demonstrated from our present and previous studies.

Data Availability

The data used to support the findings of this study are included within the article.

Conflicts of Interest

The authors declare that there is no conflict of interest regarding the publication of this paper.

Acknowledgments

References

[1] A. Moshiri, A. Oryan, and A. Meimandi-Parizi, "Role of stem cell therapy in orthopaedic tissue engineering and regenerative medicine: a comprehensive review of the literature from basic to clinical application," *Hard Tissue*, vol. 2, no. 4, 2013.

[2] D. M. Patel, J. Shah, and A. S. Srivastava, "Therapeutic potential of mesenchymal stem cells in regenerative medicine," *Stem Cells International*, vol. 2013, Article ID 496218, 15 pages, 2013.

[3] C. A. Herberts, M. S. Kwa, and H. P. Hermsen, "Risk factors in the development of stem cell therapy," *Journal of Translational Medicine*, vol. 9, no. 1, p. 29, 2011.

[4] P. P. Y. Lui, Y. F. Rui, M. Ni, and K. M. Chan, "Tenogenic differentiation of stem cells for tendon repair-what is the current evidence?," *Journal of Tissue Engineering and Regenerative Medicine*, vol. 5, no. 8, pp. e144–e163, 2011.

[5] C. Baugé and K. Boumédiene, "Use of adult stem cells for cartilage tissue engineering: current status and future developments," *Stem Cells International*, vol. 2015, Article ID 438026, 14 pages, 2015.

[6] A. Wei, B. Shen, L. Williams, and A. Diwan, "Mesenchymal stem cells: potential application in intervertebral disc regeneration," *Translational Pediatrics*, vol. 3, no. 2, pp. 71–90, 2014.

[7] M. M. Nava, M. T. Raimondi, and R. Pietrabissa, "Controlling self-renewal and differentiation of stem cells via mechanical cues," *Journal of Biomedicine and Biotechnology*, vol. 2012, Article ID 797410, 12 pages, 2012.

[8] N. Shah, Y. Morsi, and R. Manasseh, "From mechanical stimulation to biological pathways in the regulation of stem cell fate," *Cell Biochemistry and Function*, vol. 32, no. 4, pp. 309–325, 2014.

[9] L. MacQueen, Y. Sun, and C. A. Simmons, "Mesenchymal stem cell mechanobiology and emerging experimental platforms," *Journal of the Royal Society Interface*, vol. 10, no. 84, p. 20130179, 2013.

[10] A. B. Castillo and C. R. Jacobs, "Mesenchymal stem cell mechanobiology," *Current Osteoporosis Reports*, vol. 8, no. 2, pp. 98–104, 2010.

[11] L. Ramage, "Integrins and extracellular matrix in mechanotransduction," *Cell Health and Cytoskeleton*, vol. 4, pp. 1–9, 2012.

[12] J. Hao, Y. Zhang, D. Jing et al., "Mechanobiology of mesenchymal stem cells: perspective into mechanical induction of MSC fate," *Acta Biomaterialia*, vol. 20, pp. 1–9, 2015.

[13] Y. K. Wang and C. S. Chen, "Cell adhesion and mechanical stimulation in the regulation of mesenchymal stem cell differentiation," *Journal of Cellular and Molecular Medicine*, vol. 17, no. 7, pp. 823–832, 2013.

[14] H.-m. Du, X.-h. Zheng, L.-y. Wang et al., "The osteogenic response of undifferentiated human adipose-derived stem cells under mechanical stimulation," *Cells, Tissues, Organs*, vol. 196, no. 4, pp. 313–324, 2012.

[15] W. S. Leong, S. C. Wu, M. Pal et al., "Cyclic tensile loading regulates human mesenchymal stem cell differentiation into neuron-like phenotype," *Journal of Tissue Engineering and Regenerative Medicine*, vol. 6, no. S3, pp. s68–s79, 2012.

[16] Z. Li, S. J. Yao, M. Alini, and M. J. Stoddart, "Chondrogenesis of human bone marrow mesenchymal stem cells in fibrin-polyurethane composites is modulated by frequency and amplitude of dynamic compression and shear stress," *Tissue Engineering Part A*, vol. 16, no. 2, pp. 575–584, 2010.

[17] K. Hayashi, "Biomechanical studies of the remodeling of knee joint tendons and ligaments," *Journal of Biomechanics*, vol. 29, no. 6, pp. 707–716, 1996.

[18] M. Benjamin, H. Toumi, J. R. Ralphs, G. Bydder, T. M. Best, and S. Milz, "Where tendons and ligaments meet bone: attachment sites ('entheses') in relation to exercise and/or mechanical load," *Journal of Anatomy*, vol. 208, no. 4, pp. 471–490, 2010.

[19] C. K. Kuo and R. S. Tuan, "Mechanoactive tenogenic differentiation of human mesenchymal stem cells," *Tissue Engineering Part A*, vol. 14, no. 10, pp. 1615–1627, 2008.

[20] J. Y. Jang, S. W. Lee, S. H. Park et al., "Combined effects of surface morphology and mechanical straining magnitudes on the differentiation of mesenchymal stem cells without using biochemical reagents," *Journal of Biomedicine & Biotechnology*, vol. 2011, Article ID 860652, 9 pages, 2011.

[21] M. Hata, K. Naruse, S. Ozawa et al., "Mechanical stretch increases the proliferation while inhibiting the osteogenic differentiation in dental pulp stem cells," *Tissue Engineering Part A*, vol. 19, no. 5-6, pp. 625–633, 2013.

[22] W.-C. C. Lee, T. M. Maul, D. A. Vorp, J. P. Rubin, and K. G. Marra, "Effects of uniaxial cyclic strain on adipose-derived stem cell morphology, proliferation, and differentiation," *Biomechanics and Modeling in Mechanobiology*, vol. 6, no. 4, pp. 265–273, 2007.

[23] L. Dai, X. Hu, X. Zhang et al., "Different tenogenic differentiation capacities of different mesenchymal stem cells in the presence of BMP-12," *Journal of Translational Medicine*, vol. 13, no. 1, p. 200, 2015.

[24] G. Subramanian, A. Stasuk, M. Elsaadany, and E. Yildirim-Ayan, "Effect of uniaxial tensile cyclic loading regimes on matrix organization and tenogenic differentiation of adipose-derived stem cells encapsulated within 3d collagen scaffolds," *Stem Cells International*, vol. 2017, Article ID 6072406, 16 pages, 2017.

[25] T. P. Dale, S. Mazher, W. R. Webb et al., "Tenogenic differentiation of human embryonic stem cells," *Tissue Engineering Part A*, vol. 24, no. 5-6, pp. 361–368, 2018.

[26] J. Burk, A. Plenge, W. Brehm, S. Heller, B. Pfeiffer, and C. Kasper, "Induction of tenogenic differentiation mediated by extracellular tendon matrix and short-term cyclic stretching," *Stem Cells International*, vol. 2016, Article ID 7342379, 11 pages, 2016.

[27] H. Nam, P. Karunanithi, W. C. Loo et al., "The effects of staged intra-articular injection of cultured autologous mesenchymal stromal cells on the repair of damaged cartilage: a pilot study in caprine model," *Arthritis Research & Therapy*, vol. 15, no. 5, article R129, 2013.

[28] H. Y. Nam, B. Pingguan-Murphy, A. Amir Abbas, A. Mahmood Merican, and T. Kamarul, "The proliferation and tenogenic differentiation potential of bone marrow-derived mesenchymal stromal cell are influenced by specific uniaxial cyclic tensile loading conditions," *Biomechanics and Modeling in Mechanobiology*, vol. 14, no. 3, pp. 649–663, 2015.

[29] J. Zhang and J. H.-C. Wang, "Characterization of differential properties of rabbit tendon stem cells and tenocytes," *BMC Musculoskeletal Disorders*, vol. 11, no. 1, 2010.

[30] B. V. Derjaguin, V. M. Muller, and Y. P. Toporov, "Effect of contact deformations on the adhesion of particles," *Journal of Colloid and Interface Science*, vol. 53, no. 2, pp. 314–326, 1975.

[31] Y. J. Chen, C. H. Huang, I. C. Lee, Y. T. Lee, M. H. Chen, and T. H. Young, "Effects of cyclic mechanical stretching on the mRNA expression of tendon/ligament-related and osteoblast-specific genes in human mesenchymal stem cells," *Connective Tissue Research*, vol. 49, no. 1, pp. 7–14, 2008.

[32] E. Farng, A. R. Urdaneta, D. Barba, S. Esmende, and D. R. McAllister, "The effects of GDF-5 and uniaxial strain on mesenchymal stem cells in 3-D culture," *Clinical Orthopaedics and Related Research*, vol. 466, no. 8, pp. 1930–1937, 2008.

[33] J. S. Park, J. S. F. Chu, C. Cheng, F. Chen, D. Chen, and S. Li, "Differential effects of equiaxial and uniaxial strain on mesenchymal stem cells," *Biotechnology and Bioengineering*, vol. 88, no. 3, pp. 359–368, 2004.

[34] K. M. Choi, Y. K. Seo, H. H. Yoon et al., "Effects of mechanical stimulation on the proliferation of bone marrow-derived human mesenchymal stem cells," *Biotechnology and Bioprocess Engineering*, vol. 12, no. 6, pp. 601–609, 2007.

[35] C. Neidlinger-Wilke, E. S. Grood, J. H. C. Wang, R. A. Brand, and L. Claes, "Cell alignment is induced by cyclic changes in cell length: studies of cells grown in cyclically stretched substrates," *Journal of Orthopaedic Research*, vol. 19, no. 2, pp. 286–293, 2001.

[36] J. H.-C. Wang and E. S. Grood, "The strain magnitude and contact guidance determine orientation response of fibroblasts to cyclic substrate strains," *Connective Tissue Research*, vol. 41, no. 1, pp. 29–36, 2000.

[37] H. Y. Nam, H. R. Balaji Raghavendran, B. Pingguan-Murphy, A. A. Abbas, A. M. Merican, and T. Kamarul, "Fate of tenogenic differentiation potential of human bone marrow stromal cells by uniaxial stretching affected by stretch-activated calcium channel agonist gadolinium," *PLoS One*, vol. 12, no. 6, article e0178117, 2017.

[38] P. S. Mathieu and E. G. Loboa, "Cytoskeletal and focal adhesion influences on mesenchymal stem cell shape, mechanical properties, and differentiation down osteogenic, adipogenic, and chondrogenic pathways," *Tissue Engineering Part B, Reviews*, vol. 18, no. 6, pp. 436–444, 2012.

[39] G. Yourek, M. A. Hussain, and J. J. Mao, "Cytoskeletal changes of mesenchymal stem cells during differentiation," *ASAIO Journal*, vol. 53, no. 2, pp. 219–228, 2007.

[40] Y. Morita, T. Mukai, Y. Ju, and S. Watanabe, "Evaluation of stem cell-to-tenocyte differentiation by atomic force microscopy to measure cellular elastic moduli," *Cell Biochemistry and Biophysics*, vol. 66, no. 1, pp. 73–80, 2013.

[41] B. Xu, G. Song, and Y. Ju, "Effect of focal adhesion kinase on the regulation of realignment and tenogenic differentiation of human mesenchymal stem cells by mechanical stretch," *Connective Tissue Research*, vol. 52, no. 5, pp. 373–379, 2011.

[42] R. Li, L. Liang, Y. Dou et al., "Mechanical strain regulates osteogenic and adipogenic differentiation of bone marrow mesenchymal stem cells," *BioMed Research International*, vol. 2015, Article ID 873251, 10 pages, 2015.

[43] A. Charoenpanich, M. E. Wall, C. J. Tucker et al., "Cyclic tensile strain enhances osteogenesis and angiogenesis in mesenchymal stem cells from osteoporotic donors," *Tissue Engineering Part A*, vol. 20, no. 1-2, pp. 67–78, 2014.

[44] G. Friedl, R. Windhager, H. Schmidt, and R. Aigner, "The osteogenic response of undifferentiated human mesenchymal stem cells (hMSCs) to mechanical strain is inversely related to body mass index of the donor," *Acta Orthopaedica*, vol. 80, no. 4, pp. 491–498, 2009.

[45] L. A. McMahon, A. J. Reid, V. A. Campbell, and P. J. Prendergast, "Regulatory effects of mechanical strain on the chondrogenic differentiation of MSCs in a collagen-GAG scaffold: experimental and computational analysis," *Annals of Biomedical Engineering*, vol. 36, no. 2, pp. 185–194, 2008.

[46] P. Costa, F. V. M. Almeida, and J. T. Connelly, "Biophysical signals controlling cell fate decisions: how do stem cells really feel?," *The International Journal of Biochemistry & Cell Biology*, vol. 44, no. 12, pp. 2233–2237, 2012.

[47] D. Ge, X. Liu, L. Li et al., "Chemical and physical stimuli induce cardiomyocyte differentiation from stem cells," *Biochemical and Biophysical Research Communications*, vol. 381, no. 3, pp. 317–321, 2009.

[48] S. Grad, D. Eglin, M. Alini, and M. J. Stoddart, "Physical stimulation of chondrogenic cells in vitro: a review," *Clinical Orthopaedics and Related Research*, vol. 469, no. 10, pp. 2764–2772, 2011.

[49] M. Jagodzinski, Department of Trauma Surgery, Hanover Medical School (MHH), Hanover, Germany, M. Drescher et al., "Effects of cyclic longitudinal mechanical strain and dexamethasone on osteogenic differentiation of human bone marrow stromal cells," *European Cells & Materials*, vol. 7, pp. 35–41, 2004.

[50] A. L. Mackey, K. M. Heinemeier, S. O. Anneli Koskinen, and M. Kjaer, "Dynamic adaptation of tendon and muscle connective tissue to mechanical loading," *Connective Tissue Research*, vol. 49, no. 3-4, pp. 165–168, 2008.

[51] C. H. Huang, M. H. Chen, T. H. Young, J. H. Jeng, and Y. J. Chen, "Interactive effects of mechanical stretching and extracellular matrix proteins on initiating osteogenic differentiation of human mesenchymal stem cells," *Journal of Cellular Biochemistry*, vol. 108, no. 6, pp. 1263–1273, 2009.

[52] B. Lohberger, H. Kaltenegger, N. Stuendl, M. Payer, B. Rinner, and A. Leithner, "Effect of cyclic mechanical stimulation on the expression of osteogenesis genes in human intraoral mesenchymal stromal and progenitor cells," *BioMed Research International*, vol. 2014, Article ID 189516, 10 pages, 2014.

[53] Y. Wu, P. Zhang, Q. Dai et al., "Osteoclastogenesis accompanying early osteoblastic differentiation of BMSCs promoted by mechanical stretch," *Biomedical Reports*, vol. 1, no. 3, pp. 474–478, 2013.

[54] D. J. Kelly and C. R. Jacobs, "The role of mechanical signals in regulating chondrogenesis and osteogenesis of mesenchymal stem cells," *Birth Defects Research Part C, Embryo Today*, vol. 90, no. 1, pp. 75–85, 2010.

[55] J. E. Dook, C. James, N. K. Henderson, and R. I. Price, "Exercise and bone mineral density in mature female athletes," *Medicine and Science in Sports and Exercise*, vol. 29, no. 3, pp. 291–296, 1997.

[56] C. I. Buchanan and R. L. Marsh, "Effects of long-term exercise on the biomechanical properties of the Achilles tendon of guinea fowl," *Journal of Applied Physiology*, vol. 90, no. 1, pp. 164–171, 2001.

[57] C. Couppé, M. Kongsgaard, P. Aagaard et al., "Habitual loading results in tendon hypertrophy and increased stiffness of the human patellar tendon," *Journal of Applied Physiology*, vol. 105, no. 3, pp. 805–810, 2008.

[58] J. L. Olesen, K. M. Heinemeier, C. Gemmer, M. Kjaer, A. Flyvbjerg, and H. Langberg, "Exercise-dependent IGF-I, IGFBPs, and type I collagen changes in human peritendinous connective tissue determined by microdialysis," *Journal of Applied Physiology*, vol. 102, no. 1, pp. 214–220, 2007.

[59] J. H. C. Wang, "Mechanobiology of tendon," *Journal of Biomechanics*, vol. 39, no. 9, pp. 1563–1582, 2006.

[60] A. J. Engler, S. Sen, H. L. Sweeney, and D. E. Discher, "Matrix elasticity directs stem cell lineage specification," *Cell*, vol. 126, no. 4, pp. 677–689, 2006.

[61] A. A. Pitsillides, V. Das-Gupta, D. Simon, and S. C. F. Rawlinson, "Methods for analyzing bone cell responses to mechanical loading using in vitro monolayer and organ culture models," *Methods in Molecular Medicine*, vol. 80, pp. 399–422, 2003.

[62] C. R. Jacobs, H. Huang, and R. Y. Kwon, "Cell mechanics in the laboratory," in *Introduction to Cell Mechanics and Mechanobiology*, S. Scholl, Ed., pp. 151–184, Garland Science, New York, NY, USA, 2013.

[63] K. A. Lazopoulos and D. Stamenović, "A mathematical model of cell reorientation in response to substrate stretching," *Molecular & Cellular Biomechanics*, vol. 3, no. 1, pp. 43–48, 2006.

[64] T. D. Brown, "Techniques for mechanical stimulation of cells in vitro: a review," *Journal of Biomechanics*, vol. 33, no. 1, pp. 3–14, 2000.

[65] M. Taira, N. Chosa, K. Sasaki et al., "Gene expression analyses of human mesenchymal stem cells cultured in osteogenic differentiation medium for 3, 7, 14 and 21 days by genome focus DNA microarray and real-time PCR," *Journal of Oral Tissue Engineering*, vol. 5, pp. 35–47, 2007.

[66] M. Yamamoto, H. Nakata, J. Hao, J. Chou, S. Kasugai, and S. Kuroda, "Osteogenic potential of mouse adipose-derived stem cells sorted for CD90 and CD105 *in vitro*," *Stem Cells International*, vol. 2014, Article ID 576358, 17 pages, 2014.

[67] E. M. Kearney, E. Farrell, P. J. Prendergast, and V. A. Campbell, "Tensile strain as a regulator of mesenchymal stem cell osteogenesis," *Annals of Biomedical Engineering*, vol. 38, no. 5, pp. 1767–1779, 2010.

[68] M. C. Qi, J. Hu, S. J. Zou, H. Q. Chen, H. X. Zhou, and L. C. Han, "Mechanical strain induces osteogenic differentiation: Cbfa1 and Ets-1 expression in stretched rat mesenchymal stem cells," *International Journal of Oral and Maxillofacial Surgery*, vol. 37, no. 5, pp. 453–458, 2008.

Research Article

Adipose-Derived Mesenchymal Stem Cells Migrate and Rescue RPE in the Setting of Oxidative Stress

Aya Barzelay [iD],[1,2] **Shira Weisthal Algor,**[1,2] **Anat Niztan,**[1,2] **Sebastian Katz,**[1,2]
Moshe Benhamou,[1,2] **Itay Nakdimon,**[1,2] **Noam Azmon,**[1,2] **Sandy Gozlan,**[1,2]
Daphna Mezad-Koursh,[1,2] **Meira Neudorfer,**[1,2] **Michaella Goldstein,**[1,2] **Benjamin Meilik,**[2,3]
Anat Loewenstein,[1,2] **and Adiel Barak** [iD][1,2]

[1]*Department of Ophthalmology, Tel Aviv Sourasky Medical Center, Tel Aviv, Israel*
[2]*Sackler Faculty of Medicine, Tel Aviv University, Tel Aviv, Israel*
[3]*Department of Plastic and Reconstructive Surgery, Tel Aviv Sourasky Medical Center, Tel Aviv, Israel*

Correspondence should be addressed to Aya Barzelay; aya.barzelay@gmail.com

Aya Barzelay and Shira Weisthal Algor contributed equally to this work.

Oxidative stress leads to the degeneration of retinal pigment epithelial (RPE) and photoreceptor cells. We evaluated the potential of adipose-derived mesenchymal stem cells (ASCs) as a therapeutic tool by studying the migration capacity of ASCs *in vitro* and their protective effect against RPE cell death under oxidative stress *in vitro* and *in vivo*. ASCs exhibited enhanced migration when exposed to conditioned medium of oxidative stressed RPE cells obtained by hydrogen peroxide. Migration-related axis SDF-1/CXCR4 was studied, and upregulation of SDF-1 in stressed RPE and of CXCR4 in ASCs was detected. Moreover, ASCs' conditioned medium prevented H_2O_2-induced cell death of RPE cells. Early passage ASCs had high expression level of HGF, low VEGF levels, and unmodulated IL-1β levels, compared to late passage ASCs. Thus, early passage ASCs show the potential to migrate towards damaged RPE cells and protect them in a paracrine manner from cell death induced by oxidative stress. *In vivo*, mice received systemic injection of $NaIO_3$, and 72 h later, ASCs were transplanted in the subretinal space. Seven days after ASC transplantation, the eyes were enucleated fixed and frozen for immunohistochemical analysis. Under such conditions, ASC-treated mice showed preservation of nuclear layers in the outer nuclear layer and stronger staining of RPE and photoreceptor layer, compared to PBS-treated mice. Taken together, our results indicate that ASCs are able to home in on damaged RPE cells and protect against damage to the RPE and PR layers caused by oxidative stress. These data imply the potential that ASCs have in regenerating RPE under oxidative stress, providing the basis for a therapeutic approach to retinal degeneration diseases related to oxidative stress that could help save the eyesight of millions of people worldwide.

1. Introduction

Retinal degeneration diseases related to oxidative stress and inflammation, such as age-related macular degeneration (AMD), are characterized with RPE injury and cell death [1–3]. Oxidative stress is associated with the release of reactive oxygen species as a result of high oxygen tension in the macula, phagocytosis of high concentrations of polyunsaturated fatty acids from photoreceptor outer segments by the retinal pigment epithelium (RPE), and finally, decreased antioxidant capacity with advanced age [4, 5]. Degeneration, apoptosis, and necrosis of the RPE are related to both inflammation and oxidative stress by several mechanisms [6–9]. Photoreceptors (PR), whose normal function and survival are strongly related to the activity of the RPE by various metabolic functions, such as phagocytosis of PR outer segments, are highly susceptible to oxidative damage due to their constant exposure to light and oxygen. Thus, RPE

degeneration leads to secondary death of PR and their nuclei, concentrated in the outer nuclear layer (ONL).

Cell therapy for retinal degeneration diseases has recently gained attention. Among different sources of stem cells, adipose tissue-derived mesenchymal stem cells (ASCs) have emerged as a promising therapeutic modality, in light of their advantages: they can be easily isolated from subcutaneous fat by minimally invasive techniques [10], produced in larger quantities, as compared to bone marrow-derived mesenchymal stem cells [10], and additionally, characterized by high viability and reproducibility. Moreover, they serve as an autologous source for stem cells, thus precluding the need for immunosuppressive therapy, which may not be well tolerated by elderly patients [11]. Furthermore, ASCs, which bear migratory and homing abilities, also have immunomodulatory properties and secrete cytokines and growth factors [11, 12], thus facilitating replacement of dying cells, immunomodulatory capacity [12], and promotion of tissue remodeling and regeneration [11, 13]. Interestingly, mesenchymal stem cells have shown resiliency to oxidative stress, possibly due to low baseline levels of reactive oxygen species (ROS) and high levels of glutathione [14]. Therefore, this population of stem cells may serve as a therapeutic tool in the future treatment of retinal degeneration diseases that manifest with oxidative stress.

Taken together, ASCs may be a potential source of autologous stem cells with prosurvival and antioxidative activities. The aims of this study were to evaluate the migratory ability of ASCs under RPE-oxidative stress conditions, as well as the protective role of ASCs on RPE cell death and degeneration of surrounding tissues.

2. Materials and Methods

The purpose of the study and the procedures used were presented to all of the subjects, and a signed informed consent was obtained from each. This study was approved by the ethics committee for clinical trials of Tel Aviv Sourasky Medical Center, and the procedures used conformed to the tenets of the Declaration of Helsinki.

2.1. Isolation, Characterization, and Culture of ASCs

2.1.1. Isolation and Culture of Human Adipose Tissue-Derived Stem Cells (ASCs). Human adipose tissue was harvested from 5 healthy patients with a mean age of 38 ± 4.3 and body mass index of 28.2 ± 3.9 who had abdominoplasty for aesthetic reasons at Tel Aviv Sourasky Medical Center. No metabolic diseases, HIV, hepatitis, or other systemic complications were reported from these patients.

The isolation and culture of ASCs were performed as previously described [15]. Briefly, 60 to 120 ml of the raw lipoaspirates was washed with phosphate-buffered saline (PBS) and enzymatically digested with 0.75% collagenase type I (Cat. no. C1639, Sigma) at 37°C for 1 hour. The digested lipoaspirates were centrifuged at 400 g for 15 minutes, and the pellet was resuspended and passed through a 100 μm mesh filter (Cat. no. 542000, EASYstrainer, Greiner Bio-One) to remove debris. Subsequently, 1×10^6 cells were plated in 100 mm culture dishes in ADSC medium and incubated at 37°C in a humidified 8% CO_2 atmosphere [16]. The medium was changed twice weekly, and cells were passaged with 0.25% trypsin/0.1% EDTA (Biological Industries, Israel) upon reaching 90% confluency. Experiments were performed at passages 3–4.

2.1.2. Characterization of ASCs for Mesenchymal Stem Cell (MSC) Markers by Immunostaining and FACS Analysis. Characterization of cultured ASCs was performed at passage three as follows: after reaching 100% confluence, cells were trypsinized and collected in FACS tubes in aliquots (1×10^5 cells/tube). Cells were then stained with fluorescein isothiocyanate (FITC) and phycoerythrin- (PE-) conjugated monoclonal antibodies against human CD34 (Dako), CD45 (Dako), CD90 (Dako), CD105 (eBioscience), and CD73 (BD Pharmingen). Cells were subsequently analyzed by FACS Canto II flow cytometer (BD Biosciences). Isotype-matched FITC and PE-conjugated antibodies were used as controls.

2.1.3. Multipotency of ASCs by Differentiation to Osteocytes and Adipocytes. ASCs at passage 3 were studied for their ability to differentiate to osteocytes and adipocytes. Cells were seeded in a 24-well plate at a density of 1×10^4 cells per well. At confluency of 100%, differentiation media were added to the cells and changed twice a week (adipose: 10% FBS, 1 μM dexamethasone, 0.5 mM 3-isobutyl-1-methylxanthine, 10 μg/ml insulin, and 100 μM indomethacin in high glucose (HG) DMEM; bone: StemPro® osteocyte differentiation basal medium (Gibco)). Protocol lasted either two or three weeks to induce bone and adipose differentiation, respectively.

Differentiation to adipocytes was assessed using an Oil Red O stain as an indicator of intracellular lipid accumulation. The cells were fixed for 20 min at room temperature in 4% paraformaldehyde. Cells were incubated in 0.5% (wt/vol) Oil Red O reagent in 100% Isopropanol (Sigma) for 10 min at room temperature. Excess stain was removed by washing with distilled water.

Bone differentiation was assessed using Alizarin red (Sigma). Cells were fixated with 4% paraformaldehyde for 20 min and then stained with Alizarin red 2% solution adjusted to pH 4.2 for 15 min at room temperature. Excess stain was removed by washing with several changes of distilled water.

Images of stained cells with both Oil Red O and Alizarin red were taken by light microscopy. Results are presented as the percent of stained cells from the total number of cells counted in a high-power field.

2.2. Primary RPE Culture. 5.5×10^5 cells of human pRPE cells (Lonza) were plated in 100 mm culture dishes (Falcon) in RtEGM BulletKit Medium (Lonza) and incubated at 37°C in a humidified 5% CO_2 atmosphere. The medium was replaced twice weekly, and cells were passaged with 0.25% trypsin/ 0.1% EDTA (Biological Industries, Israel) upon reaching 90% confluence. Experiments were performed at passages 3–4.

2.3. Scratch Assay

2.3.1. Oxidative Stress Induction. RPE cells were seeded at 1×10^4 cells/cm^2 in RtEGM medium containing 2% FBS (Lonza). After adhesion of the cells to the dish, the medium

was changed to FBS-free RtEGM and renewed every two days until treatments. To induce oxidative stress, subconfluent RPE cells were treated for 16 h with 0.5 mM H_2O_2 (Cat. no. 216763, Sigma) in ADSC serum-free medium; the medium was collected and centrifuged at 1500 rpm for 5 min, and the supernatant was collected (stressed RPE-CM).

2.3.2. Scratch Assay.
ASCs were seeded in 6-well plates (Falcon) until confluence. Cells were cultured in ADSC serum-free conditions to prevent proliferation [17], and the monolayers were then scored with a sterile pipette tip to leave a scratch. The culture medium was immediately removed along with any detached cells and replaced with either fresh ADSC serum-free medium (non-CM), stressed RPE-CM, or conditioned medium of RPE cells not treated with H_2O_2 (RPE-CM). All scratch assays were performed in quadruplicates, and images were taken at the beginning of the treatments (time zero) and after 24 h (H_2O_2 treatments). The number of cells migrating to the scratched area was counted under high-power magnification and in a blinded fashion. ASCs as well as RPE cells were then harvested for mRNA analysis by qRT-PCR.

2.4. Quantitative RT-PCR.
Total RNA was extracted from ASCs or RPE cell cultures using High Pure RNA Isolation Kit (Roche) according to the manufacturer's instructions. Total RNA concentration was determined by NanoDrop™ 1000 Spectrophotometer (Thermo Scientific) and was reverse transcribed using Verso cDNA synthesis kit (Thermo Scientific). The mRNA expression levels of the growth factors, hepatocyte growth factor (HGF), vascular endothelial growth factor (VEGF), interleukin-1β (IL-1β), stromal-derived factor-1 (SDF-1), the chemokine receptor CXCR4, and normalizing housekeeping genes GUSB and RLP27 (see Table S1 for sequence information) were measured by real-time reverse transcription polymerase chain reaction (RT-PCR) (StepOnePlus, Applied Biosystems) using SYBR® Green qPCR Mastermix (Qiagen). The cycling RT-PCR conditions were as follows: 10 min at 95˚C, 40 cycles for 10 s at 95˚C, 15 s at 60˚C, followed by gradient stage from 60 to 95˚C to obtain a melting curve. The results were calculated by the $\Delta\Delta CT$ method of relative quantitation.

2.5. Rescue Studies

2.5.1. Preparation of ASC Conditioned Medium.
ASCs (1×10^6 cells/cm^2) at passage 3 or passage 5 were seeded on a 100 mm dish (Falcon) and cultured in ADSC BulletKit™ Medium (Lonza). At 100% confluence, ASCs were washed with phosphate-buffered saline (PBS) and cultured with ADSC serum-free medium (Lonza) for 48 h. Medium was collected, filtered using a 0.22 mm syringe filter, and either immediately transferred to RPE cells or maintained in −80˚C for further protein analysis using ELISA assay. In turn, ASCs were harvested for mRNA level detection using RT-PCR. ASCs at passage 5 showed aspects of senescence evident by low proliferation rate and morphology changes (data not shown). The condition medium of ASCs at passage 5 (P5-CM) was used in this study as negative control to the condition medium collected from ASCs at passage 3 (P3-CM).

2.5.2. Rescue Study.
RPE was preincubated with ASC-CM followed by treatment with H_2O_2. RPE cells were seeded as described above in a 6-well plate (Falcon); after reaching approximately 90% confluence, RPE cells were preincubated for 48 h with either P3-CM, P5-CM, or with nonconditioned ADSC serum-free medium (non-CM). RPE cells were then washed with PBS followed by exposure to 1 mM H_2O_2 or without H_2O_2 as a control. After 7 h, RPE cell death was monitored by propidium iodide (PI) using FACS analysis and by ethidium bromide and acridine orange fluorescent staining.

2.5.3. Propidium Iodide Staining and Flow Cytometry Analysis.
Following rescue studies as described above, RPE cells (3×10^5) at passage 3 were harvested with 0.25% trypsin/EDTA (Biological Industries). Cells were collected by centrifugation at 500g for 5 min, washed twice with PBS, and resuspended in 400 μl of PBS to which 1 μl of propidium iodide (Sigma) 1 mg/ml was added immediately before flow cytometry measurements. At least 10,000 events were collected and labeled; fluorescence cells were detected by BD FACS Canto™ II cytometer (BD Pharmingen, USA). Analysis of cell death distribution was conducted by FCS Express 4 software (De Novo Software, Canada).

2.5.4. Ethidium Bromide and Acridine Orange Fluorescent Staining.
Following rescue studies as described above, RPE cells were collected by trypsinization; the apoptosis and necrosis rates of RPE were assessed using ethidium bromide and acridine orange fluorescent staining as follows: fluorescent staining solution (0.5 μl) containing an equal volume of 100 μg/ml acridine orange and 100 μg/ml ethidium bromide (Sigma) was added to each cell suspension sample and then covered with a coverslip. 150,000 cells were counted and the morphology of cell death was examined and analyzed immediately at room temperature.

2.6. Enzyme-Linked Immunosorbent Assay (ELISA).
Conditioned media were prepared as described above; briefly, ASCs' medium was changed to serum-free medium; following 48 h of incubation, medium was collected and centrifuged at 2500 rpm for 5 min, filtered, and stored at −80˚C until it was assayed. Levels of HGF were measured by ELISA according to manufacturer protocols (HGF, R&D Systems), and results were compared to the control group comprising senescent ASCs evident by high passage, phenotype, and low proliferation.

2.7. Animal Procedure.
Wild-type C57BL mice received intraperitoneal (IP) injection of 50 mg/kg of sodium iodate (NaIO$_3$) (Sigma-Aldrich) ($n = 8$ mice in each group, ASC treatment versus PBS). The sodium iodate model manifests oxidative stress, acute injury to RPE, and consequently progressive ongoing retinal damage [18, 19]. Seventy-two hours after injection, mice were anesthetized and a small self-sealing sclerotomy was performed with the tip of a 30-gauge needle. A 33-gauge needle attached to a Hamilton syringe (Hamilton Company, Reno, Nevada, USA) was inserted through sclerotomy into the subretinal space, and an injection of 1.5 μl of PBS containing 4×10^4 cells ensued.

The injection was unilateral in all animals. To note, mice received cyclosporine in drinking water after the transplantation, at a concentration of 210 mg/l [20]. Animal handling and experiments were performed following institutional care guidelines with the approval of the Tel Aviv Sourasky Medical Center Animal Ethics Committee.

2.8. Tissue Preparation. One week following subretinal injection, mice were euthanized; the eyes were enucleated and fixed in 3.7% formaldehyde (Merck, Darmstadt, Germany) in PBS overnight. The eyes were then infiltrated for cryoprotection with 5% sucrose (Sigma-Aldrich) in PBS at room temperature for 1 h, followed by 30% sucrose in PBS overnight at 4°C. Fixed tissue was embedded in OCT Tissue Freezing Medium (Scigen Scientific, Gardena, CA, USA) and frozen on dry ice. Cross-sections ($10 \mu m$) were placed on X-tra adhesive slides (Leica Biosystems, Peterborough, UK) and stored at $-20°C$.

2.9. Immunocytochemical Analysis. Sections were washed in PBS for 20 minutes and blocked with 1% bovine serum albumin (BSA) (Sigma-Aldrich), 10% normal goat serum (NGS) (Jackson ImmunoResearch, Baltimore, MD), and 0.25% Triton X-100 (Sigma-Aldrich) in PBS for 1 h at room temperature. The sections were incubated overnight with the primary antibodies in blocking solution at 4°C. The slides were washed three times with PBS, incubated with the secondary antibodies for 1 h at room temperature, and washed again three times with PBS. The sections were then incubated with the nuclear dye DAPI (Molecular Probes, Thermo Fisher Scientific) for 10 minutes, washed once in PBS, and mounted with ProLong Gold antifade reagent (Invitrogen, Thermo Fisher Scientific). Observations and photography were carried out with a Zeiss LSM 510 confocal microscope in a blinded manner. Analysis was carried out by ImageJ software. ONL thickness was assessed by counting the number of nuclei rows at different points along the retinal length [21]. RPE65 intensity was quantified by marking the RPE layer and measuring the fluorescence intensity compared to the image's background using ImageJ software. The size of the PR layer was quantified by measuring the width of the layer at different points along the layer using ImageJ software.

2.9.1. Primary Antibodies. Mouse anti-rhodopsin monoclonal antibody, 1 : 200 (EMD Millipore, Merck, Darmstadt, Germany), and anti-RPE65 antibody, mouse monoclonal, ab78036 1 : 500 (Abcam), were used.

2.9.2. Secondary Antibodies. Alexa Fluor 488 Goat anti-mouse IgG and Alexa Fluor 546 Goat anti-mouse IgG were used. All the secondary antibodies (Invitrogen, Thermo Fisher Scientific) were diluted 1 : 400 in PBS.

2.10. Statistical Analysis. For the *in vitro* experiments, each experiment was performed a minimum of 3 samples from 3 different patients. Each experiment was performed a minimum of 3 times. For the *in vivo* experiments, each experimental group included 8 mice. Statistical analysis was performed using paired *t*-test. p value ≤ 0.05 was considered statistically significant.

3. Results

3.1. Phenotypic Characterization and Multipotency of ASCs. ASCs were isolated from lipoaspirate of donors' subcutaneous fat. Phenotypic characterization was studied at passage 3 using immunostaining and FACS analysis. ASCs expressed classic MSC markers (CD90: 100 ± 1.98, CD73: 97 ± 5.2, and CD105: $97.8 \pm 1.7\%$ of population) and were negative for hematopoietic markers (CD45:1.5 ± 0.9, CD34:0.7 ± 0.6) (Figure 1). ASCs exhibited multipotency evident by their ability to differentiate into osteocytes and adipocytes, as evidenced by the percentage of cells stained with Alizarin red and Oil Red O, respectively (Figures 1(b) and 1(c)).

3.2. Early Passage ASCs Express High Levels of the Neurotropic Protein HGF but Not the Angiogenesis-Related VEGF Factor and Proinflammatory Cytokine IL-1β. Examination using quantitative RT-PCR of the expression levels of several cytokines and growth factors secreted by ASCs revealed that ASCs at passage 3 (P3), compared to passage 5 (P5), showed consistently high levels of HGF, lower levels of VEGF, and unchanged expression levels of IL-1β (HGF: 2.55 ± 0.26-fold, VEGF: 0.31 ± 0.14-fold, and IL-β: 1.18 ± 0.1-fold) (Figure 2(a)). The expression of HGF was further validated at the protein level by ELISA and was demonstrated to increase by 2.9-fold at P3 compared to P5 (Figure 2(b)).

3.3. Enhanced Migration of ASCs following Exposure to Stressed RPE-CM Corresponds to SDF-1 and CXCR4 Upregulation in RPE Cells and ASCs, Respectively. As described above, ASCs were exposed to non-CM, RPE-CM, and stressed RPE-CM and their migration was assessed. ASC migration capacity was significantly enhanced upon exposure to stressed RPE-CM as opposed to exposure to RPE-CM or non-CM (2.33- and 2.14-fold increase, respectively, p value < 0.05) (Figures 3(a) and 3(b)).

Using qRT-PCR, we analyzed the expression levels of SDF-1 and CXCR4. In stressed RPE cells, SDF-1 was significantly upregulated when compared to the expression of SDF-1 in nonstressed RPE cells (2.4 ± 0.09-fold) (Figure 3(c)). Accordingly, exposure of ASCs to stressed RPE-CM resulted in the upregulation of the SDF-1 receptor, CXCR4, compared to non-CM (12.6 ± 4.5-fold) (Figure 3(d)).

3.4. ASCs Inhibit RPE Cell Death under Oxidative Stress. Next, we assessed the protective role of ASC-CM on RPE cells exposed to H_2O_2. RPE cells were preincubated for 48 h with either ASCs' conditioned medium at passage 3 (P3-CM), ASCs' conditioned medium at passage 5 (P5-CM), or nonconditioned ADSC serum-free medium (non-CM), followed by H_2O_2 (1 mM, 7 h) treatment. RPE cells exposed to P3-CM prior to H_2O_2 treatment exhibited a significant decrease in cell death compared to non-CM, as evidenced by FACS analysis for propidium iodide ($50.6\% \pm 1.6$ cell death reduction), while P5-CM had no effect on cell viability (Figures 4(a) and 4(b)). Furthermore, stressed RPE cells rescued by P3-CM were also detected by ethidium bromide and acridine orange staining assay (51.5% cell death reduction from total cell death counted in RPE cells exposed to H_2O_2 only) (Figure 4(c)).

(a)

(b)

(c)
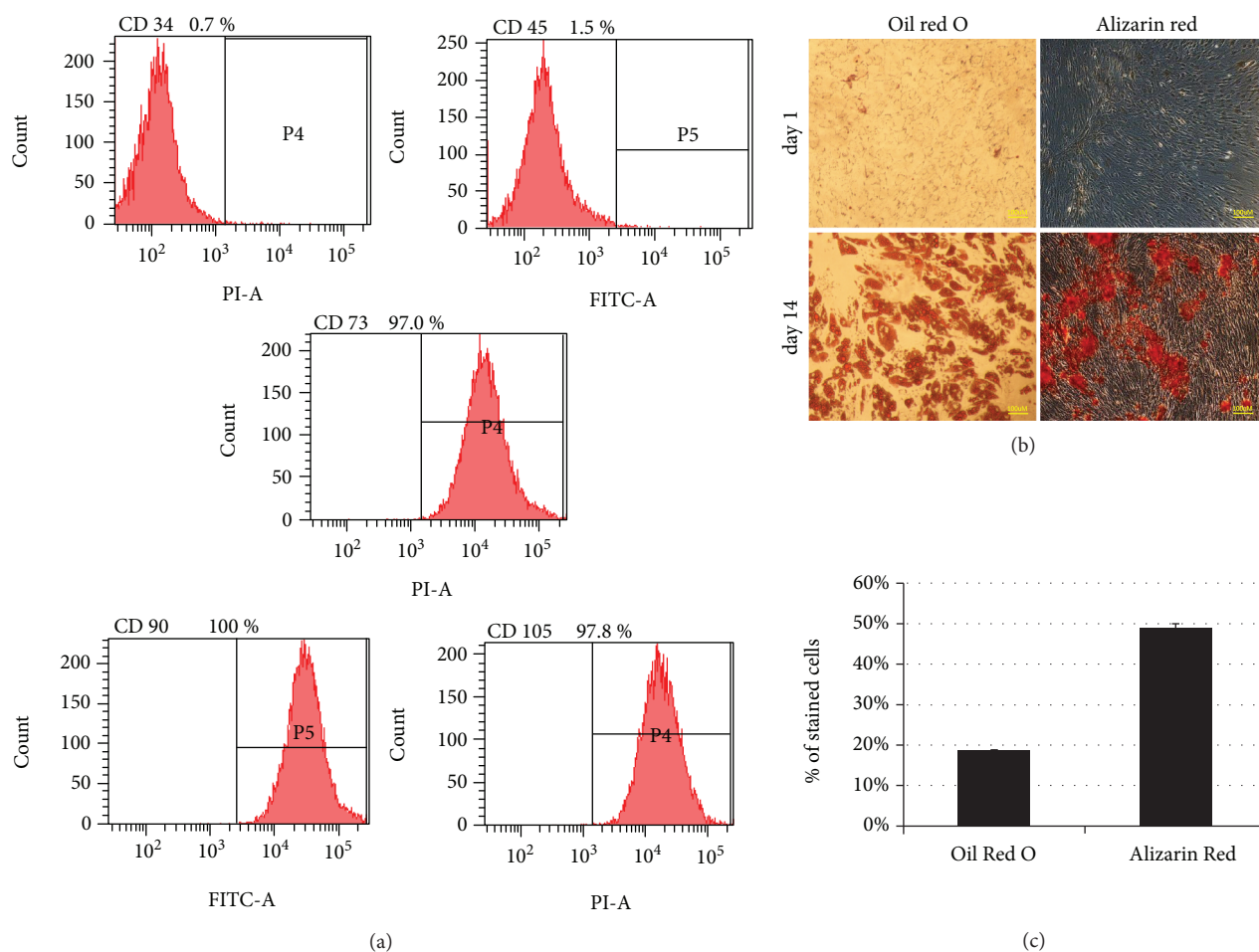
FIGURE 1: Characterization of ASCs by surface phenotype and differentiation potential at passage 3. Cultured ASCs at passage 3 were detached with trypsin, equally dispensed into FACS tubes (1×10^5 cells per tube), and incubated with monoclonal antibodies against human CD34, CD45, CD90, CD73, and CD105. Cells were then analyzed by flow cytometry for the expression of cell surface markers. CD: cluster of differentiation. Each experiment was performed a minimum of 3 samples from 3 different patients. Each experiment was performed a minimum of 3 times.

3.5. Sodium Iodate Induces RPE Damage. To examine the potential of ASCs in repairing damage caused by oxidative stress, adult C57BL mice were injected with sodium iodate (NaIO$_3$), which serves as a model for acute RPE injury and retinal degeneration by inducing oxidative stress [19] and progressive ongoing damage [18] [22]. NaIO$_3$ was injected intraperitoneally and induced damage to the RPE and PR layers in all mice examined, compared to mice that did not receive NaIO$_3$ (data not shown).

3.6. Effect of ASC Treatment on the RPE Layer. The eyes treated with ASCs showed significantly higher levels of RPE65 staining compared to PBS-treated eyes, indicating a protective effect of ASCs from NaIO$_3$-induced damage (Figure 5).

3.7. Effect of ASC Treatment on the PR Layer. NaIO$_3$ injection damages the RPE layer that nourishes the PR layer. The size of the PR layer in the eyes treated with ASCs was larger compared to that in the PBS-treated eyes (Figures 6(a) and 6(b)),

indicating that ASC treatment prevents damage not only to the RPE layer but also to the PR layer.

3.8. Effect of ASC Treatment on ONL Thickness. ONL thickness was positively affected in ASC-treated mice, evident in the preservation of nuclear layers of the ONL in ASC-treated mice when compared to the PBS-treated group (6.94 ± 1.2 ONL layers in PBS-treated mice, 8.4 ± 1.0 ONL layers in ASC-treated mice, p value $= 0.0013$) (Figure 6(c)).

4. Discussion

Oxidative stress has been shown to be one of the cardinal pathogenesis of RPE damage in several retinal degenerative diseases [3, 23], leading to the degeneration of the RPE and subsequently to PR loss [1, 2, 8]. ASC-based regenerative therapy for RPE shows great promise in providing a protective effect from oxidative stress-induced RPE cell death.

In this study, we demonstrated that oxidative stressed RPE-CM promoted ASC migration capacity, possibly by activating the migration associated-SDF-1/CXCR4 axis.

(a)

(b)
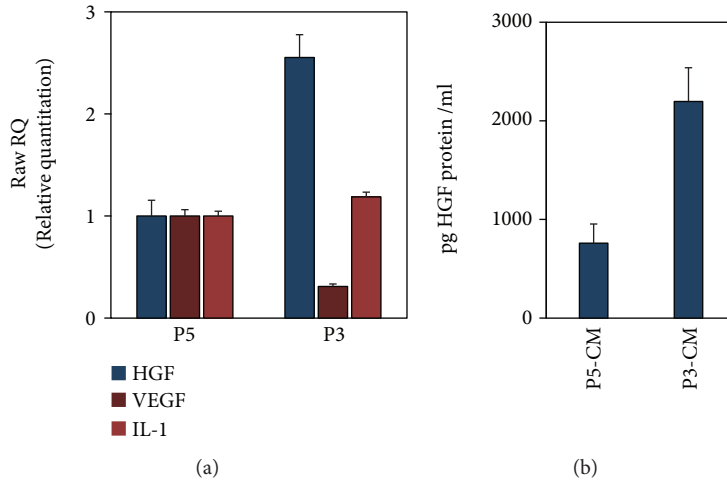
Figure 2: Early passage ASCs overexpress the neurotropic protein HGF but not VEGF nor the proinflammatory cytokine IL-1β. ASCs at passage 3 that were cultured in serum-free conditions for 48 hours were compared to the control group of ASCs at passage 5. Both cells and medium were collected and analyzed at mRNA level and at protein level by qRT-PCR and by ELISA, respectively. (a) qRT-PCR analysis of HGF, VEGF, and IL-1β. (b) ELISA for HGF protein levels. Each experiment was performed a minimum of 3 samples from 3 different patients. Each experiment was performed a minimum of 3 times.

(a)

(b)

(c)

(d)
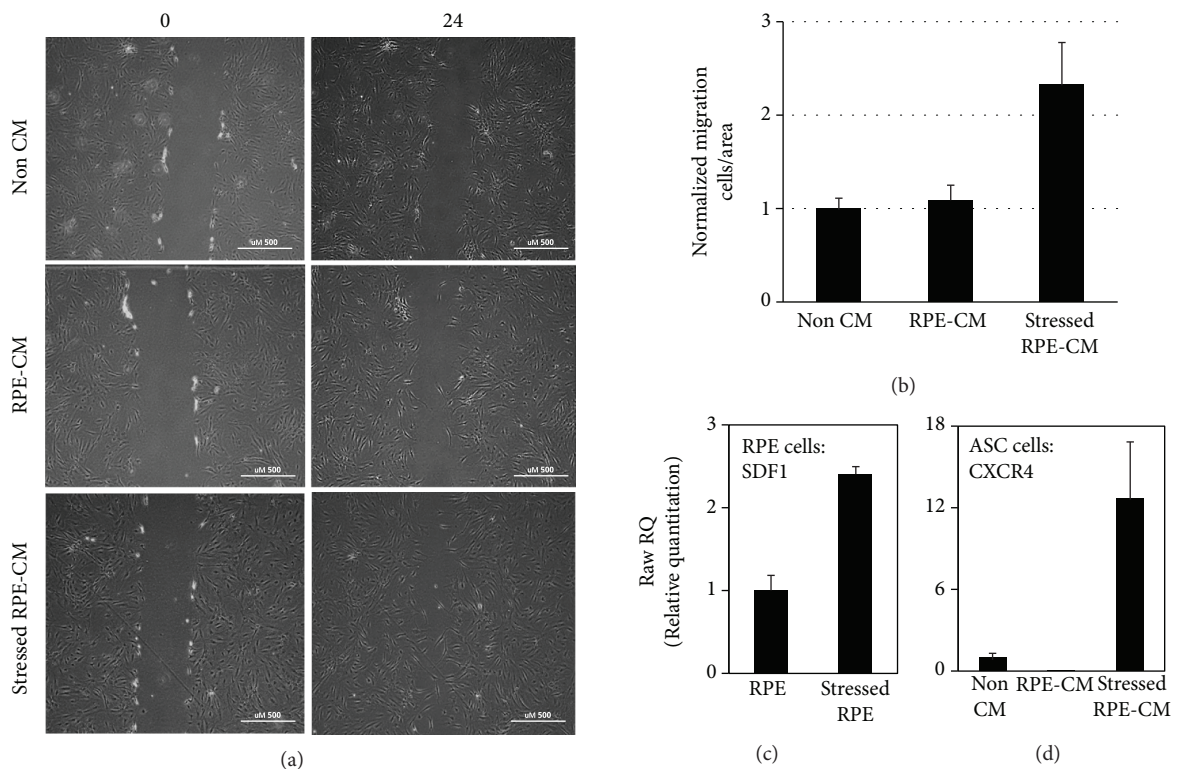
Figure 3: Enhanced migration of ASCs following exposure to stressed RPE-CM corresponds to SDF-1 and CXCR4 upregulation in RPE and ASCs, respectively. The migratory ability of ASCs was studied by scratch assay after exposure to stressed RPE-CM (RPE treated with H_2O_2) or to controls comprising ASCs exposed to RPE-CM (RPE cultured without H_2O_2) and non-CM (nonconditioned ADSC medium). (a) ASCs were monitored at 0 and 24 hours postscratch ($\times$10 magnification). (b) Quantification of ASCs' migration by counting invasive cells in scratch boundaries. All scratch assays were performed in quadruplicates, and images were taken at the beginning of the treatments (time zero) and after 24 h (H_2O_2 treatments). ASCs and RPE cells were harvested and mRNA levels were analyzed using RT-PCR. (c) SDF-1 mRNA in RPE cells incubated with or without H_2O_2. (d) CXCR4 mRNA in ASCs incubated with stressed RPE-CM, RPE-CM, or non-CM. CXCR4: chemokine receptor type 4; SDF-1: stromal cell-derived factor 1; RPE: retinal pigment epithelium; ASCs: adipose-derived stem cells; CM: conditioned medium.

(a)

(b)

(c)
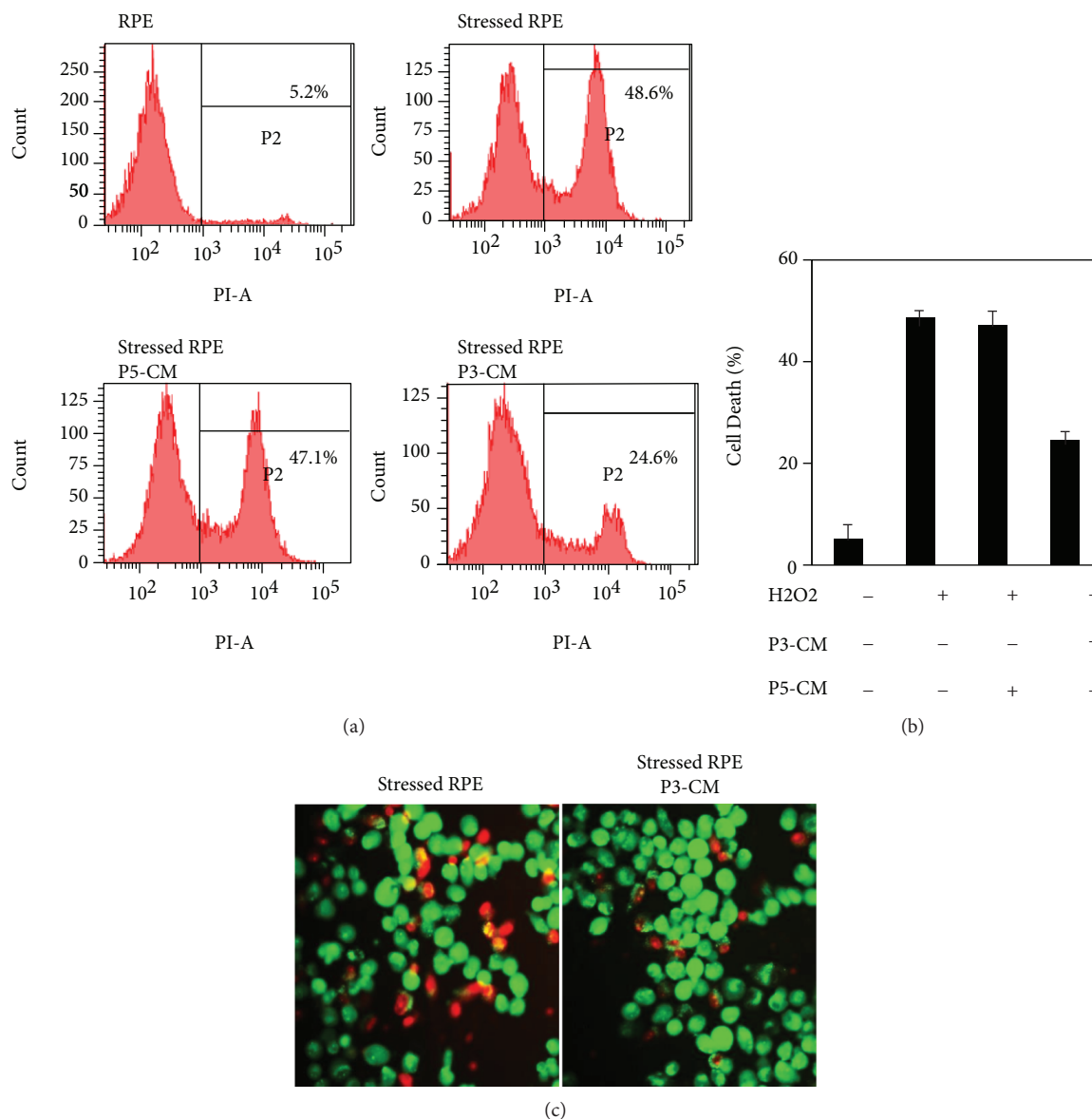
Figure 4: ASCs rescue RPE cell death under oxidative stress. RPE cells were incubated with P3-CM or with controls comprising P5-CM or non-CM for 48 hours, followed by exposure to H_2O_2 (1 mM, 7 h). Cells were harvested and cell death was analyzed. (a, b) Necrotic cell death was determined using PI staining followed by flow cytometry analysis. (c) Cell death visualized by acridine orange and ethidium bromide staining. Live cells appear green stained by acridine orange only (×20 magnification). CM: conditioned medium. Each experiment was performed a minimum of 3 samples from 3 different patients. Each experiment was performed a minimum of 3 times.

We also demonstrated that ASCs were able to prevent primary human RPE cell death caused by oxidative stress induced with H_2O_2. Interestingly, ASC-CM inhibition of RPE cell death was coupled with upregulation of the prosurvival HGF growth factor in RPE cells. Finally, transplantation of ASCs to the subretinal space in $NAIO_3$ mice resulted in the preservation of RPE and photoreceptor layers with mild preservation of the ONL at one week.

SDF-1 is a chemo-attractant known to be involved in the migration and homing of stem cells [24]. Under chronic hypoxia and oxidative stress, MSCs were shown to express the SDF-1 receptor CXCR4 in vivo and in vitro, suggesting that SDF-1 serves as a mediator in the migration and homing of MSCs [14, 24]. This study reports that consequent to incubation of ASCs with stressed RPE-CM, CXCR4 is upregulated in ASCs as a possible response to SDF-1 overexpression in oxidative stressed-RPE cells. However, this study did not examine the direct correlation between an upregulation of SDF-1/CXCR4 expression and ASC migration or the direct effect between the migration in vitro and the protective effect of ASCs seen here in vivo. This enhanced migratory capability of ASCs upon exposure to oxidative stressed RPE-CM could provide the basis for an important future study, examining whether ASCs have a potential of homing to the site of injury once transplanted in vivo.

The retina is highly susceptible to oxidative stress through the increase in reactive oxygen species (ROS) followed by RPE cell death, leading to photoreceptor degradation, which

(a)

(b)
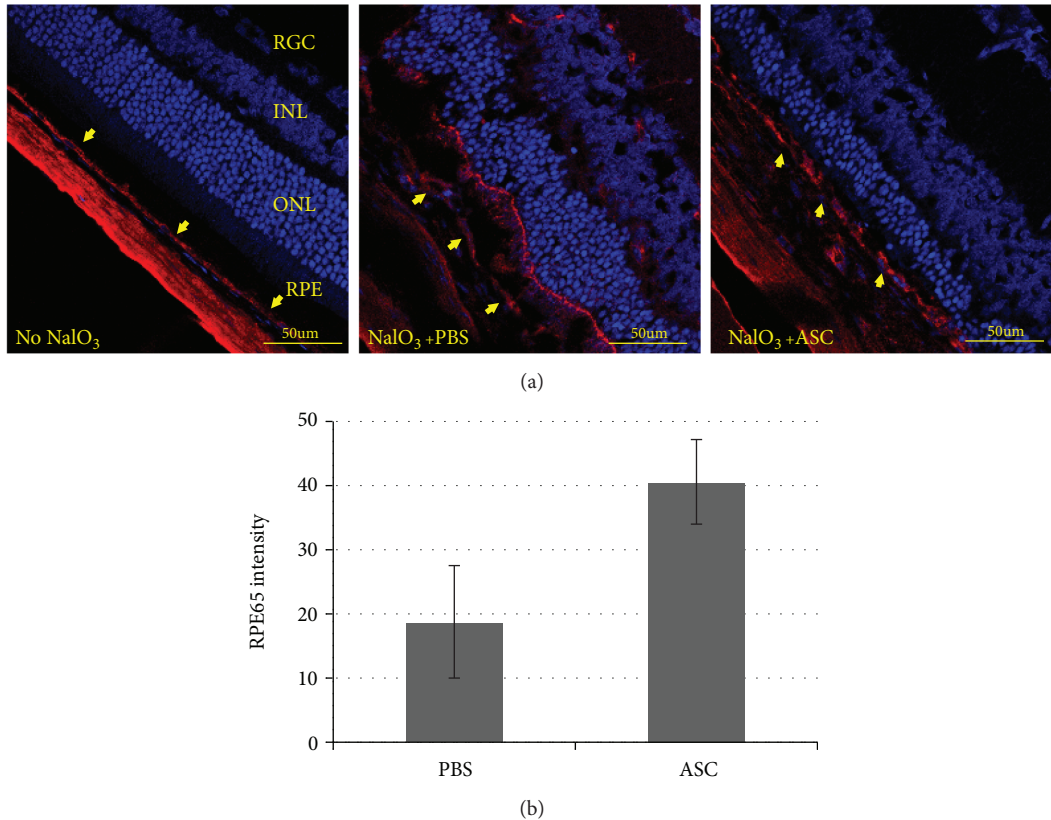
FIGURE 5: Retinal pigment epithelium layer. (a) Retinal slices were stained with RPE65 antibody (red) and the nuclear dye DAPI (blue). (b) RPE65 intensity was quantified by marking the RPE layer and measuring the fluorescence intensity compared to the image's background using ImageJ software. RPE layer staining was stronger in the eyes that received treatment with ASCs (p value = 0.0073). Yellow arrows indicate the RPE layer. Bar = 50 μm. ONL: outer nuclear layer; INL: inner nuclear layer; RGC: retinal ganglion layer. $n = 8$ for each studied group.

construct the pathophysiology of retinal degeneration [23]. Although it is recognized that RPE apoptosis is one of the major events in the pathogenesis of retinal diseases, several reports have demonstrated RPE cell death not only via apoptosis [7] but also necrosis and necroptosis [9, 25]. In the current study, the exposure of RPE to H_2O_2 induced RPE cell death, while preincubation of RPE cells with ASC-conditioned medium reduced remarkably RPE cell death caused specifically by oxidative stress. The ability of ASCs to prevent cell death was also demonstrated by Singh et al. [26]; however, cell death was induced by the proliferation inhibitor, chemotherapeutic drug, Mitomycin C, i.e., via mechanisms different from oxidative stress and using the commercially immortalized cell line ARPE19 which is known to have lost some of the key features of primary RPE [27]. Furthermore, we show that P3 ASCs overexpress the neurotropic growth factor HGF compared to P5 ASCs. HGF is well linked to the MSC regenerative activity [28, 29] and was shown to protect RPE from oxidative stress-induced cell death by various mechanisms [30, 31]. To note, it was reported that HGF correlated with CNV progression in animal laser model of choroidal neovascularization (CNV) [32]; however, clinical data failed to exhibit HGF levels in vitreous of AMD patients [33–35]. Here, we demonstrated that an increase in HGF levels in ASC-CM correlated with ASCs'

rescue of RPE from cell death, as the protective effect was abolished in the control group of ASCs at passage 5 which exhibited low HGF expression accompanied with no rescue effect on RPE. Similarly, the results of our animal experiments, in which we used P3 ASCs, provide further support to the protective, and potentially regenerative, capabilities of ASCs, possibly mediated via secretion of HGF.

Concomitant with HGF overexpression by P3 ASCs, we further demonstrate that P3 ASCs express significantly lower levels of VEGF compared to P5 ASCs. To be noted is that although a CD34+/CD90+ subpopulation of ASCs was shown to express high levels of VEGF [13, 36], ASCs used in this research were spontaneously CD34 negative, in line with low expression level of VEGF. Elevated VEGF secretion is known to contribute to additional deterioration in AMD [37]. Finally, the proinflammatory cytokine IL-1β remained unmodulated between P3 and P5. IL-1β was shown to be a neurotoxic and proinflammatory mediator in the retina [38]. High HGF secretion, accompanied with low or unmodulated VEGF and IL-1β levels, is a highly valued property in in vivo transplantation of ASCs.

Indeed, our mouse model for acute injury to RPE combined with oxidative stress [19, 39] provided further support for ASCs' ability to protect the RPE and PR layers from oxidative stress damage. The stronger staining of RPE65 in the

(a)

(b)

(c)
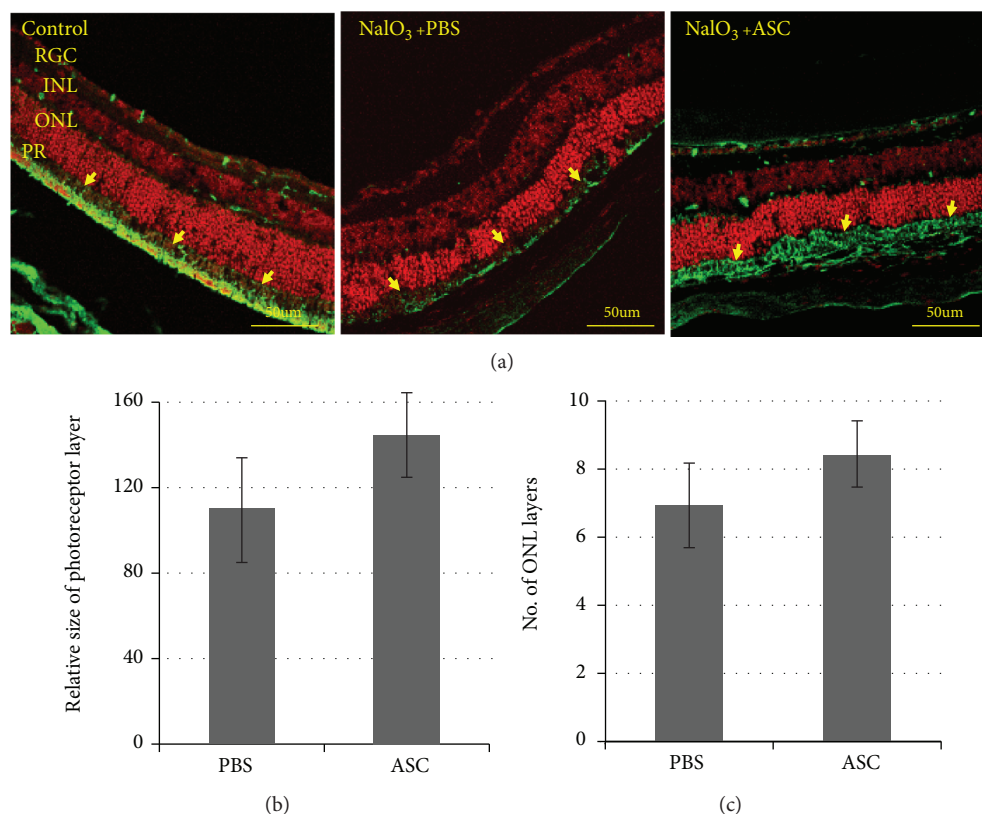
FIGURE 6: Photoreceptor layer size, rhodopsin labeling intensity, and ONL thickness. NaIO$_3$ injection damages the RPE layer that nourishes the photoreceptor layer. Rhodopsin is a light-sensitive protein found in rod cells. (a) Retinal slices were stained with propidium iodide (nuclear dye) and rhodopsin antibody (green). The size of the photoreceptor layer (b) was measured by ImageJ software. The photoreceptor layer in the retinas treated with ASCs was larger compared to that in the PBS-treated retinas (p value = 0.0505). (c) ONL thickness was assessed by counting the number of nuclei rows at different points along the retinal length. ASC-treated eyes had significantly more photoreceptor cells than PBS-treated mice (p value = 0.0013). Bar = 50 μM; yellow arrows indicate the PR layer. PR: photoreceptor layer; ONL: outer nuclear layer; INL: inner nuclear layer; RGC: retinal ganglion layer. $n = 8$ for each studied group.

RPE layer, as well as the larger size of the PR layer, compared to PBS treatment indicates that the damage induced by NaIO$_3$ was significantly reduced in the eyes treated with ASCs. Moreover, the ONL layer thickness was preserved in ASC-treated mice. However, to note, these data relate to a short treatment of 1 week, and the effect seen in RPE, PR, and ONL layers did not translate to a full recovery in retinal morphology to a healthy state. Thus, future study will include observation of the therapeutic effect of ASCs after a longer time *in vivo* as well as the addition of functional studies such as ERG recordings and fundus photographs to better characterize the protective effect shown here.

Thus, taken together, our results demonstrate the potential of ASCs in treating stressed RPE by acting in two distinct manners, one by protecting the RPE cells from oxidative stress damage and the other by preventing further damage, possibly via their regenerative capabilities, as indicated in our animal experimentation. Combined with the increase in ASCs' migration *in vitro* in response to stressed RPE medium, ASCs hold great promise as a potential therapeutic approach to treat retinal pathologies in which RPE cells suffer an oxidative stress and cell death, eventually allowing millions of people worldwide to maintain their eyesight.

Data Availability

The entire data used to support the findings of this study are included within the article.

Conflicts of Interest

The authors have no conflicts of interest to declare.

Acknowledgments

Supplementary Materials

Table S1: primers used in quantitative RT-PCR experiments. *(Supplementary Materials)*

References

[1] N. G. Bazan, "Cell survival matters: docosahexaenoic acid signaling, neuroprotection and photoreceptors," *Trends in Neurosciences*, vol. 29, no. 5, pp. 263–271, 2006.

[2] J. S. L. Tan, J. J. Wang, V. Flood, E. Rochtchina, W. Smith, and P. Mitchell, "Dietary antioxidants and the long-term incidence of age-related macular degeneration: the Blue Mountains Eye Study," *Ophthalmology*, vol. 115, no. 2, pp. 334–341, 2008.

[3] T. Masuda, M. Shimazawa, and H. Hara, "Retinal diseases associated with oxidative stress and the effects of a free radical scavenger (edaravone)," *Oxidative Medicine and Cellular Longevity*, vol. 2017, Article ID 9208489, 14 pages, 2017.

[4] N. G. Bazan, J. M. Calandria, and C. N. Serhan, "Rescue and repair during photoreceptor cell renewal mediated by docosahexaenoic acid-derived neuroprotectin D1," *Journal of Lipid Research*, vol. 51, no. 8, pp. 2018–2031, 2010.

[5] S. E. G. Nilsson, S. P. Sundelin, U. Wihlmark, and U. T. Brunk, "Aging of cultured retinal pigment epithelial cells: oxidative reactions, lipofuscin formation and blue light damage," *Documenta Ophthalmologica*, vol. 106, no. 1, pp. 13–16, 2003.

[6] F. Q. Liang and B. F. Godley, "Oxidative stress-induced mitochondrial DNA damage in human retinal pigment epithelial cells: a possible mechanism for RPE aging and age-related macular degeneration," *Experimental Eye Research*, vol. 76, no. 4, pp. 397–403, 2003.

[7] J. L. Dunaief, T. Dentchev, G. S. Ying, and A. H. Milam, "The role of apoptosis in age-related macular degeneration," *Archives of Ophthalmology*, vol. 120, no. 11, pp. 1435–1442, 2002.

[8] Y. Wang, D. Shen, V. M. Wang et al., "Enhanced apoptosis in retinal pigment epithelium under inflammatory stimuli and oxidative stress," *Apoptosis*, vol. 17, no. 11, pp. 1144–1155, 2012.

[9] J. Hanus, H. Zhang, Z. Wang, Q. Liu, Q. Zhou, and S. Wang, "Induction of necrotic cell death by oxidative stress in retinal pigment epithelial cells," *Cell Death & Disease*, vol. 4, no. 12, p. e965, 2013.

[10] A. Barzelay, R. Levy, E. Kohn et al., "Power-assisted liposuction versus tissue resection for the isolation of adipose tissue-derived mesenchymal stem cells: phenotype, senescence, and multipotency at advanced passages," *Aesthetic Surgery Journal*, vol. 35, no. 7, pp. NP230–NP240, 2015.

[11] W. Tsuji, J. P. Rubin, and K. G. Marra, "Adipose-derived stem cells: implications in tissue regeneration," *World Journal of Stem Cells*, vol. 6, no. 3, pp. 312–321, 2014.

[12] S. Ghannam, C. Bouffi, F. Djouad, C. Jorgensen, and D. Noel, "Immunosuppression by mesenchymal stem cells: mechanisms and clinical applications," *Stem Cell Research & Therapy*, vol. 1, no. 1, p. 2, 2010.

[13] G. A. Ferraro, F. De Francesco, G. Nicoletti et al., "Human adipose CD34+ CD90+ stem cells and collagen scaffold constructs grafted in vivo fabricate loose connective and adipose tissues," *Journal of Cellular Biochemistry*, vol. 114, no. 5, pp. 1039–1049, 2013.

[14] G. Y. Rochefort, B. Delorme, A. Lopez et al., "Multipotential mesenchymal stem cells are mobilized into peripheral blood by hypoxia," *Stem Cells*, vol. 24, no. 10, pp. 2202–2208, 2006.

[15] P. A. Zuk, M. Zhu, H. Mizuno et al., "Multilineage cells from human adipose tissue: implications for cell-based therapies," *Tissue Engineering*, vol. 7, no. 2, pp. 211–228, 2001.

[16] V. Morad, M. Pevsner-Fischer, S. Barnees et al., "The myelopoietic supportive capacity of mesenchymal stromal cells is uncoupled from multipotency and is influenced by lineage determination and interference with glycosylation," *Stem Cells*, vol. 26, no. 9, pp. 2275–2286, 2008.

[17] C. C. Liang, A. Y. Park, and J. L. Guan, "In vitro scratch assay: a convenient and inexpensive method for analysis of cell migration in vitro," *Nature Protocols*, vol. 2, no. 2, pp. 329–333, 2007.

[18] M. Moriguchi, S. Nakamura, Y. Inoue et al., "Irreversible photoreceptors and RPE cells damage by intravenous sodium iodate in mice is related to macrophage accumulation," *Investigative Opthalmology & Visual Science*, vol. 59, no. 8, pp. 3476–3487, 2018.

[19] B. A. Berkowitz, R. H. Podolsky, J. Lenning et al., "Sodium iodate produces a strain-dependent retinal oxidative stress response measured in vivo using QUEST MRI," *Investigative Opthalmology & Visual Science*, vol. 58, no. 7, pp. 3286–3293, 2017.

[20] J. Sun, M. Mandai, H. Kamao et al., "Protective effects of human iPS-derived retinal pigmented epithelial cells in comparison with human mesenchymal stromal cells and human neural stem cells on the degenerating retina in rd1 mice," *Stem Cells*, vol. 33, no. 5, pp. 1543–1553, 2015.

[21] H. Song, C. Vijayasarathy, Y. Zeng et al., "NADPH oxidase contributes to photoreceptor degeneration in constitutively active RAC1 mice," *Investigative Opthalmology & Visual Science*, vol. 57, no. 6, pp. 2864–2875, 2016.

[22] R. Kannan and D. R. Hinton, "Sodium iodate induced retinal degeneration: new insights from an old model," *Neural Regeneration Research*, vol. 9, no. 23, pp. 2044-2045, 2014.

[23] H. Mao, S. J. Seo, M. R. Biswal et al., "Mitochondrial oxidative stress in the retinal pigment epithelium leads to localized retinal degeneration," *Investigative Opthalmology & Visual Science*, vol. 55, no. 7, pp. 4613–4627, 2014.

[24] S. Li, Y. Deng, J. Feng, and W. Ye, "Oxidative preconditioning promotes bone marrow mesenchymal stem cells migration and prevents apoptosis," *Cell Biology International*, vol. 33, no. 3, pp. 411–418, 2009.

[25] J. Hanus, C. Anderson, and S. Wang, "RPE necroptosis in response to oxidative stress and in AMD," *Ageing Research Reviews*, vol. 24, no. Part B, pp. 286–298, 2015.

[26] A. K. Singh, G. K. Srivastava, M. T. Garcia-Gutierrez, and J. C. Pastor, "Adipose derived mesenchymal stem cells partially rescue mitomycin C treated ARPE19 cells from death in co-culture condition," *Histology and Histopathology*, vol. 28, no. 12, pp. 1577–1583, 2013.

[27] C. S. Alge, S. M. Hauck, S. G. Priglinger, A. Kampik, and M. Ueffing, "Differential protein profiling of primary versus immortalized human RPE cells identifies expression patterns associated with cytoskeletal remodeling and cell survival," *Journal of Proteome Research*, vol. 5, no. 4, pp. 862–878, 2006.

[28] S. Neuss, E. Becher, M. Woltje, L. Tietze, and W. Jahnen-Dechent, "Functional expression of HGF and HGF receptor/c-met in adult human mesenchymal stem cells suggests a role in cell

mobilization, tissue repair, and wound healing," *Stem Cells*, vol. 22, no. 3, pp. 405–414, 2004.

[29] L. Bai, D. P. Lennon, A. I. Caplan et al., "Hepatocyte growth factor mediates mesenchymal stem cell-induced recovery in multiple sclerosis models," *Nature Neuroscience*, vol. 15, no. 6, pp. 862–870, 2012.

[30] M. Jin, J. Yaung, R. Kannan, S. He, S. J. Ryan, and D. R. Hinton, "Hepatocyte growth factor protects RPE cells from apoptosis induced by glutathione depletion," *Investigative Opthalmology & Visual Science*, vol. 46, no. 11, pp. 4311–4319, 2005.

[31] R. Kannan, M. Jin, M. A. Gamulescu, and D. R. Hinton, "Ceramide-induced apoptosis: role of catalase and hepatocyte growth factor," *Free Radical Biology and Medicine*, vol. 37, no. 2, pp. 166–175, 2004.

[32] W. Hu, M. H. Criswell, S. L. Fong et al., "Differences in the temporal expression of regulatory growth factors during choroidal neovascular development," *Experimental Eye Research*, vol. 88, no. 1, pp. 79–91, 2009.

[33] E. J. Duh, H. S. Yang, J. A. Haller et al., "Vitreous levels of pigment epithelium-derived factor and vascular endothelial growth factor: implications for ocular angiogenesis," *American Journal of Ophthalmology*, vol. 137, no. 4, pp. 668–674, 2004.

[34] M. Funk, D. Karl, M. Georgopoulos et al., "Neovascular age-related macular degeneration: intraocular cytokines and growth factors and the influence of therapy with ranibizumab," *Ophthalmology*, vol. 116, no. 12, pp. 2393–2399, 2009.

[35] Y. Y. Tsai, J. M. Lin, L. Wan et al., "Interleukin gene polymorphisms in age-related macular degeneration," *Investigative Opthalmology & Visual Science*, vol. 49, no. 2, pp. 693–698, 2008.

[36] F. De Francesco, V. Tirino, V. Desiderio et al., "Human CD34/CD90 ASCs are capable of growing as sphere clusters, producing high levels of VEGF and forming capillaries," *PLoS One*, vol. 4, no. 8, article e6537, 2009.

[37] J. L. Kovach, S. G. Schwartz, H. W. Flynn, and I. U. Scott, "Anti-VEGF treatment strategies for wet AMD," *Journal of Ophthalmology*, vol. 2012, p. 7, 2012.

[38] H. Oh, H. Takagi, C. Takagi et al., "The potential angiogenic role of macrophages in the formation of choroidal neovascular membranes," *Investigative Ophthalmology & Visual Science*, vol. 40, no. 9, pp. 1891–1898, 1999.

[39] Y. Yang, T. K. Ng, C. Ye et al., "Assessing sodium iodate-induced outer retinal changes in rats using confocal scanning laser ophthalmoscopy and optical coherence tomography," *Investigative Opthalmology & Visual Science*, vol. 55, no. 3, p. 1696, 2014.

Review Article

Mesenchymal Stem Cell Therapy for Ischemic Tissues

Kar Wey Yong [iD],[1,2] **Jane Ru Choi** [iD],[3,4] **Mehdi Mohammadi,**[2,5] **Alim P. Mitha,**[6]
Amir Sanati-Nezhad,[2,7] **and Arindom Sen** [iD][1,7]

[1]*Pharmaceutical Production Research Facility, Department of Chemical and Petroleum Engineering, Schulich School of Engineering, University of Calgary, 2500 University Drive NW, Calgary, AB, T2N 1N4, Canada*
[2]*BioMEMS and Bioinspired Microfluidic Laboratory, Department of Mechanical and Manufacturing Engineering, Schulich School of Engineering, University of Calgary, 2500 University Drive NW, Calgary, AB, T2N 1N4, Canada*
[3]*Department of Mechanical Engineering, University of British Columbia, 2054-6250 Applied Science Lane, Vancouver, BC, V6T 1Z4, Canada*
[4]*Centre for Blood Research, Life Sciences Centre, University of British Columbia, 2350 Health Sciences Mall, Vancouver, BC, V6T 1Z3, Canada*
[5]*Department of Biological Sciences, University of Calgary, 2500 University Drive NW, Calgary, AB, T2N 1N4, Canada*
[6]*Department of Clinical Neurosciences, Foothills Medical Centre, University of Calgary, 3330 Hospital Drive NW, Calgary, AB, T2N 4N1, Canada*
[7]*Center of Bioengineering Research and Education, Schulich School of Engineering, University of Calgary, 2500 University Drive NW, Calgary, AB, T2N 1N4, Canada*

Correspondence should be addressed to Arindom Sen; asen@ucalgary.ca

Ischemic diseases such as myocardial infarction, ischemic stroke, and critical limb ischemia are immense public health challenges. Current pharmacotherapy and surgical approaches are insufficient to completely heal ischemic diseases and are associated with a considerable risk of adverse effects. Alternatively, human mesenchymal stem cells (hMSCs) have been shown to exhibit immunomodulation, angiogenesis, and paracrine secretion of bioactive factors that can attenuate inflammation and promote tissue regeneration, making them a promising cell source for ischemic disease therapy. This review summarizes the pathogenesis of ischemic diseases, discusses the potential therapeutic effects and mechanisms of hMSCs for these diseases, and provides an overview of challenges of using hMSCs clinically for treating ischemic diseases.

1. Introduction

Ischemic diseases are usually characterized as a reduced blood flow to a tissue or organ due to undesirable vascular conditions, such as blood vessel stenosis or aneurysm rupture [1]. Myocardial infarction, ischemic stroke, and critical limb ischemia are the three most common ischemic diseases [2]. Reperfusion therapy (pharmaceutical or surgical approach) is typically used to counteract these diseases. The clinical administration of pharmaceuticals, such as thrombolytic agents (e.g., recombinant tissue plasminogen activator or streptokinase) and anti-inflammatory agents (e.g., statins),

is a common approach to treat the symptoms of these diseases [3, 4]. However, the systemic administration of such agents can cause a host of undesirable side effects [5]. Surgical interventions are also commonly used (e.g., stent placement to block stenotic arteries) [6]. Surgical approaches also suffer from several disadvantages: surgery always has an associated risk, disease sites may be difficult to manually access, and certain conditions are prone to recurrence (e.g., restenosis of vessels). Thereby, surgical approaches need long-term mentoring and repeated surgical procedures [7]. Although both the pharmacotherapy and surgical approaches may restore the functions of arteries,
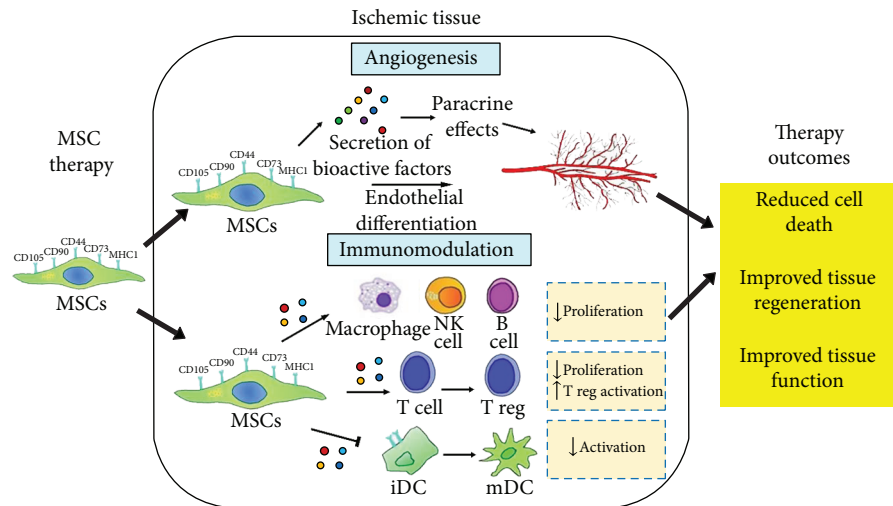
Figure 1: Main mechanisms of human mesenchymal stem cells (hMSCs) in the treatment of ischemic tissue. hMSCs repair ischemic tissues and restore the tissue function via angiogenesis and immunomodulation. NK: natural killer; reg: regulatory; iDC: immature dendritic cell; mDC: mature dendritic cell. This image is adapted from [12] published under the Creative Common Attribution License.

they cannot promote regeneration and functional recovery of the surrounding tissues affected by ischemia. Thus, alternative approaches are required.

Human mesenchymal stem cells (hMSCs) can be isolated from various locations of the human body, e.g., bone marrow, adipose, and umbilical cord [8, 9]. They are capable of secreting bioactive factors for immunomodulation and angiogenesis, which can help to promote tissue repair and regeneration [10–12]. It has been shown that hMSCs may suppress the activation and functions of leukocytes actively involved in atherosclerosis, indicating their great potential in repairing injured blood vessels for the prevention of tissue ischemia [13]. If the injured blood vessel is beyond repair, hMSCs can secrete angiogenic factors (especially vascular endothelial growth factor (VEGF)) and differentiate into endothelial cells for inducing angiogenesis in ischemic regions and promote regeneration and functional recovery of injured tissues [10, 14]. In addition, protocols to expand hMSCs in culture to clinically significant levels have been reported in both the presence and absence of animal serum [15, 16]. With such fascinating properties, hMSCs can be potentially used for clinical applications in vessel repair and ischemic diseases and may be able to successfully treat ischemic tissues (Figure 1). To date, positive outcomes have been demonstrated for the treatment utility of hMSCs in preclinical trials using animal models of ischemic diseases [17–19]. Although preclinical trials have contributed much to our understanding of the pathophysiological and therapeutic mechanisms of various diseases, translation of these results to clinical trials have remained controversial [20]. There remains a lack of published clinical trials revealing the therapeutic effectiveness of hMSCs in ischemic diseases, such as myocardial infarction, ischemic stroke, and critical limb ischemia, as most of the ongoing clinical trials still remain at phase 1 for safety evaluation (http://www .clinicaltrials.gov). Both evaluation of safety (phase 1) and

therapeutic efficacy (phase 2) are time-consuming due to the lack of a suitable human *in vitro* ischemic disease model for assessing the safety and effectiveness of stem cell therapy from different aspects of cell dosage, cell source, and cell administration methods and timing prior to clinical trials.

There exist several review articles focused on stem cell-based therapy for stroke [21], peripheral arterial diseases [22], and cardiovascular diseases [23]. In view of the rising demand for the use of hMSCs in ischemic disease therapy, there is a strong need for a timely review on therapeutic mechanisms of hMSCs in ischemic diseases and challenges in translating hMSCs to ischemic tissue-related clinical applications. In this review, the pathogenesis of ischemic diseases is first summarized. The potential therapeutic effects and mechanisms of hMSCs in treating myocardial infarction, ischemic stroke, and critical limb ischemia are highlighted. Lastly, the challenges associated with the future translation of hMSCs to the clinical settings in ischemic diseases are briefly discussed.

2. Understanding Pathogenesis of Ischemic Diseases for hMSC Therapy

Most ischemic diseases are caused by atherosclerosis, which is a chronic arterial inflammatory disease resulted from many risk factors, including hypertension, hypercholesterolemia, smoking, diabetes, and aging [24, 25]. Atherosclerosis is associated with pathologic injury and dysregulation of the endothelial cells lining the luminal wall of arteries, accumulation of lipids, smooth muscle cells, leukocytes, "foam cells", and aggregated platelets at the arterial luminal wall, resulting in plaque formation [26–28]. Both macrophages and platelets actively secrete matrix metalloproteinases (MMPs) to induce degradation of the collagenous extracellular matrix (ECM) of a blood vessel [29, 30]. To counterbalance the MMP-mediated degradation of ECM, smooth muscle cells migrate

from the outer layers of the arterial wall (tunica media and adventitia) to the tunica intima to increase the collagen production rate [31]. However, it often results in undesirable remodeling as macrophages secrete cytokines (e.g., tumor necrosis factor (TNF)-α, interleukin (IL)-6, and IL-1β) to induce apoptosis of smooth muscle cells [32]. Failure of collagen production rate to offset the ECM degradation rate results in the formation of atheromatous plaques with a thin fibrous collagenous cap [33]. At this stage, transplantation of hMSCs may suppress the functions of immune cells (MMP activity and secretion of proinflammatory cytokines) and restore collagen homeostasis, suggesting that hMSCs could be explored to treat atherosclerosis for the prevention of tissue ischemia [34].

Due to high shear stress in response to hemodynamic alteration, ruptures may easily develop in atheromatous plaques, causing bleeding which results in more recruitment of platelets and triggering of a cascade of coagulation events that leads to thrombus formation [35]. This in turn can cause stenosis of arteries, resulting in the reduction of anterograde blood flow and subsequently ischemic damage to downstream tissues [35]. For example, myocardial infarction and ischemic stroke are ischemic diseases caused by the stenosis of coronary arteries and cerebral arteries, respectively, which cause high rates of morbidity and mortality in patients [36]. Owing to the ability of hMSCs to secrete angiogenin factors and undergo endothelial differentiation, hMSCs may promote angiogenesis to restore blood flow to the ischemic tissues for tissue regeneration and functional recovery [37].

3. Potential Therapeutic Effects and Mechanisms of hMSCs in Ischemic Diseases

3.1. Myocardial Infarction. Myocardial infarction occurs upon partial or complete blockage of coronary arteries in the heart, leading to ischemia and possibly death of cardiac tissues supplied by those arteries [38]. Preclinical trials of myocardial infarction induced by coronary artery occlusion in animals have shown that hMSCs can induce angiogenesis and promote regeneration and functional recovery of the ischemic heart tissues. Local transplantation of hMSCs in animal models has been effective in inducing angiogenesis by differentiating into endothelial cells to form new blood vessels at the border zone of infarcted cardiomyocytes. These cells have shown the expression of endothelial markers CD31, CD34, CD36, Egr-3, vWf, and VEGF receptor [37, 39]. The *in vivo* differentiation of hMSCs to endothelial cells is particularly efficient when they are administered as a three-dimensional spherical cell mass (3DCM) composed of cells within a substrate containing basic fibroblast growth factor (bFGF). In fact, bFGF enhances 3D clustering of hMSCs. The cell aggregates not only support survival or persistence of hMSCs in the host but also are capable of trapping hMSC-secreted VEGF for further inducing their endothelial differentiation via the Rho/myocardin-related transcription factor-A signaling pathway [37, 40]. In addition, hMSCs may augment endogenous neovascularization through paracrine secretion of soluble factors (e.g., VEGF and bFGF) or extracellular vesicles containing proteins (e.g., platelet-derived growth factor receptor) and microRNAs that contribute to angiogenic activity [17, 41–44]. To improve the angiogenic properties (endothelial differentiation and angiogenic factor secretion), hMSCs can be genetically modified by overexpressing granulocyte chemotactic protein 2 (GCP-2), angiopoietin-1 (Ang-1), or hepatocyte growth factor to enhance their therapeutic effects on myocardial infarction [45–47]. Moreover, hMSCs may activate endogenous cardiac stem cells for myocardial regeneration through the paracrine mechanisms or direct cell-to-cell contact with cardiac stem cells [41, 48]. Combination cell therapy of hMSCs and human cardiac stem cells was more effective in reducing myocardial infarct size as compared to using either cell therapy alone [49].

On the other hand, it has been suggested that hMSCs may provide myocardial protection by suppressing inflammation within the ischemic cardiac tissue through their potent immunomodulatory capabilities [50]. hMSCs were found to promote M2 monocyte polarization (a conversion process from cardiotoxic M1 monocytes to anti-inflammatory and cardioprotective M2 monocytes) by enhancing expression of CD73 on monocytes. These CD73$^+$ monocytes produce adenosine (a strong anti-inflammatory purine nucleoside) that is capable of inhibiting activation of other immune cells [51, 52]. Evidence has demonstrated that transplanted MSCs promote CD73 expression on host macrophages in the animal models of myocardial infarction [52].

Recently, cardiac adipose tissue has been identified as a novel source of MSCs. Unlike other MSCs, they possess cardiac-like and endothelial phenotypes that may greatly enhance their therapeutic potential in myocardial infarction [53]. Interestingly, it was found that transplanted cardiac adipose-derived MSCs are superior to MSCs derived from bone marrow and subcutaneous adipose tissues in the reduction of myocardial infarct size in the animal models of myocardial infarction under similar experimental conditions [54]. Like other hMSCs, cardiac adipose-derived MSCs repair infarcted myocardial tissues by promoting endogenous neovascularization through paracrine mechanisms or endothelial differentiation [53]. Evidence has shown that cardiac adipose-derived hMSCs are more effective than those isolated from subcutaneous adipose tissues in terms of inducing neovascularization [55]. Since cardiac cells are constantly subjected to electrical and mechanical signals, electromechanically stimulated cardiac adipose-derived hMSCs could be a promising therapeutic strategy for myocardial infarction [56].

Taken together, following a successful reperfusion therapy, transplantation of hMSCs may restore blood flow to the ischemic heart, reduce infarct size, and restore the left heart ventricular function through angiogenesis, myocardial protection, and regeneration (Figure 2). To date, several published clinical trials of myocardial infarction have revealed that transplanted hMSCs reduce the infarct size, improve the heart contractility, or improve the left ventricular ejection fraction with a low risk of adverse effects [57]. The clinical trial database (http://www.clinicaltrials.gov) demonstrates 33 ongoing registered clinical trials of hMSCs at phase 1 or phase 2 for myocardial infarction.
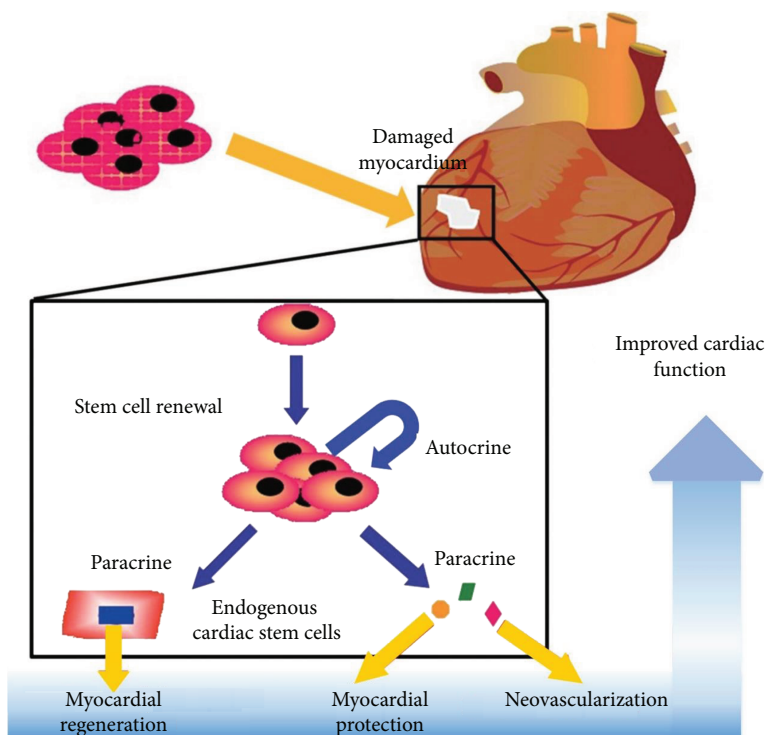
FIGURE 2: Implantation of hMSCs may repair damaged myocardium via the paracrine mechanisms. hMSCs can secrete various angiogenic factors to support neovascularization, myocardial protection, and regeneration, leading to improved cardiac function in myocardial infarction models. This image is adapted from [108] published under the Creative Common Attribution License.

3.2. Ischemic Stroke. Ischemic stroke is one of the leading causes of human mortality and morbidity (e.g., permanent neurological disability) worldwide. It is resulted from occlusion of the artery supplying the blood to the brain due to embolus or thrombus, leading to loss of neural cells and disruption of brain function [21, 58]. Preclinical trials of ischemic stroke using animal models of cerebral artery occlusion have shown that implanted hMSCs may trigger angiogenesis, which in turn can enhance neurogenesis and neurological functional recovery. Implantation of hMSCs has been demonstrated to induce angiogenesis at the border zone of ischemic neural tissues through the paracrine mechanisms. In overall, hMSCs were found to secrete various angiogenic factors, including VEGF and Ang-1, to promote endogenous neovascularization [18, 59, 60]. Upon deprivation of oxygen and glucose, neurons release γ-secretase, a protease which upregulates the expression of key Notch-1 signaling components in hMSCs, such as Notch-1, Notch-1 intercellular domain, and Hes-1, resulting in activation of Notch-1 signaling. This signaling enhances the expression of hypoxia-inducible factor (HIF)-1α and increases the secretion of VEGF from hMSCs [59]. In addition, Hes-1 may inhibit the activity of phosphatase and tension homolog (PTEN) and thus further upregulating the secretion of VEGF [61]. Ang-1 released by hMSCs stabilizes the new blood vessels formed in response to VEGF by inducing vessel sprouting and branching. These vessels become resistant to leak and damage by inflammatory cells and soluble factors [60].

Besides VEGF and Ang-1, in response to HIF-1α, hMSCs secrete neurotrophic factors (e.g., glial-derived neurotrophic factor and brain-derived neurotrophic factor) to support survival and proliferation of endogenous neural progenitor cells and subsequently mediate their differentiation into mature neurons or glial cells [62, 63]. Moreover, hMSCs may secrete platelet-derived growth factor (PDGF) to promote M2 macrophage polarization (a conversion process from neurotoxic M1 macrophage to anti-inflammatory and neuroprotective M2 macrophage) for neurovascular and neuronal remodeling [13]. PDGF may also induce proliferation of vascular smooth muscle cells for arteriogenesis [13]. In short, hMSCs may secrete various soluble factors to promote endogenous angiogenesis for restoring blood to the brain, support endogenous neurogenesis, and restore the neurological functions (as indicated by the improved motor function, coordination, and reflex response) (Figure 3). To date, several published clinical trials of ischemic stroke have shown that transplantation of hMSCs into patients with successful reperfusion therapy reduce the stroke lesion volume and promote the neurological functional recovery. This success is indicated by improvement in the human functional behavioral and sensorimotor assessments, such as modified Rankin scale score, Barthel index, Fugl-Meyer scale, European stroke scale, and National Institutes of Health Stroke Scale [64, 65]. The clinical trial database (http://www.clinicaltrials.gov) demonstrates 15 ongoing registered clinical trials of hMSCs at phase 1 or phase 2 for ischemic stroke.
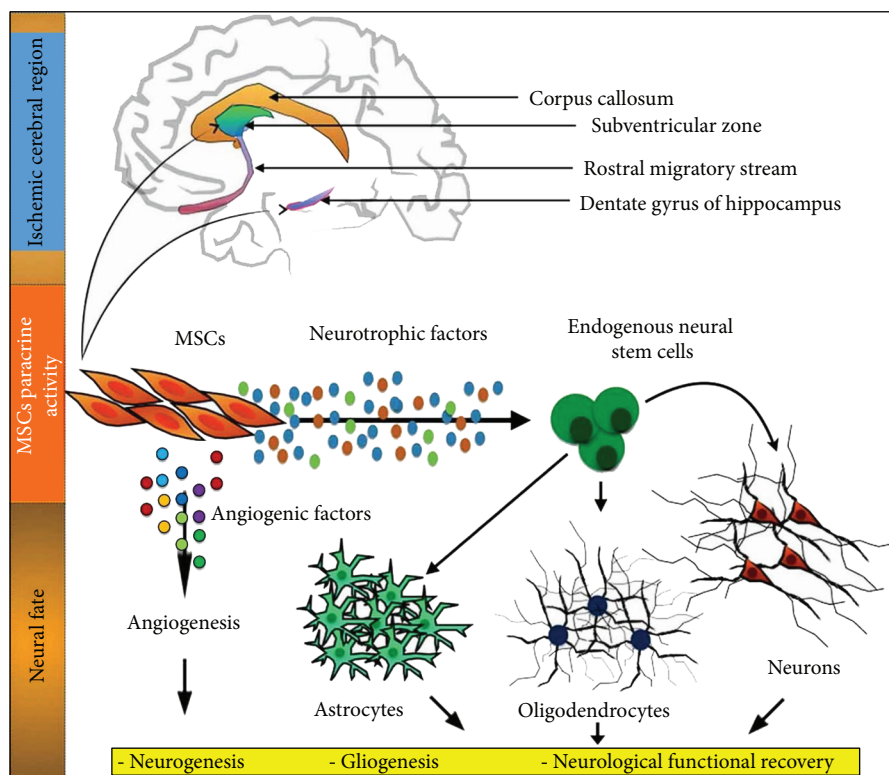
Figure 3: Implantation of hMSCs may repair damaged neural cells induced by stroke through the paracrine mechanisms. hMSCs can secrete various angiogenic and neurotrophic factors to support endogenous angiogenesis, neurogenesis, and gliogenesis, leading to improved neurological function in ischemic stroke models. This image is adapted from [109] published under the Creative Common Attribution License.

3.3. Critical Limb Ischemia. Critical limb ischemia is an obstruction of the arteries that reduces blood flow to the limbs, leading to permanent disability and eventually, limb loss [66]. Preclinical trials of critical limb ischemia using the animal models of hindlimb ischemia have demonstrated that hMSCs may induce angiogenesis and rescue the ischemic hindlimbs. For instance, transplanted hMSCs were found to undergo *in vivo* differentiation into endothelial cells, as indicated by the presence of human endothelial markers, such as CD31, CD34, vascular endothelial cadherin, endothelial nitric oxide synthase and vWf, and the formation of new blood vessels [67, 68]. It was shown that hindlimb ischemia models treated with hMSCs isolated from adipose tissues have a better recovery of blood flow and higher limb salvage rate than those treated with hMSCs derived from bone marrow [69]. It was found that hMSCs isolated from adipose tissues express a high level of MMP-3 and MMP-9, which may increase the release of VEGF, enabling hMSCs to efficiently differentiate into endothelial cells [69]. Further improvement of the limb salvage rate was observed in the ischemic hindlimb models treated with 3DCM composed of hMSCs on a substrate with immobilized bFGF [68]. Hypoxic conditioning and genetic modification of hMSCs can further increase the secretion of angiogenic factors, such as VEGF, bFGF, PDGF, and Ang-1, resulting in an enhanced angiogenesis and recovery of blood flow to the ischemic hindlimbs [19, 70–72]. Collectively, hMSCs may restore blood flow to the ischemic hindlimb and thus, prevent limb loss via

endothelial differentiation and paracrine mechanisms. To date, several published clinical trials of critical limb ischemia have shown that transplantation of hMSCs into patients with successful reperfusion therapy reduce leg ulcer size, restore limb perfusion (as indicated by improvement in ankle-brachial index and transcutaneous oxygen measurement at the limbs), or recover limb function (as indicated by improvement in pain-free walking distance and time) [22, 73]. The clinical trial database (http://www.clinicaltrials .gov) demonstrates 10 ongoing registered clinical trials of hMSCs at phase 1 or phase 2 for critical limb ischemia.

4. Challenges Associated with Future Translation of hMSCs to Ischemic Disease Therapy

There are some advantages and limitations of using hMSCs for the treatment of ischemic tissues (Table 1). Overall, many positive outcomes have been reported in preclinical trials utilizing hMSCs to treat ischemia-related medical conditions. These results have spurred ongoing clinical trials. However, the benefits observed in preclinical animal models have not yet been reproduced consistently in humans using conventional cell therapies. Conventional cell infusion approaches have been associated with complications, such as poor cell engraftment, short duration of cell persistence in the host, and low cell survival rate, in both animal models and human

TABLE 1: The advantages and limitations of hMSCs for the treatment of ischemic tissues.

Advantages	Limitations
hMSCs may repair injured vessels and ischemic tissues through their unique immunomodulation properties and paracrine mechanisms [13].	It is difficult to obtain sufficient numbers of healthy autologous hMSCs from elderly patients or patients with severe diseases [101].
hMSCs can be isolated from various locations within the human body and easily expanded *in vitro* [102].	The successful rate of differentiation of transplanted hMSCs into fully functional cardiomyocytes or neurons in a recipient remains elusive [103].
hMSCs provide a less invasive treatment procedure with low risk of adverse effects compared to surgical and pharmacological approaches [104].	hMSCs have a limited replicative lifespan [107].
hMSCs are relatively well characterized, and its clinical use can avoid the ethical concerns related to embryonic stem cells [105, 106].	

[74, 75]. These are likely due in part to the loss of homing and engraftment potential in cultured hMSCs after expanding under conventional cell culture conditions [74, 76]. Additionally, some animal models may not accurately mimic the conditions of human diseases [20]. Taken together, these may lower the successful rate of translation from animal models to clinical trials. Hence, there are increasing number of studies focused on techniques involving bioprocessing and tissue engineering (e.g., *in vitro* human tissue models, scaffold, and cellular imaging) to improve the translation rate of hMSCs. For example, a bioactive construct can be created by combining hMSCs with natural or synthetic scaffolds that possess similar characteristics as the native tissues to improve its integration into target ischemic tissues for tissue repair and regeneration. Moreover, such bioactive construct can be used on human *in vitro* ischemic disease models to evaluate its effectiveness prior to clinical trials.

4.1. *Bioprocessing of hMSCs.* There are a number of challenges that need to be addressed before hMSCs can achieve their widespread clinical applications. For example, in studies published to date, the MSC cell populations used were isolated from a number of varieties of tissues using different methodologies and expanded in culture using nonstandard protocols. In addition, many of the reported studies utilized cells exposed to animal-based serum. Standard culturing methods need to be developed, tested, and implemented to adhere to regulatory standards, achieve safe and reproducible results in a clinical setting, and make them translational. Important bioprocessing considerations include identification of proper cell source (autologous versus allogeneic), cell locations (e.g., bone marrow, adipose tissue, and synovial membrane), culture medium, static versus dynamic (bioreactor-based) culture, and long-term storage. Moreover, other considerations related to the administration of cells include optimization of cell dosage, cell administration method (cell alone versus cell-laden scaffold), and timing. Although work to address some of these important concerns is already well underway [15, 16, 77–81], it would take a considerable amount of time before these cells can be widely implemented clinically to treat ischemic tissues.

To date, significant efforts have been devoted towards the translation of hMSC-based therapy such as using bioreactors for cell population expansion and differentiation, developing animal component-free growth media, and generating cell banking protocols [82–84]. First, it is essential to optimize the procedures for isolation, expansion, and storage of hMSCs to ensure that only hMSCs are expanded within a specific duration for avoiding long-term expansion, which would increase the risk of harmful genetic transformation. For instance, a microcarrier-based stirred suspension bioreactor has demonstrated its capability to expand hMSCs from 5×10^5 cells to a clinically relevant cell number (6×10^8 cells) within a short duration (33 days) [16]. Besides that, hMSCs can be stored in master cell banks and comprehensively characterized at the time prior to clinical use. The large-scale production of safe and effective hMSCs should be in compliance with current good manufacturing practice (GMP) regulations. With the use of bioreactors incorporated with in-process control, this may automate the workflow and monitor the culture conditions, resulting in a good yield of clinical-grade cells. Additionally, the growth medium of hMSCs must be free of animal products, and the media formulations must be fully well-defined [15, 80]. For administration of hMSCs treatment in patients, a strictly accessible environment is required to reduce batch-to-batch variations of hMSCs and reduce the risk of contamination.

4.2. *Development of a Functional Human In Vitro Ischemic Disease Model.* One notable challenge has been the lack of a functional human *in vitro* ischemic disease model in which research can be easily undertaken to determine the details and efficacy of hMSC implementation. The only viable option to date has been the use of animals, which has ethical concerns and is costly and only available as an option to those who have the proper animal care facilities. Development of human *in vitro* ischemic disease tissue models is certainly a crucial need to overcome this research bottleneck. Three-dimensional biomimetic *in vitro* tissue models are conducive to the investigation of tissue or cell physiology in a systematic and repetitive manner, less time consuming, less expensive, allow high-throughput testing, and can be used in a standard manner across different research facilities [85]. This could facilitate the rapid translation of promising lab results to the clinic.

With the advances in microfluidic and hydrogel fabrication technologies, multiple techniques (e.g., needle-based molding, dissolvable network-based sacrificial molding, and bioprinting) have tremendous potential to generate 3D biomimetic blood vessels that can be used to develop

an *in vitro* ischemic disease and atherosclerotic models [86]. Among the microfabrication techniques, needle-based molding has been mostly utilized to develop biomimetic blood vessels for many applications, e.g., drug permeability testing and mechanical studies [87, 88]. A cylindrical vessel is generated by preinserting a cylindrical object (e.g., wire, needle, or rod) followed by casting a hydrogel (e.g., collagen type I and fibrin) around it and finally removing the cylindrical object after gel polymerization. This simple method is constrained to the fabrication of simple linear cylindrical vessels [89]. This vessel can, however, be functionalized with human endothelial cells cultured at the inner wall of the vessel while human perivascular cells (e.g., vascular smooth muscle cells, pericytes, and astrocytes) cultured in the wall surrounding the vessel [89, 90]. Following functionalization, this blood vessel can be subjected to biochemical cues (e.g., low-density lipoprotein, high-density lipoprotein, and human whole blood) and mechanical cues (e.g., flow-induced shear stress) to create functional human *in vitro* atherosclerotic models [91, 92]. This biomimetic model would be useful for exploring potential therapeutic effects of hMSCs in atherosclerosis for the prevention of tissue ischemia. If hMSCs can successfully treat atherosclerosis and repair injured blood vessels, hMSC transplant may be able to replace reperfusion therapy. Moreover, with the addition of organ-specific cells (e.g., cardiomyocytes and neurons) and blood components into these atherosclerotic models, *in vitro* functional human ischemic heart or brain disease tissue models can be developed. Such biomimetic *in vitro* disease models may assist in comprehensively elucidating the therapeutic mechanisms of hMSCs in the ischemic diseases, which allows for optimization of their cell processing procedures and improvement of their therapeutic benefits for ischemic diseases.

For dissolvable network-based sacrificial molding technique, a preformed cylindrical vessel made by sacrificial material (e.g., gelatin or Pluronic F127 fugitive ink) is first encapsulated in a hydrogel. Gelatin or Pluronic F127 fugitive ink is eventually liquefied by incubation at 37°C or 4°C under a modest vacuum, respectively, and removed from the hydrogel after gel polymerization to form a hollow cylindrical vessel in the hydrogel [93, 94]. In recent, bioprinting integrated with the dissolvable network-based sacrificial molding and layer-by-layer bonding technique is developed to print living cells in a 3D structure with a vessel. However, some limitations (e.g., repeatability and resolution for 3D vascular structure construction, required cell density, and cell damage due to high-speed deposition) still remain unresolved [86]. These methods can also be used to generate a functional human *in vitro* ischemic disease model for hMSC therapy.

4.3. Engraftment and Persistence of Transplanted hMSCs in the Host. Engraftment and persistence of transplanted hMSCs in a host are major challenges to be solved in stem-cell based therapy [76]. It seems that the engraftment rate of hMSCs is low, and hMSCs may not persist for longer periods in a host, thereby may reduce their therapeutic efficacy. For instance, whereas a majority of hMSCs were found to be dead within 3 days after implantation in the

animal models of myocardial infarction, positive outcomes were still observed [75, 95]. Treatment of hMSCs on a functional human ischemic disease model can enable researchers to determine hMSC engraftment rates, and evaluate the persistence of these cells within tissues by using a noninvasive cellular imaging modality. Imaging modalities, such as magnetic resonance imaging and bioluminescence imaging, have been shown to be capable of tracking transplanted stem cells in animal models of ischemic stroke and myocardial infarction, respectively, in real-time [96, 97]. This may help to explore the underlying mechanisms of stem cell therapy for ischemic diseases. Moreover, both engraftment and persistence of hMSCs can be improved with various methods (e.g., cytokines, hypoxia, and material-based approach) which may potentially improve their therapeutic efficacy [95, 98, 99]. For instance, 3D fibrin-cell patches were found to improve persistence duration and survival of transplanted hMSCs in the animal models of myocardial infarction, thereby improved the cardiac functions [100]. This scaffold may protect hMSCs from anoikis and improve interaction between hMSCs and ischemic tissues for effective stem cell therapies. By having the human *in vitro* ischemic disease models, these modified hMSCs are readily to be tested *in vitro*, which is something that is difficult to be performed in a clinical trial.

5. Conclusions

hMSCs have demonstrated their potential therapeutic effects on the ischemic diseases (including myocardial infarction, stroke, and critical limb ischemia) due to their excellent properties in immunomodulation, angiogenesis, and paracrine secretion of bioactive factors. The mode of action of hMSCs on the ischemic diseases is by means of paracrine mechanisms, endothelial differentiation, or direct cell-to-cell contact. However, their comprehensive therapeutic mechanisms in ischemic diseases, especially in attenuating atherosclerosis (main culprit for the ischemic diseases), remain elusive which requires further investigation. With the advances in microfluidic and hydrogel fabrication technologies, human *in vitro* ischemic disease tissue models are expected to be developed rapidly to accelerate the development of efficient hMSC-based therapeutics. With the exceptional and fascinating properties of hMSCs, it is envisioned that hMSCs would be an excellent cell source for a wide variety of clinical applications, including but not limited to ischemic diseases.

Conflicts of Interest

The authors declare no conflict of interest.

Authors' Contributions

Kar Wey Yong and Jane Ru Choi contributed equally to this work.

Acknowledgments

References

[1] A. S. Gupta, "Nanomedicine approaches in vascular disease: a review," *Nanomedicine: Nanotechnology, Biology and Medicine*, vol. 7, no. 6, pp. 763–779, 2011.

[2] Y. Imori, T. Akasaka, T. Ochiai et al., "Co-existence of carotid artery disease, renal artery stenosis, and lower extremity peripheral arterial disease in patients with coronary artery disease," *The American Journal of Cardiology*, vol. 113, no. 1, pp. 30–35, 2014.

[3] K. P. Rentrop and F. Feit, "Reperfusion therapy for acute myocardial infarction: concepts and controversies from inception to acceptance," *American Heart Journal*, vol. 170, no. 5, pp. 971–980, 2015.

[4] I. F. Charo and R. Taub, "Anti-inflammatory therapeutics for the treatment of atherosclerosis," *Nature Reviews Drug Discovery*, vol. 10, no. 5, pp. 365–376, 2011.

[5] A. Yamawaki-Ogata, R. Hashizume, X. M. Fu, A. Usui, and Y. Narita, "Mesenchymal stem cells for treatment of aortic aneurysms," *World Journal of Stem Cells*, vol. 6, no. 3, pp. 278–287, 2014.

[6] P. C. G. Simons, A. A. Nawijn, C. M. A. Bruijninckx, B. Knippenberg, E. H. de Vries, and H. van Overhagen, "Long-term results of primary stent placement to treat infrarenal aortic stenosis," *European Journal of Vascular and Endovascular Surgery*, vol. 32, no. 6, pp. 627–633, 2006.

[7] G. G. Stefanini and D. R. Holmes Jr, "Drug-eluting coronary-artery stents," *New england Journal of Medicine*, vol. 368, no. 3, pp. 254–265, 2013.

[8] J. R. Choi, K. W. Yong, and J. Y. Choi, "Effects of mechanical loading on human mesenchymal stem cells for cartilage tissue engineering," *Journal of Cellular Physiology*, vol. 233, no. 3, pp. 1913–1928, 2018.

[9] W. K. Z. Wan Safwani, J. R. Choi, K. W. Yong, I. Ting, N. A. Mat Adenan, and B. Pingguan-Murphy, "Hypoxia enhances the viability, growth and chondrogenic potential of cryopreserved human adipose-derived stem cells," *Cryobiology*, vol. 75, pp. 91–99, 2017.

[10] S. T. Hsiao, Z. Lokmic, H. Peshavariya et al., "Hypoxic conditioning enhances the angiogenic paracrine activity of human adipose-derived stem cells," *Stem Cells and Development*, vol. 22, no. 10, pp. 1614–1623, 2013.

[11] J. R. Choi, B. Pingguan-Murphy, W. A. B. Wan Abas et al., "*In situ* normoxia enhances survival and proliferation rate of human adipose tissue-derived stromal cells without increasing the risk of tumourigenesis," *PLoS One*, vol. 10, no. 1, article e0115034, 2015.

[12] Y.-R. Kuo, C. C. Chen, S. Goto, P. Y. Lin, F. C. Wei, and C. L. Chen, "Mesenchymal stem cells as immunomodulators in a vascularized composite allotransplantation," *Clinical and Developmental Immunology*, vol. 2012, Article ID 854846, 8 pages, 2012.

[13] T. Yan, P. Venkat, M. Chopp et al., "Neurorestorative responses to delayed human mesenchymal stromal cells treatment of stroke in type 2 diabetic rats," *Stroke*, vol. 47, no. 11, pp. 2850–2858, 2016.

[14] J. Phelps, A. Sanati-Nezhad, M. Ungrin, N. Duncan, and A. Sen, "Bioprocessing of mesenchymal stem cells and their derivatives: toward cell-free therapeutics," *Stem Cells International*, vol. 2018, Article ID 9415367, 23 pages, 2018.

[15] S. Jung, A. Sen, L. Rosenberg, and L. A. Behie, "Human mesenchymal stem cell culture: rapid and efficient isolation and expansion in a defined serum-free medium," *Journal of Tissue Engineering and Regenerative Medicine*, vol. 6, no. 5, pp. 391–403, 2012.

[16] Y. Yuan, M. S. Kallos, C. Hunter, and A. Sen, "Improved expansion of human bone marrow-derived mesenchymal stem cells in microcarrier-based suspension culture," *Journal of Tissue Engineering and Regenerative Medicine*, vol. 8, no. 3, pp. 210–225, 2014.

[17] C. Gandia, A. Armiñan, J. M. García-Verdugo et al., "Human dental pulp stem cells improve left ventricular function, induce angiogenesis, and reduce infarct size in rats with acute myocardial infarction," *Stem Cells*, vol. 26, no. 3, pp. 638–645, 2008.

[18] J. Chen, Z. G. Zhang, Y. Li et al., "Intravenous administration of human bone marrow stromal cells induces angiogenesis in the ischemic boundary zone after stroke in rats," *Circulation Research*, vol. 92, no. 6, pp. 692–699, 2003.

[19] J. Rehman, D. Traktuev, J. Li et al., "Secretion of angiogenic and antiapoptotic factors by human adipose stromal cells," *Circulation*, vol. 109, no. 10, pp. 1292–1298, 2004.

[20] H. B. van der Worp, D. W. Howells, E. S. Sena et al., "Can animal models of disease reliably inform human studies?," *PLoS Medicine*, vol. 7, no. 3, article e1000245, 2010.

[21] L. Hao, Z. Zou, H. Tian, Y. Zhang, H. Zhou, and L. Liu, "Stem cell-based therapies for ischemic stroke," *BioMed Research International*, vol. 2014, Article ID 468748, 17 pages, 2014.

[22] Y. Fujita and A. Kawamoto, "Stem cell-based peripheral vascular regeneration," *Advanced Drug Delivery Reviews*, vol. 120, pp. 25–40, 2017.

[23] V. Karantalis and J. M. Hare, "Use of mesenchymal stem cells for therapy of cardiac disease," *Circulation Research*, vol. 116, no. 8, pp. 1413–1430, 2015.

[24] P. Libby, P. M. Ridker, and A. Maseri, "Inflammation and atherosclerosis," *Circulation*, vol. 105, no. 9, pp. 1135–1143, 2018.

[25] J. Rudolf and K. B. Lewandrowski, "Cholesterol, lipoproteins, high-sensitivity C-reactive protein, and other risk factors for atherosclerosis," *Clinics in Laboratory Medicine*, vol. 34, no. 1, pp. 113–127, 2014.

[26] G. K. Hansson and P. Libby, "The immune response in atherosclerosis: a double-edged sword," *Nature Reviews Immunology*, vol. 6, no. 7, pp. 508–519, 2006.

[27] C. Weber and H. Noels, "Atherosclerosis: current pathogenesis and therapeutic options," *Nature Medicine*, vol. 17, no. 11, pp. 1410–1422, 2011.

[28] D. C. Steinl and B. A. Kaufmann, "Ultrasound imaging for risk assessment in atherosclerosis," *International Journal of Molecular Sciences*, vol. 16, no. 12, pp. 9749–9769, 2015.

[29] M. Gawaz, H. Langer, and A. E. May, "Platelets in inflammation and atherogenesis," *Journal of Clinical Investigation*, vol. 115, no. 12, pp. 3378–3384, 2005.

[30] G. K. Hansson, A.-K. L. Robertson, and C. Söderberg-Nauclér, "Inflammation and atherosclerosis," *Annual Review of Pathology: Mechanisms of Disease*, vol. 1, no. 1, pp. 297–329, 2006.

[31] A. J. Lusis, "Atherosclerosis," *Nature*, vol. 407, no. 6801, pp. 233–241, 2000.

[32] K. von Wnuck Lipinski, P. Keul, S. Lucke et al., "Degraded collagen induces calpain-mediated apoptosis and destruction of the X-chromosome-linked inhibitor of apoptosis (xIAP) in human vascular smooth muscle cells," *Cardiovascular Research*, vol. 69, no. 3, pp. 697–705, 2006.

[33] A. C. Newby, "Dual role of matrix metalloproteinases (matrixins) in intimal thickening and atherosclerotic plaque rupture," *Physiological Reviews*, vol. 85, no. 1, pp. 1–31, 2005.

[34] F. Li, X. Guo, and S.-Y. Chen, "Function and therapeutic potential of mesenchymal stem cells in atherosclerosis," *Frontiers in Cardiovascular Medicine*, vol. 4, p. 32, 2017.

[35] K. J. Woollard and F. Geissmann, "Monocytes in atherosclerosis: subsets and functions," *Nature Reviews Cardiology*, vol. 7, no. 2, pp. 77–86, 2010.

[36] Writing Group Members, W. Rosamond, K. Flegal et al., "Heart disease and stroke statistics—2008 update: a report from the American Heart Association Statistics Committee and Stroke Statistics Subcommittee," *Circulation*, vol. 117, no. 4, pp. e25–e146, 2007.

[37] J. H. Kim, I. S. Park, Y. Park, Y. Jung, S. H. Kim, and S.-H. Kim, "Therapeutic angiogenesis of three-dimensionally cultured adipose-derived stem cells in rat infarcted hearts," *Cytotherapy*, vol. 15, no. 5, pp. 542–556, 2013.

[38] P. Anversa, "Myocyte death in the pathological heart," *Circulation Research*, vol. 86, no. 2, pp. 121–124, 2000.

[39] S. Roura, J. R. Bagó, C. Soler-Botija et al., "Human umbilical cord blood-derived mesenchymal stem cells promote vascular growth *in vivo*," *PLoS One*, vol. 7, no. 11, article e49447, 2012.

[40] N. Wang, R. Zhang, S. J. Wang et al., "Vascular endothelial growth factor stimulates endothelial differentiation from mesenchymal stem cells via Rho/myocardin-related transcription factor-A signaling pathway," *The International Journal of Biochemistry & Cell Biology*, vol. 45, no. 7, pp. 1447–1456, 2013.

[41] L. Cai, B. H. Johnstone, T. G. Cook et al., "IFATS collection: human adipose tissue-derived stem cells induce angiogenesis and nerve sprouting following myocardial infarction, in conjunction with potent preservation of cardiac function," *Stem Cells*, vol. 27, no. 1, pp. 230–237, 2009.

[42] S. Bian, L. Zhang, L. Duan, X. Wang, Y. Min, and H. Yu, "Extracellular vesicles derived from human bone marrow mesenchymal stem cells promote angiogenesis in a rat myocardial infarction model," *Journal of Molecular Medicine*, vol. 92, no. 4, pp. 387–397, 2014.

[43] H.-S. Kim, D.-Y. Choi, S. J. Yun et al., "Proteomic analysis of microvesicles derived from human mesenchymal stem cells," *Journal of Proteome Research*, vol. 11, no. 2, pp. 839–849, 2012.

[44] F. Collino, M. C. Deregibus, S. Bruno et al., "Microvesicles derived from adult human bone marrow and tissue specific mesenchymal stem cells shuttle selected pattern of miRNAs," *PLoS One*, vol. 5, no. 7, article e11803, 2010.

[45] S.-W. Kim, D.-W. Lee, L.-H. Yu et al., "Mesenchymal stem cells overexpressing GCP-2 improve heart function through enhanced angiogenic properties in a myocardial infarction model," *Cardiovascular Research*, vol. 95, no. 4, pp. 495–506, 2012.

[46] A. Paul, M. Nayan, A. A. Khan, D. Shum-Tim, and S. Prakash, "Angiopoietin-1-expressing adipose stem cells genetically modified with baculovirus nanocomplex: investigation in rat heart with acute infarction," *International Journal of Nanomedicine*, vol. 7, p. 663, 2012.

[47] X.-Y. Zhu, X. Z. Zhang, L. Xu, X. Y. Zhong, Q. Ding, and Y. X. Chen, "Transplantation of adipose-derived stem cells overexpressing hHGF into cardiac tissue," *Biochemical and Biophysical Research Communications*, vol. 379, no. 4, pp. 1084–1090, 2009.

[48] V. Karantalis, V. Y. Suncion-Loescher, L. Bagno et al., "Synergistic effects of combined cell therapy for chronic ischemic cardiomyopathy," *Journal of the American College of Cardiology*, vol. 66, no. 18, pp. 1990–1999, 2015.

[49] A. R. Williams, K. E. Hatzistergos, B. Addicott et al., "Enhanced effect of combining human cardiac stem cells and bone marrow mesenchymal stem cells to reduce infarct size and to restore cardiac function after myocardial infarction," *Circulation*, vol. 127, no. 2, pp. 213–223, 2012.

[50] I. Perea-Gil, M. Monguió-Tortajada, C. Gálvez-Montón, A. Bayes-Genis, F. E. Borràs, and S. Roura, "Preclinical evaluation of the immunomodulatory properties of cardiac adipose tissue progenitor cells using umbilical cord blood mesenchymal stem cells: a direct comparative study," *BioMed Research International*, vol. 2015, Article ID 439808, 9 pages, 2015.

[51] F. S. Regateiro, S. P. Cobbold, and H. Waldmann, "CD73 and adenosine generation in the creation of regulatory microenvironments," *Clinical & Experimental Immunology*, vol. 171, no. 1, pp. 1–7, 2013.

[52] M. Monguió-Tortajada, S. Roura, C. Gálvez-Montón, M. Franquesa, A. Bayes-Genis, and F. E. Borràs, "Mesenchymal stem cells induce expression of cD73 in human monocytes *in vitro* and in a swine model of myocardial infarction *in vivo*," *Frontiers in Immunology*, vol. 8, article 1577, 2017.

[53] A. Bayes-Genis, C. Soler-Botija, J. Farré et al., "Human progenitor cells derived from cardiac adipose tissue ameliorate myocardial infarction in rodents," *Journal of Molecular and Cellular Cardiology*, vol. 49, no. 5, pp. 771–780, 2010.

[54] A. Bayes-Genis, C. Gálvez-Montón, C. Prat-Vidal, and C. Soler-Botija, "Cardiac adipose tissue: a new frontier for cardiac regeneration?," *International Journal of Cardiology*, vol. 167, no. 1, pp. 22–25, 2013.

[55] J. R. Bagó, C. Soler-Botija, L. Casaní et al., "Bioluminescence imaging of cardiomyogenic and vascular differentiation of cardiac and subcutaneous adipose tissue-derived progenitor cells in fibrin patches in a myocardium infarct model," *International Journal of Cardiology*, vol. 169, no. 4, pp. 288–295, 2013.

[56] A. Llucià-Valldeperas, C. Soler-Botija, C. Gálvez-Montón et al., "Electromechanical conditioning of adult progenitor cells improves recovery of cardiac function after myocardial infarction," *Stem Cells Translational Medicine*, vol. 6, no. 3, pp. 970–981, 2017.

[57] M. Majka, M. Sułkowski, B. Badyra, and P. Musiałek, "Concise review: mesenchymal stem cells in cardiovascular regeneration: emerging research directions and clinical applications," *Stem Cells Translational Medicine*, vol. 6, no. 10, pp. 1859–1867, 2017.

[58] J. Zhang and M. Chopp, "Cell-based therapy for ischemic stroke," *Expert Opinion on Biological Therapy*, vol. 13, no. 9, pp. 1229–1240, 2013.

[59] J. Zhu, Q. Liu, Y. Jiang, L. Wu, G. Xu, and X. Liu, "Enhanced angiogenesis promoted by human umbilical mesenchymal stem cell transplantation in stroked mouse is Notch1 signaling associated," *Neuroscience*, vol. 290, pp. 288–299, 2015.

[60] T. Onda, O. Honmou, K. Harada, K. Houkin, H. Hamada, and J. D. Kocsis, "Therapeutic benefits by human mesenchymal stem cells (hMSCs) and Ang-1 gene-modified hMSCs after cerebral ischemia," *Journal of Cerebral Blood Flow & Metabolism*, vol. 28, no. 2, pp. 329–340, 2008.

[61] J. Ma, H. Sawai, N. Ochi et al., "PTEN regulate angiogenesis through PI3K/Akt/VEGF signaling pathway in human pancreatic cancer cells," *Molecular and Cellular Biochemistry*, vol. 331, no. 1-2, pp. 161–171, 2009.

[62] D.-C. Ding, W. C. Shyu, M. F. Chiang et al., "Enhancement of neuroplasticity through upregulation of β1-integrin in human umbilical cord-derived stromal cell implanted stroke model," *Neurobiology of Disease*, vol. 27, no. 3, pp. 339–353, 2007.

[63] X. Bao, M. Feng, J. Wei et al., "Transplantation of Flk-1+ human bone marrow-derived mesenchymal stem cells promotes angiogenesis and neurogenesis after cerebral ischemia in rats," *European Journal of Neuroscience*, vol. 34, no. 1, pp. 87–98, 2011.

[64] A. Toyoshima, T. Yasuhara, and I. Date, "Mesenchymal stem cell therapy for ischemic stroke," *Acta Medica Okayama*, vol. 71, no. 4, pp. 263–268, 2017.

[65] M. A. Eckert, Q. Vu, K. Xie et al., "Evidence for high translational potential of mesenchymal stromal cell therapy to improve recovery from ischemic stroke," *Journal of Cerebral Blood Flow & Metabolism*, vol. 33, no. 9, pp. 1322–1334, 2013.

[66] M. K. Mamidi, R. Pal, S. Dey et al., "Cell therapy in critical limb ischemia: current developments and future progress," *Cytotherapy*, vol. 14, no. 8, pp. 902–916, 2012.

[67] Y. Cao, Z. Sun, L. Liao, Y. Meng, Q. Han, and R. C. Zhao, "Human adipose tissue-derived stem cells differentiate into endothelial cells in vitro and improve postnatal neovascularization in vivo," *Biochemical and Biophysical Research Communications*, vol. 332, no. 2, pp. 370–379, 2005.

[68] I. S. Park, J.-W. Rhie, and S.-H. Kim, "A novel three-dimensional adipose-derived stem cell cluster for vascular regeneration in ischemic tissue," *Cytotherapy*, vol. 16, no. 4, pp. 508–522, 2014.

[69] Y. J. Kim, H. K. Kim, H. H. Cho, Y. C. Bae, K. T. Suh, and J. S. Jung, "Direct comparison of human mesenchymal stem cells derived from adipose tissues and bone marrow in mediating neovascularization in response to vascular ischemia," *Cellular Physiology and Biochemistry*, vol. 20, no. 6, pp. 867–876, 2007.

[70] F. Yang, S.-W. Cho, S. M. Son et al., "Genetic engineering of human stem cells for enhanced angiogenesis using biodegradable polymeric nanoparticles," *Proceedings of the National Academy of Sciences of the United States of America*, vol. 107, no. 8, pp. 3317–3322, 2010.

[71] T. Yin, S. He, C. Su et al., "Genetically modified human placenta-derived mesenchymal stem cells with FGF-2 and PDGF-BB enhance neovascularization in a model of hindlimb ischemia," *Molecular Medicine Reports*, vol. 12, no. 4, pp. 5093–5099, 2015.

[72] E. K. Shevchenko, P. I. Makarevich, Z. I. Tsokolaeva et al., "Transplantation of modified human adipose derived stromal cells expressing VEGF165 results in more efficient angiogenic response in ischemic skeletal muscle," *Journal of Translational Medicine*, vol. 11, no. 1, p. 138, 2013.

[73] H. C. Lee, S. G. An, H. W. Lee et al., "Safety and effect of adipose tissue-derived stem cell implantation in patients with critical limb ischemia," *Circulation Journal*, vol. 76, no. 7, pp. 1750–1760, 2012.

[74] L. von Bahr, I. Batsis, G. Moll et al., "Analysis of tissues following mesenchymal stromal cell therapy in humans indicates limited long-term engraftment and no ectopic tissue formation," *Stem Cells*, vol. 30, no. 7, pp. 1575–1578, 2012.

[75] R. H. Lee, A. A. Pulin, M. J. Seo et al., "Intravenous hMSCs improve myocardial infarction in mice because cells embolized in lung are activated to secrete the anti-inflammatory protein TSG-6," *Cell Stem Cell*, vol. 5, no. 1, pp. 54–63, 2009.

[76] K. W. Yong, J. R. Choi, A. S. Dolbashid, and W. K. Z. Wan Safwani, "Biosafety and bioefficacy assessment of human mesenchymal stem cells: what do we know so far?," *Regenerative Medicine*, vol. 13, no. 2, pp. 219–232, 2017.

[77] M. Khurshid, A. Mulet-Sierra, A. Adesida, and A. Sen, "Osteoarthritic human chondrocytes proliferate in 3d coculture with mesenchymal stem cells in suspension bioreactors," *Journal of Tissue Engineering and Regenerative Medicine*, vol. 12, no. 3, pp. e1418–e1432, 2018.

[78] W. Ando, J. J. Kutcher, R. Krawetz et al., "Clonal analysis of synovial fluid stem cells to characterize and identify stable mesenchymal stromal cell/mesenchymal progenitor cell phenotypes in a porcine model: a cell source with enhanced commitment to the chondrogenic lineage," *Cytotherapy*, vol. 16, no. 6, pp. 776–788, 2014.

[79] H. Dry, K. Jorgenson, W. Ando, D. A. Hart, C. B. Frank, and A. Sen, "Effect of calcium on the proliferation kinetics of synovium-derived mesenchymal stromal cells," *Cytotherapy*, vol. 15, no. 7, pp. 805–819, 2013.

[80] S. Jung, A. Sen, L. Rosenberg, and L. A. Behie, "Identification of growth and attachment factors for the serum-free isolation and expansion of human mesenchymal stromal cells," *Cytotherapy*, vol. 12, no. 5, pp. 637–657, 2010.

[81] K. D. Jorgenson, D. A. Hart, R. Krawetz, and A. Sen, "Production of adult human synovial fluid-derived mesenchymal stem cells in stirred-suspension culture," *Stem Cells International*, vol. 2018, Article ID 8431053, 16 pages, 2018.

[82] M. T. Rojewski, N. Fekete, S. Baila et al., "GMP-compliant isolation and expansion of bone marrow-derived MSCs in the closed, automated device quantum cell expansion system," *Cell Transplantation*, vol. 22, no. 11, pp. 1981–2000, 2013.

[83] C. Capelli, O. Pedrini, R. Valgardsdottir, F. Da Roit, J. Golay, and M. Introna, "Clinical grade expansion of MSCs," *Immunology Letters*, vol. 168, no. 2, pp. 222–227, 2015.

[84] K. W. Yong, J. R. Choi, and W. K. Z. Wan Safwani, "Biobanking of human mesenchymal stem cells: future strategy to facilitate clinical applications," in *Biobanking and Cryopreservation of Stem Cells. Advances in Experimental Medicine and Biology*, vol. 951, pp. 99–110, Springer, 2016.

[85] N. T. Elliott and F. Yuan, "A review of three-dimensional *in vitro* tissue models for drug discovery and transport studies," *Journal of Pharmaceutical Sciences*, vol. 100, no. 1, pp. 59–74, 2011.

[86] A. Hasan, A. Paul, N. E. Vrana et al., "Microfluidic techniques for development of 3D vascularized tissue," *Biomaterials*, vol. 35, no. 26, pp. 7308–7325, 2014.

[87] H. Yoshida, M. Matsusaki, and M. Akashi, "Multilayered blood capillary analogs in biodegradable hydrogels for in vitro drug permeability assays," *Advanced Functional Materials*, vol. 23, no. 14, pp. 1736–1742, 2013.

[88] K. M. Chrobak, D. R. Potter, and J. Tien, "Formation of perfused, functional microvascular tubes in vitro," *Microvascular Research*, vol. 71, no. 3, pp. 185–196, 2006.

[89] M. I. Bogorad, J. DeStefano, J. Karlsson, A. D. Wong, S. Gerecht, and P. C. Searson, "Review: in vitro microvessel models," *Lab on a Chip*, vol. 15, no. 22, pp. 4242–4255, 2015.

[90] S. Hauser, F. Jung, and J. Pietzsch, "Human endothelial cell models in biomaterial research," *Trends in Biotechnology*, vol. 35, no. 3, pp. 265–277, 2017.

[91] J. Robert, B. Weber, L. Frese et al., "A three-dimensional engineered artery model for in vitro atherosclerosis research," *PLoS One*, vol. 8, no. 11, article e79821, 2013.

[92] F. Wolf, F. Vogt, T. Schmitz-Rode, S. Jockenhoevel, and P. Mela, "Bioengineered vascular constructs as living models for in vitro cardiovascular research," *Drug Discovery Today*, vol. 21, no. 9, pp. 1446–1455, 2016.

[93] A. P. Golden and J. Tien, "Fabrication of microfluidic hydrogels using molded gelatin as a sacrificial element," *Lab on a Chip*, vol. 7, no. 6, pp. 720–725, 2007.

[94] W. Wu, A. DeConinck, and J. A. Lewis, "Omnidirectional printing of 3D microvascular networks," *Advanced Materials*, vol. 23, no. 24, pp. H178–H183, 2011.

[95] A. Blocki, S. Beyer, J.-Y. Dewavrin et al., "Microcapsules engineered to support mesenchymal stem cell (MSC) survival and proliferation enable long-term retention of MSCs in infarcted myocardium," *Biomaterials*, vol. 53, pp. 12–24, 2015.

[96] C. Vandeputte, D. Thomas, T. Dresselaers et al., "Characterization of the inflammatory response in a photothrombotic stroke model by MRI: implications for stem cell transplantation," *Molecular Imaging and Biology*, vol. 13, no. 4, pp. 663–671, 2011.

[97] S. Roura, C. Gálvez-Montón, and A. Bayes-Genis, "Bioluminescence imaging: a shining future for cardiac regeneration," *Journal of Cellular and Molecular Medicine*, vol. 17, no. 6, pp. 693–703, 2013.

[98] S.-C. Hung, R. R. Pochampally, S. C. Hsu et al., "Short-term exposure of multipotent stromal cells to low oxygen increases their expression of CX3CR1 and CXCR4 and their engraftment in vivo," *PLoS One*, vol. 2, no. 5, article e416, 2007.

[99] J. A. Ankrum, J. F. Ong, and J. M. Karp, "Mesenchymal stem cells: immune evasive, not immune privileged," *Nature Biotechnology*, vol. 32, no. 3, pp. 252–260, 2014.

[100] S. Roura, C. Soler-Botija, J. R. Bagó et al., "Postinfarction functional recovery driven by a three-dimensional engineered fibrin patch composed of human umbilical cord blood-derived mesenchymal stem cells," *Stem Cells Translational Medicine*, vol. 4, no. 8, pp. 956–966, 2015.

[101] J. Zhang, X. Huang, H. Wang et al., "The challenges and promises of allogeneic mesenchymal stem cells for use as a cell-based therapy," *Stem Cell Research & Therapy*, vol. 6, no. 1, p. 234, 2015.

[102] W. K. Z. Wan Safwani, C. W. Wong, K. W. Yong et al., "The effects of hypoxia and serum-free conditions on the stemness properties of human adipose-derived stem cells," *Cytotechnology*, vol. 68, no. 5, pp. 1859–1872, 2016.

[103] M. Strioga, S. Viswanathan, A. Darinskas, O. Slaby, and J. Michalek, "Same or not the same? Comparison of adipose tissue-derived versus bone marrow-derived mesenchymal stem and stromal cells," *Stem Cells and Development*, vol. 21, no. 14, pp. 2724–2752, 2012.

[104] N. Kim and S.-G. Cho, "Clinical applications of mesenchymal stem cells," *The Korean Journal of Internal Medicine*, vol. 28, no. 4, pp. 387–402, 2013.

[105] M. Dominici, K. Le Blanc, I. Mueller et al., "Minimal criteria for defining multipotent mesenchymal stromal cells. The International Society for Cellular Therapy position statement," *Cytotherapy*, vol. 8, no. 4, pp. 315–317, 2006.

[106] B. Lindroos, R. Suuronen, and S. Miettinen, "The potential of adipose stem cells in regenerative medicine," *Stem Cell Reviews and Reports*, vol. 7, no. 2, pp. 269–291, 2011.

[107] H. J. Kim and J.-S. Park, "Usage of human mesenchymal stem cells in cell-based therapy: advantages and disadvantages," *Development & Reproduction*, vol. 21, no. 1, pp. 1–10, 2017.

[108] Y. Feng, Y. Wang, N. Cao, H. Yang, and Y. Wang, "Progenitor/stem cell transplantation for repair of myocardial infarction: hype or hope?," *Annals of Palliative Medicine*, vol. 1, no. 1, pp. 65–77, 2012.

[109] A. J. Salgado, J. C. Sousa, B. M. Costa et al., "Mesenchymal stem cells secretome as a modulator of the neurogenic niche: basic insights and therapeutic opportunities," *Frontiers in Cellular Neuroscience*, vol. 9, p. 249, 2015.

Research Article

Intravenous Transplantation of Mesenchymal Stem Cells Reduces the Number of Infiltrated Ly6C$^+$ Cells but Enhances the Proportions Positive for BDNF, TNF-1α, and IL-1β in the Infarct Cortices of dMCAO Rats

Yunqian Guan,[1] Xiaobo Li,[2] Wenxiu Yu,[2] Zhaohui Liang,[2] Min Huang,[2] Renchao Zhao,[2] Chunsong Zhao,[1] Yao Liu,[2] Haiqiang Zou,[3] Yanli Hao,[4] and Zhiguo Chen [1]

[1]*Cell Therapy Center, Xuanwu Hospital, Capital Medical University, and Key Laboratory of Neurodegeneration, Ministry of Education, Beijing, China*
[2]*Department of Neurology, Northern Jiangsu People's Hospital, Clinical Medical School of Yangzhou University, Yangzhou, China*
[3]*Department of Neurology, The General Hospital of Guangzhou Military Command, Guangzhou, China*
[4]*Department of Anatomy, Guangzhou Medical University, Guangzhou, China*

Correspondence should be addressed to Zhiguo Chen; chenzhiguo@gmail.com

The resident microglial and infiltrating cells from peripheral circulation are involved in the pathological processes of ischemia stroke and may be regulated by mesenchymal stem/stromal cell (MSC) transplantation. The present study is aimed at differentiating the neurotrophic and inflammatory roles played by microglial vs. infiltrating circulation-derived cells in the acute phase in rat ischemic brains and explore the influences of intravenously infused allogeneic MSCs. The ischemic brain injury was induced by distal middle cerebral artery occlusion (dMCAO) in SD rats, with or without MSC infusion in the same day following dMCAO. Circulation-derived infiltrating cells in the brain were identified by Ly6C, a majority of which were monocytes/macrophages. Without MSC transplantation, among the infiltrated Ly6C$^+$ cells, some were positive for BDNF, IL-1β, or TNF-α. Following MSC infusion, the overall number of Ly6C$^+$ infiltrated cells was reduced by 50%. In contrast, the proportions of infiltrated Ly6C$^+$ cells coexpressing BDNF, IL-1β, or TNF-α were significantly enhanced. Interestingly, Ly6C$^+$ cells in the infarct area could produce either neurotrophic factor BDNF or inflammatory cytokines (IL-1β or TNF-α), but not both. This suggests that the Ly6C$^+$ cells may constitute heterogeneous populations which react differentially to the microenvironments in the infarct area. The changes in cellular composition in the infarct area may have contributed to the beneficial effect of MSC transplantation.

1. Introduction

Mesenchymal stem/stromal cells (MSCs) have a potential for treatment of neurological diseases, such as stroke. Bone marrow-derived MSCs (BM-MSCs) show merits in that they can be allogeneically or autologously transplanted without raising ethical or immunological problems.

The therapeutic mechanisms of intravenous MSC transplantation have been mainly ascribed to the neurotrophic and anti-inflammatory effects [1]. MSCs are capable of secreting a lot of cytokines and eliciting the host to produce many kinds of neurotrophic factors, including brain-derived neurotrophic factor (BDNF) [2], glial cell-derived neurotrophic factor (GDNF) [3], and insulin growth factor-1 (IGF-1) [4].

Inflammatory responses in stroke, including immune cells, cytokines, and chemokines, are important for stroke development and recovery. Local microglial cells and periphery circulation-derived cells, such as monocytes/macrophages, are important participants in stroke-induced

inflammation and can be both beneficial and detrimental after stroke injury. Despite extensive studies on microglia in stroke, the roles of periphery-derived cells during ischemic stroke have not been fully characterized [5, 6].

We have previously shown a rapid accumulation of ionized calcium binding adaptor molecule-1- (Iba-1-) positive microglia in the injured cerebral cortex two days after dMCAO in rats [7]. After intravenous MSC transplantation, the concentrations of neurotrophin BDNF and proinflammatory cytokines TNF-α and IL-1β are all increased [7]. It will be interesting to examine the respective contribution from microglial vs. infiltrated cells in production of BDNF, TNF-α, and IL-1β.

However, microglial and infiltrating monocytes/macrophages share many features. Iba-1 expression does not allow complete discrimination of resident microglia from infiltrated monocytes/macrophages. Other commonly used pan-markers for microglia, such as CD11b, isolectin (IB4), and F4/80, are not specific enough either [6]. CD45 alone is not sufficient because although infiltrated hematopoietic cells express high levels of CD45, activated microglia express low levels of CD45 too [8].

It is therefore important to find a marker that can differentiate microglia from infiltrated monocytes/macrophages in rats. Ly6C$^+$ cells represent circulation-derived monocytes/macrophages in mice and human [9, 10]. Whether the same holds true in rats is one of the questions that will be addressed in the current study.

One of the main therapeutic effects of MSCs after stroke is the neurotrophic effects [11]. Neurotrophins, such as BDNF, may be derived from the MSCs that have migrated into the brain, the endogenous neurons, and/or microglia/macrophages. BDNF is distributed in substantial amount in the ischemic core, peri-ischemic core cortex, ipsilateral striatum, and contralateral hemisphere [2, 12]. BDNF plays a crucial role in neuronal survival and plasticity, and its importance for stroke recovery has been demonstrated in Kurozumi's study. MSCs are transfected with BDNF, ciliary neurotrophic factor (CNTF), or neurotrophin 3 (NT3) vectors. Rats that undergo middle cerebral artery occlusion (MCAO) and receive MSC-BDNF exhibit significantly better functional recovery than do control stroke rats. MCAO rats that have received MSC-CNTF and MSC-NT3 do not show significant improvement vs. control stroke rats [13, 14].

We have previously found that in the ischemic brain, BDNF is expressed in NeuN-positive neurons and CD68-positive microglia/macrophages in the peri-infarct areas, but mainly by Iba-1-positive microglia in the infarct core [7]. Whether BDNF production can be derived from infiltrated cells and regulatable by MSC treatment is still unclear, and the current study will try to address these questions as well.

The other main therapeutic mechanism underlying MSC effect in stroke is the immunosuppressive effects, including downregulation of proinflammatory cytokines produced by microglia/macrophages [15]. Macrophage infiltration is normally thought to exacerbate focal inflammatory responses and further damage the brain by producing proinflammatory cytokines, such as TNF-α and IL-1β [16, 17]. As the most studied cytokines in adult stroke, IL-1β and TNF-α have

been found to exacerbate brain damage by directly inducing neuronal injury and via consequent production of additional cytokines/chemokines and upregulation of adhesion molecules [18, 19]. Some groups found that IL-1β and TNF-α are expressed in largely segregated populations of CD11b$^+$CD45dim microglia and CD11b$^+$CD45high macrophages in mice [20].

In the current study, we will investigate whether neurotrophic factor BDNF and proinflammatory factors IL-1β and TNF-α are produced by infiltrated cells and how the production is regulated by MSC treatment.

2. Materials and Methods

2.1. Distal Middle Cerebral Artery Occlusion (dMCAO) Model, Peripheral Macrophage Depletion, and Cell Transplantation.

The performance of allogeneic bone marrow MSC culture, cell transplantation, dMCAO model establishment, and behavioral tests have been described in our previous study [7]. In brief, 1×10^6 MSCs in 1 mL 0.9% saline were administered via intravenous injection one hour after ischemia. One mL of 0.9% saline was given to the ischemia vehicle group ($n = 10$ per group).

Intravenous administration of clodronate liposomes was widely used for depletion of the monocyte/macrophage population in blood circulation. Clodronate liposomes do not affect CNS-resident microglia because they cannot pass the blood-brain barrier (BBB). In this study, clodronate liposomes (Liposoma BV, Amsterdam, Netherlands) were intraperitoneally injected 1, 2, and 3 days before the dMCAO. The dose of clodronate liposomes was 50 mg/kg according to the manufacturer's instructions. PBS injection was used as a negative control [21, 22].

The SD rats used in this study were divided into three groups, "sham" controls (skull was opened but without arterial occlusion), "ischemia + vehicle" group (dMCAO models with saline injection), and "ischemia + MSC" group (dMCAO models with MSC infusion). Three time points, 3, 24, and 48 h post-ischemia, were chosen. Under each condition, 5–10 rats were included.

2.2. Immunohistochemistry.

The rats were anesthetized and transcranially perfused with 0.9% saline, followed by cold 4% formaldehyde (PFA). The brains were removed, postfixed in 4% PFA for 24 h, and stored in 30% sucrose/PBS at 4°C. All brains were sectioned on vibrating microtome at 40 μm thickness. Free-floating sections across the entire brains were collected.

Immunohistochemistry and cell counting were performed as previously described [7]. In brief, floating brain sections were incubated in 0.3% Triton-100 PBS for 30 min and blocked with 2% donkey serum in PBS for 30 min at room temperature (RT). Sections were incubated overnight with Ly6C primary antibody (1 : 500 dilution, Santa Cruz Biotechnology, CA, USA). In the following day, sections were rinsed 3 × 15 minutes in TBS and incubated with FITC- or Cy3-conjugated secondary antibodies (1 : 300; Immune-Jackson Inc., CA, USA) for 2 h at RT. The sections were reblocked by 2% donkey serum in PBS for 30 min, then

incubated with anti-CD45 (1 : 200 dilution, eBioscience, CA, USA), anti-CD68 (1 : 500 dilution, Chemicon, Temecula, CA, USA), biotin-conjugated anti-BDNF (1 : 500 dilution, R&D Systems, Minneapolis, USA), biotin-conjugated anti-TNF-α (1 : 500 dilution, R&D Systems, Minneapolis, USA), or biotin-conjugated anti-IL-1β antibodies (1 : 500 dilution, NeoBioscience Technology Co., Ltd, Shanghai, China). Other primary antibodies used included rat anti-rat Ly6C primary antibody (1 : 500 dilution, Santa Cruz Biotechnology, CA, USA), mouse anti-rat neutrophil elastase (1 : 500 dilution, Santa Cruz Biotechnology, CA, USA), and mouse anti-rat CD3 (1 : 500 dilution, NeoBioscience Technology Co., Ltd, Shanghai, China).

After being washed by PBS for 3 times, secondary antibodies were applied for 2 hours, followed by DAPI treatment for 20 min. Control reactions for antibody specificity were performed by omission of the primary antibodies. After being mounted onto slides, the positive cells were counted using a TCS SP5 II confocal laser scanning microscope (Leica, Wetzlar, Germany) at 200x magnification. The confocal settings, such as gain and offset, were designed to ensure that all pixels of all the selected sections were within the photomultiplier detection range. The setting was maintained to ensure all images were collected with the same parameters.

2.3. Cell Counting.

In our experiments, the distribution of Ly6C, Iba-1, and BDNF was not restricted within the infarct area. For analysis, we counted the cells only in the cortical infarct areas.

The border zone between infarcted and healthy brain tissue is compartmentalized into an inner macrophage-rich part and a more peripheral zone dominated by reactive astrocytes [23, 24]. Based on this concept and the demarcation method of Gelosa et al. [25], we outlined the inner infarct boundary zone (IBZ) as within 400 μm to the boundary line between the normal and infarct areas. The counting region is a 1.6 mm × 0.8 mm rectangle (rectangle in Figure 1(i)), which is located in the infarct cortex area and adjacent to the inner IBZ.

The selection of sections for each rat was in accordance with Simsek and Duman [26]. For each section, the Ly6C-positive and Ly6C/BDNF-, Ly6C/TNF-α-, and Ly6C/IL-1β double-positive cells that were located in the counting region were counted as previously described [26, 27]. The numbers of neutrophils (neutrophil elastase^{+}) and T cells (CD3^{+}) coexpressing BDNF, TNF-α, and IL-1β were also counted. The number of labeled cells was calculated in 3 coronal sections from each rat, located between −2.0 mm and 2.0 mm to the bregma and expressed as the mean number of cells per view field (20x objective). The estimated cell numbers were determined using the method of Simsek and Duman [26]. All analyses were performed by investigators blinded to the sample identity and treatment groups.

2.4. Statistics.

The data of cell counting were expressed as mean ± SEM. The comparisons were analyzed by one-way analysis of variance (one-way ANOVA) and Bonferroni-Dunnett corrections using SPSS 10.0. The level of significance of all comparisons was set at $p < 0.05$.

3. Results

The success of ischemia model generation was validated by HE staining. The mortality rates of animals following dMCAO for the sham control, "ischemia + vehicle," and "ischemia + MSCs" groups were 0, 16.7%, and 13.3%, respectively. There was no significant difference of mortality rates between the groups.

3.1. Ly6C^{+} Cells at the Infarct Area in Rat Brains Are Circulation-Derived Cells.

Accumulation of Ly6C^{+} cells in the infarct area boundary zone (IBZ) was induced continuously over time following ischemia (Figures 1(a)–1(d)). The lineage identification is shown in Figures 1(e)–1(h), and the demarcation of inner IBZ and counting region was demonstrated in Figure 1(i).

Brain slices of naïve rats (no surgical operation, no dMCAO, and no MSC infusion) were stained, and no Ly6C^{+} cells in the cerebral cortex was detected, suggesting that the Ly6C^{+} cells observed in the dMCAO brains were derived from peripheral circulation (Figure S1A–D).

To further confirm the origin of Ly6C^{+} cells in dMCAO brains, we deleted the monocytes/macrophages in the periphery by i.p. injection of clodronate liposomes, which cannot cross BBB and therefore do not affect brain-resident microglia. Two days after dMCAO, the number of Ly6C^{+} cells in the cerebral cortex was reduced by 80–90% as compared with the sham group (Figure S1E–H).

In sham control rats, almost no Ly6C-expressing cells were found in the ischemia core cortex. Only after ischemia occurred did the Ly6C^{+} cells emerge in the infarct boundary zone (Figure 1(a)). Three hours after ischemia, Ly6C^{+} cells began to appear in the infarct area (Figure 1(b)). At 24 and 48 h, more and more Ly6C^{+} cells accumulated around almost the entire cerebral ischemia core cortex and striatum and were distributed widely in the ischemic hemisphere (Figures 1(c) and 1(d)). In contrast, few Ly6C^{+} cells were located in the ipsilateral cortex in the sham group 3, 24, and 48 h after ischemia.

At two days after the onset of ischemia, immunohistological examination showed strong expression of Ly6C in the infarct area (Figure 1(e)). The strong expression of CD45 (Figures 1(f)–1(h)) together with Ly6C reactivity confirmed that the cells were derived from periphery circulation.

3.2. Ly6C^{+} Cells Represent a Population Partly Overlapping with Iba-1^{+} Cells.

To delineate the histological distribution and find out to what extent the two markers are overlapped, we performed double immunohistochemistry for Iba-1 and Ly6C.

A large portion of Ly6C^{+} cells were found accumulated in the inner infarct boundary zone and in the infarct area (Figures 2(a)–2(d)) after ischemia induction. The distribution of Iba-1^{+} cells was wider than that of Ly6C^{+} cells. Plenty of Iba-1^{+} cells were detected not only in the infarct area but also in the intact ipsilateral cortex (Figures 2(e)–2(h)),
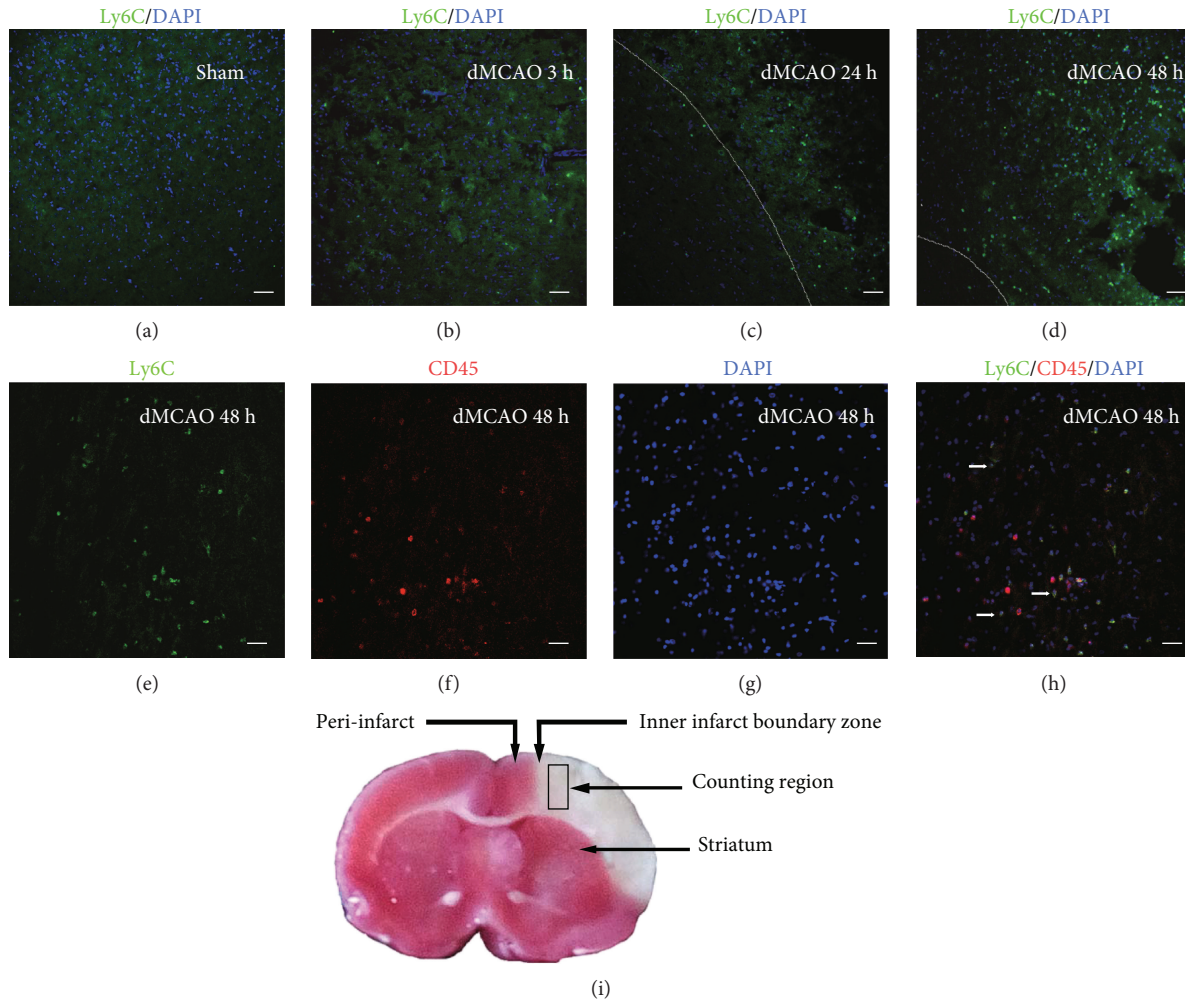
Figure 1: Ly6C$^+$ cells in the ischemic core cortex. The number of Ly6C$^+$ cells gradually increases at the IBZ of infarct dMCAO in rats. (a) Ly6C staining of the sham group. (b) Ly6C staining of the infarct area 3 h after the onset of ischemia. (c) 24 h. (d) 48 h. (e) Ly6C staining in the infarct area at 48 h. (f) CD45 staining in the same view field as (e). (g) DAPI nucleus staining. (h) Merged image of (e), (f), and (g), showing that Ly6C-positive cells are all CD45-positive. Arrow: double-labeled cells. (i) Cerebral infarct of the "ischemia + vehicle" group, as stained by triphenyltetrazolium chloride (TTC). Rectangle: the area where cell counting was performed. Dotted lines: the boundary of the infarct areas. Scale bar, 50 μm.

striatum, and corpus callosum (Figures 2(i)–2(l)) and even in the contralateral hemisphere. In the intact areas of both contra- and ipsilateral hemispheres, the majority of the Iba-1$^+$ cells were of magnified morphology, and in the infarct, the predominant morphology of Iba-1$^+$ cells was amoeboid-like round (Figures 2(d), 2(h), and 2(l)).

Only in the infarct cortex and the inner IBZ were a few Ly6C$^+$ cells reactive for Iba-1 (Figures 2(a)–2(d)). The percentage of double labeled Iba-1$^+$/Ly6C$^+$ cells in the infarct area and the inner IBZ was 30.18 ± 8.57% and 30.91 ± 15.56% among the Iba-1$^+$ cells, respectively (Figures 2(m) and 2(n)). Among the Ly6C$^+$ cells, about 25.35 ± 3.26% coexpressed Iba-1 in the infarct area and 24.68 ± 4.14% coexpressed Iba-1 in the IBZ. There was no significant difference between the numbers at the infarct area and the inner IBZ. After MSC transplantation, the overlapping percentage of Iba-1$^+$ and Ly6C$^+$ cells was not changed in the infarct area and inner IBZ.

In peri-infarct area (Figures 2(e)–2(h)), striatum, and corpus callosum (Figures 2(i)–2(l)), few Ly6C$^+$ cells were found, and they were negative for Iba-1 (Figures 2(o) and 2(p)).

When all of the Iba-1$^+$ cells, including the contra- and ipsilateral cortices, striatum, and corpus callosum, were taken into account, the overlapped proportion with Ly6C was less than 0.01% among the Iba-1$^+$ cells.

3.3. Ly6C$^+$ Cell Is One of the Major Contributors for BDNF Production.
We have shown that in the ipsilateral ischemia core cortex, Iba-1$^+$ cells are one of the main sources for the production of BDNF [7]. Other cell types, such as CD68$^+$ microglia, and NeuN$^+$ neurons, are partly responsible for production of BDNF, even after the induction of ischemia. But all of these cells together do not represent the entire BDNF$^+$ population. These results strongly suggest that there are other cell types as the source of BDNF in the infarct region.
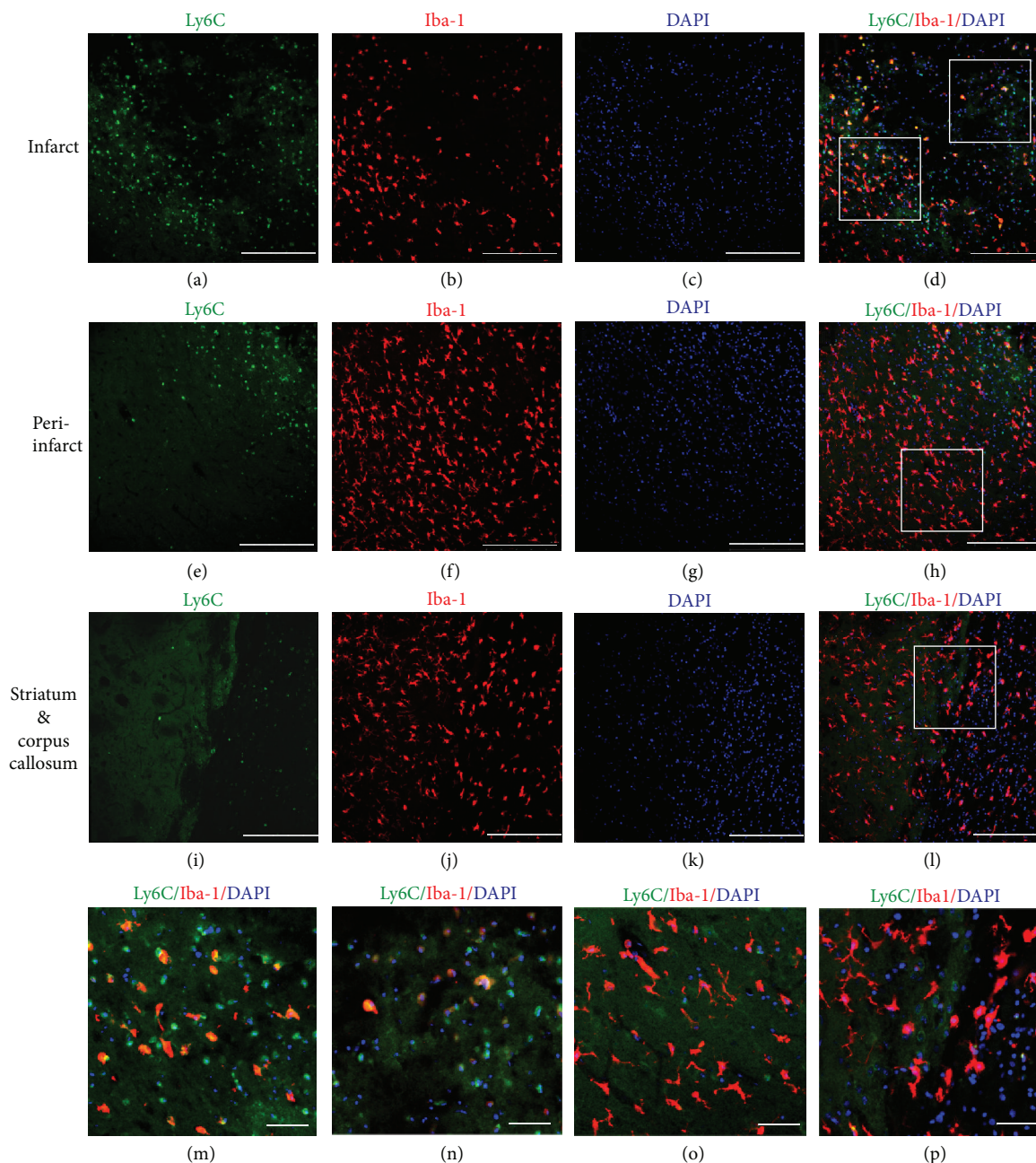
FIGURE 2: Few Ly6C$^+$ cells are double-stained with Iba-1 in the ischemia core cortex at day 2. (a–d) Distribution of Ly6C$^+$ and Iba-1$^+$ cells in the infarct areas. (e–h) Distribution of Ly6C$^+$ and Iba-1$^+$ cells in the peri-infarct area of the ipsilateral cortex. (i–l) Distribution of Ly6C$^+$ and Iba-1$^+$ cells in the ipsilateral striatum and corpus callosum. (a, e, i) Ly6C staining. (b, f, j) Iba-1. (c, g, k) DAPI nucleus staining. (d, h, l) Double-stained Ly6C$^+$/Iba-1$^+$ cells. (d) Ly6C$^+$/Iba-1$^+$ cells scattered in the infarct area (right square) and the inner infarct boundary zone (left square). (h) Very few Ly6C$^+$ cells were found in the ipsilateral peri-infarct area (to the left of the dashed line). (l) Very few Ly6C$^+$ cells were found in the ipsilateral striatum (to the left of the dashed line) and corpus callosum (to the right of the dashed line), and no double stained Ly6C$^+$/Iba-1$^+$ cells were spotted in the striatum or corpus callosum. Arrow: double-labeled cells. Scale bar, 50 μm. (m) (left square in (d)): in the inner infarct boundary zone, 30–40% of Ly6C$^+$ cells were Iba-1-positive. (n) (right square in (d)): in the infarct area, 20–30% of Ly6C$^+$ cells were Iba-1-positive. (o, p) (squares in (h) and (l)): very few or no double-stained Ly6C$^+$/Iba-1$^+$ cells was spotted in the striatum or corpus callosum. Scale bar: (a–l) 250 μm and (m–p) 50 μm.

We performed double immunohistochemistry for BDNF and Ly6C (Figure 3) and found that, two days after ischemia onset, BDNF expression was enhanced in infiltrating Ly6C$^+$ cells in the ischemia core cortex as compared with the sham control group, and only in the infarct area was BDNF staining found overlapped with Ly6C (Figures 3(a)–3(d)). The numbers of Ly6C$^+$ cells, BDNF single-positive cells, Ly6C$^+$/BDNF$^+$ double-positive cells were 93.8 $\pm$ 14.56, 40.2 $\pm$ 9.59, and 29.7 $\pm$ 6.18 per view field, respectively (Figure 3(k)).
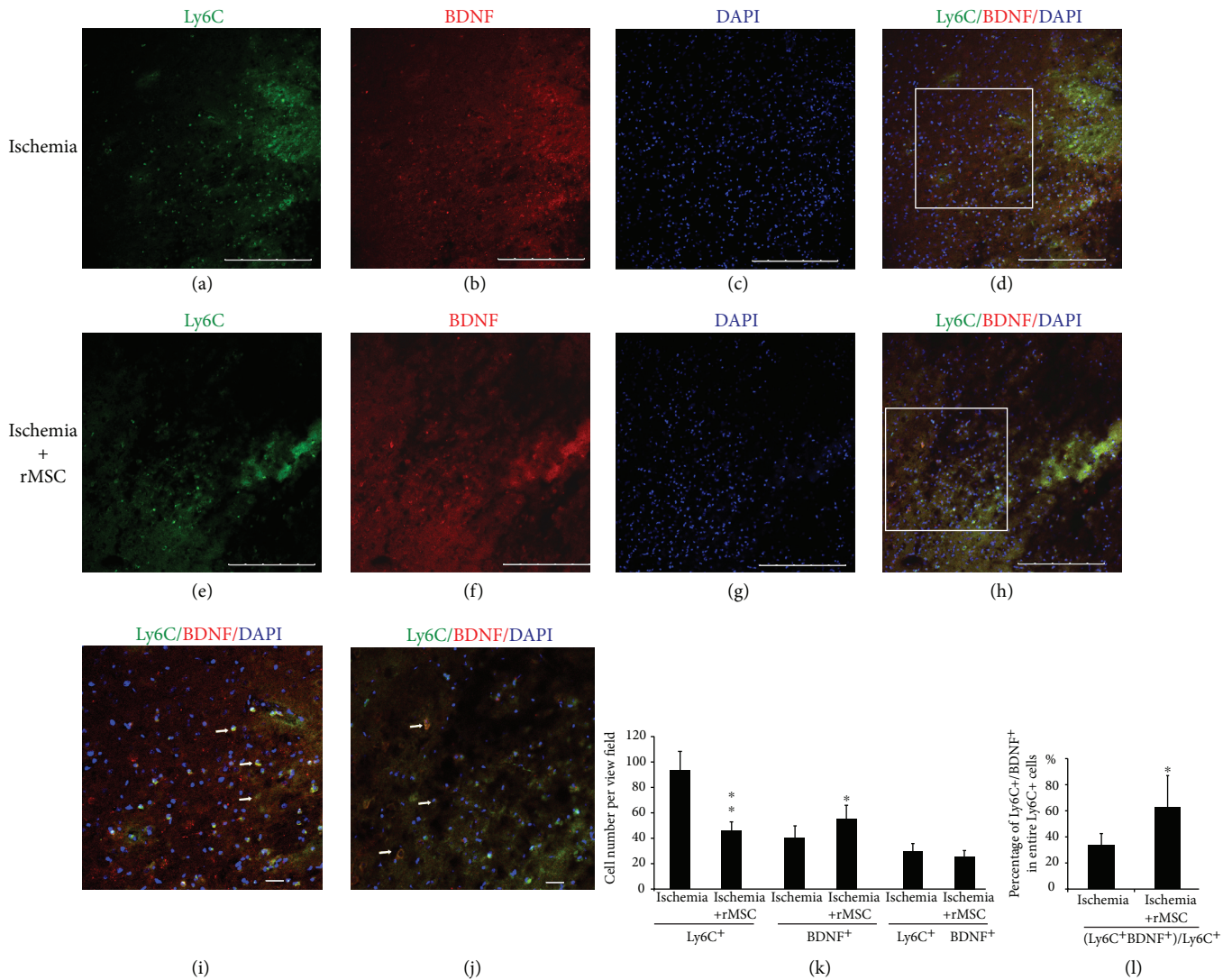
Figure 3: Ly6C$^+$ cells are one of the major contributors for BDNF production at day 2. (a–d) Distribution of Ly6C$^+$ and BDNF$^+$ cells in the infarct before MSC transplantation. (e–h) Distribution of Ly6C$^+$ and BDNF$^+$ cells in the infarct after MSC transplantation. (a, e) Ly6C staining. (b, f) BDNF. (c, g) DAPI nucleus staining. (d) Double-stained Ly6C$^+$/BDNF$^+$ cells scattered in the infarct area after dMCAO. (h) Ly6C$^+$/BDNF$^+$ cells 2 days after MSC transplantation. (i, j) Squares in (d) and (h). Ly6C$^+$ cell number was reduced in the infarct area 2 days after MSC transplantation, and the quantity and percentage of double-stained BDNF$^+$ Ly6C$^+$ cells were increased in these areas. (k) The cell counting results of Ly6C$^+$, BDNF$^+$, and Ly6C$^+$/BDNF$^+$ cells before and after MSC transplantation. (l) The percentage of Ly6C$^+$/ BDNF$^+$ cells among Ly6C$^+$ cells was increased by MSC treatment. ($^*p < 0.05$ and $^{**}p < 0.01$, as compared with the ischemia vehicle group). Arrow: double-labeled cells. $n = 5$; scale bar: (a–h) 250 μm and (i, j) 50 μm.

MSC treatment reduced the quantity of Ly6C$^+$ cells that had infiltrated into the brain to 35.7 ± 7.04 per view field, but increased the number of BDNF$^+$ cells to 55.7 ± 10.10 (Figures 3(e)–3(k)). MSC transplantation did not change the number of Ly6C$^+$/BDNF$^+$ double-positive cells ($25.5 + 4.45$), but increased the proportion of Ly6C$^+$ cells coexpressing BDNF from $32.40 \pm 7.25\%$ before MSC treatment to $71.65 \pm 4.26\%$ after treatment (Figures 3(i), 3(j), and 3(l)).

We have previously reported that BDNF expression was enhanced in Iba-1$^+$ cells following ischemia [7]. Although around 25% of Ly6C$^+$ cells were also Iba-1-positive in the infarct area, the current study strongly suggested that Ly6C$^+$ cells may be another major contributor for BDNF

production since the proportion of Ly6C$^+$ cells coexpressing BDNF was dramatically enhanced to $71.65 \pm 4.26\%$ after MSC treatment.

3.4. Ly6C$^+$ Cells Positive for IL-1β Are Upregulated by MSC Treatment.

We examined IL-1β reactivity in Ly6C$^+$ cells in the ischemia vehicle group (Figures 4(a)–4(d)) and in the ischemia + MSC group (Figures 4(e)–4(h)). The ischemia vehicle group showed a higher level of IL-1β compared to the sham control group (data not shown, $p < 0.01$), as evidenced by the increased number of IL-1β^+/Ly6C$^+$ cells in the infarct area.
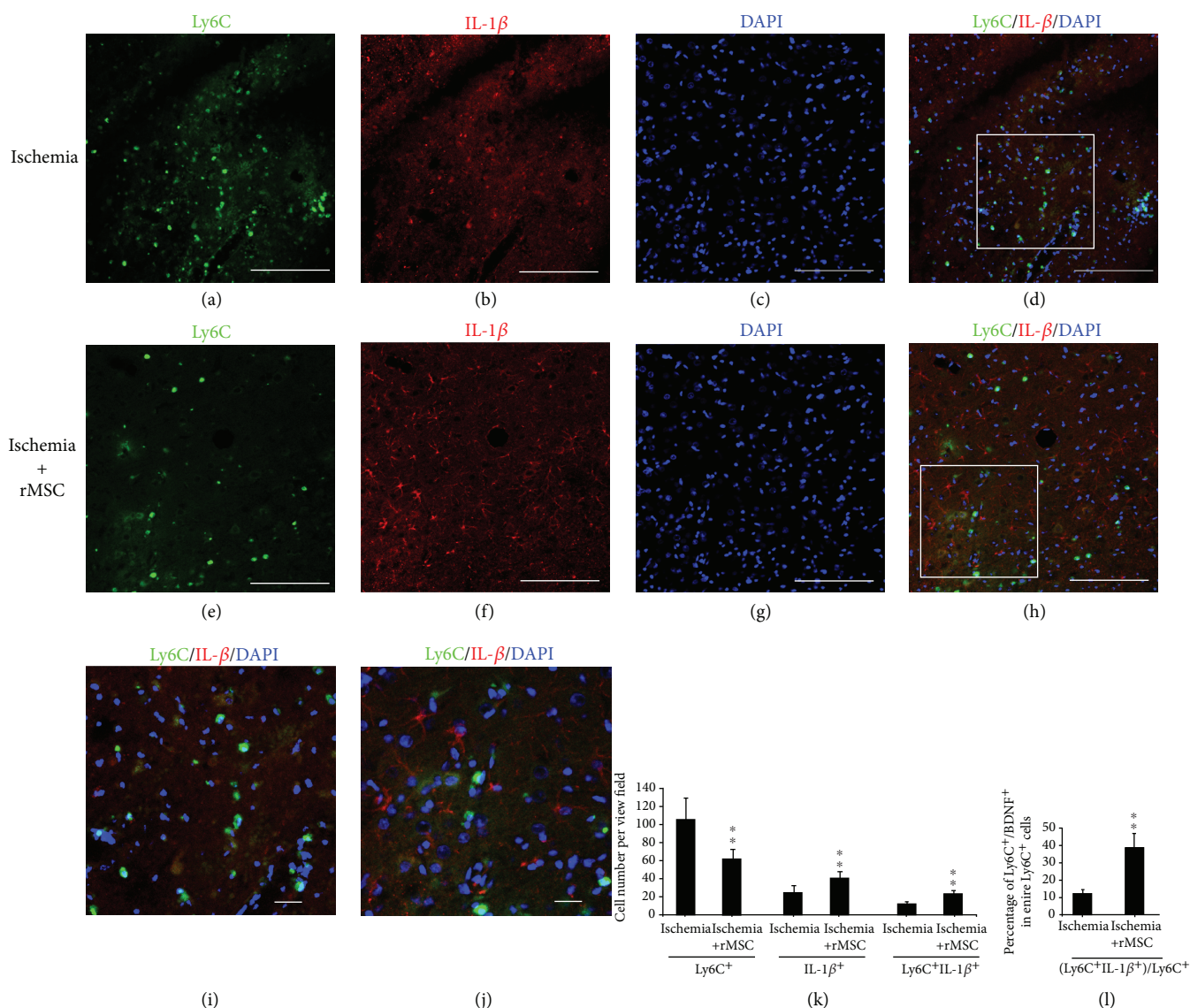
FIGURE 4: MSC treatment reduces the quantity of Ly6C$^+$ cells but increases the proportion that produces IL-1β at day 2. (a–d) Distribution of Ly6C$^+$ and IL-1β^+ cells in the infarct before MSC treatment. (e–h) Distribution of Ly6C$^+$ and IL-1β^+ cells in the infarct after MSC treatment. (a, e) Ly6C staining. (b, f) IL-1β staining. (c, g) DAPI nucleus staining. (d) Double-stained Ly6C$^+$/IL-1β^+ cells scattered in the infarct area 2 days after dMCAO. (h) Ly6C$^+$/IL-1β^+ cells in the infarct area 2 days after MSC transplantation. (i) The magnified image of the square in (d). (j) The magnified image of the square in (h). (k) Ly6C$^+$ cell number was reduced in the infarct area 2 days after MSC transplantation, but the quantity of IL-1β^+ cells and IL-1β^+/Ly6C$^+$ cells was increased in the infarct area. (l) The percentage of Ly6C/IL-1β double-positive cells among the whole Ly6C$^+$ cells was increased by MSC treatment. (*$p < 0.05$ and **$p < 0.01$, as compared with the ischemia vehicle group). Arrow: double-labeled cells. $n = 5$; scale bar: (a–h) 250 μm and (i, j) 50 μm.

MSC transplantation reduced the number of Ly6C$^+$ cells infiltrated into the brain but increased the number of IL-1β^+ cells from 24.75 ± 7.35 per view field before MSC transplantation to 41 ± 6.82 after transplantation ($p < 0.01$, Figure 4(k)). After all, the quantity of IL-1β^+/Ly6C$^+$ double-positive cells was increased by MSC treatment from 12.5 ± 2.18 to 23.75 ± 3.16 per view field ($p < 0.01$, Figure 4(k)). The percentage of IL-1β^+/Ly6C$^+$ double-positive cells in the entire Ly6C$^+$ cells was also increased by MSC treatment from $12.30 \pm 2.03\%$ to $38.62 \pm 7.99\%$ ($p < 0.01$, Figure 4(l)).

We have previously reported that IL-1β protein level was enhanced in the infarct area 48 h after MSC transplantation [7]. The results from the current study suggest that Ly6C$^+$ infiltrated cells in the brain may have contributed to this enhancement.

3.5. MSC Treatment Induces TNF-α Expression in Ly6C$^+$ Cells.
It was previously reported that in mouse stroke models, microglia are the main producer of TNF-α while macrophages are of IL-1(b) [20]. We examined TNF-α reactivity in Ly6C$^+$ cells in the ischemia vehicle group and in the
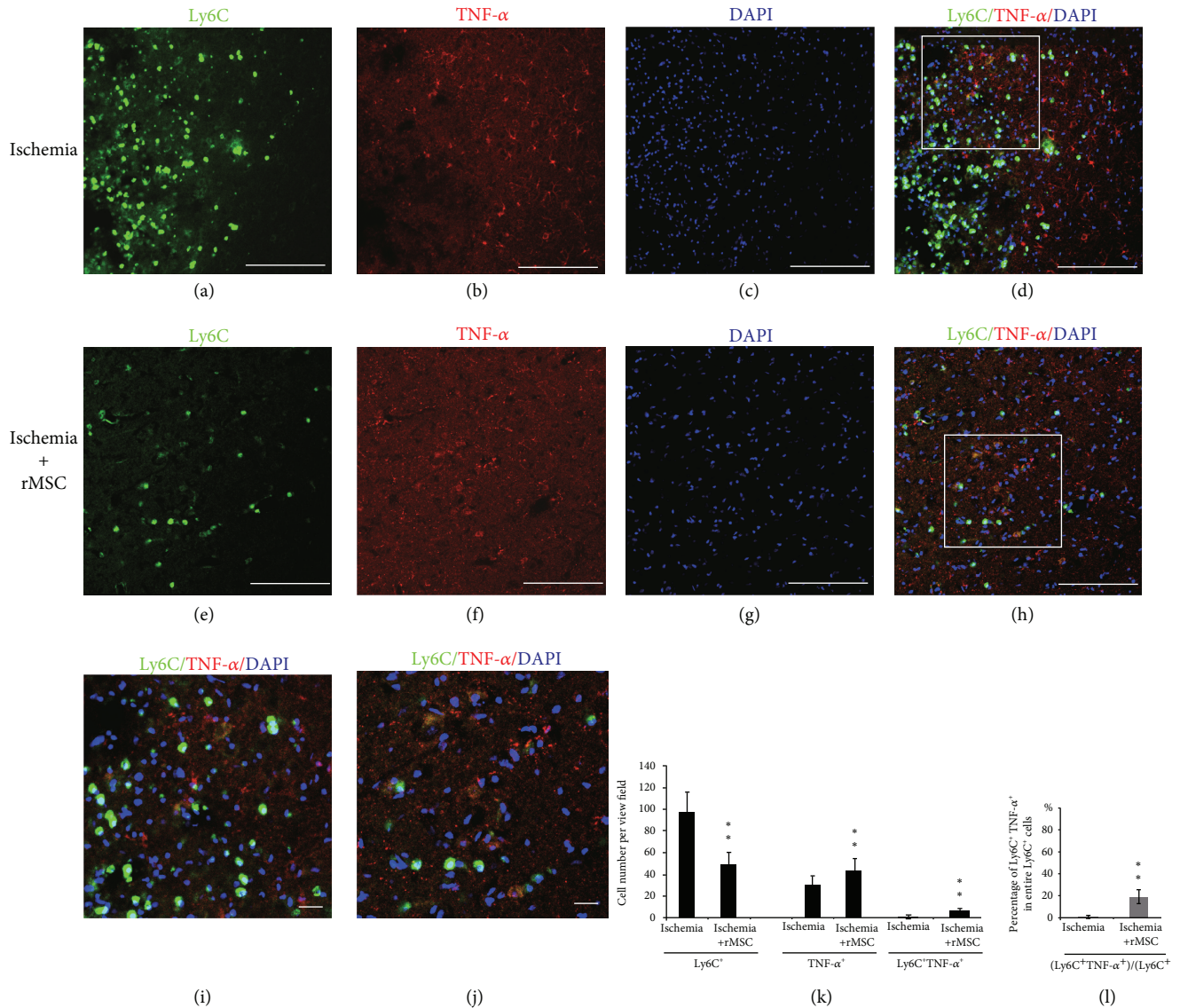
FIGURE 5: MSC increases the proportion of Ly6C$^+$ cells coexpressing TNF-α in the ischemia core of the cortex at day 2. (a–d) Distribution of Ly6C$^+$ and TNF-α^+ cells in the infarct area before MSC treatment. (e–h) Distribution of Ly6C$^+$ and TNF-α^+ cells in the infarct area after MSC treatment. (a, e) Ly6C staining. (b, f) TNF-α staining. (c, g) DAPI nucleus staining. (d) Double-stained Ly6C$^+$/TNF-α^+ cells scattered in the infarct area 2 days after dMCAO. (h) Ly6C$^+$/TNF-α^+ cells in the infarct area 2 days after MSC transplantation. (i) The magnified image of the square in (d). (j) The magnified image of the square in (h). (k) The quantities of Ly6C$^+$, TNF-α^+, and TNF-α^+/Ly6C$^+$ double-positive cells were increased in the infarct area. (l) The percentage of TNF-α^+/Ly6C$^+$ double-positive cells among the entire Ly6C$^+$ cells was increased by MSC treatment. ($^*p < 0.05$ and $^{**}p < 0.01$, as compared with the ischemia vehicle group). Arrow: double-labeled cells. $n = 5$; scale bar: (a–h) 250 μm, (i, j) 50 μm.

ischemia + MSC group. In the ischemia vehicle group (Figures 5(a)–5(d)), few TNF-α^+/Ly6C$^+$ double-positive cells were detected in the infarct area (Figures 5(d) and 5(i)). The numbers of TNF-α single-positive and TNF-α^+/Ly6C$^+$ double-positive cells were 31 ± 7.87 and 1.0 ± 1.73 per view field in the ischemia vehicle group, and the proportion of Ly6C$^+$ cells coexpressing TNF-α was 0.9 ± 1.2% (Figures 5(k) and 5(l)).

After MSC treatment, TNF-α expression was upregulated (Figures 5(e)–5(h)). The distribution of TNF-α^+/Ly6C$^+$ cells was still restricted within the infarct area and was not changed by MSC treatment (Figure 5(j)). The proportion of

Ly6C$^+$ cells coexpressing TNF-α was significantly increased (19.67 ± 6.54%) vs. the ischemia vehicle group (0.9 ± 2.2%, $p < 0.01$) (Figure 5(l)). Also, the number of TNF-α^+/Ly6C$^+$ double stained cells was enhanced to 7.5±0.87 per view field (Figure 5(k)).

3.6. Iba-1$^+$ Cells Are Not the Source of TNF-α or IL-1β Production in Rat Ischemia Brains and Cannot Be Induced by MSC Treatment. After the onset of ischemia in rats, in the contralateral hemisphere of the ischemia vehicle group, the Iba-1$^+$ cells with resting morphology were found in the intact cortex, striatum, and corpus callosum, but in these
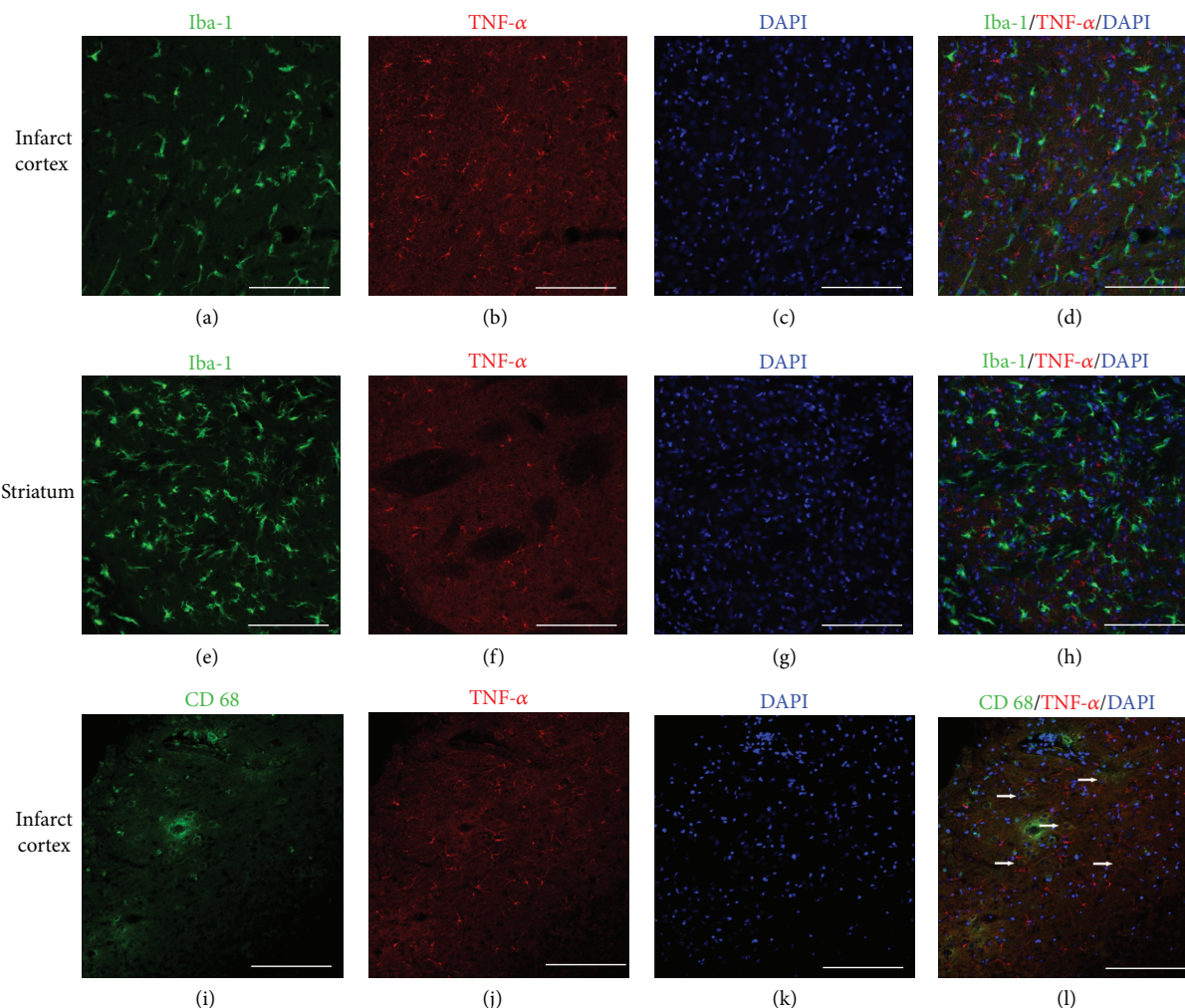
FIGURE 6: CD68$^+$ microglia but not Iba-1$^+$ cells express TNF-α in the ischemia ipsilateral hemisphere at day 2. (a–d) Distribution of Iba-1$^+$ and TNF-α^+ cells in the infarct areas after MSC transplantation. (e–h) Distribution of Iba-1$^+$ and TNF-α^+ cells in the striatum after MSC transplantation. (i–l) Distribution of CD68$^+$ and TNF-α^+ cells in the infarct areas after MSC transplantation. (a, e) Iba-1 staining. (i) CD68 staining. (b, f, j) TNF-α. (c, g, k) DAPI nucleus staining. (d) No double-stained Iba-1$^+$/TNF-α^+ cells were found in the infarct area after dMCAO. (h) No Iba-1+/TNF-α cells was found 2 days after MSC transplantation in the striatum. (l) Some CD68$^+$ cells in the infarct areas were positive for TNF-α. Arrow: double-labeled cells. Scale bar, 250 μm.

areas, TNF-α or IL-β reactivity was not detected (image not shown). In the ipsilateral hemisphere, Iba-1$^+$ microglia of both activated and resting forms were detected, but the resting phenotype existed in the infarct core cortex and intact striatum, whereas the active form was only found in the infarct core cortex.

In the infarct area, the spatial distribution of Iba-1 signals was correlated with those of TNF-α (Figures 6(a)–6(h)), although the two signals were never overlapped, whether in the infarct area (Figures 6(a)–6(d)) or the intact striatum and corpus callosum (Figures 6(e)–6(h)). Some CD68$^+$ cells in the infarct area (possibly activated microglia) were positive for TNF-α (Figures 6(i)–6(l)).

Similarly, the distribution of Iba-1$^+$ and IL-β^+ cells was spatially correlated but not overlapped (Figures 7(a)–7(h)). We have previously reported that the number of Iba-1$^+$ cells can be regulated by MSC infusion [7]. The current results indicated that in mild damage such as dMCAO, MSC treatment did not alter production levels of TNF-α or IL-β from Iba-1$^+$ cells. Iba-1$^+$ cells might not be the target of MSC regulation with respect to secretion of proinflammatory cytokines TNF-α and IL-β.

3.7. BDNF-Positive Cells Do Not Overlap with TNF-α- or IL-1β-Positive Cells.
Ischemia-induced accumulation of Ly6C$^+$ cells was localized in the ischemia core cortex and the surrounding areas, the same region where BDNF$^+$ cells resided. Here raises a question of whether BDNF and proinflammatory cytokines, such as TNF-α or IL-β, can be produced in the same cell positive for Ly6C.

We examined BDNF reactivity in TNF-α^+ and IL-β^+ cells (not restricted to macrophages) two days after stroke. No BDNF$^+$ cells were double labeled with TNF-α^+ or IL-β^+ cells in the brain, whether at the ischemia damaged areas or the intact areas (Figure 8).
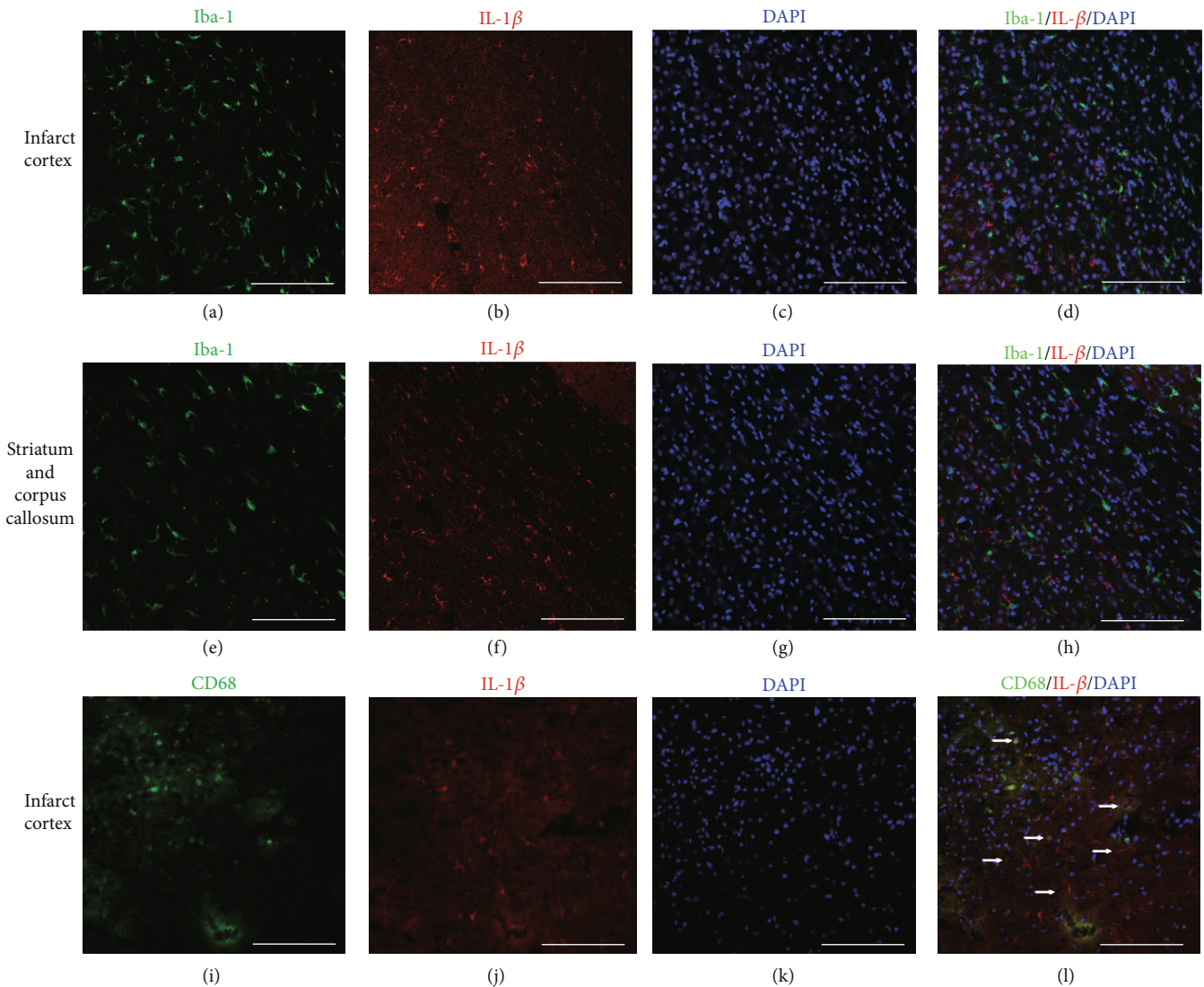
FIGURE 7: CD68^{+} microglia but not Iba-1^{+} cells express IL-β in the ischemic ipsilateral hemisphere at day 2. (a–d) Distribution of Iba-1^{+} cells and IL-β^{+} cells in the infarct areas after MSC transplantation. (e–h) Distribution of Iba-1^{+} cells and IL-β^{+} cells in the striatum after MSC transplantation. (i–l) Distribution of CD68^{+} cells and IL-β^{+} cells in the infarct areas after MSC transplantation. (a, e) Iba-1 staining. (i) CD68 staining. (b, f, j) IL-β. (c, g, k) DAPI nucleus staining. (d) No double-stained Iba-1^{+}/IL-β^{+} cells were found in the infarct area after dMCAO. (h) No Iba-1^{+}/IL-β^{+} cells were found 2 days after MSC transplantation in the striatum and corpus callosum after MSC transplantation. (i–l) Some CD68^{+} cells were positive for IL-β. Arrow: double-labeled cells. Scale bar, 250 μm.

3.8. Ly6C^{+} Cells Are Partly Positive for Neutrophil Antigen Neutrophil Elastase (NE) or T Cell Antigen CD3. We also tried to identify the cell populations that comprise the Ly6C^{+} cells in the ischemic brain. Since most of the granulocytes are neutrophils in the blood of rats, we selected neutrophil elastase (NE), to identify neutrophils in the brain. Approximately $8.62 \pm 2.62\%$ of Ly6C^{+} cells coexpressed NE in the infarct areas (Figure S2A–D). MSC transplantation did not change the proportion significantly ($9.31 \pm 2.45\%$).

We also examined the coexpression of Ly6C and T cell marker CD3. Around $15.21 \pm 4.62\%$ of Ly6C^{+} cells in the infarct areas coexpressed CD3 (Figure S2E–H). MSC transplantation did not significantly change the proportion either ($17.31 \pm 5.45\%$).

Here raised another question—could these overlapping cells also contribute to the production of BDNF, TNF-α, and IL-1β following dMCAO? We found that very few NE- or CD3-positive cells were double-stained with BDNF (<1%) (Figure S3A–H). In terms of IL-1β, it was expressed by nearly 2% NE^{+} neutrophils and 3–5% CD3^{+} T cells (Figure S4A–H). Only 1–2% NE^{+} neutrophils and 2–4% CD3^{+} T cells expressed TNF-α (Figure S5A–H).

The results suggest that it is probably the infiltrating monocytes/macrophages that are the major contributors for Ly6C^{+} cells that coexpress BDNF, TNF-α, or IL-1β.

4. Discussion

In the acute and subacute phases, resident microglial activation [28] and infiltration of circulating leukocytes to the
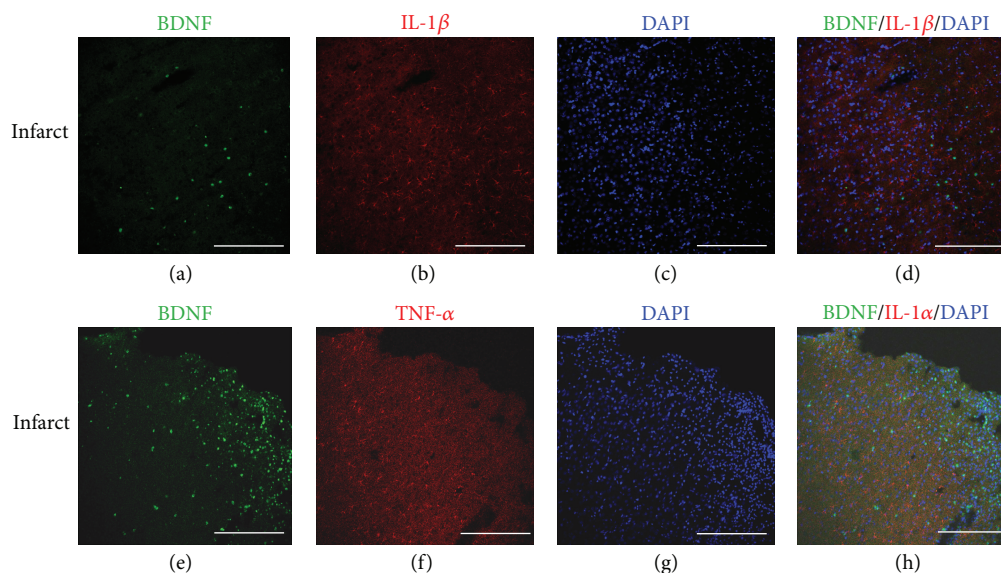
FIGURE 8: BDNF-producing cells do not overlap with TNF-α-or IL-1b-expressing cells at day 2. (a–d) Distribution of BDNF$^+$ cells and IL-β^+ cells in the infarct areas after MSC transplantation. (e–h) Distribution of BDNF$^+$ cells and TNF-α^+ cells in the infarct area after MSC transplantation. (a, e) BDNF staining. (b) IL-β. (f) TNF-α. (c, g) DAPI nucleus staining. (d) No double-stained BDNF$^+$/IL-β^+ cells were found in the infarct area after dMCAO. (h) No BDNF$^+$/TNF-α^+ cells were found 2 days after MSC transplantation in the striatum and corpus callosum after MSC transplantation. Scale bar, 250 μm.

ischemic brain [29] are the key features of the neuroimmunological responses to brain ischemia.

Previously, both microglia and infiltrated circulating leukocytes have been considered by many researchers to be harmful to the brain, since inhibition of some of these inflammatory responses improved the outcome in animal experiments. However, clinical trials aimed at inhibiting microglial activation or preventing leukocyte trafficking into the ischemic brain were unsuccessful [30]. It is nowadays accepted that the roles of inflammation in stroke are complicated in that they play both harmful and protective functions. This may be one reason why previous clinical trials of inhibiting immunological responses in stroke uniformly failed [30, 31].

Immune cells present in the healthy CNS and those recruited into stroke lesions are heterogeneous, including neutrophils, monocytes, macrophages, dendritic cells, T and B lymphocytes, and natural killer cells. Among these cells, monocytes/macrophages are important in the development of cerebral ischemia damages.

Given the importance of microglia and monocytes/macrophages in the stroke damage and that the marker "Iba-1" is normally expressed by both microglia and macrophages, it is important to identify a specific marker for infiltrated monocytes/macrophages in the ischemic brain.

Since Ly6C is widely used as the marker of mouse and human monocytes/macrophages, we selected Ly6C in this rat stroke study. Firstly, Ly6C$^+$ cells were not detected in brains of naïve rats and were only detected in brains of dMCAO rats. Secondly, depletion of peripheral immune cells by treatment with clodronate liposomes led to 80–90% reduction in the number of Ly6C$^+$ cells in dMCAO brains.

Together with the observation that Ly6C$^+$ cells were also CD45$^+$ in infarcted rat brains, it is suggested that Ly6C$^+$ cells in the brain represent circulation-derived infiltrated cells.

In ischemic brains, around 25% of Ly6C$^+$ cells were double-positive for Iba-1, and these double-stained cells were only detected inside the infarct areas. It is possible that some of the infiltrating Ly6C$^+$ immune cells may become Iba-1$^+$ over time.

CD68 is another important microglial marker. In our study, although, functionally, CD68$^+$ cells were a separated population from Iba-1$^+$ cells, morphologically, CD68$^+$ cells were part of Iba-1$^+$ cells (Figure S6). Less than 5% of Ly6C$^+$ cells were double-positive for CD68 (Figure S6), indicating that Ly6C$^+$ cells are mostly a different population than activated microglial cells.

Our results also suggest that Ly6C$^+$ cells in the ischemic brains were not purely monocytes/macrophages and included approximately 10% NE$^+$ neutrophils and 15% CD3$^+$ T cells. However, the infiltrated neutrophils and T cells did not produce BDNF, and only few of them (1–5%) were positive for TNF-α or IL-1β two days after dMCAO. Among the Ly6C$^+$ infiltrated cells, it is probably monocytes/macrophages that are the major contributors for production of BDNF, IL-1β, and TNF-α.

The spleen was reported to be a major reservoir of undifferentiated Ly6C$^+$ cells and proinflammatory cytokines that are readily mobilized during inflammatory processes, including stroke [5]. In this study, we found that dMCAO leads to infiltration of Ly6C$^+$ cells into the brain after stroke. It was reported that systemic administration of human umbilical cord blood progenitor cells (HUCBC) significantly reduces the number of macrophage/microglia in the injured brain

and maintains the size of the spleen [14]. In our study, the number of infiltrated Ly6C$^+$ cells was significantly reduced after MSC infusion. The MSCs that had migrated into the spleen may be responsible for these effects by an immune-inhibitory mechanism [32].

On the other hand, inflammation can also be seen as part of a protective response indispensable for limiting stroke-induced brain damage and inducing repair. The beneficial effects of inflammation at least include direct neuroprotection through neurotrophins.

One of the best understood trophic factors in the context of stroke is BDNF, which promotes neurological recovery following middle cerebral artery occlusion [33]. BDNF can be produced by neurons through neuronal activity-dependent exocytosis. Our previous study showed that BDNF can also be secreted by Iba-1$^+$ microglia [7]. Now we have demonstrated that monocytes/macrophages are probably another important participant that mediates the neurotrophic effects after dMCAO. At 48 h after ischemia onset, nearly 32.40% of Ly6C$^+$ cells were BDNF-positive. Although MSC infusion reduced the total number of Ly6C$^+$ cells in the brain, MSC treatment nevertheless enhanced the total number of BDNF$^+$/Ly6C$^+$ cells and increased the percentage of BDNF-producing cells among the infiltrated monocytes/macrophages in the infarct area two days after ischemia onset.

In our previous study, we have shown that in the infarct areas, proinflammatory cytokines IL-1β and TNF-α levels are increased [7]. However, the cell types that have contributed to production of these two cytokines have not been carefully examined. In the current study, we looked mainly into monocytes/macrophages and microglia for cytokine production. Quantification of cells using secretory proteins such as cytokines and growth factors by immunostaining is challenging. Perhaps a better approach to overcome the limitation is quantifying the transcript as validation, which will be employed in our future studies.

In terms of IL-1β, 12.30 ± 2.03% of infiltrated Ly6C$^+$ cells were positive for IL-1β after ischemia, and MSC treatment increased the percentage to 38.62 ± 6.99%. MSC treatment also increased the numbers of IL-1β^+ and IL-1β^+/Ly6C$^+$ cells from 24.75 ± 7.35 and 12.5 ± 2.18 to 41.00 ± 6.82 and 23.75 ± 3.16 per view field, respectively.

Interestingly, very few Ly6C$^+$ cells expressed TNF-α before MSC transplantation (0.9 ± 1.0 per view field). After MSC treatment, although the quantity of Ly6C$^+$ cells decreased in the brain, the number of TNF-α^+/Ly6C$^+$ cells and its proportion among Ly6C$^+$ cells both increased.

Ritzel et al. have shown that, in mice, 72 h after a 90 min MCAO, monocytes/macrophages accumulated in the ischemic brain compared to sham controls. Microglia produce relatively higher levels of reactive oxygen species and TNF-α, whereas monocytes/macrophages are the predominant IL-1β producer [20]. Unexpectedly, in the current study, Iba-1$^+$ microglial cells did not express any significant level of TNF-α or IL-1β, whether in the infarct area, the intact cortex and striatum, or the corpus callosum. Some CD68$^+$ cells (possibly activated microglia in our study) were positive for TNF-α or IL-1β (Figures 6 and 7). Ischemic damage and MSC transplantation after stroke did not induce the Iba-1$^+$

cells to produce TNF-α or IL-1β either. It seems that, in the current experimental setting and with respect to only microglia and monocytes/macrophages, infiltrated monocytes/macrophages, rather than microglia, are the predominant contributors for IL-1β and TNF-α production.

In our study, intravenous transplantation of mesenchymal stem cells reduces the number of infiltrated macrophages but enhances the proportions positive for BDNF, TNF-α, and IL-1β in the infarct cortices of dMCAO rats. The possible mechanisms may include, but may not be limited to, the following.

The majority of infused MSCs are trapped in the lung and spleen. Spleen is one of the organs that play an important role in the periphery after stroke. In the case of severe ischemia, the spleen contracts under the regulation of the hypothalamic-pituitary-adrenal axis and the sympathetic nervous system. This reduction in spleen size is associated with increased release of immune cells and proinflammatory cytokines into the blood, a greater extent of infiltration of leukocytes and monocytes, and a higher level of microglial activation in the brain. It seems that intravenous infusion of MSCs may suppress the "overactivated" inflammation and immune reaction in the spleen, reduce the influx of immune cells, prevent the exhaustion of immune capacities of spleen, and eventually avoid immunosuppression in stroke patients [34].

A noteworthy phenomenon was that only the Ly6C$^+$ cells located in the infarct area were positive for BDNF or proinflammatory cytokines IL-1β and TNF-α. The majority of Ly6C$^+$ cells surrounding the infarct area were negative for BDNF, TNF-α, and IL-1β. Two interesting aspects were implicated in this observation. First, after infusion, MSCs mostly accumulated at the peri-infarct areas too. The spatial correlation suggests that MSCs may have influenced the infiltrated cells through a paracrine and/or cell-cell contact mechanism. Second, Ly6C$^+$ cells in the infarct areas could be positive for either BDNF or proinflammatory cytokines (IL-1β and TNF-α), but not for both, whereas Ly6C$^+$ cells at the peri-infarct areas were mostly negative for all three. These results suggest that the infiltrated cells, including monocytes, may be intrinsically heterogeneous and can react differentially to different microenvironments. Microglia can be categorized into M1 and M2 subtypes, and the two subtypes can be switched in a certain context [34, 35]. Microglia originate from the hematopoietic lineage and are derived from the infiltrated monocytes during embryo development [21]. Like microglia, monocytes are possibly heterogeneous as well. Further efforts are warranted to identify the molecular cues in the infarct and peri-infarct areas that can induce infiltrated monocytes to assume different phenotypes. Once identified, these cues may offer a potential candidate for manipulating the functions of macrophages and improve the treatment of stroke.

Data Availability

The data used to support the findings of this study are available from the corresponding author upon request.

Conflicts of Interest

The authors declare that there is no conflict of interest regarding the publication of this paper.

Authors' Contributions

Yunqian Guan, Xiaobo Li, and Wenxiu Yu contributed equally to this work.

Acknowledgments

Supplementary Materials

Supplementary Figure 1: Ly6C$^+$ cells in ischemic brains are derived from periphery circulation at day 2. Supplementary Figure 2: a small part of Ly6C$^+$ cells costained with neutrophil elastase and CD3 at day 2. Supplementary Figure 3: infiltrated neutrophils and T cells minimally contribute to BDNF production at day 2. Supplementary Figure 4: infiltrated neutrophils and T cells minimally contribute to IL-1β production at day 2. Supplementary Figure 5: infiltrated neutrophils and T cells minimally contribute to TNF-α production at day 2. Supplementary Figure 6: the overlapping of CD68$^+$ cells with Ly6C$^+$ and Iba-1$^+$ cells, respectively, at day 2. (Supplementary Materials)

References

[1] L. Crigler, R. C. Robey, A. Asawachaicharn, D. Gaupp, and D. G. Phinney, "Human mesenchymal stem cell subpopulations express a variety of neuro-regulatory molecules and promote neuronal cell survival and neuritogenesis," *Experimental Neurology*, vol. 198, no. 1, pp. 54–64, 2006.

[2] A. Chen, L.-J. Xiong, Y. Tong, and M. Mao, "The neuroprotective roles of BDNF in hypoxic ischemic brain injury," *Biomedical Reports*, vol. 1, no. 2, pp. 167–176, 2013.

[3] P. Kaengkan, S. E. Baek, J. Y. Kim et al., "Administration of mesenchymal stem cells and ziprasidone enhanced amelioration of ischemic brain damage in rats," *Molecules and Cells*, vol. 36, no. 6, pp. 534–541, 2013.

[4] L. Du, Y. Yu, H. Ma et al., "Hypoxia enhances protective effect of placental-derived mesenchymal stem cells on damaged intestinal epithelial cells by promoting secretion of insulin-like growth factor-1," *International Journal of Molecular Sciences*, vol. 15, no. 2, pp. 1983–2002, 2014.

[5] L. N. Zhou, S. C. Li, X. Y. Li, H. Ge, and H. M. Li, "Identification of differential protein-coding gene expressions in early phase lung adenocarcinoma," *Thoracic Cancer*, vol. 9, no. 2, pp. 234–240, 2018.

[6] L. Garcia-Bonilla, G. Faraco, J. Moore et al., "Spatio-temporal profile, phenotypic diversity, and fate of recruited monocytes into the post-ischemic brain," *Journal of Neuroinflammation*, vol. 13, no. 1, p. 285, 2016.

[7] A. Gupta, M. R. Capoor, T. Shende et al., "Comparative evaluation of galactomannan test with bronchoalveolar lavage and serum for the diagnosis of invasive aspergillosis in patients with hematological malignancies," *Journal of Laboratory Physicians*, vol. 9, no. 4, pp. 234–238, 2017.

[8] B. Haghshenas, Y. Nami, A. Almasi et al., "Isolation and characterization of probiotics from dairies," *Iranian Journal of Microbiology*, vol. 9, no. 4, pp. 234–243, 2017.

[9] H. X. Chu, H. A. Kim, S. Lee, B. R. S. Broughton, G. R. Drummond, and C. G. Sobey, "Evidence of CCR2-independent transmigration of Ly6C^{hi} monocytes into the brain after permanent cerebral ischemia in mice," *Brain Research*, vol. 1637, pp. 118–127, 2016.

[10] H. Lund, M. Pieber, and R. A. Harris, "Lessons learned about neurodegeneration from microglia and monocyte depletion studies," *Frontiers in Aging Neuroscience*, vol. 9, 2017.

[11] N. Karlupia, N. C. Manley, K. Prasad, R. Schäfer, and G. K. Steinberg, "Intraarterial transplantation of human umbilical cord blood mononuclear cells is more efficacious and safer compared with umbilical cord mesenchymal stromal cells in a rodent stroke model," *Stem Cell Research & Therapy*, vol. 5, no. 2, p. 45, 2014.

[12] G. Pajenda, D. Hercher, G. Márton et al., "Spatiotemporally limited BDNF and GDNF overexpression rescues motoneurons destined to die and induces elongative axon growth," *Experimental Neurology*, vol. 261, pp. 367–376, 2014.

[13] E. Kim, J. Yang, C. D. Beltran, and S. Cho, "Role of spleen-derived monocytes/macrophages in acute ischemic brain injury," *Journal of Cerebral Blood Flow & Metabolism*, vol. 34, no. 8, pp. 1411–1419, 2014.

[14] M. Vendrame, J. Cassady, J. Newcomb et al., "Infusion of human umbilical cord blood cells in a rat model of stroke dose-dependently rescues behavioral deficits and reduces infarct volume," *Stroke*, vol. 35, no. 10, pp. 2390–2395, 2004.

[15] G. Ren, L. Zhang, X. Zhao et al., "Mesenchymal stem cell-mediated immunosuppression occurs via concerted action of chemokines and nitric oxide," *Cell Stem Cell*, vol. 2, no. 2, pp. 141–150, 2008.

[16] O. B. Dimitrijevic, S. M. Stamatovic, R. F. Keep, and A. V. Andjelkovic, "Absence of the chemokine receptor CCR2 protects against cerebral ischemia/reperfusion injury in mice," *Stroke*, vol. 38, no. 4, pp. 1345–1353, 2007.

[17] Y. Chen, J. M. Hallenbeck, C. Ruetzler et al., "Overexpression of monocyte chemoattractant protein 1 in the brain exacerbates ischemic brain injury and is associated with recruitment of inflammatory cells," *Journal of Cerebral Blood Flow & Metabolism*, vol. 23, no. 6, pp. 748–755, 2016.

[18] S. M. Allan, P. J. Tyrrell, and N. J. Rothwell, "Interleukin-1 and neuronal injury," *Nature Reviews Immunology*, vol. 5, no. 8, pp. 629–640, 2005.

[19] B. H. Clausen, M. Degn, N. A. Martin et al., "Systemically administered anti-TNF therapy ameliorates functional outcomes after focal cerebral ischemia," *Journal of Neuroinflammation*, vol. 11, no. 1, p. 203, 2014.

[20] R. M. Ritzel, A. R. Patel, J. M. Grenier et al., "Functional differences between microglia and monocytes after ischemic stroke," *Journal of Neuroinflammation*, vol. 12, no. 1, p. 106, 2015.

[21] Y. Ma, Y. Li, L. Jiang et al., "Macrophage depletion reduced brain injury following middle cerebral artery occlusion in mice," *Journal of Neuroinflammation*, vol. 13, no. 1, p. 38, 2016.

[22] M. Gliem, A. K. Mausberg, J. I. Lee et al., "Macrophages prevent hemorrhagic infarct transformation in murine stroke models," *Annals of Neurology*, vol. 71, no. 6, pp. 743–752, 2012.

[23] M. Pekny and M. Nilsson, "Astrocyte activation and reactive gliosis," *Glia*, vol. 50, no. 4, pp. 427–434, 2005.

[24] M. Schroeter, K. Schiene, M. Kraemer et al., "Astroglial responses in photochemically induced focal ischemia of the rat cortex," *Experimental Brain Research*, vol. 106, no. 1, pp. 1–6, 1995.

[25] P. Gelosa, D. Lecca, M. Fumagalli et al., "Microglia is a key player in the reduction of stroke damage promoted by the new antithrombotic agent ticagrelor," *Journal of Cerebral Blood Flow & Metabolism*, vol. 34, no. 6, pp. 979–988, 2014.

[26] M. Simsek and R. Duman, "Investigation of effect of 1,8-cineole on antimicrobial activity of chlorhexidine gluconate," *Pharmacognosy Research*, vol. 9, no. 3, pp. 234–237, 2017.

[27] Z. Chen and T. D. Palmer, "Differential roles of TNFR1 and TNFR2 signaling in adult hippocampal neurogenesis," *Brain, Behavior, and Immunity*, vol. 30, pp. 45–53, 2013.

[28] T. Mabuchi, K. Kitagawa, T. Ohtsuki et al., "Contribution of microglia/macrophages to expansion of infarction and response of oligodendrocytes after focal cerebral ischemia in rats," *Stroke*, vol. 31, no. 7, pp. 1735–1743, 2000.

[29] C. Iadecola and J. Anrather, "The immunology of stroke: from mechanisms to translation," *Nature Medicine*, vol. 17, no. 7, pp. 796–808, 2011.

[30] Y. Fu, Q. Liu, J. Anrather, and F. D. Shi, "Immune interventions in stroke," *Nature Reviews Neurology*, vol. 11, no. 9, pp. 524–535, 2015.

[31] M. Gliem, M. Schwaninger, and S. Jander, "Protective features of peripheral monocytes/macrophages in stroke," *Biochimica et Biophysica Acta (BBA) - Molecular Basis of Disease*, vol. 1862, no. 3, pp. 329–338, 2016.

[32] S. A. Acosta, N. Tajiri, J. Hoover, Y. Kaneko, and C. V. Borlongan, "Intravenous bone marrow stem cell grafts preferentially migrate to spleen and abrogate chronic inflammation in stroke," *Stroke*, vol. 46, no. 9, pp. 2616–2627, 2015.

[33] S. Yousuf, F. Atif, I. Sayeed, J. Wang, and D. G. Stein, "Post-stroke infections exacerbate ischemic brain injury in middle-aged rats: immunomodulation and neuroprotection by progesterone," *Neuroscience*, vol. 239, pp. 92–102, 2013.

[34] Y. Guan, X. Ji, J. Chen, Y. Alex Zhang, and Z. Chen, "Mesenchymal stem cells for stroke therapy," in *Bone Marrow Stem Cell Therapy for Stroke*, K. Jin, X. Ji, and Q. Zhuge, Eds., pp. 107–132, Springer Singapore, Singapore, 2017.

[35] Y. Ohya, M. Osaki, S. Sakai et al., "A case of recurrent ischemic stroke due to intravascular lymphomatosis, undiagnosed by random skin biopsy and brain imaging," *Case Reports in Neurology*, vol. 9, no. 3, pp. 234–240, 2017.

Review Article

Mesenchymal Stem Cells in Primary Sjögren's Syndrome: Prospective and Challenges

Weiqian Chen,[1] Ye Yu,[1] Jilin Ma,[2] Nancy Olsen,[3] and Jin Lin [1]

[1]*Division of Rheumatology, the First Affiliated Hospital, College of Medicine, Zhejiang University, Hangzhou, 310003 Zhejiang Province, China*
[2]*Division of Nephrology, Zhejiang Traditional Chinese Medicine and Western Medicine Hospital, Hangzhou, 310000 Zhejiang Province, China*
[3]*Division of Rheumatology, Department of Medicine, Penn State University Hershey College of Medicine Hershey, 17033, USA*

Correspondence should be addressed to Jin Lin; linjinzju@zju.edu.cn

Primary Sjögren's syndrome (pSS) is a chronic systemic inflammatory autoimmune disease characterized by lymphocytic infiltrates in exocrine glands. Current approaches do not control harmful autoimmune attacks or prevent irreversible damage and have considerable side effects. Mesenchymal stem cells (MSCs) have been effective in the treatment of several autoimmune diseases. The objective of this review is to illustrate the potential therapeutic role of MSCs in pSS. We summarize the recent advances in what is known about their immunomodulatory function and therapeutic applications in pSS. MSC transfusion can suppress autoimmunity and restore salivary gland secretory function in mouse models and patients with pSS by inducing regulatory T cells, suppressing Th1, Th17, and T follicular helper cell responses. In addition, MSCs can differentiate into salivary epithelial cells, presenting an option as a suitable alternative treatment. We also discuss current bioengineering methods which improve functions of MSCs for pSS. However, there remain many challenges to overcome before their wide clinical application.

1. Introduction

Primary Sjögren's syndrome (pSS) is a chronic, systemic autoimmune disease characterized by lymphocytic infiltrates in salivary and lacrimal glands which lead to the destruction of these glands. It affects globally 0.05–1% of people, with manifestations including xerostomia (dry mouth), dental caries, and xerophthalmia (dry eye) [1]. Activated B lymphocytes are another hallmark of the disease [2]; many antibodies appear in the circulation and tissues. Accordingly, systemic extraglandular involvement is common, including synovitis, interstitial lung disease, neuropathy, renal disease, vasculitis, and autoimmune cytopenias [3]. Furthermore, approximately 5–10% of patients may develop lymphoma, mainly the mucosa-associated lymphoid tissue non-Hodgkin lymphoma, which represents the most severe complication of the disease [4]. Although the exact etiology is unclear, it is known that adaptive and innate immune cell imbalances are involved in the pathogenesis of pSS [5–7].

Current approaches such as traditional disease-modifying antirheumatic drugs and biologic agents do not cure this disease and have considerable side and toxic effects [8]. Thus, the development of novel treatments is critically important for pSS.

Mesenchymal stem cells (MSCs), a group of mesodermal and ectodermal origin multipotent stromal cells, are first discovered by Friedenstein et al. [9]. MSCs have a capacity of self-renewal and differentiation into osteoblasts, adipocytes, and chondrocytes [10, 11]. They are of interest due to their rapid proliferation *in vitro* and strong immunomodulation [12]. Notably, MSCs have been successfully isolated from almost all adult tissues, including bone marrow, umbilical cord blood, adipose tissue, dental tissue, skin, and placenta [13–17]. Until now, bone marrow MSCs (BMSCs) and umbilical cord MSCs (UMSCs) have been most widely studied. Subsequently, other types of MSCs are reported, such as gingiva-derived MSCs (GMSCs) and adipose-derived MSCs (AMSCs). Unlike MSCs in bone marrow and umbilical cord
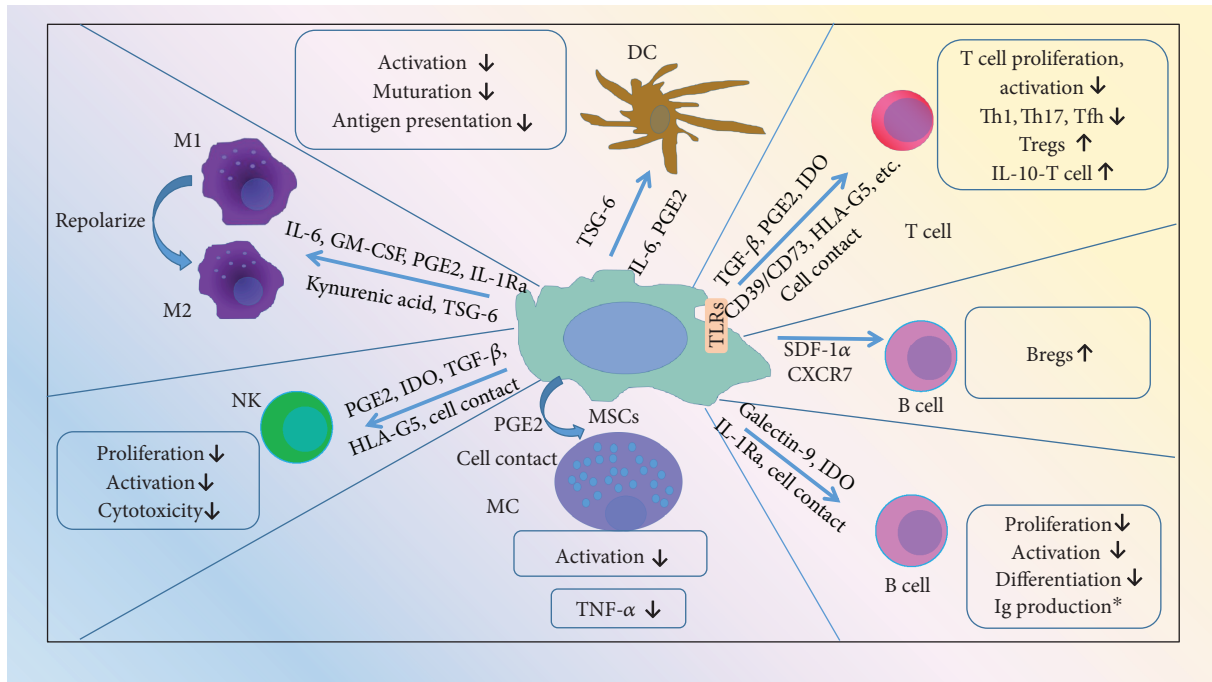
FIGURE 1: Immunomodulatory properties of mesenchymal stem cells. DC: dendritic cells; TSG-6: TNF-α-stimulated gene 6; PGE2: prostaglandin E2; M1: classically activated macrophages; M2: alternatively activated macrophages; GM-CSF: granulocyte-macrophage colony stimulating factor; IL-1Ra: IL-1 receptor antagonist; NK: natural killer T cells; IDO: indoleamine 2,3-dioxygenase; TGF-β: transforming growth factor-beta; HLA-G5: human leukocyte antigen-G5; MC: mast cells; MSCs: mesenchymal stem cells; Th: T helper; Tfh: T follicular helper cell; Tregs: regulatory T cells; TLRs: Toll-like receptors; SDF-1α: stromal derived factor-1α; CXCR7: CXC chemokine receptor 7; Bregs: regulatory B cells; *: controversial.

blood, GMSCs and AMSCs are both abundant and easily accessible, and they can often be obtained as a discarded biological sample following dental procedures or abdominal surgery. GMSCs and AMSCs are relatively easy to isolate, homogenous and proliferate rapidly *in vitro* [18]. Interestingly, no tumor is observed in the mice which are injected with GMSCs. It indicated GMSCs are nontumorigenic [19]. AMSCs also show a low tendency to develop a tumor [20].

Here, we describe the therapeutic role of MSCs in pSS based on recent relevant publications. Indeed, MSCs have been effective in treating autoimmune diseases such as systemic lupus erythematosus, rheumatoid arthritis, systemic sclerosis, and type 1 diabetes mellitus. Moreover, these treatments have no significant side effects [21–27]. Several years ago, scientists summarized the preliminary studies of MSC treatment for salivary gland dysfunction and xerostomia [28, 29]. A recently published review focuses on MSCs for treating autoimmune dacryoadenitis but not the other aspects of pSS [30]. Existing evidence supports the crucial role of MSCs in the treatment of animal models and patients with pSS. MSCs may also differentiate into salivary epithelial cells, presenting an option as a suitable alternative treatment [31, 32]. In this review, we summarize the immunomodulatory effects of MSCs both in the adaptive and the innate immune responses. The defective function of MSCs in pSS is then discussed, followed by a summary of the use of MSCs in the treatment of patients with pSS or animal models. Finally, the role of bioengineering in enhancing MSC treatment is discussed.

2. Immunomodulatory Properties of MSCs on Adaptive and Innate Immune Responses

The most attractive property of MSCs is their immunosuppression on both adaptive and innate immune responses. MSCs exert major immunomodulatory effects through cell to cell contact and release of soluble factors such as prostaglandin E2 (PGE2), indoleamine 2,3-dioxygenase (IDO), nitric oxide, transforming growth factor-beta (TGF-β), human leukocyte antigen-G5 (HLA-G5), CD39/CD73, hepatic growth factor (HGF), interleukin- (IL-) 10, IL-6, adenosine, kynurenic acid, TNF-α-stimulated gene 6 (TSG-6), heme oxygenase-1 (HO-1), IL-1 receptor antagonist (IL-1Ra), programmed death-1 ligand 1 (PD-L1), and galectins [33–36]. The mechanisms are illustrated (Figure 1).

2.1. Immunomodulatory Functions on Adaptive Immune Cells. The essential cell populations in the adaptive immune system are effector T cells, regulatory T cells (Tregs), and B cells. Abundant evidence supports a role for MSCs to exert immunoregulatory functions on T cells by suppressing proliferation and activation or regulating differentiation [15, 16, 22, 27, 35–48]. Murine BMSCs inhibit naive and memory T cell responses to their cognate antigens [37]. Murine BMSCs markedly suppress xenogeneic graft-versus-host disease (x-GVHD)-derived T helper (Th) 1 cells through adenosine accumulation [38] and also curb experimental autoimmune encephalomyelitis- (EAE-) derived Th17 cell activation in a CC chemokine ligand 2-dependent manner

[27]. Recently, it is reported that human BMSCs-derived IL-1Ra can inhibit inflammation via suppressing the Th17 differentiation [39]. Interestingly, human BMSCs and murine BMSCs themselves can produce IL-17, but IL-17+ MSC displays an impaired immunosuppressive capacity [40]. Furthermore, BMSCs could induce Tregs and IL-10-producing T cells through the release of soluble factors such as PGE2, TGF-β, and HLA-G5 or cell-cell contact [41–43]. Moreover, human BMSCs can express Toll-like receptors (TLRs). Engagement of different TLRs in MSCs enhances their immunosuppressive properties by inducing IDO or impairing Notch signaling [46, 47]. Other MSCs, for example, UMSCs and AMSCs, can also significantly suppress T cell proliferation and activation [16, 44]. AMSCs inhibit the proliferative response and the production of inflammatory cytokines by antigen-specific CD4 and CD8+ T cells. Also, the numbers of IL-10-producing T cells and monocytes are significantly augmented upon AMSC treatment [16]. It is demonstrated that GMSCs suppress T cell proliferation and activation via interferon-γ- (IFN-γ-) induced stimulation of IDO and IL-10 [15]. Moreover, GMSCs ameliorate colonic inflammation by enhancing Tregs and IL-10 expression in mice [15]. GMSCs could significantly inhibit Th1 and Th17 cells and reduce the production of inflammatory cytokines (IFN-γ, IL-17A) via CD39/CD73 signaling [22, 45].

T follicular helper cells (Tfh) are recognized as crucial effector cells for B cell maturation and immunoglobulin production. UMSCs are found to suppress the differentiation of Tfh via the secretion of IDO [26, 49]. Most importantly, BMSCs can inhibit the Tfh response in lupus-prone mice [50]. Furthermore, it is suggested that BMSCs and UMSCs could indirectly affect the maturation and immunoglobulin production of B cells by inhibiting the Tfh immune reaction.

As we know, B cell development is dependent on the interaction of B cell progenitor and stromal cells, which provides a supportive microenvironment for B cells. BMSCs can suppress B cell proliferation, differentiation toward plasmablast, and immunoglobulin production dependent on galectin-9 or IL-1Ra signaling [51, 52]. BMSCs and AMSCs both suppress activation of blood B cells by phytohemagglutinin stimulation, but UMSCs do not display an inhibitory effect [53]. Besides, BMSCs could affect chemotactic properties of B cells, because chemokine receptors (CCR) and CXC chemokine receptors (CXCR), such as CXCR4, CXCR5, and CCR7, are decreased after B cell-BMSC coculture. However, B cell costimulatory molecules CD40, CD80, and CD86 and production of various cytokines are unaffected by BMSCs [54]. Interestingly, BMSCs do not inhibit B cell proliferation but only in the presence of inflammatory cytokine IFN-γ [55]. The suppressive effect of IFN-γ is related to its ability to stimulate the release of IDO by BMSCs, which in turn inhibits the proliferation of B cells [55]. Another group finds that enhanced autoantibody production is companied by increased plasma cells after BMSC administration [56].

Several years ago, a new regulatory subset called B regulatory cells (Bregs) was identified. These cells can interact with pathogenic T cells to inhibit harmful immune responses [57]. Transfer of UMSCs ameliorates experimental colitis by inducing Bregs [58]. AMSC treatment expands the Breg population in lupus mice in vivo [59]. Further study finds that murine BMSCs promote Bregs through stromal derived factor-1α (SDF-1α) and its receptor CXCR7-mediated signaling [60].

2.2. Immunomodulatory Functions on Innate Immune Cells. The innate immune system is the first line of host defense and consists of several types of immune cells including dendritic cells (DC), macrophages, natural killer T cells (NK), and mast cells (MC). MSCs exhibit potent immunomodulatory effects on these cells which may play an important role in the pathogenesis of pSS [5]. Human BMSCs can suppress activation and maturation of DC and impair their antigen-presenting ability through the release of TSG-6 [61–63]. Other research finds that the soluble factor IL-6 is involved in the immunomodulatory mechanism mediated by murine BMSCs through partial inhibition of DC differentiation [64]. Murine BMSCs impair TLR4-induced activation of DC resulting in downregulation of antigen presentation to T cells [65]. Human GMSCs can significantly blunt the maturation and activation of DC via PGE2-dependent mechanisms [66]. Human UMSCs can facilitate the shift of monocytes toward IL-10 producing phenotypes through the production of IL-6 and HGF [67].

MSCs reprogram macrophages into the anti-inflammatory M2 phenotype through the production of IL-6, granulocyte-macrophage colony stimulating factor (GM-CSF), PGE2, kynurenic acid, TSG-6, or IL-1Ra [52, 68–71]. Human BMSCs are activated by TNF-α to produce an anti-inflammatory mediator, TSG-6, and thereby create a negative feedback loop that attenuates inflammation by reducing TLR2-mediated signaling in resident macrophages [72]. MSCs have been shown to interact with NK cells dependent on their activation state. When resting NK cells are exposed to IL-2, the expression levels of activating receptors such as NKG2D, NKp30, and NKp44 are increased. Human BMSCs could inhibit IL-2-induced proliferation of resting NK cells, whereas they partially affect proliferation of activated NK cells. Human BMSCs also downregulated the activation and cytotoxicity of NK cells by mechanisms involving PGE2, IDO, TGF-β, HLA-G5, adenosine, or cell contact [43, 53, 73–75]. Interestingly, human NK cells secrete NAP-2 (CXCL7), a chemokine that can induce MSC migration to repair damaged tissue [76]. And GMSCs are capable of exerting suppressive effects on mast cells through the release of PGE2 and cell-cell contact both in vitro and in vivo [66, 77].

Recently, it has been thought that the immunomodulatory capabilities of MSCs are not constitutive but rather are subject to the inflammatory milieu or different signals. MSCs primed with IFN-γ or the stimulation of TLR signaling is required to induce their immunosuppressive phenotype [47, 55]. Proinflammatory cytokines such as TNF-α and IL-1 have been shown to enhance the effect of IFN-γ on MSC priming through the production of IDO or PGE2 [55, 78, 79]. The activation of TLR3 may promote the polarization of MSCs into immune-suppressive phenotype, while TLR4 stimulation may induce polarization of MSCs toward

proinflammatory phenotype [80]. Therefore, MSCs show a plastic behavior and switch into an immunosuppressive phenotype depending on microenvironmental conditions.

3. BMSCs and Salivary MSCs Are Both Defective in pSS

Some evidence shows that BMSCs are defective in immuno-regulatory functions in animal models and patients with pSS [81]. BMSCs have a significantly lower proliferative capacity and less osteogenic and adipogenic differentiation potentials in nonobese diabetic (NOD) mice. BMSCs derived from NOD mice fail to suppress T cell proliferation. CD4$^+$Foxp3^{+-} Treg cells are much lower when splenocytes are cocul-tured with BMSCs from NOD mice. Furthermore, BMSCs obtained from pSS patients show an impaired suppressive effect on PBMC proliferative responses. Interestingly, acti-vated T cells can induce BMSC apoptosis via the Fas/Fas ligand pathway [82]. IFN-γ synergistically enhances TNF-α–induced BMSC apoptosis [83, 84]. Furthermore, proin-flammatory T cells inhibit the ability of BMSCs to repair damaged tissue. When the concentrations of IFN-γ and TNF-α are decreased, it significantly improves the function of BMSCs in repairing the tissue [83]. As we know, Th1 (IFN-γ and TNF-α)-mediated inflammation is a key feature in the salivary gland pathology [85]. T cells are activated in patients with pSS [86]. These findings suggest that T cell-induced BMSC apoptosis may contribute to BMSC impair-ment in pSS. Collectively, these results demonstrate that the biological and regulatory functions of BMSCs are impaired in pSS [81].

Recently, MSCs have been also found in the salivary glands of patients with pSS. Such organ-specific MSCs may have advantages for treatment of the specific tissue of origin since they could directly act on the target cell. Jeong et al. [87] efficiently isolates and amplifies MSCs in large amounts from human parotid and submandibular sal-ivary glands in vitro. These cells express the same charac-teristic MSC markers; they are negative for hematopoietic stem cell and salivary gland epithelium markers. They are able to differentiate into adipogenic, osteogenic, and chon-drogenic cells and notably into amylase-expressing cells. Transplantation of SGSCs restores salivary gland function in radiation-damaged rat salivary glands [87]. However, MSCs from the labial glands of patients with pSS have a deficiency in salivary gland-like cell differentiation [88]. Taken together, BMSCs and salivary MSCs are both defec-tive in patients with pSS disease condition, meaning that it is not ideal to treat patients using their own MSCs. We may use allogeneic MSCs for the treatment of pSS, due to non-immunogenic characteristics and low or absent expression of non-major histocompatibility complex- (MHC-) I and MHC-II [12].

4. The Application of MSCs in the Treatment of pSS

pSS is a disease triggered by the breakdown of self–nonself dis-crimination and a subsequent autoreactive immune response.

Salivary gland pathology is mainly a Th1-mediated immune reaction [85]. Th17 and Tfh cells are also associated with inflammation and clinical profiles in pSS [49, 86]. The Treg percentage is altered in the peripheral blood [89–91], and their suppressive function is compromised in pSS [92]. In contrast, another group reports that the Treg subset did not change in patients with pSS [93]. Therefore, the imbalance of these immune cells contributes to the pathogenesis of pSS. It is clear that MSCs could possess potent immuno-modulatory functions on both adaptive and innate immune cells and especially reset the immune imbalance by upregu-lating Tregs and downregulating Th1, Th17, or Tfh cells. In addition, MSCs can differentiate into salivary epithelial cells, presenting an option as a suitable alternative treatment for pSS. The unique immunomodulatory and biological proper-ties of MSCs make them candidates for cell therapy to repair tissue and organ damages caused by pSS. We have summa-rized the applications of MSCs in the treatment of patients with pSS or in animal models (Table 1).

MSC treatment ameliorates sialadenitis in the mouse model and in patients with pSS partly through reducing the proliferation of T cells, decreasing Th1, Th17, and Tfh cells, and increasing Tregs [44, 49, 81, 94–98]. The pSS patients tolerate the allogeneic UMSCs well, have an improvement in symptoms and a decrease in serum anti-SSA/anti-SSB antibody without significant adverse events [81]. Interest-ingly, infused allogeneic BMSCs could migrate toward the inflammatory regions in an SDF-1-dependent manner, as neutralization of SDF-1 ligand CXCR4 abolishes the effec-tiveness of BMSC treatment. Therefore, allogeneic BMSCs might target local sialadenitis and systemic inflammatory responses in pSS patients by a mechanism that is dependent on SDF-1/CXCR4 signaling [81]. Another team finds that treatment with BMSCs prevents a decline in the salivary flow rate and lymphocytic infiltrations in the salivary glands of NOD mice [94]. Furthermore, BMSCs enhance tear produc-tion in the NOD mouse model, due to decreased inflamma-tion and increased expression of aquaporin 5 [95]. Although the number of lymphocytic foci in the lacrimal glands of treated animals did not change, the size of the foci decreased by 40.5% [95].

As we know, bone marrow mesenchymal cells can be easily contaminated with hematopoietic cells. Researchers isolate CD45$^-$/TER119$^-$ cells from murine bone marrow by depleting CD45$^+$ cells or TER119$^+$ hematopoietic cells. CD45$^-$/TER119$^-$cells are identified as BMSCs because they are positive for stem cell surface markers and have multiple differentiation potentials. Treatment with CD45$^-$/TER119^{--} cells could prevent loss of saliva flow and reduce lymphocytic infiltrations in SG of NOD mice through downregulation of inflammatory cytokines such as TNF-α. Notably, the infiltrations of T and B cells are decreased in all foci, while the frequency of Tregs is increased. Investigators speculate enhanced Tregs inhibit the inflammation in SG. Mean-while, fibroblast growth factor-2 (FGF-2) and epidermal growth factor (EGF) involved in the growth, regeneration, and maintenance of salivary glands are both increased after CD45$^-$/TER119$^-$ MSC treatment. This suggests the CD45$^-$/TER119$^-$ BMSCs are effective in both preventing

TABLE 1: Application of MSCs in treating animal models and patients with pSS.

Types of MSCs	Treatment Cell numbers, origin	Administration	Recipient (human)	Recipient (mice)	Follow-up	Effect	Outcome	Reference
BMSCs	1×10^5, one dose, BALB/c or B6 mice	IV injection at 6 weeks age (prevention group) or 16 weeks age (treatment group)	NA	NOD mice	8 weeks or 18 weeks	Inflammatory area ↓ in SG, salivary flow rate ↑, Tregs ↑, Th2 ↑, Th17 ↓, Tfh ↓	Improvement	[81]
UMSCs	1×10^6/kg, one dose, human	IV injection	Patients with pSS	NA	12 months	SSDAI and global assessment Vas score ↓, unstimulated and stimulated salivary flow rate ↑, anti-SSA/Ro and anti-SSB/La ↓	Improvement	
BMSCs	5×10^5, four doses, mouse	IV injection	NA	NOD mice	4 weeks	Saliva flow rate ↑, lymphocytic infiltrations ↓, serum IFN-γ ↓, IL-10 ↑, TGF-β ↑	Improvement	[94]
BMSCs	1×10^6, one dose, mouse	IP injection	NA	NOD mice	4 weeks	Tear production ↑, aquaporin 5 mRNA ↑, lymphocytic score did not change	Improvement	[95]
CD45⁻TER119⁻ BMSCs	1×10^7, four doses, human	IV injection	NA	NOD mice	14 weeks	Salivary flow rate ↑, lymphocytic infiltration in SG ↓, T and B cells ↓, Tregs ↑ in all foci	Improvement	[96]
UMSCs	Human	Coculture	pSS	NA	NA	Differentiation and proliferation of Tfh ↓	Suppression	[49]
UMSCs microencapsulated	Human	Coculture	PBMC from 10 pSS	NA	NA	Proliferation of T cell ↓, Th1 ↓, Th17 ↓, Tregs ↑	Suppression	[44]
AMSCs	8×10^6, allogeneic, one dose, per eye, dog	Locally injected around lacrimal glands and gland of eyelid	NA	Dog with KCS	9 months	Schirmer tear test ↑, ocular parameter score ↓	Improvement	[97]

deterioration of saliva secretion and reducing lymphocytic influx in salivary glands with a systemic effect [96].

Tfh cells are recognized as crucial for B cell maturation and differentiation. Unlike BMSCs, UMSCs are found to suppress the differentiation of Tfh cells via the secretion of IDO in patients with pSS [49]. Therefore, UMSCs could provide a novel therapeutic approach for pSS by targeting Tfh cells. Other investigators find that human UMSCs inhibit proliferation of healthy T cells, but not T cells from pSS patients. Interestingly, they develop a new microencapsulation technique to make a coculture system separating UMSCs from T cells. This approach avoids a systemic immune reaction in the host. The specialized UMSCs could suppress pSS T cell proliferation and restore the Tregs/Th17 ratio, suggesting a drug delivery system able to enhance the immunomodulatory effects of UMSCs in pSS [44].

A small preclinical study regarding the application of AMSCs shows that when allogeneic AMSCs are implanted around the lacrimal glands in 12 dogs (24 eyes) with refractory keratoconjunctivitis sicca (KCS), improvement is observed in the Schirmer tear and ocular surface integrity tests during nine months follow-up. No systemic or local complications appear. However, a caveat is that no control cells are mentioned in this study [97].

Interestingly, it has been demonstrated that human BMSCs could temporarily change into salivary gland epithelial cells (SGEC) in a coculture system. BMSCs have comparable cellular structures and expressed several salivary genes such as aquaporin 5, E-cadherin, and α-amylase (α-AMY) when cocultured with SGEC. These BMSCs can secrete α-AMY. Moreover, they have comparable cellular structures to SGEC, such as tight junctions and numerous secretory granules, as shown by electron microscopy [99]. Some proteins such as ankryin-repeat-domain-containing-protein 56, high-mobility-group-protein 20B, and transcription factor E2a are the putative regulatory factors involved in the transdifferentiation of BMSCs into SGEC in an animal study [31]. These data suggest that cocultured BMSCs can generate a salivary gland acinar phenotype, meaning that this approach has potential application to treat salivary gland diseases such as pSS [31, 32, 99]. However, we still do not know whether pSS disease-derived BMSCs switch into acinar epithelial cells. Further study is needed to answer this question.

5. Perspectives: Learn from Bioengineering Strategies

In order to improve the function of MSCs, novel methods such as retroviral transduction, electroporation, or CRISPR-associated protein-9 nuclease (Cas9) of foreign genes have been utilized to engineer MSCs [100–103]. In cancer, MSCs have been successfully modified with a tumor suppressive gene to inhibit progress or metastasis of tumor cells. Similarly, current bioengineering strategies could be applied in pSS. For instance, IL-10 is a powerful cytokine to suppress inflammation. One team engineered mouse BMSCs with an IL-10 gene (called IL-10-BMSCs) through retroviral transduction. They demonstrated that IL-10-BMSCs, but not BMSCs alone or PBS, could modulate inflammatory arthritis

and decrease the histological scores [100]. Besides, MSCs transfected with minicircles encoding CXCR4 are more likely to migrate to the injury site [102]. Moreover, it is possible to track the MSCs which are transfected with minicircles and monitor their elastic properties with noninvasive microscopy technologies. Recently, a novel gene-editing technology based on a bacterial CRISPR-associated protein-9 nuclease (Cas9) has been successfully used to target important genes in many cell lines and organisms [103]. It may be possible to develop a successful MSCs-derived therapy for pSS if we target crucial genes involved in MSC immunomodulation, such as soluble factor production and chemokine receptors using Cas9 methods.

Recently, extracellular vesicles (EVs) have been considered as a functional molecule with their potential for treatment of pSS. As we know, extracellular vesicles are secreted by many cells, including MSCs, and are classified into two types of particles: exosomes, with a size of 50 to 100 nm derived from the endosomal compartment, and microvesicles (MVs), with a size between 100 nm and 1000 nm. It has been reported that BMSCs, UMSCs, and AMSCs may be a suitable source for therapeutic EVs [104–107]. EVs can mediate cell-to-cell communication and participate in many processes including inflammation, proliferation, cell differentiation, and immune signaling [106, 108]. They can also act directly with the target cell membrane by fusion, transferring components into intracellular compartments or causing endocytosis. MVs have a role in antigen presentation and activation of endosomal receptors such as Toll-like receptors [109]. EVs can carry autoantigens, cytokines, and tissue-degrading enzymes. Collectively, EVs could repair damaged tissue or serve as agents for drug delivery in autoimmune disease [106, 108, 110]. Recently, it has been reported that MSCs derived from human-induced pluripotent stem cells (MSCs-iPSCs) can prevent the onset of sialadenitis in NOD mice. Furthermore, EVs derived from MSCs-iPSCs are shown to suppress activation of immune cells *in vitro*. And the infusion of these EVs at the predisease stage reduces the lymphocyte infiltration in salivary glands and serum autoantibody levels in NOD mice [111].

We focus on the therapeutic effect of GMSCs in autoimmune disease, especially in pSS. GMSCs are relatively easy to isolate, homogenous and proliferate rapidly *in vitro*, and have a strong immunomodulation via suppression of Th1 and Th17 cells and enhancement of Treg differentiation [22]. We further find that GMSCs suppress human T cell-mediated diseases in the x-GVHD model via CD39/CD73/adenosine and IDO signals [112]. In addition, GMSC populations existing within the inflamed gingival tissue are functionally equivalent to those derived from healthy gingival tissue, indicating the possibility of treatment with the patient's GMSCs [113]. Furthermore, our unpublished data have documented that GMSCs could inhibit the proliferation and IFN-γ production of peripheral T cells from patients with pSS *in vitro*. Next, we plan to study whether the patient with pSS will benefit from GMSC transfusion.

There remain many challenges to overcome for clinical application of MSCs in pSS. First, there are great variations in the MSC isolation protocols, culture systems, MSC dose,

cell delivery methods, and transfusion frequency in the reported studies. Secondly, the quality control of diverse MSCs is not defined. It will be necessary to establish standardized protocols for cell culture, differentiation, and expansion, as well as recommended transfusion schedules and evaluation of responses. Thirdly, the number of enrolled patients reported in published papers is small and may not be sufficient to provide a reliable conclusion. Fourthly, another restriction in the field of clinical application of MSCs is the biosafety issues relevant to tumorigenicity [114]. Some papers report that MSCs enhance tumor angiogenesis and promote tumor formation in mice [115, 116]. Finally, whether MSC transfusion will have a long-term effect in pSS is unknown.

6. Conclusions

In summary, MSCs can be obtained from different sources and are especially abundant in adipose and dental tissues. They possess potent immunomodulatory functions and act on both adaptive and innate immune responses. They may repair damaged tissue via suppressing Th1/Th17/Tfh cell responses and upregulating Tregs. Furthermore, MSCs could induce Breg cells and modulate innate immune cells such as DC, macrophages, mast cells, and NK cells. Moreover, new bioengineering approaches, such as Cas9 methods, may improve the function of MSCs. Currently, there is no curative clinical therapy for pSS, so MSCs-based therapies show great potential in this area, with the expected capacity to significantly suppress the inflammation and preserve salivary function in pSS. As of now, no conclusive evidence to support the use of MSC-based therapies has been published. In the near future, randomized controlled trials of the therapeutic use of MSCs in pSS will be of considerable interest.

Conflicts of Interest

The authors declare that they have no competing interests.

Acknowledgments

References

[1] N. I. Maria, P. Vogelsang, and M. A. Versnel, "The clinical relevance of animal models in Sjögren's syndrome: the interferon signature from mouse to man," *Arthritis Research & Therapy*, vol. 17, no. 1, p. 172, 2015.

[2] E. A. Szyszko, K. A. Brokstad, G. Oijordsbakken, M. V. Jonsson, R. Jonsson, and K. Skarstein, "Salivary glands of primary Sjögren's syndrome patients express factors vital for plasma cell survival," *Arthritis Research & Therapy*, vol. 13, no. 1, article R2, 2011.

[3] P. C. Fox, "Autoimmune diseases and Sjögren's syndrome: an autoimmune exocrinopathy," *Annals of the New York Academy of Sciences*, vol. 1098, no. 1, pp. 15–21, 2007.

[4] G. Nocturne, A. Virone, W. F. Ng et al., "Rheumatoid factor and disease activity are independent predictors of lymphoma in primary Sjögren's syndrome," *Arthritis & Rheumatology*, vol. 68, no. 4, pp. 977–985, 2016.

[5] J. Kiripolsky, L. G. McCabe, and J. M. Kramer, "Innate immunity in Sjögren's syndrome," *Clinical Immunology*, vol. 182, pp. 4–13, 2017.

[6] A. Ambrosi and M. Wahren-Herlenius, "Update on the immunobiology of Sjögren's syndrome," *Current Opinion in Rheumatology*, vol. 27, no. 5, pp. 468–475, 2015.

[7] Y. Samuni and B. J. Baum, "Gene delivery in salivary glands: from the bench to the clinic," *Biochimica et Biophysica Acta (BBA) - Molecular Basis of Disease*, vol. 1812, no. 11, pp. 1515–1521, 2011.

[8] A. Saraux, J.-O. Pers, and V. Devauchelle-Pensec, "Treatment of primary Sjögren syndrome," *Nature Reviews Rheumatology*, vol. 12, no. 8, pp. 456–471, 2016.

[9] A. J. Friedenstein, R. K. Chailakhyan, N. V. Latsinik, A. F. Panasyuk, and I. V. Keiliss-Borok, "Stromal cells responsible for transferring the microenvironment of the hemopoietic tissues. Cloning in vitro and retransplantation in vivo," *Transplantation*, vol. 17, no. 4, pp. 331–340, 1974.

[10] M. F. Pittenger, A. M. Mackay, S. C. Beck et al., "Multilineage potential of adult human mesenchymal stem cells," *Science*, vol. 284, no. 5411, pp. 143–147, 1999.

[11] H. Y. Nam, P. Karunanithi, W. C. Loo et al., "The effects of staged intra-articular injection of cultured autologous mesenchymal stromal cells on the repair of damaged cartilage: a pilot study in caprine model," *Arthritis Research & Therapy*, vol. 15, no. 5, article R129, 2013.

[12] L. Tessier, D. Bienzle, L. B. Williams, and T. G. Koch, "Phenotypic and immunomodulatory properties of equine cord blood-derived mesenchymal stromal cells," *PLoS One*, vol. 10, no. 4, article e0122954, 2015.

[13] H. Munir and H. M. McGettrick, "Mesenchymal stem cell therapy for autoimmune disease: risks and rewards," *Stem Cells and Development*, vol. 24, no. 18, pp. 2091–2100, 2015.

[14] G. B. Tomar, R. K. Srivastava, N. Gupta et al., "Human gingiva-derived mesenchymal stem cells are superior to bone marrow-derived mesenchymal stem cells for cell therapy in regenerative medicine," *Biochemical and Biophysical Research Communications*, vol. 393, no. 3, pp. 377–383, 2010.

[15] Q. Zhang, S. Shi, Y. Liu et al., "Mesenchymal stem cells derived from human gingiva are capable of immunomodulatory functions and ameliorate inflammation-related tissue destruction in experimental colitis," *The Journal of Immunology*, vol. 183, no. 12, pp. 7787–7798, 2009.

[16] E. Gonzalez-Rey, M. A. Gonzalez, N. Varela et al., "Human adipose-derived mesenchymal stem cells reduce inflammatory and T cell responses and induce regulatory T cells in vitro in rheumatoid arthritis," *Annals of the Rheumatic Diseases*, vol. 69, no. 1, pp. 241–248, 2010.

[17] J. R. Choi, K. W. Yong, and W. K. Z. Wan Safwani, "Effect of hypoxia on human adipose-derived mesenchymal stem cells and its potential clinical applications," *Cellular and Molecular Life Sciences*, vol. 74, no. 14, pp. 2587–2600, 2017.

[18] D. Venkatesh, K. P. Mohan Kumar, and J. B. Alur, "Gingival mesenchymal stem cells," *Journal of Oral and Maxillofacial Pathology*, vol. 21, no. 2, pp. 296–298, 2017.

[19] S. Santamaria, N. Sanchez, M. Sanz, and J. A. Garcia-Sanz, "Comparison of periodontal ligament and gingiva-derived

mesenchymal stem cells for regenerative therapies," *Clinical Oral Investigations*, vol. 21, no. 4, pp. 1095–1102, 2017.

[20] J. R. Choi, B. Pingguan-Murphy, W. A. B. Wan Abas et al., "In situ normoxia enhances survival and proliferation rate of human adipose tissue-derived stromal cells without increasing the risk of tumourigenesis," *PLoS One*, vol. 10, no. 1, article e0115034, 2015.

[21] L. Sun, D. Wang, J. Liang et al., "Umbilical cord mesenchymal stem cell transplantation in severe and refractory systemic lupus erythematosus," *Arthritis & Rheumatism*, vol. 62, no. 8, pp. 2467–2475, 2010.

[22] M. Chen, W. Su, X. Lin et al., "Adoptive transfer of human gingiva-derived mesenchymal stem cells ameliorates collagen-induced arthritis via suppression of Th1 and Th17 cells and enhancement of regulatory T cell differentiation," *Arthritis & Rheumatism*, vol. 65, no. 5, pp. 1181–1193, 2013.

[23] M. Christopeit, M. Schendel, J. Föll, L. P. Müller, G. Keysser, and G. Behre, "Marked improvement of severe progressive systemic sclerosis after transplantation of mesenchymal stem cells from an allogeneic haploidentical-related donor mediated by ligation of CD137L," *Leukemia*, vol. 22, no. 5, pp. 1062–1064, 2008.

[24] L. Vija, D. Farge, J.-F. Gautier et al., "Mesenchymal stem cells: stem cell therapy perspectives for type 1 diabetes," *Diabetes & Metabolism*, vol. 35, no. 2, pp. 85–93, 2009.

[25] Y. Liu, R. Mu, S. Wang et al., "Therapeutic potential of human umbilical cord mesenchymal stem cells in the treatment of rheumatoid arthritis," *Arthritis Research & Therapy*, vol. 12, no. 6, article R210, 2010.

[26] R. Liu, X. Li, Z. Zhang et al., "Allogeneic mesenchymal stem cells inhibited T follicular helper cell generation in rheumatoid arthritis," *Scientific Reports*, vol. 5, no. 1, article 12777, 2015.

[27] M. Rafei, P. M. Campeau, A. Aguilar-Mahecha et al., "Mesenchymal stromal cells ameliorate experimental autoimmune encephalomyelitis by inhibiting CD4 Th17 T cells in a CC chemokine ligand 2-dependent manner," *The Journal of Immunology*, vol. 182, no. 10, pp. 5994–6002, 2009.

[28] Y. Sumita, Y. Liu, S. Khalili et al., "Bone marrow-derived cells rescue salivary gland function in mice with head and neck irradiation," *The International Journal of Biochemistry & Cell Biology*, vol. 43, no. 1, pp. 80–87, 2011.

[29] D. H. Jensen, R. S. Oliveri, S. F. Trojahn Kølle et al., "Mesenchymal stem cell therapy for salivary gland dysfunction and xerostomia: a systematic review of preclinical studies," *Oral Surgery, Oral Medicine, Oral Pathology and Oral Radiology*, vol. 117, no. 3, pp. 335–342.e1, 2014.

[30] X. Lu, X. Wang, H. Nian, D. Yang, and R. Wei, "Mesenchymal stem cells for treating autoimmune dacryoadenitis," *Stem Cell Research & Therapy*, vol. 8, no. 1, p. 126, 2017.

[31] Y. J. Park, J. Koh, A. E. Gauna, S. Chen, and S. Cha, "Identification of regulatory factors for mesenchymal stem cell-derived salivary epithelial cells in a co-culture system," *PLoS One*, vol. 9, no. 11, article e112158, 2014.

[32] Y.-J. Park, J. Koh, J. T. Kwon, Y.-S. Park, L. Yang, and S. Cha, "Uncovering stem cell differentiation factors for salivary gland regeneration by quantitative analysis of differential proteomes," *PLoS One*, vol. 12, no. 2, article e0169677, 2017.

[33] F. Gao, S. M. Chiu, D. A. L. Motan et al., "Mesenchymal stem cells and immunomodulation: current status and future prospects," *Cell Death & Disease*, vol. 7, no. 1, article e2062, 2016.

[34] L. A. Ortiz, M. DuTreil, C. Fattman et al., "Interleukin 1 receptor antagonist mediates the antiinflammatory and antifibrotic effect of mesenchymal stem cells during lung injury," *Proceedings of the National Academy of Sciences of the United States of America*, vol. 104, no. 26, pp. 11002–11007, 2007.

[35] L. C. Davies, N. Heldring, N. Kadri, and K. Le Blanc, "Mesenchymal stromal cell secretion of programmed death-1 ligands regulates T cell mediated immunosuppression," *Stem Cells*, vol. 35, no. 3, pp. 766–776, 2017.

[36] F. Gieseke, J. Bohringer, R. Bussolari, M. Dominici, R. Handgretinger, and I. Muller, "Human multipotent mesenchymal stromal cells use galectin-1 to inhibit immune effector cells," *Blood*, vol. 116, no. 19, pp. 3770–3779, 2010.

[37] M. Krampera, S. Glennie, J. Dyson et al., "Bone marrow mesenchymal stem cells inhibit the response of naive and memory antigen-specific T cells to their cognate peptide," *Blood*, vol. 101, no. 9, pp. 3722–3729, 2003.

[38] S. Amarnath, J. E. Foley, D. E. Farthing et al., "Bone marrow-derived mesenchymal stromal cells harness purinergenic signaling to tolerize human Th1 cells in vivo," *Stem Cells*, vol. 33, no. 4, pp. 1200–1212, 2015.

[39] K. Lee, N. Park, H. Jung et al., "Mesenchymal stem cells ameliorate experimental arthritis via expression of interleukin-1 receptor antagonist," *PLoS One*, vol. 13, no. 2, article e0193086, 2018.

[40] R. Yang, Y. Liu, P. Kelk et al., "A subset of IL-17$^+$ mesenchymal stem cells possesses anti-*Candida albicans* effect," *Cell Research*, vol. 23, no. 1, pp. 107–121, 2013.

[41] K. English, J. M. Ryan, L. Tobin, M. J. Murphy, F. P. Barry, and B. P. Mahon, "Cell contact, prostaglandin E$_2$ and transforming growth factor beta 1 play non-redundant roles in human mesenchymal stem cell induction of CD4^{+-} CD25^{high}forkhead box P3$^+$ regulatory T cells," *Clinical & Experimental Immunology*, vol. 156, no. 1, pp. 149–160, 2009.

[42] M. Najar, G. Raicevic, H. Fayyad-Kazan et al., "Bone marrow mesenchymal stromal cells induce proliferative, cytokinic and molecular changes during the T cell response: the importance of the IL-10/CD210 axis," *Stem Cell Reviews and Reports*, vol. 11, no. 3, pp. 442–452, 2015.

[43] Z. Selmani, A. Naji, I. Zidi et al., "Human leukocyte antigen-G5 secretion by human mesenchymal stem cells is required to suppress T lymphocyte and natural killer function and to induce CD4$^+$CD25^{high}FOXP3$^+$ regulatory T cells," *Stem Cells*, vol. 26, no. 1, pp. 212–222, 2008.

[44] A. Alunno, P. Montanucci, O. Bistoni et al., "In vitro immunomodulatory effects of microencapsulated umbilical cord Wharton jelly-derived mesenchymal stem cells in primary Sjögren's syndrome," *Rheumatology*, vol. 54, no. 1, pp. 163–168, 2015.

[45] L. Tang, N. Li, H. Xie, and Y. Jin, "Characterization of mesenchymal stem cells from human normal and hyperplastic gingiva," *Journal of Cellular Physiology*, vol. 226, no. 3, pp. 832–842, 2011.

[46] C. A. Opitz, U. M. Litzenburger, C. Lutz et al., "Toll-like receptor engagement enhances the immunosuppressive properties of human bone marrow-derived mesenchymal stem cells by inducing indoleamine-2,3-dioxygenase-1 via interferon-β and protein kinase R," *Stem Cells*, vol. 27, no. 4, pp. 909–919, 2009.

[47] F. Liotta, R. Angeli, L. Cosmi et al., "Toll-like receptors 3 and 4 are expressed by human bone marrow-derived mesenchymal stem cells and can inhibit their T-cell modulatory activity

by impairing notch signaling," *Stem Cells*, vol. 26, no. 1, pp. 279–289, 2008.

[48] D. Chabannes, M. Hill, E. Merieau et al., "A role for heme oxygenase-1 in the immunosuppressive effect of adult rat and human mesenchymal stem cells," *Blood*, vol. 110, no. 10, pp. 3691–3694, 2007.

[49] R. Liu, D. Su, M. Zhou, X. Feng, X. Li, and L. Sun, "Umbilical cord mesenchymal stem cells inhibit the differentiation of circulating T follicular helper cells in patients with primary Sjögren's syndrome through the secretion of indoleamine 2,3-dioxygenase," *Rheumatology*, vol. 54, no. 2, pp. 332–342, 2015.

[50] X. Yang, J. Yang, X. Li, W. Ma, and H. Zou, "Bone marrow-derived mesenchymal stem cells inhibit T follicular helper cell in lupus-prone mice," *Lupus*, vol. 27, no. 1, pp. 49–59, 2017.

[51] C. Ungerer, P. Quade-Lyssy, H. H. Radeke et al., "Galectin-9 is a suppressor of T and B cells and predicts the immune modulatory potential of mesenchymal stromal cell preparations," *Stem Cells and Development*, vol. 23, no. 7, pp. 755–766, 2014.

[52] P. Luz-Crawford, F. Djouad, K. Toupet et al., "Mesenchymal stem cell-derived interleukin 1 receptor antagonist promotes macrophage polarization and inhibits B cell differentiation," *Stem Cells*, vol. 34, no. 2, pp. 483–492, 2016.

[53] A. Ribeiro, P. Laranjeira, S. Mendes et al., "Mesenchymal stem cells from umbilical cord matrix, adipose tissue and bone marrow exhibit different capability to suppress peripheral blood B, natural killer and T cells," *Stem Cell Research & Therapy*, vol. 4, no. 5, p. 125, 2013.

[54] A. Corcione, F. Benvenuto, E. Ferretti et al., "Human mesenchymal stem cells modulate B-cell functions," *Blood*, vol. 107, no. 1, pp. 367–372, 2006.

[55] M. Krampera, L. Cosmi, R. Angeli et al., "Role for interferon-γ in the immunomodulatory activity of human bone marrow mesenchymal stem cells," *Stem Cells*, vol. 24, no. 2, pp. 386–398, 2006.

[56] M. Youd, C. Blickarz, L. Woodworth et al., "Allogeneic mesenchymal stem cells do not protect NZB × NZW F_1 mice from developing lupus disease," *Clinical & Experimental Immunology*, vol. 161, no. 1, pp. 176–186, 2010.

[57] C. Mauri and M. R. Ehrenstein, "The 'short' history of regulatory B cells," *Trends in Immunology*, vol. 29, no. 1, pp. 34–40, 2008.

[58] K. Chao, S. Zhang, Y. Qiu et al., "Human umbilical cord-derived mesenchymal stem cells protect against experimental colitis via CD5$^+$ B regulatory cells," *Stem Cell Research & Therapy*, vol. 7, no. 1, p. 109, 2016.

[59] M. J. Park, S. K. Kwok, S. H. Lee, E. K. Kim, S. H. Park, and M. L. Cho, "Adipose tissue-derived mesenchymal stem cells induce expansion of interleukin-10-producing regulatory B cells and ameliorate autoimmunity in a murine model of systemic lupus erythematosus," *Cell Transplantation*, vol. 24, no. 11, pp. 2367–2377, 2015.

[60] Y. Qin, Z. Zhou, F. Zhang et al., "Induction of regulatory B-cells by mesenchymal stem cells is affected by SDF-1α-CXCR7," *Cellular Physiology and Biochemistry*, vol. 37, no. 1, pp. 117–130, 2015.

[61] R. Ramasamy, H. Fazekasova, E. W. F. Lam, I. Soeiro, G. Lombardi, and F. Dazzi, "Mesenchymal stem cells inhibit dendritic cell differentiation and function by preventing entry into the cell cycle," *Transplantation*, vol. 83, no. 1, pp. 71–76, 2007.

[62] Y. Liu, Z. Yin, R. Zhang et al., "MSCs inhibit bone marrow-derived DC maturation and function through the release of TSG-6," *Biochemical and Biophysical Research Communications*, vol. 450, no. 4, pp. 1409–1415, 2014.

[63] X. X. Jiang, Y. Zhang, B. Liu et al., "Human mesenchymal stem cells inhibit differentiation and function of monocyte-derived dendritic cells," *Blood*, vol. 105, no. 10, pp. 4120–4126, 2005.

[64] F. Djouad, L. M. Charbonnier, C. Bouffi et al., "Mesenchymal stem cells inhibit the differentiation of dendritic cells through an interleukin-6-dependent mechanism," *Stem Cells*, vol. 25, no. 8, pp. 2025–2032, 2007.

[65] S. Chiesa, S. Morbelli, S. Morando et al., "Mesenchymal stem cells impair in vivo T-cell priming by dendritic cells," *Proceedings of the National Academy of Sciences of the United States of America*, vol. 108, no. 42, pp. 17384–17389, 2011.

[66] W. R. Su, Q. Z. Zhang, S. H. Shi, A. L. Nguyen, and A. D. Le, "Human gingiva-derived mesenchymal stromal cells attenuate contact hypersensitivity via prostaglandin E_2-dependent mechanisms," *Stem Cells*, vol. 29, no. 11, pp. 1849–1860, 2011.

[67] Y. Deng, Y. Zhang, L. Ye et al., "Umbilical cord-derived mesenchymal stem cells instruct monocytes towards an IL10-producing phenotype by secreting IL6 and HGF," *Scientific Reports*, vol. 6, no. 1, article 37566, 2016.

[68] Q. Z. Zhang, W. R. Su, S. H. Shi et al., "Human gingiva-derived mesenchymal stem cells elicit polarization of M2 macrophages and enhance cutaneous wound healing," *Stem Cells*, vol. 28, no. 10, pp. 1856–1868, 2010.

[69] A. B. Vasandan, S. Jahnavi, C. Shashank, P. Prasad, A. Kumar, and S. J. Prasanna, "Human mesenchymal stem cells program macrophage plasticity by altering their metabolic status via a PGE$_2$-dependent mechanism," *Scientific Reports*, vol. 6, no. 1, article 38308, 2016.

[70] G. Wang, K. Cao, K. Liu et al., "Kynurenic acid, an IDO metabolite, controls TSG-6-mediated immunosuppression of human mesenchymal stem cells," *Cell Death & Differentiation*, vol. 25, no. 7, pp. 1209–1223, 2018.

[71] E. Sala, M. Genua, L. Petti et al., "Mesenchymal stem cells reduce colitis in mice via release of TSG6, independently of their localization to the intestine," *Gastroenterology*, vol. 149, no. 1, pp. 163–176.e20, 2015.

[72] H. Choi, R. H. Lee, N. Bazhanov, J. Y. Oh, and D. J. Prockop, "Anti-inflammatory protein TSG-6 secreted by activated MSCs attenuates zymosan-induced mouse peritonitis by decreasing TLR2/NF-κB signaling in resident macrophages," *Blood*, vol. 118, no. 2, pp. 330–338, 2011.

[73] G. M. Spaggiari, A. Capobianco, S. Becchetti, M. C. Mingari, and L. Moretta, "Mesenchymal stem cell-natural killer cell interactions: evidence that activated NK cells are capable of killing MSCs, whereas MSCs can inhibit IL-2-induced NK-cell proliferation," *Blood*, vol. 107, no. 4, pp. 1484–1490, 2006.

[74] G. M. Spaggiari, A. Capobianco, H. Abdelrazik, F. Becchetti, M. C. Mingari, and L. Moretta, "Mesenchymal stem cells inhibit natural killer–cell proliferation, cytotoxicity, and cytokine production: role of indoleamine 2,3-dioxygenase and prostaglandin E2," *Blood*, vol. 111, no. 3, pp. 1327–1333, 2008.

[75] P. A. Sotiropoulou, S. A. Perez, A. D. Gritzapis, C. N. Baxevanis, and M. Papamichail, "Interactions between human mesenchymal stem cells and natural killer cells," *Stem Cells*, vol. 24, no. 1, pp. 74–85, 2006.

[76] C. R. Almeida, H. R. Caires, D. P. Vasconcelos, and M. A. Barbosa, "NAP-2 secreted by human NK cells can stimulate mesenchymal stem/stromal cell recruitment," *Stem Cell Reports*, vol. 6, no. 4, pp. 466–473, 2016.

[77] P. Li, Y. Zhao, and L. Ge, "Therapeutic effects of human gingiva-derived mesenchymal stromal cells on murine contact hypersensitivity via prostaglandin E_2–EP_3 signaling," *Stem Cell Research & Therapy*, vol. 7, no. 1, p. 103, 2016.

[78] G. Ren, X. Zhao, L. Zhang et al., "Inflammatory cytokine-induced intercellular adhesion molecule-1 and vascular cell adhesion molecule-1 in mesenchymal stem cells are critical for immunosuppression," *The Journal of Immunology*, vol. 184, no. 5, pp. 2321–2328, 2010.

[79] C. Bouffi, C. Bony, G. Courties, C. Jorgensen, and D. Noel, "IL-6-dependent PGE2 secretion by mesenchymal stem cells inhibits local inflammation in experimental arthritis," *PLoS One*, vol. 5, no. 12, article e14247, 2010.

[80] R. S. Waterman, S. L. Tomchuck, S. L. Henkle, and A. M. Betancourt, "A new mesenchymal stem cell (MSC) paradigm: polarization into a pro-inflammatory MSC1 or an immunosuppressive MSC2 phenotype," *PLoS One*, vol. 5, no. 4, article e10088, 2010.

[81] J. Xu, D. Wang, D. Liu et al., "Allogeneic mesenchymal stem cell treatment alleviates experimental and clinical Sjögren syndrome," *Blood*, vol. 120, no. 15, pp. 3142–3151, 2012.

[82] T. Yamaza, Y. Miura, Y. Bi et al., "Pharmacologic stem cell based intervention as a new approach to osteoporosis treatment in rodents," *PLoS One*, vol. 3, no. 7, article e2615, 2008.

[83] Y. Liu, L. Wang, T. Kikuiri et al., "Mesenchymal stem cell–based tissue regeneration is governed by recipient T lymphocytes via IFN-γ and TNF-α," *Nature Medicine*, vol. 17, no. 12, pp. 1594–1601, 2011.

[84] L. Wang, Y. Zhao, Y. Liu et al., "IFN-γ and TNF-α synergistically induce mesenchymal stem cell impairment and tumorigenesis via NFκB signaling," *Stem Cells*, vol. 31, no. 7, pp. 1383–1395, 2013.

[85] N. Singh and P. L. Cohen, "The T cell in Sjögren's syndrome: force majeure, not spectateur," *Journal of Autoimmunity*, vol. 39, no. 3, pp. 229–233, 2012.

[86] G. E. Katsifis, S. Rekka, N. M. Moutsopoulos, S. Pillemer, and S. M. Wahl, "Systemic and local interleukin-17 and linked cytokines associated with Sjögren's syndrome immunopathogenesis," *The American Journal of Pathology*, vol. 175, no. 3, pp. 1167–1177, 2009.

[87] J. Jeong, H. Baek, Y. J. Kim et al., "Human salivary gland stem cells ameliorate hyposalivation of radiation-damaged rat salivary glands," *Experimental & Molecular Medicine*, vol. 45, no. 11, article e58, 2013.

[88] S. Q. Wang, Y. X. Wang, and H. Hua, "Characteristics of labial gland mesenchymal stem cells of healthy individuals and patients with Sjögren's syndrome: a preliminary study," *Stem Cells and Development*, vol. 26, no. 16, pp. 1171–1185, 2017.

[89] M. I. Christodoulou, E. K. Kapsogeorgou, N. M. Moutsopoulos, and H. M. Moutsopoulos, "Foxp3$^+$ T-regulatory cells in Sjögren's syndrome: correlation with the grade of the autoimmune lesion and certain adverse prognostic factors," *The American Journal of Pathology*, vol. 173, no. 5, pp. 1389–1396, 2008.

[90] J. E. Gottenberg, F. Lavie, K. Abbed et al., "CD4 CD25^{high} regulatory T cells are not impaired in patients with primary Sjögren's syndrome," *Journal of Autoimmunity*, vol. 24, no. 3, pp. 235–242, 2005.

[91] X. Li, X. Li, L. Qian et al., "T regulatory cells are markedly diminished in diseased salivary glands of patients with primary Sjögren's syndrome," *The Journal of Rheumatology*, vol. 34, no. 12, pp. 2438–2445, 2007.

[92] T. G. Coursey, F. Bian, M. Zaheer, S. C. Pflugfelder, E. A. Volpe, and C. S. de Paiva, "Age-related spontaneous lacrimal keratoconjunctivitis is accompanied by dysfunctional T regulatory cells," *Mucosal Immunology*, vol. 10, no. 3, pp. 743–756, 2017.

[93] G. Sudzius, D. Mieliauskaite, A. Siaurys et al., "Distribution of peripheral lymphocyte populations in primary Sjögren's syndrome patients," *Journal of Immunology Research*, vol. 2015, Article ID 854706, 10 pages, 2015.

[94] G. F. Ruan, L. Zheng, J. S. Huang et al., "Effect of mesenchymal stem cells on Sjögren-like mice and the microRNA expression profiles of splenic CD4+ T cells," *Experimental and Therapeutic Medicine*, vol. 13, no. 6, pp. 2828–2838, 2017.

[95] H. S. Aluri, M. Samizadeh, M. C. Edman et al., "Delivery of bone marrow-derived mesenchymal stem cells improves tear production in a mouse model of Sjögren's syndrome," *Stem Cells International*, vol. 2017, Article ID 3134543, 10 pages, 2017.

[96] S. Khalili, Y. Liu, M. Kornete et al., "Mesenchymal stromal cells improve salivary function and reduce lymphocytic infiltrates in mice with Sjögren's-like disease," *PLoS One*, vol. 7, no. 6, article e38615, 2012.

[97] A. J. Villatoro, V. Fernandez, S. Claros, G. A. Rico-Llanos, J. Becerra, and J. A. Andrades, "Use of adipose-derived mesenchymal stem cells in keratoconjunctivitis sicca in a canine model," *BioMed Research International*, vol. 2015, Article ID 527926, 10 pages, 2015.

[98] G. A. Elghanam, Y. Liu, S. Khalili, D. Fang, and S. D. Tran, "Compact bone-derived multipotent mesenchymal stromal cells (MSCS) for the treatment of Sjögren's-like disease in NOD mice," *Methods in Molecular Biology*, vol. 1553, pp. 25–39, 2017.

[99] O. M. Maria and S. D. Tran, "Human mesenchymal stem cells cultured with salivary gland biopsies adopt an epithelial phenotype," *Stem Cells and Development*, vol. 20, no. 6, pp. 959–967, 2011.

[100] J. J. Choi, S. A. Yoo, S. J. Park et al., "Mesenchymal stem cells overexpressing interleukin-10 attenuate collagen-induced arthritis in mice," *Clinical & Experimental Immunology*, vol. 153, no. 2, pp. 269–276, 2008.

[101] N. Park, Y. A. Rim, H. Jung et al., "Etanercept-synthesising mesenchymal stem cells efficiently ameliorate collagen-induced arthritis," *Scientific Reports*, vol. 7, no. 1, article 39593, 2017.

[102] J.-Y. Mun, K. K. Shin, O. Kwon, Y. T. Lim, and D.-B. Oh, "Minicircle microporation-based non-viral gene delivery improved the targeting of mesenchymal stem cells to an injury site," *Biomaterials*, vol. 101, pp. 310–320, 2016.

[103] P. D. Hsu, E. S. Lander, and F. Zhang, "Development and applications of CRISPR-Cas 9 for genome engineering," *Cell*, vol. 157, no. 6, pp. 1262–1278, 2014.

[104] S. Bian, L. Zhang, L. Duan, X. Wang, Y. Min, and H. Yu, "Extracellular vesicles derived from human bone marrow mesenchymal stem cells promote angiogenesis in a rat myocardial infarction model," *Journal of Molecular Medicine*, vol. 92, no. 4, pp. 387–397, 2014.

[105] M. Franquesa, M. J. Hoogduijn, E. Ripoll et al., "Update on controls for isolation and quantification methodology of extracellular vesicles derived from adipose tissue mesenchymal stem cells," *Frontiers in Immunology*, vol. 5, p. 525, 2014.

[106] T. Katsuda, N. Kosaka, F. Takeshita, and T. Ochiya, "The therapeutic potential of mesenchymal stem cell-derived extracellular vesicles," *Proteomics*, vol. 13, no. 10-11, pp. 1637–1653, 2013.

[107] L. Kilpinen, U. Impola, L. Sankkila et al., "Extracellular membrane vesicles from umbilical cord blood-derived MSC protect against ischemic acute kidney injury, a feature that is lost after inflammatory conditioning," *Journal of Extracellular Vesicles*, vol. 2, no. 1, 2013.

[108] E. I. Buzas, B. Gyorgy, G. Nagy, A. Falus, and S. Gay, "Emerging role of extracellular vesicles in inflammatory diseases," *Nature Reviews Rheumatology*, vol. 10, no. 6, pp. 356–364, 2014.

[109] D. Turpin, M.-E. Truchetet, B. Faustin et al., "Role of extracellular vesicles in autoimmune diseases," *Autoimmunity Reviews*, vol. 15, no. 2, pp. 174–183, 2016.

[110] L. Biancone, S. Bruno, M. C. Deregibus, C. Tetta, and G. Camussi, "Therapeutic potential of mesenchymal stem cell-derived microvesicles," *Nephrology Dialysis Transplantation*, vol. 27, no. 8, pp. 3037–3042, 2012.

[111] B. Hai, T. Shigemoto-Kuroda, Q. Zhao, R. H. Lee, and F. Liu, "Inhibitory effects of iPSC-MSCs and their extracellular vesicles on the onset of sialadenitis in a mouse model of Sjögren's syndrome," *Stem Cells International*, vol. 2018, Article ID 2092315, 10 pages, 2018.

[112] F. Huang, M. Chen, W. Chen et al., "Human gingiva-derived mesenchymal stem cells inhibit xeno-graft-versus-host disease via CD39–CD73–adenosine and IDO signals," *Frontiers in Immunology*, vol. 8, p. 68, 2017.

[113] S. Ge, K. M. Mrozik, D. Menicanin, S. Gronthos, and P. M. Bartold, "Isolation and characterization of mesenchymal stem cell-like cells from healthy and inflamed gingival tissue: potential use for clinical therapy," *Regenerative Medicine*, vol. 7, no. 6, pp. 819–832, 2012.

[114] K. W. Yong, J. R. Choi, A. S. Dolbashid, and W. K. Z. Wan Safwani, "Biosafety and bioefficacy assessment of human mesenchymal stem cells: what do we know so far?," *Regenerative Medicine*, vol. 13, no. 2, pp. 219–232, 2018.

[115] K.-S. Tsai, S.-H. Yang, Y.-P. Lei et al., "Mesenchymal stem cells promote formation of colorectal tumors in mice," *Gastroenterology*, vol. 141, no. 3, pp. 1046–1056, 2011.

[116] Y. Liu, Z. P. Han, S. S. Zhang et al., "Effects of inflammatory factors on mesenchymal stem cells and their role in the promotion of tumor angiogenesis in colon cancer," *The Journal of Biological Chemistry*, vol. 286, no. 28, pp. 25007–25015, 2011.

Review Article

Mesenchymal Stromal/Stem Cells in Regenerative Medicine and Tissue Engineering

Ross E. B. Fitzsimmons [ID],[1,2] **Matthew S. Mazurek** [ID],[3] **Agnes Soos** [ID],[1,2] **and Craig A. Simmons** [ID][1,2,4]

[1]*Institute of Biomaterials and Biomedical Engineering, University of Toronto, 164 College Street, Toronto, ON, Canada M5S 3G9*
[2]*Translational Biology and Engineering Program, Ted Rogers Centre for Heart Research, 661 University Ave, Toronto, ON,*
 Canada M5G 1M1
[3]*Division of Gastroenterology and Hepatology, Department of Medicine, University of Calgary, Calgary, AB, Canada T2N 4Z6*
[4]*Department of Mechanical and Industrial Engineering, University of Toronto, 5 King's College Road, Toronto, ON,*
 Canada M5S 3G8

Correspondence should be addressed to Ross E. B. Fitzsimmons; ross.fitzsimmons@mail.utoronto.ca
and Craig A. Simmons; c.simmons@utoronto.ca

As a result of over five decades of investigation, mesenchymal stromal/stem cells (MSCs) have emerged as a versatile and frequently utilized cell source in the fields of regenerative medicine and tissue engineering. In this review, we summarize the history of MSC research from the initial discovery of their multipotency to the more recent recognition of their perivascular identity *in vivo* and their extraordinary capacity for immunomodulation and angiogenic signaling. As well, we discuss long-standing questions regarding their developmental origins and their capacity for differentiation toward a range of cell lineages. We also highlight important considerations and potential risks involved with their isolation, ex vivo expansion, and clinical use. Overall, this review aims to serve as an overview of the breadth of research that has demonstrated the utility of MSCs in a wide range of clinical contexts and continues to unravel the mechanisms by which these cells exert their therapeutic effects.

1. Introduction

By merit of their regenerative secretome and their capacity for differentiation toward multiple mesenchymal lineages, the fibroblastic cell type termed mesenchymal stromal/stem cells (MSCs) shows promise for a wide range of tissue engineering and regenerative medicine applications (Figure 1). As a result of their therapeutic versatility and the multitude of promising clinical results thus far, MSCs are poised to become an increasingly significant cell source for regenerative therapies as medicine evolves to focus on personalized and cell-based therapeutics. Given their emerging importance, this review aims to provide an overview of historical and ongoing work aimed at understanding and better utilizing these cells for therapeutic purposes.

2. Initial Discoveries and the Evolving Definition of "MSC"

The initial discovery of MSCs is attributed to Friedenstein et al. who discovered a fibroblastic cell type derived from mouse and guinea pig bone marrow that could produce clonal colonies capable of generating bone and reticular tissue when heterotopically transplanted [1, 2]. The subsequent discovery that colonies of this cell type can generate cartilage and adipose tissue, in addition to bone, gave rise to the descriptor *mesenchymal stem cells*, as originally coined by Arnold Caplan [3]. Finally, Pittenger et al. established that human bone marrow also contains a subpopulation of stromal cells that are genuinely multipotent stem cells by demonstrating single colonies have trilineage mesenchymal potential [4].
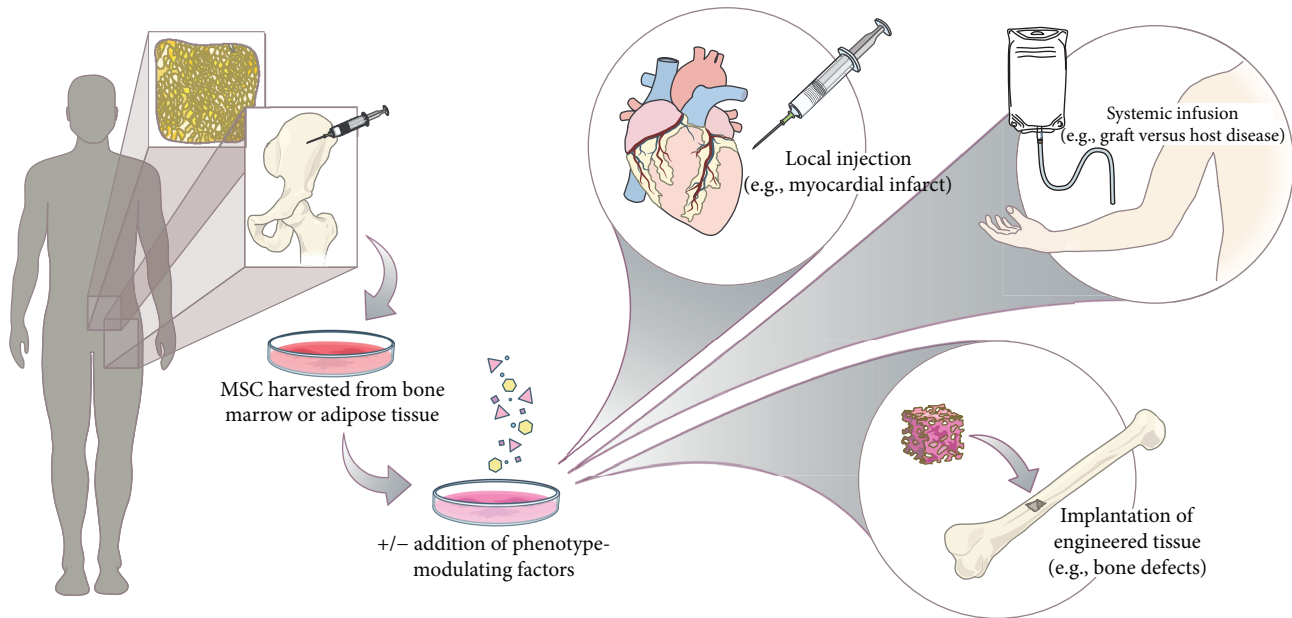
FIGURE 1: Strategies for mesenchymal stromal/stem cell- (MSC-) based therapies. MSCs may be isolated from a number of tissues (e.g., bone marrow, adipose tissue, and umbilical cord) and optionally cultured prior to clinical use. Depending on the specific application, MSC suspensions may then be introduced intravenously or by local injection to achieve the desired therapeutic effects, such as treating autoimmune diseases or stimulating local tissue repair and vascularization, respectively. MSCs may also be utilized for engineering tissues by first promoting their differentiation toward a desired cell type (e.g., osteoblasts, chondrocytes, and adipocytes) prior to being surgically implanted, often along with scaffold material.

Over time, the acronym MSC has come to take on multiple meanings including, mesenchymal stem cell, mesenchymal stromal cell, and multipotent stromal cell. To help clarify this, the International Society for Cellular Therapy (ISCT) has officially defined MSCs as *multipotent mesenchymal stromal cells* and suggests this to mean the plastic-adherent fraction from stromal tissues, while reserving the term *mesenchymal stem cells* to mean the subpopulation that actually has the two cardinal stem cell properties (*i.e.*, self-renewal and the capacity to differentiate down multiple lineages) [5]. Furthermore, ISCT has also defined MSCs as meeting several criteria including (i) being plastic adherent, (ii) having osteogenic, adipogenic, and chondrogenic trilineage differentiation potential, (iii) and being positive (>95%) and negative (<2%) for a panel of cell surface antigens. Positive markers for human MSCs include CD73 (also present on lymphocytes, endothelial cells, smooth muscle cells, and fibroblasts), CD90 (also present on hematopoietic stem cells, lymphocytes, endothelial cells, neurons, and fibroblasts), and CD105 (also found on endothelial cells, monocytes, hematopoietic progenitors, and fibroblasts) [6]. Negative markers include CD34 (present on hematopoietic progenitors and endothelial cells), CD45 (a pan-leukocyte marker), CD14 or CD11b (present on monocytes and macrophages), CD79-α or CD19 (present on B cells), and HLA-DR unless stimulated with IFN-γ (present on macrophages, B cells, and dendritic cells) [5]. It should be noted, however, that the validity of CD34 as a negative marker has recently been called into question and may require reexamination [6, 7].

As these elaborate inclusionary and exclusionary criteria highlight, no single MSC-specific epitope has been discovered, unlike for some other stem cell populations (e.g., LGR5, which labels resident stem cells in hair follicles and intestinal crypts) [8, 9]. However, some markers may be used to enrich for the stem cell population, including Stro-1, CD146, CD106, CD271, MSCA-1, and others (Table 1) [6, 10–13]. This unfortunate lack of a single definitive marker continues to confound the interpretation of a broad range of studies given that sorting out the canonical MSC population from the adherent fraction is rarely done, leading to the perennial question of which subpopulation in the adherent stromal fraction is actually eliciting the observed effects. This lack of a definitive MSC marker has also contributed to the challenge of delineating the exact *in vivo* location, function, and developmental origin of MSCs.

3. MSC Adult Anatomical Location

In the bone marrow, where MSCs were first discovered, MSCs have been reported to typically localize near the sinusoidal endothelium in close association with the resident hematopoietic stem cells (HSCs) [14, 15]. In addition to serving as osteogenic progenitors, such MSCs have been shown to play an important role in regulating HSC function by maintaining the HSC niche and by secreting trophic factors such as angiopoietin 1 (Ang1), stem cell factor (SCF), and CXC ligand 12 (CXCL12) [10]. Beyond the bone marrow, MSC/MSC-like populations have also

TABLE 1: Potential markers for MSC identification and enrichment.

Selection type (and comments)	CD No.	Name	Acronym	Reference
Negative	**CD11b**	**Integrin subunit alpha M**	**ITGAM**	[5]
Negative	**CD14**	**CD14 molecule**	**CD14**	[5]
Negative	**CD19**	**CD19 molecule**	**CD19**	[5]
Negative (not in all MSC populations)	**CD34**	**CD34 molecule**	**CD34**	[5]
Negative	**CD45**	**Protein tyrosine phosphatase, receptor type C**	**PTPRC**	[5]
Negative	**CD79a**	**CD79a molecule**	**CD79A**	[5]
Negative (unless stimulated with IFN-γ)	—	**Human leukocyte antigen, antigen D Related**	**HLA-DR**	[5]
Positive	CD9	CD9 molecule	CD9	[172]
Positive	CD10	Membrane metalloendopeptidase	MME	[173]
Positive	CD13	Alanyl aminopeptidase, membrane	ANPEP	[174]
Positive	CD29	Integrin subunit beta 1	ITGB1	[175]
Positive	CD44	CD44 molecule (Indian blood group)	CD44	[176]
Positive	CD49f	Integrin subunit alpha 6	ITGA6	[177]
Positive	CD54	Intercellular adhesion molecule 1	ICAM1	[178]
Positive	CD71	Transferrin receptor	TFRC	[179]
Positive	**CD73**	**5′-nucleotidase ecto**	**NT5E**	[5]
Positive	**CD90**	**Thy-1 cell surface antigen**	**THY1**	[5]
Positive	**CD105**	**Endoglin**	**ENG**	[5]
Positive	CD106	Vascular cell adhesion molecule 1	VCAM1	[11]
Positive	CD146	Melanoma cell adhesion molecule	MCAM	[10]
Positive	CD166	Activated leukocyte cell adhesion molecule	ALCAM	[180]
Positive	CD200	CD200 molecule	CD200	[181]
Positive	CD271	Nerve growth factor receptor	NGFR	[12]
Positive	CD349	Frizzled class receptor 9	FZD9	[173]
Positive	CD362	Syndecan 2	SDC2	[182]
Positive (a disialoganglioside, nonpeptide)	—	Ganglioside GD2	G2	[183]
Positive (also known as nucleostemin)	—	G protein nucleolar 3	GNL3	[184]
Positive (target of anti-STRO1 antibodies)	—	Heat shock protein family A (Hsp70) member 8	HSPA8	[185]
Positive	—	Heat shock protein 90 beta family member 1	HSP90B1	[186]
Positive (a glycosphingolipid, nonpeptide)	—	Stage-specific embryonic antigen-4	SSEA-4	[187]
Positive	—	Sushi domain containing 2	SUSD2	[188]
Positive	—	Alkaline phosphatase, liver/bone/kidney	ALPL	[13]

Bolded text indicates markers recommended by the International Society for Cellular Therapy (ISCT) for minimally defining human multipotent mesenchymal stromal cells by positive and negative selection.

been found in many adult tissues (*e.g.*, skin, pancreas, heart, brain, lung, kidney, adipose tissue, cartilage, and tendon) [16–19]. Such a broad anatomical distribution would suggest a common and ubiquitous MSC niche exists throughout the body. Indeed, evidence suggests that many MSC populations are specifically located near blood vessels and are in fact a subpopulation of pericytes that reside on capillaries and venules [20]. Supporting observations include the fact that pericytes and MSCs express similar surface antigens, and that cells in perivascular positions were found to express MSC markers in human bone marrow and dental pulp [16, 21]. Perhaps most definitively, Crisan et al. found that cells positive for NG2, CD146, and PDGFR-β specifically stained pericytes in multiple human tissues, and when cells with these markers were isolated, they were shown to have trilineage potential *in vitro* and were osteogenic once transplanted

in vivo [22]. The converse, that all pericytes are MSCs, is not thought to be the case [20].

In addition to being abluminal to microvessels, it should be noted that a Gli1^{+} MSC-like population has also been found to reside within the adventitia of larger vessels in mice. The Gli1^{+} population exhibits trilineage differentiation *in vitro* and is thought to play a role in arterial calcification *in vivo* [23–25]. Similarly, a MSC population with a CD34^{+} CD31^{−} CD146^{−} CD45^{−} phenotype has been discovered to reside within the adventitia of human arteries and veins suggesting that not all perivascular MSCs are pericyte-like cells in humans [7]. Furthermore, a MSC population has also been isolated from the perivascular tissue of umbilical cords (human umbilical cord perivascular cells (HUCPVCs)) which shows promise for tissue engineering applications given the cells' noninvasive extraction and their relatively

high abundance and proliferative capacity, compared to bone marrow-derived MSCs [26–28].

Finally, despite the prevalent view that MSCs reside in perivascular niches, some MSC populations may reside in avascular regions as well. For example, a lineage tracing study focused on murine tooth repair demonstrated that while some odontoblasts descend from cells expressing the pericyte marker, NG2, the majority of odontoblasts did not, suggestive of a nonpericyte origin (or at least not from NG2-positive pericytes) [29]. Additionally, MSCs have been isolated from tissues that are typically avascular, including human synovial tissue [30–32] and porcine aortic valve [33]. However, there are fenestrated capillaries localized near the synovial surface [34], and diseased sclerotic and stenotic valves can be partially vascularized [35, 36], raising the possibility of MSCs trafficking from one anatomical location to another (*e.g.*, synovium-associated vasculature to avascular cartilage) and innate differences in the local presence or absence of perivascular MSCs. Future work focused on these questions will have important implications for understanding disease progression and potential regenerative avenues.

4. MSC Developmental Origins

Presently, there are considered to be multiple developmental origins of MSCs. Unsurprisingly, given their mesenchymal differentiation potential, certain subsets of MSCs are derived from mesodermal precursors, such as lateral plate mesoderm- (LPM-) derived mesoangioblast cells from the embryonic dorsal aorta [37, 38]. Support for this comes from the observation that mesoangioblast cells isolated from the mouse dorsal aorta and then grafted into chick embryos incorporated into several mesodermal tissues (bone, cartilage, muscle, and blood) [39].

Other reports suggest MSCs partly descend from a subpopulation of neural crest cells, with the remaining MSCs descending from unknown origins. Support for this comes from the observation that a population of murine Sox1$^+$ trunk neuroepithelial cells could undergo clonogenic expansion and maintain adipogenic, chondrogenic, and osteogenic differentiation *in vitro* [40]. This neural crest origin may help explain why MSCs have neural differentiation potential and why human bone marrow-derived MSCs can be enriched for using antibodies against nerve growth factor receptor [12, 38]. Given their lineage tracing results, the authors claimed that neural crest-derived MSCs are the earliest MSCs to arise in the embryo, but they did note that other MSCs must also arise later on in development as not all MSCs detected were found to be of a neural crest origin. Corroborating this, a lineage tracing study using the promoter from Protein-0, a neural crest-associated marker, found that only a portion of bone marrow-derived MSCs were labeled in adult mice, suggestive of both a neural crest and nonneural crest origin [41].

It is possible that the indefinite nonneural crest source of MSCs observed in these studies may be mesoangioblasts or another mesoderm-derived cell type. It has also been suggested that data indicative of a mesoangioblast origin may alternatively be explained by simply "contamination" of neural crest cells as the neural tube is close to dorsal aorta at day 9.5 [38]. With regard to human MSC origins, similar dual mesoderm and neural crest origins may also exist given that human iPSCs differentiated toward these two lineages can both give rise to MSC-like cells [42, 43]. Further study will be required to resolve these issues and to elucidate if any lasting functional dissimilarities exist between MSC subpopulations that arise from differing time periods and locations during development.

5. MSC Expansion in Culture

Once isolated from their respective *in vivo* locations, human MSC populations can be expanded up to several hundredfold while maintaining their multipotency and capacity to form fibroblastic colony-forming units (CFU-F) provided the cells are seeded at a satisfactorily low seeding density ($\sim$10–100 cell/cm^2) [44]. When cultured at low clonal density, MSCs take on a highly proliferative phenotype and maintain their trilineage potential; such cells have become commonly referred to as RS-MSCs (rapidly self-renewing MSCs). This proliferative phase is thought to be dependent on Dickkopf-related protein 1 (Dkk-1) autocrine signaling which inhibits Wnt signaling that would otherwise promote differentiation [45]. Favorable for minimizing risk to patients, *in vitro* proliferation of human MSCs exhibits a relatively low frequency of oncogenic transformation ($<10^{-9}$) [46–48]. This is in stark contrast with murine MSCs which frequently gain chromosomal defects *in vitro* and often produce fibrosarcomas when injected back into mice [49].

With time, sparsely plated human MSCs create colonies with distinct *in vitro* niches with the inner cells expressing differentiation markers and the outer cells exhibiting a more RS-MSC phenotype with high motility and proliferation [50, 51]. Yet, when replated, both inner and outer regions create colonies similar to the original, implying differentiation of the inner colony is reversible to some extent [51]. If MSCs are seeded at a higher density ($\sim$1000 cell/cm^2) and/or are cultured to confluence, RS-MSCs will decrease and SR-MSCs (slowly replicating MSCs) will increase over time, while both the CFU-F and proportion of multipotent cells will gradually decline [44, 51]. This dynamic nature during culture underlines the importance of properly maintaining MSC cultures to ensure maximum self-renewal and the maintenance of differentiation potential for downstream applications.

6. MSC Differentiation Potential

As mentioned earlier, by definition, MSCs have trilineage potential with the capacity to undergo osteogenesis, adipogenesis, and chondrogenesis contingent on their exposure to the particular soluble factors in their microenvironment. Differentiation protocols for driving differentiation toward these lineages have been routinely utilized and extensively optimized [52, 53]. For example, osteogenesis typically involves the use of dexamethasone, β-glycerolphosphate, and ascorbic acid. Adipogenesis protocols also utilize

dexamethasone, in addition to isobutylmethylxanthine and indomethacin. Chondrogenesis protocols, on the other hand, typically utilize dexamethasone, ascorbic acid, sodium pyruvate, TGF-β1, and a combination of insulin-transferrin-selenium (ITS). However, variations of the components and their concentrations exist and the optimal formulations may depend on the subpopulation of MSC used and the ultimate therapeutic goal. MSCs predifferentiated toward these three lineages have been investigated extensively in the context of tissue engineering wherein cells are implanted at the site of desired repair or replacement, often along with a scaffold (Figure 1) [54–58].

Beyond the standard trilineage potential of MSCs, differentiation has also been observed toward other cell types, such as tenocytes, skeletal myocytes, cardiomyocytes, smooth muscle cells, and even neurons [59–61]. However, some of these claims have courted a degree of skepticism in regard to the frequency of differentiation and the functionality of the terminal cells produced, especially for nonmesenchymal and nonmesodermal cell types. For example, while MSCs have been shown to differentiate into neuron-like cells, the functionality of rat MSC-derived neurons has been called into question in terms of their capacity to generate normal action potentials [62, 63]. Similarly, human MSCs have also been reported to differentiate into endothelial-like cells; however, such cells have lower expression of endothelial markers compared to mature endothelial cells [64]. Further study into the differentiation frequency and normal functioning of MSC-derived terminally differentiated cells will be necessary, in addition to determining if different MSC populations are better suited to differentiate into some cell types than others. With regard to the latter, a recent study comparing human CD146$^+$/CD34$^-$/CD45$^-$ MSCs isolated from different anatomical locations (bone marrow, periosteum, and skeletal muscle) revealed that each subpopulation differed considerably in their transcriptomic signature and *in vivo* differentiation potential, hence suggesting that MSCs are not a uniform population throughout the body [65]. Moreover, MSC heterogeneity may not only exist between tissue types but also within individual tissues. For example, locationally and transcriptionally distinct subpopulations of CD34$^+$/CD146$^-$ "adventitial MSCs" and CD34$^-$/CD146$^+$ "pericyte-like MSCs" have been found to reside in human adipose tissue, a commonly used cell source for regenerative medicine [66]. Similar findings have also been noted in horses and canines, suggesting these dual perivascular subpopulations are conserved in mammals [67, 68]. Interestingly, both equine and human adipose-derived CD34$^-$/CD146$^+$ MSCs display greater angiogenicity compared to CD34$^+$/CD146$^-$ MSCs indicative of a relatively conserved functional phenotype as well, possibly due to their pericyte-like differentiation state [67, 69]. Heterogeneity among MSCs may also have important implications for treating disease resulting from inappropriate differentiation and proliferation. Of note, subsets of PDGFRβ^+ and/or PDGFRα^+ MSC-like progenitor cells with fibro-adipogenic potential have been found to be present in multiple tissues (*e.g.*, tendon, myocardium, and skeletal muscle) and may prove to be useful targets for reducing fibrotic damage after injury [70, 71].

Further investigation into MSC heterogeneity will be required to resolve if such differences are solely a result of innate differences arising from different developmental origins or if differing local microenvironments also play a role.

Unlike some other stem cell populations (e.g., hematopoietic stem cells), which have a well-established and relatively straight-forward unidirectional differentiation hierarchy, the hierarchy of MSC differentiation is currently poorly defined. To date, one of the MSC-like populations that have been most vigorously investigated in terms of hierarchy are human umbilical cord-perivascular cells (HUCPVCs). Such cells have been found to differentiate from quintipotential stem cells (with osteogenic, adipogenic, chondrogenic, myogenic, and fibrogenic potential) to a restricted fibroblast-state in a deterministic manner with a predictable order of loss in potency [72]. Whether this is true for all or some MSC populations remains to be examined, but this study should serve as a useful template for future investigation. As well, computational approaches that cluster cells according to differentially expressed genes may also help clarify the hierarchy of MSC subpopulations and their progeny cells [66] and may serve as a guide for future lineage tracing studies. That said, transdifferentiation toward nonmesodermal lineages and bidirectional phenotype switching between different mesenchymal cell types (e.g., transitions between fibroblasts and myofibroblasts or between synthetic and contractile smooth muscle cells) may further complicate any MSC hierarchical differentiation model established [73]. Regardless of any specific hierarchy and the potential for phenotypic plasticity, it should be emphasized that ultimately, the microenvironment dictates MSC behaviour, in terms of both their differentiation and their interaction with other cell types.

7. MSC Immunomodulatory Paracrine Signaling

Recently, a paradigm shift has occurred in the understanding of the therapeutic effects of MSCs. Despite the differentiation potential these cells exhibit and contrary to initial assumptions, in many therapeutic contexts, MSCs exert their healing effects not through engraftment and differentiation but rather through paracrine signaling and communication through cell-cell contacts [51, 74]. The significance of this paradigm change is reflected in the recent recommendation to rebrand MSCs as *medicinal signaling cells* by Arnold Caplan, who had originally coined the term mesenchymal stem cells [75]. Notable examples of MSC paracrine/juxtacrine-mediated treatments currently in preclinical and clinical development include injections into the myocardium after infarction, treatments for graft versus host disease (GvHD), and therapies for autoimmunity disorders (such as Crohn's disease and type I diabetes) [76–79]. Given these successes, it is becoming increasing clear that the MSC secretome has broadly beneficial effects that can be exploited for a wide range of therapeutic applications.

The MSC secretome contains a large range of molecules that are beneficial for tissue repair, including ligands that promote the proliferation and differentiation of other stem/

progenitor cells, chemoattraction, antifibrosis, antiapoptosis, angiogenesis, and immunomodulation [80]. Currently, perhaps the most impactful of these properties from a clinical perspective is their capacity for immunomodulation, which has motivated the development of intravenous injections of MSCs, such as Osiris Therapeutics' Prochymal®, which is approved for GvHD in Canada and currently in clinical trials for several autoimmune disorders in Canada and the USA. This immunomodulatory capacity has been partly attributed to the ability of MSCs to inhibit effector T-cell activation and proliferation, both directly through various cytokines and indirectly through modulating the activity of regulatory T-cells [81, 82]. MSCs have also been described as modulating the behaviors of natural killer cells, dendritic cells, B-cells, neutrophils, and monocytes/macrophages through the actions of a number of molecules, including prostaglandin E2 (PGE2), indoleamine 2,3-dioxygenase (IDO), nitric oxide (NO), interleukin-10 (IL-10), and many others [8, 80]. Notably in the context of localized tissue repair, MSCs have been implicated in promoting alternative activation of macrophages toward a regenerative and proangiogenic M2 phenotype, as opposed to a classical proinflammatory M1 phenotype [83–86]. Consequently, given the many roles MSCs play in therapeutic immunomodulation and regeneration, it is becoming increasingly acknowledged that one of the main roles of adult MSCs *in vivo* may be to coordinate healing responses and to help prevent autoimmunity after injury [8, 74, 80].

Lastly, it should be noted that MSCs are not solely anti-inflammatory. Under certain conditions, MSCs can elicit an inflammatory response by presenting antigens to induce CD8$^+$ T-cell responses, and increasing expression of MHCDII and presenting antigens to CD4$^+$ T-cells [87–89]. The "switch" between eliciting an inflammatory or anti-inflammatory response generally seems to be whether the activating signals are associated with infections or tissue injury, respectively [90].

8. MSC Angiogenic Paracrine Signaling

In addition to being proangiogenic by promoting a regenerative microenvironment via immunomodulation, MSCs also directly secrete angiogenic factors that affect endothelial cell survival, proliferation, and migration. Such factors include key growth factors critical for initial vessel formation and subsequent stabilization, such as VEGF, FGF2, SDF1, ANG1, MCP-1, HGF, and many others [91, 92]. Beyond these classical angiogenic growth factors, MSCs also secrete microvesicles (>200 μm) and exosomes (~50–200 μm) that can carry both growth factors and miRNAs and have been demonstrated to have proangiogenic activities both *in vitro* and *in vivo* [93]. Such extracellular vesicles have been shown to enhance angiogenesis and healing in a number of contexts, including murine and rat models of burn injury, cutaneous wounds, myocardial infarction, and limb ischemia [94–99]. Recent proteomic analysis has found human MSC-derived exosomes contain a number of proteins associated with angiogenesis that were upregulated when MSCs were

exposed to ischemic-like conditions, including PDGF, EGF, FGF, and NF-κB pathway-affiliated proteins [100].

Similarly, recent qPCR screening of exosomes derived from murine MSC-like cells revealed they contain a number of known proangiogenic microRNAs, several of which were found to be preferentially internalized by endothelial cells, including miR-424, miR-30c, miR-30b, and let-7f [101]. Relatedly, miR-210 has also been implicated in the therapeutic effect of MSC-derived extracellular vesicles in a mouse model of cardiac infarction, as siRNA knockdown reduced the angiogenic effect of the vesicles [102]. Delineating which specific MSC-derived exosomal miRNAs are responsible for particular aspects of angiogenesis is an ongoing area of research. Recently, for example, exosomal miRNA-125a from human adipose-derived MSCs has been implicated in enhancing angiogenesis specifically by promoting tip cell formation through the inhibition of delta-like 4 (DLL4) [103]. Ultimately, however, as is the case with angiogenic growth factors, multiple miRNAs may have to work in concert to achieve maximal effects and interrogating which subsets are critical for different stages of angiogenesis will require further inquiry.

9. Direct Cellular Involvement of MSCs in Angiogenesis

In addition to their interaction via various paracrine routes, MSCs also participate in direct cell-cell contact with endothelial cells. When cocultured on or embedded within hydrogels (e.g., fibrin or Matrigel), endothelial cells form capillary-like structures on which MSCs may adhere and assume an abluminal position akin to their perivascular position *in vivo* [104]. This maintained mural cell behavior after culture may be exploited for microvascular tissue engineering as it has beneficial effects for the nascent endothelial tubules. For example, the permeability of these *in vitro* structures is decreased in the presence of MSCs relative to simply coculturing endothelial cells with fibroblasts potentially due to tighter cell-cell junctions and VE-cadherin expression [105]. This effect may also be attributed to increased basement membrane formation, as extensive studies of pericyte-endothelial cell cocultures have demonstrated that both the expression and deposition of basement membrane proteins is upregulated through cell-cell contact *in vitro* [106, 107]. However, any specific effects of MSCs on basement membrane formation and its composition, compared to non-multipotent pericytes, has yet to be elucidated.

Under *in vivo* contexts, MSCs can also assume a perivascular cell phenotype and have beneficial effects on vessel stability and permeability. For example, when collagen-fibronectin gels containing EGFP-labeled human MSCs and HUVEC (human umbilical vein endothelial cells) were implanted in cranial windows of SCID mice, implants with MSCs resulted in a higher vessel density compared to HUVEC-only implants, and EGFP colocalized with staining for the smooth muscle cell- (SMC-) related markers, αSMA and SM22α [108]. Similarly, when embedded within submillimeter collagen rods coated with endothelial cells and then

implanted in an omental pouch within rats, GFP-labeled rat MSCs were found to migrate out of the modules and began to associate with blood vessels and express αSMA at day 7 postimplantation, while at day 21, all GFP$^+$ MSCs were found to be in a perivascular position [109]. Strikingly, when examined by microCT after Microfil® injection, including MSCs within the implant created vasculature with reduced leakiness compared to endothelial cell-only controls which exhibited a leaky core.

Similarly, after subcutaneous injection of HUVEC and fibrin hydrogel into SCID mice, HUVEC-derived vessels formed after 7 and 14 days showed decreased permeability to 70 kDa dextran in conditions including human adipose and bone marrow-derived MSCs, compared to lung fibroblasts or endothelial cells alone [110]. Correspondingly, with this improved barrier function, only implants with ASCs and BMSCs contained vessels with abluminal calponin staining, suggestive of SMC differentiation of the implanted stromal cells. Collectively, it is clear that not only is the presence of a mesenchymal cell type advantageous for vessel formation and stabilization, but the identity of the mesenchymal cell type and its propensity to take on an abluminal position and perivascular cell phenotype has an impact on the functionality of the resulting vessels.

10. Clinical Considerations for Using Bone or Adipose MSC Sources

As noted previously, MSCs can be isolated from many different human tissues; however, the most common adult sources for clinical use are bone marrow and adipose tissue. This is due to a number of reasons, including the total cell numbers that can be harvested, the frequency of the cells of interest, and the relatively small procedural risk associated with obtaining cells from these locations compared to other anatomical locations. As well, in the case of adipose tissue removal, if the procedure is being carried out for other purposes (*e.g.*, elective cosmetic surgery), there is no additional risk associated with the harvesting of progenitor cells which would otherwise be discarded.

In the case of bone marrow aspirate, the procedure is generally carried out at the bedside using a local anesthetic (*e.g.*, lidocaine) with the posterior superior iliac spine being the preferred collection site owing to its relative ease of access [111]. After sterilization of the overlying skin, a fine gauge trocar is used to gain access to the marrow space, which then permits the subsequent aspiration of marrow by syringe [111]. For the purposes of stem cell harvesting, it is possible to harvest as much as 20 mL of marrow from a single aspirate site [112].

Bone marrow sampling is generally considered to be safe but can frequently result in pain during and after the procedure [113]. Preventative measures, such as first ensuring that the periosteum is adequately anesthetized, can be used to reduce the pain to acceptable levels [113]. Other adverse events during bone marrow sampling are rare, with an estimated event rate of 5/10,000 and a fatality rate of 1-2/100,000 [114]. In a 2013 survey conducted by the British Society of Haematology, out of a total of 19,259 bone marrow

aspirates with or without trephine biopsies, clinically significant hemorrhage occurred in only 11 patients, while infections were seen in just two [114]. The risk of bleeding can be mitigated through careful patient selection and correction of underlying coagulopathies if necessary. When bleeding does occur, it is usually mild and can often be controlled by the manual application of pressure to the site [111]. In the event of more significant bleeding, arterial embolization has been demonstrated to be an effective hemostatic therapy [115]. The risk of infection can be mitigated by first ensuring an absence of any overlying skin or soft tissue infection or presence of osteomyelitis. In suspected occurrences of infectious complications, topical antimicrobials are generally considered to be adequate in most cases.

In contrast to bone marrow aspirate, adipose tissue—in the form of liquid fat from liposuction or solid fat from abdominoplasty—is obtained under general anesthetic with a greater risk of procedural morbidity and mortality [116]. In the case of liposuction, the targeted fat is removed via aspiration after injection of a sterile saline solution containing epinephrine and a topical anesthetic [116]. The process may be facilitated by the liquefaction of fat using ultrasound- or laser-assisted liposuction [116]. Conversely, abdominoplasty involves the surgical excision of excess solid adipose tissue and dermis.

Common adverse events for liposuction include postoperative nausea and vomiting, local nerve damage and paresthesias, intra- and postprocedural bleeding and hematomas, persistent edema, surgical wound infection, skin necrosis, and unplanned hospitalization or increased length of stay [117]. The risk of fatality of liposuction is conservatively estimated to be 1/5000 with deaths being attributable to pulmonary embolism, visceral perforation, cardiorespiratory complications associated with anesthesia, and hemorrhage (in order of decreasing frequency) [118]. Abdominoplasty is a more invasive procedure with higher rates of surgical complications, including wound dehiscence and necrosis, infection, and a fatality rate approaching 1/600 [119].

Given the relatively unfavorable risk profile associated with surgical collection of adipose tissue, the harvesting of adipose-derived MSCs is ideal for patients who are already planning on undergoing such a procedure. Otherwise, bone marrow aspirate remains a preferred option as it can permit the ad hoc collection of MSCs at a lower risk of morbidity and mortality. However, such clinical risks must be weighed against certain practical requirements as well.

In addition to considering the risks associated with the different anatomical sites and any contraindications specific to a certain patient, the preference for one tissue source over the other may also be affected by the number of desired cells that can be collected from a certain source and the quantity of cells requisite for a particular application. As summarized by Murphy et al., in the case of a bone marrow aspirate, approximately 109–664 CFU-F/mL can be obtained at a frequency of 10–83 CFU-F/10^6 nucleated cells [120]. In contrast, lipoaspirate typically yields far more cells of interest per milliliter of tissue, with 2058–9650 CFU-F/mL at a frequency of 205–51,000 CFU-F/10^6 nucleated cells

[120]. Hence, if the quantity of cells that can be obtained via bone marrow aspirate are insufficient for a particular autologous application, relying on an adipose cell source instead may be a sensible option. This is especially true in situations where *ex vivo* culture must be limited to preserve a desired cellular phenotype or when culture is not utilized at all (*i.e.*, immediate autologous use of the stromal vascular fraction (SVF) after harvesting).

Beyond differences in the quantity of cells obtainable from either bone or adipose tissues, innate differences in differentiation ability between cell types may also affect the preference of one MSC population over the other for a particular application. Unsurprisingly, given their developmental and anatomical origins, adipose-derived MSCs have been demonstrated to have an increased capacity for *in vitro* adipogenic differentiation by Oil Red O staining, possibly due to their relatively higher expression of the adipogenesis-regulating transcription factor, PPAR-γ, after exposure to adipogenic stimuli [121, 122]. Similarly, bone marrow-derived MSCs have been demonstrated to have an increased capacity for osteogenic differentiation over MSCs derived from adipose tissue via alizarin red staining [121, 122]. This may be partly attributable to their higher expression of the key osteogenic transcription factor, Runx2, during osteogenic differentiation [122]. Moreover, bone marrow-derived MSCs have also been shown to have a higher capacity for chondrogenic differentiation (by alcian blue staining and collagen II expression), as may be expected considering the close relationship between chondrogenesis and osteogenesis in the generation of osseous tissues [121–123]. It should be noted, however, that some conflicting reports to these general findings also exist and suggest that whether adipose or bone-derived MSCs have the higher capacity to differentiate toward a particular lineage may depend on the characteristics of the patient (*e.g.*, sex, age, and disease state), the isolation protocol, and the differentiation conditions [90].

Other notable functional differences between the two cell types have been documented. For example, in a comparison of the immunomodulatory capacity of adipose and bone marrow-derived MSCs isolated from the same donor, Valencia et al. found that MSCs from bone marrow had a higher capacity to inhibit natural killer cytotoxic activity, whereas adipose-derived MSCs had a higher capacity to inhibit dendritic cell differentiation [124]. Corroborating this, other reports have also described similar findings regarding these differential effects on natural killer cells and dendritic cell differentiation [125, 126]. Similarly, differences in growth factor expression between the two cell types have also been noted and may influence which cell type to use in clinical applications where MSCs are intended to provide trophic support. For example, bone marrow-derived MSCs have been shown to produce significantly more HGF compared to adipose-derived MSCs, which may be an important consideration for regenerative therapies involving the liver [122]. Overall, the choice of bone or adipose sources is complex and is influenced by factors specific to the application and the patient. As the use of MSCs becomes increasingly common, the

optimal choice of cell source for specific clinical circumstances will likely become clearer.

11. iPSC Sources and Epigenetic Reprogramming of MSCs

Despite the clinical promise of MSCs in allogeneic applications (or the use of HLA-matched donor cells), some therapies may necessitate an autologous approach, such as long-term implantation of MSC-derived engineered tissues. However, this presents a significant challenge in cases where the desired cell type cannot be obtained in sufficient numbers to be clinically useful. This may occur in the case of needing to engineer particularly large replacement tissues, as MSCs have limited expansion capability in culture, partly due to their low to absent expression of telomerase [127, 128]. As well, this may occur when patients have insufficient MSCs of adequate quality due to age or disease. With regard to aging, CFU-F frequency within the bone marrow generally declines with age, and the capacity of the remaining MSCs to withstand oxidative stress appears to also decline along with their function and therapeutic efficacy [129–131]. Such functional changes may be the result of progressively shortening telomeres, accumulated molecular damage, and stochastic genetic and epigenetic changes over time [132–136]. Such age-associated epigenetic dysregulation may also contribute to alterations in the differentiation potential and heterogeneity of MSCs [137, 138]. In addition to age-induced functional decline, conditions such as type 2 diabetes and metabolic syndrome may similarly limit the therapeutic potential of MSCs for autologous use due to increased oxidative stress, mitochondrial dysfunction, and increased senescence [139].

One potential solution to address this issue is iPSC (induced pluripotent stem cell) technology in which somatic cells from a patient are first reprogrammed to a pluripotent state, usually by the overexpression of transcription factors (*e.g.*, KLF4, c-MYC, OCT4, and SOX2) [140, 141]. Favorably, such cells can then be expanded *in vitro* extensively prior to differentiation, partly due to their expression of telomerase. Also favorably, especially for cells harvested from aged patients, once harvested cells are differentiated into the desired cell type after having been in a transient pluripotent state results in longer telomeres compared to the starting donor cell along with a "rejuvenated" epigenetic landscape with reduced aging-associated epigenetic marks and increased resistance to oxidative stress [142, 143].

Multiple studies have explored methods for differentiating MSC-like cells from iPSCs [143–149]. These reports have described iPSC-MSCs as being largely comparable to mature MSCs in terms of trilineage potential, immunomodulation, and trophic support. However, some minor differences have also been noted, such as differences in adipose differentiation, T-cell regulation, sensitivity to NK cells, and their expression levels of certain genes (*e.g.*, interleukin-1 and TGFβ receptors) [143, 150–153]. Interestingly, a recent study by Chin et al. reported that differentiation of human pluripotent stem cells into MSCs results in two distinct subpopulations with different trophic phenotypes [149].

One subpopulation with higher expression of CD146 and CD73 could maintain HSCs (hematopoietic stem cells) *ex vivo* and expressed HSC niche-related genes, while a second subpopulation with lower expression of CD146 and CD73 displayed poor maintenance of HSCs. Such *in vitro* findings using iPSCs are intriguingly reminiscent of *in vivo* MSC heterogeneity and may not only help provide a source of MSCs for clinical use but may also help elucidate the developmental origins of different MSC subpopulations.

While iPSCs are a promising source of MSCs, they do carry the risk of malignant transformation during culture and teratoma formation after transplantation due to residual pluripotent cells [154]. Alternative means for returning aged or diseased MSCs to a more therapeutically effective state without relying on a transient pluripotent stage may also exist. One option may consist of using the pluripotency genes used for creating iPSCs but for a shorter duration in order to elicit partial reprogramming and reverse age-associated epigenetic marks but not loss of cellular identity. Such an approach yielded impressive results in mice in terms of improving recovery from metabolic disease and increasing muscle regeneration after transient *in vivo* overexpression [155]. It remains to be seen, however, if this approach has a beneficial effect on MSCs as well. Future work will need to focus on determining the optimal dosing regimen for human cells and examining if this method is useful for the *ex vivo* rejuvenation of human MSCs.

Alternatives for rejuvenating cells that do not rely on pluripotency genes at all also exist, which may be preferable for further mitigating tumorigenic risks. One option may be to alter the levels of beneficial or detrimental miRNAs within cultured MSCs prior to transplantation. For example, Okada et al. unveiled that miR-195 plays a key role in inducing senescence in murine bone marrow-derived MSCs by inhibiting the expression of telomerase [156]. When the authors inhibited miR-195, telomere lengths and cellular proliferation were increased compared to control cells. Most importantly though, using a mouse model of acute myocardial infarction, the authors demonstrated that when transplanted the rejuvenated cells resulted in reduced infarct size and improved left-ventricle function.

Conversely, upregulation of certain molecules, such as miR-543 and miR-590-3p may also be useful in preventing senescence given their inhibitory roles in senescence onset in MSCs [157]. Upregulation of SIRT1, a NAD^+-dependent deacetylase, has also been shown to prevent MSC senescence possibly through increasing telomerase activity and reducing DNA damage [158]. Strikingly, overexpression of telomerase and myocardin in aged murine MSCs resulted in improved therapeutic efficacy when used in a model of hindlimb ischemia, in terms of stimulating arteriogenesis and increasing blood flow [159]. Regardless of whether particular factors are upregulated or downregulated, it should be stressed that any approach that alters regulators of senescence, telomere length, and/or pluripotency will require extensive investigation in order to ensure that rejuvenation of MSCs does not come at the cost of increasing tumorigenesis.

12. Clinical Risks and Challenges

As of May 2018, there are currently 82 active and recruiting trials involving "mesenchymal stem cells" listed by Clinical-Trials.gov in the United States alone, in addition to 44 already completed studies; moreover, there are also 27 active/recruiting trials involving "mesenchymal stromal cells" with 9 already completed. Of these ongoing studies, the majority are currently in phase 1 followed by phase 2 trials. Given these appreciable number of trials and their early stages, it will be crucial to discern if any patterns of adverse effects can be detected among MSC clinical trials in order to develop effective solutions to these issues. The risks involved in these trials are partly dependent on the route of administration of MSCs (Figure 1).

In terms of risks involving the systemic infusion of MSCs, Lalu et al. conducted a meta-analysis of clinical trials with both autologous and allogeneic MSCs and concluded that this route of administration appears generally safe as their analysis did not find any significant association between MSC infusion and acute toxicity, infection, organ system complications, malignancy, or death [160]. There was, however, a significant association with transient fever in some patients. Other studies have also identified chill, infection, and liver damage as potential adverse effects of systemic administration [161, 162]. Lalu et al. also commented on the frequent absence of reporting follow-up duration for long-term adverse events in the studies they examined and noted that it is critical that future studies investigate both short-term and long-term adverse events given that experimental cell-based therapies may have serious long-term consequences (*e.g.*, immunological complications, causing/enhancing neoplastic growth). Favorably for risk mitigation, however, there is evidence to suggest that MSCs that are infused systemically generally do not persist over the long-term [163]. Also favorably, of the 13 studies examined by Lalu et al. that used unmatched allogeneic MSCs, none reported acute infusional toxicity. Such findings bode well for systemically administered therapies requiring large quantities of cells that cannot be acquired from a single patient and for cases in which a patient's own MSCs may be functionally inadequate and/or inaccessible due to underlying disease.

Regardless, while MSCs themselves appear generally safe for systemic infusion, biological and chemical components associated with the *ex vivo* culture and storage of MSCs, such as fetal bovine serum (FBS) and dimethylsulfoxide (DMSO) may introduce risks in the clinical use of MSCs. Such components warrant caution due to the possibility of infectious contamination, immunogenicity, and/or infusional toxicity [164, 165]. With regard to zoonotic concerns regarding FBS, such risks may be addressed through the use of human platelet lysate in place of FBS for supporting the *ex vivo* growth of MSCs [164, 166].

Risks and their associated challenges regarding more experimental interventions involving the local injection of MSCs and implantation of engineered tissues are currently less well defined compared to the more commonly used systemic administration route. Currently, challenges associated

with these approaches often relate to first establishing clinically significant efficacy in order to justify these more invasive procedures. Some key challenges for local injections include maintaining cell viability, increasing MSC permanence after injection, and optimizing delivery to a specific location [161, 167, 168]. In regard to this, rapidly gelling injectable hydrogels have shown promise in targeting MSCs to specific anatomical locations and in maintaining their viability after injection to prolong therapeutic function [169]. Currently, investigations into generating engineered tissues are primarily focused on ensuring comparable function to native tissues (or at least, similar enough to be therapeutically useful). Key challenges include optimizing the differentiation process, developing effective scaffold materials, and ensuring sufficient maturation of the nascent tissues through chemical and mechanical cues [73, 170, 171]. As well, depending on the tissue type and its dimensions, the issue of vascularization either pre- or postimplantation must also be addressed in order to preserve function and to avoid ischemia-induced inflammation. As discussed previously in this review, MSCs themselves may be of use in this regard given their proangiogenic signaling and native perivascular phenotype. Ostensibly, some engineered tissues may be optimally composed of MSC-derived terminally differentiated cells along with angiogenic undifferentiated MSCs, in order to fully take advantage of both their differentiation and angiogenic capabilities.

13. Concluding Remarks

Efforts into understanding and exploiting MSCs for therapeutic use have garnered a multifaceted view into the capabilities of these cells, albeit sometimes in a nonlinear and even serendipitous manner. Contrary to many other clinical successes for drugs and cell therapies alike, where a comprehensive understanding of the therapeutic mechanism(s) is first established before being employed clinically, MSCs have had remarkable successes despite a limited understanding of their *in vivo* function under normal physiological conditions. To further improve and build on these early successes, future work will need to be directed toward understanding the more nuanced aspects of these cells. As alluded to earlier, this will partly involve developing an improved understanding of the differences between MSCs found in different anatomical locations and the heterogeneity that exists within these subpopulations, in addition to performing rigorous investigation into the functional differences between cells differentiated from MSCs and native terminal cells. By building on the body of MSC research that has been produced thus far, potential risks in downstream clinical applications can be mitigated and the therapeutic potential of MSCs may be further expanded upon to benefit patients in a wide range of clinical settings.

Conflicts of Interest

The authors declare that they have no conflicts of interest.

References

[1] A. J. Friedenstein, I. I. Piatetzky-Shapiro, and K. V. Petrakova, "Osteogenesis in transplants of bone marrow cells," *Development*, vol. 16, no. 3, pp. 381–390, 1966.

[2] A. J. Friedenstein, R. K. Chailakhjan, and K. S. Lalykina, "The development of fibroblast colonies in monolayer cultures of guinea-pig bone marrow and spleen cells," *Cell Proliferation*, vol. 3, no. 4, pp. 393–403, 1970.

[3] A. I. Caplan, "Mesenchymal stem cells," *Journal of Orthopaedic Research*, vol. 9, no. 5, pp. 641–650, 1991.

[4] M. F. Pittenger, A. M. Mackay, S. C. Beck et al., "Multilineage potential of adult human mesenchymal stem cells," *Science*, vol. 284, no. 5411, pp. 143–147, 1999.

[5] M. Dominici, K. le Blanc, I. Mueller et al., "Minimal criteria for defining multipotent mesenchymal stromal cells. The International Society for Cellular Therapy position statement," *Cytotherapy*, vol. 8, no. 4, pp. 315–317, 2006.

[6] C.-S. Lin, Z.-C. Xin, J. Dai, and T. F. Lue, "Commonly used mesenchymal stem cell markers and tracking labels: limitations and challenges," *Histology and Histopathology*, vol. 28, no. 9, pp. 1109–1116, 2013.

[7] M. Corselli, C.-W. Chen, B. Sun, S. Yap, J. P. Rubin, and B. Peault, "The tunica adventitia of human arteries and veins as a source of mesenchymal stem cells," *Stem Cells and Development*, vol. 21, no. 8, pp. 1299–1308, 2012.

[8] A. J. Nauta and W. E. Fibbe, "Immunomodulatory properties of mesenchymal stromal cells," *Blood*, vol. 110, no. 10, pp. 3499–3506, 2007.

[9] N. Barker and H. Clevers, "Leucine-rich repeat-containing G-protein-coupled receptors as markers of adult stem cells," *Gastroenterology*, vol. 138, no. 5, pp. 1681–1696, 2010.

[10] B. Sacchetti, A. Funari, S. Michienzi et al., "Self-renewing osteoprogenitors in bone marrow sinusoids can organize a hematopoietic microenvironment," *Cell*, vol. 131, no. 2, pp. 324–336, 2007.

[11] S. Gronthos, A. C. W. Zannettino, S. J. Hay et al., "Molecular and cellular characterisation of highly purified stromal stem cells derived from human bone marrow," *Journal of Cell Science*, vol. 116, no. 9, pp. 1827–1835, 2003.

[12] N. Quirici, D. Soligo, P. Bossolasco, F. Servida, C. Lumini, and G. L. Deliliers, "Isolation of bone marrow mesenchymal stem cells by anti-nerve growth factor receptor antibodies," *Experimental Hematology*, vol. 30, no. 7, pp. 783–791, 2002.

[13] M. Sobiesiak, K. Sivasubramaniyan, C. Hermann et al., "The mesenchymal stem cell antigen MSCA-1 is identical to tissue non-specific alkaline phosphatase," *Stem Cells and Development*, vol. 19, no. 5, pp. 669–677, 2010.

[14] S. J. Morrison and D. T. Scadden, "The bone marrow niche for haematopoietic stem cells," *Nature*, vol. 505, no. 7483, pp. 327–334, 2014.

[15] B. A. Anthony and D. C. Link, "Regulation of hematopoietic stem cells by bone marrow stromal cells," *Trends in Immunology*, vol. 35, no. 1, pp. 32–37, 2014.

[16] C. Nombela-Arrieta, J. Ritz, and L. E. Silberstein, "The elusive nature and function of mesenchymal stem cells," *Nature Reviews Molecular Cell Biology*, vol. 12, no. 2, pp. 126–131, 2011.

[17] N. Beyer Nardi and L. da Silva Meirelles, "Mesenchymal stem cells: isolation, in vitro expansion and characterization," in *Stem Cells. Handbook of Experimental Pharmacology, vol 174*, A. M. Wobus and K. R. Boheler, Eds., pp. 249–282, Springer, Berlin, Heidelberg, 2006.

[18] W. C. W. Chen, J. E. Baily, M. Corselli et al., "Human myocardial pericytes: multipotent mesodermal precursors exhibiting cardiac specificity," *Stem Cells*, vol. 33, no. 2, pp. 557–573, 2015.

[19] A. Stefanska, C. Kenyon, H. C. Christian et al., "Human kidney pericytes produce renin," *Kidney International*, vol. 90, no. 6, pp. 1251–1261, 2016.

[20] A. I. Caplan, "All MSCs are pericytes?," *Cell Stem Cell*, vol. 3, no. 3, pp. 229-230, 2008.

[21] S. Shi and S. Gronthos, "Perivascular niche of postnatal mesenchymal stem cells in human bone marrow and dental pulp," *Journal of Bone and Mineral Research*, vol. 18, no. 4, pp. 696–704, 2003.

[22] M. Crisan, S. Yap, L. Casteilla et al., "A perivascular origin for mesenchymal stem cells in multiple human organs," *Cell Stem Cell*, vol. 3, no. 3, pp. 301–313, 2008.

[23] R. Kramann, R. K. Schneider, D. P. DiRocco et al., "Perivascular Gli1+ progenitors are key contributors to injury-induced organ fibrosis," *Cell Stem Cell*, vol. 16, no. 1, pp. 51–66, 2015.

[24] R. Kramann, C. Goettsch, J. Wongboonsin et al., "Adventitial MSC-like cells are progenitors of vascular smooth muscle cells and drive vascular calcification in chronic kidney disease," *Cell Stem Cell*, vol. 19, no. 5, pp. 628–642, 2016.

[25] A. H. Baker and B. Peault, "A Gli(1) ttering role for perivascular stem cells in blood vessel remodeling," *Cell Stem Cell*, vol. 19, no. 5, pp. 563–565, 2016.

[26] R. Sarugaser, D. Lickorish, D. Baksh, M. M. Hosseini, and J. E. Davies, "Human umbilical cord perivascular (HUCPV) cells: a source of mesenchymal progenitors," *Stem Cells*, vol. 23, no. 2, pp. 220–229, 2005.

[27] J. Ennis, C. Götherström, K. Le Blanc, and J. E. Davies, "In vitro immunologic properties of human umbilical cord perivascular cells," *Cytotherapy*, vol. 10, no. 2, pp. 174–181, 2008.

[28] N. Zebardast, D. Lickorish, and J. E. Davies, "Human umbilical cord perivascular cells (HUCPVC): a mesenchymal cell source for dermal wound healing," *Organogenesis*, vol. 6, no. 4, pp. 197–203, 2010.

[29] J. Feng, A. Mantesso, C. De Bari, A. Nishiyama, and P. T. Sharpe, "Dual origin of mesenchymal stem cells contributing to organ growth and repair," *Proceedings of the National Academy of Sciences*, vol. 108, no. 16, pp. 6503–6508, 2011.

[30] Y. Sakaguchi, I. Sekiya, K. Yagishita, and T. Muneta, "Comparison of human stem cells derived from various mesenchymal tissues: superiority of synovium as a cell source," *Arthritis & Rheumatology*, vol. 52, no. 8, pp. 2521–2529, 2005.

[31] A. Nimura, T. Muneta, H. Koga et al., "Increased proliferation of human synovial mesenchymal stem cells with autologous human serum: comparisons with bone marrow mesenchymal stem cells and with fetal bovine serum," *Arthritis & Rheumatology*, vol. 58, no. 2, pp. 501–510, 2008.

[32] Y. Ogata, Y. Mabuchi, M. Yoshida et al., "Purified human synovium mesenchymal stem cells as a good resource for cartilage regeneration," *PLoS One*, vol. 10, no. 6, article e0129096, 2015.

[33] J.-H. Chen, C. Y. Y. Yip, E. D. Sone, and C. A. Simmons, "Identification and characterization of aortic valve mesenchymal progenitor cells with robust osteogenic calcification potential," *The American Journal of Pathology*, vol. 174, no. 3, pp. 1109–1119, 2009.

[34] J. R. Levick, "Microvascular architecture and exchange in synovial joints," *Microcirculation*, vol. 2, no. 3, pp. 217–233, 1995.

[35] K. L. Weind, C. G. Ellis, and D. R. Boughner, "The aortic valve blood supply," *The Journal of Heart Valve Disease*, vol. 9, pp. 1–7, 2000.

[36] Y. Soini, T. Salo, and J. Satta, "Angiogenesis is involved in the pathogenesis of nonrheumatic aortic valve stenosis," *Human Pathology*, vol. 34, no. 8, pp. 756–763, 2003.

[37] G. Sheng, "The developmental basis of mesenchymal stem/stromal cells (MSCs)," *BMC Developmental Biology*, vol. 15, no. 1, pp. 44–48, 2015.

[38] L. da Silva Meirelles, A. I. Caplan, and N. B. Nardi, "In search of the in vivo identity of mesenchymal stem cells," *Stem Cells*, vol. 26, no. 9, pp. 2287–2299, 2008.

[39] M. G. Minasi, M. Riminucci, L. de Angelis et al., "The mesoangioblast: a multipotent, self-renewing cell that originates from the dorsal aorta and differentiates into most mesodermal tissues," *Development*, vol. 129, no. 11, pp. 2773–2783, 2002.

[40] Y. Takashima, T. Era, K. Nakao et al., "Neuroepithelial cells supply an initial transient wave of MSC differentiation," *Cell*, vol. 129, no. 7, pp. 1377–1388, 2007.

[41] S. Morikawa, Y. Mabuchi, K. Niibe et al., "Development of mesenchymal stem cells partially originate from the neural crest," *Biochemical and Biophysical Research Communications*, vol. 379, no. 4, pp. 1114–1119, 2009.

[42] M. A. Vodyanik, J. Yu, X. Zhang et al., "A mesoderm-derived precursor for mesenchymal stem and endothelial cells," *Cell Stem Cell*, vol. 7, no. 6, pp. 718–729, 2010.

[43] R. Chijimatsu, M. Ikeya, Y. Yasui et al., "Characterization of mesenchymal stem cell-like cells derived from human iPSCs via neural crest development and their application for osteochondral repair," *Stem Cells International*, vol. 2017, Article ID 1960965, 18 pages, 2017.

[44] I. Sekiya, B. L. Larson, J. R. Smith, R. Pochampally, J.-G. Cui, and D. J. Prockop, "Expansion of human adult stem cells from bone marrow stroma: conditions that maximize the yields of early progenitors and evaluate their quality," *Stem Cells*, vol. 20, no. 6, pp. 530–541, 2002.

[45] C. A. Gregory, H. Singh, A. S. Perry, and D. J. Prockop, "The Wnt signaling inhibitor dickkopf-1 is required for reentry into the cell cycle of human adult stem cells from bone marrow," *Journal of Biological Chemistry*, vol. 278, no. 30, pp. 28067–28078, 2003.

[46] M. E. Bernardo, N. Zaffaroni, F. Novara et al., "Human bone marrow derived mesenchymal stem cells do not undergo

transformation after long-term *in vitro* culture and do not exhibit telomere maintenance mechanisms," *Cancer Research*, vol. 67, no. 19, pp. 9142–9149, 2007.

[47] D. J. Prockop, M. Brenner, W. E. Fibbe et al., "Defining the risks of mesenchymal stromal cell therapy," *Cytotherapy*, vol. 12, no. 5, pp. 576–578, 2010.

[48] A. Conforti, N. Starc, S. Biagini et al., "Resistance to neoplastic transformation of *ex-vivo* expanded human mesenchymal stromal cells after exposure to supramaximal physical and chemical stress," *Oncotarget*, vol. 7, no. 47, pp. 77416–77429, 2016.

[49] M. Miura, Y. Miura, H. M. Padilla-Nash et al., "Accumulated chromosomal instability in murine bone marrow mesenchymal stem cells leads to malignant transformation," *Stem Cells*, vol. 24, no. 4, pp. 1095–1103, 2006.

[50] C. A. Gregory, J. Ylostalo, and D. J. Prockop, "Adult bone marrow stem/progenitor cells (MSCs) are preconditioned by microenvironmental "niches" in culture: a two-stage hypothesis for regulation of MSC fate," *Science's STKE*, vol. 2005, no. 294, article pe37, 2005.

[51] D. J. Prockop, "Repair of tissues by adult stem/progenitor cells (MSCs): controversies, myths, and changing paradigms," *Molecular Therapy*, vol. 17, no. 6, pp. 939–946, 2009.

[52] M. C. Ciuffreda, G. Malpasso, P. Musarò, V. Turco, and M. Gnecchi, "Protocols for *in vitro* differentiation of human mesenchymal stem cells into osteogenic, chondrogenic and adipogenic lineages," in *Mesenchymal Stem Cells. Methods in Molecular Biology, vol 1416*, M. Gnecchi, Ed., pp. 149–158, Humana Press, New York, NY, USA, 2016.

[53] C. Vater, P. Kasten, and M. Stiehler, "Culture media for the differentiation of mesenchymal stromal cells," *Acta Biomaterialia*, vol. 7, no. 2, pp. 463–477, 2011.

[54] S. Bose, M. Roy, and A. Bandyopadhyay, "Recent advances in bone tissue engineering scaffolds," *Trends in Biotechnology*, vol. 30, no. 10, pp. 546–554, 2012.

[55] A. R. Amini, C. T. Laurencin, and S. P. Nukavarapu, "Bone tissue engineering: recent advances and challenges," *Critical Reviews™ in Biomedical Engineering*, vol. 40, no. 5, pp. 363–408, 2012.

[56] E. A. Makris, A. H. Gomoll, K. N. Malizos, J. C. Hu, and K. A. Athanasiou, "Repair and tissue engineering techniques for articular cartilage," *Nature Reviews Rheumatology*, vol. 11, no. 1, pp. 21–34, 2015.

[57] L. Zhang, J. Hu, and K. A. Athanasiou, "The role of tissue engineering in articular cartilage repair and regeneration," *Critical Reviews™ in Biomedical Engineering*, vol. 37, no. 1-2, pp. 1–57, 2009.

[58] J. H. Choi, J. M. Gimble, K. Lee et al., "Adipose tissue engineering for soft tissue regeneration," *Tissue Engineering Part B: Reviews*, vol. 16, no. 4, pp. 413–426, 2010.

[59] D. W. Youngstrom, J. E. LaDow, and J. G. Barrett, "Tenogenesis of bone marrow-, adipose-, and tendon-derived stem cells in a dynamic bioreactor," *Connective Tissue Research*, vol. 57, no. 6, pp. 454–465, 2016.

[60] D. Galli, M. Vitale, and M. Vaccarezza, "Bone marrow-derived mesenchymal cell differentiation toward myogenic lineages: facts and perspectives," *BioMed Research International*, vol. 2014, Article ID 762695, 6 pages, 2014.

[61] V. M. Tatard, G. D'Ippolito, S. Diabira et al., "Neurotrophin-directed differentiation of human adult marrow stromal cells to dopaminergic-like neurons," *Bone*, vol. 40, no. 2, pp. 360–373, 2007.

[62] S. Wislet-Gendebien, G. Hans, P. Leprince, J.-M. Rigo, G. Moonen, and B. Rogister, "Plasticity of cultured mesenchymal stem cells: switch from nestin-positive to excitable neuron-like phenotype," *Stem Cells*, vol. 23, no. 3, pp. 392–402, 2005.

[63] D. G. Phinney and D. J. Prockop, "Concise review: mesenchymal stem/multipotent stromal cells: the state of transdifferentiation and modes of tissue repair-current views," *Stem Cells*, vol. 25, no. 11, pp. 2896–2902, 2007.

[64] A.-C. Volz, B. Huber, and P. J. Kluger, "Adipose-derived stem cell differentiation as a basic tool for vascularized adipose tissue engineering," *Differentiation*, vol. 92, no. 1-2, pp. 52–64, 2016.

[65] B. Sacchetti, A. Funari, C. Remoli et al., "No identical "mesenchymal stem cells" at different times and sites: human committed progenitors of distinct origin and differentiation potential are incorporated as adventitial cells in microvessels," *Stem Cell Reports*, vol. 6, no. 6, pp. 897–913, 2016.

[66] W. R. Hardy, N. I. Moldovan, L. Moldovan et al., "Transcriptional networks in single perivascular cells sorted from human adipose tissue reveal a hierarchy of mesenchymal stem cells," *Stem Cells*, vol. 35, no. 5, pp. 1273–1289, 2017.

[67] C. L. Esteves, T. A. Sheldrake, S. P. Mesquita et al., "Isolation and characterization of equine native MSC populations," *Stem Cell Research and Therapy*, vol. 8, no. 1, p. 80, 2017.

[68] A. W. James, X. Zhang, M. Crisan et al., "Isolation and characterization of canine perivascular stem/stromal cells for bone tissue engineering," *PLoS One*, vol. 12, no. 5, pp. e0177308–e0177316, 2017.

[69] N. E. Lee, S. J. Kim, S.-J. Yang et al., "Comparative characterization of mesenchymal stromal cells from multiple abdominal adipose tissues and enrichment of angiogenic ability via CD146 molecule," *Cytotherapy*, vol. 19, no. 2, pp. 170–180, 2017.

[70] A. R. Jensen, B. V. Kelley, G. M. Mosich et al., "Neer Award 2018: platelet-derived growth factor receptor α co-expression typifies a subset of platelet-derived growth factor receptor β–positive progenitor cells that contribute to fatty degeneration and fibrosis of the murine rotator cuff," *Journal of Shoulder and Elbow Surgery*, vol. 27, no. 7, pp. 1149–1161, 2018.

[71] I. R. Murray, Z. N. Gonzalez, J. Baily et al., "αv integrins on mesenchymal cells regulate skeletal and cardiac muscle fibrosis," *Nature Communications*, vol. 8, no. 1, p. 1118, 2017.

[72] R. Sarugaser, L. Hanoun, A. Keating, W. L. Stanford, and J. E. Davies, "Human mesenchymal stem cells self-renew and differentiate according to a deterministic hierarchy," *PLoS One*, vol. 4, no. 8, article e6498, 2009.

[73] A. I. Caplan, "Adult mesenchymal stem cells for tissue engineering versus regenerative medicine," *Journal of Cellular Physiology*, vol. 213, no. 2, pp. 341–347, 2007.

[74] A. I. Caplan and D. Correa, "The MSC: an injury drugstore," *Cell Stem Cell*, vol. 9, no. 1, pp. 11–15, 2011.

[75] A. I. Caplan, "Mesenchymal stem cells: time to change the name!," *Stem Cells Translational Medicine*, vol. 6, no. 6, pp. 1445–1451, 2017.

[76] M. Cai, R. Shen, L. Song et al., "Bone marrow mesenchymal stem cells (BM-MSCs) improve heart function in swine

myocardial infarction model through paracrine effects," *Scientific Reports*, vol. 6, no. 1, pp. 1–12, 2016.

[77] B. Amorin, A. P. Alegretti, V. Valim et al., "Mesenchymal stem cell therapy and acute graft-versus-host disease: a review," *Human Cell*, vol. 27, no. 4, pp. 137–150, 2014.

[78] J. Dalal, K. Gandy, and J. Domen, "Role of mesenchymal stem cell therapy in Crohn's disease," *Pediatric Research*, vol. 71, no. 4–2, pp. 445–451, 2012.

[79] J. Katuchova, D. Harvanova, T. Spakova et al., "Mesenchymal stem cells in the treatment of type 1 diabetes mellitus," *Endocrine Pathology*, vol. 26, no. 2, pp. 95–103, 2015.

[80] N. G. Singer and A. I. Caplan, "Mesenchymal stem cells: mechanisms of inflammation," *Annual Review of Pathology: Mechanisms of Disease*, vol. 6, no. 1, pp. 457–478, 2011.

[81] M. M. Duffy, T. Ritter, R. Ceredig, and M. D. Griffin, "Mesenchymal stem cell effects on T-cell effector pathways," *Stem Cell Research & Therapy*, vol. 2, no. 4, p. 34, 2011.

[82] R. Haddad and F. Saldanha-Araujo, "Mechanisms of T-cell immunosuppression by mesenchymal stromal cells: what do we know so far?," *BioMed Research International*, vol. 2014, Article ID 216806, 14 pages, 2014.

[83] E. Eggenhofer and M. J. Hoogduijn, "Mesenchymal stem cell-educated macrophages," *Transplantation Research*, vol. 1, no. 1, p. 12, 2012.

[84] A. Mantovani, S. K. Biswas, M. R. Galdiero, A. Sica, and M. Locati, "Macrophage plasticity and polarization in tissue repair and remodelling," *The Journal of Pathology*, vol. 229, no. 2, pp. 176–185, 2013.

[85] M. E. Bernardo and W. E. Fibbe, "Mesenchymal stromal cells: sensors and switchers of inflammation," *Cell Stem Cell*, vol. 13, no. 4, pp. 392–402, 2013.

[86] E. Chung and Y. Son, "Crosstalk between mesenchymal stem cells and macrophages in tissue repair," *Tissue Engineering and Regenerative Medicine*, vol. 11, no. 6, pp. 431–438, 2014.

[87] W. K. Chan, A. S.-Y. Lau, J. C.-B. Li, H. K.-W. Law, Y. L. Lau, and G. C.-F. Chan, "MHC expression kinetics and immunogenicity of mesenchymal stromal cells after short-term IFN-γ challenge," *Experimental Hematology*, vol. 36, no. 11, pp. 1545–1555, 2008.

[88] M. François, R. Romieu-Mourez, S. Stock-Martineau, M.-N. Boivin, J. L. Bramson, and J. Galipeau, "Mesenchymal stromal cells cross-present soluble exogenous antigens as part of their antigen-presenting cell properties," *Blood*, vol. 114, no. 13, pp. 2632–2638, 2009.

[89] J. L. Chan, K. C. Tang, A. P. Patel et al., "Antigen-presenting property of mesenchymal stem cells occurs during a narrow window at low levels of interferon-γ," *Blood*, vol. 107, no. 12, pp. 4817–4824, 2006.

[90] M. Strioga, S. Viswanathan, A. Darinskas, O. Slaby, and J. Michalek, "Same or not the same? Comparison of adipose tissue-derived versus bone marrow-derived mesenchymal stem and stromal cells," *Stem Cells and Development*, vol. 21, no. 14, pp. 2724–2752, 2012.

[91] S. M. Nassiri and R. Rahbarghazi, "Interactions of mesenchymal stem cells with endothelial cells," *Stem Cells and Development*, vol. 23, no. 4, pp. 319–332, 2014.

[92] H. Tao, Z. Han, Z. C. Han, and Z. Li, "Proangiogenic features of mesenchymal stem cells and their therapeutic applications," *Stem Cells International*, vol. 2016, Article ID 1314709, 11 pages, 2016.

[93] D. G. Phinney and M. F. Pittenger, "Concise review: MSC-derived exosomes for cell-free therapy," *Stem Cells*, vol. 35, no. 4, pp. 851–858, 2017.

[94] A. Shabbir, A. Cox, L. Rodriguez-Menocal, M. Salgado, and E. V. Badiavas, "Mesenchymal stem cell exosomes induce proliferation and migration of normal and chronic wound fibroblasts, and enhance angiogenesis in vitro," *Stem Cells and Development*, vol. 24, no. 14, pp. 1635–1647, 2015.

[95] B. Zhang, X. Wu, X. Zhang et al., "Human umbilical cord mesenchymal stem cell exosomes enhance angiogenesis through the Wnt4/β-catenin pathway," *Stem Cells Translational Medicine*, vol. 4, no. 5, pp. 513–522, 2015.

[96] S. Bian, L. Zhang, L. Duan, X. Wang, Y. Min, and H. Yu, "Extracellular vesicles derived from human bone marrow mesenchymal stem cells promote angiogenesis in a rat myocardial infarction model," *Journal of Molecular Medicine*, vol. 92, no. 4, pp. 387–397, 2014.

[97] X. Teng, L. Chen, W. Chen, J. Yang, Z. Yang, and Z. Shen, "Mesenchymal stem cell-derived exosomes improve the microenvironment of infarcted myocardium contributing to angiogenesis and anti-inflammation," *Cellular Physiology and Biochemistry*, vol. 37, no. 6, pp. 2415–2424, 2015.

[98] J. Zhang, J. Guan, X. Niu et al., "Exosomes released from human induced pluripotent stem cells-derived MSCs facilitate cutaneous wound healing by promoting collagen synthesis and angiogenesis," *Journal of Translational Medicine*, vol. 13, no. 1, p. 49, 2015.

[99] G.-W. Hu, Q. Li, X. Niu et al., "Exosomes secreted by human-induced pluripotent stem cell-derived mesenchymal stem cells attenuate limb ischemia by promoting angiogenesis in mice," *Stem Cell Research & Therapy*, vol. 6, no. 1, p. 10, 2015.

[100] J. D. Anderson, H. J. Johansson, C. S. Graham et al., "Comprehensive proteomic analysis of mesenchymal stem cell exosomes reveals modulation of angiogenesis via nuclear factor-kappaB signaling," *Stem Cells*, vol. 34, no. 3, pp. 601–613, 2016.

[101] M. Gong, B. Yu, J. Wang et al., "Mesenchymal stem cells release exosomes that transfer miRNAs to endothelial cells and promote angiogenesis," *Oncotarget*, vol. 8, no. 28, pp. 45200–45212, 2017.

[102] N. Wang, C. Chen, D. Yang et al., "Mesenchymal stem cells-derived extracellular vesicles, via miR-210, improve infarcted cardiac function by promotion of angiogenesis," *Biochimica et Biophysica Acta (BBA) - Molecular Basis of Disease*, vol. 1863, no. 8, pp. 2085–2092, 2017.

[103] X. Liang, L. Zhang, S. Wang, Q. Han, and R. C. Zhao, "Exosomes secreted by mesenchymal stem cells promote endothelial cell angiogenesis by transferring miR-125a," *Journal of Cell Science*, vol. 129, no. 11, pp. 2182–2189, 2016.

[104] R. R. Rao, A. W. Peterson, J. Ceccarelli, A. J. Putnam, and J. P. Stegemann, "Matrix composition regulates three-dimensional network formation by endothelial cells and mesenchymal stem cells in collagen/fibrin materials," *Angiogenesis*, vol. 15, no. 2, pp. 253–264, 2012.

[105] S. J. Grainger and A. J. Putnam, "Assessing the permeability of engineered capillary networks in a 3D culture," *PLoS One*, vol. 6, no. 7, article e22086, 2011.

[106] A. N. Stratman, W. B. Saunders, A. Sacharidou et al., "Endothelial cell lumen and vascular guidance tunnel formation requires MT1-MMP-dependent proteolysis in 3-dimensional collagen matrices," *Blood*, vol. 114, no. 2, pp. 237–247, 2009.

[107] A. N. Stratman and G. E. Davis, "Endothelial cell-pericyte interactions stimulate basement membrane matrix assembly: influence on vascular tube remodeling, maturation, and stabilization," *Microscopy and Microanalysis*, vol. 18, no. 01, pp. 68–80, 2012.

[108] P. Au, J. Tam, D. Fukumura, and R. K. Jain, "Bone marrow-derived mesenchymal stem cells facilitate engineering of long-lasting functional vasculature," *Blood*, vol. 111, no. 9, pp. 4551–4558, 2008.

[109] M. D. Chamberlain, R. Gupta, and M. V. Sefton, "Bone marrow-derived mesenchymal stromal cells enhance chimeric vessel development driven by endothelial cell-coated microtissues," *Tissue Engineering Part A*, vol. 18, no. 3-4, pp. 285–294, 2012.

[110] S. J. Grainger, B. Carrion, J. Ceccarelli, and A. J. Putnam, "Stromal cell identity influences the *in vivo* functionality of engineered capillary networks formed by co-delivery of endothelial cells and stromal cells," *Tissue Engineering Part A*, vol. 19, no. 9-10, pp. 1209–1222, 2013.

[111] S. Malempati, S. Joshi, S. Lai, D. A. V. Braner, and K. Tegtmeyer, "Videos in clinical medicine. Bone marrow aspiration and biopsy," *The New England Journal of Medicine*, vol. 361, no. 15, article e28, 2009.

[112] E. M. Fennema, A. J. S. Renard, A. Leusink, C. A. van Blitterswijk, and J. de Boer, "The effect of bone marrow aspiration strategy on the yield and quality of human mesenchymal stem cells," *Acta Orthopaedica*, vol. 80, no. 5, pp. 618–621, 2009.

[113] N. Hjortholm, E. Jaddini, K. Hałaburda, and E. Snarski, "Strategies of pain reduction during the bone marrow biopsy," *Annals of Hematology*, vol. 92, no. 2, pp. 145–149, 2013.

[114] B. J. Bain, "Bone marrow biopsy morbidity and mortality," *British Journal of Haematology*, vol. 121, no. 6, pp. 949–951, 2003.

[115] B. J. Bain, "Morbidity associated with bone marrow aspiration and trephine biopsy - a review of UK data for 2004," *Haematologica*, vol. 91, no. 9, pp. 1293-1294, 2006.

[116] J. P. Hunstad and M. E. Aitken, "Liposuction: techniques and guidelines," *Clinics in Plastic Surgery*, vol. 33, no. 1, pp. 13–25, 2006.

[117] R. A. Yoho, J. J. Romaine, and D. O'Neil, "Review of the liposuction, abdominoplasty, and face-lift mortality and morbidity risk literature," *Dermatologic Surgery.*, vol. 31, no. 7, pp. 733–743, 2005.

[118] F. M. Grazer and R. H. de Jong, "Fatal outcomes from liposuction: census survey of cosmetic surgeons," *Plastic and Reconstructive Surgery*, vol. 105, no. 1, pp. 436–446, 2000.

[119] M. Chaouat, P. Levan, B. Lalanne, T. Buisson, P. Nicolau, and M. Mimoun, "Abdominal dermolipectomies: early postoperative complications and long-term unfavorable results," *Plastic and Reconstructive Surgery*, vol. 106, no. 7, pp. 1614–1618, 2000.

[120] M. B. Murphy, K. Moncivais, and A. I. Caplan, "Mesenchymal stem cells: environmentally responsive therapeutics for regenerative medicine," *Experimental & Molecular Medicine*, vol. 45, no. 11, article e54, 2013.

[121] T. M. Liu, M. Martina, D. W. Hutmacher, J. H. P. Hui, E. H. Lee, and B. Lim, "Identification of common pathways mediating differentiation of bone marrow- and adipose tissue-derived human mesenchymal stem cells into

three mesenchymal lineages," *Stem Cells*, vol. 25, no. 3, pp. 750–760, 2007.

[122] C.-Y. Li, X.-Y. Wu, J.-B. Tong et al., "Comparative analysis of human mesenchymal stem cells from bone marrow and adipose tissue under xeno-free conditions for cell therapy," *Stem Cell Research & Therapy*, vol. 6, no. 1, p. 55, 2015.

[123] Y. Jing, J. Jing, L. Ye et al., "Chondrogenesis and osteogenesis are one continuous developmental and lineage defined biological process," *Scientific Reports*, vol. 7, no. 1, p. 10020, 2017.

[124] J. Valencia, B. Blanco, R. Yáñez et al., "Comparative analysis of the immunomodulatory capacities of human bone marrow- and adipose tissue-derived mesenchymal stromal cells from the same donor," *Cytotherapy*, vol. 18, no. 10, pp. 1297–1311, 2016.

[125] B. Blanco, M. C. Herrero-Sánchez, C. Rodríguez-Serrano et al., "Immunomodulatory effects of bone marrow versus adipose tissue-derived mesenchymal stromal cells on NK cells: implications in the transplantation setting," *European Journal of Haematology*, vol. 97, no. 6, pp. 528–537, 2016.

[126] E. Ivanova-Todorova, I. Bochev, M. Mourdjeva et al., "Adipose tissue-derived mesenchymal stem cells are more potent suppressors of dendritic cells differentiation compared to bone marrow-derived mesenchymal stem cells," *Immunology Letters*, vol. 126, no. 1-2, pp. 37–42, 2009.

[127] S. Zimmermann, M. Voss, S. Kaiser, U. Kapp, C. F. Waller, and U. M. Martens, "Lack of telomerase activity in human mesenchymal stem cells," *Leukemia*, vol. 17, no. 6, pp. 1146–1149, 2003.

[128] N. Serakinci, J. Graakjaer, and S. Kolvraa, "Telomere stability and telomerase in mesenchymal stem cells," *Biochimie*, vol. 90, no. 1, pp. 33–40, 2008.

[129] A. Stolzing, E. Jones, D. McGonagle, and A. Scutt, "Age-related changes in human bone marrow-derived mesenchymal stem cells: consequences for cell therapies," *Mechanisms of Ageing and Development*, vol. 129, no. 3, pp. 163–173, 2008.

[130] G. Kasper, L. Mao, S. Geissler et al., "Insights into mesenchymal stem cell aging: involvement of antioxidant defense and actin cytoskeleton," *Stem Cells*, vol. 27, no. 6, pp. 1288–1297, 2009.

[131] P. Ganguly, J. J. El-Jawhari, P. V. Giannoudis, A. N. Burska, F. Ponchel, and E. A. Jones, "Age-related changes in bone marrow mesenchymal stromal cells: a potential impact on osteoporosis and osteoarthritis development," *Cell Transplantation*, vol. 26, no. 9, pp. 1520–1529, 2017.

[132] Y. Li, Q. Wu, Y. Wang, L. Li, H. Bu, and J. Bao, "Senescence of mesenchymal stem cells (review)," *International Journal of Molecular Medicine*, vol. 39, no. 4, pp. 775–782, 2017.

[133] B. R. Stab, L. Martinez, A. Grismaldo et al., "Mitochondrial functional changes characterization in young and senescent human adipose derived MSCs," *Frontiers in Aging Neuroscience*, vol. 8, p. 299, 2016.

[134] M. J. Peffers, J. Collins, Y. Fang et al., "Age-related changes in mesenchymal stem cells identified using a multi-omics approach," *European Cell and Materials*, vol. 31, pp. 136–159, 2016.

[135] E. G. Toraño, G. F. Bayón, Á. del Real et al., "Age-associated hydroxymethylation in human bone-marrow mesenchymal stem cells," *Journal of Translational Medicine*, vol. 14, no. 1, p. 207, 2016.

[136] J. Franzen, W. Wagner, and E. Fernandez-Rebollo, "Epigenetic modifications upon senescence of mesenchymal stem cells," *Current Stem Cell Reports*, vol. 2, no. 3, pp. 248–254, 2016.

[137] Z. Li, C. Liu, Z. Xie et al., "Epigenetic dysregulation in mesenchymal stem cell aging and spontaneous differentiation," *PLoS One*, vol. 6, no. 6, article e20526, 2011.

[138] Z. Hamidouche, K. Rother, J. Przybilla et al., "Bistable epigenetic states explain age-dependent decline in mesenchymal stem cell heterogeneity," *Stem Cells*, vol. 35, no. 3, pp. 694–704, 2017.

[139] K. Kornicka, J. Houston, and K. Marycz, "Dysfunction of mesenchymal stem cells isolated from metabolic syndrome and type 2 diabetic patients as result of oxidative stress and autophagy may limit their potential therapeutic use," *Stem Cell Reviews and Reports*, vol. 14, no. 3, pp. 337–345, 2018.

[140] K. Takahashi and S. Yamanaka, "Induction of pluripotent stem cells from mouse embryonic and adult fibroblast cultures by defined factors," *Cell*, vol. 126, no. 4, pp. 663–676, 2006.

[141] K. Takahashi, K. Tanabe, M. Ohnuki et al., "Induction of pluripotent stem cells from adult human fibroblasts by defined factors," *Cell*, vol. 131, no. 5, pp. 861–872, 2007.

[142] L. Lapasset, O. Milhavet, A. Prieur et al., "Rejuvenating senescent and centenarian human cells by reprogramming through the pluripotent state," *Genes & Development*, vol. 25, no. 21, pp. 2248–2253, 2011.

[143] J. Frobel, H. Hemeda, M. Lenz et al., "Epigenetic rejuvenation of mesenchymal stromal cells derived from induced pluripotent stem cells," *Stem Cell Reports*, vol. 3, no. 3, pp. 414–422, 2014.

[144] L. G. Villa-Diaz, S. E. Brown, Y. Liu et al., "Derivation of mesenchymal stem cells from human induced pluripotent stem cells cultured on synthetic substrates," *Stem Cells*, vol. 30, no. 6, pp. 1174–1181, 2012.

[145] L. Zou, Y. Luo, M. Chen et al., "A simple method for deriving functional MSCs and applied for osteogenesis in 3D scaffolds," *Scientific Reports*, vol. 3, no. 1, article 2243, 2013.

[146] K. Hynes, D. Menicanin, K. Mrozik, S. Gronthos, and P. M. Bartold, "Generation of functional mesenchymal stem cells from different induced pluripotent stem cell lines," *Stem Cells and Development*, vol. 23, no. 10, pp. 1084–1096, 2014.

[147] M. Moslem, I. Eberle, I. Weber, R. Henschler, and T. Cantz, "Mesenchymal stem/stromal cells derived from induced pluripotent stem cells support CD34^{pos} hematopoietic stem cell propagation and suppress inflammatory reaction," *Stem Cells International*, vol. 2015, Article ID 843058, 14 pages, 2015.

[148] K. Hynes, D. Menicanin, S. Gronthos, and M. P. Bartold, "Differentiation of iPSC to mesenchymal stem-like cells and their characterization," in *Induced Pluripotent Stem (iPS) Cells. Methods in Molecular Biology, vol 1357* Humana Press, New York, NY, USA.

[149] C. J. Chin, S. Li, M. Corselli et al., "Transcriptionally and functionally distinct mesenchymal subpopulations are generated from human pluripotent stem cells," *Stem Cell Reports*, vol. 10, no. 2, pp. 436–446, 2018.

[150] R. Kang, Y. Zhou, S. Tan et al., "Mesenchymal stem cells derived from human induced pluripotent stem cells retain adequate osteogenicity and chondrogenicity but less adipogenicity," *Stem Cell Research & Therapy*, vol. 6, no. 1, p. 144, 2015.

[151] S. Diederichs and R. S. Tuan, "Functional comparison of human-induced pluripotent stem cell-derived mesenchymal cells and bone marrow-derived mesenchymal stromal cells from the same donor," *Stem Cells and Development*, vol. 23, no. 14, pp. 1594–1610, 2014.

[152] M. Giuliani, N. Oudrhiri, Z. M. Noman et al., "Human mesenchymal stem cells derived from induced pluripotent stem cells down-regulate NK-cell cytolytic machinery," *Blood*, vol. 118, no. 12, pp. 3254–3262, 2011.

[153] Q. Zhao, C. A. Gregory, R. H. Lee et al., "MSCs derived from iPSCs with a modified protocol are tumor-tropic but have much less potential to promote tumors than bone marrow MSCs," *Proceedings of the National Academy of Sciences of the United States of America*, vol. 112, no. 2, pp. 530–535, 2015.

[154] A. S. Lee, C. Tang, M. S. Rao, I. L. Weissman, and J. C. Wu, "Tumorigenicity as a clinical hurdle for pluripotent stem cell therapies," *Nature Medicine*, vol. 19, no. 8, pp. 998–1004, 2013.

[155] A. Ocampo, P. Reddy, P. Martinez-Redondo et al., "In vivo amelioration of age-associated hallmarks by partial reprogramming," *Cell*, vol. 167, no. 7, pp. 1719–1733.e12, 2016.

[156] M. Okada, H. W. Kim, K. Matsu-ura, Y.-G. Wang, M. Xu, and M. Ashraf, "Abrogation of age-induced microRNA-195 rejuvenates the senescent mesenchymal stem cells by reactivating telomerase," *Stem Cells*, vol. 34, no. 1, pp. 148–159, 2016.

[157] S. Lee, K.-R. Yu, Y.-S. Ryu et al., "miR-543 and miR-590-3p regulate human mesenchymal stem cell aging via direct targeting of AIMP3/p18," *Age*, vol. 36, no. 6, article 9724, 2014.

[158] H. Chen, X. Liu, W. Zhu et al., "SIRT1 ameliorates age-related senescence of mesenchymal stem cells via modulating telomere shelterin," *Frontiers in Aging Neuroscience*, vol. 6, p. 103, 2014.

[159] R. Madonna, D. A. Taylor, Y. J. Geng et al., "Transplantation of mesenchymal cells rejuvenated by the overexpression of telomerase and myocardin promotes revascularization and tissue repair in a murine model of hindlimb ischemia," *Circulation Research*, vol. 113, no. 7, pp. 902–914, 2013.

[160] M. M. Lalu, L. McIntyre, C. Pugliese et al., "Safety of cell therapy with mesenchymal stromal cells (SafeCell): a systematic review and meta-analysis of clinical trials," *PLoS One*, vol. 7, no. 10, pp. e47559–e47521, 2012.

[161] G. Ren, X. Chen, F. Dong et al., "Concise review: mesenchymal stem cells and translational medicine: emerging issues," *Stem Cells Translational Medicine*, vol. 1, no. 1, pp. 51–58, 2012.

[162] L. von Bahr, B. Sundberg, L. Lönnies et al., "Long-term complications, immunologic effects, and role of passage for outcome in mesenchymal stromal cell therapy," *Biology of Blood and Marrow Transplantation*, vol. 18, no. 4, pp. 557–564, 2012.

[163] E. Eggenhofer, V. Benseler, A. Kroemer et al., "Mesenchymal stem cells are short-lived and do not migrate beyond the lungs after intravenous infusion," *Frontiers in Immunology*, vol. 3, p. 297, 2012.

[164] H. Hemeda, B. Giebel, and W. Wagner, "Evaluation of human platelet lysate versus fetal bovine serum for culture of mesenchymal stromal cells," *Cytotherapy*, vol. 16, no. 2, pp. 170–180, 2014.

[165] M. Duijvestein, A. C. W. Vos, H. Roelofs et al., "Autologous bone marrow-derived mesenchymal stromal cell treatment for refractory luminal Crohn's disease: results of a phase I study," *Gut*, vol. 59, no. 12, pp. 1662–1669, 2010.

[166] E. Fernandez-Rebollo, B. Mentrup, R. Ebert et al., "Human platelet lysate versus fetal calf serum: these supplements do not select for different mesenchymal stromal cells," *Scientific Reports*, vol. 7, no. 1, p. 5132, 2017.

[167] T. J. Kean, P. Lin, A. I. Caplan, and J. E. Dennis, "MSCs: delivery routes and engraftment, cell-targeting strategies, and immune modulation," *Stem Cells International*, vol. 2013, Article ID 732742, 13 pages, 2013.

[168] S. T. Ji, H. Kim, J. Yun, J. S. Chung, and S.-M. Kwon, "Promising therapeutic strategies for mesenchymal stem cell-based cardiovascular regeneration: from cell priming to tissue engineering," *Stem Cells International*, vol. 2017, Article ID 3945403, 13 pages, 2017.

[169] L. M. Marquardt and S. C. Heilshorn, "Design of injectable materials to improve stem cell transplantation," *Current Stem Cell Reports*, vol. 2, no. 3, pp. 207–220, 2016.

[170] S. Hanson, R. N. D'Souza, and P. Hematti, "Biomaterial-mesenchymal stem cell constructs for immunomodulation in composite tissue engineering," *Tissue Engineering Part A*, vol. 20, no. 15-16, pp. 2162–2168, 2014.

[171] A. B. Castillo and C. R. Jacobs, "Mesenchymal stem cell mechanobiology," *Current Osteoporosis Reports*, vol. 8, no. 2, pp. 98–104, 2010.

[172] A. Schäffler and C. Büchler, "Concise review: adipose tissue-derived stromal cells—basic and clinical implications for novel cell-based therapies," *Stem Cells*, vol. 25, no. 4, pp. 818–827, 2007.

[173] H.-J. Bühring, V. L. Battula, S. Treml, B. Schewe, L. Kanz, and W. Vogel, "Novel markers for the prospective isolation of human MSC," *Annals of the New York Academy of Sciences*, vol. 1106, no. 1, pp. 262–271, 2007.

[174] C. Muñiz, C. Teodosio, A. Mayado et al., "Ex vivo identification and characterization of a population of CD13^{high} CD105$^+$ CD45$^-$ mesenchymal stem cells in human bone marrow," *Stem Cell Research & Therapy*, vol. 6, no. 1, p. 169, 2015.

[175] O. G. Davies, P. R. Cooper, R. M. Shelton, A. J. Smith, and B. A. Scheven, "Isolation of adipose and bone marrow mesenchymal stem cells using CD29 and CD90 modifies their capacity for osteogenic and adipogenic differentiation," *Journal of Tissue Engineering*, vol. 6, 10 pages, 2015.

[176] H. Zhu, N. Mitsuhashi, A. Klein et al., "The role of the hyaluronan receptor CD44 in mesenchymal stem cell migration in the extracellular matrix," *Stem Cells*, vol. 24, no. 4, pp. 928–935, 2006.

[177] K.-R. Yu, S.-R. Yang, J.-W. Jung et al., "CD49f enhances multipotency and maintains stemness through the direct regulation of OCT4 and SOX2," *Stem Cells*, vol. 30, no. 5, pp. 876–887, 2012.

[178] E. G. Suto, Y. Mabuchi, N. Suzuki et al., "Prospectively isolated mesenchymal stem/stromal cells are enriched in the CD73$^+$ population and exhibit efficacy after transplantation," *Scientific Reports*, vol. 7, no. 1, p. 4838, 2017.

[179] P. A. Zuk, M. Zhu, P. Ashjian et al., "Human adipose tissue is a source of multipotent stem cells," *Molecular Biology of the Cell*, vol. 13, no. 12, pp. 4279–4295, 2002.

[180] S. Halfon, N. Abramov, B. Grinblat, and I. Ginis, "Markers distinguishing mesenchymal stem cells from fibroblasts are downregulated with passaging," *Stem Cells and Development*, vol. 20, no. 1, pp. 53–66, 2011.

[181] B. Delorme, J. Ringe, N. Gallay et al., "Specific plasma membrane protein phenotype of culture-amplified and native human bone marrow mesenchymal stem cells," *Blood*, vol. 111, no. 5, pp. 2631–2635, 2008.

[182] S. F. H. de Witte, M. Franquesa, C. C. Baan, and M. J. Hoogduijn, "Toward development of iMesenchymal stem cells for immunomodulatory therapy," *Frontiers in Immunology*, vol. 6, p. 648, 2016.

[183] C. Martinez, T. J. Hofmann, R. Marino, M. Dominici, and E. M. Horwitz, "Human bone marrow mesenchymal stromal cells express the neural ganglioside GD2: a novel surface marker for the identification of MSCs," *Blood*, vol. 109, no. 10, pp. 4245–4248, 2007.

[184] P. A. Oktar, S. Yildirim, D. Balci, and A. Can, "Continual expression throughout the cell cycle and downregulation upon adipogenic differentiation makes nucleostemin a vital human MSC proliferation marker," *Stem Cell Reviews and Reports*, vol. 7, no. 2, pp. 413–424, 2011.

[185] S. Fitter, S. Gronthos, S. S. Ooi, and A. C. W. Zannettino, "The mesenchymal precursor cell marker antibody STRO-1 binds to cell surface heat shock cognate 70," *Stem Cells*, vol. 35, no. 4, pp. 940–951, 2017.

[186] S. Gronthos, R. McCarty, K. Mrozik et al., "Heat shock protein-90 beta is expressed at the surface of multipotential mesenchymal precursor cells: generation of a novel monoclonal antibody, STRO-4, with specificity for mesenchymal precursor cells from human and ovine tissues," *Stem Cells and Development*, vol. 18, no. 9, pp. 1253–1262, 2009.

[187] E. J. Gang, D. Bosnakovski, C. A. Figueiredo, J. W. Visser, and R. C. R. Perlingeiro, "SSEA-4 identifies mesenchymal stem cells from bone marrow," *Blood*, vol. 109, no. 4, pp. 1743–1751, 2007.

[188] K. Sivasubramaniyan, A. Harichandan, S. Schumann et al., "Prospective isolation of mesenchymal stem cells from human bone marrow using novel antibodies directed against sushi domain containing 2," *Stem Cells and Development*, vol. 22, no. 13, pp. 1944–1954, 2013.

Research Article

Type III Transforming Growth Factor-β Receptor RNA Interference Enhances Transforming Growth Factor β3-Induced Chondrogenesis Signaling in Human Mesenchymal Stem Cells

Shuhui Zheng,[1] Hang Zhou [iD],[2] Zhuohui Chen,[3] Yongyong Li [iD],[1] Taifeng Zhou [iD],[2] Chengjie Lian [iD],[4] Bo Gao [iD],[4] Peiqiang Su [iD],[2] and Caixia Xu [iD][1]

[1]*Research Center for Translational Medicine, The First Affiliated Hospital of Sun Yat-sen University, Guangzhou, China*
[2]*Department of Orthopedic Surgery, The First Affiliated Hospital of Sun Yat-sen University, Guangzhou, China*
[3]*Oral and Maxillofacial Surgery, Guanghua School of Stomatology, Hospital of Stomatology, Sun Yat-sen University, Guangzhou, China*
[4]*Department of Spine Surgery, Sun Yat-Sen Memorial Hospital, Sun Yat-sen University, Guangzhou, China*

Correspondence should be addressed to Peiqiang Su; supq@mail.sysu.edu.cn and Caixia Xu; xucx3@mail.sysu.edu.cn

The type III transforming growth factor-β (TGF-β) receptor (TβRIII), a coreceptor of the TGF-β superfamily, is known to bind TGF-βs and regulate TGF-β signaling. However, the regulatory roles of TβRIII in TGF-β-induced mesenchymal stem cell (MSC) chondrogenesis have not been explored. The present study examined the effect of TβRIII RNA interference (RNAi) on TGF-β3-induced human MSC (hMSC) chondrogenesis and possible signal mechanisms. A lentiviral expression vector containing TβRIII small interfering RNA (siRNA) (SiTβRIII) or a control siRNA (SiNC) gene was constructed and infected into hMSCs. The cells were cultured in chondrogenic medium containing TGF-β3 or control medium. TβRIII RNAi significantly enhanced TGF-β3-induced chondrogenic differentiation of hMSCs, the ratio of type II (TβRII) to type I (TβRI) TGF-β receptors, and phosphorylation levels of Smad2/3 as compared with cells infected with SiNC. An inhibitor of the TGF-β signal, SB431542, not only inhibited TβRIII RNAi-stimulated TGF-β3-mediated Smad2/3 phosphorylation but also inhibited the effects of TβRIII RNAi on TGF-β3-induced chondrogenic differentiation. These results demonstrate that TβRIII RNAi enhances TGF-β3-induced chondrogenic differentiation in hMSCs by activating TGF-β/Smad2/3 signaling. The finding points to the possibility of modifying MSCs by TβRIII knockdown as a potent future strategy for cell-based cartilage tissue engineering.

1. Introduction

Cell-based cartilage tissue engineering provides a feasible way of regenerating damaged cartilage tissue caused by trauma or joint diseases. Mesenchymal stem cells (MSCs), common precursor cells of chondrocytes, are the basis for the development of cartilage and represent promising cells for use in stem cell therapy [1, 2]. However, cartilage tissue formed by MSC-derived chondrocytes is not the same as that of native articular cartilage and has poor functional properties [3, 4]. Understanding the molecular mechanisms that control chondrogenic differentiation of MSCs and enhancing chondrogenic activities of cells are crucial to improve cartilage regeneration by MSCs.

Chondrogenic differentiation is potently induced by growth factors [2, 5]. Transforming growth factor-β3 (TGF-β3), a member of the transforming growth factor-β (TGF-β) superfamily, induces chondrogenic differentiation of MSCs [6]. TGF-β signaling is initiated by the binding of TGF-β to type II TGF-β receptors (TβRII) and then forms heteromeric complexes with type I receptors (TβRI) [7]. These complexes further phosphorylate cytoplasmic effector

molecules Smad2 and Smad3, which are translocated to the nucleus, where they modulate the expression of target genes, such as SOX9 and collagen type II (COL II) [8].

In addition to kinase receptors, the type III TGF-β receptor (TβRIII), also known as betaglycan, participates in ligand binding of the TGF-β superfamily and signaling [9, 10]. TβRIII is a membrane-anchored proteoglycan found in many cell types. The main function of this receptor was thought to be binding members of the TGF-β family, including TGF-β isoforms TGF-β1–TGF-β3, and presenting them to type II receptors [11, 12]. However, according to the recent literature, TβRIII seems to play complex roles in cellular processes. For example, studies reported that in some cell lines, TβRIII significantly enhanced the response to TGF-β by increasing the affinity of TβRII for TGF-β [12, 13]. Studies also showed that TβRIII functioned as a potent inhibitor of TGF-β signaling in other types of cells, such as renal epithelial cells [14, 15]. Our previous study demonstrated that human MSCs (hMSCs) expressed abundant TβRIII and that TGF-β3 stimulation clearly repressed TβRIII expression in MSCs and induced MSC chondrogenic differentiation [16]. These results suggested that the effect of TGF-β3 on MSC chondrogenesis might be associated with low expression of TβRIII. However, the role of TβRIII in TGF-β-induced chondrogenic differentiation of MSCs is unknown.

In the present study, we studied the biological effects of TβRIII on TGF-β3-induced MSC chondrogenesis. We demonstrated that TβRIII RNA interference (RNAi) enhanced TGF-β-induced chondrogenic differentiation of hMSCs by activating TGF-β and Smad2/3 signaling.

2. Materials and Methods

2.1. Isolation and Culture of hMSCs. The study was approved by the ethics committee of the First Affiliated Hospital of Sun Yat-sen University in accordance with the Declaration of Helsinki, and all the subjects provided written informed consent. hMSCs were isolated and purified from bone marrow samples of 3 healthy volunteer donors by density gradient centrifugation, as described previously [17]. Briefly, bone marrow samples (8–10 ml) were diluted with 10 ml phosphate-buffered saline (PBS). Cells were then fractionated using a Lymphoprep (MP Biomedicals LLC., Santa Ana, CA, USA) density gradient by centrifugation at 500 ×g for 20 minutes. Interfacial mononuclears were collected and cultured in low-glucose Dulbecco's modified Eagle medium (L-DMEM) (Gibco; Invitrogen Corporation, NY, USA), supplemented with 10% fetal bovine serum (FBS) (Gibco; Invitrogen Corporation, NY, USA) under 37°C and 5% CO_2. Cells were passaged when they reached approximately 80% confluence. Passages 3 to 5 cells were used for the experimental protocols.

2.2. TβRIII Small Interfering RNA (siRNA) Design and Lentiviral Vector Construction. The human TβRIII cDNA sequence (GenBank accession number: NM_003243) was searched for siRNA target sequences. Four target sequences were selected, AAGCATGAAGGAACCAAAT, TGCTTT ATCTCTCCATATT, ACCTGAAATCGTGGTGTTT, and

AGTTGGTAAAGGGTTAATA. A scrambled sequence, TTCTCCGAACGTGTCACGT, was used as a negative control (NC). DNA oligos containing the target sequence were synthesized, annealed, and inserted into a green fluorescent protein (GFP) lentiviral expression vector GV248 (GeneChem, Shanghai, China). The ligated production was transformed into *Escherichia coli* DH5α cells. Briefly, 100 μl of DH5α cells was mixed with 2 μl ligated product at 42°C for 90 s. The mixtures were added on Luria-Bertani (LB) media (ATCC, USA) containing ampilillin (50 μg/ml) and incubated at 37°C for 16 h. The transformant was identified by polymerase chain reaction (PCR) and DNA sequencing.

2.3. Lentiviral Production and Infection. A lentivirus TβRIII (LV-TβRIII) siRNA-mix and lentivirus normal control (LV-NC) virus were produced by plasmid cotransfection of 293T cells. Briefly, 293T cells were transfected with DNA mix (pGC-LV vector, 20 μg; pHelper 1.0 vector, 15 μg; and pHelper 2.0 vector, 10 μg) (GeneChem, Shanghai, China) and 100 μl of Lipofectamine 2000 reagent (Invitrogen, NY, USA), according to the manufacturer's instructions. The viral supernatant was harvested 48 hours (h) after transfection, and the concentrated viral titer was determined. The viral supernatant was added into target MSCs at multiplicity of infection (MOI 10). Before infection, 5×10^4/ml of MSCs were seeded onto a 60 cm^2 cell culture dish overnight. The cells were then infected with 100 μl of 1×10^8 TU/ml virus and 5 μg/ml of polybrene, following the manufacturer's instructions. Then, 10 h after infection, the cells were incubated with L-DMEM containing 10% FBS. Three days after infection, GFP expression in cells was observed by a fluorescence microscope (Olympus, Japan). TβRIII expression was detected by the real-time polymerase chain reaction (PCR) and Western blot analysis.

2.4. Chondrogenic Differentiation of hMSCs in Micromass Culture. Chondrogenic differentiation of hMSCs was performed using a modified micromass culture system according to a previously described method [18]. Briefly, MSCs being infected with TβRIII siRNA (SiTβRIII) or control siRNA (SiNC), or without infection, were harvested and resuspended at 2×10^7 cells/ml. Cell droplets (4×10^5/20 μl) were placed carefully in each well of 24-well plates for 2 h, followed by the addition of control medium or chondrogenic medium at 37°C/5% CO_2. The control medium consisted of high-glucose DMEM (H-DMEM), supplemented with 50 μg/ml of vitamin C, 100 nM dexamethasone, 1 mM sodium pyruvate, 40 μg/ml of proline, and ITS+Universal Culture Supplement Premix (BD Biosciences, NY, USA). The chondrogenic medium consisted of the control medium, added by 10 ng/ml of TGF-β3 (PeproTech, Rocky Hill, USA). After 24 h, the cell droplets became spherical. The medium was changed every 3 days.

Cell pellets from uninfected MSCs were divided into a control group and TGF-β3 group according to the control medium and chondrogenic medium and used for TβRIII analysis. The cells were harvested on day 7 after chondrogenic induction. The pellets from infected MSCs were divided into the following four groups for identification of

Table 1: Primers used for real-time PCR.

Gene	Forward primer (5′ to 3′)	Reverse primer (5′ to 3′)
GAPDH	5′-AGAAAAACCTGCCAAATATGATGAC-3′	5′-TGGGTGTCGCTGTTGAAGTC-3′
β-Actin	5′-GACTTAGTTGCGTTACACCCTTTC-3′	5′-GCTGTCACCTTCACCGTTCC-3′
Col2A1	5′-GGCAATAGCAGGTTCACGTACA-3′	5′-CGATAACAGTCTTGCCCCACTT-3′
SOX 9	5′-AGCGAACGCACATCAAGAC-3′	5′-GCTGTAGTGTGGGAGGTTGAA-3′
TβRI	5′-ATTACCAACTGCCTTATTATGA-3′	5′-CATTACTCTCAAGGCTTCAC-3′
TβRII	5′-ATGGAGGCCCAGAAAGATG-3′	5′-GACTGCACCGTTGTTGTCAG-3′
TβRIII	5′GTGTTCCCTCCAAAGTGCAAC-3′	5′-AGCTCGATGATGTGTACTTCCT-3′

GAPDH: glyceraldehyde-3-phosphate dehydrogenase; COL2A1: collagen type II; SOX9: SRY- (sex determining region Y-) box 9; TβRI/II/III: recombinant human transforming growth factor-β receptor type I/II/III.

chondrogenic differentiation and TGF-β/Smad signaling: C-SiNC group (SiNC-infected cells cultured in control medium), C-SiTβRIII group (SiTβRIII-infected cells cultured in control medium), T-SiNC group (SiNC-infected cells cultured in chondrogenic medium), and T-SiTβRIII group (SiTβRIII-infected cells cultured in chondrogenic medium). The cells were harvested on day 14 for identification of chondrogenic differentiation, and on day 7 for TβRI and TβRII analysis. All experiments were performed by using 3 biological replicate samples each group.

2.5. RNA Extraction and Real-Time PCR Analysis. Total RNA was isolated from transfected MSCs or pellets using an RNAsimple Total RNA Kit (Tiangen, Beijing, China). Total RNA was then converted into cDNA using a PrimeScript® RT Reagent Kit (Takara, Osaka, Japan) according to the manufacturer's instructions. Real-Time PCR assay was performed in triplicate in a Real-Time PCR system (Bio-Rad Laboratories, Hercules, CA, USA) by using SYBR Green I Master Mix (Takara, Osaka, Japan). The following genes were examined: COL II, alpha 1 (COL2A1), SRY- (sex determining region Y-) box 9 [SOX9], TβRI, TβRII, and TβRIII. The primer sequences are listed in Table 1. The relative expression levels for each target gene were calculated by referencing to the internal controls glyceraldehyde-3-phosphate dehydrogenase (GAPDH) and β-actin using the $2^{-\Delta\Delta CT}$ method.

2.6. Histology and Immunohistochemistry. The pellets were fixed in 4% paraformaldehyde and embedded in paraffin. 4 μm sections were deparaffinized, rehydrated through decreasing concentrations of ethanol, and stained with 0.1% Alcian blue (Sigma-Aldrich, St. Louis, USA) for glycosaminoglycan (GAG) analysis. For immunohistochemistry analysis, the sections were blocked with 1/100 diluted goat serum for 15 min and then reacted overnight at 4°C with the appropriate primary antibody against human COL II polyclonal antibodies (Abzoom Biolabs, Dallas, TX, USA) and human TβRIII antibody (Santa Cruz, Dallas, USA) followed by biotinylated goat anti-rabbit immunoglobulin G (IgG) (EarthOx, SFO, USA) for 30 min. The sections were incubated with peroxide-conjugated streptavidin and

stained with 3,3′-diaminobenzidine tetrahydrochloride (DAB) (Jinshan Jinqiao, Beijing, China).

For fluorescent immunohistochemistry, the pellets from transfected MSCs were frozen and then sectioned using a Leica CM1950 microtome (Leica, Germany) on day 7 after chondrogenic induction. Tissue sections that were 4 μm thick were permeabilized with 0.1% Triton X for 5 min and blocked with 5% BSA for 1 h. The sections were then incubated with primary antibodies against TβRI (Santa Cruz, Dallas, USA) and human TβRII antibody (RD Systems, USA), diluted at 1 : 50 at 4°C overnight. FITC-conjugated secondary antibody (K00018968; Dako North America Inc., Dako, Denmark) diluted at 1 : 100 was applied for 1 h. The sections were then stained with 4′-6-diamidino-2-phenylindole (1 mg/ml) and visualized using a Zeiss LSM 710 confocal microscope (Carl Zeiss, Heidelberg, Germany).

2.7. Glycosaminoglycan (GAG) Quantitation. The pellets were harvested on day 14 and papain-digested for 16 h at 65°C. An aliquot of 40 μl lysate was reacted with 1,9-dimethyl-methylene blue (DMMB) (Sigma-Aldrich, St. Louis, USA) for GAG analysis. The absorbance at 525 nm was measured using an Automatic Microplate Reader (Bio-Tek, Winooski, Vermont, USA). Total GAG was calculated by a standard curve obtained with shark chondroitin sulfate (Sigma-Aldrich, MO, USA). The total amount of DNA was quantified by reacting with 0.7 μg/ml Hoechst 33258 solution (Sigma-Aldrich, St. Louis, USA). The reaction product was measured using a Synergy Microplate Reader (BioTek, Winooski, Vermont, USA). The results of GAG quantification were normalized to the DNA content.

2.8. Western Blot. For TβRIII RNAi identification, proteins were extracted from MSCs 72 h after transfection. For detection of Smad2/3 phosphorylation, proteins were extracted from pellets after 24 h of chondrogenic induction. The protein concentration was quantified by a BCA Protein Assay Kit (CWBio, Beijing, China). 100 μg proteins was subjected to 6% SDS-PAGE and electrotransferred onto PVDF membrane (Millipore, Boston, USA) at 250 mV for 100 min. After blocking with 5% skim milk and Tris-buffered saline containing 0.1% Tween-20, the PVDF membranes were incubated with antibodies against human TβRIII antibody (Santa Cruz,

(a)

(b)
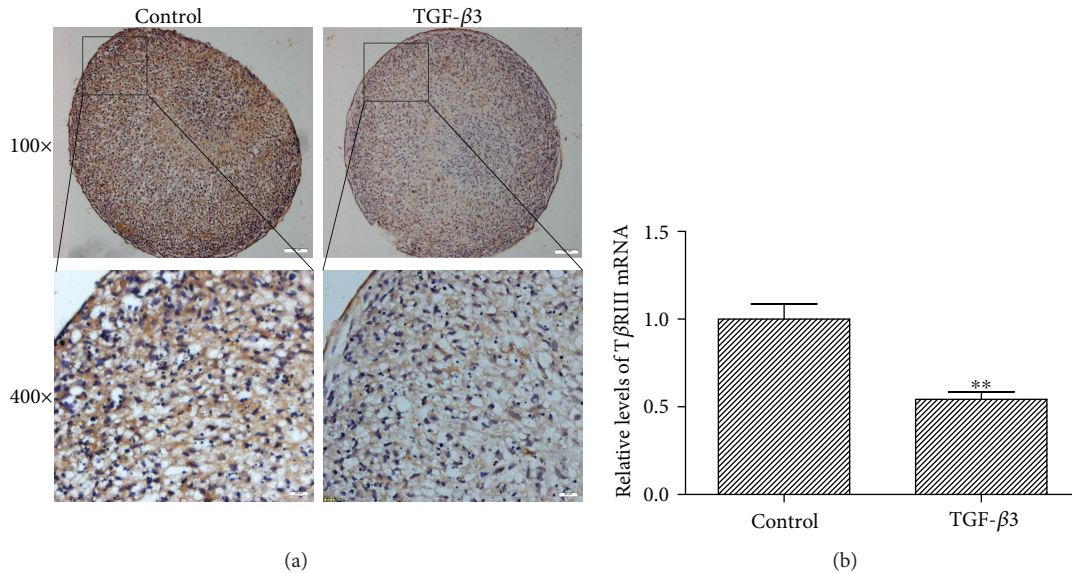
Figure 1: TGF-β3 inhibited the expression of TβRIII during chondrogenic differentiation of hMSCs. (a) hMSCs were cultured in chondrogenic medium including TGF-β3 or control medium without TGF-β3 for 7 days and subjected to immunohistochemistry analysis for TβRIII (upper panel, scale bar = 100 μm; lower panel, scale bar = 20 μm; the TβRIII is stained in brown, cell nucleus is stained in blue). (b) qPCR analysis of TβRIII mRNA level in hMSCs cultured in chondrogenic medium or control medium for 7 days. The TβRIII mRNA level was lower in hMSCs cultured in chondrogenic medium containing TGF-β3 as compared with that of cells cultured in control medium. Error bars represent the means ± SD, n = 3. $^{**}P < 0.01$ versus control.

Dallas, USA), rabbit anti-phospho-Smad2 (Ser465/467)/Smad3 (Ser423/425) (Cell Signaling, Danvers, USA), rabbit anti-Smad2/3 (Cell Signaling, Danvers, USA), and anti-GAPDH monoclonal antibody (EarthOx, SFO, USA) followed by incubation with HRP-conjugated corresponding secondary antibodies. The signals were detected using SuperSignal West Pico Chemiluminescent Substrate (Pierce, NY, USA). Protein levels in phosphorylated-Smad2/3 (P-Smad2/3) were normalized to those of total Smad2/3 quantities or GAPDH.

2.9. Inhibition of TGF-β/Smad Signaling. The infected cells were treated with or without SB431542 (Sigma-Aldrich, St. Louis, USA), a selective inhibitor of activin receptor-like kinase 5 (ALK5) (TβRI) [19], for 2 h before being cultured in chondrogenic medium or control medium. After 24 h of chondrogenic induction, the cells were collected, and the expression of P-Smad2/3 and that of Smad2/3 was detected by a Western blot. After 14 days of chondrogenic induction, the chondrogenic differentiation ability of hMSCs was assayed by detecting protein and gene expression.

2.10. Statistical Analysis. All quantitative data were presented as mean values ± standard errors (S.E.). All the statistical analysis was performed using SPSS 16.0 statistical software (SPSS, Chicago, IL, USA). For comparisons of two groups, independent student's t-test was performed; for comparisons of multiple groups, one-way ANOVA followed by an LSD t-test was performed. $P < 0.05$ was chosen as the threshold of significance.

3. Results

3.1. TGF-β3 Inhibited the Expression of TβRIII in hMSCs. To ascertain whether hMSCs express TβRIII and TGF-β3 could regulate TβRIII expression level, we detected the expression of TβRIII during TGF-β3-induced hMSC chondrogenesis by immunohistochemistry staining and quantitative PCR. The results showed that hMSCs expressed abundant TβRIII protein (Figure 1(a), left panels) and high TβRIII mRNA ($P < 0.01$, Figure 1(b)). Exogenous TGF-β3 clearly reduced TβRIII expression in hMSCs at protein and mRNA levels (Figures 1(a) and 1(b)).

3.2. Viral Infection and Suppression of TβRIII Expression at mRNA and Protein Levels. In order to investigate the role of TβRIII in hMSC chondrogenesis, we infected hMSCs with LV-TβRIII siRNA-mix and identified the silencing effect on TβRIII. Following viral infection for 72 h, most of the cells exhibited high GFP expression under fluorescence microscopy (Figure 2(a)). As compared with the control group, the expression profile of TβRIII mRNA and that of the TβRIII protein decreased significantly in the SiTβRIII groups, with mRNA expression decreased by 77.65% (Figures 2(b) and 2(c)).

3.3. TβRIII RNAi Enhanced TGF-β3-Induced Chondrogenic Differentiation of hMSCs. We then investigated the effects of TβRIII RNAi on the TGF-β3-induced chondrogenic differentiation of hMSCs. As shown in Figure 3, TβRIII RNAi had no obvious effects on GAG and COL II secretion (Figures 3(a) and 3(b); $P > 0.05$) or any noticeable effects on the expression of cartilage-specific genes (SOX9 and

(a)

(b)

(c)
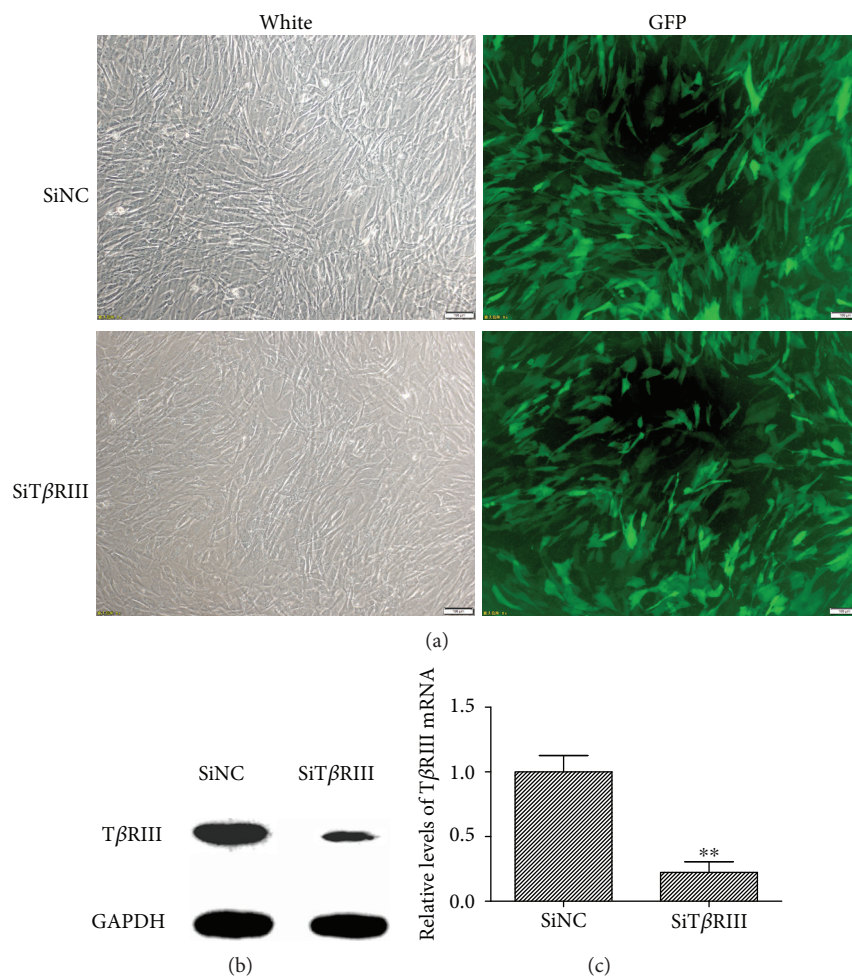
FIGURE 2: Identification and efficiency of lentiviral infection. (a) GFP fluorescence imaging confirmed that the majority of hMSCs were GFP positive 72 h after they were infected by TβRIII siRNA (SiTβRIII) or SiNC virus. Scale bar = 100 μm. (b) Western blot showed that TβRIII siRNA clearly inhibited the expression of the TβRIII protein. (c) qPCR confirmed that the expression profiles of TβRIII mRNA decreased significantly in the SiTβRIII groups as compared with those in the SiNC group. Error bars represent the means $\pm$ SD, $n = 3$. $^{**}P < 0.01$ versus SiNC group.

COL2A1) when hMSCs were cultured in control medium (Figure 3(c); $P > 0.05$). However, TβRIII RNAi significantly enhanced TGF-β3-induced chondrogenic differentiation of hMSCs as compared with that of cells infected with SiNC (Figures 3(a)–3(c); $P < 0.05$).

3.4. TβRIII RNAi Increased the Ratio of TβRII to TβRI. To explore the mechanism on TβRIII RNAi regulating TGF-β3-induced chondrogenic differentiation of hMSCs, we further analyzed the effect of TβRIII RNAi on TβRI and TβRII expression and downstream Smad2/3 signaling during TGF-β3-induced chondrogenesis. Analysis of TβRI and TβRII expression revealed that both TβRI mRNA levels and protein expression had no difference between the cells in the C-SiNC, C-SiTβRIII, and T-SiNC groups (Figures 4(a) and 4(b); $P > 0.05$). However, TβRI mRNA and protein expression levels were decreased in the T-SiTβRIII group as compared with those in the other groups (Figures 4(a) and 4(b); $P < 0.05$). Neither the expression of the TβRII gene (Figure 4(a)) nor that of the protein (Figure 4(b)) was

increased in the C-SiTβRIII group as compared with that in the C-SiNC group ($P > 0.05$). However, as compared with the C-SiNC group, both the T-SiNC and T-SiTβRIII groups had enhanced mRNA levels of TβRII (Figure 4(a); $P < 0.05$) and TβRII expression (Figure 4(b)). The expression of the TβRII gene, as well as that of the TβRII protein, was higher in the T-SiTβRIII group as compared with that in the T-SiNC group. The ratio of TβRII to TβRI in the T-SiNC and T-SiTβRIII groups was higher than that in the C-SiNC and C-SiTβRIII groups (Figure 4(a); $P < 0.05$ and $P < 0.01$, resp.). TβRII/TβRI levels increased dramatically in the T-SiTβRIII groups as compared with those in other groups (Figure 4(a); $P < 0.05$).

3.5. TβRIII RNAi Strengthened TGF-β3-Mediated Phosphorylation of Smad2/3. Analysis of phosphorylation of Smad2/3 revealed that TβRIII-RNAi did not affect the expression of P-Smad2/3 in control medium. However, phosphorylation of Smad2/3 was obviously activated in T-SiNC and T-SiTβRIII groups. Interestingly, when cells

(a)

(b)

(c)
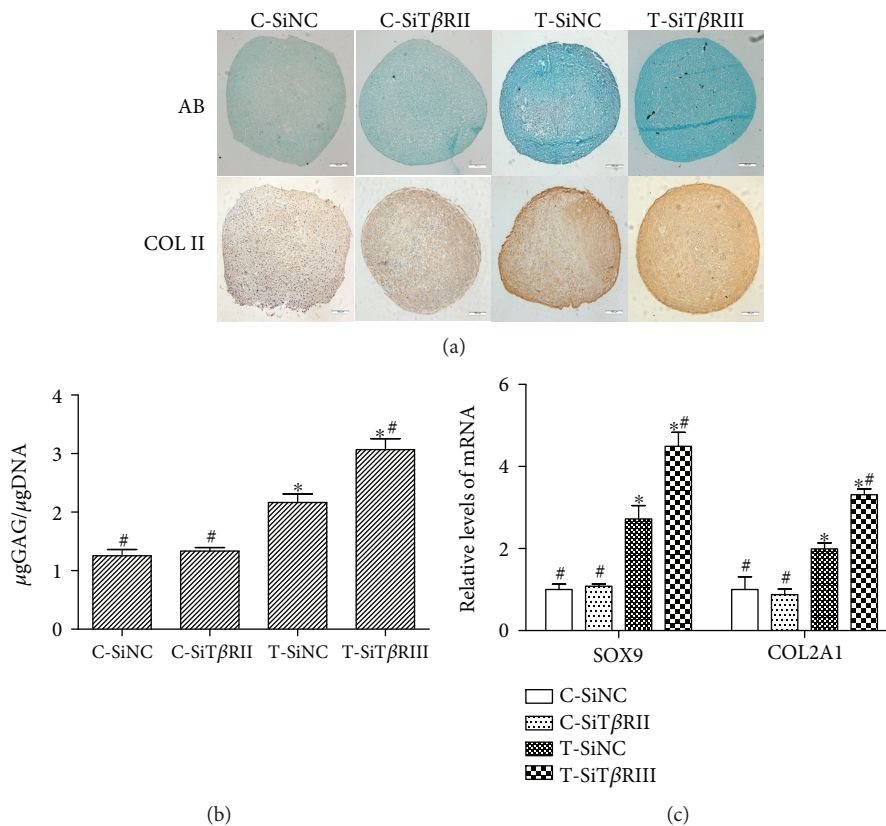
FIGURE 3: TβRIII RNAi enhanced TGF-β3-induced chondrogenic differentiation of hMSCs. SiNC- or SiTβRIII-infected cells were cultured in control medium (C-SiNC group; C-SiTβRIII group) or chondrogenic medium containing TGF-β3 (T-SiNC group; T-SiTβRIII group) for 14 days. (a) Upper panels show glycosaminoglycan (GAG) expression by Alcian blue staining; lower panels show COL II expression by immunohistochemistry. Scale bar = 100 μm. (b) GAG content was quantitatively analyzed and normalized by DNA content. (c) Real-time PCR analysis of COL2A1 and SOX9 mRNA levels in hMSCs from different groups. Error bars represent the means ± SD, $n = 3$. $^{*}P < 0.05$ versus C-SiNC group; $^{\#}P < 0.05$ versus T-SiNC group.

were infected with SiTβRIII, the activation of P-Smad2/3 was further enhanced (Figures 5(a) and 5(b)).

3.6. SB431542 Blocked TβRIII RNAi-Activated TGF-β3-Mediated Phosphorylation of Smad2/3. SB431542 was identified as a specific inhibitor of TβRI and TGF-β signaling [19]. Therefore, we tested whether SB431542 blocked TβRIII RNAi-activated TGF-β signaling. The results showed that SB431542 inhibited both TGF-β3-activated Smad2/3 phosphorylation and TβRIII RNAi-activated TGF-β3-mediated Smad2/3 phosphorylation (Figure 6(a)). The results of the statistical analysis revealed decreased ratios of P-Smad2/3 to Smad2/3 and P-Smad2/3 to GAPDH in the T-SiNC + SB and T-SiTβRIII + SB groups as compared with those in the T-SiNC and T-SiTβRIII groups ($P < 0.05$), as shown in Figure 6(b). There was no statistical difference in P-Smad2/3 levels in the T-SiNC + SB group versus those in the T-SiTβRIII + SB group ($P > 0.05$) (Figure 6(b)). These data showed that SB431542 completely inhibited TGF-β3-mediated Smad2/3 phosphorylation, activated by TβRIII RNAi.

3.7. SB431542 Inhibited TβRIII RNAi-Enhanced TGF-β3-Induced Chondrogenic Differentiation of hMSCs. We have shown that SB431542 blocked TβRIII RNAi-activated TGF-

β signaling. We next investigated whether it was sufficient to inhibit the ability of TβRIII RNAi-enhanced TGF-β3-induced chondrogenic differentiation of hMSCs. As shown in Figure 7, GAG and COL II secretion increased significantly in the T-SiTβRIII group (Figures 7(a) and 7(b)), as well as mRNA levels of cartilage-specific genes (SOX9 and COL2A1), as compared with that in the T-SiNC group (Figure 7(c); $P < 0.05$). Cartilage-specific protein and gene expression decreased in the T-SiNC + SB and T-SiTβRIII + SB groups as compared with cartilage-specific protein and gene expression in the T-SiNC and T-SiTβRIII groups (Figures 7(a)–7(c); $P < 0.05$).

4. Discussion

TβRIII is an abundant TGF-β receptor, which is present in many cell types [9, 13]. We previously demonstrated that hMSCs expressed high levels of TβRIII and that TGF-β3 reduced the expression of TβRIII at mRNA and protein levels [15]. Other studies demonstrated the specific role of TGF-β1 in decreasing TβRIII mRNA and protein levels in cancer cells [20, 21]. These findings were similar to those of our own study. Hempel et al. [21] showed the TGF-β1-mediated downregulation of TβRIII mRNA expression by
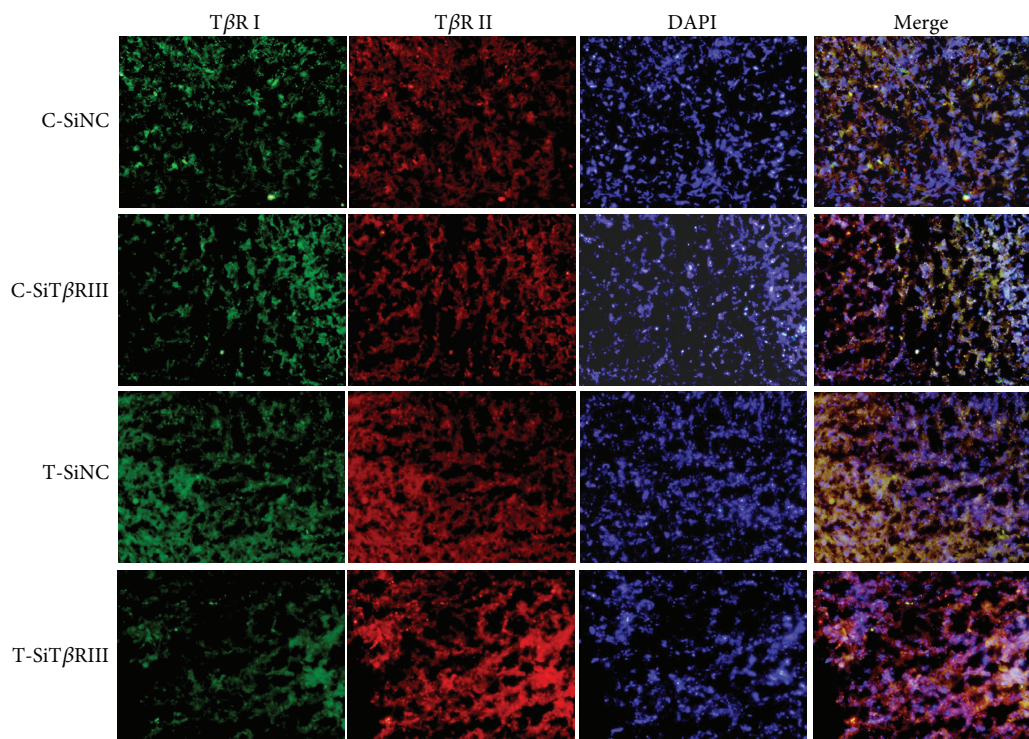
(a)
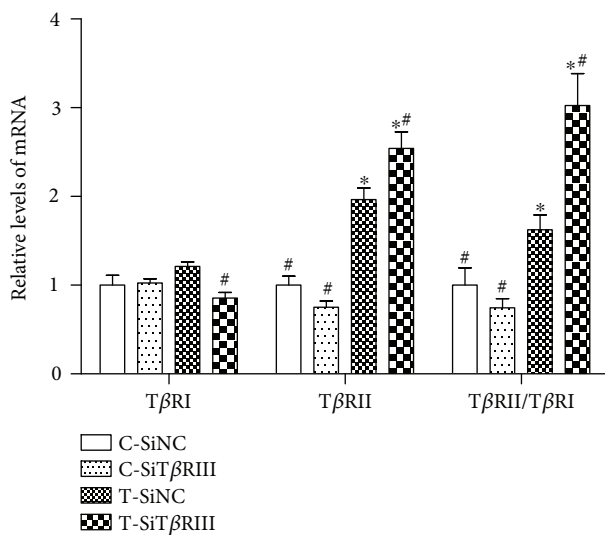
(b)

FIGURE 4: TβRIII RNAi increased the ratio of TβRII to TβRI. SiNC- or SiTβRIII-infected cells were cultured in control medium (C-SiNC group; C-SiTβRIII group) or chondrogenic medium containing TGF-β3 (T-SiNC group; T-SiTβRIII group) for 7days ($n = 3$). (a) The expression of TβRI and that of TβRII were visualized by immunofluorescence staining using anti-TβRI (green) and anti-TβRII (red) antibodies. Nuclei were counterstained using DAPI (blue). The far right panels show merged images. Scale bar = $20\,\mu$m. (b) mRNA expression of TβRI and TβRII and the ratio of TβRII to TβRI by real-time RT-PCR. $^*P < 0.05$ versus C-SiNC group; $^\#P < 0.05$ versus T-SiNC group.

exerting effects on the ALK5/Smad2/3 pathway of the TGFβR3 gene proximal promoter. Three highly homologous isoforms of TGF-β in humans (TGF-β1, TGF-β2, and TGF-β3) share a similar receptor complex and signaling pathway [20]. Therefore, the mechanism underlying the suppression by TGF-β3 on TβRIII may be the same as that involved in TGF-β1-mediated downregulation of TβRIII.

In recent years, many studies have investigated the effects of altering the expression level of TβRIII and its roles on mediating cell migration, invasion, growth, and differentiation in several cell types, including cancer and epithelial cells [13, 20, 22, 23]. However, the regulatory roles of TβRIII in MSCs have not been explored. RNAi is a powerful tool for studying protein function [24]. Lentiviral vectors encoding

(a)   (b)
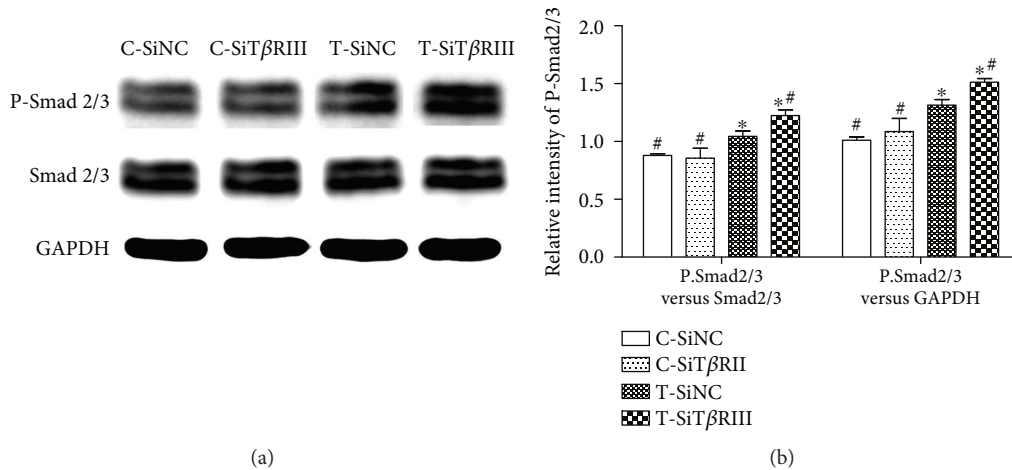
FIGURE 5: TβRIII RNAi strengthened TGF-β3-mediated Smad2/3 phosphorylation. SiNC- or SiTβRIII-infected cells were cultured in control medium (C-SiNC group; C-SiTβRIII group) or chondrogenic medium containing TGF-β3 (T-SiNC group; T-SiTβRIII group) and harvested after 24 h. (a) A Western blot of protein levels of P-Smad2/3, total Smad2/3, and GAPDH. (b) Quantification of protein levels of P-Smad2/3 normalized to total levels of Smad2/3 or GAPDH. Error bars represent the means $\pm$ SD, $n = 3$. $^{*}P < 0.05$ versus C-SiNC group; $^{\#}P < 0.05$ versus T-SiNC group.

(a)   (b)
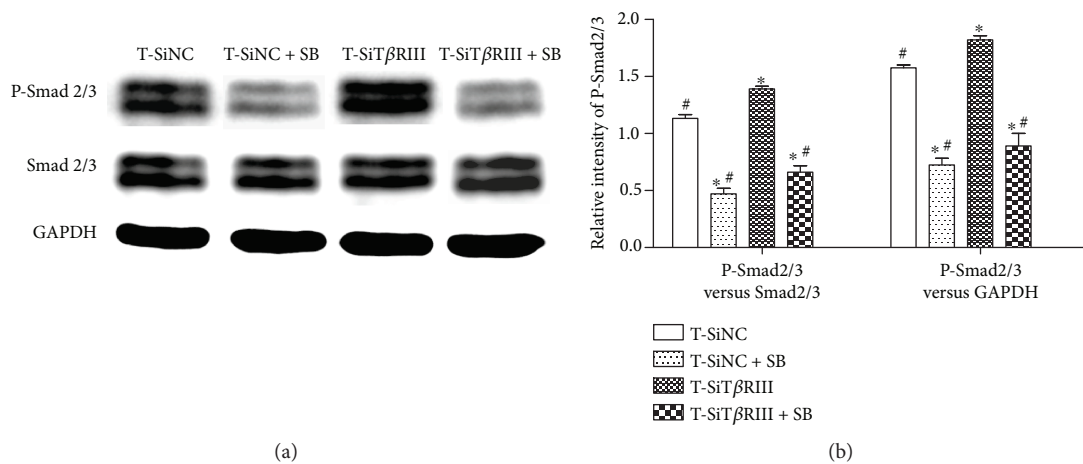
FIGURE 6: SB431542 blocked TβRIII RNAi-activated TGF-β3-mediated phosphorylation of Smad2/3. SiNC- or SiTβRIII-infected hMSCs were cultured in chondrogenic medium, supplemented with TGF-β3 (T-SiNC group or T-SiTβRIII group) and exposed to SB431542 treatment for 2 h before treatment with TGF-β3 (T-SiNC + SB group or T-SiTβRIII + SB group). Samples were harvested after 24 h. (a) Western blot of protein levels of P-Smad2/3, total Smad2/3, and GAPDH. (b) Quantification of protein levels of P-Smad2/3 normalized to total levels of Smad2/3 and GAPDH. Error bars represent the means $\pm$ SD, $n = 3$. $^{*}P < 0.05$ versus T-SiNC group, $^{\#}P < 0.05$ versus T-SiTβRIII group.

short hairpin RNAs (shRNAs) or microRNAs (miRNAs) can be used to specifically knock down target mRNAs [25]. Besides the ability to transfer vectors in primary and nondividing cells, the reverse-transcribed lentiviral vector is integrated in the genome, allowing stable expression of the gene or shRNA of interest [26]. We used GV248-based lentiviral vectors for delivery of shRNAs, precursors of TβRIII siRNA, into MSCs to suppress TβRIII gene expression. This vector coexpressed enhanced GFP, a reporter gene, permitting infected cells to be detected by fluorescence microscopy. Three days after infection with Lenti-siTβRIII or Lenti-NC, fluorescence microscopy images revealed efficient infection of MSCs with lentiviral vectors. The data also demonstrated

that the lentiviral vector-based shRNA vector effectively downregulated mRNA and protein expression of TβRIII. These data indicated that Lenti-siTβRIII MSCs could be used as a powerful tool for studying the effect of the siTβRIII gene on MSC chondrogenesis.

Our study is the first to demonstrate that TβRIII knockdown in MSCs enhanced TGF-β3-induced chondrogenic differentiation, indicating a role for TβRIII as a negative modulator of MSC chondrogenesis. Previous research reported that the functional impact of TβRIII on TGF-β ligand signaling was cell-type dependent [9]. Li et al. [13] demonstrated that transfection of TβRIII-containing plasmid DNA dramatically promoted a TGF-β1-induced

(a)

(b)

(c)
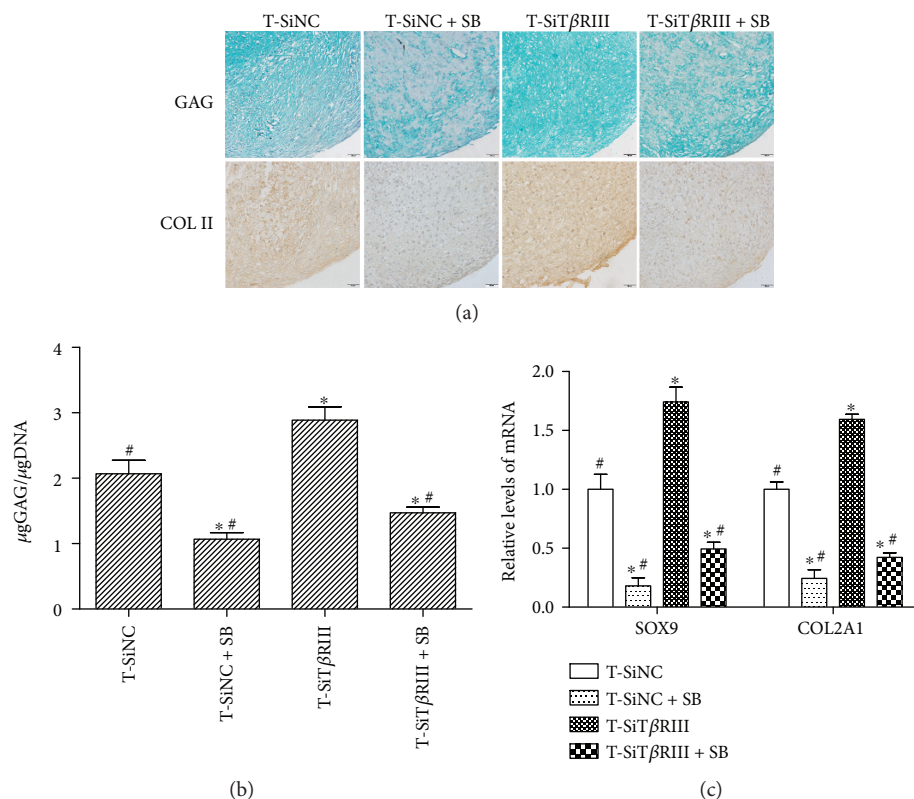
FIGURE 7: SB431542 inhibited TβRIIIRNAi-enhanced TGF-β3-induced chondrogenic differentiation of hMSCs. Cells from T-SiNC, T-SiNC + SB, T-SiTβRIII, and T-SiTβRIII + SB groups were cultured for 14 days. (a) Alcian blue staining for GAG expression and immunohistochemistry staining for COL II expression. $n = 3$, scale bar $= 50\,\mu$m. (b) GAG content was quantitatively analyzed and normalized by DNA content. (c) mRNA levels of SOX9 and COL2A1 were measured by real-time PCR. Error bars represent the means $\pm$ SD, $n = 3$. $^*P < 0.05$ versus T-SiNC group, $^\#P < 0.05$ versus T-SiTβRIII group.

decrease in cell viability, apoptosis, and cell arrest. On the other hand, Eickelberg et al. indicated that the expression of TβRIII in renal epithelial LLC-PK1 cells resulted in inhibition of TGF signaling [27]. They also suggested that TβRIII with larger proteoglycans negatively modulated TGF-β1-induced cellular responses, whereas TβRIII containing smaller proteoglycans enhances TGF-β1-induced cellular responses [27]. These results suggested that TβRIII in MSCs may contain larger proteoglycans.

TGF-βs (TGF-β1, TGF-β2, and TGF-β3, resp.) are small secreted signaling proteins, each of which signals through TβRI and TβRII. In contrast to TβRI and TβRII, TβRIII is a membrane-anchored nonsignaling receptor, and its function is to bind and concentrate TGF-β isoforms on the cell surface and promote the binding of TβRII and recruitment of TβRI [11]. Chen et al. [15] demonstrated that TβRI was recruited to form TβRIII/TβRII/TβRI ternary complexes that it had two forms: complex I and complex II. Complex I contained more TβRII than TβRI, underwent clathrin-mediated endocytosis, and transduced signals in endosomes. Complex II, which contained more TβRI than TβRII, underwent caveolae/lipid-raft-mediated endocytosis and rapid degradation. The formation of these complexes was regulated by the proteoglycan moiety of TβRIII and altered the expression of TβRII or TβRI [15]. Herein, we demonstrated that TβRIII RNAi decreased TβRI expression and increased

TβRII expression in the T-SiTβRIII group when MSCs were cultured with TGF-β3 as compared with the T-SiNC group (Figure 4). The data, combined with the findings of previous reports [15], indicated that TβRIII RNAi increased the ratio of TβRII to TβRI of the receptor complex and formed complex I, therefore enhancing TGF-β3 signaling in MSC chondrogenesis.

TGF-β signals predominantly bind to the ALK5 receptor (TβRI) and subsequently activate C-terminal Smad 2/3 phosphorylation. This signaling route stimulates the production of matrix components [19]. The present study also showed that TβRIII RNAi further enhanced the TGF-β3-activated downstream Smad2/3 signaling pathway (Figure 5). In addition, SB431542, a TβRI inhibitor, as well as dominant negative Smad2/3 specifically [28], significantly reversed TβRIII RNAi-mediated increases in TGF-β3-induced MSC chondrogenesis (Figures 6 and 7). These data indicated that TβRIII knockdown enhanced TGF-β3-induced MSC chondrogenesis via the Smad2/3 signaling pathway.

5. Conclusions

This study demonstrated that TGF-β3 inhibited the expression of TβRIII. TβRIII RNAi enhanced TGF-β3-induced chondrogenic differentiation of hMSCs by increasing the ratio of TβRII to TβRI in the receptor complex and further

activating downstream Smad2/3 signaling. These findings contribute to the understanding of the molecular mechanisms that control chondrogenic differentiation of MSCs and provide a potential strategy (i.e., modification of MSCs by TβRIII knockdown for cell-based cartilage tissue engineering).

Data Availability

The data used to support the findings of this study are available from the corresponding author upon request.

Conflicts of Interest

The authors declare that there is no conflict of interests regarding the publication of this paper.

Authors' Contributions

Shuhui Zheng and Hang Zhou contributed equally to this work.

Acknowledgments

References

[1] Y. Wang, M. Yuan, Q.-Y. Guo, S.-B. Lu, and J. Peng, "Mesenchymal stem cells for treating articular cartilage defects and osteoarthritis," *Cell Transplantation*, vol. 24, no. 9, pp. 1661–1678, 2015.

[2] S. W. Huh, A. A. Shetty, S. Ahmed, D. H. Lee, and S. J. Kim, "Autologous bone-marrow mesenchymal cell induced chondrogenesis (MCIC)," *Journal of Clinical Orthopaedics and Trauma*, vol. 7, no. 3, pp. 153–156, 2016.

[3] S. Yamasaki, H. Mera, M. Itokazu, Y. Hashimoto, and S. Wakitani, "Cartilage repair with autologous bone marrow mesenchymal stem cell transplantation: review of preclinical and clinical studies," *Cartilage*, vol. 5, no. 4, pp. 196–202, 2014.

[4] A. R. Tan and C. T. Hung, "Concise review: mesenchymal stem cells for functional cartilage tissue engineering: taking cues from chondrocyte-based constructs," *Stem Cells Translational Medicine*, vol. 6, no. 4, pp. 1295–1303, 2017.

[5] S. Yoshiya and A. Dhawan, "Cartilage repair techniques in the knee: stem cell therapies," *Current Reviews in Musculoskeletal Medicine*, vol. 8, no. 4, pp. 457–466, 2015.

[6] Q. O. Tang, K. Shakib, M. Heliotis et al., "TGF-β3: a potential biological therapy for enhancing chondrogenesis," *Expert Opinion on Biological Therapy*, vol. 9, no. 6, pp. 689–701, 2009.

[7] J. Nickel, P. ten Dijke, and T. D. Mueller, "TGF-β family co-receptor function and signaling," *Acta Biochimica et Biophysica Sinica*, vol. 50, no. 1, pp. 12–36, 2018.

[8] K. B. Marcu, L. M. G. de Kroon, R. Narcisi et al., "Activin receptor-like kinase receptors ALK5 and ALK1 are both required for TGFβ-induced chondrogenic differentiation of human bone marrow-derived mesenchymal stem cells," *PLoS One*, vol. 10, no. 12, article e0146124, 2015.

[9] M. Bilandzic and K. L. Stenvers, "Betaglycan: a multifunctional accessory," *Molecular and Cellular Endocrinology*, vol. 339, no. 1-2, pp. 180–189, 2011.

[10] F. López-Casillas, H. M. Payne, J. L. Andres, and J. Massagué, "Betaglycan can act as a dual modulator of TGF-beta access to signaling receptors: mapping of ligand binding and GAG attachment sites," *Journal of Cell Biology*, vol. 124, no. 4, pp. 557–568, 1994.

[11] M. M. Villarreal, S. K. Kim, L. Barron et al., "Binding properties of the transforming growth factor-β coreceptor betaglycan: proposed mechanism for potentiation of receptor complex assembly and signaling," *Biochemistry*, vol. 55, no. 49, pp. 6880–6896, 2016.

[12] S. McLean and G. M. Di Guglielmo, "TGFβ (transforming growth factor β) receptor type III directs clathrin-mediated endocytosis of TGFβ receptor types I and II," *Biochemical Journal*, vol. 429, no. 1, pp. 137–145, 2010.

[13] D. Li, D. Xu, Z. Lu, X. Dong, and X. Wang, "Overexpression of transforming growth factor type III receptor restores TGF-β1 sensitivity in human tongue squamous cell carcinoma cells," *Bioscience Reports*, vol. 35, no. 4, article e00243, 2015.

[14] K. Tazat, M. Hector-Greene, G. C. Blobe, and Y. I. Henis, "TβRIII independently binds type I and type II TGF-β receptors to inhibit TGF-β signaling," *Molecular Biology of the Cell*, vol. 26, no. 19, pp. 3535–3545, 2015.

[15] C.-L. Chen, S. S. Huang, and J. S. Huang, "Cellular heparan sulfate negatively modulates transforming growth factor-β_1(TGF-β_1) responsiveness in epithelial cells," *Journal of Biological Chemistry*, vol. 281, no. 17, pp. 11506–11514, 2006.

[16] J. Chen, Y. Wang, C. Chen et al., "Exogenous heparan sulfate enhances the TGF-β3-induced chondrogenesis in human mesenchymal stem cells by activating TGF-β/Smad signaling," *Stem Cells International*, vol. 2016, Article ID 1520136, 10 pages, 2016.

[17] C. Xu, Z. Zheng, L. Fang et al., "Phosphatidylserine enhances osteogenic differentiation in human mesenchymal stem cells via ERK signal pathways," *Materials Science and Engineering: C*, vol. 33, no. 3, pp. 1783–1788, 2013.

[18] L. Zhang, P. Su, C. Xu, J. Yang, W. Yu, and D. Huang, "Chondrogenic differentiation of human mesenchymal stem cells: a comparison between micromass and pellet culture systems," *Biotechnology Letters*, vol. 32, no. 9, pp. 1339–1346, 2010.

[19] A. van Caam, W. Madej, A. Garcia de Vinuesa et al., "TGFβ1-induced SMAD2/3 and SMAD1/5 phosphorylation are both ALK5-kinase-dependent in primary chondrocytes and mediated by TAK1 kinase activity," *Arthritis Research & Therapy*, vol. 19, no. 1, p. 112, 2017.

[20] S. E. N. Zhang, W.-Y. Sun, J.-J. Wu, Y.-J. Gu, and W. E. I. Wei, "Decreased expression of the type III TGF-β receptor enhances metastasis and invasion in hepatocellullar carcinoma progression," *Oncology Reports*, vol. 35, no. 4, pp. 2373–2381, 2016.

[21] N. Hempel, T. How, S. J. Cooper et al., "Expression of the type III TGF-β receptor is negatively regulated by TGF-β," *Carcinogenesis*, vol. 29, no. 5, pp. 905–912, 2008.

[22] D. Xu, D. U. O. Li, Z. Lu, X. Dong, and X. Wang, "Type III TGF-β receptor inhibits cell proliferation and migration in salivary glands adenoid cystic carcinoma by suppressing NF-κB signaling," *Oncology Reports*, vol. 35, no. 1, pp. 267–274, 2016.

[23] L. M. Jenkins, P. Singh, A. Varadaraj et al., "Altering the proteoglycan state of transforming growth factor β type III

receptor (TβRIII)/Betaglycan modulates canonical Wnt/β-catenin signaling," *Journal of Biological Chemistry*, vol. 291, no. 49, pp. 25716–25728, 2016.

[24] L. Zhang, H.-j. Liu, T.-j. Li et al., "Lentiviral vector-mediated siRNA knockdown of SR-PSOX inhibits foam cell formation *in vitro*," *Acta Pharmacologica Sinica*, vol. 29, no. 7, pp. 847–852, 2008.

[25] Y. P. Liu, M. A. Vink, J. T. Westerink et al., "Titers of lentiviral vectors encoding shRNAs and miRNAs are reduced by different mechanisms that require distinct repair strategies," *RNA*, vol. 16, no. 7, pp. 1328–1339, 2010.

[26] C. Albrecht, S. Hosiner, B. Tichy, S. Aldrian, S. Hajdu, and S. Nürnberger, "Comparison of lentiviral packaging mixes and producer cell lines for RNAi applications," *Molecular Biotechnology*, vol. 57, no. 6, pp. 499–505, 2015.

[27] O. Eickelberg, M. Centrella, M. Reiss, M. Kashgarian, and R. G. Wells, "Betaglycan inhibits TGF-β signaling by preventing type I-type II receptor complex formation: glycosaminoglycan modifications alter betaglycan function," *Journal of Biological Chemistry*, vol. 277, no. 1, pp. 823–829, 2002.

[28] H. J. You, M. W. Bruinsma, T. How, J. H. Ostrander, and G. C. Blobe, "The type III TGF-β receptor signals through both Smad3 and the p38 MAP kinase pathways to contribute to inhibition of cell proliferation," *Carcinogenesis*, vol. 28, no. 12, pp. 2491–2500, 2007.

Research Article

Alginate/Hydroxyapatite-Based Nanocomposite Scaffolds for Bone Tissue Engineering Improve Dental Pulp Biomineralization and Differentiation

Silvia Sancilio [ID],[1] **Marialucia Gallorini** [ID],[2,3] **Chiara Di Nisio,**[1] **Eleonora Marsich** [ID],[4] **Roberta Di Pietro** [ID],[5] **Helmut Schweikl,**[3] **and Amelia Cataldi**[1]

[1]Department of Pharmacy, University G. d'Annunzio, Chieti-Pescara, Italy
[2]Department of Medical, Oral and Biotechnological Sciences, University G. d'Annunzio, Chieti-Pescara, Italy
[3]Department of Conservative Dentistry and Periodontology, University Hospital Regensburg, University of Regensburg, Regensburg, Germany
[4]Department of Medical, Surgical and Health Sciences, University of Trieste, Trieste, Italy
[5]Department of Medicine and Ageing Sciences, G. d'Annunzio University, Chieti, Italy

Correspondence should be addressed to Silvia Sancilio; s.sancilio@unich.it

Tissue engineering is widely recognized as a promising approach for bone repair and reconstruction. Several attempts have been made to achieve materials that must be compatible, osteoconductive, and osteointegrative and have mechanical strength to provide a structural support. Composite scaffolds consisting in biodegradable natural polymers are very promising constructs. Hydroxyapatite (HAp) can support alginate as inorganic reinforcement and osteoconductive component of alginate/HAp composite scaffolds. Therefore, HAp-strengthened polymer biocomposites offer a solid system to engineer synthetic bone substitutes. In the present work, HAp was incorporated into an alginate solution and internal gelling was induced by addition of slowly acid-hydrolyzing D-gluconic acid delta-lactone for the direct release of calcium ions from HAp. It has been previously demonstrated that alginate-based composites efficiently support adhesion of cancer bone cell lines. Human dental pulp stem cells (DPSCs) identified in human dental pulp are clonogenic cells capable of differentiating in multiple lineage. Thus, this study is aimed at verifying the mineralization and differentiation potential of human DPSCs seeded onto scaffolds based on alginate and nano-hydroxyapatite. For this purpose, gene expression profile of early and late mineralization-related markers, extracellular matrix components, viability parameters, and oxidative stress occurrence were evaluated and analyzed. In summary, our data show that DPSCs express osteogenic differentiation-related markers and promote calcium deposition and biomineralization when growing onto Alg/HAp scaffolds. These findings confirm the use of Alg/HAp scaffolds as feasible composite materials in tissue engineering, being capable of promoting a specific and successful tissue regeneration as well as mineralized matrix deposition and sustaining natural bone regeneration.

1. Introduction

Tissue engineering is widely recognized as one of the most promising approaches for bone repair and reconstruction in orthopaedics [1]. Bone is a complex and hierarchical tissue with nano-hydroxyapatite and collagen representing the major portions [2]. Several attempts have been made in order to achieve feasible materials with osteoconductive and osteointegrative properties to provide a structural support [3]. Indeed, the major role of bone is to provide a morphological framework, mechanical strength, blood pH regulation, and maintenance of calcium and phosphate levels to assist metabolic processes [2]. As far as dental restoration is concerned, regenerative endodontics is a promising field of tissue engineering that is aimed at achieving results using stem cells associated with responsive molecules and scaffolds.

In particular, the combination of composite materials and stem cells in the site of implantation is considered an ideal alternative treatment to traditional root canal therapy [4]. Thus, growing cells from a small biopsy, followed by their culture in porous scaffold to form a new tissue, is the goal of tissue engineering [3]. Artificial scaffolds are temporary structures designed to sustain and promote cell adhesion, migration, proliferation, and differentiation through their chemical and physical properties [2]. Both bioactive ceramics and polymers have been developed for use as bone composite scaffolds. Composite scaffolds consisting in biodegradable natural polymers are very promising constructs, endowed with excellent biocompatibility and suitable mechanical properties. Moreover, they can be loaded with growth and differentiation factors involved in bone formation. Natural polymers offer the advantage of being very similar to the physiological macromolecular environment of cells [1, 5]. Among natural polymers, polysaccharides are very versatile, able to be decorated with signal molecules and to interact with inorganic components. Alginates belong to a family of linear copolymers capable of forming stable gels in the presence of millimolar concentrations of calcium or other divalent cations [6]. Alginates can be effectively manufactured into porous three-dimensional biodegradable networks, and, in combination with hydroxyapatite (HAp) as inorganic reinforcement and osteoconductive element and/or with other bioactive components, they can constitute solid systems sustaining natural bone regeneration [1, 7, 8].

Over the last decade, the discovery of different types of multipotent stem cells from human adult tissues has led to a rapid breakthrough in the field of regenerative medicine. They can potentially regenerate different types of tissues when loaded on suitable scaffolding structures that direct stem cell fate [9]. Adult mesenchymal stem cells (MSCs), primarily isolated from the bone marrow, were identified to be multipotent stem cells with the ability of differentiating into cells of mesodermal (osteocytes, chondrocytes, and adipocytes), ectodermal (neurons), and endodermal origins. Other eminent sources of adult MSCs include placenta, umbilical cord, amniotic fluid, adipose tissue, dental pulp, breast milk, and synovium [10]. The oral cavity as well as the extracted teeth constitute a remarkable source since they produce a variety of somatic stem cells [11]. The major differences in the stem cells arising from different sources are exhibited in their immunophenotypes. These differences have implications on proliferation, differentiation, and immunomodulation of MSCs from the respective sources. Dental pulp stem cells (DPSCs) have been reported to have higher proliferative ability than bone marrow- and adipose tissue-derived MSCs [10, 12–14]. They continuously divide and differentiate into various cell types, for instance, cells belonging to osteogenic, dentinogenic, adipogenic, neurogenic, chondrogenic, and myogenic lineage. Moreover, dental pulp can be easily isolated from the surgical waste derived from deciduous tooth or wisdom tooth extraction [15]. The very low morbidity of the anatomical site after the collection of the pulp, the high efficiency of the extraction procedure of stem cells from the pulp tissue, the differentiation ability, and the demonstrated interactivity of stem cells derived from dental pulp with biomaterials for tissue engineering applications hold to DPSCs a great potential for clinical purposes [11, 16]. Although it has been well demonstrated that MSCs from various sources are able to sustain bone regeneration [17], only recent tissue engineering approaches have shown that DPSCs constitute a valuable cell source for the healing of bone tissue when supported by a suitable scaffold [18–20].

Also compared to equal volumes of bone marrow, dental pulp contains a higher number of mesenchymal stem cells [21, 22]. In this light, due to the presence of a higher undifferentiated population, DPSCs are a suitable stem cell source in order to obtain different kinds of tissue including dental pulp tissues, dentin, or bone. These cells proliferate and differentiate into mature cells that produce an extracellular mineralized matrix. Remarkably, it seems that redox homeostasis might be essential for osteogenic differentiation [23]. MSCs are known to have low levels of intracellular ROS and high levels of glutathione, a key antioxidant. They also constitutively express high levels of enzymes required to manage oxidative stress. In terms of redox regulation, numerous recent reports describe the importance of oxidants on MSC differentiation into osteoblast-like cells. Elevated levels of ROS, defined as oxidative stress, lead to arrest of the MSC cell cycle and apoptosis [23, 24].

The differentiation stage of DPSCs greatly influences both the speed of matrix deposition and the quality of the newly formed one [22, 25]. Among several components, water with some dissolved noncollagenous organic matter is the third component of the mineralized matrix, while the ratios of hydroxyapatite-to-collagen-to-water volume and weight fraction are not constant. Wet collagen and hydroxyapatite mineral crystal agglomerations interpenetrate each other, forming the mineralized fibril at a scale of several hundred nanometers [2]. The aim of this study is to verify the mineralization potential of human DPSC growth in the presence of composite scaffolds based on alginate and nano-hydroxyapatite, which has been already described and characterized by Turco et al. [1]. It has been shown that these scaffolds can efficiently sustain adhesion, colonization, and matrix deposition of osteoblast-like cells without any additional chemical modification of alginate. Moreover, they have adequate structural and physical-chemical properties for being used as scaffolds in bone tissue engineering strategies. In the present paper, the gene expression profile of early and late mineralization-related markers, extracellular matrix components, viability parameters of DPSCs, and expression of bone sialoprotein II (BSP II) were evaluated and analyzed. We further provide experimental evidence that the activation of the enzymatic antioxidant catalase is crucial for cell survival.

2. Materials and Methods

2.1. Preparation of Alginate and HAp Composites (Alg/HAp Scaffolds).
Alg/HAp composite scaffolds were prepared after having mixed alginate 2% (*w/v*) and HAp at different concentrations in water using the calcium release method. HAp in powder was homogenously dissolved into a stirred

solution of alginate in water, followed by the addition of GDL 60 mM to release calcium ions from HAp. Aliquots of this gel were then pipetted and incubated in a 24-well tissue culture plate (Costar, Cambridge, MA) for 24 h at room temperature in order to achieve a complete gelification. Hydrogels were then stepwise cooled, immersing tissue culture plates in a liquid cryostat using an aqueous solution of ethylene glycol (3 : 1 in water) as refrigerant fluid. Temperature was lowered stepwise from 20 up to −20°C using 5°C steps with a 30 min interval for equilibration. Samples were then freeze-dried for 24 h to obtain porous scaffolds. As a control, pure alginate gels (HAp-free) were prepared by replacing HAp with $CaCO_3$ (30 mM of Ca^{2+}). Hap-free gels were then processed as their counterpart with HAp. Alg/HAp scaffolds were further characterized as previously described [1].

2.2. Alg/HAp Scaffold Sterilization and Preparation for Cell Culture.
Alg/HAp scaffolds underwent two cycles of sterilization under a UV light (15 W) for 1 hour. After that, they were rehydrated in a sterile aqueous solution of 5 mM $CaCl_2$ and 1% penicillin/streptomycin under weak magnetic agitation for 20 minutes. Next, every scaffold was gently squeezed by means of a clamp and placed in a Falcon® 12-Well Clear Flat Bottom Not Treated Multiwell Cell Culture Plate. MEM ALPHA medium supplemented with 10% FBS and 1% penicillin/streptomycin (all purchased by EuroClone, Milan, Italy) was immediately added up to the brim of each well in order to cover up the entire scaffold surface. Then scaffolds were conditioned by the medium overnight, placing the multiwell plate at 37°C and 5% CO_2.

2.3. Isolation and Cultivation of DPSCs.
According to the Italian Legislation and the code of ethical principles for medical research involving human subjects of the World Medical Association (Declaration of Helsinki), young donors who underwent extraction of the third molar signed an informed consent. This project has received the approval of the Local Ethical Committee of the University of Chieti-Pescara (approval number 1173, date of approval 31/03/2016). After having obtained dental pulp samples from surgical procedures, DPSCs were handled and cultivated as previously described [22].

DPSCs were then analyzed by flow cytometry in order to characterize the cells by their immunophenotype. Molecular markers commonly applied to identify mesenchymal stem cells were detected as described in a previous work from our group [26].

2.4. Cell Seeding on Alg/HAp Scaffolds.
After being characterized by flow cytometry, DPSCs were cultured and expanded in MEM ALPHA medium supplemented with 10% FBS and 1% penicillin/streptomycin (all purchased by EuroClone, Milan, Italy) up to passage 7. Cell cultures were then trypsinized (Trypsin/EDTA 1x, EuroClone, Milan, Italy), and cells were collected by centrifugation at 1200 rpm for 10 minutes at room temperature. DPSCs were counted by Trypan blue dye exclusion, and 5×10^4 cells resuspended in 130 μl of complete MEM ALPHA medium were used for cell seeding on each scaffold. The same cell number was used to seed DPSCs on polystyrene (named in figures as DPSCs). After having discarded the medium from the overnight conditioning, scaffolds were once again squeezed to eliminate the excess of medium and placed on a fresh Falcon 12-Well Clear Flat Bottom Not Treated Multiwell Cell Culture Plate. Next, DPSCs were seeded drop by drop on the scaffolds and immediately placed at 37°C and 5% CO_2 for 3 h. Finally, a complete MEM ALPHA medium was added (named in figures as "Scaffold", i.e., DPSC-laden scaffolds). Where necessary, the complete MEM ALPHA medium supplemented by differentiation agents (named in figures as DPSCs + DM and Scaffold + DM, i.e., DPSC-laden scaffolds in the presence of differentiation medium) was added. Complete DM was supplemented by L-ascorbic acid 100 μM, dexamethasone 10 nM, β-glycerol phosphate disodium salt pentahydrate 5 mM (all purchased by Sigma-Aldrich, MI, USA), and potassium phosphate monohydrate 1.8 mM (Alfa Aesar, MA, USA). DPSCs seeded on polystyrene and DPSCs onto Alg/HAp scaffolds with or without DM were incubated for 1, 3, 7, 14, 21, and 28 days, refreshing the medium every 72 h.

2.5. Alizarin Red S Staining.
To assess calcium deposition, Alizarin Red S staining was carried out on DPSC cultures. On days 7, 14, 21, and 28, the cell supernatant was discarded and cells were washed twice with PBS with Ca/Mg. After that, cultures were fixed with 4% paraformaldehyde (PFA) for 30 minutes and then washed with PBS. Samples were afterwards incubated with Alizarin Red S (40 mM in deionized water) for 30 minutes in the dark. After that, DPSCs were washed three times with deionized water and samples were observed under a phase-contrast light microscope (Leica, Wetzlar, Germany) equipped with a CoolSNAP camera to acquire computerized images (Photometrics, Tucson, AZ).

2.6. Alkaline Phosphatase Activity.
Alkaline phosphatase (ALP) catalyzes the hydrolysis of phosphate esters in alkaline buffer and produces an organic radical and inorganic phosphate. The activity of ALP was analyzed in cell supernatants using the Alkaline Phosphatase Assay Kit (Colorimetric) (Abcam, Cambridge, UK). The kit uses p-nitrophenyl phosphate (pNPP) as a phosphatase substrate which turns yellow ($\lambda_{max} = 405$ nm) when dephosphorylated by ALP. Cell supernatants were collected after 1, 3, 7, 14, 21, and 28 days of culture. After collection, 80 μl/well of sample was loaded in a Falcon 96-Well Clear Flat Bottom TC-Treated Culture Microplate in duplicate. Next, 50 μl of pNPP 5 mM/well was added and the plate was incubated for 1 hour at room temperature in the dark. After that, 20 μl of stop solution was pipetted into each well and the absorbance output was measured at 405 nm by means of a microplate reader (Multiskan GO, Thermo Scientific, MA, USA). Each test was performed in triplicate. The calculation of ALP activity (U/l/min) was carried out following the manufacturer's specifications, and each obtained value was normalized on its protein content (μg of proteins/sample) measured by the BCA assay.

2.7. Quantification of Human Collagen Type I.
Levels of collagen type I in the culture medium were quantified by

means of ELISA (human collagen type 1 ELISA, Cosmo Bio, Tokyo, Japan). After 1, 3, 7, 14, 21, and 28 days, cell supernatants were collected and ELISA assay was performed. Cell supernatants were pipetted, and the blue conjugate and the yellow antibody were added. After 2 h of incubation at room temperature on a plate shaker, wells were washed and then incubated with the pNPP substrate for 45 min. Finally, a stop solution was added and optical density (OD) was measured at 450 nm by means of a microplate reader (Multiskan GO, Thermo Scientific, MA, USA). Each test was performed in triplicate. The concentration of collagen type I was calculated using a standard curve generated with specific standards provided by the manufacturers. Each obtained collagen concentration (μg/ml) was normalized on the protein content (μg of proteins/sample) measured by the BCA assay.

2.8. Protein Extraction and BCA Assay. After having discarded the supernatants, DPSCs cultured on polystyrene were washed twice with PBS, trypsinized, and collected by centrifugation at 1200 rpm for 10 minutes. Pellets were then washed twice with cool PBS and kept on ice. As regard DPSCs' growth onto scaffolds, they were put in a sodium citrate buffer solution at pH = 7.4 under vigorous magnetic agitation in order to decompose scaffolds without damaging cells. This buffer solution was made by 50 mM sodium citrate tribasic dehydrate, 100 mM sodium chloride, and 10 mM sucrose (all purchased from Sigma-Aldrich, MI, USA). After being dissolved in the buffer solution, scaffolds and DPSCs were collected by centrifugation at 1500 rpm for 10 minutes and pellets were washed twice with cool PBS. After having discarded the washing solution, 0.5 ml of lysis buffer enriched with a protein inhibitor cocktail (PBS, 1% IGEPAL CA-630, 0.5% sodium deoxycholate, 0.1% SDS, 10 mg/ml PMSF, 1 mg/ml aprotinin, 100 mM sodium orthovanadate, and 50 μg/ml leupeptin, all purchased from Sigma-Aldrich, MI, USA) was added and samples were kept on ice for 30 min. Then, the lysed pellets were resuspended and kept on ice for a further 30 min. Following centrifugation for 15 min at 20,000g, the supernatant was collected as the whole cell fraction. Protein concentration in the whole cell lysate was determined using bicinchoninic acid assay (QuantiPro™ BCA Assay Kit for 0.5–30 μg/ml protein, Sigma-Aldrich, Milan, Italy) following the manufacturer's instructions. Briefly, cell lysates were diluted 1 : 150 in 150 μl of deionized water and an equal volume of QuantiPro BCA assay mix was added. Samples were incubated 2 h at 37°C, and the absorbance signal generated was measured at 562 nm in a microplate reader (Multiskan GO, Thermo Scientific, MA, USA). Each test was performed in triplicate. Analyses of the obtained OD were carried out using GraphPad Prism version 5.01 for Windows (GraphPad Software, San Diego, CA). The concentration of protein was calculated using a standard curve generated with specific standards provided by the manufacturers.

2.9. Cytotoxicity Assay. Cytotoxicity occurrence was assessed by means of the CytoTox 96® Non-Radioactive Cytotoxicity Assay (Promega, WI, USA). The kit measures lactate dehydrogenase (LDH), a stable cytosolic enzyme that is released upon cell lysis. Released LDH in culture supernatants is measured with coupled enzymatic assay, which results in the conversion of a tetrazolium salt (iodonitrotetrazolium violet (INT)) into a red formazan product. The amount of color formed is proportional to the number of lysed cells. After having collected supernatants at days 1, 3, 7, 14, 21, and 28, 50 μl was transferred to a Falcon 96-Well Clear Flat Bottom TC-Treated Culture Microplate in triplicate. An equal volume of CytoTox 96 Reagent is added to each well and incubated for 30 minutes. When a provided stop solution was added, the absorbance signal was measured at 490 nm and 690 nm (background) in a microplate reader (Multiskan GO, Thermo Scientific, MA, USA). Each test was carried out in triplicate. Assessment of the percentage of relative cytotoxicity was calculated subtracting the background value and normalizing the obtained OD with the protein content (μg of proteins/sample) measured by the BCA assay.

2.10. Catalase Activity. To indirectly assess oxidative stress occurrence, the analysis of the antioxidant enzyme catalase activity was carried out. For this purpose, the Amplex® Red Catalase Assay Kit was used (Molecular Probes, Invitrogen Corporation, CA, USA). Catalase is a heme-containing redox protein which prevents excess of intracellular hydrogen peroxide (H_2O_2) converting this compound to water and oxygen. In the assay, catalase—if working in samples—first reacts with H_2O_2 to produce water and oxygen (O_2). Next, the Amplex Red reagent reacts with a 1 : 1 stoichiometry with any unreacted H_2O_2 in the presence of horseradish peroxidase (HRP) to produce the highly fluorescent oxidation product, resorufin. Therefore, as catalase activity increases, the signal from resorufin decreases. The absorbance was measured at 560 nm in a microplate reader (Multiskan GO, Thermo Scientific, MA, USA). The results are typically plotted by subtracting the observed fluorescence from that of a no-catalase control (complete MEM ALPHA medium and complete medium with DM). Assessment of the relative catalase activity (mU/ml) was calculated using a standard curve generated with specific standards provided by the manufacturers and normalizing the obtained values with the protein content (μg of proteins/sample) measured by the BCA assay.

2.11. RNA Extraction. Total RNA was extracted using TRI Reagent (Sigma-Aldrich, St. Louis, MO). Briefly, cell growth onto Alg/HAp scaffolds was suspended in 500 μl of TRI Reagent and then centrifuged at 10,000 rpm for 10 min at 4°C. The supernatant was added to 100 μl of chloroform, then shaken vigorously, incubated on ice for 15 min, and centrifuged at 13,200 rpm for 20 min at 4°C. RNA in aqueous phase was precipitated with 250 μl of isopropanol, stored for 30 min at −20°C, and pelletted by centrifugation at 13,200 rpm for 20 min at 4°C. RNA pellet was washed with 500 μl of 75% ethanol, air-dried, and finally resuspended in RNAse-free water. In order to avoid the contamination of samples, DNA was removed using a DNA-free kit (Life Technologies, Carlsbad, CA). RNA concentration was determined by spectrophotometer reading at 260 nm, and its purity was assessed by the ratio at 260 and 280 nm readings (BioPhotometer Eppendorf, Hamburg, Germany). Samples were afterwards tested by

| | 7 days | 14 days | 21 days | 28 days |
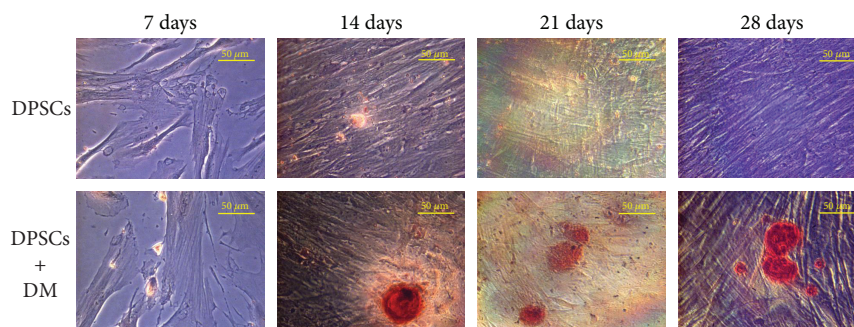
FIGURE 1: Mineralization of dental pulp stem cells (DPSCs) assessed by Alizarin Red staining. The upper panel shows the Alizarin Red staining of pulp cells after 7, 14, 21, and 28 days of culture without differentiation medium (DM). The presence of mineralized nodules in cultures exposed to DM after 7, 14, 21, and 28 days is displayed in the lower panel. Magnification 40x.

electrophoresis through agarose gels and visualized by staining with ethidium bromide, under UV light.

2.12. Reverse Transcription (RT) and Real-Time RT-Polymerase Chain Reaction (Real-Time RT-PCR). In order to reverse-transcribe 1 μg of RNA, a high-capacity cDNA Reverse Transcription Kit (Life Technologies) was used. Twenty microliters of these solutions was stepwise incubated in a 2720 Thermal Cycler (Life Technologies) initially at 25°C for 10 min, then at 37°C for 2 h and finally at 85°C for 5 min. Gene expression was determined by quantitative PCR using TaqMan probe-based chemistry. Reactions were performed in 96-well plates on an ABI PRISM 7900 HT Fast Real-Time PCR System (Life Technologies). TaqMan probes and PCR primers were obtained from Life Technologies (TaqMan Gene Expression Assays (20x): Hs00154192_m1 for BMP2, Hs00231692_m1 for RUNX2, and Hs01866874_s1 for SP7), and glyceraldehyde 3-phosphate dehydrogenase (GAPDH) (Life Technologies, part number 4333764 F) was used as a housekeeping gene. Each amplification reaction was performed with 10 μl of TaqMan Fast Universal PCR Master Mix (2x), No AmpErase UNG (Life Technologies), 1 μl of primer-probe mixture, 1 μl of cDNA, and 8 μl of nuclease-free water. No-template control was used to check for contamination. A reverse transcriptase minus control was included for SP7 gene assay. Thermal cycling conditions were 95°C for 20 s, followed by 40 cycles of amplification at 95°C for 1 s and 60°C for 20 s. Sequence Detection System software, ver. 2.3 (Life Technologies), elaborated gene expression data. The comparative $2^{-\Delta\Delta Ct}$ method was used to quantify the relative abundance of mRNA (relative quantification). Real-time PCR analysis was performed in three independent experiments. In each experiment, we included one cDNA sample for each experimental condition. Amplification was carried out in triplicate for each cDNA sample in relation to each of the investigated genes.

2.13. Immunoblotting. DPSC lysates (20 μg/sample) were electrophoresed on a 4–20% SDS-PAGE gel (ExpressPlus™ 10x8, GenScript Biotech Corporation, China) and transferred to nitrocellulose membranes further blocked in 5% of nonfat milk, 10 mmol/l Tris pH 7.5, 100 mM NaCl, and 0.1% Tween 20. Membranes were then probed for mouse anti-β-actin monoclonal antibody (Sigma-Aldrich, St. Louis, MO, USA) (primary antibody dilution 1 : 10,000) and mouse monoclonal anti-BSP II (Santa Cruz Biotechnology, CA, USA) (primary antibody dilution 1 : 200) and incubated in the presence of specific conjugated IgG horseradish peroxidase. Immunoreactive bands were identified using the ECL detection system (Amersham Int., Buckinghamshire, UK) and analyzed by densitometry. Densitometric values, expressed as the percentage of the integrated optical intensity ratio of BSP II and β-actin, were estimated by the ChemiDoc XRS system using the QuantiOne 1-D analysis software (Bio-Rad, Richmond, CA, USA).

2.14. Statistics. Statistical analysis was performed using the analysis of variance (one-way ANOVA) with post hoc test (Tukey) for RT-PCR analysis and the *t*-test. Results were expressed as mean ± SD. Values of $p < 0.05$ were considered statistically significant.

3. Results

3.1. Formation of Mineralized Nodules in DPSCs Exposed to Differentiation Medium. The production of the extracellular mineralized matrix by DPSCs was evaluated through Alizarin Red S staining. As shown in Figure 1, cells cultured in the presence of differentiation agents (DM) are crowded by a mineralized matrix rich in calcium precipitates stained in red (lower panel), revealing that the generation of calcium precipitates is time-dependent. Quite the opposite, cells from the control group show fewer Alizarin Red-positive regions starting from 7 days of culture up to 28 days (upper panel).

3.2. Alkaline Phosphatase Activity and Collagen Type I Release in DPSCs Exposed to Medium Enriched with Mineralizing Agents. In order to evaluate mineralization occurrence and to confirm Alizarin Red S staining observation, ALP activity was quantified in DPSCs committed to osteogenic differentiation (DPSCs + DM) compared to cells cultivated in normal growth medium (DPSCs) (Figure 2(a)). After 1 day of culture, only a slight difference among DPSCs and DPSCs + DM in terms of ALP activity is detectable (5.33×10^{-4} U/l/min and 4.6×10^{-4} U/l/min, resp.). As far as DPSC culture is concerned, ALP activity decreases

(a)

(b)
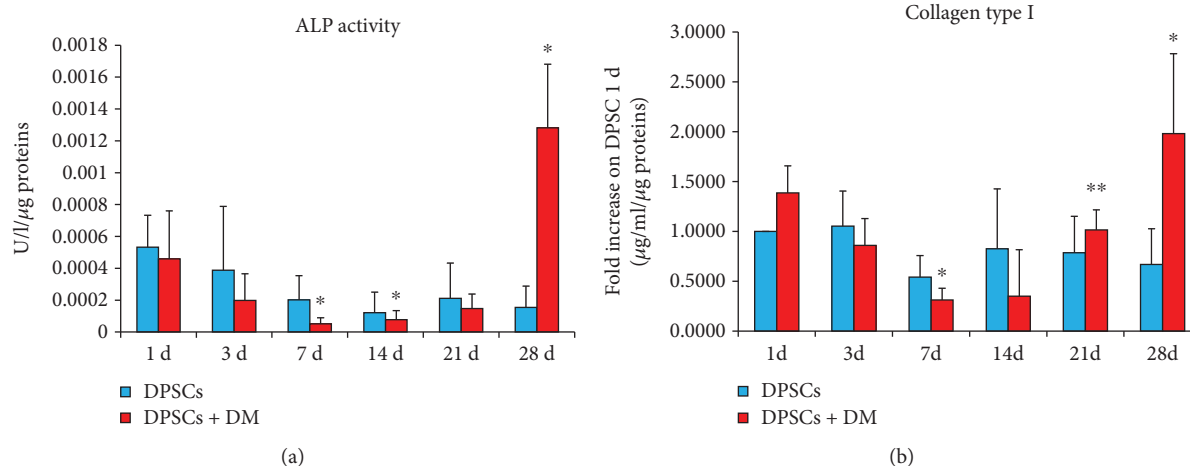
FIGURE 2: Alkaline phosphatase (ALP) activity and collagen type I release in dental pulp stem cells (DPSCs). (a) Bar graph showing the enzymatic activity of ALP (U/ml) normalized on the protein content (μg/sample) after 1, 3, 7, 14, 21, and 28 days of culture. $^*p < 0.05$, 7, 14, and 28 d of DPSCs + DM versus DPSCs. (b) The bar graph represents collagen type I secretion from DPSCs with or without DM after 1, 3, 7, 14, 21, and 28 days of culture. Results are normalized on values obtained from DPSCs cultured for 1 day without DM after being proportioned on the protein content (μg/sample). $^*p < 0.05$ 28 d DPSCs + DM versus DPSCs. $^{**}p < 0.01$ 21 d DPSCs + DM versus DPSCs.

in a time-dependent manner, being assessed at 3.88×10^{-4} U/l/min after 3 days of culture and at 1.54×10^{-4} U/l/min after 28 days. A similar tendency can be observed for DPSCs exposed to DM, being significantly dropped after 7 and 14 days (5.13×10^{-5} U/l/min and 7.75×10^{-5} U/l/min, resp.). Cells exposed to differentiation agents for 28 days produce the highest peak in terms of ALP activity, being significantly increased compared to DPSCs cultivated in normal growth medium (1.28×10^{-3} U/l/min versus 1.54×10^{-4}).

After that, collagen type I secretion was quantified to evaluate the extracellular matrix modifications and the osteogenic commitment (Figure 2(b)). As regard DPSCs cultivated in normal growth medium, after a slight decrease occurred up to 7 days, the levels of secreted collagen type I arise again to the level of the first day of culture. In parallel, cells exposed to differentiation agents show a decrease in collagen type I production reaching the lowest values after 7 and 14 days ($0.311\,\mu$g/ml and $0.349\,\mu$g/ml). After 21 days, this tendency is reversed and the production of collagen type I is significantly higher with respect to the first day of culture ($1.98\,\mu$g/ml).

3.3. Protein Quantification and Cytotoxicity. As a measure of cell seeding efficiency, the BCA assay was performed on the whole cell lysates derived from DPSCs cultivated onto Alg/HAp scaffolds compared to the ones from DPSCs under normal cell conditions with or without differentiation agents (Figure 3(a)). As regards control group (DPSCs), the protein content gradually arises over the time of the experiments, being almost 9-fold augmented after 28 days compared to 1 and 3 days of culture ($315.17\,\mu$g, $36.57\,\mu$g, and $47.40\,\mu$g, resp.). A similar tendency can be observed for DPSCs cultivated in the presence of differentiation agents up to 14 days when the absolute highest protein content is registered ($27.97\,\mu$g, $51.18\,\mu$g, $238.45\,\mu$g, and $251.87\,\mu$g). After that, a slight decrease occurs, with the protein content assessed at

$171.35\,\mu$g after 21 days and at $203.84\,\mu$g after 28 days. Although this fall is significant compared to 14 and 7 days of culture, the amount of proteins remains consistent with respect to early stages (Figure 3(a)). When DPSCs were cultivated onto Alg/HAp scaffolds, the protein pool is significantly reduced compared to DPSCs alone after 1 day of culture ($11.95\,\mu$g and $36.57\,\mu$g, resp.). The shrinkage in terms of protein content can be observed up to 14 days, when the absolute lower value is registered ($7.64\,\mu$g). Surprisingly, a 7-fold increase is detected ($54.61\,\mu$g) after 21 days of culture. Nevertheless, the protein pool is once again lowered after 28 days. A similar tendency can be registered when DPSCs are cultivated onto scaffolds in the presence of differentiation agents (scaffold + DM). For instance, the amount of protein after 21 days, when there is the peak for DPSCs and scaffold, is even lower ($44.57\,\mu$g).

After having monitored cell seeding efficiency by means of protein quantification, the cytotoxicity of Alg/HAp scaffolds on DPSCs was assessed in terms of LDH release (Figure 3(b)). There are no significant changes in the percentage of LDH released from cells exposed to DM or cultivated alone, as the highest peaks for these experimental conditions are assessed at 1.18% after 28 days of culture of DPSCs alone. Quite the opposite, a substantial elevation in the percentage of LDH released can be detected when DPSCs are grown onto Alg/HAp scaffolds. More in detail, the amount of enzyme secreted after 1 day is 11-fold higher than the one released from DPSCs alone (11.06% versus 1.06%). After 3 days of cell culture on the scaffold, this rise is even more enhanced, reaching a 32.7-fold increase if compared to DPSCs alone (26.20% versus 0.80%). After this peak, the percentage of LDH released gradually decreases, being assessed at 0.68% after 21 days of culture (Figure 3(b)). Once again, a rise in terms of LDH release is observed after 28 days of culture (15.57%). A similar progress can be registered when DPSCs are cultivated onto scaffolds in the presence of
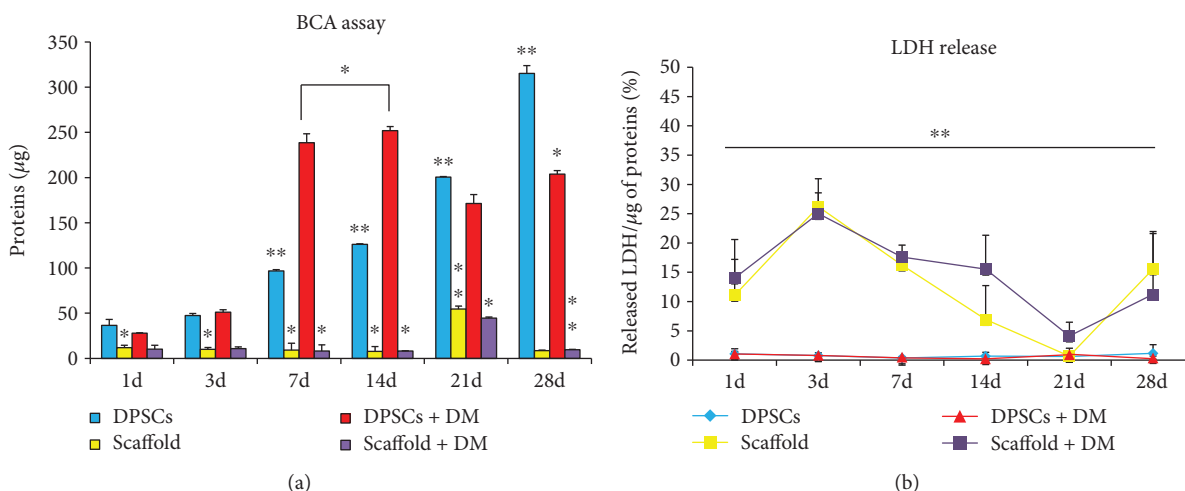
FIGURE 3: Protein content and cytotoxicity assay on dental pulp stem cells (DPSCs) in the presence of alginate/hydroxyapatite scaffolds. (a) The bar graph represents the quantification of protein content (μg/sample) measured by the bicinchoninic acid (BCA) assay of DPSCs in the presence of alginate/hydroxyapatite scaffolds over the different experimental conditions. $^*p < 0.05$ 7, 14, and 28 d DPSCs + DM versus DPSCs; 1, 3, 7, and 14 d scaffold versus DPSCs; 7, 14, and 21 d scaffold + DM versus DPSCs + DM. $^{**}p < 0.01$ 7, 14, 21, and 28 d DPSCs versus 1 d DPSCs; 21 d scaffold versus DPSCs; 28 d scaffold + DM versus scaffold. (b) Lactate dehydrogenase (LDH) released from DPSCs seeded on alginate/hydroxyapatite scaffolds with or without DM. $^{**}p < 0.01$ 1, 3, 7, 14, 21, and 28 d scaffold versus DPSCs; 1, 3, 7, 14, 21, and 28 d scaffold + DM versus DPSCs + DM. Scaffold = DPSC-laden scaffolds; scaffold + DM = DPSC-laden scaffolds in the presence of differentiation medium.

DM, with the exception of the 14 days of culture, when the percentage of LDH is quite higher with respect to DPSCs and scaffold alone (15.52% versus 6.93%).

3.4. Formation of Oxidative Stress. To correlate the elevated cytotoxicity to an oxidative stress occurrence, the activity of catalase was monitored and quantified (Figure 4). When DPSCs are cultured alone, the activity of the antioxidant enzyme gradually decreases, being 27.04 mU/ml after 1 day of culture and 1.31 mU/ml after 28 days. Very likely, when DPSCs are exposed to DM, the activity of catalase lowers with respect to DPSCs without DM up to 14 days of culture. After 21 days of culture in the presence of DM, catalase activity is doubled with respect to DPSCs alone (4.54 mU/ml versus 2.14 mU/ml) and the difference is even more enhanced after 28 days (4.31 mU/ml versus 1.31 mU/ml). Observing catalase activity in DPSCs growth onto scaffolds, a dramatic rise can be detected compared to both DPSCs exposed to DM and DPSCs alone (Figure 4). More in detail, values appear similar as regard 1 and 3 days of culture (38.21 mU/ml and 37.58 mU/ml, resp.). At 7 days of culture onto scaffolds, the absolute highest value of catalase activity is registered (91.12 mU/ml). After that peak, the activity of the enzyme progressively decreases, reaching 24.94 mU/ml after 28 days. When DM is added to the DPSCs/scaffold culture, the tendency results to be very similar to the previous one. The catalase activity after 7 days is slightly lower (87.70 mU/ml) but still consistent compared to DPSCs + DM. As above, the activity of the enzyme lessens, being 21.05 mU/ml after 28 days of culture.

3.5. Gene Expression Profile of Mineralization-Related Markers. To demonstrate that a commitment to mineralization is

established, relative gene expression of BMP2, RUNX2, and SP7 was analyzed by RT-PCR on DPSCs alone and growth onto Alg/HAp scaffolds along with their counterpart exposed to DM (Figure 5). At length, the expression of the early differentiation gene BMP2 (Figure 5(a)) is not significantly changed after 3 days of cell culture in the presence of DM. Notably, there is a consistent elevation of BMP2 when DPSCs are exposed to DM for 7 days. After that, values revert to the ones of the control group. When cells grow onto scaffolds, a significant positive peak is registered after 7 days of culture (1.805 fold increase). As regard DPSCs/scaffold culture + DM, the expression of BMP2 is dramatically increased earlier than 7 days, being elevated already after 1 day of culture and even more after 3 and 7 days (1.357-, 1.402-, and 2.798-fold increase, resp.).

Next, gene expression of RUNX2 was analyzed, which is found expressed here at later stages than BMP2 (Figure 5(b)). For instance, there is a climax after 21 days when DPSCs are grown onto scaffold (1.479-fold increase) with respect to both DPSCs alone and DPSCs + DM. When cells are cultivated in the presence of the scaffold and exposed to DM, two positive pulses of RUNX2 gene expression can be registered. The first one is after 3 days of culture, and the second—more dramatic—is observed after 21 days (1.910- and 3.233-fold increase, resp.).

Finally, the expression of the late differentiation gene SP7 was evaluated. Generally speaking, there are no significant differences up to 21 days of culture. After 28 days, the expression of SP7 is consistently enhanced when DPSCs are cultivated onto scaffolds (1.390-fold increase) and this tendency is even more evident when DM is added to the DPSC/scaffold model (2.272-fold increase).
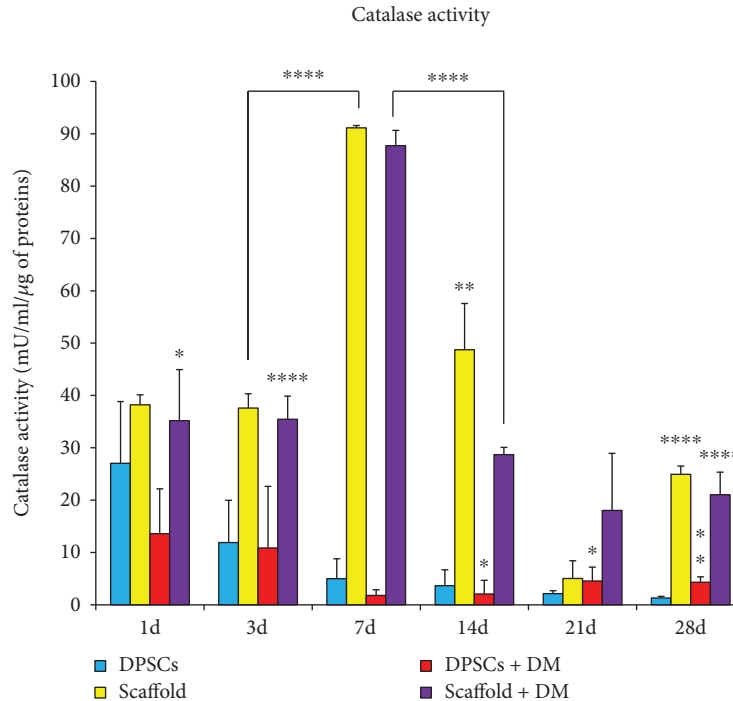
Catalase activity

FIGURE 4: Catalase activity of dental pulp stem cells (DPSCs) in the presence of alginate/hydroxyapatite scaffolds. Bars display the modulation of catalase activity (mU/ml) normalized on the protein content (μg/sample) of DPSCs over the different experimental conditions. $^*p < 0.05$ 14 and 21 d DPSCs + DM versus DPSCs; 1 d scaffold + DM versus DPSCs + DM. $^{**}p < 0.01$ 28 d DPSCs + DM versus DPSCs; 14 d scaffold versus DPSCs. $^{****}p < 0.005$ 14 d scaffold + DM versus scaffold; 3, 7, and 28 d scaffold versus DPSCs; 3, 7, 14, and 28 d scaffold + DM versus DPSCs + DM. Scaffold = DPSC-laden scaffolds; scaffold + DM = DPSC-laden scaffolds in the presence of differentiation medium.

3.6. ALP Activity and Collagen Type I Release in DPSC Growth onto Alg/HAp Scaffolds. Finally, to further confirm DPSCs' osteogenic commitment when cultured onto Alg/HAp scaffolds in the presence or not of DM, the activity of ALP and the release of collagen type I were monitored (Figure 6). The presence of DM does not influence ALP activity after 1 day of culture, with U/l/min being very similar to the one of DPSCs on scaffold alone (Figure 6(a)). A positive peak can be observed when DPSCs are cultured onto scaffolds for 3 days. As deduced from the bar graph, this is the highest absolute value registered, being assessed at 0.0493 U/l/min. When DM is added to the culture, ALP activity slightly lowers, but remaining consistent (0.0401 U/l/min). After 7, 14, and 21 days of culture, there are only weak fluctuations of ALP activity, while it is quite elevated after 28 days when DPSCs are cultured onto scaffolds without DM.

In parallel, the concentration of collagen type I in cell supernatants was evaluated comparing all the values to the concentration after 1 day of culture of DPSCs on scaffold without DM (Figure 6(b)). A time-dependent concentration increase can be detected for DPSC growth onto scaffolds, with the release of collagen 1.32-fold higher after 3 days and 6.50-fold higher after 28 days with respect to 1 day of culture. Very likely but even more consistently, the secretion of collagen type I when DPSCs are grown onto scaffolds in the presence of DM is time-dependently increased. Indeed, the release of collagen after 28 days is 13-fold higher if compared to the one after 3 days (3.01-fold versus 39.46-fold, resp.).

3.7. BSP II Expression in DPSCs Seeded on HAp/Alg Scaffolds. To confirm the osteogenic differentiation of DPSCs grown onto scaffolds in the presence or not of DM, the expression of the noncollagenous protein BSP II, implied in the regulation of bone mineralization, was analyzed by means of Western blotting. Densitometric values show a peak after 7 days of culture, registering a significant increased value when DPSCs are grown onto scaffolds without DM (Figure 7). After that, BSP II is notably expressed after 21 and 28 days when the DM is present.

4. Discussion

DPSCs isolated from human postnatal dental pulp tissues can give rise to multilineage differentiation *in vitro* and generate related mineralized tissues *in vivo* [27]. Bone and dentine extracellular matrix proteins are similar, consisting primarily of type I collagen, acidic proteins, and proteoglycans. Although collagen forms the lattice for deposition of calcium and phosphate assisting formation of carbonate apatite, noncollagenous proteins are believed to control initiation and growth of the crystals [28]. For this purpose, Alizarin Red S staining was carried out on our system. More in detail, DPSCs cultured on polystyrene exposed to medium enriched by differentiation agents show calcium nodule deposition from 7 days of culture compared to cells from the control group (Figure 1). The dimension of calcium nodules arises in a time-dependent manner in DPSCs cultured in the presence of DM with
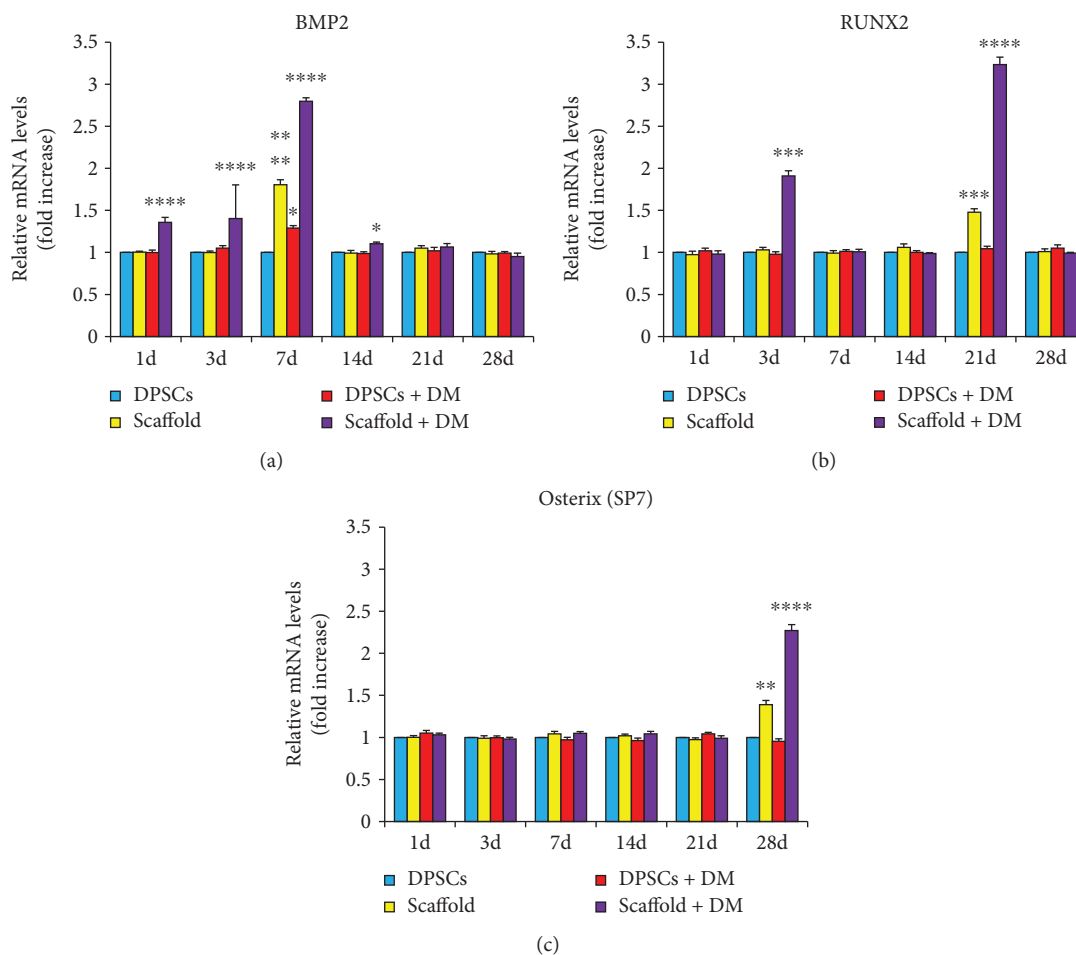
FIGURE 5: Gene expression profiles of differentiation- and mineralization-associated marker genes in dental pulp stem cells (DPSCs) in the presence of alginate/hydroxyapatite scaffolds. Graphs represent the relative gene expression of BMP2 (a), RUNX2 (b), and Osterix (SP7) (c) in DPSCs over the various experimental conditions. Data are expressed as fold increase on relative mRNA levels of DPSCs cultivated in growth medium not enriched with differentiation agents. (a) $^*p < 0.05$ 14 d scaffold + DM versus DPSCs; 7 d DPSCs + DM versus DPSCs. $^{****}p < 0.001$ 7 d scaffold versus DPSCs; 1, 3, and 7 d scaffold + DM versus DPSCs. (b) $^{***}p < 0.005$ 21 d scaffold versus DPSCs; 3 and 21 d scaffold + DM versus DPSCs. (c) $^{**}p < 0.01$ 28 d scaffold versus DPSCs. $^{****}p < 0.001$ scaffold + DM versus DPSCs. Scaffold = DPSC-laden scaffolds; scaffold + DM = DPSC-laden scaffolds in the presence of differentiation medium.

respect to DPSCs' growth in normal medium. In parallel, we evaluated ALP activity and secretion of collagen type I in the same experimental conditions. Despite different fluctuations, both parameters increased at late stages of culture, for instance, at 28 days. This is coherent with previous studies and literature [29], and the authors of the present work are quite confident on the functionality of the experimental system in committing cells to mineralized matrix deposition.

For most regenerative strategies, an organic scaffold is used to provide a surface on which cells may adhere, grow, and spatially organize [30]. In the present paper, a 3D biodegradable porous scaffold prepared from a binary mixture composed by alginate and HAp was used. DPSCs have to interpenetrate this porous structure and proliferate to give birth to newly produced mineralized tissue. Due to the difficult handling of this experimental 3D cell culture and the difficulty in obtaining data on cell seeding efficiency and viability with classical and commercially available assays,

we measured the amount of proteins to indirectly evaluate DPSC attachment and interpolation into scaffolds. Not surprisingly, DPSCs better adhered on polystyrene, with the amount of proteins increased over the time of the culture. In the DPSC/scaffold system, an increment in the amount of protein was consistent after 21 days. In parallel, the protein pool was slightly lowered when DM is added. This let us speculate that DPSCs were more proliferating on scaffolds alone. Next, to evaluate the cytotoxic response of DPSCs on Alg/HAp scaffolds, the LDH assay was carried out. Observing in parallel the amount of proteins and the release of LDH, it is plausible to assume that nonproliferating DPSCs in the presence of scaffolds fit on necrotic cell death, especially after 3 days of culture. Quite the opposite, the LDH release, which gradually lowered from 7 days up to 21 days, let us hypothesize a compensatory mechanism. Data on LDH release agreed with the rise in protein amount at 21 days, when the release of LDH is very low and very close to the one of the control group (Figure 3). The hypothesized compensatory

(a)

(b)
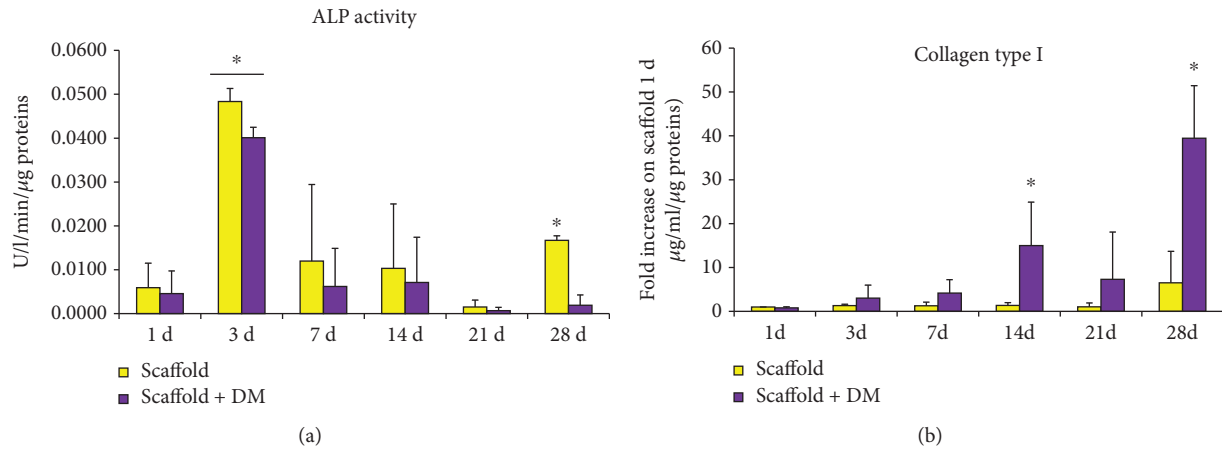
FIGURE 6: Alkaline phosphatase (ALP) activity and collagen type I release in dental pulp stem cells (DPSCs) in the presence of alginate/ hydroxyapatite scaffolds. (a) Bar graph showing the enzymatic activity of ALP (U/ml) normalized on the protein content (μg/sample) after 1, 3, 7, 14, 21, and 28 days of culture of DPSC growth onto scaffolds. $^*p < 0.05$ 3 and 28 d scaffold versus 1 d scaffold; 3 d scaffold + DM versus 1 d scaffold + DM. (b) The bar graph represents collagen type I secretion from DPSCs cultured on scaffolds with or without DM after 1, 3, 7, 14, 21, and 28 days. Results are normalized on values obtained from DPSCs cultured on scaffolds for 1 day without DM after being proportioned on the protein content (μg/sample). $^*p < 0.05$ 14 and 28 d scaffold + DM versus scaffold and scaffold + DM. Scaffold = DPSC-laden scaffolds; scaffold + DM = DPSC-laden scaffolds in the presence of differentiation medium.
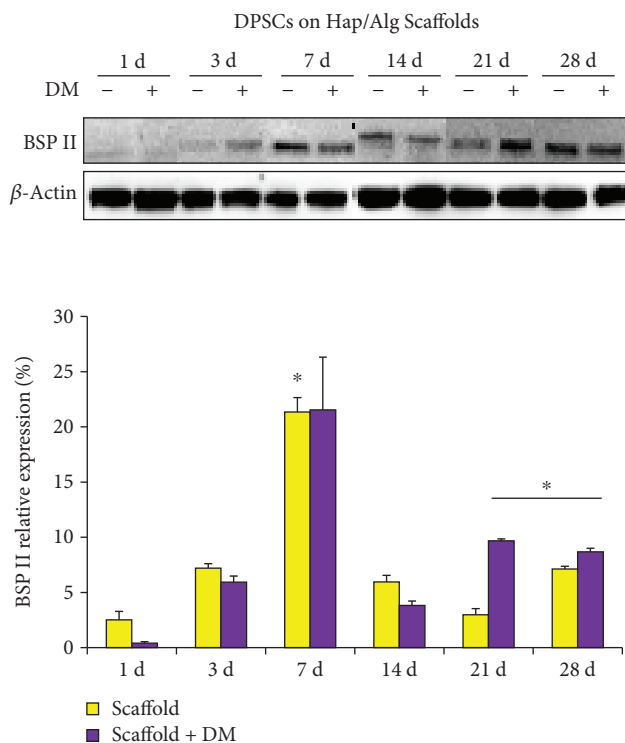
FIGURE 7: Bone sialoprotein II (BSP II) protein expression in dental pulp stem cells (DPSCs) in the presence of alginate/ hydroxyapatite scaffolds by Western blotting analysis. Graph represents densitometric values (%) of BSP II expression normalized on β-actin expression. $^*p < 0.05$ 7 days scaffold versus 1 day scaffold; $^*p < 0.05$ 21 and 28 days scaffold + DM versus 1 day scaffold + DM. Scaffold = DPSC-laden scaffolds; scaffold + DM = DPSC-laden scaffolds in the presence of differentiation medium.

mechanism seems to default after 28 days in the same experimental conditions when a rise of LDH released and a decrease in the protein amount is registered. Most relevantly, DM seems to even enhance the reduction of the protein amount and rise of LDH release as evidenced by bar and trend graphs after 14 days of culture.

Hydrogen peroxide scavenging is governed by catalase, which is the enzyme that converts H_2O_2 in H_2O and O_2 [31]. To correlate the dramatic LDH release from DPSCs cultured onto scaffolds for 3 days and the recovering of the system after 7 days and on, we evaluated the activity of the antioxidant enzyme catalase (Figure 4). As shown by the bar graph, oxidative stress was not occurring in both DPSCs from the control group and the one exposed to DM, with the activity of catalase being physiologically compatible. On the other way round, the activity of catalase in DPSCs cultivated on Alg/HAp scaffolds was consistent already from early stages. Indeed, after 7 days, the highest absolute value is registered, making plausible the hypothesis that DPSCs produced a large amount of H_2O_2 when growing onto scaffolds. To counteract oxidative stress occurrence, cells respond by activating antioxidant molecules; among them, catalase is one of the terminal regulators [32]. Redox homeostasis is crucial for osteogenic commitment, differentiation, and cell survival [23]. Likewise, here DPSCs escaped from necrotic cell death, through the activation of catalase, as evidenced by the decrement of LDH released and the massive increase of catalase activity after 7 days (Figures 3 and 4).

The tissue engineering goal is not only cell proliferation and the lack of cell cytotoxic responses against the foreign material, but overall the production of newly born tissues and then stem cell commitment to osteogenic differentiation. Data from literature has demonstrated that seven days after H_2O_2 treatment, DPSCs showed significant reduction

in ALP activity compared with negative control and no mineralized nodule deposition [34]. Hence, the evaluation of the gene profile of mineralization-related markers was mandatory. We therefore analyzed the expression of BMP2, RUNX2, and Osterix (SP7). The gene expression of BMP2 is recognized to stimulate mineralization, and it is considered the most osteogenic bone morphogenetic protein which implies the early induction of differentiation [35]. RUNX2 is an important transcriptional modulator of differentiation, maturation, and homeostasis, downstream from the BMP2 differentiation pathway [36]. In turn, Osterix (SP7) is a transcription factor which plays a pivotal role during the differentiation of progenitors into mature cells in a step downstream of RUNX2 [37]. In our system, expression of early, intermediate, and late differentiation markers is consistent with data in literature [22]. More in detail, BMP2 expression increased after 3 and 7 days in DPSCs cultured on scaffolds indifferently from the presence of DM, in accordance with data of catalase activity. Beside a spike after 3 days, RUNX2 was enhanced after 21 days mostly when DM is present, in agreement with LDH release after the same experimental time. As regards Osterix gene expression, it was clearly increased after 28 days mainly in DPSCs/ scaffolds + DM, when the LDH amount was slightly decreased with respect to scaffolds alone (Figure 5). Several studies have reported the synthesis of many scaffolds capable of sustaining pulp stem cell differentiation in vitro in the presence of differentiation media, but only two of them, namely, a polyvinyl alcohol- (PVA-) poly(ε) caprolactone- (PCL-) hydroxyapatite-based bioceramic [38] and a calcium phosphate cement scaffold loaded with iron oxide nanoparticles [39], have been found to enhance cell differentiation compared to cell monolayers cultured on polystyrene due to the osteoinductive property of the material.

To confirm if DPSC enhanced mineralization when cultured on Alg/HAp scaffolds, we reevaluated ALP activity and collagen type I secretion. Data supported gene expression results, with ALP activity being strongly enhanced after 3 days of culture where DM was not influencing the activity of the enzyme. This tendency was similar over the experimental time, up to 28 days of culture (Figure 6(a)). Conversely, the release of collagen type I seemed to be consistently influenced by DM as shown in Figure 6(b). It is plausible to assume that this enhancement could be ascribed to the presence of ascorbic acid present in the DM medium. This is in agreement with data on literature which correlates the release of collagen and extracellular matrix deposition with exposures to ascorbate [40]. Finally, to strengthen DPSC's ability to differentiate into osteoblast-like cells, the expression of BSP II was analyzed. Among all, the dentin-bone noncollagenous proteins consist in small integrin-binding ligand N-linked glycoproteins (SIBLINGs). SIBLINGs are secreted during the formation and mineralization of both dentin and bone, and BSP is a highly posttranslationally modified protein that is an abundant noncollagenous component of the bone matrix. Moreover, in situ hybridization and immunolocalization experiments have shown that BSP is expressed in teeth during mineralization [41–43]. Our data show that BSP II is highly expressed after 7, 21, and 28 days on DPSCs grown onto scaffolds in the presence of DM in line with PCR results.

In summary, we provide evidence for osteoconductivity of alginate/hydroxyapatite scaffolds that are able of efficiently sustaining adhesion, colonization, and matrix deposition of osteoblast-like cells. [1]. We show that DPSCs express mineralization-related markers and proteins, definitely promoting matrix deposition. Most importantly, this physiological function is here related to redox homeostasis controlled by the activation of catalase which as an enzymatic antioxidant enhances cell survival.

4.1. Limitations of the Study. Although the cellular response towards oxidative stress is driven by a multidimensional network of transcription factors and enzymes and the measurement of catalase activity is only one aspect of the molecular scenario occurring intracellularly, catalase plays a crucial role in adaptive response to H_2O_2 and it has been suggested that its role is somehow auxiliary to that of glutathione peroxidase [33]. Furthermore, the differentiation of osteoblasts implies the formation of an extracellular matrix, which is rich in proteins. Due to the difficulty in the experimental design, in the handling of the three-dimensional cell culture and the specific properties of the material, to normalize ELISA and LDH results with the amount of proteins was the only appropriate experimental procedure because any other proliferation assays are not feasible.

Data Availability

The data used to support the findings of this study are available from the corresponding author upon request.

Conflicts of Interest

The authors declare that they have no conflicts of interest.

Authors' Contributions

Silvia Sancilio and Marialucia Gallorini contributed equally to the work.

Acknowledgments

Supplementary Materials

S1. DPSC immunophenotyping: data reported show the representative immunophenotype profile of DPSCs isolated from the third molar at passage 4. Cells were found negative for the lymphocyte-related CD45 (protein tyrosine phosphatase) and slightly positive for SSEA4 (stage-specific embryonic

antigen 4), while they significantly express CD90 (Thy-1), CD73 ($5'$ nucleotidase), CD29 (integrin $\beta1$), and CD105 (endoglin), thus identifying a mesenchymal stem cell population. *(Supplementary Materials)*

References

[1] G. Turco, E. Marsich, F. Bellomo et al., "Alginate/hydroxyapatite biocomposite for bone ingrowth: a trabecular structure with high and isotropic connectivity," *Biomacromolecules*, vol. 10, no. 6, pp. 1575–1583, 2009.

[2] J. Venkatesan, I. Bhatnagar, P. Manivasagan, K. H. Kang, and S. K. Kim, "Alginate composites for bone tissue engineering: a review," *International Journal of Biological Macromolecules*, vol. 72, pp. 269–281, 2015.

[3] H. H. Jin, D. H. Kim, T. W. Kim et al., "In vivo evaluation of porous hydroxyapatite/chitosan-alginate composite scaffolds for bone tissue engineering," *International Journal of Biological Macromolecules*, vol. 51, no. 5, pp. 1079–1085, 2012.

[4] T. Gong, B. C. Heng, E. C. M. Lo, and C. Zhang, "Current advance and future prospects of tissue engineering approach to dentin/pulp regenerative therapy," *Stem Cells International*, vol. 2016, Article ID 9204574, 13 pages, 2016.

[5] L. E. Niklason, "Engineering of bone grafts," *Nature Biotechnology*, vol. 18, no. 9, pp. 929-930, 2000.

[6] O. Smidsrød, A. Haug, B. Larsen et al., "The influence of pH on the rate of hydrolysis of acidic polysaccharides," *Acta Chemica Scandinavica*, vol. 20, no. 4, pp. 1026–1034, 1966.

[7] H. Oguchi, K. Ishikawa, K. Mizoue, K. Seto, and G. Eguchi, "Long-term histological evaluation of hydroxyapatite ceramics in humans," *Biomaterials*, vol. 16, no. 1, pp. 33–38, 1995.

[8] K. M. Tohamy, M. Mabrouk, I. E. Soliman, H. H. Beherei, and M. A. Aboelnasr, "Novel alginate/hydroxyethyl cellulose/hydroxyapatite composite scaffold for bone regeneration: In vitro cell viability and proliferation of human mesenchymal stem cells," *International Journal of Biological Macromolecules*, vol. 112, pp. 448–460, 2018.

[9] V. V. Hiew, S. F. B. Simat, and P. L. Teoh, "The advancement of biomaterials in regulating stem cell fate," *Stem Cell Reviews and Reports*, vol. 14, no. 1, pp. 43–57, 2018.

[10] D. Macrin, J. P. Joseph, A. A. Pillai, and A. Devi, "Eminent sources of adult mesenchymal stem cells and their therapeutic imminence," *Stem Cell Reviews and Reports*, vol. 13, no. 6, pp. 741–756, 2017.

[11] I. Mortada, R. Mortada, and M. al Bazzal, "Dental pulp stem cells and the management of neurological diseases: an update," *Journal of Neuroscience Research*, vol. 96, no. 2, pp. 265–272, 2018.

[12] P. Stanko, K. Kaiserova, V. Altanerova, and C. Altaner, "Comparison of human mesenchymal stem cells derived from dental pulp, bone marrow, adipose tissue, and umbilical cord tissue by gene expression," *Biomedical Papers*, vol. 158, no. 3, pp. 373–377, 2014.

[13] J. Wang, X. Liu, X. Jin et al., "The odontogenic differentiation of human dental pulp stem cells on nanofibrous poly (L-lactic acid) scaffolds in vitro and in vivo," *Acta Biomaterialia*, vol. 6, no. 10, pp. 3856–3863, 2010.

[14] A. Almushayt, K. Narayanan, A. E. Zaki, and A. George, "Dentin matrix protein 1 induces cytodifferentiation of dental pulp stem cells into odontoblasts," *Gene Therapy*, vol. 13, no. 7, pp. 611–620, 2006.

[15] H. Egusa, W. Sonoyama, M. Nishimura, I. Atsuta, and K. Akiyama, "Stem cells in dentistry – part I: stem cell sources," *Journal of Prosthodontic Research*, vol. 56, no. 3, pp. 151–165, 2012.

[16] E. P. Chalisserry, S. Y. Nam, S. H. Park, and S. Anil, "Therapeutic potential of dental stem cells," *Journal of Tissue Engineering*, vol. 8, 2017.

[17] S. Toosi, N. Behravan, and J. Behravan, "Nonunion fractures, mesenchymal stem cells and bone tissue engineering," *Journal of Biomedical Materials Research Part A*, 2018.

[18] Y. Gu, Y. Bai, and D. Zhang, "Osteogenic stimulation of human dental pulp stem cells with a novel gelatin-hydroxyapatite-tricalcium phosphate scaffold," *Journal of Biomedical Materials Research Part A*, vol. 106, no. 7, pp. 1851–1861, 2018.

[19] K. Nakajima, R. Kunimatsu, K. Ando et al., "Comparison of the bone regeneration ability between stem cells from human exfoliated deciduous teeth, human dental pulp stem cells and human bone marrow mesenchymal stem cells," *Biochemical and Biophysical Research Communications*, vol. 497, no. 3, pp. 876–882, 2018.

[20] N. Wongsupa, T. Nuntanaranont, S. Kamolmattayakul, and N. Thuaksuban, "Assessment of bone regeneration of a tissue-engineered bone complex using human dental pulp stem cells/poly(ε-caprolactone)-biphasic calcium phosphate scaffold constructs in rabbit calvarial defects," *Journal of Materials Science: Materials in Medicine*, vol. 28, no. 5, p. 77, 2017.

[21] S. Gronthos, M. Mankani, J. Brahim, P. G. Robey, and S. Shi, "Postnatal human dental pulp stem cells (DPSCs) in vitro and in vivo," *Proceedings of the National Academy of Sciences*, vol. 97, no. 25, pp. 13625–13630, 2000.

[22] M. Radunovic, M. De Colli, P. De Marco et al., "Graphene oxide enrichment of collagen membranes improves DPSCs differentiation and controls inflammation occurrence," *Journal of Biomedical Materials Research Part A*, vol. 105, no. 8, pp. 2312–2320, 2017.

[23] F. Atashi, A. Modarressi, and M. S. Pepper, "The role of reactive oxygen species in mesenchymal stem cell adipogenic and osteogenic differentiation: a review," *Stem Cells and Development*, vol. 24, no. 10, pp. 1150–1163, 2015.

[24] Q. Li, Z. Gao, Y. Chen, and M. X. Guan, "The role of mitochondria in osteogenic, adipogenic and chondrogenic differentiation of mesenchymal stem cells," *Protein & Cell*, vol. 8, no. 6, pp. 439–445, 2017.

[25] O. G. Davies, P. R. Cooper, R. M. Shelton, A. J. Smith, and B. A. Scheven, "A comparison of the in vitro mineralisation and dentinogenic potential of mesenchymal stem cells derived from adipose tissue, bone marrow and dental pulp," *Journal of Bone and Mineral Metabolism*, vol. 33, no. 4, pp. 371–382, 2015.

[26] M. D. Colli, M. Radunovic, V. L. Zizzari et al., "Osteoblastic differentiating potential of dental pulp stem cells in vitro cultured on a chemically modified microrough titanium surface," *Dental Materials Journal*, vol. 37, no. 2, pp. 197–205, 2018.

[27] M. Lei, K. Li, B. Li, L. N. Gao, F. M. Chen, and Y. Jin, "Mesenchymal stem cell characteristics of dental pulp and periodontal ligament stem cells after in vivo transplantation," *Biomaterials*, vol. 35, no. 24, pp. 6332–6343, 2014.

[28] W. T. Butler, H. H. Ritchie, and A. L. J. J. Bronckers, *Extracellular Matrix Proteins of Dentine*, Novartis Foundation Symposia, 1997.

[29] H. S. Ching, N. Luddin, I. A. Rahman, and K. T. Ponnuraj, "Expression of odontogenic and osteogenic markers in DPSCs and SHED: a review," *Current Stem Cell Research & Therapy*, vol. 12, no. 1, pp. 71–79, 2017.

[30] K. M. Galler, R. N. D'Souza, J. D. Hartgerink, and G. Schmalz, "Scaffolds for dental pulp tissue engineering," *Advances in Dental Research*, vol. 23, no. 3, pp. 333–339, 2011.

[31] F. Ahmadinejad, S. Geir Møller, M. Hashemzadeh-Chaleshtori, G. Bidkhori, and M. S. Jami, "Molecular mechanisms behind free radical scavengers function against oxidative stress," *Antioxidants*, vol. 6, no. 3, 2017.

[32] M. Gallorini, C. Petzel, C. Bolay et al., "Activation of the Nrf2-regulated antioxidant cell response inhibits HEMA-induced oxidative stress and supports cell viability," *Biomaterials*, vol. 56, pp. 114–128, 2015.

[33] H. Sepasi Tehrani and A. A. Moosavi-Movahedi, "Catalase and its mysteries," *Progress in Biophysics and Molecular Biology*, 2018.

[34] D. G. Soares, F. Gonçalves Basso, J. Hebling, and C. A. de Souza Costa, "Effect of hydrogen-peroxide-mediated oxidative stress on human dental pulp cells," *Journal of Dentistry*, vol. 43, no. 6, pp. 750–756, 2015.

[35] D. L. Cochran and J. M. Wozney, "Biological mediators for periodontal regeneration," *Periodontology 2000*, vol. 19, no. 1, pp. 40–58, 1999.

[36] S. Vimalraj, B. Arumugam, P. J. Miranda, and N. Selvamurugan, "Runx 2: structure, function, and phosphorylation in osteoblast differentiation," *International Journal of Biological Macromolecules*, vol. 78, pp. 202–208, 2015.

[37] K. Nakashima, X. Zhou, G. Kunkel et al., "The novel zinc finger-containing transcription factor osterix is required for osteoblast differentiation and bone formation," *Cell*, vol. 108, no. 1, pp. 17–29, 2002.

[38] R. D. Prabha, D. C. E. Kraft, L. Harkness et al., "Bioactive nano-fibrous scaffold for vascularized craniofacial bone regeneration," *Journal of Tissue Engineering and Regenerative Medicine*, vol. 12, no. 3, pp. e1537–e1548, 2018.

[39] Y. Xia, H. Chen, F. Zhang et al., "Injectable calcium phosphate scaffold with iron oxide nanoparticles to enhance osteogenesis via dental pulp stem cells," *Artificial Cells, Nanomedicine, and Biotechnology*, pp. 1–11, 2018.

[40] V. di Giacomo, M. Berardocco, M. Gallorini et al., "Combined supplementation of ascorbic acid and thyroid hormone T3 affects tenocyte proliferation. The effect of ascorbic acid in the production of nitric oxide," *Muscle, Ligaments and Tendons Journal*, vol. 7, no. 1, pp. 11–18, 2017.

[41] M. MacDougall, J. Dong, and A. C. Acevedo, "Molecular basis of human dentin diseases," *American Journal of Medical Genetics Part A*, vol. 140A, no. 23, pp. 2536–2546, 2006.

[42] J. Chen, H. S. Shapiro, and J. Sodek, "Developmental expression of bone sialoprotein mRNA in rat mineralized connective tissues," *Journal of Bone and Mineral Research*, vol. 7, no. 8, pp. 987–997, 1992.

[43] J. Chen, C. A. G. McCulloch, and J. Sodek, "Bone sialoprotein in developing porcine dental tissues: cellular expression and comparison of tissue localization with osteopontin and osteonectin," *Archives of Oral Biology*, vol. 38, no. 3, pp. 241–249, 1993.

Research Article

Bidirectional Transcriptome Analysis of Rat Bone Marrow-Derived Mesenchymal Stem Cells and Activated Microglia in an *In Vitro* Coculture System

Da Yeon Lee,[1] Moon Suk Jin,[1] Balachandran Manavalan,[1] Hak Kyun Kim,[2] Jun Hyeok Song,[2] Tae Hwan Shin [iD],[1,3] and Gwang Lee [iD][1,3]

[1]Department of Physiology and Department of Biomedical Sciences, Ajou University School of Medicine, Suwon, Republic of Korea
[2]Ajou University School of Medicine, Suwon, Republic of Korea
[3]Institute of Molecular Science and Technology, Ajou University, Suwon, Republic of Korea

Correspondence should be addressed to Tae Hwan Shin; catholicon@ajou.ac.kr and Gwang Lee; glee@ajou.ac.kr

Academic Editor: Jane Ru Choi

Microglia contribute to the regulation of neuroinflammation and play an important role in the pathogenesis of brain diseases. Thus, regulation of neuroinflammation triggered by activated microglia in brain diseases has become a promising curative strategy. Bone marrow-derived mesenchymal stem cells (BM-MSCs) have been shown to have therapeutic effects, resulting from the regulation of inflammatory conditions in the brain. In this study, we investigated differential gene expression in rat BM-MSCs (rBM-MSCs) that were cocultured with lipopolysaccharide- (LPS-) stimulated primary rat microglia using microarray analysis and evaluated the functional relationships through Ingenuity Pathway Analysis (IPA). We also evaluated the effects of rBM-MSC on LPS-stimulated microglia using a reverse coculture system and the same conditions of the transcriptomic analysis. In the transcriptome of rBM-MSCs, 67 genes were differentially expressed, which were highly related with migration of cells, compared to control. The prediction of the gene network using IPA and experimental validation showed that LPS-stimulated primary rat microglia increase the migration of rBM-MSCs. Reversely, expression patterns of the transcriptome in LPS-stimulated primary rat microglia were changed when cocultured with rBM-MSCs. Our results showed that 65 genes were changed, which were highly related with inflammatory response, compared to absence of rBM-MSCs. In the same way with the aforementioned, the prediction of the gene network and experimental validation showed that rBM-MSCs decrease the inflammatory response of LPS-stimulated primary rat microglia. Our data indicate that LPS-stimulated microglia increase the migration of rBM-MSCs and that rBM-MSCs reduce the inflammatory activity in LPS-stimulated microglia. The results of this study show complex mechanisms underlying the interaction between rBM-MSCs and activated microglia and may be helpful for the development of stem cell-based strategies for brain diseases.

1. Introduction

Microglia are resident immune cells of the brain that participate in various physiological functions, such as pruning, regulating plasticity, and neurogenesis, to maintain homeostasis [1]. Multibranched resting microglia exist in a quiescent state in healthy conditions; however, upon sensing a disturbance in homeostasis, microglia become more rounded and amoeboid-shaped and increase phagocytosis and secretion of proinflammatory cytokines [2]. Activated microglia induce inflammatory environments that are related to neurological diseases such as neurodegenerative disorders, multiple sclerosis (MS), stroke, and neuropathic pain disease [3–6].

Regulation of microglia-mediated inflammation has been considered a therapeutic strategy in brain diseases. Several anti-inflammatory drugs such as glucocorticoids, minocycline, endocannabinoids, and nonsteroidal anti-inflammatory

drugs are effective in controlling microglial activation and exert neuroprotective effects in the brain following different types of injuries and neurodegenerative diseases [7, 8]. Although several drugs reduce the symptoms of brain diseases, they are frequently associated with side effects [9, 10]. For the last two decades, the ability of bone marrow-derived mesenchymal stem cells (BM-MSCs) to reduce symptoms of brain diseases such as stroke, Parkinson's disease, and multiple system atrophy has been investigated [11–14].

In addition, BM-MSCs have a therapeutic effect owing to their ability to downregulate inflammatory conditions in the brain [12, 15, 16]. Particularly, the immunomodulatory properties of BM-MSCs play an important role in the treatment of inflammatory diseases, including neurodegenerative disorders. Importantly, this immunomodulatory capacity is highly plastic in response to complex changes in the inflammatory niche. Given the dynamic inflammation in neurodegenerative diseases, BM-MSC-mediated immunomodulation in cell therapy for these diseases deserves more attention [17].

Although many studies have reported the effects of BM-MSC transplantation in animal models of brain disease in reducing neuroinflammation induced by microglia [15, 18, 19], the underlying mechanisms of BM-MSCs in targeting microglia-mediated neuroinflammation and the cellular network of activated microglia are still unclear. In addition, even though mutual reactions between BM-MSC and activated microglia were investigated *in vitro* [20], their interactions were analysed in targeted approaches with limitations to elucidate the corresponding mechanisms. In this study, we evaluated the relationship between rat bone marrow-derived mesenchymal stem cells (rBM-MSCs) and activated microglia using bidirectional transcriptomic analysis.

2. Materials and Methods

2.1. Isolation and Maintenance of rBM-MSCs. rBM-MSCs were isolated from 8–12-week-old Sprague Dawley (SD) rats and characterised as previously described [21]. Briefly, cells were isolated from the tibias and femurs and separated using 80% Percoll gradient centrifugation at 1300 rpm for 10 min at RT. Cells in the low-density fraction were washed with Dulbecco's modified Eagle's medium (DMEM; Gibco, USA) supplemented with 10% foetal bovine serum (FBS), 100 U/mL penicillin, and 100 μg/mL streptomycin sulphate (HyClone, USA). Next, 1.6×10^5 cells were seeded onto 10 cm culture dishes (SPL, South Korea) containing a control medium and cultured as adherent cells in a humidified chamber at 5% CO_2 and 37°C for 3–4 weeks. The media was replenished every 3 days. Upon reaching a confluence of 70–80%, cells were subcultured at a ratio of 1 : 4 for up to four passages. We characterised with anti-CD34 monoclonal antibody as negative control and anti-CD29 and CD44 antibodies as positive marker for the characterisation of rBM-MSCs from SD rat. rBM-MSC was highly stained with only positive markers (data not shown), which is consistent with previous report [21].

2.2. Rat Microglia Primary Cultures. Microglial primary cultures were obtained from the midbrain of one-day-old Sprague Dawley (SD) rat pups purchased from Nara Bio (Gyeonggi, South Korea). Briefly, mid-brain tissues were isolated from rat pups and rinsed with minimum essential medium (MEM; HyClone, USA) containing 10% FBS, 100 U/mL penicillin, and 100 μg/mL streptomycin sulphate (HyClone, USA). Tissues were mechanically dissociated, and the cells were plated in 10 cm culture dishes (SPL, South Korea). After 13–15 days, the microglia were detached from the flasks and applied to a nylon mesh to remove astrocytes. The collected microglia were cultured in control media in a humidified chamber at 5% CO_2 and 37°C. Microglia were trypsinized and washed twice with PBS and fixed in Cytofix buffer (BD, USA) for 30 min at room temperature. Cells were incubated 1 h at room temperature with anti-Iba1 mouse monoclonal antibody (1 : 100, Santa Cruz Biotechnology, USA) for characterisation of microglia. Cells were washed twice with PBS and incubated with FITC-conjugated anti-mouse goat antibody (1 : 100, Vector Laboratories, USA) in PBS for 1 h in ice. After washing twice with PBS, labeled cells were analysed by a flow cytometer (FACS Aria II™, BD, USA). Cells showed high expression (~86.5%) of positive marker (Supplementary Figure 1).

2.3. Coculture of LPS-Stimulated or Nonstimulated Microglia and rBM-MSCs. To evaluate the effects of LPS-stimulated microglia on rBM-MSCs and of rBM-MSCs on LPS-stimulated microglia, we used a Costar transwell system as previously reported [15], which consists of coculture without direct cell contact between both populations. Subject groups of cells ($1–2 \times 10^5$ cells/well) were seeded in the bottom chamber, and effector groups of cells (1×10^4 cells/well) were seeded in the insert (0.4 μm pore size; Corning, USA). LPS stimulation of microglia was performed with 100 ng/mL LPS (Sigma, USA) for 4 h prior to coculture. After coculture for 12 h, rBM-MSCs or microglia of subject groups were isolated and processed for further evaluations. Microglial activation was estimated by their morphological differences. Swelled microglia cells with rounder morphology were considered as activated microglia based on criteria for activated microglia [22, 23]. Images were acquired with an optical lens and an Axiovert 200M fluorescence microscope (Zeiss, Jena, Germany).

2.4. Transcriptomic Analysis. Differences in gene expression in subject groups of rBM-MSCs or microglia were examined using the Illumina system (Illumina, USA) in conjunction with Sentrix Rat-Ref-12-v1 Expression Bead Chips containing gene-specific oligonucleotides (~22,000 genes, Illumina, USA). Differences in data distribution were analysed using BeadStudio software (Illumina, USA). Probe signals were quantile normalised, and those with a p value of less than 0.05 were selected for further analysis. Gene ontology and biological pathways and functions were determined using the web-based bioinformatics software Ingenuity Pathway Analysis (IPA; Ingenuity Systems, USA). A fold change of ±1.2 in expression levels was used as a cut-off to generate data sets of genes with a significantly altered expression.

When we applied a stringent cut-off of ±1.5, we cannot compare the groups (experimental and control) and the biological function of the gene network cannot be predicted. This is mainly due to the low abundance of changed genes (Supplementary Figures 2, 3, and 4). Genes with similar molecular functions were grouped and depicted as a network with indicated direct and indirect relationships as previously described [24, 25].

2.5. Quantitative Real-Time PCR (qPCR). The expression levels of genes were quantified with qPCR using SsoAdvanced Universal SYBR Green Supermix real-time PCR kit (Bio-Rad, USA) and cDNA and gene-specific primer pairs (Supplementary Tables 1 and 2) on a Rotor-Gene Q system (Qiagen, USA). Reaction conditions were as follows: 95°C for 5 min, followed by 50 cycles of 95°C for 5 s and 60°C for 30 s. The threshold/quantification cycle (Ct/Cq) value was determined as the point where the detected fluorescence was statistically higher than the background levels. PCR products were analysed using melting curves constructed with Rotor-Gene 1.7 software (Qiagen, USA). PCR reactions were prepared independently in triplicates. Relative quantification of target gene expression was calculated using the $2^{-\Delta\Delta Ct}$ method.

2.6. Migration Assay. Migratory activity of rBM-MSCs was determined using an $8\,\mu m$ pore-size transwell system (Corning, USA). The upper side of the insert was coated with Matrigel (1 : 10 dilution in 0.01 M Tris (pH 8.0), 0.7% NaCl, Corning, USA) for 2 h at 37°C. The bottom chambers contained one of five different conditions for comparison: MEM with 10% FBS as positive control, MEM without FBS as negative control, MEM with 100 ng/mL LPS, 5×10^4 microglia with MEM, and LPS-stimulated 5×10^4 microglia with MEM. Inserts containing 2.5×10^4 rBM-MSCs were overlaid onto each conditioned well and incubated for 12 h. The inserts were carefully washed with cold phosphate-buffered saline (PBS), and nonmigrating cells remaining in the upper side of the inserts were removed with a cotton swab. The insert was fixed in Cytofix buffer (BD, San Jose, CA, USA) at 4°C for 30 min and stained with $10\,\mu g/mL$ Hoechst 33342 at RT for 10 min. After washing twice with PBS, images were acquired using an Axiovert 200M fluorescence microscope (Zeiss, Jena, Germany). The excitation wavelength for Hoechst 33342 was 405 nm. Migrating cells were counted in ten random $378.27\,mm^2$ $(710.52\,\mu m \times 532.38\,\mu m)$ microscopic fields using ImageJ software.

2.7. Statistical Analysis. Results were analysed using one-way analysis of variance (ANOVA) with Bonferroni's multiple-comparison test as a post hoc test and IBM-SPSS software (IBM, USA). We performed more than three independent experiments and carried out statistical analysis. Differences were considered significant for p values < 0.05.

3. Results

3.1. Cellular Movement-Related Transcriptomic Changes in rBM-MSCs Cocultured with LPS-Stimulated Microglia. To investigate the effects of LPS-stimulated microglia on rBM-MSCs, we used an *in vitro* coculture system (Figure 1(a)). For this study, we isolated rBM-MSCs from 8–12-week-old SD rats and primary microglia from the midbrain of 1-day-old rat pups. Groups of rBM-MSCs were seeded onto the bottom chamber and subjected to 4 different conditions (groups 1–4). Group 1 was the rBM-MSC-only control, group 2 was the coculture with microglia, group 3 was the LPS-treated rBM-MSCs, and group 4 was the coculture with LPS-stimulated microglia. There were no significant changes in cell density of rBM-MSCs (data not shown). In a microarray distribution analysis, gene expression was altered in groups 2, 3, and 4 compared to that of the control (Supplementary Figure 5). In addition, the most pronounced variation in the pattern of gene expression was observed in group 4. Gene ontology analysis of the transcriptome from group 4 revealed that genes from several canonical pathways such as interferon signalling, death receptor signalling, hepatic fibrosis, and neuroinflammation showed variation in expression levels (Supplementary Table 3). Expression of genes related to cellular functions, including death, survival, cell cycle, and cellular movement, was also highly altered in group 4 (Supplementary Figure 6). We focused on the cellular movement function, because the homing of MSCs to the injury site is important for exerting anti-inflammatory effects [26]. For detailed transcriptomic analysis of cellular movement, we selected genes related to cellular movement with altered expression (Figure 1(b)). Heat map analysis showed clear differences in the gene expression pattern in group 4 compared to that of the control (Figure 1(c)).

3.2. Functional Prediction of Transcriptomic Networks in rBM-MSCs Cocultured with LPS-Stimulated Microglia. To obtain detailed information of the genes showing variation in expression, we generated cell movement-related gene expression networks of groups 2, 3, and 4 compared to the network of group 1 using IPA (Supplementary Figure 7). The most pronounced changes in the gene expression networks were also observed in group 4, and the related genes were linked with direct relationships. Based on up- or down-regulation and stream relationships, prediction analysis of the networks showed that cell migration is predicted to be activated in group 4 (Figure 2(a)). Four genes with altered expression levels were identified as being highly related to the migratory activity of cells, which was confirmed using quantitative qPCR (Figure 2(b)). The expression levels of matrix metallopeptidases 3 and 9 (Mmp3 and Mmp9, resp.), vascular cell adhesion protein 1 (Vcam1), and intercellular adhesion molecule 1 (Icam1) were significantly higher in group 4 than in group 2.

3.3. Increased Migratory Activity in rBM-MSCs Cocultured with LPS-Stimulated Microglia. Based on the transcriptomic analysis and prediction, we assumed that there were changes in migratory activity of rBM-MSC influenced by LPS-stimulated microglia. To test the prediction, FBS-containing media condition was used as positive control, and the number of migrating cells was significantly increased in
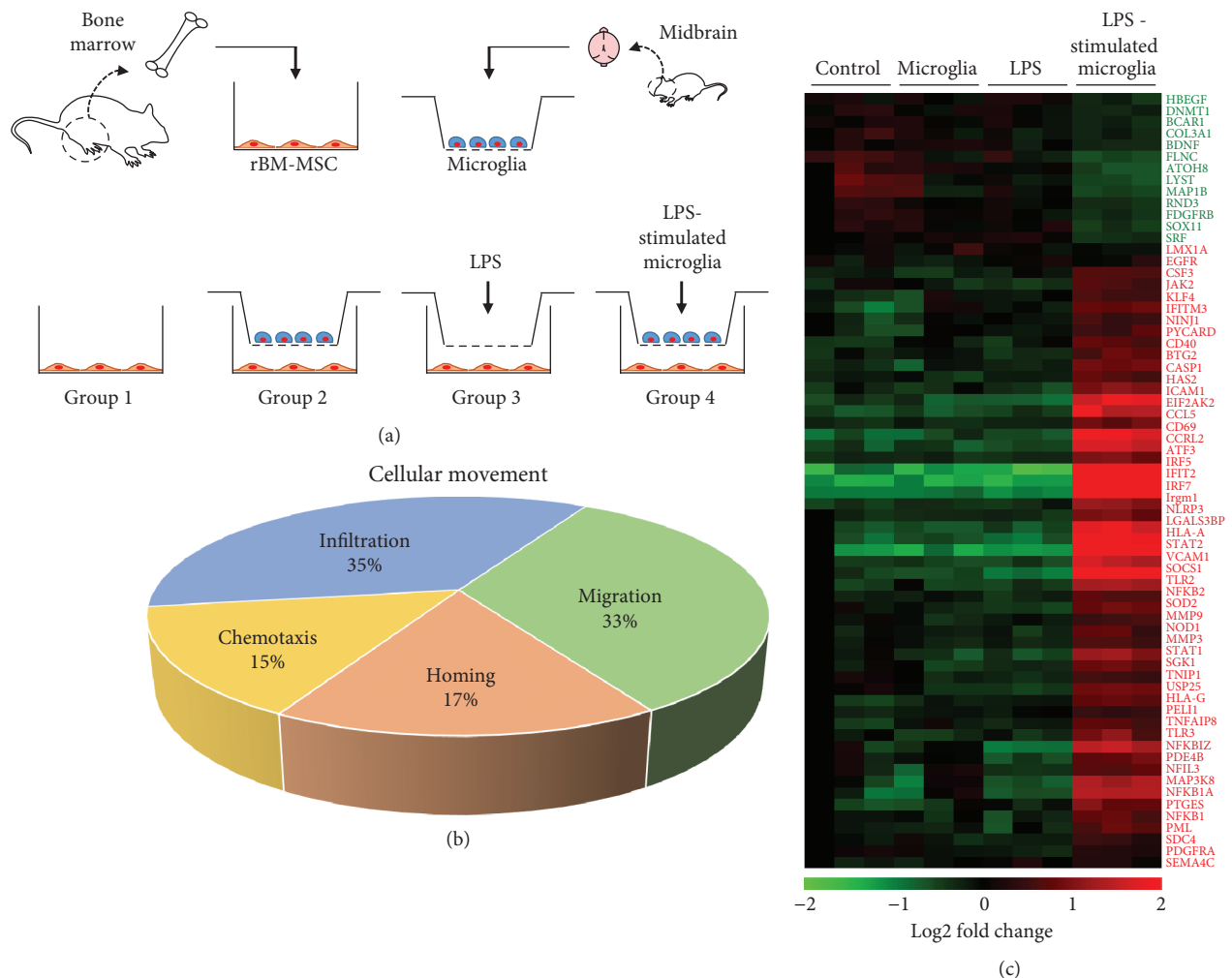
FIGURE 1: Cellular movement-related gene expression variation in rat bone marrow-derived mesenchymal stem cells (rBM-MSCs) cocultured with LPS-stimulated microglia. (a) *In vitro* coculture experimental design. Four different conditions were used (groups 1–4): group 1, rBM-MSCs only (control); group 2, rBM-MSCs cocultured with microglia; group 3, LPS-treated rBM-MSCs; and group 4, rBM-MSCs cocultured with LPS-stimulated microglia. (b) Gene categorisation according to subgroups related to cellular movement. Genes involved with cellular movement were categorised in subgroups (chemotaxis, homing, migration, and infiltration) based on microarrays and Ingenuity Pathway Analysis. (c) Heat map of genes related to cell migration in the 4 different groups with altered expression levels. Gene expression values are coloured from green (downregulated) to red (upregulated).

rBM-MSCs when cocultured with LPS-stimulated microglia (Figures 3(a) and 3(b)).

3.4. Transcriptomic Analysis in LPS-Stimulated Microglia Cocultured with rBM-MSCs.

The effects of rBM-MSCs on LPS-stimulated microglia were also determined via reversed conditions of the aforementioned coculture system *in vitro*. To that end, microglia were seeded on the bottom chamber as subject groups and subjected to 3 different conditions: control, LPS stimulation, and LPS stimulation with rBM-MSC coculture (Figure 4(a)). There were no significant changes in cell density of microglia (data not shown). The transcriptome of subject groups was analysed using microarrays and IPA. Comparison between LPS stimulation and LPS stimulation with rBM-MSC coculture showed changes in expression levels of genes related to cancer, organismal injury and abnormalities, and cell death (Supplementary Figure 8).

Gene ontology analysis of the transcriptome revealed altered expression levels of genes related to inflammatory response-related canonical pathways such as triggering receptor expressed on myeloid cell 1 (TREM1) signalling, neuroinflammation, and rheumatoid arthritis (Supplementary Table 4 and Figure 4(b)). Expression of genes related to TREM1 signalling and neuroinflammation was especially suppressed, as predicted (negative z-score). Focused gene expression analysis of the inflammatory response showed significantly altered levels in 65 genes between groups (Figure 4(c)). Although the differences were more pronounced after LPS stimulation, remarkable changes were also observed between the presence and absence of rBM-MSCs.

3.5. Functional Prediction of Transcriptomic Networks and Reduced Inflammatory Response in LPS-Stimulated Microglia Cocultured with rBM-MSCs.

To investigate

(a)

(b)
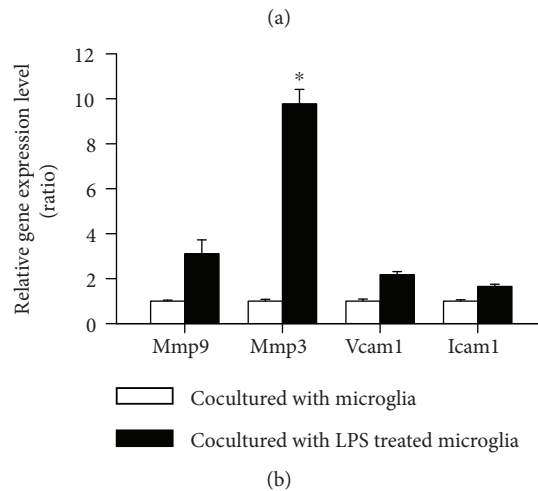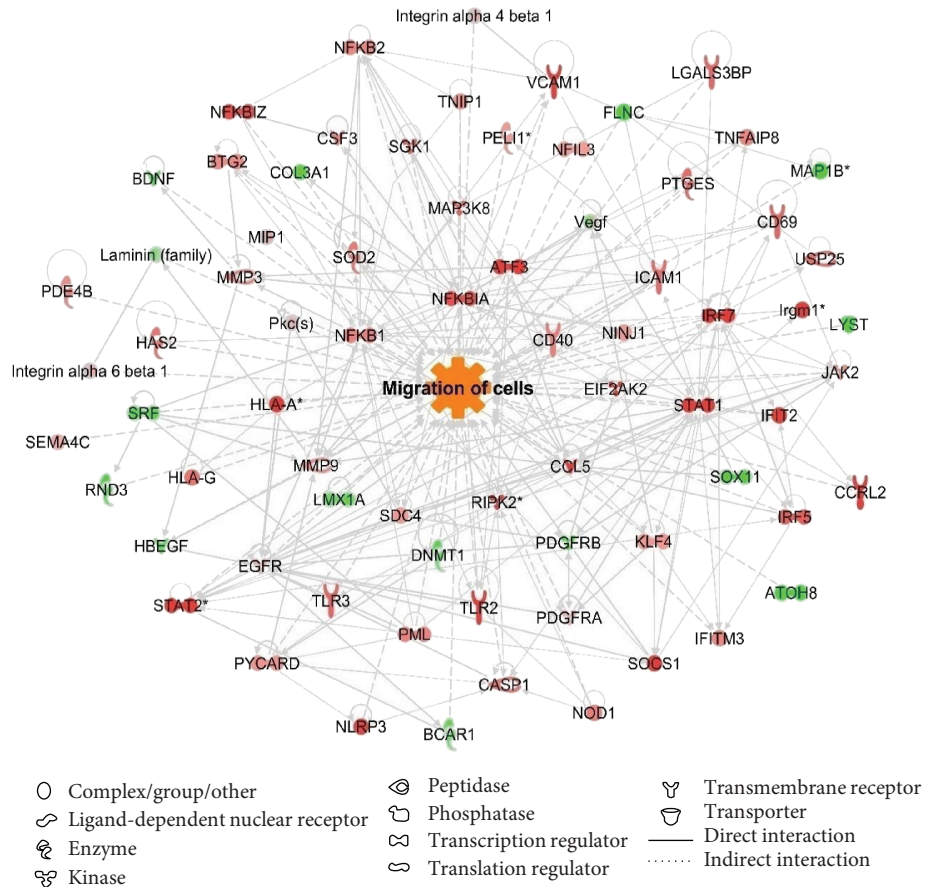
Figure 2: Increase in migration of rat bone marrow-derived mesenchymal stem cells (rBM-MSCs) cocultured with LPS-stimulated microglia. (a) Gene network related to cell migration was constructed, and cellular function was predicted algorithmically using Ingenuity Pathway Analysis. Red and green areas indicate up- and downregulated genes, respectively. Differentially expressed genes were obtained from microarray data (>1.2 fold change). (b) quantitative RT-PCR analysis of gene expression related to cell migration in rBM-MSCs cocultured with LPS-stimulated microglia compared to rBM-MSCs cocultured with microglia. Data represent the mean of three independent experiments. (mean ± SD) $^*p < 0.05$ versus rBM-MSCs cocultured with microglia.

differences in transcriptomes between LPS-stimulated microglia with and without rBM-MSCs, we generated inflammatory response-related gene expression networks using IPA in the corresponding groups (Supplementary Figure 9). A total of 65 genes highly related to the inflammatory response were identified, and the genes

were directly linked. Based on the differential expression (upregulation or downregulation), prediction analysis of networks showed that the inflammatory response is predicted to be inhibited by rBM-MSCs (Figure 5(a)). Three genes with altered expression levels were highly related to inflammation, which was confirmed using

(a)

(b)
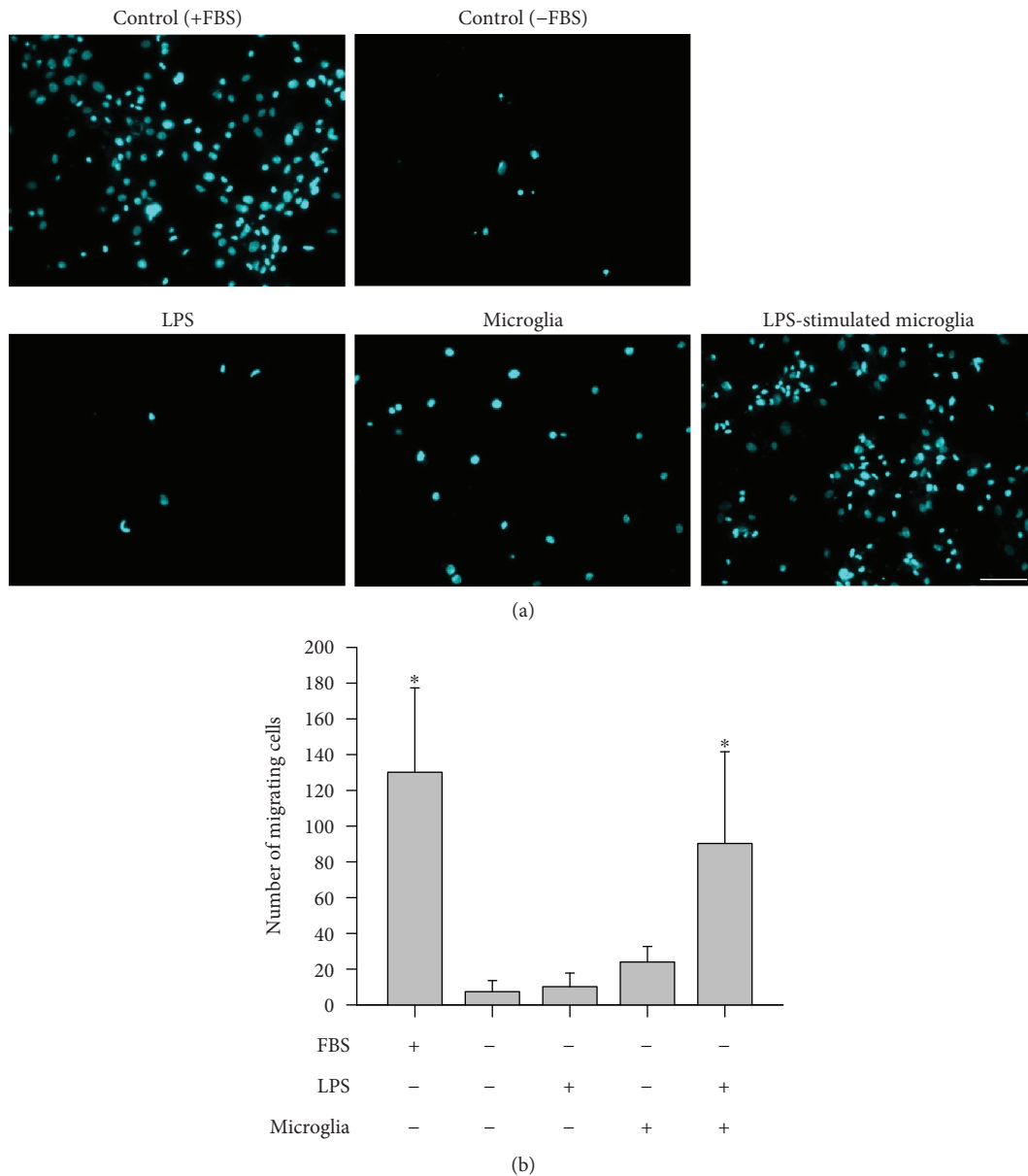
Figure 3: Migration assays with rat bone marrow-derived mesenchymal stem cells (rBM-MSCs) cocultured with LPS-stimulated microglia. (a) Images of migrating rBM-MSCs. Migration of rBM-MSCs was investigated in 5 different conditions: media containing foetal bovine serum (FBS) (positive control), media without FBS (negative control), LPS-treated, cocultured with microglia, and coculture with LPS-stimulated microglia. Migrating cells are cyan in colour (10x magnification). Representative images of migration for each condition are shown. Scale bar: 100 μm. (b) Quantification of migrating cells was performed by counting coloured dots in the images. Data represent the mean of ten random 372.23 mm^2 (710.52 μm × 532.38 μm) microscopic fields (mean ± SD). $^*p < 0.05$ versus negative control (media without FBS).

qPCR (Figure 5(b)). LPS-induced upregulated levels of tumor necrosis factor (Tnf), C-C motif chemokine ligand 2 (Ccl2), and toll-like receptor 2 (Tlr2) genes were significantly decreased after coculture with rBM-MSCs. These predicted functional results were confirmed in experiments using cell cultures, where the number of activated cells induced by LPS stimulation showing swelled and round morphology was significantly decreased by rBM-MSCs (Figure 5(c)). Moreover, the levels of protein markers for microglial activation, CD40 and CD74, were also lower in the presence of rBM-MSC than after LPS

stimulation without rBM-MSC, indicating that direct phenotypical activation of microglia was reduced by rBM-MSCs (Supplementary Figure 10).

4. Discussion

To the best of our knowledge, this study is the first bidirectional comprehensive investigation of the interaction between activated microglia and MSCs through transcriptomic analysis. We showed that activated microglia increase migration of rBM-MSCs and that rBM-MSCs reduce

(a)

(b)

(c)
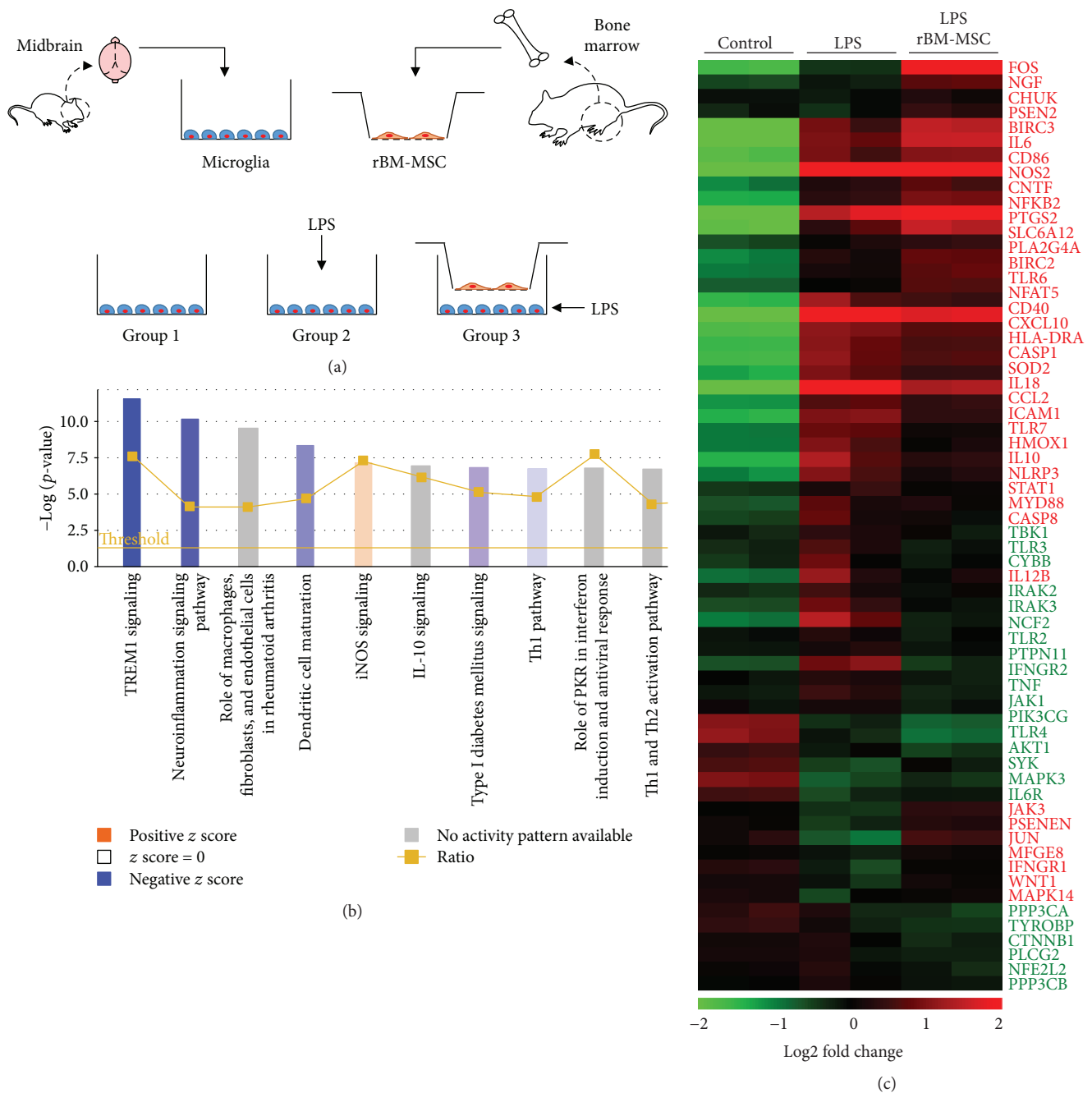
FIGURE 4: Inflammation-related gene expression variation in LPS-stimulated microglia cocultured with rat bone marrow-derived mesenchymal stem cells (rBM-MSCs). (a) *In vitro* reverse coculture experimental design. Three different conditions were used (group 1–3): group 1, control (microglia only); group 2, LPS-stimulated microglia; and group 3, LPS-stimulation with rBM-MSC coculture. (b) Canonical pathway analysis was constructed algorithmically using Ingenuity Pathway Analysis based on microarray data. Bars indicate canonical pathways containing genes with significantly altered expression. Bar graph colours from blue (inhibition) to orange (activation) represent gene activity of the corresponding pathway according to *z*-score. (c) Heat map of genes related to inflammation with altered expression levels. Gene expression values are coloured from green (downregulated) to red (upregulated).

inflammation of activated microglia at the cellular network level. We analysed the bidirectional cellular interaction that occur between rBM-MSCs and LPS-stimulated microglia using transcriptomics (Figure 6). The results show that (i) LPS-stimulated microglia facilitate homing of rBM-MSCs via inducing transcriptomic changes and that (ii)

rBM-MSCs reduce the inflammatory response of microglia by decreasing the expression of the relevant genes.

Transplanted BM-MSCs migrate to the ischaemic border zone in animal models of stroke [27, 28] and to the *substantia nigra* (SN) induced by LPS and MPTP administration in animal models of Parkinson's

(a)

(b)

(c)
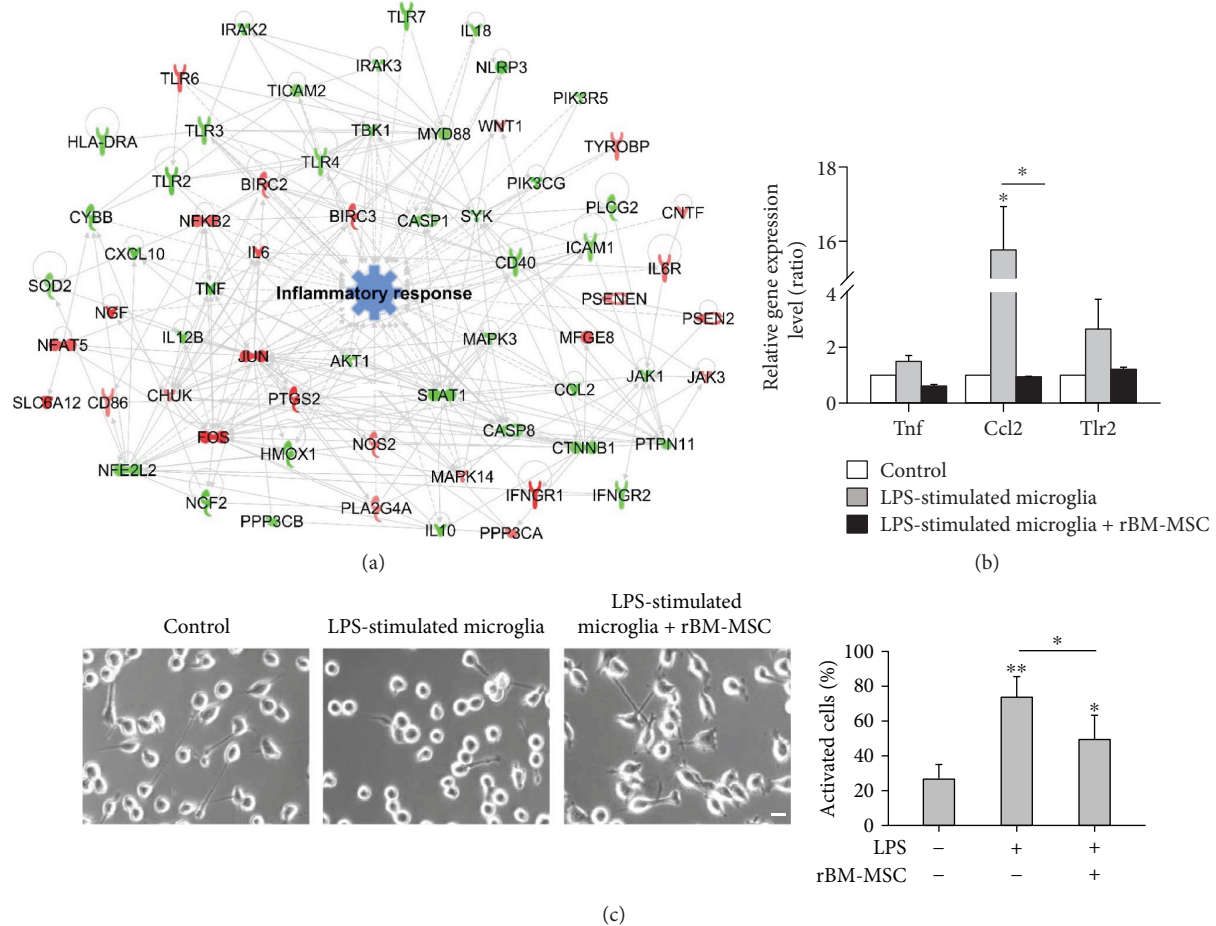
FIGURE 5: Reduced inflammatory response in LPS-stimulated microglia cocultured with rat bone marrow-derived mesenchymal stem cells (rBM-MSCs). (a) Gene network related to inflammatory response was constructed, and cellular function was predicted algorithmically using Ingenuity Pathway Analysis. Red and green areas indicate up- and downregulated genes, respectively. Differentially expressed genes were obtained from microarray data (>1.2 fold-change). (b) Quantitative real-time PCR analysis of gene expression-related inflammation in LPS-stimulated microglia cocultured with rBM-MSCs compared to control (microglia only). (c) Activated microglia were counted in light microscopy images and quantified as the percentage of activated microglia/total cell number. Cells at the edge of the images were not counted. Scale bar: 20 μm. $^{*}p < 0.05$ and $^{**}p < 0.01$ versus control (microglia only).

disease [15], in which inflammatory regions contain activated microglia. In addition, BM-MSCs migrate to LPS-stimulated microglia *in vitro* in response to chemotactic factors [20]. These reports indicate that activated microglia are a possible cause of movement of rBM-MSCs to the site of injury. However, detailed transcriptomic mechanisms of how activated microglia induce the movement of BM-MSCs are not well understood. In this study, we show that the expression levels of 67 genes were significantly altered and that network analysis predicted an increase in migration activity. Meanwhile, CXCR4 receptor and its ligand stromal cell-derived factor-1 (SDF-1a) play an important role in homing of MSCs to brain lesions [29]. However, there were no changes in microarray data and RT-PCR (data not shown). Further studies concerning the homing effects of rBM-MSC on microglia in coculture systems are needed.

The prediction was confirmed experimentally in rBM-MSCs cocultured with LPS-stimulated microglia compared with control and cells cocultured with microglia. Especially, Mmp3 and 9 are essential enzymes for migratory activity

and the corresponding genes are induced in inflammatory conditions via proinflammatory cytokines and oxidative substrates [30, 31]. Thus, LPS-stimulated microglia might form a locally conditioned inflammatory region in the coculture system, and rBM-MSCs move toward this region.

It has been reported that human BM-MSCs (hBM-MSCs) dramatically reduce neural damages in a LPS-stimulated mouse brain and reduce inflammation of microglia owing to the production of cytokines and trophic factors [32]. In addition, cocultured BM-MSCs reduce the expression of TNF-alpha and iNOS and NO production in LPS-stimulated microglia compared with noncocultured BM-MSCs [15, 20]. However, the detailed mechanism of how BM-MSCs downregulate activated microglia has not been well studied. In this study, we show that the expression levels of 65 genes were significantly altered, and network analysis predicted the suppression of the inflammatory response. This prediction was experimentally verified in LPS-stimulated microglia cocultured with rBM-MSCs. The results show that the levels of most proinflammatory genes
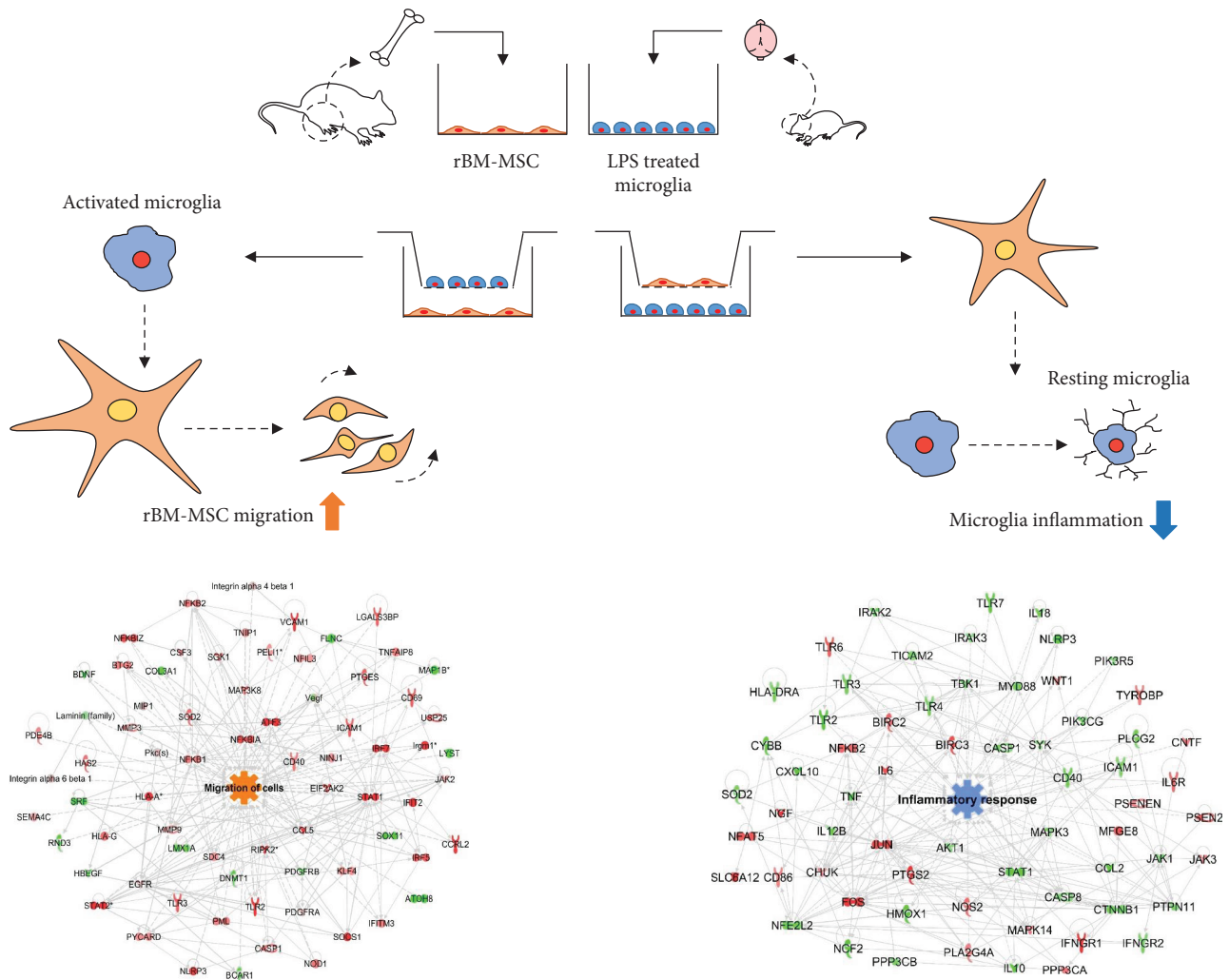
FIGURE 6: Schematic representation of bidirectional interaction between rat bone marrow-derived mesenchymal stem cells (rBM-MSCs) and activated microglia. Activated microglia increased migration of rBM-MSCs in rBM-MSCs cocultured with LPS-stimulated microglia in an *in vitro* coculture system. rBM-MSCs decreased the inflammatory response of activated microglia in a reverse coculture system.

were reduced when cocultured with rBM-MSCs. The expression levels of Ccl2, a key mediator of microglial activation [33, 34], were significantly decreased in the presence of rBM-MSCs, indicating anti-inflammatory effects by rBM-MSC. These phenomena may occur as a result of secreted molecules from both rBM-MSCs and LPS-stimulated microglia. Further studies are needed to identify the secreted molecules, that is, the secretome, that increase invasive migratory activity of rBM-MSCs and decrease the inflammatory response of LPS-stimulated microglia.

There are several limitations to our study. First, we used a fold change of ±1.2 in expression levels as a cut-off and identified low level of abundant genes due to the limitation in an *in vitro* coculture system. In general, the transwell coculture system has fundamental limitations, such as cell density, fluid concentration, and cell-other cell direct interaction, compared to that *in vivo* [35]. However, our transcriptomic analysis for bidirectional effect of each cells and the above approach cannot be done in the *in vivo*

system, due to diversity of cells in the organ. We expect that the implied biological effect in our results might be more strongly expressed in *in vivo*. Second, fundamental limitations reside in microarray and bioinformatics analysis. Although microarray is performed with an additional probe for compensation of inaccuracies and statistically analysed, the reduction of false positive or negative is a challenging task [36]. In addition, bioinformatics tool is constructed with existing knowledge, hence novel finding is limited [37]. As a result, a unique pathway cannot be deduced in our analysis system and individual analysis for genes can be biased, which could bring about false positive or negative results. Thus, we focused more in cellular processes than target molecules. Finally, analysing specific pathway/s or molecule/s is beyond our limitation in this study. To find novel pathway/s or molecule/s, responsible for attracting rBM-MSCs or inflammatory response of microglia identified, other methodological biomolecular approaches are required.

In conclusion, we performed bidirectional transcriptomic analysis of activated microglia and BM-MSCs. The results

show that activated microglia in a neuroinflammatory condition modulate the migration of BM-MSCs and that BM MSCs reduce inflammatory response in microglia. This study enhances our understanding of the relationship between activated microglia and transplanted stem cells and may lead to a new therapeutic strategy using stem cell therapy for brain diseases.

Data Availability

The data used to support the findings of this study are available from the corresponding author upon request.

Conflicts of Interest

The authors declare no conflict of interests.

Acknowledgments

Supplementary Materials

Supplementary Table 1: quantitative RT-PCR primer sequences for genes encoding the transcriptomic network related to cell migration. Supplementary Table 2: quantitative RT-PCR primer sequences for genes encoding the transcriptomic network related to inflammatory response. Supplementary Table 3: top 20 canonical pathways constructed algorithmically by Ingenuity Pathway Analysis in rBM-MSCs cocultured with LPS-stimulated microglia compared to rBM-MSCs cocultured with microglia. Supplementary Table 4: top 20 canonical pathways constructed algorithmically by Ingenuity Pathway Analysis in LPS-stimulated microglia cocultured with rBM-MSCs compared to LPS-stimulated microglia. Supplementary Figure 1: flow cytometry analysis of Iba1-positive cells in primary microglia isolated from SD rat pups. Supplementary Figure 2: transcriptomic network analysis in four different culture conditions of rBM-MSCs (>1.5 fold change). Supplementary Figure 3: gene network related to cell migration in rBM-MSCs cocultured with LPS-stimulated microglia compared to rBM-MSCs cocultured with microglia was constructed algorithmically using Ingenuity Pathway Analysis (>1.5 fold change). Supplementary Figure 4: gene network related to inflammatory response in LPS-stimulated microglia cocultured with rBM-MSCs compared to control (microglia only) was constructed algorithmically using Ingenuity Pathway Analysis (>1.5 fold change). Supplementary Figure 5: plotting of signal intensities in three different culture conditions of rBM-MSCs compared to control (rBM-MSCs only). Supplementary Figure 6: top 20 list of function or diseases constructed algorithmically by Ingenuity Pathway Analysis in rBM-MSCs cocultured with LPS-stimulated microglia compared to rBM-MSCs cocultured with microglia. Supplementary Figure 7: transcriptomic network analysis in four different culture conditions of rBM-MSCs (>1.2 fold change). Supplementary Figure 8: top 20 list of function or diseases constructed algorithmically by Ingenuity Pathway Analysis in LPS-stimulated microglia cocultured with rBM-MSCs compared to LPS-stimulated microglia. Supplementary Figure 9: transcriptomic network analysis in two different culture conditions of LPS-stimulated microglia (>1.2 fold change). Supplementary Figure 10: Western blot analysis in LPS-stimulated microglia cocultured with rBM-MSCs using anti CD40 and CD74 antibodies. *(Supplementary Materials)*

References

[1] M. W. Salter and B. Stevens, "Microglia emerge as central players in brain disease," *Nature Medicine*, vol. 23, no. 9, pp. 1018–1027, 2017.

[2] M. Colonna and O. Butovsky, "Microglia function in the central nervous system during health and neurodegeneration," *Annual Review of Immunology*, vol. 35, no. 1, pp. 441–468, 2017.

[3] L. Xu, D. He, and Y. Bai, "Microglia-mediated inflammation and neurodegenerative disease," *Molecular Neurobiology*, vol. 53, no. 10, pp. 6709–6715, 2016.

[4] K. Inoue and M. Tsuda, "Microglia in neuropathic pain: cellular and molecular mechanisms and therapeutic potential," *Nature Reviews. Neuroscience*, vol. 19, no. 3, pp. 138–152, 2018.

[5] R. Beschorner, H. J. Schluesener, F. Gozalan, R. Meyermann, and J. M. Schwab, "Infiltrating CD14$^+$ monocytes and expression of CD14 by activated parenchymal microglia/macrophages contribute to the pool of CD14$^+$ cells in ischemic brain lesions," *Journal of Neuroimmunology*, vol. 126, no. 1-2, pp. 107–115, 2002.

[6] P. L. McGeer, S. Itagaki, B. E. Boyes, and E. G. McGeer, "Reactive microglia are positive for HLA-DR in the substantia nigra of Parkinson's and Alzheimer's disease brains," *Neurology*, vol. 38, no. 8, pp. 1285–1291, 1988.

[7] S. Thameem Dheen, C. Kaur, and E. A. Ling, "Microglial activation and its implications in the brain diseases," *Current Medicinal Chemistry*, vol. 14, no. 11, pp. 1189–1197, 2007.

[8] M. A. Ajmone-Cat, A. Bernardo, A. Greco, and L. Minghetti, "Non-steroidal anti-inflammatory drugs and brain inflammation: effects on microglial functions," *Pharmaceuticals*, vol. 3, no. 6, pp. 1949–1965, 2010.

[9] B. L. Jacobs, H. van Praag, and F. H. Gage, "Adult brain neurogenesis and psychiatry: a novel theory of depression," *Molecular Psychiatry*, vol. 5, no. 3, pp. 262–269, 2000.

[10] Y. L. Feng and X. L. Tang, "Effect of glucocorticoid-induced oxidative stress on the expression of Cbfa1," *Chemico-Biological Interactions*, vol. 207, pp. 26–31, 2014.

[11] O. Y. Bang, J. S. Lee, P. H. Lee, and G. Lee, "Autologous mesenchymal stem cell transplantation in stroke patients," *Annals of Neurology*, vol. 57, no. 6, pp. 874–882, 2005.

[12] T. H. Shin, G. Phukan, J. S. Shim et al., "Restoration of polyamine metabolic patterns in *in vivo* and *in vitro* model of ischemic stroke following human mesenchymal

stem cell treatment," *Stem Cells International*, vol. 2016, Article ID 4612531, 11 pages, 2016.

[13] N. K. Venkataramana, R. Pal, S. A. V. Rao et al., "Bilateral transplantation of allogenic adult human bone marrow-derived mesenchymal stem cells into the subventricular zone of Parkinson's disease: a pilot clinical study," *Stem Cells International*, vol. 2012, Article ID 931902, 12 pages, 2012.

[14] P. H. Lee, J. W. Kim, O. Y. Bang, Y. H. Ahn, I. S. Joo, and K. Huh, "Autologous mesenchymal stem cell therapy delays the progression of neurological deficits in patients with multiple system atrophy," *Clinical Pharmacology and Therapeutics*, vol. 83, no. 5, pp. 723–730, 2007.

[15] Y. J. Kim, H. J. Park, G. Lee et al., "Neuroprotective effects of human mesenchymal stem cells on dopaminergic neurons through anti-inflammatory action," *Glia*, vol. 57, no. 1, pp. 13–23, 2009.

[16] M. A. Matthay, S. Pati, and J. W. Lee, "Concise review: mesenchymal stem (stromal) cells: biology and preclinical evidence for therapeutic potential for organ dysfunction following trauma or Sepsis," *Stem Cells*, vol. 35, no. 2, pp. 316–324, 2017.

[17] Z. Cheng, H. L. Peng, R. Zhang, X. M. Fu, and G. S. Zhang, "Bone marrow-derived innate macrophages attenuate oxazolone-induced colitis," *Cellular Immunology*, vol. 311, pp. 46–53, 2017.

[18] Y. Jaimes, Y. Naaldijk, K. Wenk, C. Leovsky, and F. Emmrich, "Mesenchymal stem cell-derived microvesicles modulate lipopolysaccharides-induced inflammatory responses to microglia cells," *Stem Cells*, vol. 35, no. 3, pp. 812–823, 2017.

[19] K. Yan, R. Zhang, C. Sun et al., "Bone marrow-derived mesenchymal stem cells maintain the resting phenotype of microglia and inhibit microglial activation," *PLoS One*, vol. 8, no. 12, article e84116, 2013.

[20] Z.'a. Rahmat, S. Jose, R. Ramasamy, and S. Vidyadaran, "Reciprocal interactions of mouse bone marrow-derived mesenchymal stem cells and BV2 microglia after lipopolysaccharide stimulation," *Stem Cell Research & Therapy*, vol. 4, no. 1, p. 12, 2013.

[21] H. J. Park, P. H. Lee, O. Y. Bang, G. Lee, and Y. H. Ahn, "Mesenchymal stem cells therapy exerts neuroprotection in a progressive animal model of Parkinson's disease," *Journal of Neurochemistry*, vol. 107, no. 1, pp. 141–151, 2008.

[22] G. W. Kreutzberg, "Microglia: a sensor for pathological events in the CNS," *Trends in Neurosciences*, vol. 19, no. 8, pp. 312–318, 1996.

[23] A. D. Bachstetter, L. J. van Eldik, F. A. Schmitt et al., "Disease-related microglia heterogeneity in the hippocampus of Alzheimer's disease, dementia with Lewy bodies, and hippocampal sclerosis of aging," *Acta Neuropathologica Communications*, vol. 3, no. 1, p. 32, 2015.

[24] T. H. Shin, S. Lee, K. R. Choi et al., "Quality and freshness of human bone marrow-derived mesenchymal stem cells decrease over time after trypsinization and storage in phosphate-buffered saline," *Scientific Reports*, vol. 7, no. 1, article 1106, 2017.

[25] T. H. Shin, D. Y. Lee, H. S. Lee et al., "Integration of metabolomics and transcriptomics in nanotoxicity studies," *BMB Reports*, vol. 51, no. 1, pp. 14–20, 2018.

[26] B. de Lucas, L. M. Perez, and B. G. Galvez, "Importance and regulation of adult stem cell migration," *Journal of Cellular and Molecular Medicine*, vol. 22, no. 2, pp. 746–754, 2018.

[27] M. J. Paik, W. Y. Li, Y. H. Ahn et al., "The free fatty acid metabolome in cerebral ischemia following human mesenchymal stem cell transplantation in rats," *Clinica Chimica Acta*, vol. 402, no. 1-2, pp. 25–30, 2009.

[28] D. Kalladka and K. W. Muir, "Brain repair: cell therapy in stroke," *Stem Cells and Cloning: Advances and Applications*, vol. 7, pp. 31–44, 2014.

[29] G. Chamberlain, J. Fox, B. Ashton, and J. Middleton, "Concise review: mesenchymal stem cells: their phenotype, differentiation capacity, immunological features, and potential for homing," *Stem Cells*, vol. 25, no. 11, pp. 2739–2749, 2007.

[30] S. G. Almalki and D. K. Agrawal, "Effects of matrix metalloproteinases on the fate of mesenchymal stem cells," *Stem Cell Research & Therapy*, vol. 7, no. 1, p. 129, 2016.

[31] R. L. Warner, N. Bhagavathula, K. C. Nerusu et al., "Matrix metalloproteinases in acute inflammation: induction of MMP-3 and MMP-9 in fibroblasts and epithelial cells following exposure to pro-inflammatory mediators in vitro," *Experimental and Molecular Pathology*, vol. 76, no. 3, pp. 189–195, 2004.

[32] C. Zhou, C. Zhang, S. Chi et al., "Effects of human marrow stromal cells on activation of microglial cells and production of inflammatory factors induced by lipopolysaccharide," *Brain Research*, vol. 1269, pp. 23–30, 2009.

[33] M. A. Thacker, A. K. Clark, T. Bishop et al., "CCL2 is a key mediator of microglia activation in neuropathic pain states," *European Journal of Pain*, vol. 13, no. 3, pp. 263–272, 2009.

[34] A. E. Hinojosa, B. Garcia-Bueno, J. C. Leza, and J. L. Madrigal, "CCL2/MCP-1 modulation of microglial activation and proliferation," *Journal of Neuroinflammation*, vol. 8, no. 1, p. 77, 2011.

[35] M. J. Carroll, L. E. Stopfer, and P. K. Kreeger, "A simplified culture system to examine soluble factor interactions between mammalian cells," *Chemical Communications*, vol. 50, no. 40, pp. 5279–5281, 2014.

[36] A. V. Tinker, A. Boussioutas, and D. D. L. Bowtell, "The challenges of gene expression microarrays for the study of human cancer," *Cancer Cell*, vol. 9, no. 5, pp. 333–339, 2006.

[37] L. Jin, X. Y. Zuo, W. Y. Su et al., "Pathway-based analysis tools for complex diseases: a review," *Genomics, Proteomics & Bioinformatics*, vol. 12, no. 5, pp. 210–220, 2014.

Review Article

Stem Cells in Dentistry: Types of Intra- and Extraoral Tissue-Derived Stem Cells and Clinical Applications

Ana Gomes Paz (ID),[1] **Hassan Maghaireh** (ID),[2] **and Francesco Guido Mangano** (ID)[3]

[1]*Department of Endodontics, Lisbon, Dental School, University of Lisbon, Lisbon, Portugal*
[2]*Clinical Teaching Fellow, University of Manchester, Manchester, UK*
[3]*Department of Medicine and Surgery, Dental School, University of Varese, Varese, Italy*

Correspondence should be addressed to Ana Gomes Paz; anagpaz20@gmail.com

Received 9 February 2018; Revised 5 April 2018; Accepted 7 June 2018; Published 2 July 2018

Academic Editor: Jane Ru Choi

Stem cells are undifferentiated cells, capable of renewing themselves, with the capacity to produce different cell types to regenerate missing tissues and treat diseases. Oral facial tissues have been identified as a source and therapeutic target for stem cells with clinical interest in dentistry. This narrative review report targets on the several extraoral- and intraoral-derived stem cells that can be applied in dentistry. In addition, stem cell origins are suggested in what concerns their ability to differentiate as well as their particular distinguishing quality of convenience and immunomodulatory for regenerative dentistry. The development of bioengineered teeth to replace the patient's missing teeth was also possible because of stem cell technologies. This review will also focus our attention on the clinical application of stem cells in dentistry. In recent years, a variety of articles reported the advantages of stem cell-based procedures in regenerative treatments. The regeneration of lost oral tissue is the target of stem cell research. Owing to the fact that bone imperfections that ensue after tooth loss can result in further bone loss which limit the success of dental implants and prosthodontic therapies, the rehabilitation of alveolar ridge height is prosthodontists' principal interest. The development of bioengineered teeth to replace the patient's missing teeth was also possible because of stem cell technologies. In addition, a "dental stem cell banking" is available for regenerative treatments in the future. The main features of stem cells in the future of dentistry should be understood by clinicians.

1. Introduction

Stem cells are undifferentiated cells, capable of renewing themselves. Via differentiation, they have the potential to develop into many different cell lineages. There are different kinds of stem cells, depending on the type of cells they can create and the location in the body. In recent years, studies have shown that oral tissues are a source of stem cells. Structuring of tissue in dentistry has revealed promising results in the regeneration of oral tissue or organs. There are multiple factors that can produce alveolar bone resorption due to tooth extraction or loss because of severe cavities, trauma, or root fracture or even because of periodontal diseases. In edentulous patients, bone resorption continues throughout life particularly in the mandible, which makes it difficult to substitute the missing teeth with dental implants [1].

Tissue engineering therapies and stem cells are a promising way to achieve alveolar bone regeneration and solve large periodontal tissue defects and finally to substitute a lost tooth itself. Organs and tissues such as tongue, salivary glands, the temporomandibular joint condylar cartilage, and skeletal muscles are set to be used in regenerative dental medicine.

To develop the concept of oral tissue and organ regeneration for clinical application in dentistry, several studies have been carried out in animals including key elements of tissue engineering such as extracellular matrix scaffolds and stem cells [2]. Furthermore, clinical trials about jaw bone regeneration applied in dental areas such as implantology using stem cells and tissue engineering strategies have demonstrated positive results.

Considering the new role of regenerative biology and stem cells in dentistry, especially regarding the ideal stem cells for oral regeneration, some confusion can be made

depending on the various oral and maxillofacial locations where stem cells can be obtained [3].

The aim of this review is to explain the different kinds and sources of stem cells from a clinical perspective in dentistry, regarding their accessibility, immunomodulatory properties, and differentiation capacity, as well as their clinical applications. We will focus on the ongoing analysis and clinical studies in dentistry.

2. Origins

2.1. Pluripotent Stem Cells. The pluripotent stem cells when applied in dentistry can include investigation on the biology and regenerative treatments due to their pluripotency and unlimited self-renewal. Dental research is focused on obtaining oral lineages from the differentiation of pluripotent stem cells to be applied clinically [4].

2.1.1. ES Cells (Embryonic Stem Cells). ES cells are produced from the culturing cells, which precede from the blastocyst, particularly from its undifferentiated inner cell mass (the early stage of embryonic development after fertilization) [5]. They are of great interest because of their particular distinguishing quality of differentiating in vitro into all somatic cell lineages and germ cells [6]. The main reason why there are moral and ethical questions about the use of human ES cells has to do with the embryonic origin.

Research about pluripotent stem cells and its differentiation may help to understand the oral developmental biology and in future can be useful to create strategies in regenerative dentistry to fulfill the clinical demands [7]. Nevertheless, these kinds of studies are expensive, and researchers still have to deal with ethical issues, unless experts, who can routinely deal with patient embryos, were included in the team.

2.1.2. iPS Cells (Pluripotent Stem Cells). iPS cells have the aptitude to develop into various types tissue and organs. This stem cell technology is very promising, which can revolutionize medicine and create a biocompatible medicine that uses patients' cells to supply individual and biocompatible treatments.

IPS cells can be obtained from multiple oral mesenchymal cells: SCAP, DPSCs and SHED, TGPCs, buccal mucosa fibroblasts, gingiva fibroblasts, and periodontal ligament fibroblasts [8]. It is expected that oral cells can be an ideal iPS cell source, which can be applied in regenerative procedures for periodontal tissue, salivary glands, missing jaw bone, and tooth loss [9].

iPSCs are obtained by introducing reprogramming factors or specific products of pluripotency-associated genes into a given cell type. The original set of reprogramming factors are the transcription factors Oct4 (encoded by the gene POU5F1), Sox2 (sex-determining region Y-box 2), cMyc, and Klf4 (Kruppel-like factor 4). Each of these factors can be replaced by related transcription factors, miRNAs, small molecules, or even nonrelated genes such as lineage specifiers [10].

Duan et al. described that making the combination between iPS cells and enamel matrix derivatives can enhance

periodontal regeneration and the cementum formation of the periodontal ligament and alveolar bone [11]. Other studies suggested that the ability of iPS cells to differentiate into ameloblasts and odontogenic mesenchymal cells is promising in tooth bioengineering [9, 12].

Further research is necessary to understand how to control their differentiation. It is still unclear whether iPS and ES cells are equal.

It is necessary to identify iPS cell origins to achieve adequate guided differentiation. Furthermore, if iPS cells are clinically applied, it is important to prevent tumor formation upon in vivo implantation, since its protocol of implantation uses the oncogene c-Myc, which can raise concerns about possible carcinogenic properties. However, this problem can be solved by using L-Myc replacing c-Myc and reprogramming using components which are not viral, such as proteins, microRNA, synthetic mRNA, or episomal plasmids. Nevertheless, remaining undifferentiated iPS cells that stay among the differentiated target cells can uncontrollably proliferate to form teratomas in the transplanted location, being an important clinical problem. To solve this concern, different methods such as a cell sorting approach or a selective ablation procedure have been investigated [1].

2.2. Adult Stem Cells. Embryonic stem (ES) and adult stem cells are two of the leading sources of stem cells present in humans. Further sources can be obtained synthetically from somatic cells, which are known as pluripotent stem (iPS) cells.

Adult stem cells can only develop into a certain number of kinds of cells. On the other hand, ES cells or IPS cells are pluripotent stem cells, which means that they can differentiate into all kinds of cells from all three germinal layers.

There are very few adult stem cells existing in adult tissues that go through self-regeneration and differentiation to maintain healthy tissue and repair damage tissues. They are known to be somatic stem cells or postnatal stem cells [13, 14] that undergo into self-renewal and differentiation to repair injured tissues. Studies on stem cells have revealed that there are in the oral and maxillofacial location a number of adult stem cell sources [15].

2.2.1. Introduction to MSCs. Even though bone marrow was the original source of MSCs, there are alternatives which have been drawn from other adult tissues [16–18]. Thanks to their capacity of self-renewing and their ability to differentiate along specific lines on stimulation, these types of cells present promising characteristics for the development of cell-based approaches in bone regeneration [17].

Friedenstein et al. described in the 70s the approach of using adherent fibroblastic cells that were drawn from the bone marrow [19] and their capacity to differentiate into several mesenchymal tissues. Years later, Pittenger et al. described human mesenchymal stem cells from the iliac crest bone marrow as multipotent cells, explaining their isolation, expansion in culture, and differentiation into chondrogenic, adipogenic, and osteogenic lineages [20]. Nevertheless, due to the lack of homogeneity of the population of bone marrow isolated adherent cells and the inability to identify definitive

markers for MSCs, this concept of MSCs is still controversial [21]. Mesenchymal stem cells can be attached to tissue culture-treated plastic when maintained in standard culture conditions [22] as stated in ISCT criteria. In addition, MSCs should express CD105, CD73, and CD90 and lack the expression of CD45, CD34, CD14 or CD11b, CD79a or CD19, and HLA-DR surface molecules. In vitro, MSCs must also be able to differentiate into chondroblasts, adipocytes, and osteoblasts [23]. In 2007, studies have identified other cell surface markers for human MSCs like CD271 [24] and MSC antigen-1 [25]. Finally, the selection of MSC's fixed mRNA markers shown in MSCs [26, 27] has been reported.

2.2.2. Bone Marrow-Derived MSCs (BMSCs).

BMSCs are multipotent progenitor cells present in adult bone marrow. Due to their replicative capacity, they can also differentiate into numerous cells of the connective tissue. BMSCs can be isolated from the iliac crest [28].

Many studies have demonstrated that BMSCs from the iliac crest can differentiate into myogenic, osteogenic, chondrogenic, adipogenic, and nonmesenchymal neurogenic lineages [29]. Even though the process of isolating BMSCs from the bone marrow is a relatively simple process, a major surgical and invasive operation will be needed, and this is considered one of the great drawbacks of BMSCs from the iliac crest. Nevertheless, this procedure is the most common and it has been used in dental bone regeneration for many years.

Thanks to the high potential for regenerating bone [30], BMSCs from the human iliac crest are important for bone tissue engineering notwithstanding patient age [31, 32].

Still, various reports have described a relation between age and the reduction in the osteogenic potential of BMSCs when extracted from the femur and iliac crest [32–34] and delineate that the age of the donor is an important factor for bone formation. Furthermore, the expansion capacity seems to be restricted, since cells tend to age and lose their properties with repeated passaging and culture time in their multidifferentiation potential. The disadvantages must be overcome to apply with success BMSCs for bone regeneration and tissue engineering.

We can obtain BMSCs from orofacial bones as well. Human BMSCs can be isolated from the maxilla and mandible bone marrow suctioned during dental treatments like dental implantation, third molar extraction, orthodontic osteotomy, or cyst extirpation [35].

These cells have the possibility to be attained from both young patients (6–53 years old [36]) and from older patients (57–62 years old [36]), taking into consideration that the age of the donor can have some influence on the gene expression pattern of BMSC [37].

Animal [37–39] and human studies [40–42] have described that grafted bone from the craniofacial area for autologous bone grafting at craniofacial locations produces greater results and considerably higher bone volume than bone extracted from the edochondral bone, such as rib or iliac crest.

Depending on the BMSC niche and type present in the graft, distinct skeletal different skeletal tissues have distinguishing regenerative qualities.

Following embryology, cranial neural crest cells create maxilla and mandible bones, and the mesoderm originates the iliac crest bone. This embryological explanation may be the reason why there are functional differences between the iliac crest human and orofacial BMSCs [41–44].

Studies revealed that orofacial BMSCs have functional and phenotype differences compared to the iliac crest BMSCs. In 2007, a group of researchers described that BMSCs derived from the orofacial site have a reduced differentiation potential with distinct expression patterns for several MSC marker genes when compared to the ones derived from the ilium, femur, and tibia [26]. Authors like Akintoye et al. reported specific site properties of the BMSCs derived from the orofacial and iliac crest of the same individual, where a greater proliferation and osteogenic differentiation ability was observed from the BMSCs derived from the orofacial site compared to the ones from the iliac crest. Furthermore, orofacial BMSCs' adipogenic potential is lower than those of the iliac, [43] which can lower the production of fat during bone tissue regeneration. The properties described from the orofacial BMSCs can be considered advantageous for bone regeneration. Nevertheless, the volume collected from the iliac crest bone marrow is higher than that from the orofacial bone marrow (0.03–0.5 ml) [36–45]. To sum up, authors suggest that, when applying BMSCs in clinical trials, a safe cell expansion and more reliable protocol must be rooted.

2.2.3. Dental Tissue-Derived Stem Cells.

Epithelial stem cells and MSC-like cells have been described in dental tissues. In 1999, through organ culture of the apical end of the mouse incisor, the first epithelial stem cell niche was established. The cervical loop of the tooth apex where the niche is located possibly contains dental epithelial stem cells, which have the ability to turn into enamel-producing amelobasts. There is no information available about human dental epithelial stem cells. This niche can be particular to rodents, since their incisors are different from all human dentition, erupting continuously throughout the animal's life.

Having the suitable conditions after dental procedures, dental tissues such as dental pulp and periodontal tissues are able to regenerate and form reparative dentine. We can find mesenchymal progenitor or stem cells in these types of tissues [46].

Various sources of MSC were verified in dental tissues, and isolated stem cells were also studied [47].

2.2.4. Periosteum-Derived Stem/Progenitor Cells.

Periosteum is the name given to the specialized connective tissue whose function is to cover the outer surface of the bone tissue. In 1932, author Fell firstly described the osteogenic potential of long bones periosteum and its membrane, having suggested its capacity to form a mineralized extracellular matrix if there were the suitable in vitro circumstances [48]. The histological periosteum composition is based on 2 different tears and up to 5 very distinct functional locations when dissociated enzymatically and cultured [49]. The external area contains elastic fibers and fibroblasts, and the interior area is constituted by MSCs, fibroblasts and osteoblasts,

osteogenic progenitor cells, microvessels, and sympathetic nerves [50].

These cells have the ability to differentiate into adipocytes, osteoblasts, and chondrocytes and to express the typical MSC markers. Furthermore, it was described that single-cell-derived clonal populations of adult human periosteal cells have a multipotential mesenchymal property, since they can turn into adipocytes, chondrocytes, osteoblasts, and skeletal myocyte lineages in vivo and in vitro. This can explain why periosteum-derived cells could be used in tissue engineering, in particular for bone regeneration.

Clinical research has demonstrated positive results when cells derived from the periosteum were applied for sinus or alveolar ridge augmentation, which showed reliable implant insertion, with improved bone remodeling and lamellar bone production, and also demonstrated that shorter postoperative waiting time was needed after implantation.

As a result, in case of large bone defects, the periosteum could be a source of stem/progenitor cells [51].

2.2.5. Salivary Gland-Derived Stem Cells.
Salivary gland-derived stem cells have been studied to be used for autologous transplantation treatment, for gland tissue engineering, and for cell treatments. The endoderm originates from the salivary glands, which compose the epithelial cells from the ductus and acinar cells with exocrine capacity. The epithelium proliferates when the link of the salivary gland duct occurs, and the acinar cells undergo apoptosis.

Stem cells that can differentiate into all kinds of epithelial cells within the gland have not yet been identified in literature [52, 53]. Salivary gland stem/progenitor cells were isolated from a rat submandibular gland, and it was found that these cells are highly proliferative and have the ability to express acinar, myoepithelial, and ductal cell lineage markers [54].

Studies suggest that salivary glands are a promising source for stem cells that can be used for therapy in patients that suffer from cancer to the head and neck and who have undergone radiotherapy.

Human salivary gland primitive MSC-like cells were isolated that evidence embryonic and adult stem cell markers and can be guided to differentiate into chondrogenic, osteogenic, and adipogenic cells [55]. The selection of a cell's particular marker or label with induced reporter proteins is essential to obtaining a considered actual stem cell culture for the salivary gland [56].

2.2.6. Adipose Tissue-Derived Stem Cells (ASCs).
Adipose tissue has been studied as a stem cell source in regenerative medicine, and it is considered an abundant MSC source. ASCs can be obtained through lipectomy or from lipoaspiration from areas such as the chin, hips, upper arms, and abdomen with low donor-site morbidity, as liposuction is a very common cosmetic procedure [57].

ASCs are expected to be an alternative source of MSCS in bone regeneration in the dental field, as they present a robust osteogenesis [58].

The practicability of using ASCs in GBR and implant surgery has already been tested [59].

More studies are needed, focusing on ASCs to be used clinically with efficacy in periodontal and bone regeneration.

2.3. Regenerative Dentistry with Stem Cell Application.
A suitable stem cell must carry out the control of cell outcome, guaranteeing patient safety in regenerative medicine.

MSCs currently have been described to have a clinical potential, since their regeneration potential in bone and periodontal tissue has been evaluated, and there are some clinical studies already published.

2.3.1. Differentiation Capacity.
BMSCs, especially periosteum-derived stem cells or bone marrow-derived stem cells, are appropriate for alveolar bone growth due to their compatibility with the target tissue. MSCs can also present promising results for dental mesenchymal-derived tissue regeneration, like periodontal tissues, pulp, or dentin. Nevertheless, MSCs' capacity of differentiating is restricted to mesenchymal lineages, which can retard the regeneration of complex oral organ application, since they are formed during development by epithelial and mesenchymal tissue interaction.

An option to achieve organ regeneration is to identify specific organ stem cells based on the ability of a single tissue-specific stem cell to form gastric units or epithelial components of the mammary glands [60, 61].

Studies have already demonstrated that pluripotent stem cells are a solution for complex organ renewal [62, 63], since there are no postnatal stem cells with organogenic capacity in teeth or salivary glands. Nevertheless, it is necessary to understand how it leads iPS cells to achieve specific progenitor cells for the tissue and organs targeted for renewal to obtain successful results. Further studies based on the development of iPS cell technology are necessary.

2.3.2. Immunomodulation.
Immunomodulation has been identified in MSCs with therapeutic effects in angiogenesis, anti-inflammation, and antiapoptosis. Studies also described that MSCs have a short inherent immunogenicity [64]. Other studies described that MSCs derived from human oral tissue (SHED, PDLSCs, SCAP, and GMSCs) have immunomodulatory characteristics equal to BMSCs [65–68].

Gingiva can be considered a promising origin of stem cells with future potential for immune-related therapies as well as for regenerative medicine, since GMSCs promote the oral mucosa progenitor cells to have a fetal phenotype with immunomodulation to be recognized by our immune system [69].

2.3.3. Regeneration.
MSCs hold promise in regenerative therapies due to their multipotency and availability. MSCs are being considered for the treatment of a wide range of pathologies, and researchers are especially interested in their potential to treat musculoskeletal disorders such as osteoarthritis, osteoporosis, and osteonecrosis [70].

An important MSC application in dentistry is pulp and dentin regeneration. Cell-based approaches in endodontic regeneration based on pulpal MSCs have demonstrated promising results in terms of pulp-dentin regeneration in vivo through autologous transplantation. Despite that pulpal regeneration requires the cell-based approach, several

challenges in clinical translation must be overcome including aging-associated phenotypic changes in pulpal MSCs, availability of tissue sources, and safety and regulation involved with expansion of MSCs in laboratories. Allotransplantation of MSCs can be an alternative in going through these obstacles; more research needs to be carried out on the long-term stability of MSCs and efficacy in pulp-dentin regeneration [71].

3. Clinical Applications

3.1. Evolution in Regenerative Therapy in Dentistry. Stem cell action contributes as a main factor to the capacity of self-renewal and differentiation of every organ and tissue.

The regeneration of lost oral tissue is the target of stem cell research. Owing to the fact that bone imperfections [72] that ensue after tooth loss can result in further bone loss which limits the success of dental implants and prosthodontic therapies, the rehabilitation of alveolar ridge height is prosthodontists' principal interest.

There are already different regenerative therapies based on stem cell technology available, namely, mesenchymal stem/stromal cells (MSCs). Although these cells have already been used in the clinic for alveolar bone augmentation, hardly anything is known about their in vivo biology [73].

In the clinic, the main approach to the treatment was the material-based reconstruction without major surgical procedures; nonetheless, the clinical concept was expanded, including stem cell-based regeneration, as a consequence of the emerging stem cell technologies and the requirements of alveolar ridge augmentation associated with implant dentistry [73].

The development of bioengineered teeth to replace the patient's missing teeth was also possible because of stem cell technologies.

The approach of regenerative dentistry has already been applied in implantology and periodontology [74]. In this text, we are going to do an assessment of the progress in regenerative therapies associated to periodontal tissue and alveolar bone.

3.1.1. Tissue Regeneration Based on Scaffolds. The periodontal regenerative therapy concept is based on the principal that, firstly, the source of infection must be removed and, secondly, a space for the cells to grow must be provided [75]. Guided tissue regeneration (GTR) is the most documented material used in periodontal regeneration [76, 77]. In this kind of regeneration, biocompatible barrier membranes are used to cover the bone defects. Using this technique, connective tissue and bone regeneration occurs within the bone defect. The bone defect is protected by a barrier with migration of epithelial tissues into the wound [78]. Bioinert materials, such as pure titanium membranes, PLGA, and ePTFE, cannot stimulate bone formation [79]. GBR and socket preservation are alveolar bone augmentation and preservation techniques that demand the application of bioactive materials to raise the activity of bone formation and therefore provide direct bonding with the bone. Hydroxyapatite, tricalcium phosphate (b-TCP: OSferion 1,

Olympus, Japan), biphasic calcium phosphate, and bovine bone mineral are CaP-based biomaterials. These materials are not osteoinductive materials since they cannot stimulate production of new bone in locations with lack of bone [80]. To permit and speed up bone formation and augment osteointegration of implants (underrating implant failure), the osteoinduction using bone grafting substitutes can be a solution when titanium implants are applied. For that reason, osteoinductive scaffolds based on CaP were engineered through osteogenic bioactive factor incorporation and have been reported to stimulate bone formation [81, 82].

Due to the fact that natural extracellular matrix (ECM) components modulate MSC osteogenic differentiation, adhesion, migration, and proliferation, it is beneficial for scaffolds to mimic the ECM [83].

Nevertheless, due to safety issues, it is not possible to apply them in the clinic animal-derived ECM. Other encouraging alternatives are synthetic peptide analogues of ECM components or bioactive small molecules [84].

For ECM-based biomimetic material acquisition, cell-derived decellularized extracellular matrices are likely to yield favorable results [85].

3.1.2. Growth Factor Delivery-Based Tissue Regeneration. Approaches which combine with scaffold-based tissue regeneration options have been increased by the growth factor delivery [86, 87]. The usage of platelet-rich plasma (PRP) is a well-known therapy which applies growth factor release to obtain periodontal regeneration. PRP can be utilized to regenerate periodontal defects, since it contains a variety of matrix components and growth factors. To obtain predictable periodontal regeneration, there is high interest in considering the application of PRP in combination with bone grafts or autologous stem cells [88].

A recent innovation in the field of medicine and dentistry is the development of autologous platelet-rich fibrin (PRF) as a growth factor delivery system. PRF is a platelet concentrate next to platelet-rich plasma with an advantage of simplified preparation and no biochemical blood handling. PRF represents a new step in the platelet gel therapeutic concept with simplified processing without artificial biochemical modification. The combined properties of fibrin, platelets, leucocytes, growth factors, and cytokines make platelet-rich fibrin a healing biomaterial with tremendous potential for bone and soft tissue regeneration. Interestingly, in 2014, a new protocol for PRF was introduced (termed Advanced-PRF or A-PRF) whereby centrifugal forces were decreased and total spin times were increased. This modification to centrifugation protocol has previously been shown to increase platelet cell number and monocyte/macrophage behavior [89].

Differences in growth factor components and platelet count between different PRP preparation procedures may be the reason why there are inconclusive results of clinical trials of PRP [90]. Enamel matrix derivative (EMD) product has also been extensively applied in periodontology for regeneration procedures [90, 91].

Some studies already described that EMD inhibits epithelial cell growth and induce periodontal fibroblast growth which may help in periodontal tissue regeneration [90–92].

Recombinant growth factors such as PDGF-BB and FGF-2 and BMP-2 were introduced for bone and periodontal regenerative treatments [93]. BMPs are known for their ability to induce bone formation and for playing an important role in embryonic patterning and early skeletal formation.

Another major factor in platelet-rich plasma is PDGF, which is known to induce angiogenesis [94, 95].

FGF-2 is a growth factor delivery, as it has several biological functions in tissue regeneration, inducing formation and growth of blood vessels and stem cell proliferation [93, 96].

MSC cultures are reported to stimulate bone formation in rats [97].

3.2. Stem Cells' Regenerative Therapy Requirements

3.2.1. Augmentation of Alveolar Bone. Taking into consideration that regular bone grafting materials have no osteoinductive properties, it is difficult to accomplish through material/growth factor-based procedures such as bone augmentation of the acutely atrophic alveolar ridge, especially vertical bone augmentation during guided bone regeneration or sinus-lifting. Activated osteoclasts bring out an unavoidable resorption which is the immune response against the transplants; even when used in combination with scaffolds, host cells are not able to migrate into a large defect area.

Due to the fact that autologous cancellous bone contains osteogenic, osteoconductive, and osteoinductive features provided by a suitable cellular content, it has been applied for big bone defects [98]. Nevertheless, the limited intraoral supply and difficulty in harvesting for autologous grafts have inspired another alternative method: the development of stem cell-based tissue engineering treatment [99]. Since the increasing demand of dental implants, there has also been an increasing demand for techniques related to bone augmentation in atrophic alveolar ridge and maxillary sinus.

Stem cells present an encouraging strategy to accomplish the regeneration of large alveolar bone defects, accelerate bone formation, and stimulate osteointegration in implant treatments.

3.3. Treatments Based on Stem Cells. The clinical application of stem cells has been analyzed in cases of alveolar ridge augmentation in dental implant rehabilitation. The clinical applications of stem cell-based bone augmentation are split into two groups: the chair-side cellular grafting and the tissue engineering approach. In either case, the most frequently applied stem cells are BMSCs from the iliac crest [100].

3.3.1. Approach of Tissue Engineering. The regenerative strategies using stem cells have utilized cell culture techniques to achieve bone tissue engineering [101].

Dental pulp-derived MSCs in combination with a collagen sponge scaffold can be used to restore human mandible bone defects. Regardless of the fact that stem cell-based tissue engineering has been suggested to be beneficial, there is criticism on the absence of characterization of the cellular component of the graft which can foreseeably produce consistent cell populations [102].

It is necessary to verify if tissue engineering based on cells ultimately has advantages for patients and to decide

definitive protocols for stem/osteoprogenitor cell preparation. Further studies on this subject are needed.

3.3.2. Approach of Chair-Side Cellular Grafting. Cellular graft derived from patients and prepared clinically or an allograft bone matrix that contains native MSCs is another alternative of bone regeneration based on stem cells [103].

There is evidence and good documentation about cellular grafting methods applying the mononuclear fraction obtained from processed fresh marrow. One of these methods is called "bone marrow aspirate concentrate (BMAC)." Stem cells that have the function of hematopoiesis and MSC population are two of the principal lineages of stem cells present in the mononuclear fraction [104].

The cells in freshly processed grafts may contain a variety of cell types, that is, stromal cells, angiogenic cells, MSCs, osteogenic cells, and hematopoietic cells. Some studies have reported that when BMSCs are administrated to an injured tissue or intravenously, it can have a positive anti-inflammatory effect [105, 106].

Further studies and research are needed to explain in detail the precise mechanisms of implanting BMSC population.

3.3.3. Tissue Regeneration Based on Cell Sheet. Cell sheet-based tissue regeneration has been applied successfully in tissue regeneration [107–110]. Enzymatic cell digestion and cell-to-cell contact are not needed since they remain intact, which is an advantage for regeneration of tissue. In addition, ECM proteins can be applied without requiring an additional scaffold.

A variety of cell sheets in tissue engineering have been described, for instance, using the cell sheet as a source of 3D pellet, applying multilayered cell sheet, and using the cell sheet to wrap a scaffold [111–116].

This technology has already been applied in periodontal and alveolar bone tissue regeneration [117–119].

Researchers reported that dental follicle cells (DFCs) could be an alternative for root and periodontal regeneration [120].

3.4. Regenerative Therapy Based on Stem Cells: Influencing Factors. The therapy based on stem cells is a new technology that has shown promising results for orofacial bone regeneration; nevertheless, these procedures are still poorly understood.

More clinical evidence is needed to understand if the new bone that was formed was provided by the implanted cells which survived or is from host osteogenic cells [121].

3.4.1. Transplanted Cells' Survival. Osteogenic cells which have the ability to retain the cellular activity to allow the cells that are transplanted to be able to produce ECMs for tissue regeneration are required for tissue engineering to be successful through cell transplantation [120].

Nevertheless, the destiny of cells and their clinical results are still unknown.

It was observed in animal studies that the cells that are transplanted can migrate out of the transplanted location or die quickly [122, 123].

In 2010, Tasso et al. demonstrated in an animal study that distinct waves of cells (CD31$^+$ endothelial progenitors and CD146$^+$ pericyte-like cells) migrated from the host to the BMSC-seeded ceramic to develop new tissue [124].

One year later, Boukhechba et al. proved that BMSC cells which were grafted did not survive more than a month after they were implanted [125].

More studies are needed to help understand the interaction of cells in bone regeneration treatment.

3.4.2. Donor Cells: The Preculture Condition. The preculture condition of cells that are transplanted was widely analyzed on bone formation.

It has been suggested that human BMSCs lose their in vivo osteogenic capacity in in vitro expansion, when cultured not regarding the osteogenic induction length [126].

Preculture periosteum-derived cells with biomimetic calcium and phosphate supplementation resulted in partial or complete ectopic bone formation, although CaP-based biomaterials have significant potential for bone regeneration [127].

The period is an important factor of in vitro preculture to regenerate the bone using BMSCs.

In majority of cases, undifferentiated MSCs were found; nevertheless, osteogenically induced MSCs were solely found in fewer cases. Thus, we can conclude that the host immune system can destroy these.

Optimal conditions for human BMSCs should be established once the protocol for bone regeneration based on stem cells is designed.

3.4.3. Cellular Grafting: Local Immune Responses. Ectopic bone formation applying stem cells that are transplanted in animal models does not have clinically predictable results for orthotopic bone formation in individuals.

The donor BMSCs can produce several anti-inflammatory factors to restrict the capacities of the various types of immune cells [128]. Even though the results of MSC-mediated immunosuppression are a restriction of T cell activation and proliferation, MSCs have also been shown to induce T cell differentiation into immunosuppressive Tregs [129, 130]. Furthermore, MSCs provoke recipient T cell apoptosis, resulting in an augmentation in the number of Tregs [131]. MSCs may also stimulate dendritic cells and macrophages to secrete IL, which in turn has an immunosuppressive effect on T cells [132].

Future clinical applications will be guided by BMSC biology, environment, and interactions.

3.5. Complex Oral Tissue/Organ Regeneration: Preclinical Studies. Due to their developmental and structural complexity, it was not possible to do a clinical trial about regeneration technologies for complex oral organs and tissues on the head and neck. Nevertheless, there are some advances based on animal research that have been known as good strategies to regenerate these tissues.

3.5.1. Root/Tooth Regeneration. The aim of tooth regeneration is to obtain a functional tooth which can replace the lost one [133]. Root regeneration is now a more clinical

applicable approach. Studies reported that using the root/periodontal complex constructed using periodontal and apical papilla stem cells would be able to support an artificial crown to provide normal tooth function in a model of a swine [134]. Additionally, DFCs were successfully used for tooth root reconstruction together with dentin matrix scaffold.

Tooth regeneration is one of the most important achievements in dentistry. Tooth structures from mice, rats, and pigs have been used in tooth engineering [135].

Bioengineered tooth transplantation has been proven to be a solution for tooth regenerative treatments, especially when an important alveolar bone loss exists [136].

This procedure is still an obstacle clinically when using tooth regeneration technology, and iPS cells can be considered a cell source [12].

3.5.2. Regeneration of Salivary Glands. Salivary gland regeneration is an interesting topic especially for head and neck oncology experts. Two regenerative approaches to restore the function of salivary glands have been applied. The first application is to obtain an artificial salivary gland by tissue engineering. The second application is to use stem cells in the damaged salivary tissue. There are some reports in specialized literature that refer that stem cells such as MSCs and BMSCS can be applied to reestablish the function of the damaged salivary glands [137].

A recent review article describes that using genetic lineage tracing in mice, the DNA label application to mark label-retaining quiescent cells, in vitro floating sphere assays, and two-dimensional (2D) or three-dimensional (3D) cultures of both human and rodent salivary glands cells demonstrated multiple stem/progenitor-like cells in the salivary glands. These cells can be identified and isolated, thanks to the expression of proteins and enzymes. These stem/progenitor cells present at different occasions during organ development and may compensate cell loss to allow suitable organ formation. Even during adult salivary gland homeostasis, multiple reservoir cell types in compartments have the ability to duplicate, maintain, and/or expand themselves [138].

3.5.3. Regeneration of Mandible Condyle. Tissue regeneration can be a solution to temporomandibular joint disc condyle defects or trauma. El-Bialy et al. reported in their study that BMSCs could increasingly regenerate a rabbit condyle that was enhanced by using pulsed ultrasound [139]. All these findings can help develop the concept for stem cell-based tissue engineering if there is condyle degeneration in case of disorders like rheumatoid arthritis.

3.5.4. Tongue Regeneration. Tongue regeneration has already been reported in animal studies with the objective of reconstructing tongue defects and reestablishing speech, swallowing function, and air protection [140, 141]. Cell-based reconstruction of the tongue was reported in a rat model, in which myoblast-progenitor cells were implanted in a hemiglossectomized tongue for muscle regeneration [140]. Nevertheless, functional regeneration is difficult in

the tongue. In 2013, Egusa et al. reported in their study that the application of cyclic strain to BMSCs stimulates the achievement of aligned myotube structures [142]. More advanced studies in stem cell engineering may help develop the regenerative techniques of the damaged or resected tongue and reestablish its role [142].

3.6. Immunotherapy with MSCs. MSCs have been expanded for the therapy of immune diseases.

3.6.1. Application BMSCs in Immune-Mediated Diseases. BMSCs constitute an important HSC niche component in the bone marrow [143].

They act in the repair process, thanks to cytokine and growth factors' secretion and endogenous progenitor cells' proliferation and differentiation [144]. Thus, transplanted or endogenous MSCs are stimulated by inflammatory cytokines (TNF-α) [145]. In addition, MSCs express matrix metalloproteinase to come through ECM barriers [146]. Some studies reported that BMSCs present an important immunomodulatory action. Therefore, it can be applied as a treatment for immune disorders [147, 148]. Thus, peripheral tolerance is induced by the administration of BMSCs, and the BMSCs then move to damaged tissues, where the release of proinflammatory cytokines is inhibited and cell survival is encouraged [148].

Several animal studies have examined BMSCs' effect in immune-mediated inflammatory diseases [149]. Additionally, MSCs' immunosuppressive effect in patients in case of refractory inflammatory bowel disease and graft versus host disease (GVHD) [150, 151] has been proven.

More studies are needed to explain MSCs' immunomodulatory effect before applying these cells therapeutically.

3.6.2. Immunotherapy with MSCs in Dentistry: Possible Applications. Reports demonstrated that transplanted allogeneic PDLSC sheets show decreased immunogenicity and marked immunosuppressive ability [151].

Studies reported the systemic delivery of dental MSCs to be applied in therapeutic strategies, since they can curb Th17 cell differentiation and an augmentation in the number of Treg cells [66, 152, 153].

All new MSCs' immunomodulatory features may be interesting to dental experts since they can be used for regenerative therapy and immunotherapy.

3.7. Banking of Stem Cells in Dentistry. Specialized studies have demonstrated that dental tissues are a rich source of MSCs, which can be applied in medical fields, particularly in immune and regenerative therapies [154].

The process of storing stem cells acquired from patients' deciduous teeth and wisdom teeth, called dental stem cell banking, is a strategy to realize the potential of dental stem cell-based regenerative therapy [155].

Stem cell-containing tissues are acquired from the patient and can be cryopreserved for many years to retain their regenerative capacity. Whenever required, dental stem cells, which are tolerated by the immune system, can be isolated from the cryopreserved tissue/tooth for future regenerative therapies [156, 157].

4. Conclusions

The oral and maxillofacial regions have been described as a promising source of adult stem cells. Dental clinicians should recognize the evolution of the regenerative dentistry field and take into consideration the possibility of acquiring stem cells during dental treatments (from deciduous teeth, third molars, and the gingiva), which can be stored for future autologous therapeutics.

We obtain iPS cells from discarded oral tissues that can be used in patient-specific modeling of oral diseases and the development of tailor-made diagnostic and drug screening tools for alveolar bone augmentation and oral cancer treatment, apart from the autologous cell-based regeneration of complex oral tissues. Nevertheless, more studies are needed to justify the application of these cells in autologous regenerative cells in the dental field.

Further studies on adult MSCs and BMSCs are needed to identify factors that have the responsibility to achieve successful results of stem cell-based bone and periodontal tissue regeneration. It is also important that researchers investigate more about the immunomodulatory properties of the stem cells, thus facilitating the grafting of transplanted cells at inflamed sites.

Further studies on adult stem cells and pluripotent stem cells should be developed to obtain more effective outcomes in the regenerative dentistry field.

Since it has more predictable regenerative results, future research areas of stem cell-based therapy in dentistry should be focused on tissue engineering and chair-side cellular grafting approaches.

To achieve more scientific evidence, more studies, such as clinical randomized controlled trials with long follow-ups, must be carried out.

There must also be a complete understanding of biological processes on both donor and recipient sides during bone regeneration which is extremely important to be able to structure more effective clinical strategies for stem cell-based bone regeneration.

MSCs' immunomodulatory function is important in suppressing the local immune response during transplantation and in achieving optimal tissue regeneration.

Prosthodontists are being motivated to get involved in stem cell biology by the increased requirement for new technologies for implant dentistry.

Authorized organizations should establish a link between stem cell-based dentistry, with standard protocols, so it can more often be applied in the dental field.

Conflicts of Interest

The authors have no conflict of interest related to the preparation and submission of this review.

References

[1] H. Egusa, "iPS cells in dentistry," *Clinical Calcium*, vol. 22, pp. 67–73, 2012.

[2] T. Kubo, K. Doi, K. Hayashi et al., "Comparative evaluation of bone regeneration using spherical and irregularly shaped granules of interconnected porous hydroxylapatite. A beagle dog study," *Journal of Prosthodontic Research*, vol. 55, no. 2, pp. 104–109, 2011.

[3] C. Jakobsen, J. A. Sørensen, M. Kassem, and T. H. Thygesen, "Mesenchymal stem cells in oral reconstructive surgery: a systematic review of the literature," *Journal of Oral Rehabilitation*, vol. 40, no. 9, pp. 693–706, 2013.

[4] J. Wray, T. Kalkan, and A. G. Smith, "The ground state of pluripotency," *Biochemical Society Transactions*, vol. 38, no. 4, pp. 1027–1032, 2010.

[5] J. A. Thomson, J. Itskovitz-Eldor, S. S. Shapiro et al., "Embryonic stem cell lines derived from human blastocysts," *Science*, vol. 282, no. 5391, pp. 1145–1147, 1998.

[6] A. M. Wobus and K. R. Boheler, "Embryonic stem cells: prospects for developmental biology and cell therapy," *Physiological Reviews*, vol. 85, no. 2, pp. 635–678, 2005.

[7] Y. Shamis, K. J. Hewitt, M. W. Carlson et al., "Fibroblasts derived from human embryonic stem cells direct development and repair of 3D human skin equivalents," *Stem Cell Research & Therapy*, vol. 2, no. 1, p. 10, 2011.

[8] N. Wada, B. Wang, N. H. Lin, A. L. Laslett, S. Gronthos, and P. M. Bartold, "Induced pluripotent stem cell lines derived from human gingival fibroblasts and periodontal ligament fibroblasts," *Journal of Periodontal Research*, vol. 46, no. 4, pp. 438–447, 2011.

[9] K. Otsu, R. Kishigami, A. Oikawa-Sasaki et al., "Differentiation of induced pluripotent stem cells into dental mesenchymal cells," *Stem Cells and Development*, vol. 21, no. 7, pp. 1156–1164, 2012.

[10] C. H. Hackett and L. A. Fortier, "Embryonic stem cells and iPS cells: sources and characteristics," *Veterinary Clinics of North America Equine Practice*, vol. 27, no. 2, pp. 233–242, 2011.

[11] X. Duan, Q. Tu, J. Zhang et al., "Application of induced pluripotent stem (iPS) cells in periodontal tissue regeneration," *Journal of Cellular Physiology*, vol. 226, no. 1, pp. 150–157, 2011.

[12] M. Arakaki, M. Ishikawa, T. Nakamura et al., "Role of epithelial-stem cell interactions during dental cell differentiation," *The Journal of Biological Chemistry*, vol. 287, no. 13, pp. 10590–10601, 2012.

[13] H. E. Young and A. C. Black Jr, "Adult stem cells," *The Anatomical Record. Part A, Discoveries in Molecular, Cellular, and Evolutionary Biology*, vol. 276A, no. 1, pp. 75–102, 2004.

[14] H. Egusa, W. Sonoyama, M. Nishimura, I. Atsuta, and K. Akiyama, "Stem cells in dentistry – part I : stem cell sources," *Journal of Prosthodontic Research*, vol. 56, no. 3, pp. 151–165, 2012.

[15] C. Mangano, F. Paino, R. d'Aquino et al., "Human dental pulp stem cells hook into biocoral scaffold forming an engineered biocomplex," *PLoS One*, vol. 6, no. 4, article e18721, 2011.

[16] H. H. Ahn, K. S. Kim, J. H. Lee et al., "*In vivo* osteogenic differentiation of human adipose-derived stem cells in an injectable *in situ*–forming gel scaffold," *Tissue Engineering Part A*, vol. 15, no. 7, pp. 1821–1832, 2009.

[17] A. Cicconetti, B. Sacchetti, A. Bartoli et al., "Human maxillary tuberosity and jaw periosteum as sources of osteoprogenitor cells for tissue engineering," *Oral Surgery, Oral Medicine, Oral Pathology, Oral Radiology, and Endodontics*, vol. 104, no. 5, pp. 618.e1–618.e12, 2007.

[18] G. J. Meijer, J. D. de Bruijn, R. Koole, and C. A. van Blitterswijk, "Cell based bone tissue engineering in jaw defects," *Biomaterials*, vol. 29, no. 21, pp. 3053–3061, 2008.

[19] A. J. Friedenstein, R. K. Chailakhjan, and K. S. Lalykina, "The development of fibroblast colonies in monolayer cultures of guinea-pig bone marrow and spleen cells," *Cell and Tissue Kinetics*, vol. 3, no. 4, pp. 393–403, 1970.

[20] M. F. Pittenger, A. M. Mackay, S. C. Beck et al., "Multilineage potential of adult human mesenchymal stem cells," *Science*, vol. 284, no. 5411, pp. 143–147, 1999.

[21] M. Ishii, C. Koike, A. Igarashi et al., "Molecular markers distinguish bone marrow mesenchymal stem cells from fibroblasts," *Biochemical and Biophysical Research Communications*, vol. 332, no. 1, pp. 297–303, 2005.

[22] E. M. Horwitz, K. le Blanc, M. Dominici et al., "Clarification of the nomenclature for MSC: the International Society for Cellular Therapy position statement," *Cytotherapy*, vol. 7, no. 5, pp. 393–395, 2005.

[23] M. Dominici, K. le Blanc, I. Mueller et al., "Minimal criteria for defining multipotent mesenchymal stromal cells. The International Society for Cellular Therapy position statement," *Cytotherapy*, vol. 8, no. 4, pp. 315–317, 2006.

[24] H.-J. Buhring, V. L. Battula, S. Treml, B. Schewe, L. Kanz, and W. vogel, "Novel markers for the prospective isolation of human MSC," *Annals of the New York Academy of Sciences*, vol. 1106, no. 1, pp. 262–271, 2007.

[25] V. L. Battula, S. Treml, P. M. Bareiss et al., "Isolation of functionally distinct mesenchymal stem cell subsets using antibodies against CD56, CD271, and mesenchymal stem cell antigen-1," *Haematologica*, vol. 94, no. 2, pp. 173–184, 2009.

[26] A. Igarashi, K. Segoshi, Y. Sakai et al., "Selection of common markers for bone marrow stromal cells from various bones using real-time RT-PCR: effects of passage number and donor age," *Tissue Engineering*, vol. 13, no. 10, pp. 2405–2417, 2007.

[27] H. Kubo, M. Shimizu, Y. Taya et al., "Identification of mesenchymal stem cell (MSC)-transcription factors by microarray and knockdown analyses, and signature molecule-marked MSC in bone marrow by immunohistochemistry," *Genes to Cells*, vol. 14, no. 3, pp. 407–424, 2009.

[28] A. R. Derubeis and R. Cancedda, "Bone marrow stromal cells (BMSCs) in bone engineering: limitations and recent advances," *Annals of Biomedical Engineering*, vol. 32, no. 1, pp. 160–165, 2004.

[29] H. Egusa, F. E. Schweizer, C. C. Wang, Y. Matsuka, and I. Nishimura, "Neuronal differentiation of bone marrow-derived stromal stem cells involves suppression of discordant phenotypes through gene silencing," *The Journal of Biological Chemistry*, vol. 280, no. 25, pp. 23691–23697, 2005.

[30] M. Dezawa, H. Ishikawa, Y. Itokazu et al., "Bone marrow stromal cells generate muscle cells and repair muscle degeneration," *Science*, vol. 309, no. 5732, pp. 314–317, 2005.

[31] M. Dezawa, H. Kanno, M. Hoshino et al., "Specific induction of neuronal cells from bone marrow stromal cells and application for autologous transplantation," *The Journal of Clinical Investigation*, vol. 113, no. 12, pp. 1701–1710, 2004.

[32] K. Stenderup, J. Justesen, E. F. Eriksen, S. I. S. Rattan, and M. Kassem, "Number and proliferative capacity of

osteogenic stem cells are maintained during aging and in patients with osteoporosis," *Journal of Bone and Mineral Research*, vol. 16, no. 6, pp. 1120–1129, 2001.

[33] S. C. Mendes, J. M. Tibbe, M. Veenhof et al., "Bone tissue-engineered implants using human bone marrow stromal cells: effect of culture conditions and donor age," *Tissue Engineering*, vol. 8, no. 6, pp. 911–920, 2002.

[34] S. Nishida, N. Endo, H. Yamagiwa, T. Tanizawa, and H. E. Takahashi, "Number of osteoprogenitor cells in human bone marrow markedly decreases after skeletal maturation," *Journal of Bone and Mineral Metabolism*, vol. 17, no. 3, pp. 171–177, 1999.

[35] S. M. Mueller and J. Glowacki, "Age-related decline in the osteogenic potential of human bone marrow cells cultured in three-dimensional collagen sponges," *Journal of Cellular Biochemistry*, vol. 82, no. 4, pp. 583–590, 2001.

[36] T. Matsubara, K. Suardita, M. Ishii et al., "Alveolar bone marrow as a cell source for regenerative medicine: differences between alveolar and iliac bone marrow stromal cells," *Journal of Bone and Mineral Research*, vol. 20, no. 3, pp. 399–409, 2005.

[37] J. E. Zins and L. A. Whitaker, "Membranous vs endochondral bone autografts: implications for craniofacial reconstruction," *Surgical Forum*, vol. 30, pp. 521–523, 1979.

[38] J. E. Zins and L. A. Whitaker, "Membranous versus endochondral bone: implications for craniofacial reconstruction," *Plastic and Reconstructive Surgery*, vol. 72, no. 6, pp. 778–784, 1983.

[39] C. M. G. Donovan, L. N. C. Dickerson, M. J. W. Hellstein, and M. L. J. Hanson, "Autologous calvarial and iliac onlay bone grafts in miniature swine," *Journal of Oral and Maxillofacial Surgery*, vol. 51, no. 8, pp. 898–903, 1993.

[40] R. Crespi, R. Vinci, P. Cappare, E. Gherlone, and G. E. Romanos, "Calvarial versus iliac crest for autologous bone graft material for a sinus lift procedure: a histomorphometric study," *The International Journal of Oral & Maxillofacial Implants*, vol. 22, no. 4, pp. 527–532, 2007.

[41] W. A. Borstlap, K. L. W. M. Heidbuchel, H. P. M. Freihofer, and A. M. Kuijpers-Jagtman, "Early secondary bone grafting of alveolar cleft defects. A comparison between chin and rib grafts," *Journal of Cranio-Maxillofacial Surgery*, vol. 18, no. 5, pp. 201–205, 1990.

[42] R. Koole, H. Bosker, and F. N. van der Dussen, "Late secondary autogenous bone grafting in cleft patients comparing mandibular (ectomesenchymal) and iliac crest (mesenchymal) grafts," *Journal of Cranio-Maxillo-Facial Surgery*, vol. 17, Supplement 1, pp. 28–30, 1989.

[43] S. O. Akintoye, T. Lam, S. Shi, J. Brahim, M. T. Collins, and P. G. Robey, "Skeletal site-specific characterization of orofacial and iliac crest human bone marrow stromal cells in same individuals," *Bone*, vol. 38, no. 6, pp. 758–768, 2006.

[44] I. H. Chung, T. Yamaza, H. Zhao, P. H. Choung, S. Shi, and Y. Chai, "Stem cell property of postmigratory cranial neural crest cells and their utility in alveolar bone regeneration and tooth development," *Stem Cells*, vol. 27, no. 4, pp. 866–877, 2009.

[45] J. Han, H. Okada, H. Takai, Y. Nakayama, T. Maeda, and Y. Ogata, "Collection and culture of alveolar bone marrow multipotent mesenchymal stromal cells from older individuals," *Journal of Cellular Biochemistry*, vol. 107, no. 6, pp. 1198–1204, 2009.

[46] D. W. Kao and J. P. Fiorellini, "Regenerative periodontal therapy," *Frontiers of Oral Biology*, vol. 15, pp. 149–159, 2012.

[47] K. Akiyama, C. Chen, S. Gronthos, and S. Shi, "Lineage differentiation of mesenchymal stem cells from dental pulp, apical papilla, and periodontal ligament," *Methods in Molecular Biology*, vol. 887, pp. 111–121, 2012.

[48] H. B. Fell, "The osteogenic capacity *in vitro* of periosteum and endosteum isolated from the limb skeleton of fowl embryos and young chicks," *Journal of Anatomy*, vol. 66, Part 2, pp. 157–180, 1932.

[49] M. R. Allen, J. M. Hock, and D. B. Burr, "Periosteum: biology, regulation, and response to osteoporosis therapies," *Bone*, vol. 35, no. 5, pp. 1003–1012, 2004.

[50] M. D. Ball, I. C. Bonzani, M. J. Bovis, A. Williams, and M. M. Stevens, "Human periosteum is a source of cells for orthopaedic tissue engineering: a pilot study," *Clinical Orthopaedics and Related Research*, vol. 469, no. 11, pp. 3085–3093, 2011.

[51] S. J. Zhu, B. H. Choi, J. Y. Huh, J. H. Jung, B. Y. Kim, and S. H. Lee, "A comparative qualitative histological analysis of tissue-engineered bone using bone marrow mesenchymal stem cells, alveolar bone cells, and periosteal cells," *Oral Surgery, Oral Medicine, Oral Pathology, Oral Radiology, and Endodontics*, vol. 101, no. 2, pp. 164–169, 2006.

[52] P. C. Denny and P. A. Denny, "Dynamics of parenchymal cell division, differentiation, and apoptosis in the young adult female mouse submandibular gland," *The Anatomical Record*, vol. 254, no. 3, pp. 408–417, 1999.

[53] Y. G. Man, W. D. Ball, L. Marchetti, and A. R. Hand, "Contributions of intercalated duct cells to the normal parenchyma of submandibular glands of adult rats," *The Anatomical Record*, vol. 263, no. 2, pp. 202–214, 2001.

[54] T. Kishi, T. Takao, K. Fujita, and H. Taniguchi, "Clonal proliferation of multipotent stem/progenitor cells in the neonatal and adult salivary glands," *Biochemical and Biophysical Research Communications*, vol. 340, no. 2, pp. 544–552, 2006.

[55] E. Gorjup, S. Danner, N. Rotter et al., "Glandular tissue from human pancreas and salivary gland yields similar stem cell populations," *European Journal of Cell Biology*, vol. 88, no. 7, pp. 409–421, 2009.

[56] R. P. Coppes and M. A. Stokman, "Stem cells and the repair of radiation-induced salivary gland damage," *Oral Diseases*, vol. 17, no. 2, pp. 143–153, 2011.

[57] H. Mizuno, M. Tobita, and A. C. Uysal, "Concise review: adipose-derived stem cells as a novel tool for future regenerative medicine," *Stem Cells*, vol. 30, no. 5, pp. 804–810, 2012.

[58] S. Kern, H. Eichler, J. Stoeve, H. Kluter, and K. Bieback, "Comparative analysis of mesenchymal stem cells from bone marrow, umbilical cord blood, or adipose tissue," *Stem Cells*, vol. 24, no. 5, pp. 1294–1301, 2006.

[59] K. Mesimäki, B. Lindroos, J. Törnwall et al., "Novel maxillary reconstruction with ectopic bone formation by GMP adipose stem cells," *International Journal of Oral and Maxillofacial Surgery*, vol. 38, no. 3, pp. 201–209, 2009.

[60] J. Stingl, P. Eirew, I. Ricketson et al., "Purification and unique properties of mammary epithelial stem cells," *Nature*, vol. 439, no. 7079, pp. 993–997, 2006.

[61] N. Barker, M. Huch, P. Kujala et al., "Lgr5^{+ve} stem cells drive self-renewal in the stomach and build long-lived gastric units in vitro," *Cell Stem Cell*, vol. 6, no. 1, pp. 25–36, 2010.

[62] M. Eiraku, N. Takata, H. Ishibashi et al., "Self-organizing optic-cup morphogenesis in three-dimensional culture," *Nature*, vol. 472, no. 7341, pp. 51–56, 2011.

[63] H. Suga, T. Kadoshima, M. Minaguchi et al., "Self-formation of functional adenohypophysis in three-dimensional culture," *Nature*, vol. 480, no. 7375, pp. 57–62, 2011.

[64] I. Rasmusson, M. Uhlin, K. Le Blanc, and V. Levitsky, "Mesenchymal stem cells fail to trigger effector functions of cytotoxic T lymphocytes," *Journal of Leukocyte Biology*, vol. 82, no. 4, pp. 887–893, 2007.

[65] L. Pierdomenico, L. Bonsi, M. Calvitti et al., "Multipotent mesenchymal stem cells with immunosuppressive activity can be easily isolated from dental pulp," *Transplantation*, vol. 80, no. 6, pp. 836–842, 2005.

[66] T. Yamaza, A. Kentaro, C. Chen et al., "Immunomodulatory properties of stem cells from human exfoliated deciduous teeth," *Stem Cell Research & Therapy*, vol. 1, no. 1, p. 5, 2010.

[67] N. Wada, D. Menicanin, S. Shi, P. M. Bartold, and S. Gronthos, "Immunomodulatory properties of human periodontal ligament stem cells," *Journal of Cellular Physiology*, vol. 219, no. 3, pp. 667–676, 2009.

[68] G. Ding, W. Wang, Y. Liu et al., "Effect of cryopreservation on biological and immunological properties of stem cells from apical papilla," *Journal of Cellular Physiology*, vol. 223, no. 2, pp. 415–422, 2010.

[69] L. C. Davies, H. Lönnies, M. Locke et al., "Oral mucosal progenitor cells are potently immunosuppressive in a dose-independent manner," *Stem Cells and Development*, vol. 21, no. 9, pp. 1478–1487, 2012.

[70] O. S. Beane, V. C. Fonseca, L. L. Cooper, G. Koren, and E. M. Darling, "Impact of aging on the regenerative properties of bone marrow-, muscle-, and adipose-derived mesenchymal stem/stromal cells," *PLoS One*, vol. 9, no. 12, article e115963, 2014.

[71] Y. Cao, M. Song, E. Kim et al., "Pulp-dentin regeneration: current state and future prospects," *Journal of Dental Research*, vol. 94, no. 11, pp. 1544–1551, 2015.

[72] H. G. Moghadam, "Vertical and horizontal bone augmentation with the intraoral autogenous J-graft," *Implant Dentistry*, vol. 18, no. 3, pp. 230–238, 2009.

[73] B. J. Costello, G. Shah, P. Kumta, and C. S. Sfeir, "Regenerative medicine for craniomaxillofacial surgery," *Oral and Maxillofacial Surgery Clinics of North America*, vol. 22, no. 1, pp. 33–42, 2010.

[74] J.-I. Sasaki, T.-A. Asoh, T. Matsumoto et al., "Fabrication of three-dimensional cell constructs using temperature-responsive hydrogel," *Tissue Engineering. Part A*, vol. 16, no. 8, pp. 2497–2504, 2010.

[75] I. G. Needleman, H. V. Worthington, E. Giedrys-Leeper, and R. J. Tucker, "Guided tissue regeneration for periodontal infra-bony defects," *Cochrane Database of Systematic Reviews*, no. 2, article CD001724, 2006.

[76] J. Gottlow, S. Nyman, J. Lindhe, T. Karring, and J. Wennstrom, "New attachment formation in the human periodontium by guided tissue regeneration. Case reports," *Journal of Clinical Periodontology*, vol. 13, no. 6, pp. 604–616, 1986.

[77] S. Nyman, J. Gottlow, J. Lindhe, T. Karring, and J. Wennstrom, "New attachment formation by guided tissue regeneration," *Journal of Periodontal Research*, vol. 22, no. 3, pp. 252–254, 1987.

[78] T. Karring, S. Nyman, J. Gottlow, and L. Laurell, "Development of the biological concept of guided tissue regeneration – animal and human studies," *Periodontology 2000*, vol. 1, no. 1, pp. 26–35, 1993.

[79] R. Z. LeGeros, "Calcium phosphate-based osteoinductive materials," *Chemical Reviews*, vol. 108, no. 11, pp. 4742–4753, 2008.

[80] R. Z. LeGeros, "Properties of osteoconductive biomaterials: calcium phosphates," *Clinical Orthopaedics and Related Research*, vol. 395, pp. 81–98, 2002.

[81] B. Klinge and T. F. Flemmig, "Tissue augmentation and esthetics (Working Group 3)," *Clinical Oral Implants Research*, vol. 20, no. 4, pp. 166–170, 2009.

[82] I. Darby, "Periodontal materials," *Australian Dental Journal*, vol. 56, Supplement 1, pp. 107–118, 2011.

[83] A. Ode, G. N. Duda, J. D. Glaeser et al., "Toward biomimetic materials in bone regeneration: functional behavior of mesenchymal stem cells on a broad spectrum of extracellular matrix components," *Journal of Biomedial Materials Research Part A*, vol. 95A, no. 4, pp. 1114–1124, 2010.

[84] H. Egusa, M. Saeki, M. Doi et al., "A small-molecule approach to bone regenerative medicine in dentistry," *Journal of Oral Biosciences*, vol. 52, no. 2, pp. 107–118, 2010.

[85] M. L. Decaris, A. Mojadedi, A. Bhat, and J. K. Leach, "Transferable cell-secreted extracellular matrices enhance osteogenic differentiation," *Acta Biomaterialia*, vol. 8, no. 2, pp. 744–752, 2012.

[86] F. Long, "Building strong bones: molecular regulation of the osteoblast lineage," *Nature Reviews Molecular Cell Biology*, vol. 13, no. 1, pp. 27–38, 2012.

[87] A. Teti, "Bone development: overview of bone cells and signaling," *Current Osteoporosis Reports*, vol. 9, no. 4, pp. 264–273, 2011.

[88] G. Intini, "The use of platelet-rich plasma in bone reconstruction therapy," *Biomaterials*, vol. 30, no. 28, pp. 4956–4966, 2009.

[89] R. J. Miron and J. Choukroun, *Regenerative Dentistry: Biological Background and Clinical Indications*, Wiley, Hoboken, NJ, USA, 1st edition, 2017.

[90] L. Hammarstrom, "Enamel matrix, cementum development and regeneration," *Journal of Clinical Periodontology*, vol. 24, no. 9, pp. 658–668, 1997.

[91] A. Sculean, F. Schwarz, J. Becker, and M. Brecx, "The application of an enamel matrix protein derivative (Emdogain) in regenerative periodontal therapy: a review," *Medical Principles and Practice*, vol. 16, no. 3, pp. 167–180, 2007.

[92] T. Kawase, K. Okuda, H. Yoshie, and D. M. Burns, "Cytostatic action of enamel matrix derivative (EMDOGAIN) on human oral squamous cell carcinoma-derived SCC25 epithelial cells," *Journal of Periodontal Research*, vol. 35, no. 5, pp. 291–300, 2000.

[93] S. Murakami, "Periodontal tissue regeneration by signaling molecule(s): what role does basic fibroblast growth factor (FGF-2) have in periodontal therapy?," *Periodontology 2000*, vol. 56, no. 1, pp. 188–208, 2011.

[94] J. Andrae, R. Gallini, and C. Betsholtz, "Role of platelet-derived growth factors in physiology and medicine," *Genes & Development*, vol. 22, no. 10, pp. 1276–1312, 2008.

[95] D. Ribatti, B. Nico, and E. Crivellato, "The role of pericytes in angiogenesis," *The International Journal of Developmental Biology*, vol. 55, no. 3, pp. 261–268, 2011.

[96] Y. Akagawa, T. Kubo, K. Koretake et al., "Initial bone regeneration around fenestrated implants in Beagle dogs using basic fibroblast growth factor-gelatin hydrogel complex with varying biodegradation rates," *Journal of Prosthodontic Research*, vol. 53, no. 1, pp. 41–47, 2009.

[97] M. Osugi, W. Katagiri, R. Yoshimi, T. Inukai, H. D. P. Hibi, and M. Ueda, "Conditioned media from mesenchymal stem cells enhanced bone regeneration in rat calvarial bone defects," *Tissue Engineering. Part A*, vol. 18, no. 13-14, pp. 1479–1489, 2012.

[98] W. Becker, B. E. Becker, and R. Caffesse, "A comparison of demineralized freeze-dried bone and autologous bone to induce bone formation in human extraction sockets," *Journal of Periodontology*, vol. 65, no. 12, pp. 1128–1133, 1994.

[99] M. Ueda, Y. Yamada, H. Kagami, and H. Hibi, "Injectable bone applied for ridge augmentation and dental implant placement: human progress study," *Implant Dentistry*, vol. 17, no. 1, pp. 82–90, 2008.

[100] A. De Rosa, V. Lanza, V. Tirino et al., "Human mandible bone defect repair by the grafting of dental pulp stem/progenitor cells and collagen sponge biocomplexes," *European Cells & Materials*, vol. 18, pp. 75–83, 2009.

[101] R. Schmelzeisen, R. Schimming, and M. Sittinger, "Making bone: implant insertion into tissue-engineered bone for maxillary sinus floor augmentation- a preliminary report," *Journal of Cranio-Maxillo-Facial Surgery*, vol. 31, no. 1, pp. 34–39, 2003.

[102] D. Kaigler, G. Pagni, C. H. Park, S. A. Tarle, R. L. Bartel, and W. V. Giannobile, "Angiogenic and osteogenic potential of bone repair cells for craniofacial regeneration," *Tissue Engineering. Part A*, vol. 16, no. 9, pp. 2809–2820, 2010.

[103] A. Gonshor, B. McAllister, S. S. Wallace, and H. Prasad, "Histologic and histomorphometric evaluation of an allograft stem cell-based matrix sinus augmentation procedure," *The International Journal of Oral & Maxillofacial Implants*, vol. 26, no. 1, pp. 123–131, 2011.

[104] A. I. Caplan, "Mesenchymal stem cells," *Journal of Orthopaedic Research*, vol. 9, no. 5, pp. 641–650, 1991.

[105] A. Mahmood, D. Lu, and M. Chopp, "Marrow stromal cell transplantation after traumatic brain injury promotes cellular proliferation within the brain," *Neurosurgery*, vol. 55, no. 5, pp. 1185–1193, 2004.

[106] Y. Zhou, S. Wang, Z. Yu et al., "Direct injection of autologous mesenchymal stromal cells improves myocardial function," *Biochemical and Biophysical Research Communications*, vol. 390, no. 3, pp. 902–907, 2009.

[107] T. Shimizu, M. Yamato, A. Kikuchi, and T. Okano, "Two-dimensional manipulation of cardiac myocyte sheets utilizing temperature-responsive culture dishes augments the pulsatile amplitude," *Tissue Engineering*, vol. 7, no. 2, pp. 141–151, 2001.

[108] K. Nishida, M. Yamato, Y. Hayashida et al., "Corneal reconstruction with tissue-engineered cell sheets composed of autologous oral mucosal epithelium," *The New England Journal of Medicine*, vol. 351, no. 12, pp. 1187–1196, 2004.

[109] M. Kanzaki, M. Yamato, H. Hatakeyama et al., "Tissue engineered epithelial cell sheets for the creation of a bioartificial trachea," *Tissue Engineering*, vol. 12, no. 5, pp. 1275–11283, 2006.

[110] T. Ohki, M. Yamato, D. Murakami et al., "Treatment of oesophageal ulcerations using endoscopic transplantation of tissue-engineered autologous oral mucosal epithelial cell sheets in a canine model," *Gut*, vol. 55, no. 12, pp. 1704–1710, 2006.

[111] Z. Yang, F. Jin, X. Zhang et al., "Tissue engineering of cementum/periodontal-ligament complex using a novel three-dimensional pellet cultivation system for human periodontal ligament stem cells," *Tissue Engineering. Part C, Methods*, vol. 15, no. 4, pp. 571–581, 2009.

[112] T. Iwata, M. Yamato, H. Tsuchioka et al., "Periodontal regeneration with multi-layered periodontal ligament-derived cell sheets in a canine model," *Biomaterials*, vol. 30, no. 14, pp. 2716–2723, 2009.

[113] M. G. Flores, M. Hasegawa, M. Yamato, R. Takagi, T. Okano, and I. Ishikawa, "Cementum-periodontal ligament complex regeneration using the cell sheet technique," *Journal of Periodontal Research*, vol. 43, no. 3, pp. 364–371, 2008.

[114] Y. Zhou, F. Chen, S. Ho, M. Woodruff, T. Lim, and D. Hutmacher, "Combined marrow stromal cell-sheet techniques and high-strength biodegradable composite scaffolds for engineered functional bone grafts," *Biomaterials*, vol. 28, no. 5, pp. 814–824, 2007.

[115] B. Yang, G. Chen, J. Li et al., "Tooth root regeneration using dental follicle cell sheets in combination with a dentin matrix-based scaffold," *Biomaterials*, vol. 33, no. 8, pp. 2449–2461, 2012.

[116] Z. Gao, F. Chen, J. Zhang et al., "Vitalisation of tubular coral scaffolds with cell sheets for regeneration of long bones: a preliminary study in nude mice," *The British Journal of Oral & Maxillofacial Surgery*, vol. 47, no. 2, pp. 116–122, 2009.

[117] T. Akizuki, S. Oda, M. Komaki et al., "Application of periodontal ligament cell sheet for periodontal regeneration: a pilot study in beagle dogs," *Journal of Periodontal Research*, vol. 40, no. 3, pp. 245–251, 2005.

[118] Y. Tsumanuma, T. Iwata, K. Washio et al., "Comparison of different tissue-derived stem cell sheets for periodontal regeneration in a canine 1-wall defect model," *Biomaterials*, vol. 32, no. 25, pp. 5819–5825, 2011.

[119] M. Nagata, H. Hoshina, M. Li et al., "A clinical study of alveolar bone tissue engineering with cultured autogenous periosteal cells: coordinated activation of bone formation and resorption," *Bone*, vol. 50, no. 5, pp. 1123–1129, 2012.

[120] Y. Bai, Y. Bai, K. Matsuzaka et al., "Cementum- and periodontal ligament-like tissue formation by dental follicle cell sheets co-cultured with Hertwig's epithelial root sheath cells," *Bone*, vol. 48, no. 6, pp. 1417–1426, 2011.

[121] F. Pieri, E. Lucarelli, G. Corinaldesi et al., "Dose-dependent effect of adipose-derived adult stem cells on vertical bone regeneration in rabbit calvarium," *Biomaterials*, vol. 31, no. 13, pp. 3527–3535, 2010.

[122] C. E. Zimmermann, M. Gierloff, J. Hedderich, Y. Acil, J. Wiltfang, and H. Terheyden, "Survival of transplanted rat bone marrow-derived osteogenic stem cells in vivo," *Tissue Engineering. Part A*, vol. 17, no. 7-8, pp. 1147–1156, 2011.

[123] J. Quintavalla, S. Uziel-Fusi, J. Yin et al., "Fluorescently labeled mesenchymal stem cells (MSCs) maintain multilineage potential and can be detected following implantation into articular cartilage defects," *Biomaterials*, vol. 23, no. 1, pp. 109–119, 2002.

[124] R. Tasso, F. Fais, D. Reverberi, F. Tortelli, and R. Cancedda, "The recruitment of two consecutive and different waves of

host stem/progenitor cells during the development of tissue-engineered bone in a murine model," *Biomaterials*, vol. 31, no. 8, pp. 2121–2129, 2010.

[125] F. Boukhechba, T. Balaguer, S. Bouvet-Gerbettaz et al., "Fate of bone marrow stromal cells in a syngenic model of bone formation," *Tissue Engineering. Part A*, vol. 17, no. 17-18, pp. 2267–2278, 2011.

[126] H. Agata, I. Asahina, N. Watanabe et al., "Characteristic change and loss of in vivo osteogenic abilities of human bone marrow stromal cells during passage," *Tissue Engineering. Part A*, vol. 16, no. 2, pp. 663–673, 2010.

[127] Y. C. Chai, S. J. Roberts, E. Desmet et al., "Mechanisms of ectopic bone formation by human osteoprogenitor cells on CaP biomaterial carriers," *Biomaterials*, vol. 33, no. 11, pp. 3127–3142, 2012.

[128] A. J. Nauta and W. E. Fibbe, "Immunomodulatory properties of mesenchymal stromal cells," *Blood*, vol. 110, no. 10, pp. 3499–3506, 2007.

[129] S. Aggarwal and M. F. Pittenger, "Human mesenchymal stem cells modulate allogeneic immune cell responses," *Blood*, vol. 105, no. 4, pp. 1815–1822, 2005.

[130] R. Maccario, M. Podestà, A. Moretta et al., "Interaction of human mesenchymal stem cells with cells involved in alloantigen-specific immune response favors the differentiation of CD4+ T-cell subsets expressing a regulatory/suppressive phenotype," *Haematologica*, vol. 90, no. 4, pp. 516–525, 2005.

[131] K. Akiyama, C. Chen, D. Wang et al., "Mesenchymal- stem-cell-induced immunoregulation involves FAS-ligand-/FAS-mediated T cell apoptosis," *Cell Stem Cell*, vol. 10, no. 5, pp. 544–555, 2012.

[132] S. Beyth, Z. Borovsky, D. Mevorach et al., "Human mesenchymal stem cells alter antigen-presenting cell maturation and induce T-cell unresponsiveness," *Blood*, vol. 105, no. 5, pp. 2214–2219, 2005.

[133] E. Ikeda and T. Tsuji, "Growing bioengineered teeth from single cells: potential for dental regenerative medicine," *Expert Opinion on Biological Therapy*, vol. 8, no. 6, pp. 735–744, 2008.

[134] W. Sonoyama, Y. Liu, D. Fang et al., "Mesenchymal stem cell-mediated functional tooth regeneration in swine," *PLoS One*, vol. 1, no. 1, article e79, 2006.

[135] C. S. Young, H. Abukawa, R. Asrican et al., "Tissue-engineered hybrid tooth and bone," *Tissue Engineering*, vol. 11, no. 9-10, pp. 1599–1610, 2005.

[136] M. Oshima, M. Mizuno, A. Imamura et al., "Functional tooth regeneration using a bioengineered tooth unit as a mature organ replacement regenerative therapy," *PLoS One*, vol. 6, no. 7, article e21531, 2011.

[137] L. S. Y. Nanduri, M. Maimets, S. A. Pringle, M. van der Zwaag, R. P. van Os, and R. P. Coppes, "Regeneration of irradiated salivary glands with stem cell marker expressing cells," *Radiotherapy and Oncology*, vol. 99, no. 3, pp. 367–372, 2011.

[138] I. Lombaert, M. M. Movahednia, C. Adine, and J. N. Ferreira, "Concise review: salivary gland regeneration: therapeutic approaches from stem cells to tissue organoids," *Stem Cells*, vol. 35, no. 1, pp. 97–105, 2017.

[139] T. El-Bialy, H. Uludag, N. Jomha, and S. F. Badylak, "In vivo ultrasound-assisted tissue-engineered mandibular condyle: a pilot study in rabbits," *Tissue Engineering. Part C, Methods*, vol. 16, no. 6, pp. 1315–1323, 2010.

[140] T. Luxameechanporn, T. Hadlock, J. Shyu, D. Cowan, W. Faquin, and M. Varvares, "Successful myoblast transplantation in rat tongue reconstruction," *Head & Neck*, vol. 28, no. 6, pp. 517–524, 2006.

[141] T. Bunaprasert, T. Hadlock, J. Marler et al., "Tissue engineered muscle implantation for tongue reconstruction: a preliminary report," *Laryngoscope*, vol. 113, no. 10, pp. 1792–1797, 2003.

[142] H. Egusa, M. Kobayashi, T. Matsumoto, J. I. Sasaki, S. Uraguchi, and H. Yatani, "Application of cyclic strain for accelerated skeletal myogenic differentiation of mouse bone marrow-derived mesenchymal stromal cells with cell alignment," *Tissue Engineering. Part A*, vol. 19, no. 5-6, pp. 770–782, 2013.

[143] S. Méndez-Ferrer, T. V. Michurina, F. Ferraro et al., "Mesenchymal and haematopoietic stem cells form a unique bone marrow niche," *Nature*, vol. 466, no. 7308, pp. 829–834, 2010.

[144] J. M. Karp and G. S. Leng Teo, "Mesenchymal stem cell homing: the devil is in the details," *Cell Stem Cell*, vol. 4, no. 3, pp. 206–216, 2009.

[145] W. Böcker, D. Docheva, W. C. Prall et al., "IKK-2 is required for TNF-alpha-induced invasion and proliferation of human mesenchymal stem cells," *Journal of Molecular Medicine*, vol. 86, no. 10, pp. 1183–1192, 2008.

[146] C. Ries, V. Egea, M. Karow, H. Kolb, M. Jochum, and P. Neth, "MMP-2, MT1- MMP, and TIMP-2 are essential for the invasive capacity of human mesenchymal stem cells: differential regulation by inflammatory cytokines," *Blood*, vol. 109, no. 9, pp. 4055–4063, 2007.

[147] A. Uccelli, V. Pistoia, and L. Moretta, "Mesenchymal stem cells: a new strategy for immunosuppression?," *Trends in Immunology*, vol. 28, no. 5, pp. 219–226, 2007.

[148] A. Uccelli, L. Moretta, and V. Pistoia, "Mesenchymal stem cells in health and disease," *Nature Reviews Immunology*, vol. 8, no. 9, pp. 726–736, 2008.

[149] L. Sun, K. Akiyama, H. Zhang et al., "Mesenchymal stem cell transplantation reverses multiorgan dysfunction in systemic lupus erythematosus mice and humans," *Stem Cells*, vol. 27, no. 6, pp. 1421–1432, 2009.

[150] K. Le Blanc, I. Rasmusson, B. Sundberg et al., "Treatment of severe acute graft-versus-host disease with third party haploidentical mesenchymal stem cells," *Lancet*, vol. 363, no. 9419, pp. 1439–1441, 2004.

[151] J. Liang, H. Zhang, D. Wang et al., "Allogeneic mesenchymal stem cell transplantation in seven patients with refractory inflammatory bowel disease," *Gut*, vol. 61, no. 3, pp. 468-469, 2012.

[152] T. Kikuiri, I. Kim, T. Yamaza et al., "Cell-based immunotherapy with mesenchymal stem cells cures bisphosphonate-related osteonecrosis of the jaw-like disease in mice," *Journal of Bone and Mineral Research*, vol. 25, no. 7, pp. 1668–1679, 2010.

[153] Q. Zhang, S. Shi, Y. Liu et al., "Mesenchymal stem cells derived from human gingiva are capable of immunomodulatory functions and ameliorate inflammation-related tissue destruction in experimental colitis," *Journal of Immunology*, vol. 183, no. 12, pp. 7787–7798, 2009.

[154] H. El-Menoufy, L. A. A. Aly, M. T. A. Aziz et al., "The role of bone marrow-derived mesenchymal stem cells in treating formocresol induced oral ulcers in dogs," *Journal of Oral Pathology & Medicine*, vol. 39, no. 4, pp. 281–289, 2010.

[155] M. Kaku, H. Kamada, T. Kawata et al., "Cryopreservation of periodontal ligament cells with magnetic field for tooth banking," *Cryobiology*, vol. 61, no. 1, pp. 73–78, 2010.

[156] V. Tirino, F. Paino, R. d'Aquino, V. Desiderio, A. De Rosa, and G. Papaccio, "Methods for the identification, characterization and banking of human DPSCs: current strategies and perspectives," *Stem Cell Reviews*, vol. 7, no. 3, pp. 608–615, 2011.

[157] H. Egusa, W. Sonoyama, M. Nishimura, I. Atsuta, and K. Akiyama, "Stem cells in dentistry – part II : clinical applications," *Journal of Prosthodontic Research*, vol. 56, no. 4, pp. 229–248, 2012.

Research Article

Comparative Effects of Umbilical Cord- and Menstrual Blood-Derived MSCs in Repairing Acute Lung Injury

Haitao Ren [ID],[1] Qiang Zhang [ID],[2,3] Jinfu Wang [ID],[4] and Ruolang Pan [ID][2,3]

[1]*Department of Burns and Wound Center, The Second Affiliated Hospital, School of Medicine, Zhejiang University, Hangzhou 310009, China*
[2]*Key Laboratory of Cell-Based Drug and Applied Technology Development in Zhejiang Province, Hangzhou 311121, China*
[3]*Institute for Cell-Based Drug Development of Zhejiang Province, S-Evans Biosciences, Hangzhou 311121, China*
[4]*Institute of Cell and Development, College of Life Science, Zhejiang University, Hangzhou 310058, China*

Correspondence should be addressed to Jinfu Wang; wjfu@zju.edu.cn and Ruolang Pan; ruolang_pan@163.com

Mesenchymal stem cells (MSCs) can effectively relieve acute lung injury (ALI) in several *in vivo* models. However, the underlying mechanisms and optimal sources of MSCs are unclear. In the present study, we investigated the effects of umbilical cord- (UC-) and menstrual blood- (MB-) derived MSCs on ALI. MSCs were transplanted into a lipopolysaccharide-induced ALI mouse model, and the therapeutic effects were determined by histological, cellular, and biochemical analyses. Our results showed that both UCMSC and MBMSC transplantation inhibited the inflammatory response and promoted lung tissue repair. UCMSC treatment resulted in reduced damage and inflammation in the lung tissue and enhanced protection of lung function. Furthermore, we found that UCMSCs secreted higher levels of anti-inflammatory cytokines (interleukin-10 and keratinocyte growth factor) in ALI-related conditions, which may be due to the greater therapeutic capacity of UCMSCs compared with MBMSCs. These findings suggest that MSCs protected the lipopolysaccharide-induced ALI model by regulating inflammation, most likely via paracrine factors. Moreover, MSCs derived from the UC may be a promising alternative for ALI treatment.

1. Introduction

Mesenchymal stem cells (MSCs) are stromal cells that can differentiate into various cell types such as osteoblasts, chondrocytes, adipocytes, myocytes, and hepatocytes [1, 2]. In addition to their presence in the bone marrow, MSCs have been found in multiple tissues, including umbilical cord blood, adipose tissue, placenta, adult muscle, and even menstrual blood [3, 4]. Promising features such as multipotency, secretion of growth factors, and immunoregulatory properties make MSCs suitable candidates for cell-based therapies [5]. Numerous studies have demonstrated the beneficial effects of MSC-based therapy for various diseases in animal models and clinical trials, such as in liver fibrosis, cartilage regeneration, nerve injury, and wound healing [6–9].

Acute lung injury (ALI) is a major cause of acute respiratory failure and has a high mortality rate in critical care medicine [10]. Although ALI pathophysiology and treatments have been investigated in many studies, effective pharmacotherapies or therapeutic strategies are limited [11]. MSCs may be a promising alternative for treating lung diseases [12, 13], as increasing evidence supports the therapeutic effects of MSCs in pulmonary fibrosis, bronchopulmonary dysplasia, chronic obstructive pulmonary disease, and ALI. Recent studies have also shown that transplantation of MSCs from the bone marrow, umbilical cord (UC), menstrual blood (MB), and adipose tissue can attenuate lung injury and inflammatory responses [14–16]. Mechanistic studies revealed that MSCs can differentiate into lung tissue cells or exhibit paracrine functions [17–19]. For further application in ALI therapy, additional studies are needed to optimize several parameters of MSC therapy, such as cell sources, infusion routes, and doses.

In the present study, we compared the effects of UC- and MB-derived MSCs (UCMSCs and MBMSCs, resp.) on ALI using a lipopolysaccharide- (LPS-) induced mouse model.

MSCs were intravenously transplanted into ALI animals, and their therapeutic effects were determined by histological, cellular, and biochemical analyses. We also preliminarily investigated the underlying mechanism by examining several cytokines secreted from these two types of MSCs.

2. Materials and Methods

2.1. Animals and Cells. Six- to eight-week-old imprinting control region (ICR) male mice were obtained from the Laboratory Animal Unit of Zhejiang Academy of Medical Sciences (Hangzhou, China). All animal experiments were performed in accordance with legal regulations and were approved by a local ethics committee. UCMSCs and MBMSCs were provided by S-Evans Biosciences (Hangzhou, China) and characterized as described previously [20]. Briefly, for UCMSC isolation, umbilical cord tissues (5–10 cm) were procured from healthy women during labor ($n = 3$) and cut into approximately 1 mm^3 pieces for primary adherent culturing. MBMSCs were isolated from menstrual blood samples collected from healthy female donors ($n = 3$) with a menstruation cup (S-Evans Biosciences). Cells that reached 80–90% confluence was digested with 0.25% trypsin-EDTA (Gibco, Carlsbad, CA) for passaging. UCMSCs and MBMSCs of passage 3 were characterized by morphology, surface marker expression, and mesenchymal lineage differentiation (osteogenic, adipogenic, and chondrogenic differentiation), after which they were used for further experiments.

2.2. Experimental Models and Treatments. For the ALI model, ICR mice were treated with LPS as described previously [21], with some modifications. Briefly, animals were anesthetized with pentobarbital (60 mg/kg) intraperitoneally and then intratracheally injected with either 2 mg/kg LPS (*Escherichia coli* O55 : B5, Sigma-Aldrich, St. Louis, MO) dissolved in 100 μL phosphate-buffered saline (PBS) or vehicle (PBS). After 6 h, 1×10^6 UCMSCs or MBMSCs in 100 μL PBS were transplanted intravenously into ALI mice through the tail vein and were defined as UCMSC- or MBMSC-treated groups. The animals were sacrificed 72 h posttransplantation, and samples were collected for further analysis.

2.3. Histological Analysis. Lung tissues were fixed with 4% paraformaldehyde and embedded in paraffin. Next, 5 μm tissue sections were deparaffinized and stained with hematoxylin and eosin. The extent of lung injury was assessed under a light microscope (Carl Zeiss, Oberkochen, Germany) and semiquantified by determining the lung injury score as described previously [22].

2.4. Wet/Dry Ratio Determination. Lung tissues were collected and weighed immediately to determine wet weight. The tissues were dried in an oven at 60°C for 48 h to determine dry weight. The wet/dry ratio was then calculated and defined as the W/D ratio [15].

2.5. Arterial Blood Gas Analysis. Arterial blood gas was analyzed as descried previously [23, 24]. Briefly, mice were anesthetized with pentobarbital (60 mg/kg) intraperitoneally. All animals breathed spontaneously during the experiment.

Then, blood samples were obtained from the celiac artery by heparinized syringes and immediately analyzed for oxygen partial pressure and oxygen saturation (sO$_2$) using an ABL700 blood gas analyzer (Radiometer, Copenhagen, Denmark). The oxygen partial pressure/fractional inspired oxygen (pO$_2$/FiO$_2$) ratio was also calculated.

2.6. Measurements of Bronchoalveolar Lavage Fluid (BALF). Mice were sacrificed, and the lungs were washed twice with 1 mL PBS for BALF sample collection. BALF was centrifuged at 300 ×g for 10 min. Cell pellets were resuspended in 200 μL PBS for total cell and neutrophil count using a Countstar IC1000 (Beijing, China). The supernatants were collected to detect total protein concentrations using a Bicinchoninic Acid (BCA) Protein Assay kit (Beyotime Biotechnology, Jiangsu, China), and myeloperoxidase (MPO) activity was determined using an MPO kit (Nanjing Jiancheng Technology, Ltd., Nanjing, China) according to the manufacturer's instructions.

2.7. Enzyme-Linked Immunosorbent Assay (ELISA) Analysis. The concentrations of interleukin- (IL-) 1β and tumor necrosis factor α (TNFα) in BALF and serum as well as IL-10 and keratinocyte growth factor (KGF) in lung tissues were measured using ELISA kits (RayBiotech Inc., Norcross, GA) according to the manufacturer's instructions.

2.8. Treatment of MSCs with BALF-S. BALF from ALI mice were collected and centrifuged as described above. The supernatants were then passed through a 0.22 μm filter and defined as BALF-S. Next, 1×10^6 UCMSCs or MBMSCs of passage 3 were cultured and treated with 5% (v/v) BALF-S for 12 h. The cells were further placed in serum-free medium for another 24 h. Cultured media were collected and passed through a 0.22 μm filter. Secreted IL-10 and KGF in the filtrate were examined using ELISA kits (RayBiotech) according to the manufacturer's instructions. Media from normal cultured UCMSCs or MBMSCs were used as controls. Furthermore, cell viability was measured using a Cell Counting Kit-8 assay (Beyotime Biotechnology) according to the manufacturer's instructions.

2.9. Statistical Analysis. All experiments were conducted at six times. Data are presented as the mean ± standard deviation. Statistical evaluation of differences between the values was determined by independent multiple Student's t-tests. P values of less than 0.05 were considered statistically significant.

3. Results

3.1. MSC Transplantation Attenuated Lung Injury in LPS-Induced ALI. UCMSCs and MBMSCs of passage 3 were characterized (Supplementary Figures 1 and 2) and transplanted intravenously into ALI mice. The therapeutic effects of MSCs on ALI were first evaluated by scoring hematoxylin and eosin-stained lung histological sections. The results showed that LPS-induced inflammatory infiltrates, interalveolar septal thickening, and other structural destruction were reduced by treatment with both UCMSCs and MBMSCs (Figure 1(a)). The degree of lung injury was further assessed

(a)

(b)
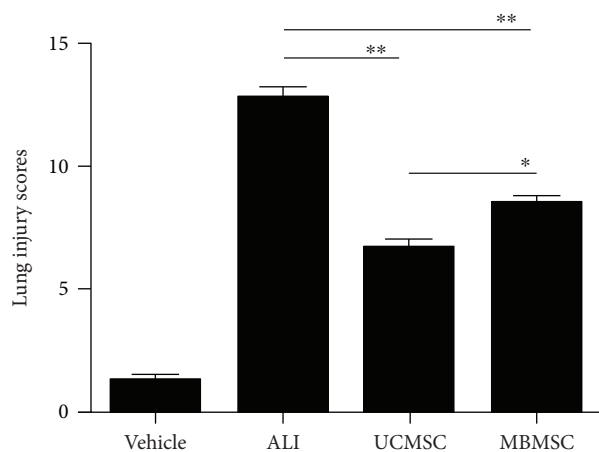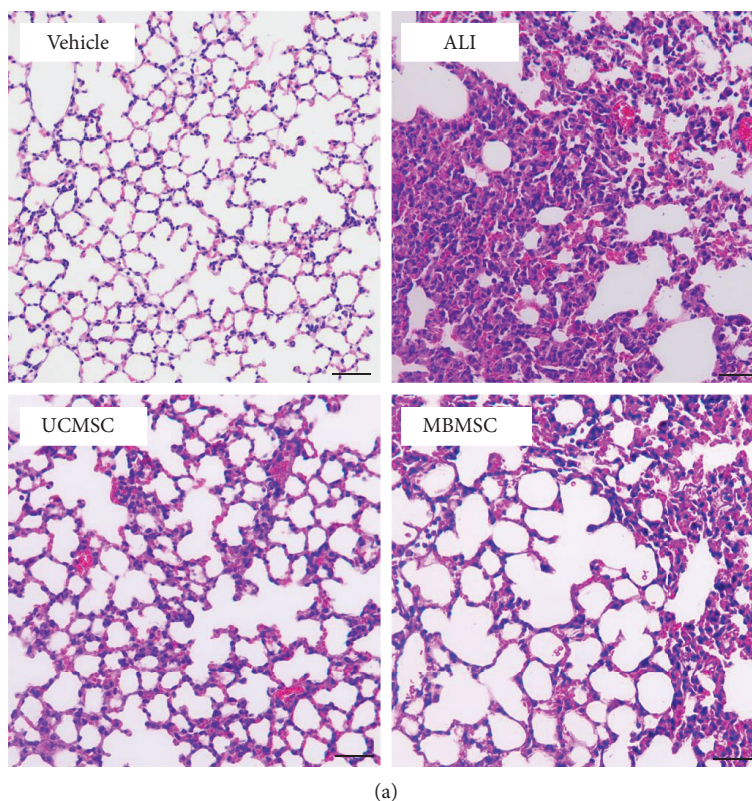
Figure 1: Assessment of histological changes in lung tissue. (a) HE-stained lung histological sections and representative lung histological changes. (b) Assessment of lung injury scores. The degree of lung injury was assessed from six sections, which conclude atelectasis, alveolar and interstitial inflammation, alveolar and interstitial hemorrhage, alveolar and interstitial edema, necrosis, and overdistension. Vehicle: normal mice with PBS injection; ALI: LPS-induced ALI model; UCMSC: ALI mice with UCMSC transplantation; MBMSC: ALI mice with MBMSC transplantation; HE: hematoxylin and eosin. Scale bars 50 μm. $*p < 0.05$, $**p < 0.01$; $n = 6$.

by lung injury score evaluation based on atelectasis, alveolar and interstitial inflammation, alveolar and interstitial hemorrhage, alveolar and interstitial edema, necrosis, and overdistension. UCMSC administration resulted in a more significant reduction in lung injury compared with that in the MBMSC-treated group, as determined by lung injury score (6.7 ± 0.3 versus 8.5 ± 0.2, resp.; Figure 1(b)). These results suggest that MSCs can improve damaged lung tissue in ALI, with UCMSCs showing greater efficiency.

3.2. MSC Treatment Improved Pulmonary Function. To evaluate the role of MSCs in the repair of pulmonary function [15, 23], W/D ratios and arterial blood gases were measured. We found that ALI mice treated with UCMSCs and MBMSCs showed significantly lower W/D ratios (Figure 2(a)) of 4.7 and 5.3, respectively, versus 7.0 in ALI animals. This result indicates that treatment with either type of MSCs can decrease the degree of LPS-induced lung edema. Arterial blood gas analysis (Figure 2(b)) showed that LPS
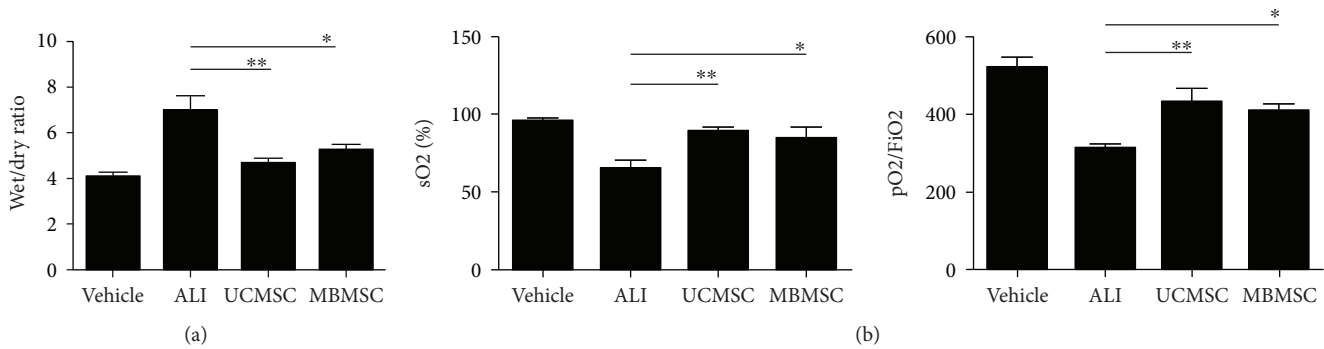
FIGURE 2: Indicator detections of pulmonary function. (a) Wet/dry ratio analysis. (b) The percentage of sO2 and the pO2/FiO2 ratio. Vehicle: normal mice with PBS injection; ALI: LPS-induced ALI model; UCMSC: ALI mice with UCMSC transplantation; MBMSC: ALI mice with MBMSC transplantation. $^{*}p < 0.05$, $^{**}p < 0.01$; $n = 6$.

decreased the sO_2 percentage (65.0%) and pO_2/FiO_2 ratio (314) compared with that of the vehicle group (95.5% and 519, resp.), whereas UCMSC and MBMSC treatments resulted in increased levels of both parameters, suggesting improvements in lung function recovery. Moreover, these results revealed that UCMSCs and MBMSCs have similar effects on lung function protection.

3.3. MSC Administration Reduced the Degree of Changes in BALF. To further analyze lung damage and inflammation, cellular counts and protein concentrations in BALF were examined. Total protein levels and cell numbers in BALF increased in LPS-induced ALI mice but decreased in UCMSC- and MBMSC-treated groups (Figures 3(a) and 3(b)). The numbers of neutrophils in BALF were significantly elevated by LPS induction but decreased in both MSC-treated groups. Moreover, we found that UCMSC transplantation resulted in a greater reduction in neutrophil numbers compared with MBMSCs $(0.6 \pm 0.08) \times 10^6/mL$ versus $(1.6 \pm 0.41) \times 10^6/mL$, respectively (Figure 3(c)). This was further supported by MPO activity measurements, which gave values of 0.7 ± 0.11 U/L for the UCMSC group and 1.1 ± 0.22 U/L for the MBMSC group (Figure 3(d)). These results suggest not only that both types of MSCs do improve lung damage in ALI but also that UCMSCs can reduce cellular infiltration in an efficient manner.

3.4. MSCs Regulate the Expression of Inflammatory Cytokines. To investigate inflammatory regulation by MSCs, we analyzed expression levels of the proinflammatory cytokines IL-1β and TNFα in serum (Figure 4(a)) and BALF (Figure 4(b)) via ELISA. The concentration of IL-1β and TNFα in serum and BALF was clearly elevated in the LPS-induced group and significantly reduced after MSC transplantation. The UCMSC-treated group showed a greater reduction in serum IL-1β $(323 \pm 23.9$ ng/L) and BALF TNFα $(692 \pm 53.9$ ng/L) levels compared with the MBMSC-treated group $(368 \pm 36.4$ ng/L and 850 ± 25.4 ng/L, resp.). These results indicate that both types of MSCs decrease the expression of inflammatory cytokines.

3.5. MSC Treatment Upregulated the Expression of IL-10 and KGF in Lung Tissues. The expression of IL-10 (Figure 5(a)), a

representative anti-inflammatory cytokine, was elevated both in MSC-treated groups and in the LPS-induced group. The results also showed that UCMSCs induced much higher levels of IL-10 in lung tissues compared with MBMSCs. Similarly, KGF, a potent mitogenic factor in alveolar epithelial cells, also showed increased expression in the MSC group, particularly in the UCMSC-treated group (Figure 5(b)). These findings suggest that MSCs attenuate lung injury and the inflammatory response by regulating the expression of several crucial factors.

3.6. BALF-S Stimulates IL-10 and KGF Secretion by MSCs. We further investigated the secretion of soluble factors by MSCs which may contribute to the upregulation of IL-10 and KGF in lung tissues after MSC treatment. Paracrine factors IL-10 and KGF secreted by UCMSCs and MBMSCs after BALF-S stimulation were measured in culture media (Figure 6). The results showed that both types of MSCs secreted the two factors at comparable levels under normal culture conditions. After BALF-S treatment, expression levels of IL-10 and KGF increased to different extents and without any significant changes in cell viability (Supplementary Figure 3). BALF-S stimulation resulted in significantly enhanced secretion of IL-10 and KGF by UCMSCs (from 731 to 1316 pg/mL and 700 to 976 pg/mL, resp.) but not by MBMSCs. These results indicate that paracrine factors secreted by MSCs may partially contribute to the increased levels of IL-10 and KGF in MSC-treated lung tissues. Moreover, UCMSCs produced increased levels of cytokines or paracrine factors in response to the inflammatory condition, resulting in the more efficient in anti-inflammatory regulation observed in the UCMSC-treated group.

4. Discussion

The main findings of this study were that MSCs from both sources reduced lung injury and improved lung function in LPS-induced ALI mice to different extents, that MSCs may inhibit inflammatory responses by secreting anti-inflammatory cytokines to relieve lung injury, and that UCMSCs exhibited greater therapeutic effects than MBMSCs.
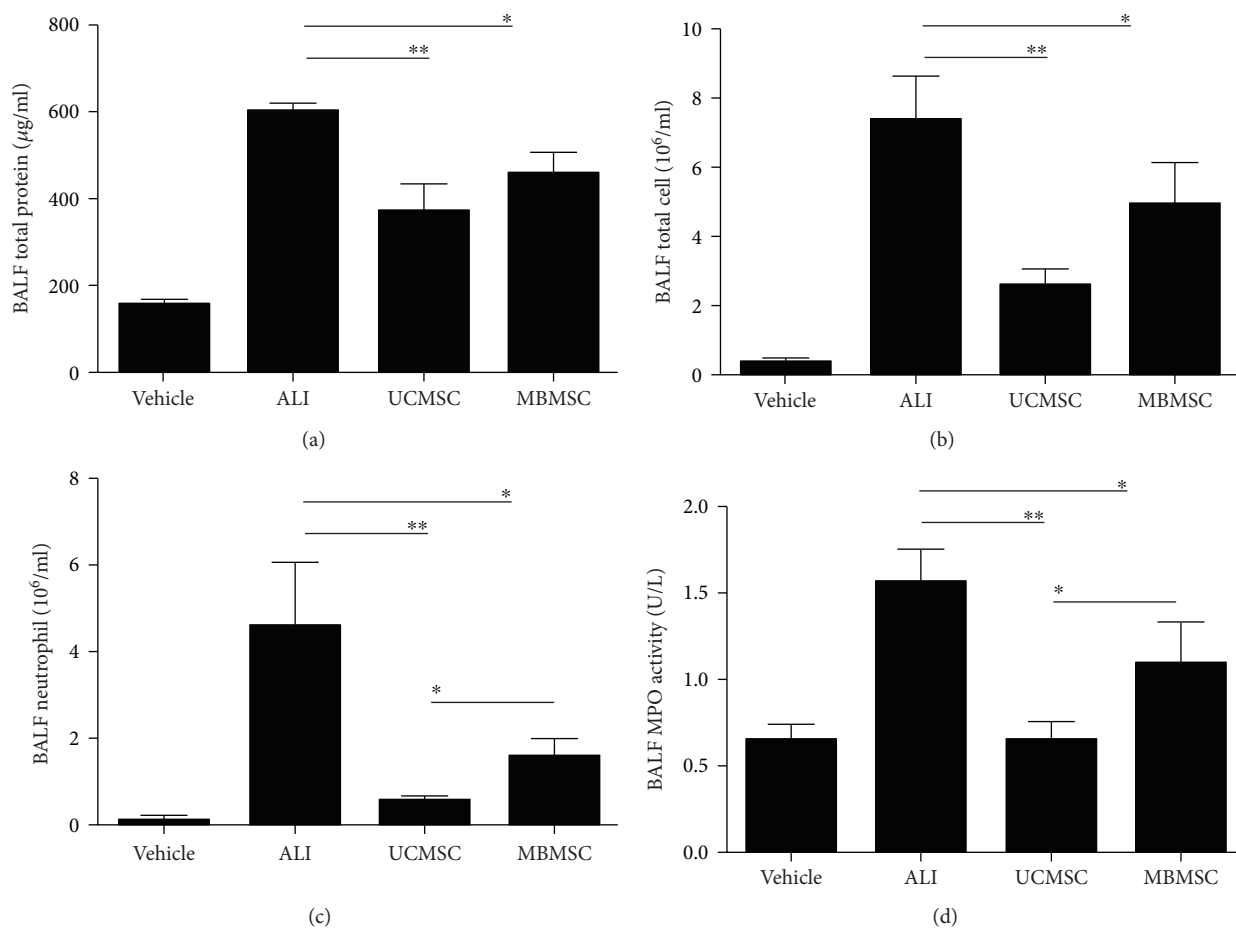
FIGURE 3: Detection of cell numbers and protein levels in BALF. (a) The concentrations of total protein in BALF. (b) Total cell counts in BALF. (c) Neutrophil counts in BALF. (d) Evaluation of MPO activity in BALF. Vehicle: normal mice with PBS injection; ALI: LPS-induced ALI model; UCMSC: ALI mice with UCMSC transplantation; MBMSC: ALI mice with MBMSC transplantation. $^*p < 0.05$, $^{**}p < 0.01$; $n = 6$.

This difference may be due to the increased secretion of anti-inflammatory cytokines by UCMSCs after transplantation in an inflammatory environment rather than differences in cell retention between MBMSCs and UCMSCs in injured lung tissue (Supplementary Figure 4). However, the underlying mechanism regarding whether secretion of other anti-inflammatory cytokines or exosomes by UCMSCs are involved requires further analysis.

Over the past decades, numerous preclinical studies on MSC-based therapies have been conducted due to the promising features of MSCs. Studies on lung disease therapies have focused on the ability of MSCs to secrete soluble factors, such as anti-inflammatory and cytokine growth factors, which can stabilize the alveolocapillary barrier, enhance alveolar fluid clearance, and decrease infection [25–28]. Clinical trials of lung disease therapies have also been conducted in recent years. In a double-blind randomized single-center trial, Zheng et al. [26] found that it is safe to inject human MSCs intravenously in 12 acute respiratory distress syndrome patients. In 2015, Wilson et al. [27] showed that intravenous administration of human MSCs was well tolerated in 9 patients with acute respiratory distress syndrome in a phase 1 clinical trial;

based on these promising results, a phase 2 clinical study is currently underway.

Although the results are promising, the optimal dose, route of MSC administration, MSC sources, and precise mechanisms remain unclear. As a potential mechanism, the therapeutic effect of MSCs may be due to the secretion of soluble factors [28]. In ALI models, IL-10, prostaglandin E2, and KGF were shown to be secreted by MSCs to inhibit lung inflammation or protect against alveolar epithelium injury [29–32]. Our findings support the notion that MSCs secrete paracrine anti-inflammatory cytokines (IL-10 and KGF) to attenuate the inflammatory response and ameliorate lung injury. More importantly, we found that UCMSCs are more sensitive to inflammatory conditions and produced more cytokines or paracrine factors for lung repair in ALI. Although it is theoretically easy to obtain MBMSCs from monthly menstrual blood, we found that menstrual blood is prone to microbial contamination during the collection process (unpublished data). It was also found that MBMSCs have a weaker amplification capability compared with UCMSCs [20]. Taking these findings into consideration, UCMSCs appear to be more feasible for application in future
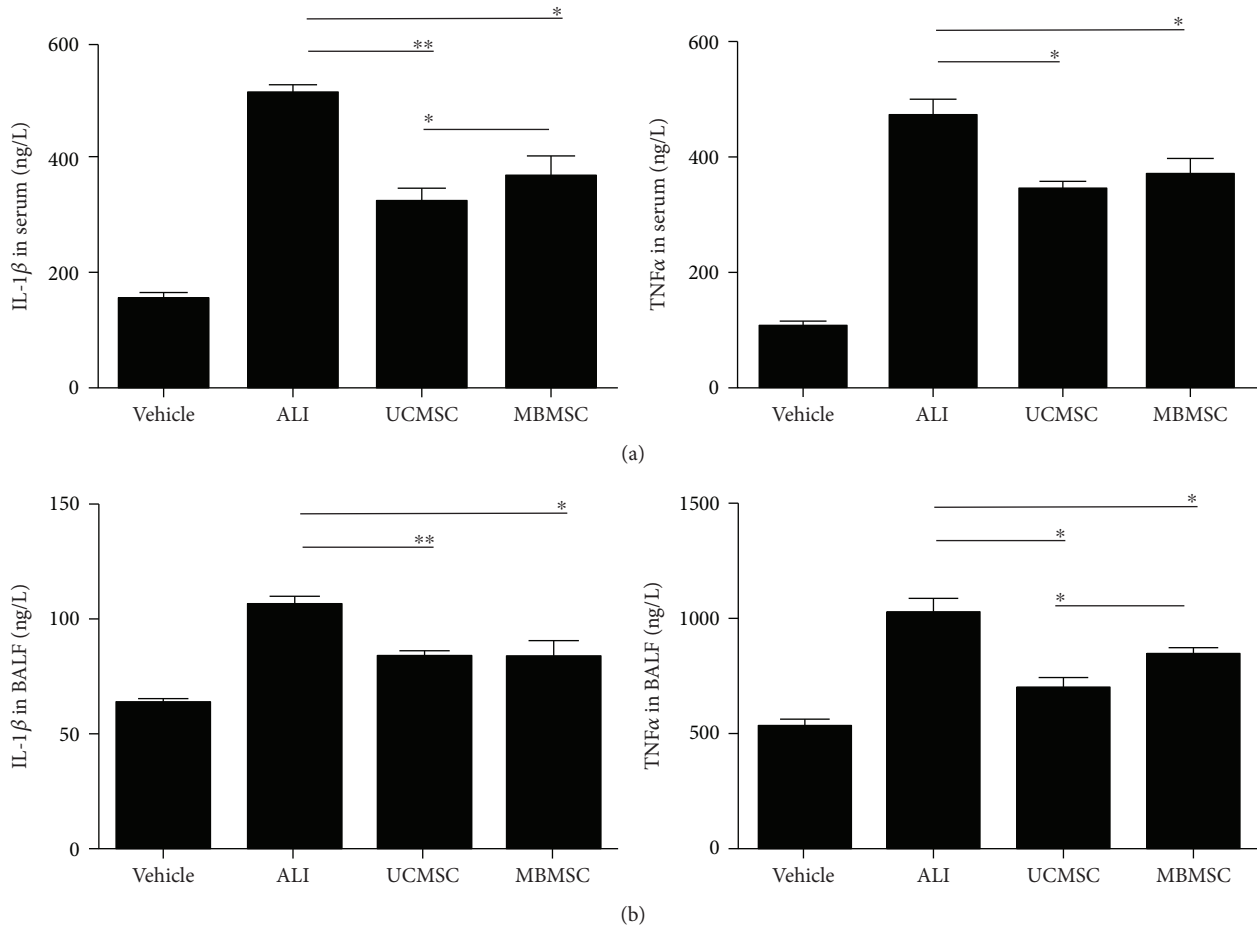
FIGURE 4: Analysis of inflammatory cytokines in serum and BALF. (a, b) The expression levels of IL-1β and TNFα in serum and BALF were detected by ELISA. Vehicle: normal mice with PBS injection; ALI: LPS-induced ALI model; UCMSC: ALI mice with UCMSC transplantation; MBMSC: ALI mice with MBMSC transplantation. $^*p < 0.05$, $^{**}p < 0.01$; $n = 6$.
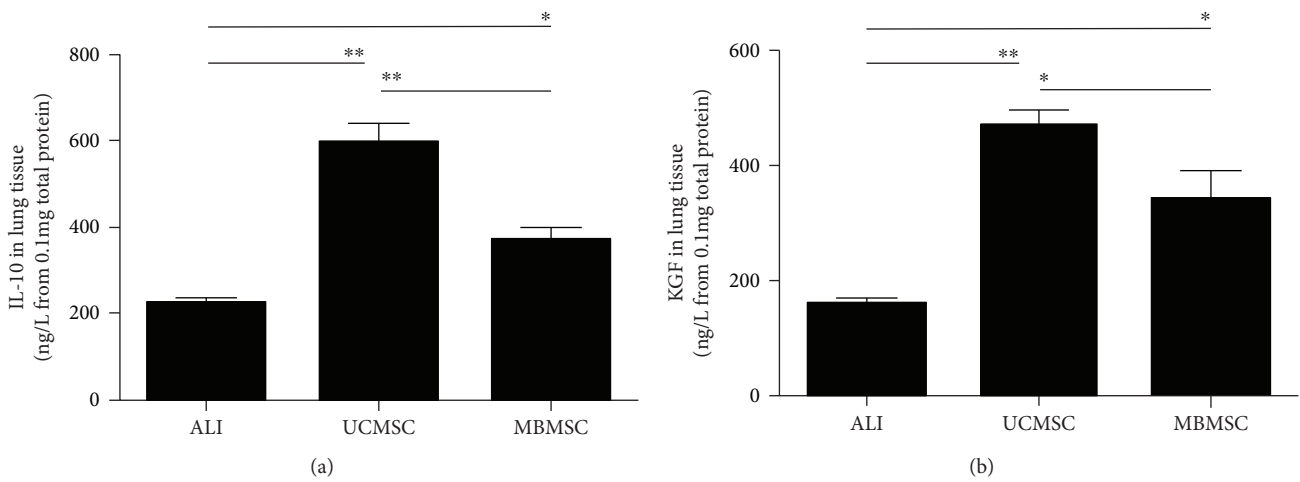
FIGURE 5: Examine the anti-inflammatory factor levels in lung tissues. (a, b) Expression levels of IL-10 and KGF in the lung tissues were detected by ELISA. ALI: LPS-induced ALI model; UCMSC: ALI mice with UCMSC transplantation; MBMSC: ALI mice with MBMSC transplantation. $^*p < 0.05$, $^{**}p < 0.01$; $n = 6$.

(a)

(b)
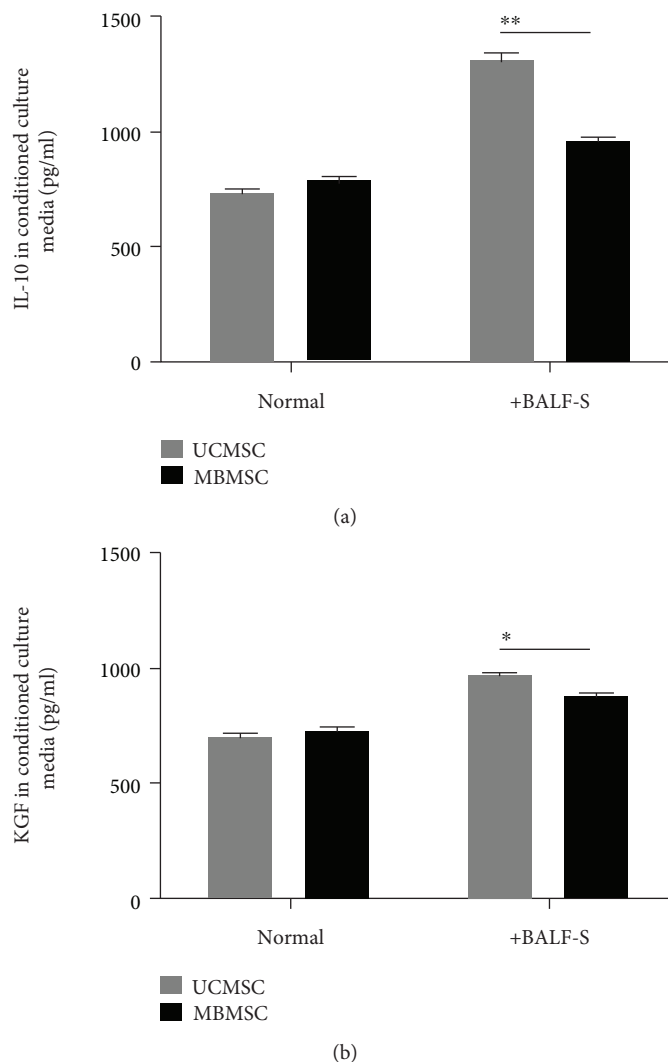
FIGURE 6: BALF-S-induced production of anti-inflammatory cytokines in cultured MSCs. (a, b) UCMSCs and MBMSCs were stimulated by 5% BALF-S (v/v), and the paracrine secretions of IL-10 and KGF in culture media were detected by ELISA. Normal: normal cultured groups; +BALF-S: 5% BALF-S-treated groups. $^*p < 0.05$, $^{**}p < 0.01$; $n = 6$.

ALI therapies. However, uncovering the precise mechanisms requires further investigation.

5. Conclusions

Our findings strongly support the use of UCMSCs and MBMSCs in ALI and other inflammatory lung disease therapies. Moreover, UCMSCs showed enhanced therapeutic effects compared with MBMSCs, indicating that UCMSCs are more promising for ALI treatment. Nevertheless, the specific mechanism underlying MSC-based ALI therapy requires further investigation.

Data Availability

The datasets generated during and/or analyzed during the current study are available from the corresponding author on a reasonable request.

Conflicts of Interest

The authors declare that they have no conflicts of interest.

Authors' Contributions

Haitao Ren and Qiang Zhang designed and performed the study. Ruolang Pan analyzed the data and wrote the manuscript. Jinfu Wang revised the manuscript. All authors read and approved the final manuscript.

Acknowledgments

Supplementary Materials

Supplementary Figure 1: characterization of UCMSC and MBMSC by morphological analysis and measurement of representative surface markers. Supplementary Figure 2: characterization of UCMSC and MBMSC by mesenchymal lineage differentiation. Supplementary Figure 3: cell viability assay for BALF-S-treated UCMSC and MBMSC. Supplementary Figure 4: detection of retained UCMSC and MBMSC in lung tissues at 72 h posttransplantation. *(Supplementary Materials)*

References

[1] J. A. Ankrum, J. F. Ong, and J. M. Karp, "Mesenchymal stem cells: immune evasive, not immune privileged," *Nature Biotechnology*, vol. 32, no. 3, pp. 252–260, 2014.

[2] R. S. Mahla, "Stem cells applications in regenerative medicine and disease therapeutics," *International Journal of Cell Biology*, vol. 2016, Article ID 6940283, 24 pages, 2016.

[3] S. Wang, X. Qu, and R. C. Zhao, "Clinical applications of mesenchymal stem cells," *Journal of Hematology & Oncology*, vol. 5, no. 1, p. 19, 2012.

[4] M. J. Branch, K. Hashmani, P. Dhillon, D. R. E. Jones, H. S. Dua, and A. Hopkinson, "Mesenchymal stem cells in the human corneal limbal stroma," *Investigative Ophthalmology & Visual Science*, vol. 53, no. 9, pp. 5109–5116, 2012.

[5] T. Squillaro, G. Peluso, and U. Galderisi, "Clinical trials with mesenchymal stem cells: an update," *Cell Transplantation*, vol. 25, no. 5, pp. 829–848, 2016.

[6] Y. W. Eom, K. Y. Shim, and S. K. Baik, "Mesenchymal stem cell therapy for liver fibrosis," *The Korean Journal of Internal Medicine*, vol. 30, no. 5, pp. 580–589, 2015.

[7] D. Cui, H. Li, X. Xu et al., "Mesenchymal stem cells for cartilage regeneration of TMJ osteoarthritis," *Stem Cells International*, vol. 2017, Article ID 5979741, 11 pages, 2017.

[8] S. Sayad Fathi and A. Zaminy, "Stem cell therapy for nerve injury," *World Journal of Stem Cells*, vol. 9, no. 9, pp. 144–151, 2017.

[9] M. Li, Y. Zhao, H. Hao, W. Han, and X. Fu, "Mesenchymal stem cell-based therapy for nonhealing wounds: today and tomorrow," *Wound Repair and Regeneration*, vol. 23, no. 4, pp. 465–482, 2015.

[10] S. Han and R. K. Mallampalli, "The acute respiratory distress syndrome: from mechanism to translation," *Journal of Immunology*, vol. 194, no. 3, pp. 855–860, 2015.

[11] C. F. Su, S. J. Kao, and H. I. Chen, "Acute respiratory distress syndrome and lung injury: pathogenetic mechanism and therapeutic implication," *World Journal of Critical Care Medicine*, vol. 1, no. 2, pp. 50–60, 2012.

[12] R. Guillamat-Prats, M. Camprubi-Rimblas, J. Bringue, N. Tantinya, and A. Artigas, "Cell therapy for the treatment of sepsis and acute respiratory distress syndrome," *Annals of Translational Medicine*, vol. 5, no. 22, p. 446, 2017.

[13] Y. Zhu, X. Chen, X. Yang, J. Ji, and A. El-Hashash, "Stem cells in lung repair and regeneration: current applications and future promise," *Journal of Cellular Physiology*, 2018.

[14] Q. Hao, Y. G. Zhu, A. Monsel et al., "Study of bone marrow and embryonic stem cell-derived human mesenchymal stem cells for treatment of Escherichia coli endotoxin-induced acute lung injury in mice," *Stem Cells Translational Medicine*, vol. 4, no. 7, pp. 832–840, 2015.

[15] B. Xiang, L. Chen, X. Wang, Y. Zhao, Y. Wang, and C. Xiang, "Transplantation of menstrual blood-derived mesenchymal stem cells promotes the repair of LPS-induced acute lung injury," *International Journal of Molecular Sciences*, vol. 18, no. 4, 2017.

[16] R. J. Cho, Y. S. Kim, J. Y. Kim, and Y. M. Oh, "Human adipose-derived mesenchymal stem cell spheroids improve recovery in a mouse model of elastase-induced emphysema," *BMB Reports*, vol. 50, no. 2, pp. 79–84, 2017.

[17] A. Monsel, Y. G. Zhu, V. Gudapati, H. Lim, and J. W. Lee, "Mesenchymal stem cell derived secretome and extracellular vesicles for acute lung injury and other inflammatory lung diseases," *Expert Opinion on Biological Therapy*, vol. 16, no. 7, pp. 859–871, 2016.

[18] M. S. H. Ho, S. H. J. Mei, and D. J. Stewart, "The immunomodulatory and therapeutic effects of mesenchymal stromal cells for acute lung injury and sepsis," *Journal of Cellular Physiology*, vol. 230, no. 11, pp. 2606–2617, 2015.

[19] S. Horie and J. G. Laffey, "Recent insights: mesenchymal stromal/stem cell therapy for acute respiratory distress syndrome," *F1000Res*, vol. 5, 2016.

[20] J. Y. Chen, X. Z. Mou, X. C. Du, and C. Xiang, "Comparative analysis of biological characteristics of adult mesenchymal stem cells with different tissue origins," *Asian Pacific Journal of Tropical Medicine*, vol. 8, no. 9, pp. 739–746, 2015.

[21] L. Pedrazza, A. A. Cunha, C. Luft et al., "Mesenchymal stem cells improves survival in LPS-induced acute lung injury acting through inhibition of NETs formation," *Journal of Cellular Physiology*, vol. 232, no. 12, pp. 3552–3564, 2017.

[22] X. D. Tang, L. Shi, A. Monsel et al., "Mesenchymal stem cell microvesicles attenuate acute lung injury in mice partly mediated by Ang-1 mRNA," *Stem Cells*, vol. 35, no. 7, pp. 1849–1859, 2017.

[23] M. Jin, C. Y. Sun, C. Q. Pei, L. Wang, and P. C. Zhang, "Effect of safflor yellow injection on inhibiting lipopolysaccharide-induced pulmonary inflammatory injury in mice," *Chinese Journal of Integrative Medicine*, vol. 19, no. 11, pp. 836–843, 2013.

[24] Y. Li, J. Xu, W. Shi et al., "Mesenchymal stromal cell treatment prevents H9N2 avian influenza virus-induced acute lung injury in mice," *Stem Cell Research & Therapy*, vol. 7, no. 1, p. 159, 2016.

[25] L. B. Ware and M. A. Matthay, "The acute respiratory distress syndrome," *The New England Journal of Medicine*, vol. 342, no. 18, pp. 1334–1349, 2000.

[26] G. Zheng, L. Huang, H. Tong et al., "Treatment of acute respiratory distress syndrome with allogeneic adipose-derived mesenchymal stem cells: a randomized, placebo-controlled pilot study," *Respiratory Research*, vol. 15, no. 1, p. 39, 2014.

[27] J. G. Wilson, K. D. Liu, H. Zhuo et al., "Mesenchymal stem (stromal) cells for treatment of ARDS: a phase 1 clinical trial," *The Lancet Respiratory Medicine*, vol. 3, no. 1, pp. 24–32, 2015.

[28] J. W. Lee, X. Fang, A. Krasnodembskaya, J. P. Howard, and M. A. Matthay, "Concise review: mesenchymal stem cells for acute lung injury: role of paracrine soluble factors," *Stem Cells*, vol. 29, no. 6, pp. 913–919, 2011.

[29] B. P. Guery, C. M. Mason, E. P. Dobard, G. Beaucaire, W. R. Summer, and S. Nelson, "Keratinocyte growth factor increases transalveolar sodium reabsorption in normal and injured rat

lungs," *American Journal of Respiratory and Critical Care Medicine*, vol. 155, no. 5, pp. 1777–1784, 1997.

[30] J. W. Lee, X. Fang, N. Gupta, V. Serikov, and M. A. Matthay, "Allogeneic human mesenchymal stem cells for treatment of E. coli endotoxin-induced acute lung injury in the ex vivo perfused human lung," *Proceedings of the National Academy of Sciences of the United States of America*, vol. 106, no. 38, pp. 16357–16362, 2009.

[31] J. W. Lee, A. Krasnodembskaya, D. H. McKenna, Y. Song, J. Abbott, and M. A. Matthay, "Therapeutic effects of human mesenchymal stem cells in ex vivo human lungs injured with live bacteria," *American Journal of Respiratory and Critical Care Medicine*, vol. 187, no. 7, pp. 751–760, 2013.

[32] Y. G. Zhu, X. M. Feng, J. Abbott et al., "Human mesenchymal stem cell microvesicles for treatment of Escherichia coli endotoxin-induced acute lung injury in mice," *Stem Cells*, vol. 32, no. 1, pp. 116–125, 2014.

Research Article

In Vitro Uptake of Hydroxyapatite Nanoparticles and Their Effect on Osteogenic Differentiation of Human Mesenchymal Stem Cells

Xing Yang,[1] Yuanyuan Li,[2] Xujie Liu,[1,3] Ranran Zhang,[1] and Qingling Feng [1,4]

[1]*State Key Laboratory of New Ceramics and Fine Processing, School of Materials Science and Engineering, Tsinghua University, Beijing 100084, China*
[2]*Department of Stomatology, Shengli Oilfield Central Hospital, Dongying 257034, China*
[3]*Graduate School at Shenzhen, Tsinghua University, Shenzhen 518055, China*
[4]*Key Laboratory of Advanced Materials of Ministry of Education of China, School of Materials Science and Engineering, Tsinghua University, Beijing 100084, China*

Correspondence should be addressed to Qingling Feng; biomater@mail.tsinghua.edu.cn

There have been many applications in biomedical fields based on hydroxyapatite nanoparticles (HA NPs) over the past decades. However, the biocompatibility of HANPs is affected by exposure dose, particle size, and the way of contact with cells. The objective of this study is to investigate the effect of HA NPs with different sizes on osteogenesis using human mesenchymal stem cells (hMSCs). Three different-sized HA NPs (~50, ~100, and ~150 nm, resp.) were synthesized to study the cytotoxicity, cellular uptake, and effect on osteogenic differentiation of hMSCs. The results clearly showed that each size of HA NPs had dose-dependent cytotoxicity on hMSCs. It was found that HA NPs could be uptaken into hMSCs. The osteogenic differentiation of hMSCs was evaluated through alkaline phosphatase (ALP) activity measurement, ALP staining, immunofluorescent staining for osteopontin (OPN), and real-time polymerase chain reaction (RT-PCR) examination. As expected, HA NPs of all sizes could promote the differentiation of hMSCs towards osteoblast lineage. Among the three sizes, smaller-sized HA NPs (~50 and ~100 nm) appeared to be more effective in stimulating osteogenic differentiation of hMSCs.

1. Introduction

Over the past few decades, nanotechnology and nanoscience have been emerging with the rise in manufacture of various nanomaterials [1]. Recently, biomaterials based on nanoparticles have become a very popular research field for applications in biomedicine, tissue engineering, and health care system [2–4]. Compared with traditional medicine, nanoparticles exhibit new possibilities for many technological applications [5]. Hydroxyapatite (HA) with chemical formula of $Ca_{10}(PO_4)_6(OH)_2$ is the major mineral constituent of human hard tissue (bones and teeth) [6]. Owing to the excellent biocompatibility [7], hydroxyapatite nanoparticles (HA NPs) play an important role in various biomedical applications. For instance, HA NPs can be used for bioimaging, photodynamic therapy, gene/drug delivery, and hard tissue repair [8–12]. In order to meet the requirements of various applications in the biomedical field, HA NPs with different sizes and aspect ratios have been prepared by using surfactant molecules as structure-directing agents [13–15]. These surfactants are normally toxic for biomedical applications. To remove the cytotoxic surfactants, several methods have been proposed [16, 17]. For example, calcination is a common strategy for removing surfactant molecules from HA NPs, which will change their morphology and size distribution [16], while the reaction-dissolution approach can clean

the surface of HA NPs with unchanged topographic characteristics (shape and size distribution) and improved biocompatibility [17].

Many researchers have focused on the potential of HA NPs used for bone repair and regeneration. In a previous study, Wang et al. prepared the HA NPs/polyamide composite scaffolds and found that the scaffolds had no negative effects on osteogenic differentiation of rabbit bone marrow-derived mesenchymal stem cells [18]. He et al. prepared micropatterns composed of HA NPs, and osteoblasts were proven to be well localized on the HA microislands [19]. In addition, HA NPs were not only used for investigation of osteogenic differentiation in vitro but also bone defect repair in vivo as well. Liu et al. confirmed the osteoinductivity of HA NPs/silk fibroin composite scaffolds through both cell experiment in vitro and calvarial defect model in vivo [20]. Zhang et al. found that 3D porous scaffold composed of HA NPs (surface grafted with PLLA) and PLGA enhanced the in vivo mineralization and osteogenesis through investigation of intramuscular implantation and repairing radius defects of rabbits [21]. Similarly, the HA NP-coated PLGA scaffolds have exhibited improved biocompatibility and facilitated the bone defect restoration of rabbits [22].

As noted above, HA NPs have been a very attractive material used in bone repair and regeneration because of appropriate physicochemical properties and biological characteristics. However, previous researches involving HA NPs and osteogenesis mainly focused on the influence of coatings or scaffolds incorporated with HA NPs on osteogenic differentiation of bone-related cells. On the other hand, due to the different physicochemical characteristics and bioactivity from bulk materials, HA NPs have also been applied for a number of applications in biomedicine, such as drug delivery, transfection, and gene silencing [8]. Among these applications, HA NPs interacted directly with the related cells and then were internalized into the cells. Due to the internalization of HA NPs, cells incubated with HA NPs directly may show different responses compared with that cultured on the surface of HA NPs containing coatings or scaffolds. Some recent studies showed that the biocompatibility of HA NPs varied as exposure dose, particle size, and the way of contact with cells [1, 23–25]. There is a lack of information concerning the bioactivity in the human tissue cells as it relates to the size of HA NPs. Therefore, it is of great interest to investigate the effect of internalization of different-sized HA NPs on human tissue cells. Understanding the cell response to different-sized HA NPs is beneficial to choose the effective candidates for bone tissue regeneration.

In the bone tissue, hMSCs play a key role because they are multipotent cells which can renew themselves and differentiate into osteoblast [26, 27]. Osteogenesis is a part of bone cellular metabolism, which is essential to bone remodeling [28]. The hMSCs are usually applied as seed cells for bone tissue engineering. For these reasons, hMSCs, derived from bone marrow, are one of the best in vitro model systems for investigating the osteogenesis potential of nanobiomaterials in human.

Hence, the aim of this study is to evaluate the in vitro uptake of HA NPs with different sizes and their effect on osteogenic differentiation of bone marrow-derived hMSCs. Three different-sized HA NPs were prepared by chemical precipitation method. The hMSCs were exposed to different concentrations of HA NPs for 24 h and then induced to osteogenic differentiation. The potential effects of these HA NPs on cell viability and expression of several osteogenic were analyzed.

2. Materials and Methods

2.1. Preparation and Characterization of HA NPs.
HA NPs with three different sizes (designated herein as S50, S100, and S150, resp.) were prepared by the conventional chemical precipitation [6, 29]. In brief, calcium chloride ($CaCl_2$) solution was dropwise added to diammonium hydrogen phosphate (($NH_4)_2HPO4$) solution under continuous and gentle stirring, while the molar ratio of Ca/P was kept at 1.67. During the precipitation, aqueous ammonia was added to adjust the pH value to 7 for S50, 8 for S100, and 10 for S150. The temperature was maintained at 30°C for S50, 50°C for S100, and 90°C for S150. After precipitation, the resultant suspension was aged at room temperature for 16 h. Finally, the resulting powders were collected, rinsed with deionized water, and dried by vacuum freeze drying.

The morphology and size of the synthesized powders were characterized by transmission electron microscope (TEM, Tecnai G20, USA). The crystalline phases of the synthesized powders were determined using X-ray diffraction (XRD, Rigaku D/max-2500 PC, Japan). The Brunauer–Emmett–Teller (BET) surface area was measured by Autosorb-IQ2-MP (Quantachrome Instruments, USA). The hydrodynamic diameter of S50, S100, and S150, dispersed in basal medium (Cyagen Biosciences Inc., China) with 10% fetal bovine serum, was measured by dynamic light scattering (DLS, Zetasizer Nano ZS90, UK).

2.2. Cell Culture.
Bone marrow-derived hMSCs were cultured in a growth medium (Cyagen Biosciences Inc., USA) containing 10% fetal bovine serum (FBS), 1% glutamine, and 1% penicillin-streptomycin at 37°C in humid air containing 5% CO_2. The growth medium was changed every 48 h.

To induce osteogenic differentiation, the culture medium was changed to osteogenic inductive medium (Cyagen Biosciences Inc., USA) after hMSCs treated with HA NPs for 24 h. The inductive medium was refreshed every 48 h.

2.3. Cell Viability Assay.
The Cell Counting Kit-8 (CCK-8, Dojindo, Japan) assay was used to evaluate the effect of HA NPs on cell viability of hMSCs. Cells were cultured with different concentrations (0, 5, 10, and 50 μg/ml) of HA NPs for 24 h at 5% CO_2, 37°C. After 1, 3, and 5 days of osteoinduction, the cells were incubated with CCK-8 solution (consisting of 90% growth medium and 10% CCK-8) for 3 h at 37°C. Afterwards, the absorbance (OD) of the incubation solution was measured at 450 nm.

2.4. Cellular Uptake of HA NPs.
TEM was employed to observe cellular uptake of HA NPs by hMSCs. After incubation with 10 μg/ml of HA NPs for 24 h, the cells were harvested and fixed in 2.5% glutaraldehyde at 4°C overnight.

Then, the cells were postfixed in 0.1 M cacodylate buffer containing 1% osmium tetroxide for 1 h at 4°C, dehydrated stepwise in ethanol, and embedded in epoxy resin. Ultra-thin sections (70 nm) were cut using an ultramicrotome (Lecia, Germany), collected on copper grids, and observed by TEM (Hitachi H-7650B, Japan).

2.5. ALP Activity Assay. The cells were incubated with 0 and 10 μg/ml HA NPs for 24 h and then induced into osteogenic differentiation. ALP activity assay was performed on days 7 and 14 after osteogenic induction. Briefly, the cells were lysed in 100 μl RIPA lysis buffer (Beyotime, China). The lysate was then analyzed according to the manufacturer's protocol (ALP assay kit, Jiancheng, China). The ALP activity was normalized by the total protein content, which was measured by a bicinchoninic acid assay kit (Aidlab, China).

2.6. Immunofluorescent Staining for Osteopontin (OPN). Immunofluorescent staining was applied to evaluate the expression of OPN at protein level. The cells were incubated with 0 and 10 μg/ml HA NPs for 24 h and then induced into osteogenic differentiation. On day 14 of differentiation, the cells were washed with PBS, fixed with 4% paraformaldehyde, permeabilized with 0.3% Triton X-100, and blocked with 10% goat serum for 2 h. Thereafter, the cells were incubated with the rabbit polyclonal antibodies against OPN (Abcam, USA) at 4°C overnight and treated with Dylight 594-conjugated goat anti-rabbit IgG (Abbkine, USA) for 1 h. The cell nuclei were then stained with 4′,6-diamidino-2-phenylindole (DAPI) at room temperature for 15 min. Subsequently, the samples were viewed using a laser scanning confocal microscope (LSCM, Zeiss710 META, Germany).

2.7. Real-Time Polymerase Chain Reaction (RT-PCR). The expression of ALP, OPN, runt-related transcription factor 2 (Runx2), and osteocalcin (OCN) at gene level were quantitatively analyzed by RT-PCR (the primers used for the RT-PCR study are shown in Table 1). The cells were incubated with 0 and 10 μg/ml HA NPs for 24 h and then induced into osteogenic differentiation. On day 14 after osteogenic induction, total RNA of the cells was extracted using TRNzol Reagent (Tiangen, China). Then, 400 ng of total RNA was reverse transcribed into cDNA using FastQuant RT kit (Tiangen, China). RT-PCR was performed on T100 Thermal Cycler (BioRad, USA) using iTaq Universal SYBR Green Supermix (BioRad, USA).

2.8. Calcium Ion Release. The degradation experiment *in vitro* was performed by immersing 10 μg/ml of HA NPs in Dulbecco's phosphate-buffered saline (DPBS) at 37°C for 14 days. The concentration of calcium ions released by HA NPs was measured by inductively coupled plasma optical emission spectrometer (ICP-OES).

2.9. Medium pH Measurement. In order to investigate the effect of HA NPs on the pH of culture medium, 10 μg/ml of HA NPs was immersed in the osteogenic inductive medium (Cyagen Biosciences Inc., USA) at 37°C in humid air containing 5% CO_2. Since the osteogenic inductive medium was

TABLE 1: Primers used for RT-PCR study.

Gene	Primer ($5' \to 3'$)
ALP	F: AGCACTCCCACTTCATCTGGAA
	R: GAGACCCAATAGGTAGTCCACATTG
OPN	F: CTCAGGCCAGTTGCAGCC
	R: CAAAAGCAAATCACTGCAATTCTC
Runx2	F: GCCTTCAAGGTGGTAGCCC
	R: CGTTACCCGCCATGACAGTA
OCN	F: CACTCCTCGCCCTATTGGC
	R: CCCTCCTGCTTGGACACAAAG
GAPDH	F: GAAGGTGAAGGTCGGAGTC
	R: GAAGATGGTGATGGGATTTC

changed every 2 days, the pH of medium with and without HA NPs was measured after 2 days of incubation.

2.10. Statistical Analysis. All data were expressed as the mean ± standard deviation (SD) of three independent experiments and analyzed using one-way analysis of variance (ANOVA) by SPSS software (15.0.1). A $p < 0.05$ was considered statistically significant.

3. Results

3.1. Characterization of HA NPs. Figure 1 shows the TEM images of HA NPs (S50, S100, and S150). The length of S50, S100, and S150 was approximately 50, 100, and 150 nm (Figure 1(c)), while the width was around 8, 15, and 20 nm, respectively. The hydrodynamic diameter from DLS analysis was 567.86 ± 19.71 nm for S50, 626.10 ± 14.95 nm for S100, and 1262.33 ± 46.5 nm for S150 (Table 2), which revealed that HA NPs were aggregated in the cell culture medium. As shown in Table 2, S50 and S100 showed similar specific surface area, which is much larger than that of S150.

XRD patterns of S50, S100, and S150 (Figure 2) display typical characteristic diffraction peaks of crystalline HA phase (25.87°, 31.78°, 46.71°, 49.47°, and 53.14°) according to the standard card of HA (JCPDS 09-0432) [30, 31]. Moreover, S50 and S100 showed broadening diffraction peaks, indicating that they consisted of poorly crystalline and small crystals. In contrast, the diffraction peaks of S150 were sharper than those of S50 and S100, implying the higher crystallinity of S150.

3.2. Cell Viability Assay. To evaluate the effect of HA NPs on cell viability of hMSCs, CCK8 assay was applied on days 1, 3, and 5 after osteogenic induction. As shown in Figure 3, the cell viability of hMSCs treated with 5 and 10 μg/ml of HA NPs was comparable to the control group. However, there were significant decreases in cell viability of hMSCs treated with 50 μg/ml of HA NPs compared with that of the control group at each time point. The result indicated that HA NPs showed cytotoxicity to hMSCs in a concentration-dependent manner. Based on the result of cell viability assay, the maximum safety concentration, that is, 10 μg/ml, was selected for subsequent experiments.

(a)   (b)   (c)
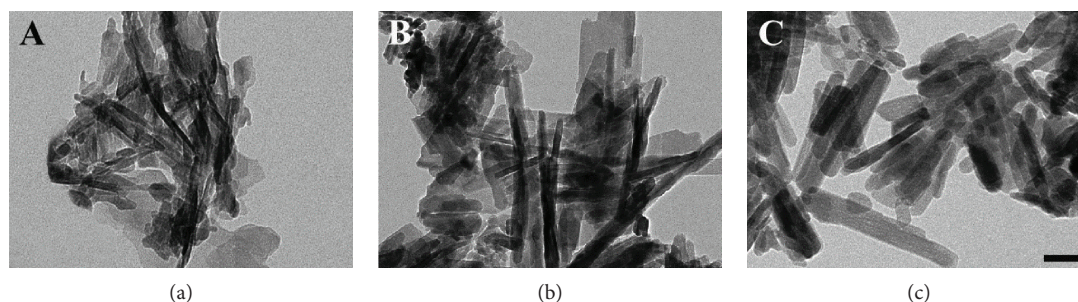
FIGURE 1: TEM images of S50 (a), S100 (b), and S150 (c). The bar is 50 nm.

TABLE 2: Hydrodynamic diameter and surface area of HA NPs. Values are expressed as mean ± SD ($n = 3$ for each sample).

Particle	Hydrodynamic diameter (nm)	Surface area (m^2/g)
S50	568 ± 20	63.30 ± 0.94
S100	626 ± 15	66.73 ± 0.95
S150	1262 ± 47	46.80 ± 1.19
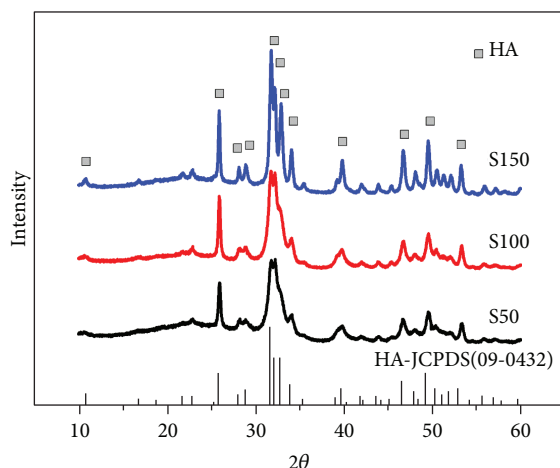
FIGURE 2: XRD patterns of S50 (black line), S100 (red line), and S150 (blue line).

3.3. Cellular Uptake of HA NPs. As shown in Figure 4, S50, S100, and S150 were uptaken into hMSCs after incubation for 24 h at the concentration of 10 μg/ml, and they distributed in some different-sized vesicles in cell cytoplasm. The HA NPs were irregularly aggregated, and the size of some aggregation reached several microns (Figures 4(a)–4(c)). The size and morphology of the HA NPs were further confirmed in Figures 4(d)–4(f).

3.4. Osteogenic Differentiation. ALP activity of hMSCs was qualitatively and quantitatively assayed on days 7 and 14 after osteogenic induction. The ALP activity of hMSCs increased from days 7 to 14 (Figure 5). As shown in Figure 5(a), more intense color was observed for cells of HA NP treatment groups in comparison with that of the control group. Furthermore, for the cells treated with S50, S100 seemed to stain more strongly and homogenously than those treated with S150. The quantitative result (Figure 5(b)) also showed that

the addition of HA NPs increased the ALP activity of hMSCs. In addition, the cells incubated with smaller HA NPs (S50 and S100) showed higher ALP activity compared with the S150 group at each time point.

The expression of OPN at protein level was detected by immunofluorescent staining. On day 14 after osteogenic induction, the cells were strongly positive to OPN for all groups (Figure 6). Cells incubated with 10 μg/ml HA NPs displayed higher fluorescence intensity compared with those of the control group. Moreover, the cells showed higher expression extent of OPN treated with S50 and S100 than those exposed to S150.

To further investigate the effect of HA NPs on osteogenic differentiation of hMSCs, the expression of ALP, OPN, Runx2, and OCN was assessed using RT-PCR after 14 days of induction (Figure 7). In agreement with the ALP activity and immunofluorescent staining results, HA NPs increased the expression of all four bone-related genes. For the cells incubated with of S50 and S100, the expression levels of ALP, OPN, Runx2, and OCN all displayed significant increases compared with that of S150 group.

3.5. Calcium Ion Release. The release of calcium ion (Ca^{2+}) form HA NPs in DPBS was investigated using ICP-OES. As shown in Figure 8, Ca^{2+} concentrations of S50, S100, and S150 groups were significantly higher than that of the control group (DPBS only). Moreover, after 14 days of soaking, the Ca^{2+} release form S50 and S100 showed a significant increment of 147% and 117% as compared with that of S150. The result indicates that HA NPs of all sizes possess degradability and smaller-sized HA NPs (S50 and S100) appear to degrade faster than larger-sized S150.

3.6. The Effect of HA NPs on Medium pH. After 2 days of incubation under standard cell culture condition, the pH of the control group (medium without HA NPs) was 7.23 ± 0.02, while the pH of medium with S50, S100, and S150 was 7.23 ± 0.02, 7.24 ± 0.01, and 7.26 ± 0.02, respectively, all displaying no significant differences compared with the control group. The result indicates that the addition of HA NPs does not change the pH of culture medium.

4. Discussion

HA NPs have been widely used for applications in the field of biomedicine and tissue engineering [8, 32], such as hard

(a)

(b)

(c)
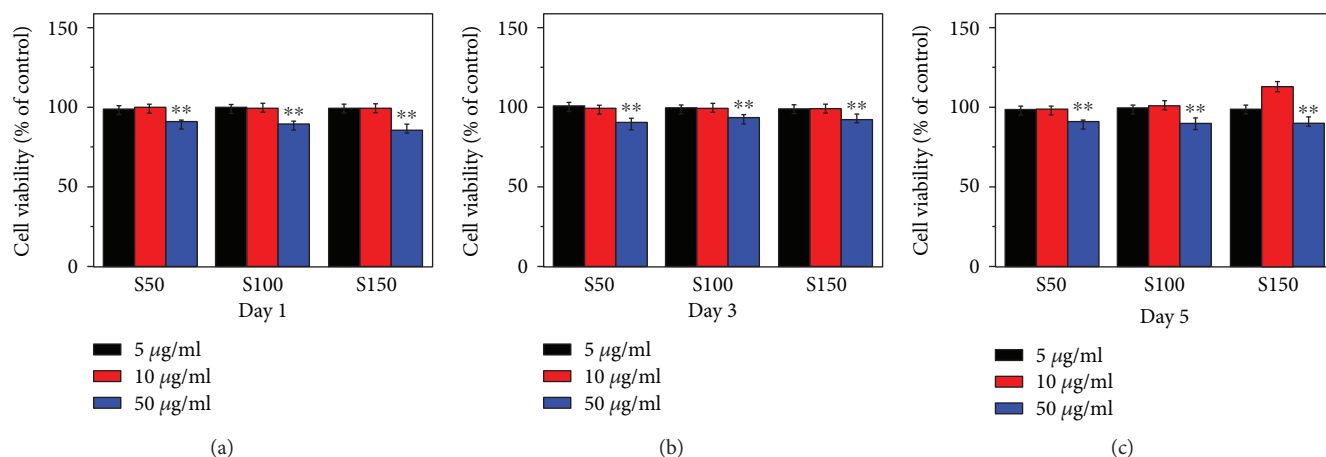
FIGURE 3: Cell viability detected by CCK-8 assay on days 1, 3, and 5 after osteoinduction. The hMSCs were treated with different concentrations (0, 5, 10, and 50 μg/ml) of HA NPs for 24 h at 5% CO_2, 37°C. Values are expressed as mean $\pm$ SD ($n = 3$ for each sample). $^{**}p < 0.01$ compared to the control group (hMSCs without HA NP treatment).

(a)

(b)

(c)

(d)

(e)

(f)
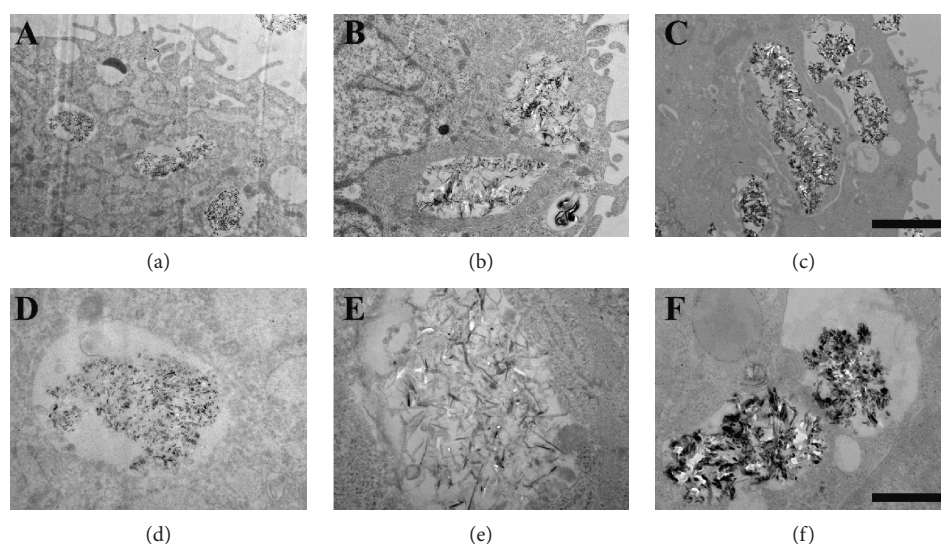
FIGURE 4: TEM images of cellular uptake of HA NPs in hMSCs. The cells were incubated with 10 μg/ml of S50 (a, d), S100 (b, e), and S150 (c, f) for 24 h. The bar is 2 μm for (a–c), 500 nm for (d–f).

tissue repair, biomedical imaging, and drug delivery. These applications associated with HA NPs require that they have different shapes and sizes. In this study, HA NPs with three different sizes were prepared by chemical precipitation method via altering the temperature and pH of reaction solution (Figure 1). Calcium ions and phosphate anions firstly formed amorphous calcium phosphate (CaP) or hydrated orthophosphates, which can subsequently transform to HA through phase transformation at suitable conditions [33]. Thus, the growth process of HA was prolonged and slow [34]. Higher precipitation temperature, supplying higher amounts of energy, allowed HA NPs grow faster. The diffraction peaks S50 and S100 were wide and low, while S150 showed well-differentiated peaks (Figure 2), which may be caused by the increased c-axis of the unit cells of S150 under higher precipitation temperature. Murakoshi et al. also prepared different-sized hexagonal CdS nanoparticles through varying the preparation temperature [35]. In addition, due

to the different pH value, crystallite facets of HA NPs absorbed different amounts of OH^- [36]. The shielding effect of OH^- on the interface could control the growth rate of the OH^--absorbed crystallite facets [37]. Taken together, the different sizes and aspect ratios of S50, S100, and S150 were caused by altering pH value and precipitation temperatures.

Cytocompatibility assessment result in this study showed that S50, S100, and S150 were cytotoxic to hMSCs in a dose-dependent manner. Many previous researches have already reported the dose-dependent cytotoxicity of HA NPs to several cell types through inducing necrosis or apoptosis [1, 23, 24, 38, 39]. The degree of cell death caused by HA NPs had a strong correlation with the amount of particle load [23, 38]. The HA NPs were degraded in cell lysosomes to increase intracellular Ca^{2+} concentrations, which might cause lysosomal rupture to induce cell necrosis [40]. On the other hand, the anticipated agglomeration and subsequent sedimentation of HA NPs at relative high concentrations

(a)

(b)
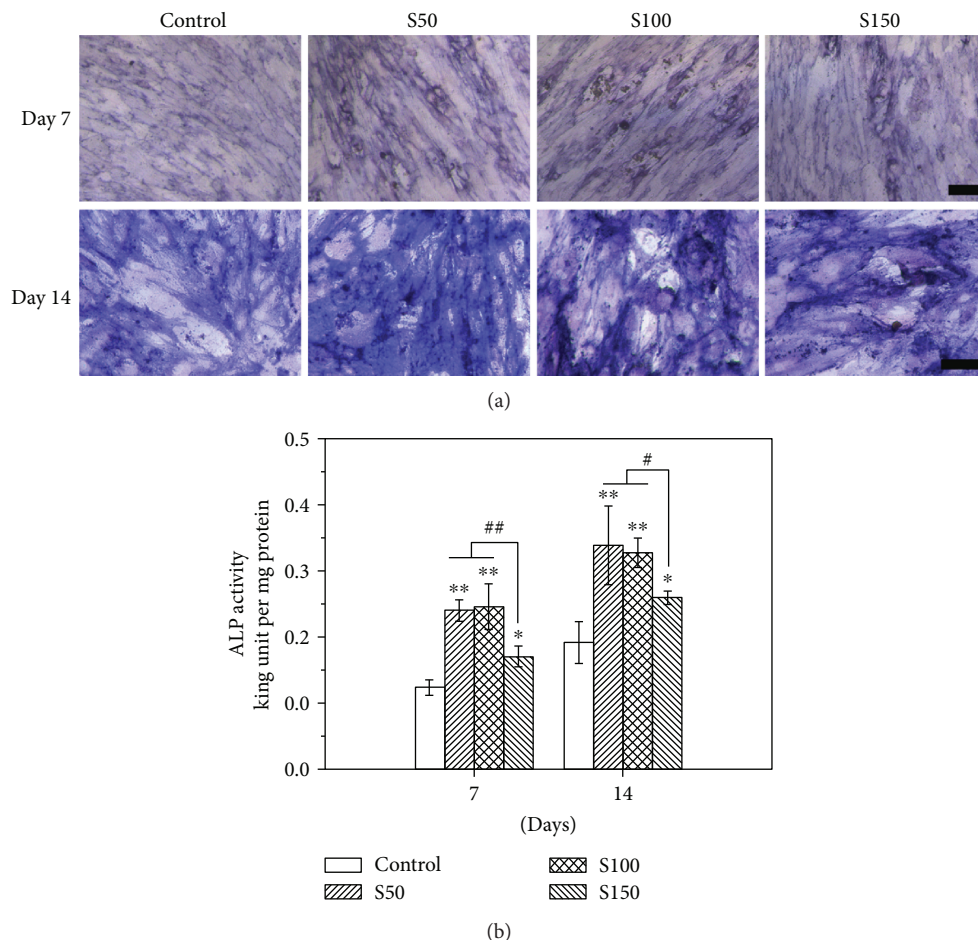
FIGURE 5: ALP staining (a) and ALP activity (b) of hMSCs after 7 and 14 days of osteoinduction. The hMSCs were incubated with 0 and 10 μg/ml of HA NPs for 24 h. $^*p < 0.05$, $^{**}p < 0.01$ comparison between the control group (hMSCs without HA NP treatment) and other groups. $^{\#}p < 0.05$, $^{\#\#}p < 0.01$ comparison between S50 group, S100 group, and S150 group.

(a)   (b)   (c)   (d)
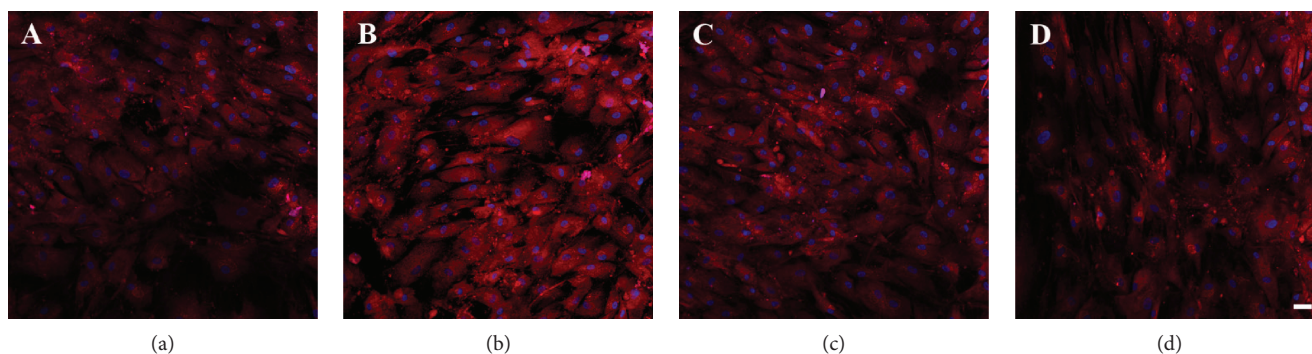
FIGURE 6: Immunofluorescent staining for OPN on day 14 after osteogenic induction (scale bar is 50 μm). The cells were exposed to HA NPs for 24 h (a) 0 μg/ml, (b) S50—10 μg/ml, (c) S100—10 μg/ml, and (d) S150—10 μg/ml.

might result in mechanical damage to the cells, which could cause cytotoxicity [1, 41]. These reasons may be possible mechanisms for the concentration-dependent cytotoxicity of S50, S100, and S150 to hMSCs.

Previous researches involving HA NPs and osteogenesis mainly focused on the effect of coatings or scaffolds doped with HA NPs on osteogenic differentiation of bone-related cells [18, 20, 21]. For instance, Wang et al. found that the

hydroxyapatite nanoparticles/polyamide (HA NPs/PA) composite scaffolds had no negative effects on the adhesion, proliferation, and osteogenic differentiation of rabbit bone marrow-derived mesenchymal stem cells (rBMSCs) [18]. In contrast, this study investigated the *in vitro uptake* of HA NPs with different sizes and their influence on differentiation of hMSCs into osteoblastic phenotype. A major finding of the present study is that S50, S100, and S150 have stimulatory
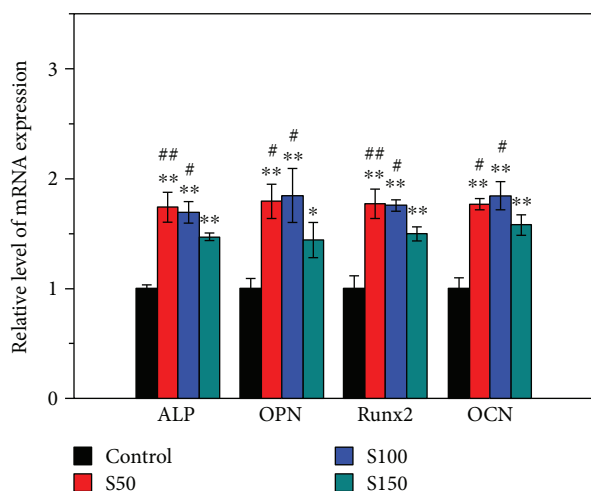
FIGURE 7: mRNA expression levels of ALP, OPN, Runx2, and OCN on day 14 after osteogenic induction. The cells were incubated with 0 and $10 \mu g/ml$ HA NPs for 24 h. Values are expressed as mean $\pm$ SD ($n = 3$ for each sample). $^*p < 0.05$, $^{**}p < 0.01$ compared to the control group (hMSCs without HA NP treatment). $^#p < 0.05$, $^{##}p < 0.01$ comparison between S50 group, S100 group, and S150 group.
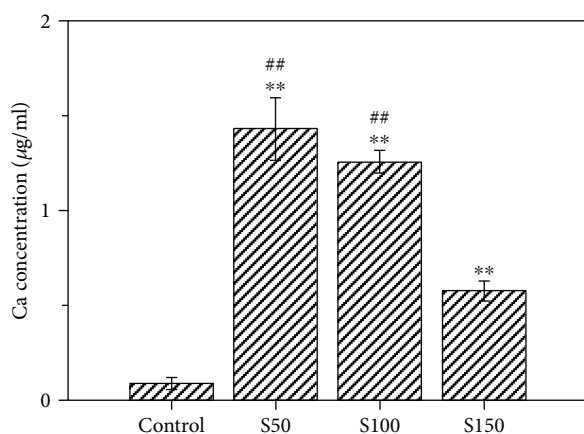
FIGURE 8: Release of calcium ions from $10 \mu g/ml$ of S50, S100, and S150 in DPBS at $37°C$ for 7 days. Values are expressed as mean $\pm$ SD ($n = 3$ for each sample). $^{**}p < 0.01$ compared to the control group (hMSCs without HA NP treatment). $^{##}p < 0.01$ comparison between S50 group, S100 group, and S150 group.

effect on osteogenic differentiation of hMSCs reflected by increased ALP activity and enhanced expression of bone-related markers (Figures 5–7). ALP is an early marker during the osteogenic differentiation, which can provide phosphate groups for subsequent hydroxyapatite deposition [42]. Runx2 acts as the initial and most specific marker that can activate and regulate osteogenic differentiation [43]. OCN, synthesized only by fully differentiated osteoblasts, is a specific marker of mature osteoblasts [44]. OPN, which can enhance mineralization by its calcium and collagen-binding properties, is also a marker of osteoblasts [45]. Similar results have been found in previous studies, where HA NPs showed positive effects on osteogenesis [25, 46, 47]. For instance, HA

NPs with a diameter of about 20 nm have been reported to promote the type I collagen, OCN, and OPN expressions of rabbit mesenchymal stem cells [25]. Moreover, Wang et al. prepared HA nanospheres (~50 nm in diameter) and HA nanorods (~50 nm in length) through the induction of protein template and found that both nanoparticles could significantly enhance the osteoblastic differentiation of rat mesenchymal stem cells, especially the HA nanospheres [46]. The enhancement of osteogenic differentiation of hMSCs may be related to the changes of culture medium condition caused by HA NPs [25]. HA NP-conditioned medium (obtained by soaking HA NPs in culture medium for 3 days and centrifuging to remove HA NPs) has been proven to promote the osteogenic differentiation of bone marrow-derived mesenchymal stem cells [48]. Small shifts in extracellular pH could result in significant changes in the ability of hMSCs to express markers of the osteoblast phenotype [49]. The activity of human osteoblasts has been proven to increase with the increasing medium pH during the range from 7.0 to 7.6 [49–51]. It is known that the original pH of culture medium of most cells varies in the range of 7.2–7.4 due to the physiological pH. In this study, after 2 days of incubation, the pH of culture medium with and without HA NPs was comparable during the range of 7.2–7.3. The addition of HA NPs did not change the medium pH. Therefore, the positive effects of HA NPs on osteogenesis may be related to other condition changes of culture medium, such as the concentration of calcium ions, caused by HA NPs rather than the medium pH.

Another major finding is that S50 and S150 appear to have stronger role in stimulating the osteogenic differentiation of hMSCs than S150. The cells treated with S50 and S100 expressed more ALP, OPN, and Runx2 compared with that treated with S150 (Figures 5–7). Similar results could be found in a previous study, where rat bone marrow-derived mesenchymal stem cells (rBMSCs) expressed higher levels of osteoblast-related markers by the stimulation of smaller HA NPs than that of larger ones [33]. The size of HA NPs is an important factor for affecting the biological behavior of bone-related cells [32, 52, 53]. Smaller-sized HA NPs may change the microenvironments of cell culture which can greatly enhance osteogenesis [54]. Smaller-sized HA NPs adsorb proteins forming a neomatrix different with that formed by larger-sized HA, which can greatly impact osteogenesis [33]. Calcium ions (Ca^{2+}) have been shown to affect the growth and osteogenic differentiation of stem cells [55, 56]. Greater concentrations of Ca^{2+} significantly increased the extent of cell mineralization [56]. Ca^{2+} plays an essential role in maintaining the cell growth and functions [57]. Futhermore, Ca^{2+} can activate MAPK signaling pathway, which is important for inducing cell differentiation [58, 59]. S50 and S100 released more than two times of Ca^{2+} as S150 after 14 days of soaking in DPBS (Figure 8). The larger specific surface area and aggregation size of S150 (Table 2) may result in its lower degradation speed. Due to the differences in degradation speed, smaller-sized HA NPs (S50 and S100) release higher concentration of Ca^{2+} than larger-sized HA NPs (S150), which may result in their different effects on osteogenic differentiation of stem cells. These

may be the reasons why the smaller-sized HA NPs show greater stimulatory effect on osteogenic differentiation of stem cells.

5. Conclusions

In this study, HA NPs with three sizes (S50, S100, and S150) were prepared. All the data demonstrated that HA NPs of all sizes had stimulatory effect on the osteogenic differentiation of hMSCs in vitro. The hMSCs incubated with smaller-sized HA NPs (S50 and S100) seemed to have higher differentiation rate compared with that treated with S150, indicating that the efficiency of osteogenic differentiation of hMSCs was dependent on the size of HA NPs. This difference may be caused by the different concentrations of Ca^{2+} released by S50, S100, and S150. These suggest that the size of nanoparticles is an important factor needed for consideration in biological environment and will provide a reference for HA NPs in biomedical applications.

Data Availability

The data used to support the findings of this study are available from the corresponding author upon request.

Conflicts of Interest

The authors declare that they have no conflicts of interest.

Acknowledgments

References

[1] N. S. Remya, S. Syama, V. Gayathri, H. K. Varma, and P. V. Mohanan, "An in vitro study on the interaction of hydroxyapatite nanoparticles and bone marrow mesenchymal stem cells for assessing the toxicological behaviour," Colloids and Surfaces, B: Biointerfaces, vol. 117, pp. 389–397, 2014.

[2] M. De, P. S. Ghosh, and V. M. Rotello, "Applications of nanoparticles in biology," Advanced Materials, vol. 20, no. 22, pp. 4225–4241, 2008.

[3] J. Xie, S. Lee, and X. Chen, "Nanoparticle-based theranostic agents," Advanced Drug Delivery Reviews, vol. 62, no. 11, pp. 1064–1079, 2010.

[4] A. Tautzenberger, A. Kovtun, and A. Ignatius, "Nanoparticles and their potential for application in bone," International Journal of Nanomedicine, vol. 7, pp. 4545–4557, 2012.

[5] W.-K. Ko, D. N. Heo, H.-J. Moon et al., "The effect of gold nanoparticle size on osteogenic differentiation of adipose-derived stem cells," Journal of Colloid and Interface Science, vol. 438, pp. 68–76, 2015.

[6] M. Sadat-Shojai, M.-T. Khorasani, E. Dinpanah-Khoshdargi, and A. Jamshidi, "Synthesis methods for nanosized hydroxyapatite with diverse structures," Acta Biomaterialia, vol. 9, no. 8, pp. 7591–7621, 2013.

[7] L. Chen, J. M. Mccrate, J. C.-M. Lee, and H. Li, "The role of surface charge on the uptake and biocompatibility of hydroxyapatite nanoparticles with osteoblast cells," Nanotechnology, vol. 22, no. 10, article 105708, 2011.

[8] M. Epple, K. Ganesan, R. Heumann et al., "Application of calcium phosphatenanoparticles in biomedicine," Journal of Materials Chemistry, vol. 20, no. 1, pp. 18–23, 2010.

[9] E. H. Chowdhury, M. Kunou, M. Nagaoka, A. K. Kundu, T. Hoshiba, and T. Akaike, "High-efficiency gene delivery for expression in mammalian cells by nanoprecipitates of Ca–Mg phosphate," Gene, vol. 341, pp. 77–82, 2004.

[10] E. I.˙. Altınoğlu, T. J. Russin, J. M. Kaiser et al., "Near-infrared emitting fluorophore-doped calcium phosphate nanoparticles for in vivo imaging of human breast cancer," ACS Nano, vol. 2, no. 10, pp. 2075–2084, 2008.

[11] M. Kester, Y. Heakal, T. Fox et al., "Calcium phosphate nanocomposite particles for in vitro imaging and encapsulated chemotherapeutic drug delivery to cancer cells," Nano Letters, vol. 8, no. 12, pp. 4116–4121, 2008.

[12] M. Sadat-Shojai, M. Atai, A. Nodehi, and L. N. Khanlar, "Hydroxyapatite nanorods as novel fillers for improving the properties of dental adhesives: synthesis and application," Dental Materials, vol. 26, no. 5, pp. 471–482, 2010.

[13] S. Manafi and M. R. Rahimipour, "Synthesis of nanocrystalline hydroxyapatite nanorods via hydrothermal conditions," Chemical Engineering & Technology, vol. 34, no. 6, pp. 972–976, 2011.

[14] X. Wang, J. Zhuang, Q. Peng, and Y. D. Li, "Liquid–solid–solution synthesis of biomedical hydroxyapatite nanorods," Advanced Materials, vol. 18, no. 15, pp. 2031–2034, 2006.

[15] M. Uota, H. Arakawa, N. Kitamura, T. Yoshimura, J. Tanaka, and T. Kijima, "Synthesis of high surface area hydroxyapatite nanoparticles by mixed surfactant-mediated approach," Langmuir, vol. 21, no. 10, pp. 4724–4728, 2005.

[16] Y. T. Huang, M. Imura, Y. Nemoto, C. H. Cheng, and Y. Yamauchi, "Block-copolymer-assisted synthesis of hydroxyapatite nanoparticles with high surface area and uniform size," Science and Technology of Advanced Materials, vol. 12, no. 4, article 045005, 2016.

[17] B. Cao, M. Yang, L. Wang, H. Xu, Y. Zhu, and C. Mao, ""Cleaning" the surface of hydroxyapatite nanorods by a reaction-dissolution approach," Journal of Materials Chemistry B, vol. 3, no. 39, pp. 7667–7672, 2015.

[18] H. Wang, Y. Li, Y. Zuo, J. Li, S. Ma, and L. Cheng, "Biocompatibility and osteogenesis of biomimetic nano-hydroxyapatite/polyamide composite scaffolds for bone tissue engineering," Biomaterials, vol. 28, no. 22, pp. 3338–3348, 2007.

[19] Y. He, X. Wang, L. Chen, and J. Ding, "Preparation of hydroxyapatite micropatterns for the study of cell–biomaterial interactions," Journal of Materials Chemistry B, vol. 2, no. 16, pp. 2220–2227, 2014.

[20] H. Liu, G. W. Xu, Y. F. Wang et al., "Composite scaffolds of nano-hydroxyapatite and silk fibroin enhance mesenchymal stem cell-based bone regeneration via the interleukin 1 alpha autocrine/paracrine signaling loop," Biomaterials, vol. 49, pp. 103–112, 2015.

[21] P. Zhang, Z. Hong, T. Yu, X. Chen, and X. Jing, "In vivo mineralization and osteogenesis of nanocomposite scaffold of poly(lactide-co-glycolide) and hydroxyapatite surface-grafted with poly(l-lactide)," Biomaterials, vol. 30, no. 1, pp. 58–70, 2009.

[22] D. Wang, Y. He, L. Bi et al., "Enhancing the bioactivity of poly(lactic-co-glycolic acid) scaffold with a nano-hydroxyapatite coating for the treatment of segmental bone defect in a rabbit model," *International Journal of Nanomedicine*, vol. 8, pp. 1855–1865, 2013.

[23] K. H. Müller, M. Motskin, A. J. Philpott et al., "The effect of particle agglomeration on the formation of a surface-connected compartment induced by hydroxyapatite nanoparticles in human monocyte-derived macrophages," *Biomaterials*, vol. 35, no. 3, pp. 1074–1088, 2014.

[24] R. Meena, K. K. Kesari, M. Rani, and R. Paulraj, "Effects of hydroxyapatite nanoparticles on proliferation and apoptosis of human breast cancer cells (MCF-7)," *Journal of Nanoparticle Research*, vol. 14, no. 2, 2012.

[25] Y. Liu, G. Wang, Y. Cai et al., "In vitro effects of nanophase hydroxyapatite particles on proliferation and osteogenic differentiation of bone marrow-derived mesenchymal stem cells," *Journal of Biomedical Materials Research Part A*, vol. 90A, no. 4, pp. 1083–1091, 2009.

[26] X. Yang, X. Liu, Y. Li et al., "The negative effect of silica nanoparticles on adipogenic differentiation of human mesenchymal stem cells," *Materials Science and Engineering: C*, vol. 81, pp. 341–348, 2017.

[27] W. He, A. Kienzle, X. Liu, W. E. G. Müller, T. A. Elkhooly, and Q. Feng, "In vitro effect of 30 nm silver nanoparticles on adipogenic differentiation of human mesenchymal stem cells," *Journal of Biomedical Nanotechnology*, vol. 12, no. 3, pp. 525–535, 2016.

[28] R. Ravichandran, J. R. Venugopal, S. Sundarrajan, S. Mukherjee, and S. Ramakrishna, "Precipitation of nanohydroxyapatite on PLLA/PBLG/collagen nanofibrous structures for the differentiation of adipose derived stem cells to osteogenic lineage," *Biomaterials*, vol. 33, no. 3, pp. 846–855, 2012.

[29] M. Sadat-Shojai, M.-T. Khorasani, and A. Jamshidi, "Hydrothermal processing of hydroxyapatite nanoparticles-A Taguchi experimental design approach," *Journal of Crystal Growth*, vol. 361, pp. 73–84, 2012.

[30] S. K. Swain, S. V. Dorozhkin, and D. Sarkar, "Synthesis and dispersion of hydroxyapatite nanopowders," *Materials Science and Engineering: C*, vol. 32, no. 5, pp. 1237–1240, 2012.

[31] H. Peng, J. Wang, S. Lv, J. Wen, and J. F. Chen, "Synthesis and characterization of hydroxyapatite nanoparticles prepared by a high-gravity precipitation method," *Ceramics International*, vol. 41, no. 10, pp. 14340–14349, 2015.

[32] C. Zhou, Y. Hong, and X. Zhang, "Applications of nanostructured calcium phosphate in tissue engineering," *Biomaterials Science*, vol. 1, no. 10, pp. 1012–1028, 2013.

[33] Y. Huang, G. Zhou, L. Zheng, H. Liu, X. Niu, and Y. Fan, "Micro-/nano- sized hydroxyapatite directs differentiation of rat bone marrow derived mesenchymal stem cells towards an osteoblast lineage," *Nanoscale*, vol. 4, no. 7, pp. 2484–2490, 2012.

[34] S. Sarig and F. Kahana, "Rapid formation of nanocrystalline apatite," *Journal of Crystal Growth*, vol. 237-239, pp. 55–59, 2002.

[35] K. Murakoshi, H. Hosokawa, M. Saitoh et al., "Preparation of size-controlled hexagonal CdS nanocrystallites and the characteristics of their surface structures," *Journal of the Chemical Society, Faraday Transactions*, vol. 94, no. 4, pp. 579–586, 1998.

[36] W.-J. Li, E.-W. Shi, W.-Z. Zhong, and Z.-W. Yin, "Growth mechanism and growth habit of oxide crystals," *Journal of Crystal Growth*, vol. 203, no. 1-2, pp. 186–196, 1999.

[37] J. Liu, K. Li, H. Wang, M. Zhu, and H. Yan, "Rapid formation of hydroxyapatite nanostructures by microwave irradiation," *Chemical Physics Letters*, vol. 396, no. 4-6, pp. 429–432, 2004.

[38] M. Motskin, D. M. Wright, K. Muller et al., "Hydroxyapatite nano and microparticles: correlation of particle properties with cytotoxicity and biostability," *Biomaterials*, vol. 30, no. 19, pp. 3307–3317, 2009.

[39] C. He, Y. Hu, L. Yin, C. Tang, and C. Yin, "Effects of particle size and surface charge on cellular uptake and biodistribution of polymeric nanoparticles," *Biomaterials*, vol. 31, no. 13, pp. 3657–3666, 2010.

[40] Z. Liu, Y. Xiao, W. Chen et al., "Calcium phosphate nanoparticles primarily induce cell necrosis through lysosomal rupture: the origination of material cytotoxicity," *Journal of Materials Chemistry B*, vol. 2, no. 22, pp. 3480–3489, 2014.

[41] A. K. Gaharwar, S. M. Mihaila, A. Swami et al., "Bioactive silicate nanoplatelets for osteogenic differentiation of human mesenchymal stem cells," *Advanced Materials*, vol. 25, no. 24, pp. 3329–3336, 2013.

[42] X. Yang, Y. Li, X. Liu et al., "The stimulatory effect of silica nanoparticles on osteogenic differentiation of human mesenchymal stem cells," *Biomedical Materials*, vol. 12, no. 1, article 015001, 2017.

[43] X. Liu, W. He, Z. Fang, A. Kienzle, and Q. Feng, "Influence of silver nanoparticles on osteogenic differentiation of human mesenchymal stem cells," *Journal of Biomedical Nanotechnology*, vol. 10, no. 7, pp. 1277–1285, 2014.

[44] X. Zan, P. Sitasuwan, S. Feng, and Q. Wang, "Effect of roughness on in situ biomineralized CaP-collagen coating on the osteogenesis of mesenchymal stem cells," *Langmuir*, vol. 32, no. 7, pp. 1808–1817, 2016.

[45] Y. Chen, B. S. Bal, and J. P. Gorski, "Calcium and collagen binding properties of osteopontin, bone sialoprotein, and bone acidic glycoprotein-75 from bone," *Journal of Biological Chemistry*, vol. 267, no. 34, pp. 24871–24878, 1992.

[46] J. Wang, G. Yang, Y. Wang et al., "Chimeric protein template-induced shape control of bone mineral nanoparticles and its impact on mesenchymal stem cell fate," *Biomacromolecules*, vol. 16, no. 7, pp. 1987–1996, 2015.

[47] S. M. Zakaria, S. H. Sharif Zein, M. R. Othman, F. Yang, and J. A. Jansen, "Nanophase hydroxyapatite as a biomaterial in advanced hard tissue engineering: a review," *Tissue Engineering Part B: Reviews*, vol. 19, no. 5, pp. 431–441, 2013.

[48] X. Yao, H. J. Ji, Y. K. Liu et al., "Hydroxyapatite conditioned medium enhance the osteogenic differentiation of mesenchymal stem cells," *Minerva Biotecnologica*, vol. 22, pp. 9–15, 2010.

[49] D. H. Kohn, M. Sarmadi, J. I. Helman, and P. H. Krebsbach, "Effects of pH on human bone marrow stromal cells in vitro: implications for tissue engineering of bone," *Journal of Biomedical Materials Research*, vol. 60, no. 2, pp. 292–299, 2002.

[50] W. K. Ramp, L. G. Lenz, and K. K. Kaysinger, "Medium pH modulates matrix, mineral, and energy metabolism in cultured chick bones and osteoblast-like cells," *Bone and Mineral*, vol. 24, no. 1, pp. 59–73, 1994.

[51] K. K. Kaysinger and W. K. Ramp, "Extracellular pH modulates the activity of cultured human osteoblasts," *Journal of Cellular Biochemistry*, vol. 68, no. 1, pp. 83–89, 1998.

[52] Z. Shi, X. Huang, Y. Cai, R. Tang, and D. Yang, "Size effect of hydroxyapatite nanoparticles on proliferation and apoptosis of osteoblast-like cells," *Acta Biomaterialia*, vol. 5, no. 1, pp. 338–345, 2009.

[53] Y. Cai, Y. Liu, W. Yan et al., "Role of hydroxyapatite nanoparticle size in bone cell proliferation," *Journal of Materials Chemistry*, vol. 17, no. 36, pp. 3780–3787, 2007.

[54] T. Yuan, H. Luo, J. Tan, H. Fan, and X. Zhang, "The effect of stress and tissue fluid microenvironment on allogeneic chondrocytes in vivo and the immunological properties of engineered cartilage," *Biomaterials*, vol. 32, no. 26, pp. 6017–6024, 2011.

[55] Q. Lei, J. Chen, W. Huang, D. Wu, H. Lin, and Y. Lai, "Proteomic analysis of the effect of extracellular calcium ions on human mesenchymal stem cells: implications for bone tissue engineering," *Chemico-Biological Interactions*, vol. 233, pp. 139–146, 2015.

[56] Y. K. Liu, Q. Z. Lu, R. Pei et al., "The effect of extracellular calcium and inorganic phosphate on the growth and osteogenic differentiation of mesenchymal stem cells *in vitro*: implication for bone tissue engineering," *Biomedical Materials*, vol. 4, no. 2, article 025004, 2009.

[57] M. Zayzafoon, "Calcium/calmodulin signaling controls osteoblast growth and differentiation," *Journal of Cellular Biochemistry*, vol. 97, no. 1, pp. 56–70, 2006.

[58] C. J. Marshall, "Specificity of receptor tyrosine kinase signaling: transient versus sustained extracellular signal-regulated kinase activation," *Cell*, vol. 80, no. 2, pp. 179–185, 1995.

[59] N. Agell, O. Bachs, N. Rocamora, and P. Villalonga, "Modulation of the Ras/Raf/MEK/ERK pathway by Ca^{2+}, and calmodulin," *Cellular Signalling*, vol. 14, no. 8, pp. 649–654, 2002.

Review Article

Autologous Stem Cell Therapy in Critical Limb Ischemia: A Meta-Analysis of Randomized Controlled Trials

Baocheng Xie ⓘ,[1] Houlong Luo ⓘ,[2] Yusheng Zhang ⓘ,[1] Qinghui Wang ⓘ,[1] Chenhui Zhou ⓘ,[3] and Daohua Xu ⓘ[1,4]

[1]*Department of Pharmacology, Guangdong Medical University, Dongguan 523808, China*
[2]*Institute of Laboratory Medicine, Guangdong Medical University, Dongguan 523808, China*
[3]*School of Nursing, Guangdong Medical University, Dongguan 523808, China*
[4]*Institute of Traditional Chinese Medicine and New Pharmacy Development, Guangdong Medical University, Dongguan 523808, China*

Correspondence should be addressed to Daohua Xu; daohuax108@163.com

Objective. Critical limb ischemia (CLI) is the most dangerous stage of peripheral artery disease (PAD). Many basic researches and clinical treatment had been focused on stem cell transplantation for CLI. This systematic review was performed to review evidence for safety and efficacy of autologous stem cell therapy in CLI. *Methods.* A systematic literature search was performed in the SinoMed, PubMed, Embase, ClinicalTrials.gov, and Cochrane Controlled Trials Register databases from building database to January 2018. *Results.* Meta-analysis showed that cell therapy significantly increased the probability of ulcer healing (RR = 1.73, 95% CI = 1.45–2.06), angiogenesis (RR = 5.91, 95% CI = 2.49–14.02), and reduced the amputation rates (RR = 0.59, 95% CI = 0.46–0.76). Ankle-brachial index (ABI) (MD = 0.13, 95% CI = 0.11–0.15), TcO_2 (MD = 12.22, 95% CI = 5.03–19.41), and pain-free walking distance (MD = 144.84, 95% CI = 53.03–236.66) were significantly better in the cell therapy group than in the control group ($P < 0.01$). *Conclusions.* The results of this meta-analysis indicate that autologous stem cell therapy is safe and effective in CLI. However, higher quality and larger RCTs are required for further investigation to support clinical application of stem cell transplantation.

1. Introduction

Critical limb ischemia (CLI) is the most dangerous stage of peripheral artery disease (PAD) caused by distal tissue hypoxia injury and lack of blood supply, including distal extremity ischemia, ulcers, or gangrene [1, 2]. The prevalence of PAD in the general population is 3% to 10% [3, 4]. The data showed that 11.2% of patients with PAD would deteriorate to CLI each year, and the patient with CLI had the high amputation and mortality rates [5]. Currently, patients in PAD could be treated by percutaneous transluminal angioplasty (PTA) or intravascular thrombolysis [6, 7]; however, 10%–30% of patients with CLI are not candidates for revascularization surgery. Many patients lose the chance of PTA, and the prognosis is poor after surgery, because the patients have

peripheral atherosclerosis obliterans, extensive vascular disease, and/or serious damage caused by severe ischemic lesions of limbs [8, 9]. The studies [3, 10] found that vascular remodeling and other means still cannot alleviate the symptoms of ischemia. The amputation rate is 10%–40%, and the mortality rate is up to 20% in patients with CLI within 6 months [11]. The angiogenesis is the optimal treatment for CLI, and autologous stem cell therapy is an emerging alternative treatment [12, 13].

Since 2002, Tateishi-Yuyama et al. [14] have reported that bone marrow mononuclear cell transplantation was safe and effective for therapeutic angiogenesis in patients with CLI and it could significantly promote ulcer healing and reduce the amputation rate. During the past decades, a large number of basic researches and clinical treatment had been

focused on stem cell transplantation for CLI [15]. The stem cell transplantation may improve pathophysiologic processes by stimulating the activities of tissue repair cells and inducing into vascular endothelial cells [16, 17]. However, only few evidences were available regarding safety and efficacy of autologous stem cell therapy in CLI. Meta-analyses have already become supporting evidence-based medicine. Although, there were some meta-analyses of stem cell therapy in CLI, the small amount of studies or incomplete indicators lead to the results of deviation and unconvinced [18, 19]. Therefore, this study of 23 RCTs with a total of 962 patients was included in order to acquire high-quality evidence for the clinical efficacy and safety of autologous stem cell therapy in CLI.

2. Methods

2.1. Literature Search. We searched the clinical studies, including SinoMed, PubMed, Embase, http://ClinicalTrials.gov, and Cochrane Controlled Trials Register databases from building database to January 2018. Using the terms number 1 "stem cells," "mononuclear cells," "granulocyte colony-stimulating factor," "G-CSF," "peripheral blood," and "bone marrow," the above search terms were connected with "OR". Number 2 "critical limb ischemia," "peripheral arterial disease," "peripheral vascular disease," "diabetic foot," "revascularization," "angiogenesis," or "arteriogenesis", the above search terms were connected with "OR". Number 3 "randomized controlled". Then, the above search terms of number 1, number 2, and number 3 were connected with "AND". We manually searched the references of the original and review articles for possible related studies.

2.2. Study Selection. For the systematic review, we searched 23 clinical studies that met the following criteria: (1) patients with PAD or CLI, (2) received autologous stem cell therapy, (3) reported as randomized controlled trials (RCTs), (4) the control group received standard therapy with or without sham injections, (5) at least 1-month follow-up, and (6) reported efficacy and safety issues.

2.3. Data Extraction and Quality Assessment. Two of the authors independently extracted the data of literature and made a quality assessment process according to the predefined inclusion criteria. Difference among the two authors was solved by discussion with the third author. We used the Cochrane risk of bias tool for the quality evaluation of the included studies. This quality evaluating strategy included criteria concerning aspects of random sequence generation, allocation concealment, blinding of participants and personnel, blinding of outcome assessors, incomplete outcome data, selective reporting, and other biases [20].

2.4. Statistical Analysis. In this meta-analysis, statistical analysis was performed using RevMan software version 5.3 and we used risk ratio (RR) with 95% confidence interval (CI) for the analysis of dichotomous data, whereas the continuous data were presented as weighted mean difference (MD) or standardized mean difference (SWD) with 95% CI. Heterogeneity between the studies was determined using the chi-square test, with the I^2 statistic, where $I^2 < 25\%$ represent mild inconsistency, values between 25% and 50% represent moderate inconsistency and values $> 50\%$ suggest severe heterogeneity between the studies. We defined $I^2 > 50\%$ as an indicator of significant heterogeneity among the trials. We used random effects' models to estimate the pooled results to minimize the influence of potential clinical heterogeneity among the studies, and the statistical significance was assumed at $P < 0.05$. Subgroup analysis was assessed using the χ^2 test. Sensitivity analysis was performed to evaluate the robustness of merged results, by removing individual study. Publication bias was assessed by means of funnel plots.

3. Results

3.1. Search Results. A systematic search of studies published until January 2018 was performed through SinoMed, PubMed, Embase, http://ClinicalTrials.gov, and Cochrane Controlled Trials Register databases from building database. A total of 1130 literatures were searched, 23 RCTs were included in the inclusion criteria, and the literature search procedure was shown in Figure 1.

3.2. Study Characteristics. The general characteristics of the included studies were listed in Table 1. The included studies were 23 RCTs with a total of 962 patients. In these studies, the cell therapy group was one of the following stem cells: bone marrow mononuclear cells (BMMNCs, $n = 7$ studies), bone marrow mesenchymal stem cells (BMMSCs, $n = 4$ studies), bone marrow stem cells (BMSCs, $n = 5$ studies), peripheral blood mononuclear cells (PBMNCs, $n = 2$ studies), peripheral blood stem cells (PBSCs, $n = 4$ studies), CD34+ ($n = 1$ study), or CD133+ stem cells ($n = 1$ study). The transplantation method of stem cell was intramuscular ($n = 20$ studies) or intra-arterial ($n = 3$ studies). The patients in the control group received either placebo or standard care ($n = 23$ studies). The dose of stem cells was divided into three groups: high dose (10^9, $n = 5$ studies), medium dose (10^8, $n = 5$ studies), and low dose (10^7, $n = 5$ studies). The mean follow-ups of the studies were 3 months ($n = 9$ studies), 6 months ($n = 8$ studies), and 12 months ($n = 3$ studies).

3.3. Quality Assessment. The risks of biases of the included studies were evaluated by the Cochrane assessment tool, and these results were summarized in Table 2. Three of the studies were at high risk of bias for blinding of participants and personnel and other biases according to the Cochrane Collaboration tool. Five studies reported methods of random sequence, and three studies reported the details of allocation concealment.

3.4. Amputation Rate. Amputation rate was reported in 18 studies with a total of 512 patients treated with cell therapy and 525 patients in the control groups (Figure 2). Cell therapy was associated with a significant 41% reduction in the amputation rate, compared with control groups (RR = 0.59, 95% CI = 0.46–0.76, $P < 0.0001$). Subgroup analyses indicated that peripheral blood stem cell (PBSC) was more beneficial than bone marrow stem cell (BMSC) on the amputation rate ($P = 0.03$, $I^2 = 78.6\%$). Intramuscular of autologous stem
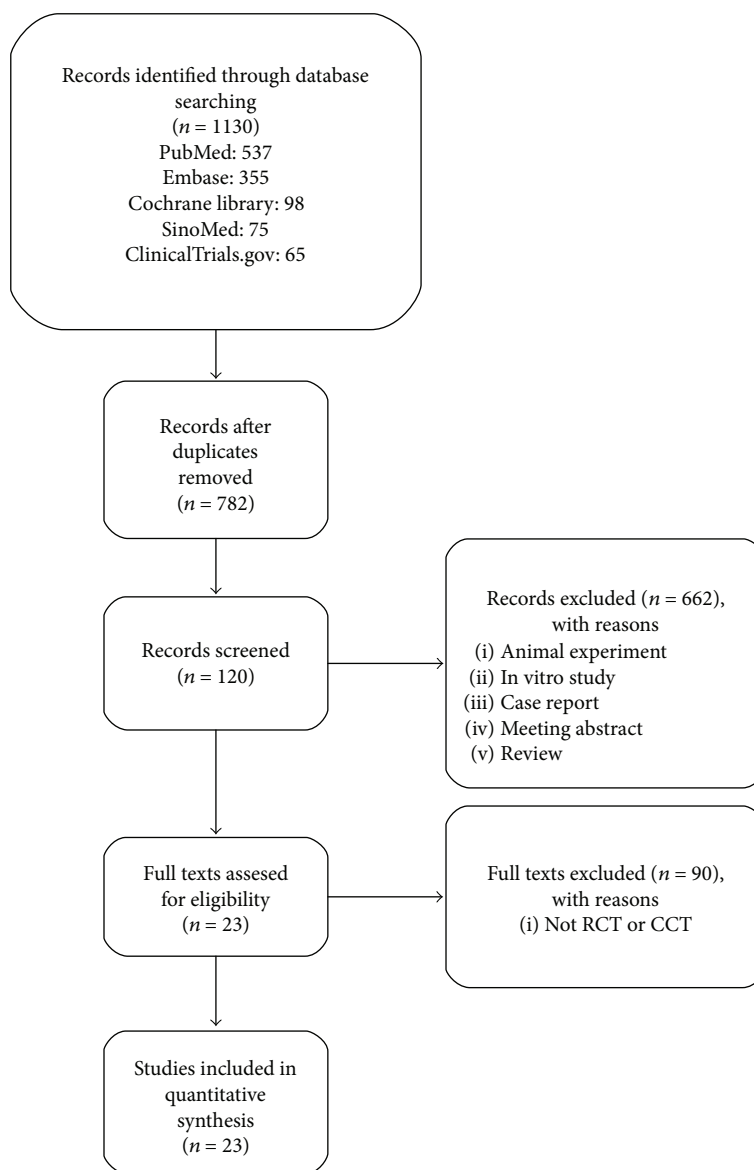
FIGURE 1: Flow chart and strategy of the meta-analysis.

cell transplantation was better than intra-arterial in reducing the amputation rate ($P = 0.05$, $I^2 = 75\%$). The mean follow-ups of the studies were divided into 3 months, 6 months, and 12 months, and the group of 3 months was a significant difference compared with 6 months and 12 months ($P = 0.03$). Subgroup analysis among high dose (10^9), medium dose (10^8), and low dose (10^7) showed that the group of low dose (10^7) had a significant effect in reducing the amputation rate.

3.5. Ulcer Healing and Pain-Free Walking Distance.
Ulcer healing was included in the analysis of 18 studies (Figure 3). Results of analysis showed that cell therapy could significantly increase the probability of ulcer healing (RR = 1.73, 95% CI = 1.45–2.06, $P < 0.00001$). Subgroup analyses indicated that the low dose (10^7) group of autologous stem cell transplantation was better than the other groups in ulcer healing (RR = 3.55, 95% CI = 1.95–6.48, $P = 0.02$). Pain-free

walking distance significantly increased in cell therapy (MD = 144.84, 95% CI = 53.03–236.66, $P = 0.002$) (Figure 4).

3.6. Ankle-Brachial Index (ABI) and Transcutaneous Oxygen Tension (TcO_2).
ABI with 15 studies was included in the analysis (Figure 5). Results indicated that cell therapy significantly improved the ABI by 0.13 (MD = 0.13, 95% CI = 0.11–0.15, $P < 0.00001$). Subgroup analyses indicated that bone marrow mesenchymal stem cells (BMMSCs) were superior to bone marrow mononuclear cells (BMMNCs), but there was no significant difference between bone marrow stem cells (BMSCs) and peripheral blood stem cells (PBSCs) in improving the ABI. The TcO_2 with 8 studies was included in the analysis. Results indicated that cell therapy significantly improved TcO_2 by 12.22 mmHg (MD = 12.22, 95% CI = 5.03–19.41, $P = 0.0009$). Subgroup analyses showed that there was no beneficial effect between BMSCs and PBSCs on the TcO_2 (Figure 6).

TABLE 1: Characteristics of included clinical studies.

Study	Sample (T/C)	Age (T/C)	Intervention T	Intervention C	Injection	Follow-up	Number of cells	Evaluation
Huang et al. [37]	14/14	71.1/70.9	PBMNCs	Standard care	IM	12 w	3×10^9	①, ②, ③, ④, ⑥, ⑦
Arai et al. [23]	13/12	62/68	BMMNCs	Standard care	IM	1 mo	$1\text{--}3 \times 10^9$	②, ⑤
Barć et al. [24]	14/15	Unclear	BMMNCs	Standard care	IM	6 mo	Unclear	①, ②
Lu et al. [38]	22/23	66.6/65.5	BMMSCs	Standard care	IM	12 w	$7.32 \times 10^8 - 5.61 \times 10^9$	①, ②, ③, ④, ⑥
Dash et al. [39]	12/12	40	BMMSCs	Standard care	IM	12 w	$4.5\text{-}6 \times 10^7$	②, ⑥
Shi et al. [40]	25/25	Unclear	BMSCs	Standard care	IM	3 mo	Unclear	②, ④, ⑦
Procházka et al. [30]	42/54	66.2/64.1	BMSCs	Standard care	IA	4 mo	1.96×10^8	①, ②, ③
Wen and Huang [34]	30/30	63	PBSCs	Standard care	IM	3 mo	3×10^9	①, ②, ③, ④, ⑦
Lu [15]	21/41	63	BMMNCs	Standard care	IM	24 w	9.3×10^8	①, ②, ③, ④, ⑤
Lu et al. [15]	20/41	65	BMMSCs	Standard care	IM	24 w	9.6×10^8	①, ②, ③, ④, ⑤
Walter et al. [25]	19/21	64.4/64.5	BMMNCs	Standard care	IA	6 mo	1.53×10^8	①, ④, ⑤
Jain et al. [41]	25/23	54/58	BMSCs	Standard care	IM	3 mo	Unclear	②
Benoit et al. [42]	34/14	65.7/72.5	BMSCs	Standard care	IM	6 mo	Unclear	①, ②
Losordo et al. [43]	16/12	66.2/67.1	CD34+	Standard care	IM	12 mo	1×10^6 1×10^5	①, ④
Powell et al. [44]	48/24	67.3/69.2	BMSCs	Standard care	IM	12 mo	$0.35\text{--}2.95 \times 10^8$	①
Ozturk et al. [31]	20/20	71.9/70.8	PBMNCs	Standard care	IM	3 mo	2.48×10^7	①, ②, ③, ④, ⑤, ⑥
Gupta et al. [29]	10/10	43/47.6	BMMSCs	Standard care	IM	6 mo	2×10^9	①, ②, ④
Li et al. [26]	29/29	61/63	BMMNCs	Standard care	IM	6 mo	1×10^7	①, ②
Mohammadzadeh et al. [32]	7/14	63.5/64.2	PBSCs	Standard care	IM	3 mo	2×10^7	①, ②, ④
Szabo et al. [33]	10/10	60.6/63	PBSCs	Standard care	IM	24 mo	6.64×10^7	②, ⑤
Raval et al. [9]	7/3	65/85	CD133+	Standard care	IM	12 mo	$5\text{--}40 \times 10^7$	①
Teraa et al. [5]	81/79	69/65	BMMNCs	Standard care	IA	6 mo	$5\text{-}6 \times 10^8$	①, ②, ④, ⑤
Skóra et al. [45]	16/16	66.7/68.3	BMMNCs	Pentoxifylline	IM	3 mo	1.58×10^9	①, ③, ④
Lu et al. [46]	20/21	67.2	PBSCs	Standard care	IM	6 mo	Unclear	④, ⑤

Note: T = cell therapy; C = control group; IM = intramuscular; IA = intra-arterial; w = week; mo = month; PBMNCs = peripheral blood mononuclear cells; BMMNCs = bone marrow mononuclear cells; BMMSCs = bone marrow mesenchymal stem cells; BMSCs = bone marrow stem cells; PBSCs = peripheral blood stem cells; ① = amputation; ② = ulcer healing; ③ = angiographic; ④ = ABI; ⑤ = TcO₂; ⑥ = pain-free walking distance; ⑦ = the blood flow of 10 toes.

3.7. Angiogenesis and Blood Flow of 10 Toes. There were 8 studies included in the analysis with angiogenesis (Figure 7). Analysis by digital subtraction angiography revealed that autologous stem cell transplantation significantly improved the new vessel form (RR = 5.91, 95% CI = 2.49–14.02, $P < 0.0001$). The number of ischemic limbs with rich new collateral vessels in the transplant patients was significantly higher than that in the control group. Meanwhile, the blood flow of 10 toes significantly increased in cell therapy (SMD = 0.83, 95% CI = 0.48–1.18, $P < 0.00001$) (Figure 8).

3.8. Publication Bias and Heterogeneity. According to this meta-analysis, the significant symmetry showed that the ABI did not have obvious publication bias. Furthermore, the Egger's test funnel plot also indicated that there was no obvious publication bias in the ABI ($P > 0.363$, 95% CI = −0.57–1.45) (Figure 9). Sensitivity analysis was performed using a Galbraith plot for all the indicators. The results showed that there was no substantial change in the ABI and amputation rate, indicating that the results of meta-analysis were credible (Figure 10).

4. Discussion

4.1. Main Outcome. The registrations of stem cell clinical trials were retrieved on USA National Institutes of Health (NIH) clinical trial registration website (http://ClinicalTrials.gov). We performed the databases from building database to January 2018. There were 4715 clinical trial registration information for stem cells all over the world, and there were 2399 studies in America, 1027 studies in Europe, and 574 studies in China. We analyzed the disease of stem cell therapy and found that there were 1767 studies on neoplasms by histologic type, 1279 studies on immune system diseases, 607 studies on vascular diseases, and 513 studies on bone marrow diseases. The data showed that stem cell therapy has been used in various diseases, and stem cell therapy is approved in the globe. This meta-analysis included 23 RCTs with a total of 962 patients with CLI who were ineligible for surgical or percutaneous revascularization. Results indicated that autologous stem cell therapy had the potential effect to reduce the risk of amputation by 41% and significantly increased the probability effect of ulcer healing by 73% compared with the control group. ABI and TcO₂ are the basic

TABLE 2: Cochrane risk of bias assessment.

Study	Random sequence generation	Allocation concealment	Blinding of participants and personnel	Blinding of outcome assessment	Incomplete outcome data	Selective reporting	Other biases
Huang et al. [37]	Unclear	Unclear	Unclear	Unclear	Low	Unclear	Low
Arai et al. [23]	Unclear	Unclear	High	Unclear	Low	Low	Low
Barć et al. [24]	Unclear	Unclear	High	Unclear	Low	Low	Low
Lu et al. [38]	Unclear	Unclear	Unclear	Unclear	Low	Low	Low
Dash et al. [39]	Unclear	Unclear	High	Unclear	Low	Unclear	Low
Shi et al. [40]	Unclear	Unclear	High	Unclear	Low	Low	High
Procházka et al. [30]	Low	Low	High	Unclear	Low	Low	Low
Wen and Huang [34]	Unclear	Unclear	Unclear	Unclear	Low	Low	High
Lu [15]	Unclear	Unclear	Low	Unclear	Low	Unclear	Low
Lu et al. [15]	Low	Unclear	Low	Low	Low	Low	Low
Walter et al. [25]	Unclear	Unclear	Low	Unclear	Low	Unclear	Low
Jain et al. [41]	Low	Low	Low	Unclear	Low	Unclear	Low
Benoit et al. [42]	Unclear	Unclear	Low	Unclear	Low	Low	Low
Losordo et al. [43]	Unclear	Unclear	Low	Low	Low	Unclear	Low
Powell et al. [44]	Unclear	Unclear	Low	Unclear	Low	Unclear	Low
Ozturk et al. [31]	Unclear	Unclear	High	Unclear	Low	Low	Low
Gupta et al. [29]	Low	Low	Low	Low	Low	Low	Low
Li et al. [26]	Unclear	Unclear	Unclear	Unclear	Low	Unclear	Low
Mohammadzadeh et al. [32]	Unclear	Unclear	Unclear	Unclear	Low	Low	Low
Szabo et al. [33]	Unclear	Unclear	High	Low	Low	Low	Low
Raval et al. [9]	Unclear	Unclear	Low	Low	Low	Low	Low
Teraa et al. [5]	Low	Unclear	Low	Low	Low	Low	Low
Skóra et al. [45]	Low	Unclear	Low	Low	Low	Low	Low
Lu et al. [46]	Unclear	Unclear	High	Low	Low	Low	High

Note: low = low risk of bias; unclear = unclear risk of bias; high = high risk of bias.

indicators of CLI, and the results indicated that cell therapy significantly improved the ABI by 0.13 and TcO_2 by 12.22 mmHg. Moreover, the value of the increased ABI and TcO_2 level were meaningful to confirm the truth of the improvements of amputation and wound healing rates. In addition, cell therapy could improve the endpoints of limb perfusion, and the blood flow of 10 toes significantly increased in cell therapy, compared with the control group. We speculated that the main reason for the increases of limb perfusion was angiogenesis. The studies reported that endothelial progenitor cells (EPCs) derived from the bone marrow can facilitate microvasculature regeneration by paracrine or direct mechanisms in regions of blood vessel formation [21, 22]. Therefore, we made a statistics on the use of angiography in patients with CLI. There were 8 studies with RCTs in the analysis, revealing a significant effect of angiogenesis after autologous stem cell transplantation.

4.2. Subgroup Analysis. A study by Tateishi-Yuyama et al. [14] reported that transplantation of bone marrow stem cell therapy in patients with CLI significantly improved TcO_2, ABI, and pain-free walking distance. Hereafter, many studies with RCTs had investigated the safety and feasibility of autologous stem cells of BMMNC therapy in CLI [5, 15, 23–26]. In

recent years, a variety of cell types have been studied for treatment of PAD or CLI, including PBSCs, BMSCs, BMMNCs, PBMNCs, and BMMSCs. Our subgroup analyses indicated that PBSCs were more beneficial than BMSCs on the amputation rates. Dubsky et al. [13, 27] suggested that there was no significant difference in long-term prognosis between patients treated with BMMNCs and those treated with PBMNCs. The trials reported that transplantation of BMMSCs was safe and no serious adverse events by cell injection after the follow-up period [28, 29]. RCTs by Lu et al. [15] suggested that ulcer healing, ABI, TcO_2, painless walking time, and magnetic resonance angiography (MRA) in the BMMSC group were significantly higher than that in the BMMNC group in diabetic patients with CLI. The subgroup analyses indicated that BMMSCs showed beneficial effect than BMMNCs in improving the ABI. Therefore, BMMSCs could be more effective than BMMNCs in the treatment of CLI.

In RCTs of patients with CLI, the most common route of stem cell therapy administration was intramuscular. But, the potential route of intra-arterial was also injected therapy [5, 25, 30]. In order to find suitable and beneficial injection therapy, we conducted subgroup analysis. The results showed that the amputation rate in the intramuscular group was significantly lower than that in the intra-arterial group. The
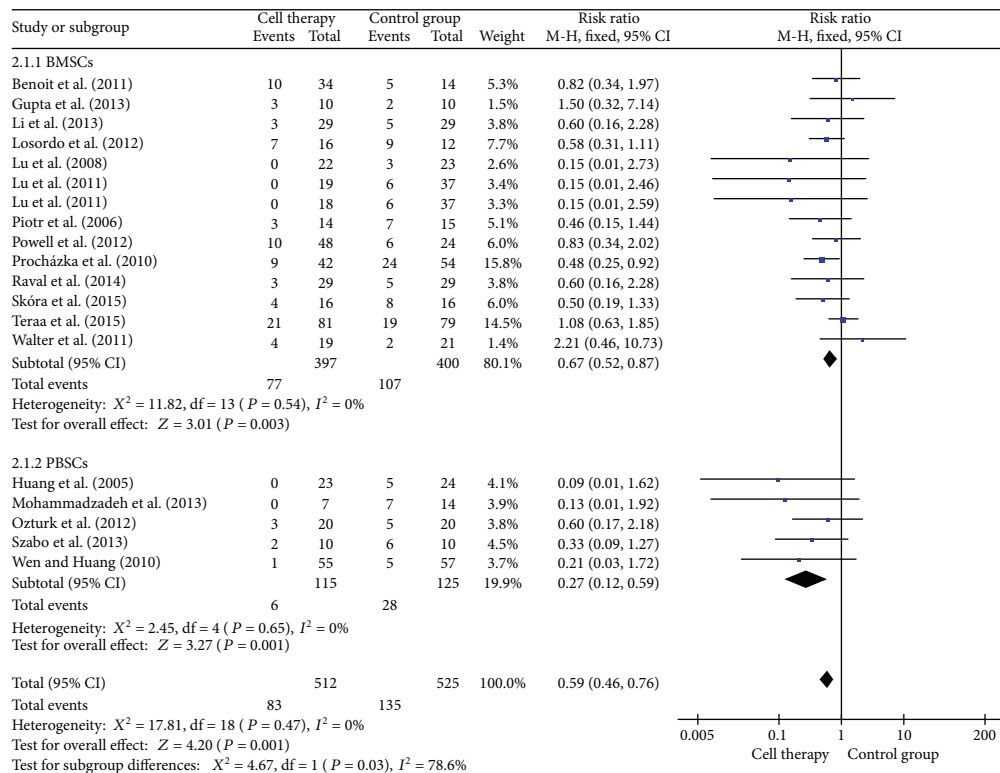
(a)
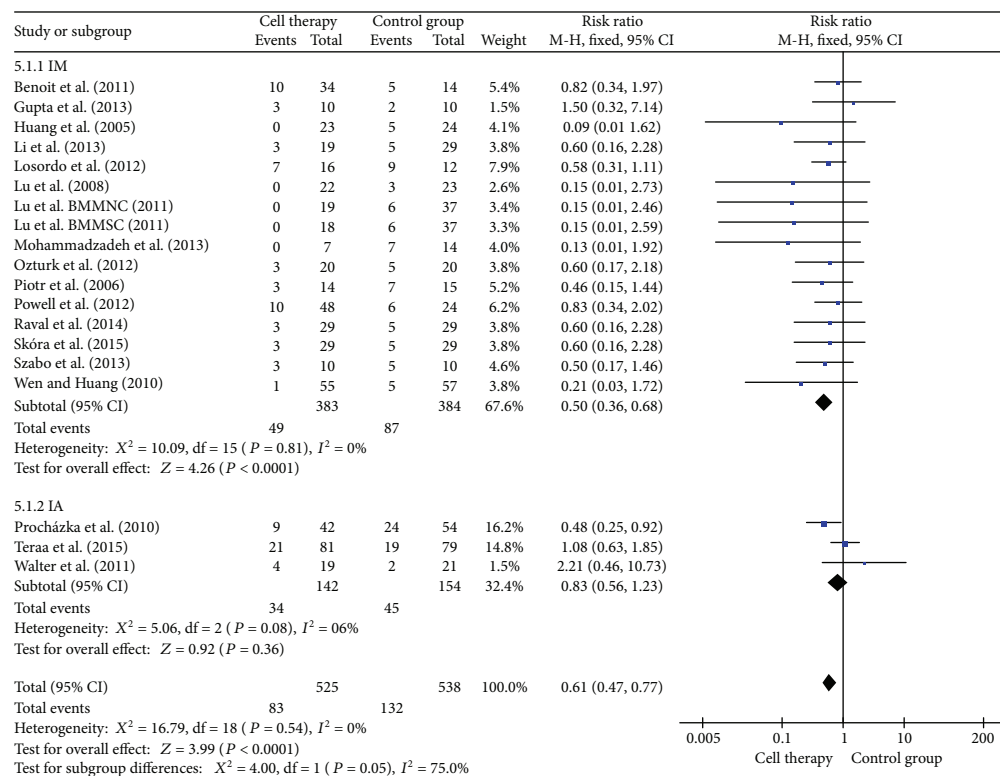
(b)

FIGURE 2: Forest plot of meta-analysis of the amputation rate in cell therapy and standard care for critical limb ischemia. (a) Subgroup analyses of bone marrow stem cells (BMSCs) versus peripheral blood stem cells (PBSCs). (b) Subgroup analyses of intramuscular (IM) versus intra-arterial (IA). Squares indicate the risk ratio, and horizontal lines represent 95% confidence intervals.
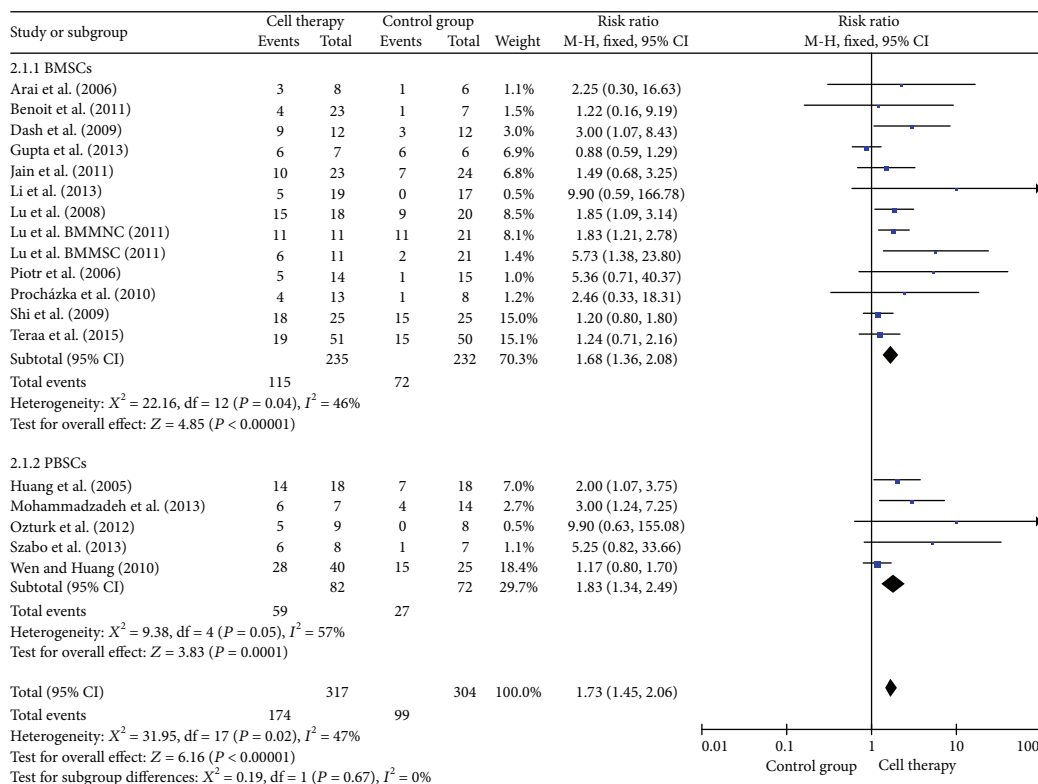
(a)
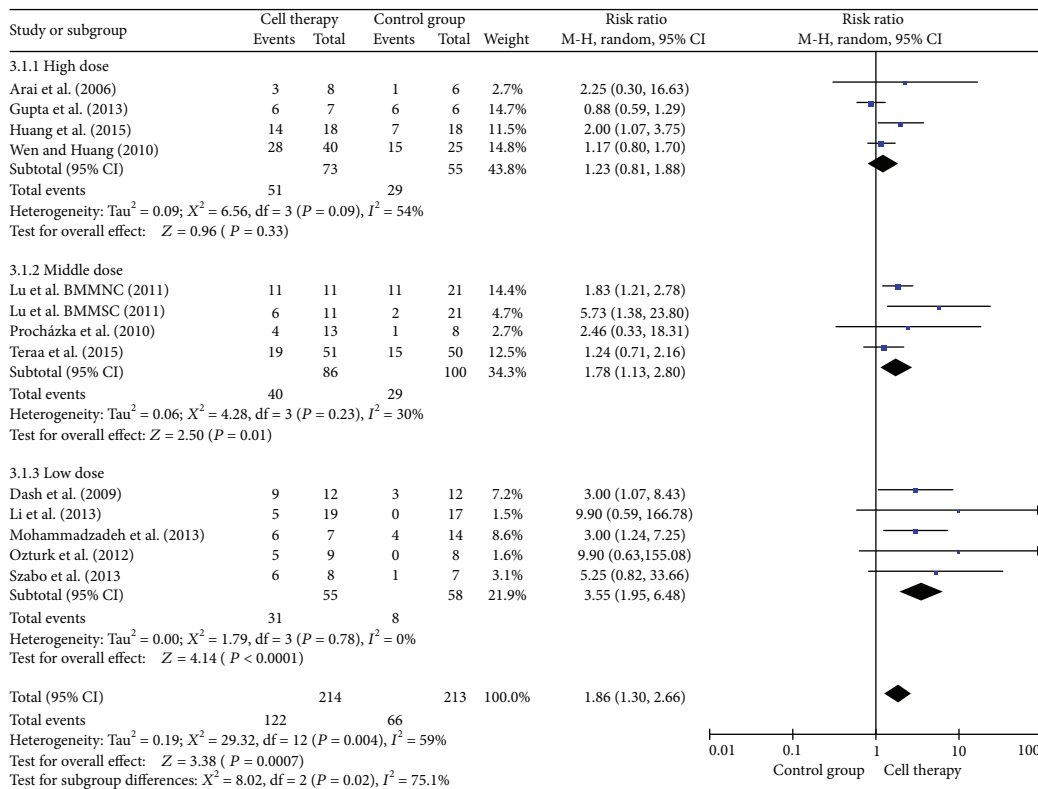
(b)

FIGURE 3: Forest plot of meta-analysis of ulcer healing in cell therapy and standard care for critical limb ischemia. (a) Subgroup analyses of bone marrow stem cells (BMSCs) versus peripheral blood stem cells (PBSCs). (b) Subgroup analyses among high dose (10^9), medium dose (10^8), and low dose (10^7). Squares indicate the risk ratio, and horizontal lines represent 95% confidence intervals.

| Study or subgroup | Cell therapy | | | Control group | | | Weight | Mean difference | Mean difference |
	Mean	SD	Total	Mean	SD	Total		IV, random, 95% CI	IV, random, 95% CI
Dash et al. (2009)	284.44	212.12	12	78.22	35.35	12	22.1%	206.22 (84.55, 327.89)	
Huang et al. (2005)	306.4	289.1	14	78.6	142.3	14	16.3%	227.80 (59.01, 396.59)	
Lu et al. (2008)	369.38	111.01	22	203.38	85.55	23	31.6%	166.00 (107.91, 224.09)	
Ozturk et al. (2012)	338	98	11	306	63	10	29.9%	32.00 (−37.85, 101.85)	
Total (95% CI)			59			59	100.0%	144.84 (53.03, 236.66)	

Heterogeneity: Tau^2 = 6058.60, X^2 = 11.83 df = 3 (P = 0.008), I^2 = 75%
Test for overall effect: Z = 3.09 (P = 0.002)

FIGURE 4: Forest plot of meta-analysis of pain-free walking distance in cell therapy and standard care for critical limb ischemia. Squares indicate the weighted mean difference, and horizontal lines represent 95% confidence intervals.

| Study or subgroup | Cell therapy | | | Control group | | | Weight | Mean difference | Mean difference |
	Mean	SD	Total	Mean	SD	Total		IV, fixed, 95% CI	IV, fixed, 95% CI
2.1.1 BMSCs									
Gupta et al. (2013)	0.77	0.15	7	0.6	0.14	10	2.2%	0.17 (0.03, 0.31)	
Losordo et al. H (2012)	0.6	0.05	5	0.4	0.17	5	1.8%	0.20 (0.04, 0.36)	
Losordo et al. L (2012)	0.7	0.23	4	0.4	0.17	4	0.5%	0.30 (0.02, 0.58)	
Lu et al. (2008)	0.74	0.11	22	0.61	0.11	23	10.4%	0.13 (0.07, 0.19)	
Lu et al. BMMNC (2011)	0.65	0.035	19	0.54	0.09	37	39.6%	0.11 (0.08, 0.14)	
Lu et al. BMMSC (2011)	0.72	0.078	18	0.54	0.09	37	20.2%	0.18 (0.13, 0.23)	
Shi et al. (2009)	1.08	0.16	25	0.96	0.13	25	6.6%	0.12 (0.04, 0.20)	
Skóra et al. (2015)	0.52	0.52	16	0.3	0.29	16	0.5%	0.22 (−0.07, 0.51)	
Teraa et al. (2015)	0.61	0.24	40	0.58	0.3	37	2.9%	0.03 (−0.09, 0.15)	
Walter et al. (2011)	0.75	0.23	11	0.66	0.42	15	0.7%	0.09 (−0.16, 0.34)	
Subtotal (95% CI)			167			209	85.4%	0.13 (0.11, 0.15)	
Heterogeneity: X^2 = 11.47, df = 9 (P = 0.24), I^2 = 22%									
Test for overall effect: Z = 11.53 (P < 0.00001)									
2.1.2 PBSCs									
Huang et al. (2015)	0.63	0.25	23	0.51	0.28	24	1.9%	0.12 (−0.03, 0.27)	
Lu et al. (2016)	0.45	0.17	20	0.31	0.16	21	4.2%	0.14 (0.04, 0.24)	
Mohammadzadeh et al. (2013)	0.92	0.15	7	0.65	0.25	14	1.5%	0.27 (0.10, 0.44)	
Ozturk et al. (2012)	0.87	0.24	20	0.73	0.28	20	1.7%	0.14 (−0.02, 0.30)	
Wen and Huang (2010)	0.59	0.27	55	0.51	0.21	57	5.4%	0.08 (−0.01, 0.17)	
Subtotal (95% CI)			125			136	14.6%	0.13 (0.07, 0.18)	
Heterogeneity: X^2 = 3.81, df = 4 (P = 0.43), I^2 = 0%									
Test for overall effect: Z = 4.62 (P < 0.00001)									
Total (95% CI)			292			345	100.0%	0.13 (0.11, 0.15)	

Heterogeneity: X^2 = 15.30, df = 14 (P = 0.36), I^2 = 8%
Test for overall effect: Z = 12.42 (P < 0.00001)
Test for subgroup differences: X^2 = 0.02, df = 1 (P = 0.90), I^2 = 0%

(a)

| Study or subgroup | Cell therapy | | | Control group | | | Weight | Mean difference | Mean difference |
	Mean	SD	Total	Mean	SD	Total		IV, fixed, 95% CI	IV, fixed, 95% CI
4.1.1 BMMNCs									
Lu et al. BMMNC (2011)	0.65	0.035	19	0.54	0.09	37	51.8%	0.11 (0.08, 0.14)	
Skóra et al. (2015)	0.52	0.52	16	0.3	0.29	16	0.7%	0.22 (−0.07, 0.51)	
Teraa et al. (2015)	0.61	0.24	40	0.58	0.3	37	3.8%	0.03 (−0.09, 0.15)	
Walter et al. (2011)	0.75	0.23	11	0.66	0.42	15	0.9%	0.09 (−0.16, 0.34)	
Subtotal (95% CI)			86			105	57.2%	0.11 (0.07, 0.14)	
Heterogeneity: X^2 = 2.15, df = 3 (P = 0.54), I^2 = 0%									
Test for overall effect: Z = 6.59 (P < 0.00001)									
4.1.2 BMMSC									
Gupta et al. (2013)	0.77	0.15	7	0.6	0.14	10	2.8%	0.17 (0.03, 0.31)	
Lu et al. (2008)	0.74	0.11	22	0.61	0.11	23	13.6%	0.13 (0.07, 0.19)	
Lu et al. BMMSC (2011)	0.72	0.078	18	0.54	0.09	37	26.4%	0.18 (0.13, 0.23)	
Subtotal (95% CI)			47			70	42.8%	0.16 (0.13, 0.20)	
Heterogeneity: X^2 = 1.54, df = 2 (P = 0.46), I^2 = 0%									
Test for overall effect: Z = 8.83 (P < 0.00001)									
Total (95% CI)			133			175	100.0%	0.13 (0.11, 0.15)	

Heterogeneity: X^2 = 9.25, df = 6 (P = 0.16), I^2 = 35%
Test for overall effect: Z = 10.76 (P < 0.00001)
Test for subgroup differences: X^2 = 5.56, df = 1 (P = 0.02), I^2 = 82.0%

(b)

FIGURE 5: Forest plot of meta-analysis with the ankle-brachial index (ABI) in cell therapy and standard care for critical limb ischemia. (a) Subgroup analyses of bone marrow stem cells (BMSCs) versus peripheral blood stem cells (PBSCs). (b) Subgroup analyses among bone marrow mononuclear cells (BMMNCs) and bone marrow mesenchymal stem cells (BMMSCs). Squares indicate the weighted mean difference, and horizontal lines represent 95% confidence intervals.

Study or subgroup	Cell therapy			Control group			Weight	Mean difference IV, random, 95% CI	Mean difference IV, random, 95% CI
	Mean	SD	Total	Mean	SD	Total			
2.1.1 BMSCs									
Arai et al. (2006)	32	8	13	26	5	12	13.8%	6.00 (0.81, 11.19)	
Lu et al. BMMNC (2011)	61	9	19	44	13	37	13.6%	17.00 (11.18, 22.82)	
Lu et al. BMMSC (2011)	67	8	18	44	13	37	13.7%	23.00 (17.41, 28.59)	
Teraa et al. (2015)	10.4	3.1	57	6.7	2.7	56	14.9%	3.70 (2.63, 4.77)	
Walter et al. (2011)	40.5	23	6	39.7	17	10	6.5%	0.80 (−20.41, 22.01)	
Subtotal (95% CI)			113			152	62.5%	11.07 (2.42, 19.71)	

Heterogeneity: Tau^2 = 80.36; X^2 = 62.02 df = 4 (P < 0.00001), I^2 = 94%
Test for overall effect: Z = 2.51 (P = 0.01)

2.1.2 PBSCs									
Lu et al. (2016)	39.4	1.31	20	21.37	2.04	21	14.9%	18.03 (16.99, 19.07)	
Ozturk et al. (2012)	44.31	10.03	20	31.35	14.7	20	12.7%	12.96 (5.16, 20.76)	
Szabo et al. (2013)	6.6	12.64	10	−3.5	9.3	3	10.0%	10.10 (−3.02, 23.22)	
Subtotal (95% CI)			50			44	37.5%	16.35 (12.28, 20.41)	

Heterogeneity: Tau^2 = 5.72; X^2 = 2.96, df = 2 (P = 0.23), I^2 = 32%
Test for overall effect: Z = 7.89 (P < 0.00001)

Total (95% CI)			163			196	100.0%	12.22 (5.03, 19.41)	

Heterogeneity: Tau^2 = 90.18; X^2 = 378.48, df = 7 (P < 0.00001), I^2 = 98%
Test for overall effect: Z = 3.33 (P = 0.0009)
Test for subgroup differences: X^2 = 1.17, df = 1 (P = 0.28), I^2 = 14.8%

FIGURE 6: Forest plot of meta-analysis with transcutaneous oxygen tension (TcO$_2$) in cell therapy and standard care for critical limb ischemia. Subgroup analyses of bone marrow stem cells (BMSCs) versus peripheral blood stem cells (PBSCs). Squares indicate the weighted mean difference, and horizontal lines represent 95% confidence intervals.

Study or subgroup	Cell therapy		Control group		Weight	Risk ratio M-H, random, 95% CI	Risk ratio M-H, random, 95% CI
	Events	Total	Events	Total			
Huang et al. (2005)	10	13	2	11	17.0%	4.23 (1.17, 15.35)	
Lu et al. (2008)	11	15	2	14	16.7%	5.13 (1.37, 19.19)	
Lu et al. BMMNC (2011)	8	19	0	37	7.1%	32.30 (1.96, 531.32)	
Lu et al. BMMSC (2011)	15	18	0	37	7.2%	62.00 (3.92, 981.34)	
Ozturk et al. (2012)	9	20	5	20	21.1%	1.80 (0.73, 4.43)	
Procházka et al. (2010)	4	42	0	54	6.7%	11.51 (0.64, 208.04)	
Skóra et al. (2015)	12	16	0	16	7.3%	25.00 (1.61, 389.35)	
Wen et al. (2010)	7	10	2	9	17.0%	3.15 (0.87, 11.42)	
Total (95% CI)		153		198	100.0%	5.91 (2.49, 14.02)	
Total events	76		11				

Heterogeneity: Tau^2 = 0.71, X^2 = 14.55, df = 7 (P = 0.04), I^2 = 52%
Test for overall effect: Z = 4.04 (P < 0.0001)
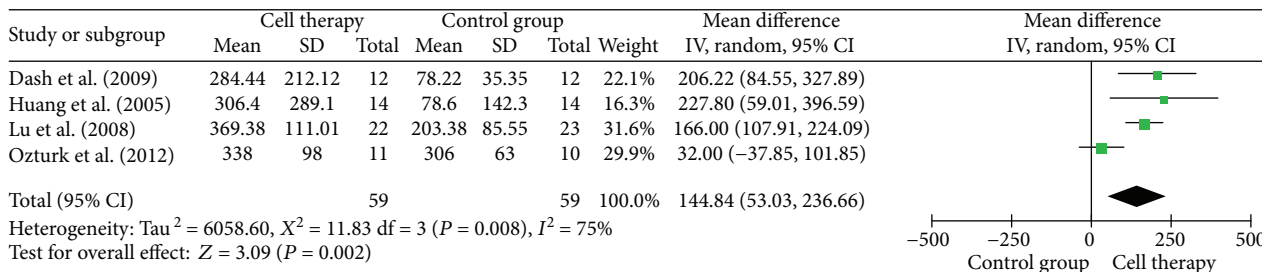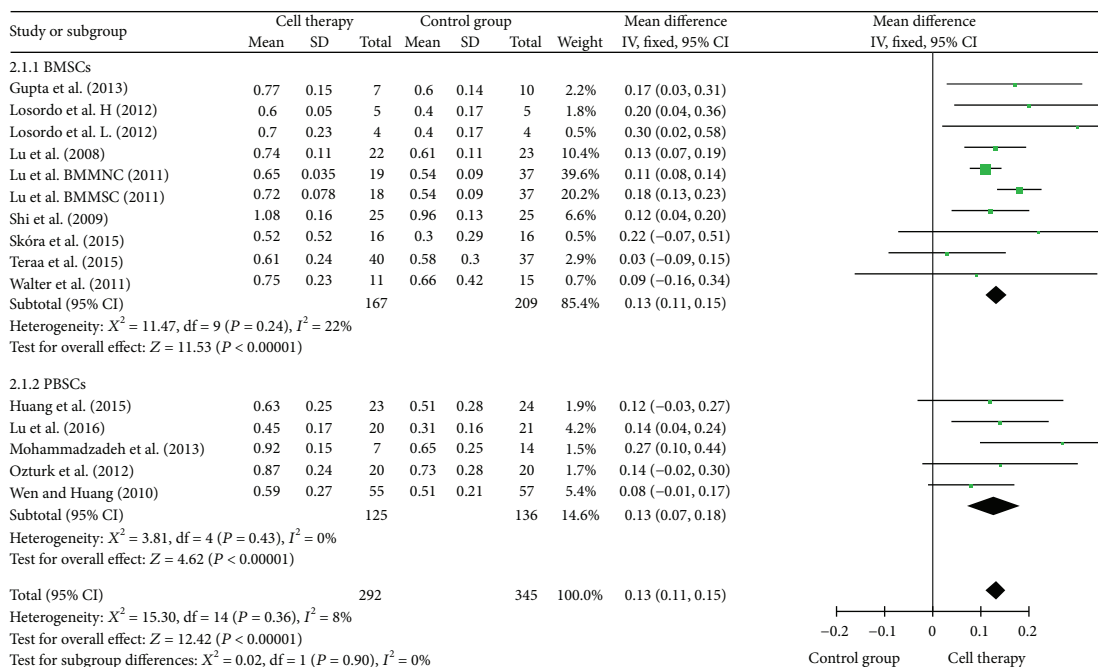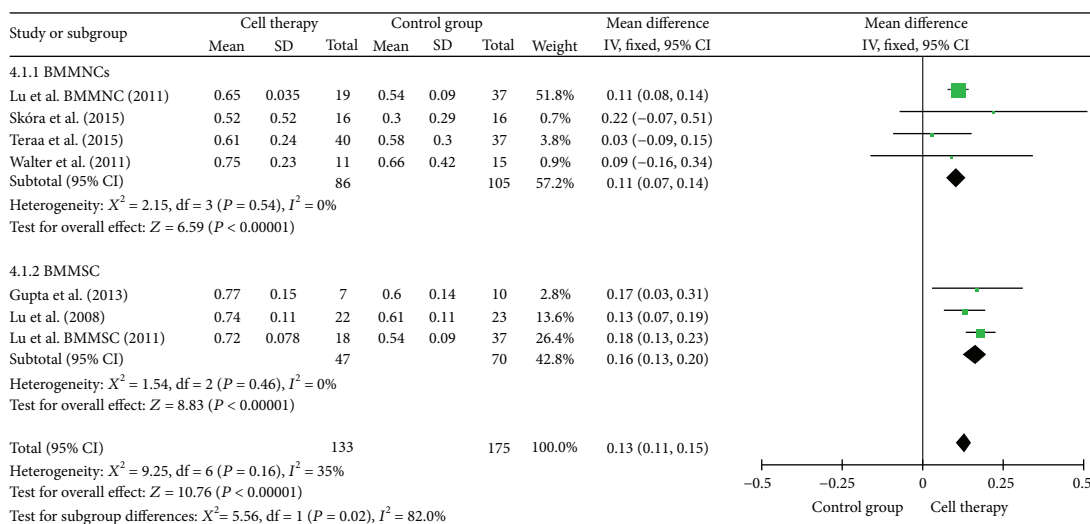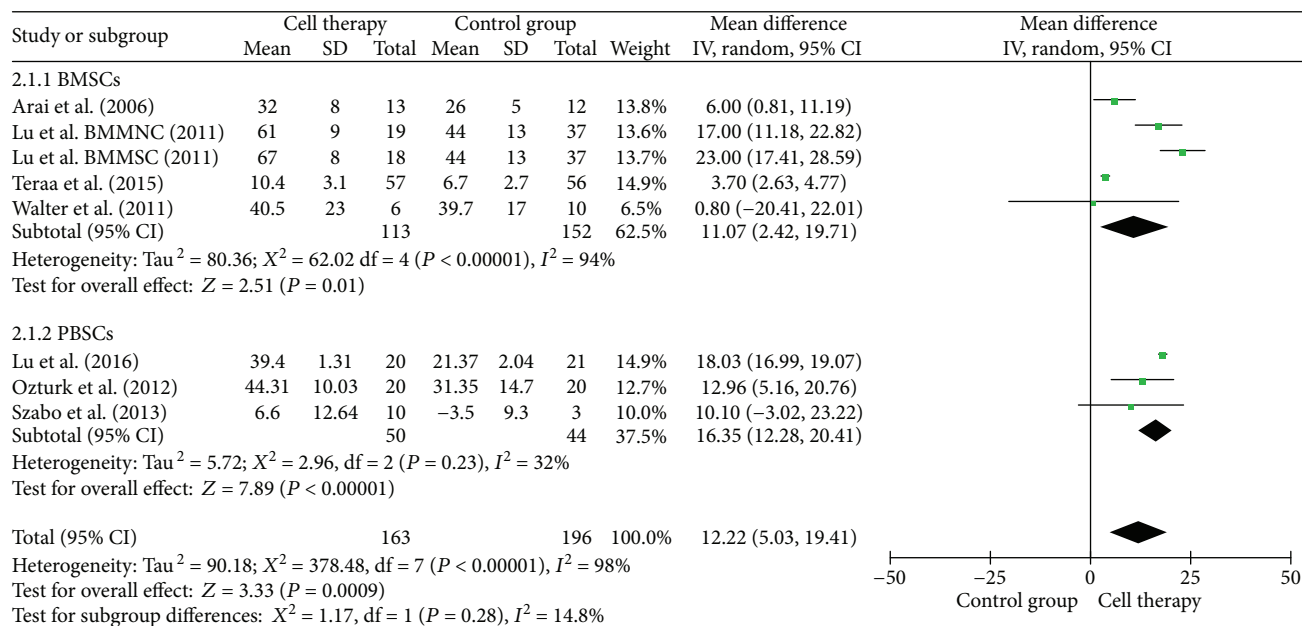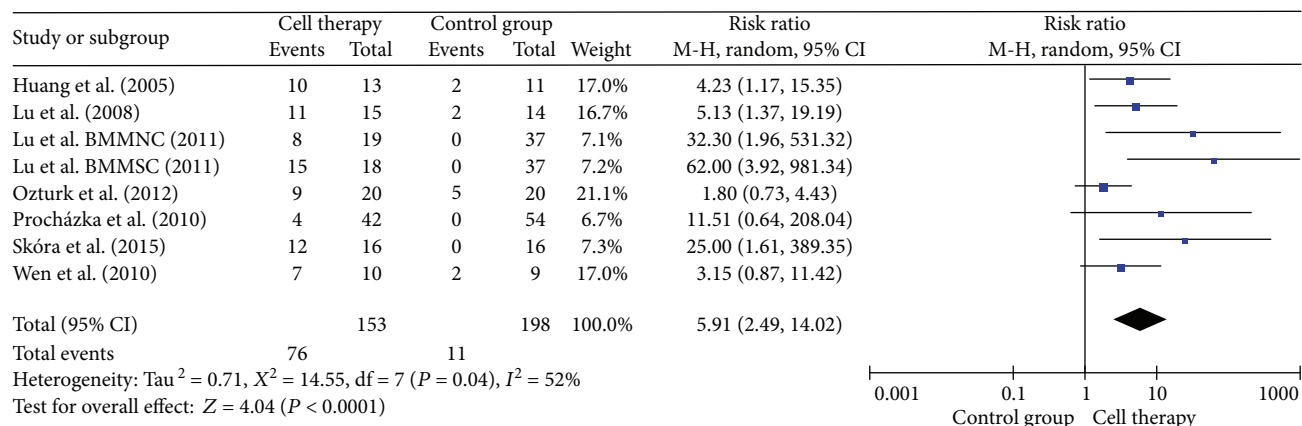

FIGURE 7: Forest plot of meta-analysis with angiogenesis in cell therapy and standard care for critical limb ischemia. Squares indicate the risk ratio, and horizontal lines represent 95% confidence intervals.

Study or subgroup	Cell therapy			Control group			Weight	Std. mean difference IV, fixed, 95% CI	Std. mean difference IV, fixed, 95% CI
	Mean	SD	Total	Mean	SD	Total			
Huang et al. (2005)	4.34	3.84	14	1.21	1.54	14	19.4%	1.04 (0.24, 1.84)	
Shi et al. (2009)	29	9	25	25	7	25	38.8%	0.49 (−0.07, 1.05)	
Wen et al. (2010)	3.89	2.94	30	1.43	1.38	30	41.8%	1.06 (0.51, 1.60)	
Total (95% CI)			69			69	100.0%	0.83 (0.48, 1.18)	

Heterogeneity: X^2 = 2.35 df = 2 (P = 0.31), I^2 = 15%
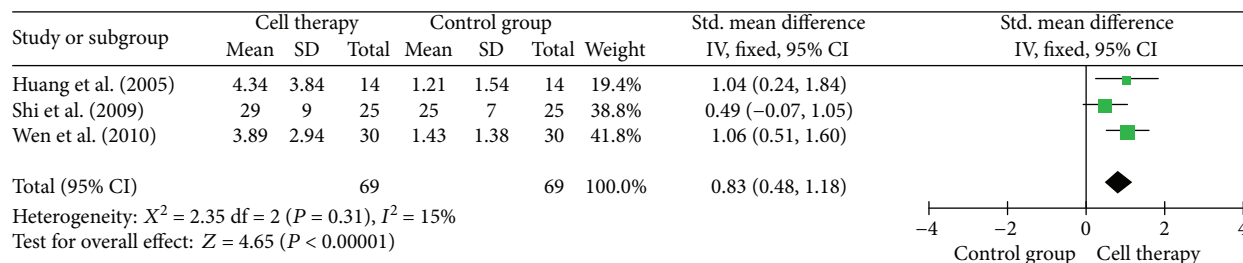Test for overall effect: Z = 4.65 (P < 0.00001)

FIGURE 8: Forest plot of meta-analysis with blood flow of 10 toes in cell therapy and standard care for critical limb ischemia. Squares indicate the standardized mean difference, and horizontal lines represent 95% confidence intervals.

JUVENTAS trial is the largest RCT to investigate the effects of BMMNCs by intra-arterial [5]. The study [5] reported that repetitive intra-arterial of autologous BMMNCs was not effective in reducing the primary outcome of the amputation rate at 6 months, ABI, ulcer healing, and TcO$_2$. Therefore, we suggest that stem cell administration is suitable and beneficial
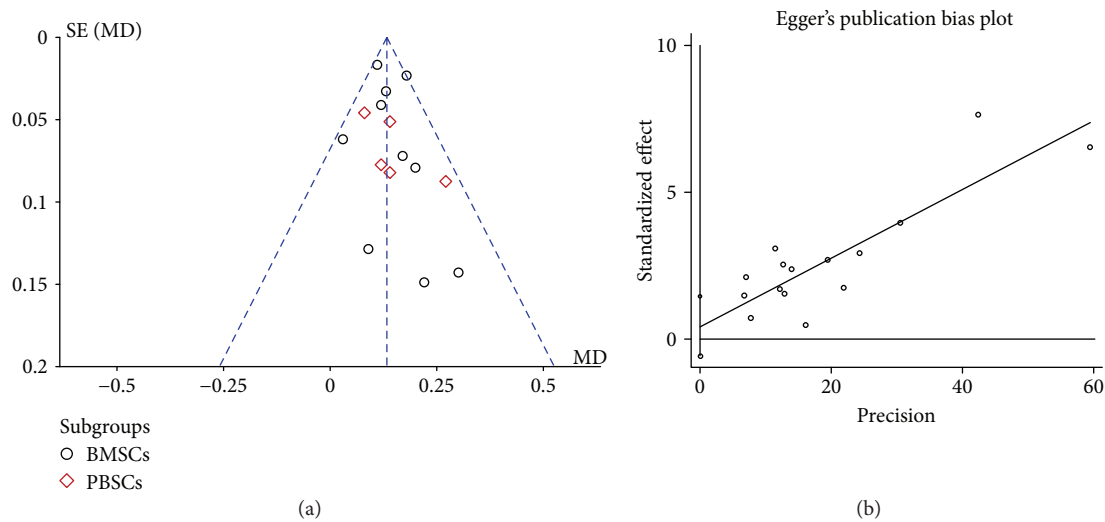
FIGURE 9: Meta-analysis of publication bias of the ankle-brachial index (ABI) in cell therapy and standard care for critical limb ischemia. (a) Funnel plot of the ABI. (b) Egger's funnel plot of the ABI.
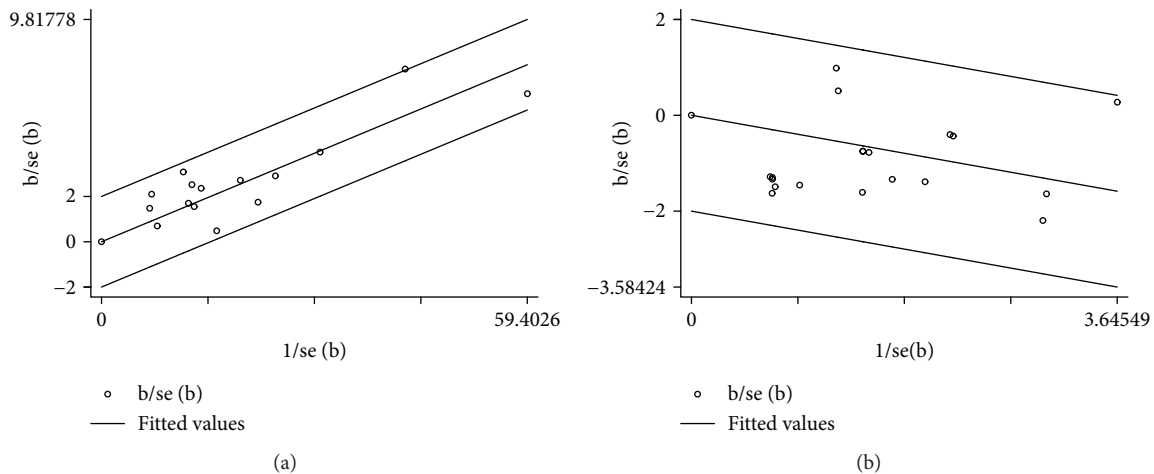

FIGURE 10: Meta-analysis of sensitivity in cell therapy and standard care for critical limb ischemia. (a) Galbraith plot of the ankle-brachial index (ABI). (b) Galbraith plot of the amputation rate.

choice by intramuscular injection. In addition, we found that the low dose (10^7) group was a significant difference on the amputation rate compared with high dose (10^9) and medium dose (10^8) groups ($P = 0.03$), and cell therapy with low dose (10^7) significantly reduced the amputation rate. The cell therapy with low dose (10^7) showed a significant improvement in ulcer healing in patients with CLI [26, 31, 32]. However, a degree of heterogeneity may be generated in subgroup analysis, which could negatively impinge upon the assessment on efficacy of cell therapy. The generated heterogeneity could mask the true effect of cell therapy [10]. So we think that the results of subgroup analysis need the large clinical trials as evidence to support.

4.3. Safety. The studies of 23 RCTs showed that cell therapy was relatively safe, and the adverse events were mostly mild and transient. Teraa et al. [5] reported that there was a patient with inguinal hematoma due to intra-arterial injection, and the study of Szabo et al. [33] found that the cell

therapy group had three adverse events during 3 months, but there was no evidence that the adverse events were attributed to stem cell transplantation. Li et al. [26] reported that there are three patients with fever in the cell therapy group, and they were cured after treatment. Lu et al. [15] showed that a few patients had a short-term response of mild pain 2 hours after cell transplantation, but no complications were detected, such as immune rejection and allergic reactions. Wen and Huang [34] reported that some patients felt uncomfortable of their limbs after intramuscular injection of PBSCs within 1 week, and the intramuscular injection site did not appear infected during 3-month follow-up. Similarly, many studies reported that stem cell transplantation was safe in long-term follow-up [28, 35]. The study by Molavi et al. [36] showed no adverse events during the 24-week follow-up period after cell delivery. No serious adverse events were found in the 23 studies included in this meta-analysis. Therefore, autologous stem cell transplantation is safe in the treatment of CLI.

In conclusion, this meta-analysis suggests that autologous stem cell therapy is safe and effective in CLI. Subgroup analysis indicates that cell types, cell dosage, route of administration, and follow-up time are the very important factors in stem cell therapy. However, we still lack high quality and large scale of RCTs to explore the influence of factors and the effect of autologous stem cell therapy in CLI.

Conflicts of Interest

The authors declare that they have no competing interests.

Authors' Contributions

Baocheng Xie and Daohua Xu designed the research. Baocheng Xie, Houlong Luo, Yusheng Zhang, Qinghui Wang, and Chenhui Zhou reviewed the literatures. Baocheng Xie, Houlong Luo, Yusheng Zhang, Qinghui Wang, and Chenhui Zhou collected the data. Baocheng Xie, Houlong Luo, and Yusheng Zhang analyzed the data. Baocheng Xie and Daohua Xu wrote the paper.

Acknowledgments

References

[1] R. W. Sprengers, M. Teraa, F. L. Moll, G. Ardine de Wit, Y. van der Graaf, and M. C. Verhaar, "Quality of life in patients with no-option critical limb ischemia underlines the need for new effective treatment," *Journal of Vascular Surgery*, vol. 52, no. 4, pp. 843–849.e1, 2010.

[2] Á. Cequier, C. Carrascosa, E. Diez-Tejedor et al., "Comments on the ESC guidelines on the diagnosis and treatment of peripheral artery diseases. A report of the Task Force of the Clinical Practice Guidelines Committee of the Spanish Society of Cardiology," *Revista Española de Cardiología (English Edition)*, vol. 65, no. 2, pp. 119–124, 2012.

[3] L. Norgren, W. R. Hiatt, J. A. Dormandy, M. R. Nehler, K. A. Harris, and F. G. R. Fowkes, "Inter-society consensus for the management of peripheral arterial disease (TASC II)," *Journal of Vascular Surgery*, vol. 45, no. 1, pp. S5–S67, 2007.

[4] M. R. Nehler, S. Duval, L. Diao et al., "Epidemiology of peripheral arterial disease and critical limb ischemia in an insured national population," *Journal of Vascular Surgery*, vol. 60, no. 3, pp. 686–695.e2, 2014.

[5] M. Teraa, R. W. Sprengers, R. E. G. Schutgens et al., "Effect of repetitive intra-arterial infusion of bone marrow mononuclear cells in patients with no-option limb ischemia: the randomized, double-blind, placebo-controlled rejuvenating endothelial progenitor cells via transcutaneous intra-arterial supplementation (JUVENTAS) trial," *Circulation*, vol. 131, no. 10, pp. 851–860, 2015.

[6] S. D. Patel, L. Biasi, I. Paraskevopoulos et al., "Comparison of angioplasty and bypass surgery for critical limb ischaemia in patients with infrapopliteal peripheral artery disease," *British Journal of Surgery*, vol. 103, no. 13, pp. 1815–1822, 2016.

[7] M. Pave, L. Benadiba, L. Berger, D. Gouicem, M. Hendricks, and D. Plissonnier, "Below-the-knee angioplasty for critical limb ischemia: results of a series of 157 procedures and impact of the angiosome concept," *Annals of Vascular Surgery*, vol. 36, pp. 199–207, 2016.

[8] F. Becker, H. Robert-Ebadi, J. B. Ricco et al., "Chapter I: definitions, epidemiology, clinical presentation and prognosis," *European Journal of Vascular and Endovascular Surgery*, vol. 42, pp. S4–S12, 2011.

[9] A. N. Raval, E. G. Schmuck, G. Tefera et al., "Bilateral administration of autologous CD133+ cells in ambulatory patients with refractory critical limb ischemia: lessons learned from a pilot randomized, double-blind, placebo-controlled trial," *Cytotherapy*, vol. 16, no. 12, pp. 1720–1732, 2014.

[10] M. Rigato, M. Monami, and G. P. Fadini, "Autologous cell therapy for peripheral arterial disease: systematic review and meta-analysis of randomized, non-randomized, and non-controlled studies," *Circulation Research*, vol. 120, no. 8, pp. 1326–1340, 2017.

[11] R. Compagna, B. Amato, S. Massa et al., "Cell therapy in patients with critical limb ischemia," *Stem Cells International*, vol. 2015, Article ID 931420, 13 pages, 2015.

[12] B. Lehalle, "Stem cells as a new treatment for peripheral artery disease: hype or hope? The point of view of a vascular surgeon," *Bio-medical Materials and Engineering*, vol. 25, 1 Supplement, pp. 73–78, 2015.

[13] M. Dubsky, A. Jirkovska, R. Bem et al., "Both autologous bone marrow mononuclear cell and peripheral blood progenitor cell therapies similarly improve ischaemia in patients with diabetic foot in comparison with control treatment," *Diabetes/Metabolism Research and Reviews*, vol. 29, no. 5, pp. 369–376, 2013.

[14] E. Tateishi-Yuyama, H. Matsubara, T. Murohara et al., "Therapeutic angiogenesis for patients with limb ischaemia by autologous transplantation of bone-marrow cells: a pilot study and a randomised controlled trial," *The Lancet*, vol. 360, no. 9331, pp. 427–435, 2002.

[15] D. Lu, B. Chen, Z. Liang et al., "Comparison of bone marrow mesenchymal stem cells with bone marrow-derived mononuclear cells for treatment of diabetic critical limb ischemia and foot ulcer: a double-blind, randomized, controlled trial," *Diabetes Research and Clinical Practice*, vol. 92, no. 1, pp. 26–36, 2011.

[16] C. A. Hart, J. Tsui, A. Khanna, D. J. Abraham, and D. M. Baker, "Stem cells of the lower limb: their role and potential in management of critical limb ischemia," *Experimental Biology and Medicine*, vol. 238, no. 10, pp. 1118–1126, 2013.

[17] M. Yang, L. Sheng, T. R. Zhang, and Q. Li, "Stem cell therapy for lower extremity diabetic ulcers: where do we stand?," *BioMed Research International*, vol. 2013, Article ID 462179, 8 pages, 2013.

[18] S. M. O. Peeters Weem, M. Teraa, G. J. de Borst, M. C. Verhaar, and F. L. Moll, "Bone marrow derived cell therapy in critical limb ischemia: a meta-analysis of randomized placebo controlled trials," *European Journal of Vascular and Endovascular Surgery*, vol. 50, no. 6, pp. 775–783, 2015.

[19] X. Sun, J. Ying, Y. Wang et al., "Meta-analysis on autologous stem cell transplantation in the treatment of limb ischemic," *International Journal of Clinical and Experimental Medicine*, vol. 8, no. 6, pp. 8740–8748, 2015.

[20] D. Moher, B.'. Pham, A. Jones et al., "Does quality of reports of randomised trials affect estimates of intervention efficacy

reported in meta-analyses?," *The Lancet*, vol. 352, no. 9128, pp. 609–613, 1998.

[21] H. Lawall, P. Bramlage, and B. Amann, "Treatment of peripheral arterial disease using stem and progenitor cell therapy," *Journal of Vascular Surgery*, vol. 53, no. 2, pp. 445–453, 2011.

[22] M. Teraa, R. W. Sprengers, P. E. Westerweel et al., "Bone marrow alterations and lower endothelial progenitor cell numbers in critical limb ischemia patients," *PLoS One*, vol. 8, no. 1, article e55592, 2013.

[23] M. Arai, Y. Misao, H. Nagai et al., "Granulocyte colony-stimulating factor: a noninvasive regeneration therapy for treating atherosclerotic peripheral artery disease," *Circulation Journal*, vol. 70, no. 9, pp. 1093–1098, 2006.

[24] P. Barć, J. Skóra, A. Pupka et al., "Bone-marrow cells in therapy of critical limb ischemia of lower extremities-own experience," *Acta Angiologica*, vol. 12, no. 4, pp. 155–166, 2006.

[25] D. H. Walter, H. Krankenberg, J. O. Balzer et al., "Intraarterial administration of bone marrow mononuclear cells in patients with critical limb ischemia: a randomized-start, placebo-controlled pilot trial (PROVASA)," *Circulation: Cardiovascular Interventions*, vol. 4, no. 1, pp. 26–37, 2011.

[26] M. Li, Department of Cardiology Provincial Hospital affiliated to Shandong University, Shandong Province, China, H. Zhou et al., "Autologous bone marrow mononuclear cells transplant in patients with critical leg ischemia: preliminary clinical results," *Experimental and Clinical Transplantation*, vol. 11, no. 5, pp. 435–439, 2013.

[27] M. Dubsky, A. Jirkovska, R. Bem et al., "Comparison of two different methods of stem cell therapy of critical limb ischemia in patients with diabetic foot disease," *Diabetes*, 2010.

[28] G. P. Lasala, J. A. Silva, P. A. Gardner, and J. J. Minguell, "Combination stem cell therapy for the treatment of severe limb ischemia: safety and efficacy analysis," *Angiology*, vol. 61, no. 6, pp. 551–6, 2010.

[29] P. K. Gupta, A. Chullikana, R. Parakh et al., "A double blind randomized placebo controlled phase I/II study assessing the safety and efficacy of allogeneic bone marrow derived mesenchymal stem cell in critical limb ischemia," *Journal of Translational Medicine*, vol. 11, no. 1, p. 143, 2013.

[30] V. Procházka, J. Gumulec, F. Jalůvka et al., "Cell therapy, a new standard in management of chronic critical limb ischemia and foot ulcer," *Cell Transplantation*, vol. 19, no. 11, pp. 1413–1424, 2010.

[31] A. Ozturk, Y. Kucukardali, F. Tangi et al., "Therapeutical potential of autologous peripheral blood mononuclear cell transplantation in patients with type 2 diabetic critical limb ischemia," *Journal of Diabetes and its Complications*, vol. 26, no. 1, pp. 29–33, 2012.

[32] L. Mohammadzadeh, S. H. Samedanifard, A. Keshavarzi et al., "Therapeutic outcomes of transplanting autologous granulocyte colony-stimulating factor-mobilised peripheral mononuclear cells in diabetic patients with critical limb ischaemia," *Experimental and Clinical Endocrinology & Diabetes*, vol. 121, no. 1, pp. 48–53, 2013.

[33] G. V. Szabo, Z. Kovesd, J. Cserepes, J. Daroczy, M. Belkin, and G. Acsady, "Peripheral blood-derived autologous stem cell therapy for the treatment of patients with late-stage peripheral artery disease-results of the short- and long-term follow-up," *Cytotherapy*, vol. 15, no. 10, pp. 1245–1252, 2013.

[34] J. C. Wen and P. P. Huang, "Autologous peripheral blood mononuclear cells transplantation in treatment of 30 cases of

critical limb ischemia: 3-year safety follow-up," *Journal of Clinical Rehabilitative Tissue Engineering Research*, vol. 14, no. 45, pp. 8526–8530, 2010.

[35] V. Ponemone, S. Gupta, D. Sethi et al., "Safety and effectiveness of bone marrow cell concentrate in the treatment of chronic critical limb ischemia utilizing a rapid point-of-care system," *Stem Cells International*, vol. 2017, Article ID 4137626, 16 pages, 2017.

[36] B. Molavi, M. R. Zafarghandi, E. Aminizadeh et al., "Safety and efficacy of repeated bone marrow mononuclear cell therapy in patients with critical limb ischemia in a pilot randomized controlled trial," *Archives of Iranian Medicine*, vol. 19, no. 6, pp. 388–396, 2016.

[37] P. Huang, S. Li, M. Han, Z. Xiao, R. Yang, and Z. C. Han, "Autologous transplantation of granulocyte colony-stimulating factor-mobilized peripheral blood mononuclear cells improves critical limb ischemia in diabetes," *Diabetes Care*, vol. 28, no. 9, pp. 2155–2160, 2005.

[38] L. Debin, J. Youzhao, L. Ziwen, L. Xiaoyan, Z. Zhonghui, and C. Bing, "Autologous transplantation of bone marrow mesenchymal stem cells on diabetic patients with lower limb ischemia," *Journal of Medical Colleges of PLA*, vol. 23, no. 2, pp. 106–115, 2008.

[39] N. R. Dash, S. N. Dash, P. Routray, S. Mohapatra, and P. C. Mohapatra, "Targeting nonhealing ulcers of lower extremity in human through autologous bone marrow-derived mesenchymal stem cells," *Rejuvenation Research*, vol. 12, no. 5, pp. 359–366, 2009.

[40] J. Shi, Z. R. Yang, X. Hu, L. H. Cao, X. Y. Zhang, and X. X. Ma, "Clinical study of autologous bone marrow hematopoietic stem cell transplantation for treatment of diabetic lower limb vascular lesions," *Chinese Journal of Postgraduates of Medicine*, vol. 32, no. 12, pp. 50–52, 2009.

[41] P. Jain, B. Perakath, M. R. Jesudason, and S. Nayak, "The effect of autologous bone marrow-derived cells on healing chronic lower extremity wounds: results of a randomized controlled study," *Ostomy/Wound Management*, vol. 57, no. 7, pp. 38–44, 2011.

[42] E. Benoit, T. F. O'Donnell, M. D. Iafrati et al., "The role of amputation as an outcome measure in cellular therapy for critical limb ischemia: implications for clinical trial design," *Journal of Translational Medicine*, vol. 9, no. 1, p. 165, 2011.

[43] D. W. Losordo, M. R. Kibbe, F. Mendelsohn et al., "A randomized, controlled pilot study of autologous CD34+ cell therapy for critical limb ischemia," *Circulation: Cardiovascular Interventions*, vol. 5, no. 6, pp. 821–830, 2012.

[44] R. J. Powell, W. A. Marston, S. A. Berceli et al., "Cellular therapy with Ixmyelocel-T to treat critical limb ischemia: the randomized, double-blind, placebo-controlled RESTORE-CLI trial," *Molecular Therapy*, vol. 20, no. 6, pp. 1280–6, 2012.

[45] J. Skóra, A. Pupka, D. Janczak et al., "Combined autologous bone marrow mononuclear cell and gene therapy as the last resort for patients with critical limb ischemia," *Archives of Medical Science*, vol. 2, no. 2, pp. 325–331, 2015.

[46] A. J. Lu, J. Zhao, S. P. Zhang, D. M. Li, L. J. Zhang, and J. L. Nan, "The clinical observation of 20 cases of diabetic vascular lesion of lower limbs treated with autologous peripheral blood stem cell transplant after bone marrow mobilization," *Inner Mongolia Medical Journal*, vol. 48, no. 4, pp. 402–404, 2016.